

STATUS OF THESIS

Title of thesis

DESIGN AND DEVELOPMENT OF A SMART ADVISORY  
SYSTEM FOR HAZARDOUS MATERIALS  
TRANSPORTATION RISK ANALYSIS VIA QUANTITATIVE  
APPROACHES

I ZULKIFLI BIN ABDUL RASHID

hereby allow my thesis to be placed at the Information Resource Center (IRC) of  
Universiti Teknologi PETRONAS (UTP) with the following conditions:

1. The thesis becomes the property of UTP
2. The IRC of UTP may make copies of the thesis for academic purposes only.
3. This thesis is classified as

☐

Confidential

☐

Non-confidential

If this thesis is confidential, please state the reason:

---

The content of the thesis will remain confidential for \_\_\_\_\_ years.

Remarks on disclosure:

---

Endorsed by

\_\_\_\_\_  
(Signature of Author)

Permanent address:

No. 17 Jalan BTK 5/8, Section 5,  
Bandar Teknologi Kajang,  
43500 Semenyih, Selangor

Date : \_\_\_\_\_

\_\_\_\_\_  
(Signature of Supervisor)

Dr. Mohanad A.A. El Harbawi

Date : \_\_\_\_\_



UNIVERSITI TEKNOLOGI PETRONAS

DESIGN AND DEVELOPMENT OF A SMART ADVISORY SYSTEM FOR  
HAZARDOUS MATERIALS TRANSPORTATION RISK ANALYSIS VIA  
QUANTITATIVE APPROACHES

by

ZULKIFLI BIN ABDUL RASHID

The undersigned certify that they have read, and recommend to the Postgraduate Studies Program for acceptance, for the fulfillment of the requirements for the degree stated.

Signature:

---

Supervisor:

Dr. Mohanad A.A. El Harbawi

---

Signature:

---

Head of Department:

Assoc. Prof. Dr.Mohamad Azmi Bustam

---

Date:

---



DESIGN AND DEVELOPMENT OF A SMART ADVISORY SYSTEM FOR  
HAZARDOUS MATERIALS TRANSPORTATION RISK ANALYSIS VIA  
QUANTITATIVE APPROACHES

by

ZULKIFLI BIN ABDUL RASHID

A Thesis

Submitted to the Postgraduate Studies Programme  
as a Requirement for the Degree of

DOCTOR OF PHILOSOPHY  
CHEMICAL ENGINEERING PROGRAMME  
UNIVERSITI TEKNOLOGI PETRONAS  
BANDAR SERI ISKANDAR,  
PERAK

JUNE, 2013



## DECLARATION OF THESIS

Title of thesis

DESIGN AND DEVELOPMENT OF A SMART ADVISORY  
SYSTEM FOR HAZARDOUS MATERIALS TRANSPORTATION  
RISK ANALYSIS VIA QUANTITATIVE APPROACHES

I ZULKIFLI BIN ABDUL RASHID

I hereby declare that the thesis is based on my original work except for quotations and citations which have been duly acknowledged. I also declare that it has not been previously or concurrently submitted for any other degree at UTP or other institutions.

Witnessed by

\_\_\_\_\_  
(Signature of Author)

Permanent address:

No. 17 Jalan BTK 5/8, Section 5,

Bandar Teknologi Kajang,

43500 Semenyih, Selangor

\_\_\_\_\_  
(Signature of Supervisor)

Dr. Mohanad A.A. El Harbawi

Date : \_\_\_\_\_

Date : \_\_\_\_\_



## ACKNOWLEDGEMENT

In the name of Allah the Most Gracious and the Most Merciful, I hereby express my warmest gratitude and appreciation to my supervisor, Dr. Mohanad A.A. El-Harbawi for his continuous encouragement, valuable suggestions and supports throughout my research progress from February 2009.

My biggest appreciation to Postgraduate coordinator, Dr. Nurlidia and all UTP Chemical Engineering Department lecturers for the favour and beneficial professional guidance to me. Thousand thanks for Puan Kamaliah for patiently checking my thesis format according to the UTP thesis guideline. Warmest thanks for all my colleagues in UITM for the encouragement and support especially to Encik Azil Bahari, Dr. Sherif and Prof. Dr. Sharifah.

Thanks to Allah with His guidance, finally I able to complete my thesis even though I had an illness during the last 1 year which gave a major impact to my study. Therefore, a million thanks to all the Specialists in Hospital Pakar Sultanah Fatimah Muar, all Islamic alternative medicine practitioner from Darul Shifa', Dato' Dr. Haron Din Al-Hajj and Ustaz Anuar Al-Hafiz. My biggest appreciation and love to my dear beloved wife Dr. Mastura Binti Mokhtar, all my children and my parents for their sacrifice, patience and support during my illness and during the completion of my thesis.

A special thanks to the MOHE for sponsored my PhD scholarship. Last but certainly not the least, I wish everyone the very best future and continue to provide excellent guidance and support for the future innovative research. Thank you.



## DEDICATION

*for my beloved wife, children and parents*



## ABSTRACT

Safe transportation of hazardous materials is critical as it has a high potential of catastrophic accidents depending on the amount of transported product, its hazardous characteristics and the environmental conditions. Consequently, an efficient, smart and reliable intervention is essential to enhance prediction on the impacts of transportation hazards. Although various risk assessment techniques have been used in industry and regulatory bodies, they were developed for evaluating risk of hazardous materials for fixed installation cases instead of moving risk sources. This study applies the Transportation Risk Analysis (TRA), which is an extension of a well-known Quantitative Risk Analysis (QRA) technique in developing and design a Smart Advisory Systems (SAS), to determine the safest routes for transportation of hazardous materials according to Malaysia scenario. Although a number of Smart Advisory Systems (SAS) TRA simulation tools have been developed to assess transportation risks, these tools are not user friendly due to the large number of variables, complexity of the models and lack of available data for TRA. The proposed TRA model in this study aims at minimizing the problems related to SAS simulation faced by the previous researchers resulting in an optimum TRA model that is both practical and marketable. Several researchers integrate Geographic Information System (GIS) with mathematical and simulation models, to develop the required databases and expert systems. However, the advantage of using GIS tool is very dependent on the functional capability of the latest GIS version to generate a comprehensive and updated map. This newly developed SAS simulation software is called SMACTRA software, which is designed to be compatible with windows operating system. It utilizes Esri and ArcGIS 9.4 to review, analyse and evaluate the potential hazards consequences from transportation accidents at any points and locations resulting in accurate and precise hazards consequences, and it also predicts the survival capability by taking into consideration age and total burn body surface



area (TBS) factors. Moreover, some of the hazards consequences from transportation accident can also be simulated online.



## ABSTRAK

Pengangkutan bahan berbahaya dengan selamat adalah kritikal memandangkan ia amat berpotensi untuk mengundang bencana sekiranya berlaku kemalangan. Secara umumnya kesan bencana dari kemalangan pengangkutan bahan berbahaya bergantung kepada beberapa faktor umpamanya jumlah produk yang diangkut, jenis bahan berbahaya dan keadaan persekitaran sekeliling. Oleh yang demikian, satu kaedah atau pembangunan perkakas yang cekap, pintar dan boleh dipercayai untuk meramal kesan-kesan bencana dari pengangkutan bahan-bahan berbahaya amat penting untuk direkabentuk. Pelbagai teknik penilaian risiko telah digunakan dalam industri dan badan-badan yang mengawal selia undang-undang berkaitan keselamatan dan analisa risiko, bagi menilai tahap risiko serta mengenalpasti peluang mengurangkan risiko kemalangan dari bahan berbahaya ini. Walaubagaimanapun sebahagian besar keputusan penggunaan teknik-teknik penilaian risiko ini didapati lebih berjaya dan tepat bagi kes-kes risiko punca statik berbanding risiko daripada punca-punca bergerak. Di dalam kajian ini, Transportation Risk Analysis (TRA), iaitu lanjutan daripada teknik analisis risiko kuantitatif (QRA) diaplikasi bagi menentukan laluan-laluan paling selamat ketika pengangkutan bahan berbahaya. Seterusnya melalui penggunaan TRA model ini, suatu Sistem Penasihat Pintar akan direkabentuk untuk menilai risiko kemalangan pengangkutan bahan berbahaya berdasarkan senario di Malaysia. Oleh itu garis-garis panduan sedia ada bagi model TRA dikaji semula dan dianalisis, supaya TRA model yang lebih sesuai dan lebih tepat boleh dihasilkan untuk digunakan menurut senario Malaysia. Beberapa Sistem Penasihat Pintar (SAS) atau Peralatan simulasi TRA telah dibangunkan untuk menilai risiko pengangkutan bahan berbahaya walaubagaimanapun, kebanyakan daripada yang perkakas-perkakas tersedia tidak mudahpakai. Ini adalah disebabkan oleh bilangan pembolehubah yang digunakan di dalam model yang terlalu banyak, sifat punca-punca bergerak yang



terlalu rumit, kekurangan data tersedia / pangkalan data untuk TRA dan kesukaran untuk memahami perhubungan yang kompleks di antara unsur- unsur yang terlibat semasa analisis.

TRA model yang dicadangkan di dalam kajian adalah bertujuan untuk mengurangkan masalah-masalah berkaitan dengan simulasi SAS seperti yang dihadapi oleh penyelidik-penyelidik sebelumnya selain memoptimumkan penggunaan TRA model di dalam pembangunan perisian simulasi SAS supaya lebih praktikal dan mudah dipasarkan. Dalam penilaian risiko beberapa penyelidik telah menggunakan GIS, dengan mengintegrasikan GIS dengan formula matematik dan model simulasi, untuk membangunkan suatu sistem pengkalan data yang cekap dan sistem pintar. Walau bagaimanapun, keupayaan untuk menghasilkan maklumat yang komprehensif kepada peta digital amat bergantung kepada kebolehan fungsi- fungsi yang ada pada setiap versi GIS yang telah dikemaskini. Perisian simulasi SAS yang baru dibangunkan ini dipanggil perisian SMACTRA di mana ia direka bentuk supaya serasi dengan sistem pengendalian computer windows. Perisian ini juga menggunakan Esri iaitu ArcGIS 9.4 bagi semakan semula, analisis dan menilai bahaya akibat kemalangan pengangkutan dimana- mana titik dan lokasi berdasarkan peta yang dijanakan oleh komputer dan berupaya untuk mengenal pasti keupayaan mangsa untuk hidup dengan mengambilkira pertimbangan keatas faktor umur dan jumlah luas permukaan badan yang terbakar (TBS. Sebahagian keputusan dari TRA juga boleh disimulasikan secara talian.



## COPYRIGHT PAGE

In compliance with the terms of the Copyright Act 1987 and the IP Policy of the university, the copyright of this thesis has been reassigned by the author to the legal entity of the university,

Institute of Technology PETRONAS Sdn. Bhd.

Due acknowledgement shall always be made of the use of any material contained in, or derived from, this thesis.

© ZULKIFLI ABDUL RASHID, 2013

Institute of Technology PETRONAS Sdn Bhd

All rights reserved.



## TABLE OF CONTENTS

|   |       |
|---|-------|
| STATUS OF THESIS.....   | i     |
| UNIVERSITI TEKNOLOGI PETRONAS.....                            | ii    |
| DECLARATION OF THESIS.....                                    | iv    |
| ACKNOWLEDGEMENT.....  | v     |
| DEDICATION.....   | vi    |
| ABSTRACT.....   | vii   |
| COPYRIGHT PAGE.....   | xi    |
| TABLE OF CONTENTS.....  | xii   |
| LIST OF FIGURES.....  | xix   |
| LIST OF TABLES.....   | xxxii |
| <br>CHAPTER 1: INTRODUCTION.....                              | <br>1 |
| 1.1 Background.....   | 1     |
| 1.2 Problem Statement.....                                    | 3     |
| 1.3 Objectives of the study.....                              | 4     |
| 1.4 Scope of Study.....                                       | 5     |
| 1.5 Layout of the thesis.....                                 | 6     |
| <br>CHAPTER 2 : LITERATURE REVIEW.....                        | <br>8 |
| 2.1 Background.....   | 8     |
| 2.2 Hazardous Materials.....                                  | 10    |
| 2.3 Hazardous Materials (HazMat) Transportation Incident..... | 14    |



|         |   |    |
|---------|---|----|
| 2.4.    | Transportation Quantitative Risk Analysis .....   | 15 |
| 2.4.1   | Risk Assessment.....  | 15 |
| 2.4.2   | The Public and Risk Assessment.....   | 22 |
| 2.5     | The Quantitative Risk Analysis Procedure.....   | 22 |
| 2.5.1   | Framework of TRA.....   | 22 |
| 2.5.2   | Comparison to Stationary Facility of Chemical Process Risk Analysis.....                                      | 24 |
| 2.5.3   | Reason in Conducting TRA.....   | 26 |
| 2.6     | Review of Previous Work on Transport Risk Analysis Models and Guideline.....                                  | 27 |
| 2.6.1   | Swiss Methodology (BUWAL) for Assessing the Risk of Hazardous Materials Transportation by Road.....           | 27 |
| 2.6.1.1 | Subdivision of the Road Tracks into Road ad Segments.....   | 27 |
| 2.6.1.2 | Data information.....   | 28 |
| 2.6.1.3 | Estimation of the likelihood of an Incident with Severe Consequences to People or Environment.....            | 30 |
| 2.6.1.4 | Frequency of incident with severe damages.....  | 31 |
| 2.6.1.5 | Ratio of the relevant Product of the SDR- class Applicable to the representative Incident Scenario (RRP)..... | 31 |
| 2.6.1.6 | Assumptions concerning the representative incident scenario for the “Population”.....                         | 31 |
| 2.6.1.7 | Comparison risk by two routes only at one time.....   | 31 |
| 2.6.2   | Rhyne Methodology for Assessing the Risk of Hazardous Materials Transportation by Road.....                   | 32 |
| 2.6.3   | CCPS-TRA Methodology for Assessing the Risk of Hazardous Materials Transportation by Road.....                | 35 |
| 2.6.4   | Previous Trend on Development of Transportation Risk Analysis Model.....                                      | 38 |



|                              |  |     |
|------------------------------|--|-----|
| 2.7                          | Application of Geographic Information System in TRA.....   | 45  |
| 2.8                          | The Application of GIS for HazMat Transportation.....  | 47  |
| 2.9                          | Application of GIS for Air Dispersion Consequences.....  | 47  |
| 2.10                         | Transportation Accident Trends based on Available Accident Database.....   | 50  |
| 2.11                         | Smart Advisory System in HazMat TRA.....   | 54  |
| 2.12                         | Discussions Analysis for Proposed A Smart Advisory System of Hazardous Materials Transportations Risk Analysis Based on Malaysia Scenario..... | 62  |
| 2.12.1                       | Analysis from the existing TRA model of hazardous Materials.....   | 63  |
| 2.12.2                       | Requirement to develop and design proposed SAS for Hazardous materials transportation.....   | 71  |
| 2.13                         | Summary.....   | 72  |
| CHAPTER 3 : METHODOLOGY..... |  | 75  |
| 3.1                          | Review the Existing TRA Model of Hazardous Materials.....  | 78  |
| 3.2                          | Modification of TRA Model for Malaysia.....  | 78  |
| 3.2.1                        | Accident Rates.....  | 81  |
| 3.2.2                        | Number of Road Tanker Trip.....  | 86  |
| 3.2.3                        | Probability Event from the Accident.....   | 86  |
| 3.2.4                        | Probability Damage Calculation.....  | 86  |
| 3.2.5                        | Probit Analysis.....   | 87  |
| 3.2.5.1                      | The damage to human from thermal radiation.....  | 91  |
| 3.2.5.2                      | The impact of Thermal Radiation to Human from the of burn size distribution and ages.....  | 97  |
| 3.3                          | Consequence Analysis.....  | 99  |
| 3.4                          | Route Segmentation.....  | 103 |



|         |  |     |
|---------|--|-----|
| 3.5     | Risk Estimation.....                             | 105 |
| 3.5.1   | Individual Risk.....                             | 105 |
| 3.5.2   | Societal Risk Analysis.....                      | 111 |
| 3.5.3   | Acceptability Risk.....                          | 113 |
| 3.6     | Population Density.....                          | 115 |
| 3.6.1   | Population Data.....                             | 115 |
| 3.6.1.1 | Population Data for Residential Area.....        | 116 |
| 3.6.1.2 | Population Data for Commercial Area.....         | 116 |
| 3.6.1.3 | Population Data for Industrial Area.....         | 117 |
| 3.6.1.4 | Population Data for Recreational Area.....       | 117 |
| 3.6.2   | Population Present.....                          | 117 |
| 3.6.2.1 | Day- time and Night- time population.....        | 117 |
| 3.6.2.2 | Indoor and Outdoor.....                          | 119 |
| 3.6.3   | Corrected Population Present.....                | 119 |
| 3.6.4   | Population Mapping.....                          | 120 |
| 3.7     | Meteorology Condition.....                       | 120 |
| 3.8     | SMACTRA Description.....                         | 122 |
| 3.8.1   | Planning the Application.....                    | 123 |
| 3.8.2   | Designing Database.....                          | 124 |
| 3.8.3   | Building the Graphical User Interface (GUI)..... | 127 |
| 3.8.4   | General Interface.....                           | 127 |
| 3.8.7   | Incident Frequency Interface.....                | 132 |
| 3.8.8   | Fire Interface.....                              | 134 |
| 3.8.9   | Explosion Interface.....                         | 137 |



|            |   |     |
|------------|---|-----|
| 3.8.5      | Toxic Release Interface.....  | 140 |
| 3.8.6      | Risk Impact Interface.....  | 140 |
| 3.8.10     | Transportation Risk Analysis Simulation (TRIS) in<br>SMACTRA.....   | 141 |
| 3.8.11     | SMACTRA Contour Panel for GIS Presentation.....   | 143 |
| 3.9        | Writing the Computer Programme.....   | 144 |
| 3.10       | Development of GIS.....   | 144 |
| 3.10.1     | Integrating SMACTRA Application with GIS.....   | 145 |
| 3.10.1.1   | Database Design.....  | 145 |
| 3.10.1.2   | Data Processing.....  | 147 |
| 3.10.2     | Integrate VB Output to ArcGIS Model Builder.....  | 148 |
| 3.11       | Map Projection with Georeferencing.....   | 154 |
| 3.12       | SMACTRA Validation and Verification.....  | 159 |
| 3.13       | Summary.....  | 159 |
| CHAPTER 4: | RESULT & DISCUSSION.....  | 162 |
| 4.1        | Software Validation.....  | 162 |
| 4.1.1      | Case Studies.....   | 165 |
| 4.2        | Accident Scenario (Sequence of Event).....  | 167 |
| 4.3        | Output from the Case Studies.....   | 170 |
| 4.3.1      | Results of the Vapour Cloud Explosion Consequences of LPG<br>Transportation Accident (at the container capacity 34.5m <sup>3</sup> ).....               | 170 |
| 4.3.2      | Results of the Vapour Cloud Explosion from LPG<br>Transportation Accident at various truck capacities.....  | 175 |
| 4.3.3      | Results of the Vapour Cloud Consequences of LPG<br>Transportation Accident to Human and Structural Building<br>Effects of Exposure to Overpressure..... | 180 |



|        |  |     |
|--------|--|-----|
| 4.3.4  | Comparison results of the vapour cloud explosion consequences using SMACTRA with published case studies and software risk analysis results.....  | 197 |
| 4.3.5  | Results of the radiant heat from pool and torch fires of LPG transportation accident (at the container capacity 34.5 m <sup>3</sup> ).....   | 200 |
| 4.3.6  | The effect from the radiant heat pool fire of LPG transportation accident (at the container capacity 34.5m <sup>3</sup> ) to receptor.....   | 205 |
| 4.3.7  | The pool fire time exposure effect on thermal radiation dose load for LPG tanker incident (in capacity of 34.5m <sup>3</sup> ) to Receptor.....  | 207 |
| 4.3.8  | Results of the BLEVE fireball consequences of LPG transportation accident.....   | 212 |
| 4.3.9  | The BLEVE time exposure effect over age and thermal radiation dose load for LPG tanker incident (in capacity of 34.5m <sup>3</sup> ) to receptor.....  | 216 |
| 4.3.10 | The BLEVE probit analysis and Thermal Radiation dose load as a function of distance for LPG tanker incident (in capacity of 34.5m <sup>3</sup> ) to Receptor.....                                    | 227 |
| 4.3.11 | The Effect of fireball height, fireball diameter and emissive power as a function of BLEVE fireball formation time for the LPG tanker incident (in capacity of 34.5m <sup>3</sup> ) to Receptor..... | 231 |
| 4.3.12 | The Effect of toxic gas dispersion as the results of propane and ammonia release from transportation accident by using SMACTRA Map API online.....   | 233 |
| 4.4    | Risk Analysis for Hazardous Materials Transportation.....  | 239 |
| 4.4.1  | Results of the road tanker accident analysis carrying 13,000kg of LPG (at the container capacity 34.5m <sup>3</sup> ).....   | 240 |
| 4.4.2  | Comparing results of societal risk route from LPG transportation accident (at the container capacity 34.5m <sup>3</sup> ).....   | 243 |
| 4.4.3  | Analyze the effect of route length over societal risk from LPG accident (at the container capacity 34.5m <sup>3</sup> ) by using SMACTRA.....  | 247 |



|  |  |     |
|--|--|-----|
| 4.4.4                                    | The trips effect over the societal risk for five routes of LPG tanker incident (in capacity of 34.5m <sup>3</sup> ) to receptor..... | 252 |
| 4.4.5                                    | Comparison the individual risk and societal risk results between SMACTRA, BUWAL and CCPS.....  | 253 |
| 4.5                                      | Hazard Mapping Analysis.....   | 256 |
| 4.5.1                                    | The effect of population distribution to transportation risk hazards during day and night activities.....                            | 261 |
| 4.5.2                                    | The effect of LPG capacity during transportation accident using GIS application.....   | 262 |
| 4.6                                      | Summary.....   | 266 |
| CHAPTER 5: CONCLUSION & FUTURE WORK..... |  | 269 |
| RECOMMENDATION FOR FUTURE WORK.....      |  | 276 |
| REFERENCES.....                          |  | 277 |
| LIST OF PUBLICATIONS AND AWARDS.....     |  | 298 |
| APPENDIX 1.....                          |  | 301 |
| APPENDIX 2.....                          |  | 314 |
| APPENDIX 3.....                          |  | 315 |
| APPENDIX 4.....                          |  | 323 |
| APPENDIX 5.....                          |  | 349 |



## LIST OF FIGURES

|             |  |     |
|-------------|--|-----|
| Figure 3.1  | Flowchart shows the summary of the development of smart advisory system for transportation risk analysis (HazMat).....   | 76  |
| Figure 3.2  | Overview flowchart of proposed TRA methodology for Malaysia HazMat Scenario.....   | 77  |
| Figure 3.3  | Route Segmentation.....  | 104 |
| Figure 3.4  | Diagram shows the relationships between link (l), point of release Q (x,y) and point of exposure Exp (x,y).....  | 105 |
| Figure 3.5  | The individual risk for receptor at x, y coordinate of one scenario such as toxic release occurring at several locations.....                                    | 109 |
| Figure 3.6  | The individual risk for receptors at (x, y) and (x <sub>1</sub> , y <sub>1</sub> ) coordinates of one scenario such as BLEVE occurring at several locations..... | 110 |
| Figure 3.7  | Shows how the societal risk are calculated over the all routes to find the safest road.....  | 114 |
| Figure 3.8  | Malaysian Meteorological Department Homepage.....  | 121 |
| Figure 3.9  | Flowchart of SMACTRA.....  | 126 |
| Figure 3.10 | The main general interface.....  | 128 |
| Figure 3.11 | File submenus.....   | 128 |
| Figure 3.12 | TRA interface form.....  | 129 |
| Figure 3.13 | Edit submenus.....   | 129 |
| Figure 3.14 | View submenus.....   | 129 |
| Figure 3.15 | Scenario submenus.....   | 130 |
| Figure 3.16 | shows consequences analysis model menu.....  | 130 |



|             |   |     |
|-------------|---|-----|
| Figure 3.17 | Shows vulnerability main menu.....  | 131 |
| Figure 3.18 | shows the risk assessment menu.....   | 131 |
| Figure 3.19 | Accident scenario and frequency selection profile.....  | 132 |
| Figure 3.20 | Final frequency output from the propagation sequence of the accident scenario.....  | 133 |
| Figure 3.21 | Consequences analysis interface.....  | 133 |
| Figure 3.22 | shows the pool fire forms.....  | 134 |
| Figure 3.23 | illustrates the calculation of pool fire hazard results via Casal Method.....   | 135 |
| Figure 3.24 | shows the pool fire hazard calculation following CCPS method.....   | 136 |
| Figure 3.25 | shows the wind influence to pool fire.....  | 136 |
| Figure 3.26 | illustrates the calculation of jet fire hazard.....   | 137 |
| Figure 3.27 | illustrates the calculation of BLEVE hazard with its graph analysis and output results for the incident scenario.....   | 137 |
| Figure 3.28 | illustrates peak overpressure impact over the receptor distance to predict the effects of explosion to human, structure and building.....   | 138 |
| Figure 3.29 | shows comparison analysis of the explosion effects calculation of road tanker carrying varies capacity of hazardous material over distance impact on human, structure and building..... | 139 |
| Figure 3.30 | shows the BLEVE fireball and its vulnerability interface.....   | 139 |
| Figure 3.31 | illustrates the toxic release interface.....  | 140 |
| Figure 3.32 | illustrates the risk impact interface.....  | 141 |
| Figure 3.33 | shows the online driving simulator.....   | 142 |
| Figure 3.34 | shows the BLEVE fireball impact using online simulation....   | 142 |
| Figure 3.35 | Shows the BLEVE fireball impact at panoramic view.....  | 142 |



|             |   |     |
|-------------|---|-----|
| Figure 3.36 | shows GIS map analyzing using SMACTRA.....  | 143 |
| Figure 3.37 | Work Flow of GIS Integration.....   | 145 |
| Figure 3.38 | Database design VB to Arc GIS.....  | 146 |
| Figure 3.39 | GIS Data Processing VB to ArcGIS Model builder tool.....  | 146 |
| Figure 3.40 | shows Model builder ArcGIS submenu properties.....  | 149 |
| Figure 3.41 | shows Hazard region analysis environment settings.....  | 150 |
| Figure 3.42 | shows the boundary polygon and hazard point location.....   | 150 |
| Figure 3.43 | show the input setting parameter from VB calculation integrated into GIS model builder.....                         | 151 |
| Figure 3.44 | shows the selected coordinate x, y in VB which represent the Accident point data on GIS.....                        | 151 |
| Figure 3.45 | shows the selected coordinate x, y in VB is converted to GIS point data location at shape file.....                 | 152 |
| Figure 3.46 | shows the buffer radius from the tanker accident will generated on GIS map via the input coordinate x, y in VB..... | 152 |
| Figure 3.47 | shows the Clip gathered the risk input data and buffer result.....  | 153 |
| Figure 3.48 | shows the process flow to integrate the VB output to ArcGIS.....  | 154 |
| Figure 3.49 | Google satellite image.....   | 155 |
| Figure 3.50 | Search location of accident occurs (at Middle West Coast Refinery in Port Dickson) and zoom out the image.....      | 156 |
| Figure 3.51 | Add the lating of the position coordinate in decimal degree unit (at least 4 points).....                           | 156 |
| Figure 3.52 | Projection Map from Different Spatial Reference World Geographic Coordinate System.....                             | 156 |
| Figure 3.53 | Adding Control from Reference Object.....   | 157 |



|             |   |     |
|-------------|---|-----|
| Figure 3.54 | Checked the coordinate residual (e.g 0.00001) subjected to Georeferencing analysis.....   | 157 |
| Figure 3.55 | Result after Map projection and Georeferencing analysis processes (image as background layer).....  | 157 |
| Figure 3.56 | Illustrate Inverse Distance Weighted (IDW) interpolation based on Weighted sample point distance (left) from population density point over route.....   | 158 |
| Figure 4.1  | Software Validation.....  | 164 |
| Figure 4.2  | shows the sequence of events based on LPG road tanker accident case study at Port Dickson.....  | 168 |
| Figure 4.3  | Comparison of the overpressure at a given scenario predicted as a function of distance for the three methods (SMACTRA – TNT - equivalency ( $\eta=10\%$ at <b>13000kg</b> propane); Multi Energy method: blast strength = 7 (interpolation from scaled overpressure); TNO Multi Energy method using blast wave chart; Baker Strehlow -Tang method: $M_f = 0.662$ flame speed in Mach number)..... | 172 |
| Figure 4.4  | Comparison of the overpressure in a given scenario predicted as a function of distance for the three methods (SMACTRA – TNT- equivalency ( $\eta=10\%$ at <b>1000kg</b> propane); Multi Energy method: blast strength= 7 (interpolation from scaled overpressure); TNO Multi Energy method using blast wave chart; Baker Strehlow-Tang method: $M_f= 0.662$ flame speed in Mach number).....      | 176 |
| Figure 4.5  | Comparison of the overpressure at a given scenario predicted as a function of distance for the three methods (SMACTRA – TNT- equivalency ( $\eta=10\%$ at <b>2000kg</b> propane); Multi Energy method: blast strength= 7 (interpolation from scaled overpressure); TNO Multi Energy method using blast wave chart; Baker Strehlow-Tang method: $M_f= 0.662$ flame speed in Mach number).....      | 176 |
| Figure 4.6  | Comparison of the overpressure at a given scenario predicted as a function of distance for the three methods (SMACTRA – TNT- equivalency ( $\eta=10\%$ at <b>3000kg</b> propane); Multi Energy method: blast strength= 7 (interpolation from scaled overpressure); TNO Multi Energy method using blast wave chart; Baker Strehlow-Tang method: $M_f= 0.662$ flame speed in Mach number).....      | 177 |



|             |   |     |
|-------------|---|-----|
| Figure 4.7  | Comparison of the overpressure at a given scenario predicted as a function of distance for the three methods (SMACTRA – TNT- equivalency ( $\eta=10\%$ at <b>5000kg</b> propane); Multi Energy method: blast strength= 7 (interpolation from scaled overpressure); TNO Multi Energy method using blast wave chart; Baker Strehlow-Tang method: $M_f= 0.662$ flame speed in Mach number).....  | 177 |
| Figure 4.8  | Comparison of the overpressure at a given scenario predicted as a function of distance for the three methods (SMACTRA – TNT- equivalency ( $\eta=10\%$ at <b>7000kg</b> propane); Multi Energy method: blast strength= 7 (interpolation from scaled overpressure); TNO Multi Energy method using blast wave chart; Baker Strehlow-Tang method: $M_f= 0.662$ flame speed in Mach number).....  | 178 |
| Figure 4.9  | Comparison of the overpressure at a given scenario predicted as a function of distance for the three methods (SMACTRA – TNT- equivalency ( $\eta=10\%$ at <b>32000kg</b> propane); Multi Energy method: blast strength= 7 (interpolation from scaled overpressure); TNO Multi Energy method using blast wave chart; Baker Strehlow-Tang method: $M_f= 0.662$ flame speed in Mach number)..... | 178 |
| Figure 4.10 | Comparison of the overpressure at a given scenario predicted as a function of distance for the three methods (SMACTRA – TNT- equivalency ( $\eta=10\%$ at <b>8500 kg</b> propane); Multi Energy method: blast strength= 7 (interpolation from scaled overpressure); TNO Multi Energy method using blast wave chart; Baker Strehlow-Tang method: $M_f= 0.662$ flame speed in Mach number)..... | 179 |
| Figure 4.11 | Comparison of the overpressure probit relation generated from an explosion of a road tanker containing 13000kg of LPG as a function of distance predicted by SACTRA with others software.....   | 181 |
| Figure 4.12 | Comparison of the overpressure probit relation generated from an explosion of a road tanker containing 2000kg of LPG as a function of distance predicted by SACTRA with others software.....  | 183 |
| Figure 4.13 | Comparison of the overpressure probit relation generated from an explosion of a road tanker containing 3000kg of LPG as a function of distance predicted by SACTRA with others software.....  | 183 |



|             |   |     |
|-------------|---|-----|
| Figure 4.14 | Comparison of the overpressure probit relation generated from an explosion of a road tanker containing 5000kg of LPG as a function of distance predicted by SACTRA with others software.....  | 184 |
| Figure 4.15 | Comparison of the overpressure probit relation generated from an explosion of a road tanker containing 7000kg of LPG as a function of distance predicted by SACTRA with others software.....  | 184 |
| Figure 4.16 | Comparison of the overpressure probit relation generated from an explosion of a road tanker containing 8500kg of LPG as a function of distance predicted by SACTRA with others software.....  | 185 |
| Figure 4.17 | Comparison of the overpressure probit relation generated from an explosion of a road tanker containing 9119 kg of LPG as a function of distance predicted by SACTRA with others software.....   | 185 |
| Figure 4.18 | Consequences of an explosion from a road tanker containing 13000 kg of LPG as a function of distance predicted by SACTRA software.....  | 195 |
| Figure 4.19 | Consequences of an explosion from a road tanker containing 9119 kg of LPG as a function of distance predicted by SACTRA software.....   | 195 |
| Figure 4.20 | Consequences of an explosion from a road tanker containing 2000 kg of LPG as a function of distance predicted by SACTRA software.....   | 196 |
| Figure 4.21 | Thermal radiation intensity, view factor and transmissivity as a function of distance generated from consequences of pool fire from a road tanker containing 13000 kg of LPG at leakage rate 0.0707m <sup>3</sup> /s or 43.5 kg/s (predicted by SACTRA software)..... | 206 |
| Figure 4.22 | Thermal radiation intensity as a function of leakage rate release generated from consequences of pool fire from a road tanker containing 13000 kg of LPG (predicted by SACTRA software).....  | 207 |
| Figure 4.23 | Thermal radiation dose loads as a function of distance generated from consequences of pool fire from a road tanker containing 13000 kg of LPG at leakage rate 0.0707m <sup>3</sup> /s or 43.5 kg/s (predicted by SACTRA software).....                                | 207 |



|             |   |     |
|-------------|---|-----|
| Figure 4.24 | Probit functions for pool fire thermal radiation (at exposure time 43.5sec. and Dose <sub>human</sub> (kW/m <sup>2</sup> ) <sup>4/3</sup> s (predicted by SMACTRA software).....  | 209 |
| Figure 4.25 | Probit functions for pool fire thermal radiation (at exposure time 60 sec. and Dose <sub>human</sub> (kW/m <sup>2</sup> ) <sup>4/3</sup> s (predicted by SMACTRA software).....   | 209 |
| Figure 4.26 | Probit functions for pool fire thermal radiation (at exposure time 90 sec.. and Dose <sub>human</sub> (kW/m <sup>2</sup> ) <sup>4/3</sup> s (predicted by SMACTRA software).....  | 210 |
| Figure 4.27 | Probit functions for pool fire thermal radiation (at exposure time 180 sec.. and Dose <sub>human</sub> (kW/m <sup>2</sup> ) <sup>4/3</sup> s (predicted by SMACTRA software). ....  | 210 |
| Figure 4.28 | Probit functions for pool fire thermal radiation (at exposure time 900 sec. and Dose <sub>human</sub> (kW/m <sup>2</sup> ) <sup>4/3</sup> s (predicted by SMACTRA software).....  | 211 |
| Figure 4.29 | Probit functions for pool fire thermal radiation (at exposure time 1200 sec. and Dose <sub>human</sub> (kW/m <sup>2</sup> ) <sup>4/3</sup> s (predicted by SMACTRA software).....   | 211 |
| Figure 4.30 | Time before one feels pain as a function of thermal radiation at 43.5kg/s or 0.0707m <sup>3</sup> /s caused from pool fire (predicted by SMACTRA software).....   | 212 |
| Figure 4.31 | Comparison of Fireball diameters between SMACTRA over EFFECT 8.01 software and experimental and calculated relationship as function of mass fuel.....   | 214 |
| Figure 4.32 | Comparison of Fireball duration time (s) between SMACTRA over EFFECT 8.01 software and experimental and calculated relationship as function of mass fuel.....   | 214 |
| Figure 4.33 | Time before one feels pain as a function of BLEVE fireball thermal radiation at truck tanker containing 13,000kg (predicted by SMACTRA software).....   | 215 |
| Figure 4.34 | Probit functions for BLEVE fireball thermal radiation (at exposure time 9.61sec. and Dose <sub>human</sub> (kW/m <sup>2</sup> ) <sup>4/3</sup> s at truck containing 13,000 kg of LPG (predicted by SMACTRA software): b1=1 <sup>st</sup> degree burn; b2=2 <sup>nd</sup> degree burn; unP = lethality (unprotected); P= protected..... | 216 |



|             |  |     |
|-------------|--|-----|
| Figure 4.35 | Probability of surviving from 2 <sup>nd</sup> degree burn at the age of 69 for BLEVE fireball thermal radiation (at exposure time 10.01sec. and Dose <sub>human</sub> (kW/m <sup>2</sup> ) <sup>4/3</sup> s at truck containing 13,000 kg of LPG (predicted by SACTRA software): b1=1 <sup>st</sup> degree burn; b2=2 <sup>nd</sup> degree burn survived; unP <sup>new</sup> = lethality after revised (unprotected); P= protected ..... | 219 |
| Figure 4.36 | Probability of surviving from 2 <sup>nd</sup> degree burn at the age of 55 for BLEVE fireball thermal radiation (at exposure time 10.01sec. and Dose <sub>human</sub> (kW/m <sup>2</sup> ) <sup>4/3</sup> s at truck containing 13,000 kg of LPG (predicted by SACTRA software): b1=1 <sup>st</sup> degree burn; b2=2 <sup>nd</sup> degree burn survived; unP <sup>new</sup> = lethality after revised (unprotected); P= protected.....  | 219 |
| Figure 4.37 | Probability of surviving from 2 <sup>nd</sup> degree burn at the age of 45 for BLEVE fireball thermal radiation (at exposure time 10.01sec. and Dose <sub>human</sub> (kW/m <sup>2</sup> ) <sup>4/3</sup> s at truck containing 13,000 kg of LPG (predicted by SACTRA software): b1=1 <sup>st</sup> degree burn; b2=2 <sup>nd</sup> degree burn survived; unP <sup>new</sup> = lethality after revised (unprotected); P= protected.....  | 220 |
| Figure 4.38 | Probability of surviving from 2 <sup>nd</sup> degree burn at the age of 35 for BLEVE fireball thermal radiation (at exposure time 10.01sec. and Dose <sub>human</sub> (kW/m <sup>2</sup> ) <sup>4/3</sup> s at truck containing 13,000 kg of LPG (predicted by SACTRA software): b1=1 <sup>st</sup> degree burn; b2=2 <sup>nd</sup> degree burn survived; unP <sup>new</sup> = lethality after revised (unprotected); P= protected.....  | 220 |
| Figure 4.39 | Probability of surviving from 2 <sup>nd</sup> degree burn at the age of 15 for BLEVE fireball thermal radiation (at exposure time 10.01sec. and Dose <sub>human</sub> (kW/m <sup>2</sup> ) <sup>4/3</sup> s at truck containing 13,000 kg of LPG (predicted by SACTRA software): b1=1 <sup>st</sup> degree burn; b2=2 <sup>nd</sup> degree burn survived; unP <sup>new</sup> = lethality after revised (unprotected); P= protected.....  | 221 |
| Figure 4.40 | Probability of surviving from 2 <sup>nd</sup> degree burn at the age of 14 for BLEVE fireball thermal radiation (at exposure time 10.01sec., 50% total burn surface area (TBS) and Dose <sub>human</sub> (kW/m <sup>2</sup> ) <sup>4/3</sup> s ) for a truck containing 13,000 kg of LPG (predicted by SACTRA software):.....  | 222 |
| Figure 4.41 | Probability of surviving from 2 <sup>nd</sup> degree burn at the age of 45 for BLEVE fireball thermal radiation (at exposure time 10.01sec., 50% total burn surface area (TBS) and Dose <sub>human</sub> (kW/m <sup>2</sup> ) <sup>4/3</sup> s at truck containing 13,000 kg of LPG (predicted by SACTRA software):.....   | 222 |



|             |   |     |
|-------------|---|-----|
| Figure 4.42 | Probability of surviving from 2 <sup>nd</sup> degree burn at the age of 69 for BLEVE fireball thermal radiation (at exposure time 10.01sec., 50% total burn surface area (TBS) and Dose <sub>human</sub> (kW/m <sup>2</sup> ) <sup>4/3</sup> s at truck containing 13,000 kg of LPG (predicted by SACTRA software):.....  | 223 |
| Figure 4.43 | Probability of surviving from 2 <sup>nd</sup> degree burn at the age of 69 for BLEVE fireball thermal radiation (at exposure time 10.01sec., 10% total burn surface area (TBS) and Dose <sub>human</sub> (kW/m <sup>2</sup> ) <sup>4/3</sup> s at truck containing 13,000 kg of LPG (predicted by SACTRA software):.....  | 223 |
| Figure 4.44 | Probability of surviving from 2 <sup>nd</sup> degree burn at the age of 45 for BLEVE fireball thermal radiation (at exposure time 10.01sec., 10% total burn surface area (TBS) and Dose <sub>human</sub> (kW/m <sup>2</sup> ) <sup>4/3</sup> s) for a truck containing 13,000 kg of LPG (predicted by SACTRA software):.....  | 224 |
| Figure 4.45 | Probability of surviving from 2 <sup>nd</sup> degree burn at the age of 14 for BLEVE fireball thermal radiation (at exposure time 10.01sec., 10% total burn surface area (TBS) and Dose <sub>human</sub> (kW/m <sup>2</sup> ) <sup>4/3</sup> s) for a truck containing 13,000 kg of LPG (predicted by SACTRA software):.....  | 224 |
| Figure 4.46 | Probability of surviving from 2 <sup>nd</sup> degree burn at the age of 14 for BLEVE fireball thermal radiation (at exposure time 10.01sec., 30% total burn surface area (TBS) and Dose <sub>human</sub> (kW/m <sup>2</sup> ) <sup>4/3</sup> s) for a truck containing 4,000 kg of LPG (predicted by SACTRA software):.....   | 225 |
| Figure 4.47 | Probability of surviving from 2 <sup>nd</sup> degree burn at the age of 80 for BLEVE fireball thermal radiation (at exposure time 10.01sec., 10% total burn surface area (TBS) and Dose <sub>human</sub> (kW/m <sup>2</sup> ) <sup>4/3</sup> s) for a truck containing 4,000 kg of LPG (predicted by SACTRA software):.....   | 227 |
| Figure 4.48 | Consequences of BLEVE fireball thermal radiation as a function of the dose received by a person in Dose <sub>human</sub> (kW/m <sup>2</sup> ) <sup>4/3</sup> s , exposure distance (m) and probit functions at truck containing 13,000 kg of LPG (predicted by SACTRA software): b1=1 <sup>st</sup> degree burn; b2=2 <sup>nd</sup> degree burn; unP = lethality (unprotected); P= protected..... | 228 |



|             |  |     |
|-------------|--|-----|
| Figure 4.49 | Consequences of BLEVE fireball thermal radiation as a function of the dose received by a person in $\text{Dose}_{\text{human}} (\text{kW}/\text{m}^2)^{4/3}\text{s}$ , exposure distance (m) and probit functions (10% below) at truck containing 13,000 kg of LPG (predicted by SMACTRA software): b1=1 <sup>st</sup> degree burn; b2=2 <sup>nd</sup> degree burn; unP = lethality (unprotected); P= protected..... | 229 |
| Figure 4.50 | Consequences of BLEVE fireball thermal radiation as a function of the dose received by a person in $\text{Dose}_{\text{human}} (\text{kW}/\text{m}^2)^{4/3}\text{s}$ , exposure distance (m) and probit functions at truck containing 9119kg of LPG (predicted by SMACTRA software): b1=1 <sup>st</sup> degree burn; b2=2 <sup>nd</sup> degree burn; unP = lethality (unprotected); P= protected.....                | 229 |
| Figure 4.51 | Consequences of BLEVE fireball thermal radiation as a function of the dose received by a person in $\text{Dose}_{\text{human}} (\text{kW}/\text{m}^2)^{4/3}\text{s}$ , exposure distance (m) and probit functions (10% below) at truck containing 9119 kg of LPG (predicted by SMACTRA software): b1=1 <sup>st</sup> degree burn; b2=2 <sup>nd</sup> degree burn; unP = lethality (unprotected); P= protected.....   | 230 |
| Figure 4.52 | Consequences of BLEVE fireball thermal radiation as a function of the dose received by a person in $\text{Dose}_{\text{human}} (\text{kW}/\text{m}^2)^{4/3}\text{s}$ , exposure distance (m) and probit functions at truck containing 3000 kg of LPG (predicted by SMACTRA software): b1=1 <sup>st</sup> degree burn; b2=2 <sup>nd</sup> degree burn; unP = lethality (unprotected); P= protected.....               | 230 |
| Figure 4.53 | Consequences of BLEVE fireball thermal radiation as a function of the dose received by a person in $\text{Dose}_{\text{human}} (\text{kW}/\text{m}^2)^{4/3}\text{s}$ , exposure distance (m) and probit functions (10% below) at truck containing 3000 kg of LPG (predicted by SMACTRA software): b1=1 <sup>st</sup> degree burn; b2=2 <sup>nd</sup> degree burn; unP = lethality (unprotected); P= protect.....     | 232 |
| Figure 4.54 | Emissive Power, fireball height and fireball diameter as a function of time, for BLEVE of 3,000kg of LPG (1195mmX2480mmX 3500mm) truck tanker.....   | 233 |
| Figure 4.55 | Emissive Power, fireball height and fireball diameter as a function of time, for BLEVE of 9119kg of LPG (1195mmX2480mmX 3500mm) truck tanker.....  | 234 |
| Figure 4.56 | Emissive Power, fireball height and fireball diameter as a function of time, for BLEVE of 13,000kg of LPG (1195mmX2480mmX 3500mm) truck tanker.....  | 234 |



|             |  |     |
|-------------|--|-----|
| Figure 4.57 | shows the accident location at Jalan Ampang involving a road tanker carrying hazardous materials.....  | 236 |
| Figure 4.58 | represents buffer zone from the impact of truck tanker explosion.....  | 237 |
| Figure 4.59 | shows thermal radiation dose load from fireball impact .....   | 237 |
| Figure 4.60 | demonstrates an instantaneous case from ammonia gas release  | 228 |
| Figure 4.61 | shows continuous case from ammonia gas release .....   | 238 |
| Figure 4.62 | shows the outcome map API online at Petronas Twin Tower, Jln Pinang, Kuala Lumpur.....   | 240 |
| Figure 4.63 | Individual risk vs. the distance from the route 1 for the LPG transport case varies with time.....   | 244 |
| Figure 4.64 | Societal risk for the LPG transport case at route 1; dashed lines: limits of the Dutch ALARP zone; dotted lines: limits of the U.K. ALARP zone.....    | 245 |
| Figure 4.65 | F-N curves for LPG tank truck via five routes as comparison  | 245 |
| Figure 4.66 | Societal risk for the LPG transport case at route 2; dashed lines: limits of the Dutch ALARP zone; dotted lines: limits of the U.K. ALARP zone.....    | 246 |
| Figure 4.67 | Societal risk for the LPG transport case at route 3; dashed lines: limits of the Dutch ALARP zone; dotted lines: limits of the U.K. ALARP zone.....    | 246 |
| Figure 4.68 | 68 Societal risk for the LPG transport case at route 4; dashed lines: limits of the Dutch ALARP zone; dotted lines: limits of the U.K. ALARP zone..... | 247 |
| Figure 4.69 | Societal risk for the LPG transport case at route 5; dashed lines: limits of the Dutch ALARP zone; dotted lines: limits of the U.K. ALARP zone.....    | 247 |
| Figure 4.70 | F-N curves for LPG tank truck via five routes as comparison on route 2 at length 34 km.....  | 250 |
| Figure 4.71 | F-N curves for LPG tank truck via five routes as comparison with route 2 at length 20 km .....   | 250 |



|             |  |     |
|-------------|--|-----|
| Figure 4.72 | F-N curves for LPG tank truck via five routes as comparison on route 2 at length 14 km.....  | 251 |
| Figure 4.73 | F-N curves for LPG tank truck via five routes as comparison on route 2 at length 10.458 km.....  | 251 |
| Figure 4.74 | F-N curves for LPG tank truck via five routes as comparison on route 2 at length 4.458 km.....   | 252 |
| Figure 4.75 | Societal risk for the LPG transport case at route 2, 4.458 km; dashed lines: limits of the Dutch ALARP zone; dotted lines: limits of the U.K. ALARP zone.....        | 252 |
| Figure 4.76 | F-N curves for LPG tank truck via five routes as comparison on route 2 at 600 trips per day.....   | 254 |
| Figure 4.77 | F-N curves for LPG tank truck via five routes as comparison on route 2 at 50 trips per day.....  | 254 |
| Figure 4.78 | comparison the total individual risk results SMACTRA/ BUWAL/ CCPS (AIChE).....   | 255 |
| Figure 4.79 | comparison the total individual risk results SMACTRA/ BUWAL/ CCPS (AIChE).....   | 256 |
| Figure 4.80 | comparison the individual risk results SMACTRA/ BUWAL/ CCPS (AIChE).....   | 256 |
| Figure 4.81 | comparison the societal risk results SMACTRA/ BUWAL/ CCPS (AIChE) for route 1 at 3.2s.....   | 257 |
| Figure 4.82 | Vulnerable zone at the 300 m buffer from route 5 at 4.4024 km length (Grey color = residential zone, orange color= commercial zone, magenta = industrial zone).      | 259 |
| Figure 4.83 | Vulnerable zone at the 300 m buffer from route 4 at 9.16 km length (Grey color = residential zone, orange color= commercial zone, cyan color = industrial zone).     | 259 |
| Figure 4.84 | Vulnerable zone at the 300 m buffer from route 3 at 9.7 km length (Grey color = residential zone, orange color= commercial zone, dark blue color = industrial zone). | 260 |
| Figure 4.85 | Vulnerable zone at the 300 m buffer from route 2 at 7.548 km length (Grey color = residential zone, orange color= commercial zone, green color = industrial zone).   | 260 |



|             |  |     |
|-------------|--|-----|
| Figure 4.86 | Vulnerable zone at the 300 m buffer from route 1 at 10 km length (Grey color = residential zone, orange color= commercial zone, yellow color = industrial zone)..... | 261 |
| Figure 4.87 | show the transportation risk hazards based on population density point at night.....   | 263 |
| Figure 4.88 | show the transportation risk hazards based on population density point at day time .....   | 264 |
| Figure 4.89 | shows the buffer hazard impact from 13,000 kg of LPG tanker explosion.....   | 265 |
| Figure 4.90 | shows the buffer hazard impact from 50,000 kg of LPG tanker explosion.....   | 265 |
| Figure 4.91 | showing the detail characteristics of land use activities within the possible series sources of hazard point buffer along the transportation route.....              | 266 |
| Figure 4.92 | showing the detail characteristics of land use activities within the possible series sources of hazard point buffer along the transportation route.....              | 267 |
| Figure 4.93 | showing the detail characteristics of land use activities within the possible series sources of hazard point buffer (two rings) along the transportation route.....  | 267 |
| Figure 4.94 | showing the effect of land use activities within the possible series sources of hazard point buffer along the transportation route at 100,000 kg of LPG.....         | 268 |



## LIST OF TABLES

|           |  |     |
|-----------|--|-----|
| Table 2.1 | List of major accidents based on the available database.....   | 17  |
| Table 2.2 | Ratio of the different SDR-classes to the dangerous goods traffic (RSC).....   | 29  |
| Table 2.3 | Accident rates for the total traffic (average values AR-total).....  | 29  |
| Table 2.4 | Shows selected list of major accident database.....  | 53  |
| Table 2.5 | Software and their features involved in chemical transportation risk analysis and routing management.....                      | 60  |
| Table 3.1 | Shows the structure and definition of independent variables for applying Eq. (3-6).....  | 85  |
| Table 3.2 | Probit Correlations for a variety of exposure (The Causative variable is representative of the magnitude of the exposure)..... | 89  |
| Table 3.3 | Probit equations for the different degrees of damage to buildings and structures caused by explosions.....                     | 90  |
| Table 3.4 | Probit equations for different types of damage from explosions on human outdoors.....  | 91  |
| Table 3.5 | Approximate levels of damage for different radiation intensity.....  | 93  |
| Table 3.6 | Shows the effect results of LPG transportation accident [182].....   | 95  |
| Table 3.7 | Burn Mortality.....  | 98  |
| Table 3.8 | Acceptability Risk Criteria of Some Foreign Countries.....   | 113 |
| Table 3.9 | Meteorological Conditions Defining the Pasquill- Gifford Stability Classes [20].....   | 121 |
| Table 4.1 | Population distribution.....   | 169 |



|            |  |     |
|------------|--|-----|
| Table 4.2  | Peak overpressure vs. scaled distance for blast wave pressure from an explosion using SMACTRA.....   | 171 |
| Table 4.3  | Peak overpressure vs. scaled distance for blast wave pressure from an explosion (SMACTRA over other two models Baker Strehlow Tang and TNO Multi Energy Model at 13,000 kg of LPG.....   | 174 |
| Table 4.4  | Summary of the comparison between the peak overpressure result region for SMACTRA and the two models (TNO Multi Energy and Baker Strehlow Tang).....   | 180 |
| Table 4.5  | Comparison of mortality percentage (1%, 50% and 99%) to human from an explosion of a vessel containing various capacities of LPG as function of distance by using SMACTRA and EFFECT Version 8.0 software.....   | 182 |
| Table 4.6  | Comparison of probabilities impacts to human and structural building generated from an explosion of a vessel containing 13000kg of LPG as function of distance by using SMACTRA and CANARY software.....   | 190 |
| Table 4.7  | Comparison of probabilities impacts to human and structural building generated from an explosion of a vessel containing 2000 kg of LPG as function of distance by using SMACTRA and EFFECT Version 8.0 software.....   | 191 |
| Table 4.8  | Comparison between SMACTRA result probabilities impacts to human and structural building generated from an explosion of a vessel containing 2000 and 13000kg of LPG as function of distance over CANARY and EFFECT Version 8.0 software (within 20% difference from SMACTRA region value)..... | 192 |
| Table 4.9  | Comparison between predicted peak side on overpressure versus distance curves for vessel containing 13000 kg of LPG using three models SMACTRA, CANARY and EFFECT Version 8.0 software.....  | 193 |
| Table 4.10 | Comparison of peak overpressure from an explosion of propane, LPG, and butadiene with previous software and published data.....  | 198 |
| Table 4.11 | Comparison the probabilities of fatalities from lung haemorrhage for a given overpressure.....   | 199 |



|            |  |     |
|------------|--|-----|
| Table 4.12 | Comparison the probabilities of glass breakage for a given overpressure.....                                       | 199 |
| Table 4.13 | Comparison of the probabilities for construction damage at a given overpressure.....                               | 199 |
| Table 4.14 | Effect of burning rate of pool fire to pool fire diameter using SMACTRA.....                                       | 201 |
| Table 4.15 | Effect of time spillage to pool fire diameter at constant burning rate using SMACTRA.....                          | 202 |
| Table 4.16 | SMACTRA input and output parameters for Pool fire hazard (34.5m <sup>3</sup> LPG).....                             | 204 |
| Table 4.17 | Comparison of the pool fire output results between SMACTRA and FRED software.....                                  | 205 |
| Table 4.18 | SMACTRA input and output parameters for ammonia gas release.....   | 241 |
| Table 4.19 | Comparison results of five routes societal risk from BLEVE impact using SMACTRA.....                               | 248 |
| Table 4.20 | Comparison results of five routes based on area affected using SMACTRA and GIS Application.....                    | 262 |
| Table 4.21 | Comparison results of five routes based on area affected per km using SMACTRA and GIS Application.....             | 262 |
| Table 4.22 | showing the characteristics of land use activities within the hazard point buffer for 13,000 kg of LPG tanker..... | 266 |



# CHAPTER 1

## INTRODUCTION

This chapter represents an overview of the entire thesis. Section 1.1 covers the background for the Transportation Risk Analysis (TRA). Current trend of TRA implementations are presented in section Section 1.2 states the problems that need to be solved, aiming for a better designed and reliable Smart Advisory System for the transportation of hazardous materials. In the light of that, section 1.3 defines the research objectives undertaken in the thesis. Section 1.4 briefly presents the approach used, the scope and brief methodology of the performance evaluation and testing of the proposed technique.

### **1.1 Background**

During the last few decades, we have seen a rapid development in chemical industries including those related to hazardous materials either explosive, flammable liquids or solids, corrosive or poisonous materials [1-4]. These materials sometimes need to be transported from one place to another via roads, railways, pipelines or waterways which can be extremely harmful to the environment and human health since unpredictable accidents may occur along the route [5-7]. Therefore, risk potential related to hazardous material transportation has drawn considerable attention from local, national and international safety authorities. For instance, Advisory Committee on Major Hazards (ACMH) United Kingdom in its report [8-10] suggested the government to enforce on safety policy toward company or agency involved with any activities related to hazardous materials transportation. This serious attention by ACMH towards risk related to hazardous material transportation attracted attention from other countries which produce chemical, oil and gas. Previously, to reduce risk during transportation of hazardous materials, many governments allow them to use



only on designated roads, which avoid heavily populated areas. However, hazardous material transportation accidents do happen occasionally throughout the world, which may lead to a very undesirable consequence including fatalities and injuries especially when it happens at a congested population area or sensitive zone area such as in a country with limited land space. Therefore, several techniques have been introduced in order to identify the safest route for hazardous material transportation. Result from transportation risk analysis by using qualitative method has been shown to be less accurate since the risk potential from HazMat transportation accident has become more complex and the parameters involve not only limited to population density but also include accident rate, length route, meteorological condition and etc.

Among the various technique, quantitative risk analysis (QRA) has been successfully applied in a studied risk area to analyze, assess and evaluate hazards from fixed facility of chemical process industries (CPI) [8-10]. In the United Kingdom, probabilistic safety assessment is not mandatory in the safety report but the Health and Safety Executive (HSE) find it is easier to accept the conclusion if the risk assessment is supported by quantified risk arguments [8]. Up to now, quantitative risk criteria have been published most in the UK, as far as the control of land use in the vicinity of industrial facilities is concerned. Due to the strength of the QRA technique, a similar approach has been established to analyze and to evaluate the impact from transportation of hazardous material. However, they are not capable to analyse the impact derived from a moving risk source. As the results, transportation risk analysis (TRA) is developed as an extension of the QRA techniques, which initially utilize for assessing risk in nuclear processes, and then adapted to process industry [11]. However, for the risk source which is moving in a continuously changing environment prevents the large diffusion of this technique compared with that of fixed installations [8, 12]. To perform an accurate TRA, detail information of the area is importance such as data on local distribution of population, accident rates and weather conditions. This information is gathered by using geographic information system (GIS), which can relate the data of interest to its geographical co-ordinates.



GIS technology integrates common database operations such as query and statistical analysis with unique visualization and geographic analysis capabilities. These functions make GIS distinguish from other information systems and make it valuable for explaining events, predicting outcomes and planning strategies. Tools for GIS spatial risk assessment can externally generated risk contours results (by displaying as buffer and multiple ring buffer and others) and links to models describing accidental, continuous atmospheric releases and dispersion spills into surface water systems, and transportation risk analysis. Therefore by using GIS, hazards from transportation accident, can be viewed and evaluated the potential consequences at any points and locations based on computer maps generated. Results of consequences such as fire, explosion, fireball, BLEVE from transportation accidents will be more accurate, precise and more details, depending on how far the very comprehensive maps (spatial and non-spatial) in formations can be generated.

Therefore, it is apparent that transportation risk assessment can be made feasible by using computer aided technologies. The complex development of transportation accident scenarios which transported hazardous materials can be achieved by using the consequence modelling combined with various computer softwares.

## **1.2 Problem Statement**

Malaysia also had experienced some major accidents for instance accidents at Km 20.8 New Klang Valley Expressway (carrying 21,600 liters of petrol), North South highway near Damansara Perdana (LPG tanker), Batu Klawang Ulu Klawang involving a truck carrying 33,000liter (21,000 litres of petrol and 10,000 litres of diesel) caused 3 fatalities, and property damaged [13-16]. Due to the above matter, the safe transportation of hazardous materials from place of origin to place of destination has become a major concern to the public and government policy makers. Pressure has been placed on the transportation agencies to designate safe routes for hazardous materials transport that minimize risk. One of the methods to identify safest route is by using smart advisory system (SAS) as transportation risk



analysis. However, most of the current SAS for hazardous material (HazMat) transportation is lacking of practical application. This is due to most of those available tools are not user friendly especially when involving large number of variables or a more complex risk sources models. Other reasons are due to lack of available data/database for TRA and difficulty to understand the complex relationships amongst many elements involved during the analysis. Various elements involved in the construction of the SAS must be integrated and optimised in order to produce a viable model that is marketable and has practical application.

Currently, most of companies in Malaysia are adopting chain business processes supply to streamline and automate the distribution of petroleum products per year to its customers across peninsular Malaysia. PETRONAS for instance distributes more than 7.5 billion liters of petroleum products per year to its customers across peninsular Malaysia with more than 600 retail service stations [17]. For that matter, PETRONAS Dagangan Berhad (PDB) is implementing Aspen Tech's solution for fuels marketing as the central element of a project to create an Automated Road Tanker Scheduling System (ARTSS), [18] which can create a single system capable of managing and optimizing the distribution of all petroleum products – including vehicle gasoline, aviation fuel, diesel, fuel oil, liquefied petroleum gas (LPG), lubricants and bitumen – from bulk terminals or plants to the end-customer. However the system is incapable to analyze the accident risk related to the transportation of hazardous material such as (petrochemical/oil/ gas/chemical).

### **1.3 Objectives of the Study**

The main objectives of this study are:

- i) Analyze the existing TRA model to rectify and identify the possible parameters for the proposed TRA model according to Malaysia scenario.
- ii) Based on the above identification as in (i), proposed suitable TRA model for Malaysia transportation risk of hazardous materials.
- iii) Integrate and compute the proposed TRA model, with established consequences model and databases to develop a smart advisory system for transportation risk analysis



- iv) Develop a user-friendly software package using Visual Basic application for analyzing the transportation of hazardous material accidents.
- v) Customize a GIS desktop application through integrated Visual Basic with ArcGIS Engine Developer Kit to assess the chemical transportation hazards with its geographical locations.
- vi) Confirm the validity and verification of the software by comparing the results from the current software with other results from established data, published literature, laboratory and numerical data sets and various risk assessment software.

#### **1.4 Scope of Study**

The aim of this study is to develop a smart advisory system (SAS) which is capable of estimating the risk from transportation of hazardous material according to Malaysia scenario. Therefore to estimate the hazards risk from transportation, there are several TRA models which will be reviewed and analysed to identify the weaknesses and the strength of the model. Based on the loopholes of existing models, the improvise TRA model will be utilized in SAS to assess the transportation risk consequence scenarios. All calculations involving the proposed TRA model, established consequences model, with related databases are computerised in the proposed smart advisory system software. To develop and to design a SAS which assesses the consequences accidents from transportation of chemical is created by integrating the models in the system with GIS tools and by using Visual Basic programming language to simulate the consequences models and perform advanced calculations of the data input for the selected field.

It is also known that SMACTRA software calculations are limited to:

- Applied the proposed TRA model
- Most of databases such accident rate, road network, topology, weather and meteorology condition, and etc are based on Malaysia scenario
- Consequence hazards from explosion, fire and toxic release.



- Light buoyant gas.
- Toxic release in horizontal direction.
- Outdoor consequences caused by chemical transportation accidents.
- Two dimension of visualisation for hazard mapping.
- Online risk analysis simulation
- Calculate individual risk
- Calculate the societal risk
- Risk estimation for acceptability risk
- Transportation Risk analysis Potential Safest Route Solution to the Complex Hazardous Materials (Hazmat) Release Consequences in Major Transportation Accident

## **1.5 Layout of the thesis**

This thesis is consists of five chapters. Chapter 1 provides an introduction. Chapter 2 of the thesis outlines the literature review related to hazardous materials and the risk involved in road transportation, overview of the importance of TRA, TRA procedure, general framework of TRA, comparison of hazardous material transportation and fixed facility risk analysis characteristics, presents preliminary work in this discipline which has been categorized as TRA methodology guidelines, applications, procedures, data availability such as accident database, application of Geographic Information System (GIS) transportation, and trend of TRA software and their limitation. This chapter ends with summary to point out several important considerations for the present research work. Chapter 3 presents some issues and factors affecting transportation risk analysis for Malaysia scenario, a description of modified TRA model. Since most of QRA software do not distinguish for specific age, amount of burnt skin and survival rate of the victim based on the depth of burn injury, and risk outcome is represent by number of fatality. In this chapter, the assessment of thermal radiation consequences has been extended to include a methodology describing the prognosis of burn injury victims, therefore it is possible



to estimate the mortality probability of a victim knowing the victim's age and percentage body area suffering from burn injury and also avoid double counting on effect calculation. A description of GIS integration with SAS simulation is provided in this chapter. The analysis of results and conclusions will be discussed in chapter 4. The case study involving 5 selected routes of interest in Port Dickson. In this chapter, the SACTRA calculation results, are tested by using an established data, and compared with the results from published literature and chemical risk software. Finally some conclusions, suggestions and directions for future research is provided in chapter 5.



















## CHAPTER 2

### LITERATURE REVIEW

#### 2.1 Background

Over the last three decades process industries has developed a distinctive approach to prevent and control hazards that can cause loss of life and property. This approach is called loss prevention. Since 1960s, modern technologies contributed a great changes in the chemical, oil and petrochemical industries. The energy which derived from the chemical process and the chemical process activities may possess high pressure and temperature which may expose a great hazards during accident. These hazards from chemical process technology not only happen at chemical plants, but it may become more complex and severe if accident occur during transportation of this hazardous material which has high pressure, very reactive chemicals and highly toxic. Therefore there is an absolute requirement for a reliable risk, safety and loss prevention technology which is parallel with the advancement of chemical process technology. The first UK IChemE symposium in Chemical process hazards with special reference to chemical process plant design in 1960, is the pioneer to a serious discussion on the implementation of safety and loss prevention aspects into chemical plant design and process operation [8-10]. This effort by Intitute of Chemical Engineers (IChemE) UK is then continued by American Institute of Chemical Engineers (AIChE) in 1967 which initiate the first AIChE loss prevention symposium. Meanwhile European Federation of Chemical Engineering (EFCE) in 1972 which introduced the major loss prevention in the process industries.

Risk analysis is a concept that is vaguely understood by many researchers. In 1662, mathematicians in the Port Royal monastery in Paris whom first described the modern concept of risk analysis define risk as “Fear of harm ought to be proportional



not merely to the gravity of harm, but also to the probability of the event” [19]. This definition of risk has not changed till 350 years. Correspondingly, the Center for Chemical Process Safety (CCPS) define risk as ‘a measure of potential economic loss, human injury, or environmental damage in terms of both the incident likelihood and magnitude of the loss, injury, or damage’ [11, 20] and transportation risk analysis (TRA) defined as the ‘development of a qualitative or quantitative estimate of (transportation) risk based on engineering evaluations and possibly mathematical techniques for combining estimates of incident consequences and frequencies’ [21, 22]. The UK Health and Safety Executive provides an analogous definition of risk [24] as ‘the likelihood of a specified undesired event occurring within a specified period or in specified circumstances’. As a conclusion, in TRA, risk is defined as a measure of the possible undesirable consequences and frequencies of a release of HazMats during their use, storage, transportation and disposal either caused by an accident or without an accident. Risk assessment is defined as the process by which the results of risk analysis are used to make decisions, either through relative ranking of risk reduction strategies or through comparison with risk targets [19].

Even though loss, damage, or injuries resulting from the incident are the consequences of the event [19], but in most of the transportation hazard assessment, these consequences are not well presented. For example, most of the risk analysis does not include the magnitude of human injury, disability and fatality or some studies only include fatality risk in their TRA. Historical evidence has shown that incidents due to hazardous materials (HazMat) releases during transportation can lead to severe consequences. Therefore, these hazards need to be identified, controlled or eliminated through the use of risk analysis or assessment tool.

Apart from that, previous TRA researchers faced problems to estimate or predict consequences towards impact zone. This is probably due to enormous data are required and each of them must be analyzed before they can be applied in the TRA model calculations. For example, in order to generate the best route with the least risk if an accident happens, data such as accident rate and population along the route are essential. However, these data cannot be utilized directly into the model unless they have been analyzed such as the total route involved, the number of accident in a year



along the route, the number of accidents related to transportation of hazardous material, the traffic condition, the topology and socio-economic status of the studied area. Even though researchers have established the simplified assumptions in order to ensure an accurate impact calculation for the safest route, they are only capable to calculate risk for a limited number of routes. This chapter describes an overview of the existing literatures related to risk assessment for transportation of hazardous material and discuss on the current capabilities of TRA guidelines, databases and softwares development. Various SAS techniques for the hazardous materials transportation risk analysis have been developed, is also reviewed in this chapter.

## **2.2 Hazardous Materials**

The chemicals transportation is unavoidable for the manufacturing and distribution of products within and across regional and international borders. These transportations must comply to the country transportation regulation which are referred as “dangerous goods” or “hazardous materials”. The federal Hazardous Materials Transportation Act of 1975 (HMTA) of United States of America and its re-authorizing legislation define hazardous material as a substance or material that, if not regulated, may pose an unreasonable risk to health, safety, or property when transported in commerce. Department of Transportation (DOT) has identified more than 3,300 hazardous materials which need to be regulated. Thousands of unnamed materials are also identified for regulation based on their characteristic such as explosive, flammable, corrosive or infectious [1].

According to the United States Department of Transportation, gasoline and other petroleum products contributed to about 40 percent of all hazardous materials shipments in US [2-4] with more than two-thirds of petroleum products are transported using road tanker [3,6-7]. In Europe, concern is now being voiced about HAZMAT transportation risk to the public, so that the legislators have begun to pay more attention to it [21, 22, 29].

In view of the rise in the advancement of industrialization in Malaysia as with the rest of the world, the numbers of stationary installations (i.e. process plants, liquefied petroleum gas (LPG) terminal, refineries, petrol stations etc.) have grown significant over the past few years. Furthermore, since the discovery of oil and gas in the country, the growth of chemical related industries had further spurred and it is became one of



the major focuses for expansion [30, 31]. As a result, this scenario has indirectly caused an increase in the number of HAZMAT transportations from one stationary installations to another for further processing or for product distribution. From the previous hazmat risk assessment based on facility location, routing and network design literature, it is obvious that, since 1982 there are numbers of papers published by the researchers focus on identifying a lesser risk route either by road [39-48, 53], rail [49, 50], marine [51] and combine road and rail [52]. However, many researcher still facing problems to precisely estimate or predict the consequences towards the impact zone. This is probably due to enormous data required and each of them must be analyzed before they can be applied in the consequences calculations. Secondly, this is due to lack of available data or databases, relevant to the transportation risk area. Quantitative Risk Analysis (QRA) approaches and its use have grown significant over the past twenty years and is now widely used and incorporated into safety legislation for a number of industries. However, most developments and use of QRA are mainly on fixed installations. Since HAZMAT transportation is not a fixed source therefore the magnitude of risk related to accident is unpredictable. Road transportation of dangerous goods carries risk to the surrounding people and environment at any point along its routes. Previous review on the transportation HAZMAT accidents have also shown that the accident related to hazardous materials transportation may also give additional consequences due to its chemical and physical properties [21, 22, 26, 27]. The amount of destruction is expected to be worse if the accident occur at high population density area [28].

Due to enormous numbers of HAZMAT, an effective controlled systems such as engineering codes, checklists and process safety management (PSM) is needed to ensure safety and reduce risk related to HAZMAT. It is also important to identify and analyze the risk first then a reliable management systems need to be developed that involve procedures and actions to support strategic, tactical and operational decisions, including the transportation route selection, facility selection, emergency response in case an incident would occur [11, 17, 18, 21, 22, 32-35].

So far there are some recognized regulations and rules which have been set to regulate HazMat transportation activities. For instance in USA, the Hazardous Material Transportation Act (HMTA) enacted in 1975 [4], is to provide adequate protection against the risks to life and property inherent in the transportation of



hazardous material, in Singapore the transportation of hazardous chemical and petroleum products is controlled by the Ministry of Environment and the Ministry of Home Affairs through the Poisons (Hazardous Substances) Rule enacted in 1986 and the Petroleum Act 1985, which aim to reduce the consequences that may occur from loss of containment of the hazardous chemical during transit through the road network. In Malaysia there are also laws and regulations such as Environmental Quality Act 1974 to regulate the environmental management of chemical substance in air, land, water and Scheduled Waste Regulation, 2005 to control hazardous waste management [36] and Petroleum (Safety Measures) Act 1984 [38]. However, those regulations are mainly addressing definition, hardware, procedures and compliance with those regulations do not necessarily guarantee the desired reduction on risk transportation for hazardous material. New innovative means and measures need to be devised by which these complex HazMat transportation risk problems can be dealt with more effectively in the future [36].

The conventional way to evaluate risk assessment is by using mathematical models. However, it is essential to know that the HAZMAT transportation risk assessment is complex and difficult to be implemented manually by using the mathematical technique due to the following reasons:

- The calculations are difficult to perform,
- A large number of calculations are required,
- Trained users are required as most people cannot understand, or utilised mathematical risk assessments,
- There may be several event outcomes from a single accident; thus it is difficult to keep track of these outcomes as the road tanker is moving along the road,
- The summation of risk required much effort even though it would be for an individual risk. For societal risk, the effort required for manual calculation would be overwhelming, even more worse for transportation risk analysis.

For these reasons, there is no doubt that a user friendly computer-aided technology is required for risk assessment. Casal et al. [37] have proven that implementation of computerised models has led to a powerful and easy-to-use tool for the prediction of the effects of hazardous material releases. He also concluded the designed tool



application can also be used by introducing less complete information, for the real-time prediction of the evolution of accidental releases.

As mentioned earlier, there are many undesirable consequences of HazMat transportation. The geometric shape and size of an impact area are not only depending on the substance being transported but also on other factors, such as topology, weather, population density, accident rate, traffic volume, wind speed and wind direction. Apart from that, any changes in the route selected require both the acquisition of data and the calculations for the new route, to examine alternative with possibly less hazardous route. Therefore the application of TRA via manually calculation will introduces additional uncertainties in the risk estimated. Geographic Information Systems (GIS) has a great potential in effectively handled in those TRA data, since they allow managing databases related to territorial entities such as towns, roads, rivers, hills, weather, population and etc., along the route or associated to their respective geographical location. Due to this, the integration of risk assessment program with a GIS appears as a suitable mean for performing TRA based on accurate territorial information, in order to obtain reliable risk measure.

Some numerical methodologies have been developed to assess the transportation risk; however, most of those methodologies were hard to employ directly by decision or policy makers. One reason is that the methodologies were proposed without input data, or the methodology was too complicated to obtain available input data. For example, incident frequency and conditional release probability data were assumed to be available in most of the methodologies, but in fact the acquisition of the required data calls for considerable effort. In many cases not all the data required by the TRA are available, thus some mathematical methodologies are needed to assess the required data based on expert experience or other information sources. The lack of the match between the data/database analysis and the numerical methodologies for TRA has prevented decision makers from making sound actions quickly. Therefore, a smart advisory system should be developed, so that the decisions on HazMat transportation risk could be made quickly, effectively and accurately test the suitability of alternative choices using valid acceptability criteria.



### **2.3 Hazardous Materials (HazMat) Transportation Incident**

A major goal of the safe and secure transportation of hazardous materials is a reduction in incidents that could lead to a release or to misuse. To date, the achievements in safety are the result of regulations, industry standards, individual company initiatives, and emergency response preparedness, as well as investments in training, systems, and technology. Even with the foundation that these programs and activities supporting the day-to-day operating practices provide, the safe transportation of hazardous materials is still a complex matter due to a number of issues [11, 21, 22]:

- Number of regulated hazardous materials (thousands are listed in regulations worldwide),
- Regulations that vary by mode, region, and country,
- Different hazards classes including toxicity, flammability, corrosivity, and reactivity,
- Various modes of transportation including road, rail, marine (including bulk vessels), pipeline, and air,
- Multiple packaging types including bulk and non-bulk,
- Use of more than one mode during a shipment (intermodal),
- Complexity of the supply chain including multiple parties and changes of custody during transit,
- Overlapping and potentially unclear responsibility of various parties and
- Transport routes where the risk profiles change depending on proximity to the public or other sensitive areas.

As a result, even with the availability of current safety regulations and operating practices, accidents involving the transportation of hazardous materials accident still occur [21, 22, 25, 34, 54]. For example, in 1978, at San Carlos de la Rapita, Spain, fireballs from a tanker containing 23.5 ton of propylene caused about 200 fatalities [32, 38, 56-64].

Nevertheless, HAZMAT accident do happen and in many cases have severe consequences such as accident involving chlorine leaking from damaged tank cars



due to a derailment in Mississauga, Ontario in 1979 leading to an enormous loss of properties and forced the evacuation of 200,000 people [56-58].

In another accident, that resulted from BLEVE impact from a tanker vehicle on June 22, 2002, near the city of Tivisa in Catalonia, Spain [66]. The driver died while two persons (at a distance of 200 m) suffered from 1st and 2nd degree burns. The pressure developed during BLEVE was estimated to be about 10 bar. Hence, it is necessary to design and develop SAS to assist the authorities in the control of transportation of hazardous materials to ensure the accidents damages are minimized in the future.

Although the liability cost of an average hazmat incident is not significantly higher than the cost of a non-Hazmat incident, but many cases studies involving major HazMat transportation incident show that the cost of a hazmat accident especially when it is resulting in fire or explosion is significantly higher [55]. Therefore, HazMat transportation accidents are perceived as low probability–high consequence (LPHC) events and so far the current data seem to support this statement [55]. In fact, according to the DOT of United States of America statistics, 156,483 HazMat transportation incidents have occurred between 1995 to 2004, resulting in a total of 226 fatalities and 3,218 injuries [62, 63].

Table (2-1) illustrates list of selected major transportation accident in various countries, across different modes of transportation.

## **2.4 Transportation Quantitative Risk Analysis**

### **2.4.1 Risk Assessment**

Few definitions need to be clarified to assist in further discussion for risk assessment. Risk involves in most fields and activities including economies, business, sport, industry, also in our daily life. Risk associated with probability and consequence of an undesirable event [67]. Risk and hazard are often used synonymously, but they are actually two different entity. Hazard is the inherent characteristic of a material, condition, or activity that has the potential to cause harm to people, property, or the



environment [13, 34]. The Center of Chemical Process Safety (CCPS) characterized hazard into inherent physical and chemical characteristic [11, 68] with the potential for causing harm. Some authors define risk as the product of probability and expected consequence of the undesirable event [25, 69].

Probability can be defined as a number between zero and one that expresses the degree of belief concerning the possible occurrence of an event. Conditional probability is a probability of an event that should be preceded by another specific event. Consequence is considered to be the direct effect, usually undesirable, of an event such as a rail accident involving hazardous materials. The consequences of risk analysis begin with the release of hazardous material from the container and involve three-step procedure: (i) the release amount and mode of release; (ii) the extent to which people is exposed to the source term; and (iii) assessment of the health effect [25].



Table 2-1: List of major accidents based on the available database

| Date of accident | Location         | Transport mode | Substance and quantity released   | Initiating Event   | Outcome | Deaths/injuries/evacuated | Property/environment impact  | References       |
|------------------|------------------|----------------|-----------------------------------|--|---------|---------------------------|--|------------------|
| 1969             | Mississippi, USA | Rail tank car  | Anhydrous ammonia, 29,200 gallons | Derailment, a gas cloud was formed which blanketed the surrounding area  | F/E     | 64/53/0                   | Yes  | [56, 59, 60-63]  |
| 1971             | Texas, USA       | Rail tank car  | Vinyl chloride                    | Derailed cars included six tank cars containing vinyl chloride monomer and two cars containing other hazardous materials. Two tank cars were punctured in the derailment. The vinyl chloride monomer escaped and ignited | F       | 6/50/0                    | Yes, tank car ruptured violently and another tank car “rocketed” approximately 300 feet from its initial resting place | [56,59, 60-63]   |
| 1972             | Lynchburg, USA   | Road tanker    | Propane                           | Overturning, the vehicle slid on its side and struck a rock embankment, which ruptured the tank shell and permitted the propane to escape  | F/E     | 1/5/0                     | Yes  | [57,59, 62]      |
| 1974             | Illinois, USA    | Rail tank car  | Isobutene                         | Collisions and punctured the tank. Isobutene escaped and vaporized for 8 to 10 minutes before it exploded. The yard, surrounding residences, and commercial facilities were damaged extensively by fire and shock waves. | F/E     | 7/349/0                   | Yes, property damage was estimated at \$18 million,  | [21, 61]         |
| 1974             | Eagle Pass, USA  | Road tanker    | LPG                               | Leakage LPG during transport   | F/E     | 17/34/0                   | Yes  | [56-59]          |
| 1974             | Yokkaichi, Japan | Transshipment  | Chlorine                          | Leakage of chlorine during transshipment   | VCE     | 0/521/0                   | Yes  | [56-59]          |
| 1976             | Deer Park, USA   | Road tanker    | Ammonia                           | Collision during road transportation ammonia   | TG      | 5/200/0                   | Yes  | [56-59]          |
| 1976             | Illinois, USA    | Rail tank car  | Ammonia                           | Derailment and collisions  | TG      | 0/14/0                    | Yes, damage from the accident was estimated to be \$1,914,600.   | [61, 63]         |
| 1976             | Texas, USA       | Rail tank car  | Anhydrous ammonia, 7,509 gallons  | The tractor and trailer left the ramp, struck a support column of an adjacent overpass, and fell onto the Southwest Freeway, approximately 15 feet below   | TG      | 6/178/0                   | Yes  | [56, 61, 63, 64] |

Note: F = fire, E = explosions, VCE= vapor cloud explosion, TG = toxic gases



| Date of accident | Location            | Transport mode | Substance and quantity released   | Initiating Event   | Outcome | Deaths/injuries/evacuated                            | Property/environment impact                         | References       |
|------------------|---------------------|----------------|---|--|---------|--|---|------------------|
| 1977             | USA                 | Rail tank car  | Anhydrous ammonia   | Derailment and puncture  | TG      | 2/46/1000  | Yes, property damage was estimated to be \$724,000. | [61, 63]         |
| 1978             | USA                 | Rail tank car  | Ammonium nitrate (liquid), Caustic soda (liquid), Chlorine, Turpentine, Lpg | Derailment of 44 tank wagons caused by sabotage<br>Big chlorine release  | F/E     | 8/153  | Yes   | [57-59]<br>[64]  |
| 1978             | Florida, USA        | Rail tank car  | Chlorine  | Leakage of chlorine during rail transportation   | TG      | 8/138/0  | Environment   | [56-58]          |
| 1978             | Los Alfaques, Spain | Road tanker    | Propylene   | Unknown  | E       | 216/200/0  | Yes   | [21,56-58, 64]   |
| 1979             | Suda Bay, Greece    | Road tanker    | Propane   | Unknown  | E       | 7/140/0  | Yes   | [56, 57]         |
| 1979             | Mississauga, Canada | Rail tank car  | Chlorine, Propane, LPG  | Derailment of a train carrying dangerous goods<br>3cars (propane) exploded, chlorine tank punctured, release chlorine in the air | F/E/TG  | 0/0/250,000<br>evacuated from surrounding urban area | Yes   | [56, 57]         |
| 1981             | Montannas, Mexico   | Road tanker    | Chlorine  | Accident during transportation of chlorine   | TG      | 28/1000/5000   | Yes   | [21, 56, 57, 64] |
| 1983             | USA                 | Rail transport | Nitric acid fuming, Sodium carbonate (soda ash)                             | Drive, Collision, Penetrate/Puncture<br>Release, Chemical reaction, Ignition<br>Fire, Vaporize                                   | F/E     | 0/34/0   | Yes   | [57-59]          |
| 1983             | Nile, Egypt         | Marine         | LPG   | Explosion during transportation  | F/E     | 317/44/0   | Yes   | [56, 57]         |
| 1984             | Matamoros, Mexico   | Unknown        | Ammonia   | Accident during transportation of ammonia  | TG      | 0/182/3000   | Yes   | [56, 57]         |
| 1987             | USSR, Annau         | Unknown        | Chlorine  | Accident during transportation of chlorine   | TG      | 0/200/0  | Yes   | [21, 56, 57]     |

Note: F = fire, E = explosions, VCE= vapor cloud explosion, TG = toxic gases



| Date of accident | Location          | Transport mode | Substance and quantity released | Initiating Event   | Outcome                      | Deaths/injuries/evacuated | Property/environment impact   | References |
|------------------|-------------------|----------------|---------------------------------|--|------------------------------|---------------------------|---|------------|
| 1998             | South Korea       | Marine, tanker | Butane, LPG, Propane            | During unattended unloading a hose ruptured and Fire heated up 2 lpg tank vehicles causing bleve and 84 casualties including firefighters  | Overheating /BLEVE/ fireball | 1/83/0                    | Yes   | [57]       |
| 1998             | Kyrgyzstan        | Road tanker    | Cyanide (1800kg)                | Sodium cyanide were spilled into a river upstream of several villages  | TL                           | 0/>1000/0                 | Yes, polluted a river , symptom after 100 days  | [56]       |
| 1999             | France            | Marine         | Fuel oil (8,000 tones)          | Fuel oil escaped from the tanker of Africa   | TL                           | 0/0/0                     | Environment highly polluted, when 100kms of coast were affected. Major economic effects on fishing, oyster farming, and tourism | [56, 57]   |
| 1999             | Malaysia          | Road tanker    | 21,850 liters of petrol         | Crash of a lorry carrying petrol hit house and overturn  | F/E                          | 0/2/0                     | House and car total damage  | [15]       |
| 2002             | Malaysia          | Road tanker    | 21,600 liters of petrol         | Crash of a lorry carrying petrol at km 20.8new Klang Valley Expressway   | F/E/                         | 12/50/0                   | Yes, traffic more than 5 hours  | [16]       |
| 2003             | Japan             | Road tanker    | Benzene (fp< 21deg. C           | Collision on slight bend of tunnel caused huge Explosion, fire, damage to tunnel and 2 casualties  | Ignition/F/E                 | 2/0/0                     | Yes   | [57]       |
| 2004             | Zahedan City,Iran | Road tanker    | Gasoline (17,000 litres)        | Truck carrying gasoline was lost control and hit one of the buses and burst into flames while the leaking gasoline, which turned the whole area into an inferno, incinerating the buses and the fireball then enveloped five other buses | F/E (fireball)               | 90/110/0                  | Yes, firemen took more than 2 hours to extinguish the fire.   | [56]       |
| 2003             | Malaysia          | Road tanker    | Gasoline (38,000liters)         | Petrol tanker skidded before landing on its side and caught fire.  | F/E                          | 0/1/0                     | Yes   | [13]       |
| 2007             | Malaysia          | Road tanker    | Petrol (21,840 liters           | Petrol tanker skidded and overturn   | F/E                          | 0/1/0                     | Yes, traffic for 3.5 hours and 2km  | [38]       |

Note: F = fire, E = explosions, VCE= vapor cloud explosion, TG = toxic gases



| Date of accident | Location       | Transport mode  | Substance and quantity released               | Initiating Event   | Outcome           | Deaths/injuries/evacuated  | Property/environment impact   | References |
|------------------|----------------|-----------------|---|--|-------------------|--|---|------------|
| 2007             | Ukraine        | Rail tanker car | Phosphorus                                    | Train derailed   | F/TG/             | 0/190/ unknown. The highly toxic substance, which can catch fire spontaneously on contact with air at temperatures higher than 104 degrees, can cause liver damage | Yes, Six of the tankers caught fire and smoke from the burning phosphorous spread over 35 square miles. | [57, 58]   |
| 2007             | Mexico         | Road tanker     | Ammonium nitrate                              | Truck loaded with ammonium nitrate has exploded in Mexico after a traffic accident, creating a huge fireball   | Fireball/F 20mx3m | 28 people, including rescue workers and photographers. People stuck in the traffic jam caused by the accident were also killed                                     | Yes   | [57-59]    |
| 2008             | Mexico         | Road tanker     | Ammonium nitrate                              | Emergency crews were on the scene of a propane tanker accident in Chelsea for more than 24 hours. The truck was carrying 2,400 gallons of propane when it slid off the road-- spilling gas into a nearby stream. Officials say about 1,800 gallons of fuel leaked into the waterway. And because the flammable fuel could catch fire | No                | 0/0/40 homes   | Environment   | [57-59]    |
| 2009             | Malaysia       | Road tanker     | 21,000 liters petrol and 10,000 liters diesel | Oil tanker skid  | F/VCE             | 3/1/1 homes  | Property  | [6,7]      |
| 2010             | Malaysia Bahau | Road tanker     | 21,000liters petrol                           | Collision  | F/E               | 4/0/0  | Property  | [38]       |

Note: F = fire, E = explosions, VCE= vapor cloud explosion, TG = toxic gases



An initiating event is the first in a sequence of events that may lead to an undesirable consequence. In transportation risk analysis, the initiating event is the first event which initiate a particular accident that requires notification to the regulatory agencies. An undesirable event that results in the release of a hazardous substance is called an incident. Although there can be many undesirable consequences of an incident (such as damage to wildlife, economic losses, and injuries), the prime concern is incidence fatalities. It is common to assume that the undesirable consequence is proportionate to the size of the population surrounding the incident and the type of substance carried by the HAZMAT [21, 22].

By considering fatalities as the prime concern, this will simplify the risk assessment process even though its end result might be far then from the absolute risk of a potentially transportation hazards activity. Saccomanno and Chan [48] have described the assessment of risk with the financial loss (US dollar) related to fatalities and other type of injuries. However it is difficult to be implemented, since most of HazMat direct impact on human life is difficult to be quantified and valued [11, 19, 23].

Risk assessment has been accepted as the determination of risk acceptability and CCPS define risk assessment as the process by which the results of a risk analysis are used to make decisions, either through relative ranking of risk reduction strategies or through comparison with risk criteria [19]. In TRA, risk assessment is define as the process by which the results of a risk analysis are used to make decisions, either through a relative ranking of risk reduction strategies or through comparison with risk targets [21,22, 70].

While taking action to reduce risks is called as risk management [7]. Risk assessment should quantify the transportation risk, identify sources of greatest risk, and examine specific issues in risk reduction. It should identify risks associated with accidents on transportation of hazardous materials and determine the levels of risk that are acceptable, affordable and comparable with HazMat transportation risks present in Malaysia. Most of this depends on probabilistic estimates of a release from an incident. Risk assessment also estimates the frequency and consequences of undesirable events, then evaluating the associated risk in quantitative terms. The final outcomes of risk assessment provide knowledge essential to informed decision making.



### **2.4.2 The Public and Risk Assessment**

The techniques of risk assessment address two fundamental questions: i) what is the actual level of risk? , ii) what level of risk is acceptable to those affected? [25]. Qualitative judgments are important to the second question. The public creates its own unscientific risk assessments and still raised their concern regarding HAZMAT transportation incidence even though the safety record of hazardous material being transported is excellent. This is due to unpredictability and the disaster that can happen in accident involving HAZMAT transportation. Risk acceptability is complicated by the fact that the public may have risk perceptions that differ substantially from the actual risks.

## **2.5 The Quantitative Risk Analysis Procedure**

Quantitative risk assessment (QRA) is the development of a quantitative estimation of risk based on engineering evaluation and mathematical techniques by combining estimation of incident consequences and its frequencies [11]. The QRA procedure is basically consists of a set of methods to estimate the risk posed by any given condition in terms of human loss or economic loss [67]. The QRA also able to identify incident scenarios and evaluate the risk by defining the probability of failure, the probability of various consequences and the potential impact of those consequences Various publications provide information on QRA methodologies. Two of the most important examples are the “Purple book” published by TNO [71] and the guidelines published by CCPS [11].

In the past, the techniques of chemical process quantitative risk analysis (CPQRA) are more recognised than those of TRA. CPQRA is a method designed to provide management tool to evaluate overall process safety in the chemical process industry [11, 72]. The tool such as engineering codes, checklists and process safety management (PSM) provide layers of protection against incidents. However, the potential for serious incidents cannot be totally eliminated. CPQRA provides a quantitative method to evaluate risk and to identify areas for cost-effective risk reduction.



### 2.5.1 Framework of TRA

Transportation risk analysis (TRA) methods have existed for about the same time period as CPQRA, but yet they are far less widely used and understood [32, 33]. TRA can be conducted on a qualitative or quantitative basis [35, 67]. Qualitative approaches include risk-screening methodologies, which are generally unique for each company. Other qualitative approaches include carrier screening programs, route and container selection, driver training and selection programs. The quantitative approach in TRA is similar to CPQRA, which is used to help to evaluate potential risks when qualitative methods cannot provide adequate understanding of the risks and more information is needed for risk management. It can also be used to evaluate alternative risk reduction strategies.

In CPQRA, risk is defined as a function of probability or frequency and consequence of a particular incident scenario and calculated as below:

$$\text{Risk} = F(s, c, f) \quad (2-1)$$

where,

$s$  = hypothetical scenario,

$c$  = estimated consequence(s), and

$f$  = estimated frequency.

This function can be extremely complex and there can be many numerically different risk measures (using different risk functions) calculated from a given set of  $s$ ,  $c$ ,  $f$ , which will be further discussed in section 2.6.

The general steps of TRA are described below [11, 21, 22, 72, 73]:

- **TRA Scope Definition** converts user requirements into study goals and objectives. Risk measurement and risk presentation formats are chosen in final step in TRA. The depth of study is based on the specific objectives defined and the resources available.
- **Movement Description** is the compilation of the transportation activity information needed for the risk analysis. For an example, mode, container specification, weather data, number of trips, volume per container, material, shipping conditions, route or origin and destination, and population data. This data information is then used throughout the TRA.



- **Hazard or Initiating Event Identification** is a critical step in TRA. The incident-initiating events of concern can generally be identified based on previous data. Non-incident-initiating events can be identified through hazard identification techniques described in CPQRA Guidelines [17, 39].
- **Likelihood Estimation** is the method used to estimate the frequency or probability of occurrence of an incident. Estimation may be obtained from historical incident data on failure frequencies or from failure sequence models such as fault trees and event trees or from special failure models.
- **Consequence Estimation** is the methodology used to determine the potential damage, fatality or injury from specific incidents. A single incident (e.g., leakage from pressurized liquid tank) may have many distinct incident outcomes, e.g., vapor cloud explosion (VCE), boiling liquid and so on.
- **Risk Estimation** combines the consequences and likelihood of all incident outcomes from all selected incidents to provide risk measurement. The risks of all selected incidents are individually estimated and summed to give an overall measure of risk.
- **Utilization of Risk Estimates** is the process by which the results of a risk analysis are used to make decisions, either through relative ranking of risk reduction strategies or through comparison with specific risk targets.

Other qualitative analyses do not comply to these steps completely. Risk screening can be developed by adopting one or more of these steps into account. Level analysis can be conducted by comparing the data set for the transportation of concern with the data set and results for another transportation for which a quantitative TRA has been conducted, and simply determining if the transportation of concern poses more or less risk than the previously evaluated one. In quantitative risk analyses it may be possible to take the results of other studies and use them as the basis of one or more of the steps in the TRA, but these other results may first need to be scaled or adjusted before using them, and usually all steps need to be performed to get the quantitative results.



### **2.5.2 Comparison to Stationary Facility of Chemical Process Risk Analysis**

There are similarities and differences between HAZMAT transportation and fixed facility risk evaluations. As an example, for the usual singular focus on a single vehicle with a single hazardous cargo, the identification of the hazard, the consequences interest, and the initiating events are very much simplified for transportation. Both TRA and fixed facility risk evaluations can be qualitative or semi-quantitative compared to quantitative. In these Qualitative or semi-quantitative estimate risk by taking into account experience, judgment, good practices, training, procedures, inspection and maintenance, codes and standards, past performance, etc., whether one is dealing with fixed facilities or transportation movements.

The modelling of release consequences is largely independent on the cause of the release and is therefore directly transferable from CPQRA method to TRA. Risk measurement are also commonly utilised in these two types of quantitative risk analyses. The most fundamental difference between CPQRA and TRA is that TRA deals with a linear source of risk, while CPQRA deals with relatively discrete point. This linear source may be static such as pipelines or may be a moving source for other modes of transport.

The nature of TRA data can be different from CPQRA data. They are often expressed as a function of distance travelled or per trip, transit, or visit. External event causes of accidents are generally included in the data including such items as vandalism for rail transport, adverse weather for marine transport, and third-party damage for road. Other difference between transportation and fixed facility risk evaluations is the nature of the risk reduction and mitigation alternatives available. By virtue of the unknown location of transportation release (prior to its occurrence), it is much more difficult to identify and implement effective mitigative (post-release) strategies. Secondary containment via water sprays, foams, evacuations, etc. are either not feasible, or can only be initiated some significant amount of time after the release has occurred. Given the rapid dispersion of many large releases, such mitigation measures may be totally infeasible or untimely. The result is to make mitigation modelling more uncertain for a transport accident than it is for plant accident.



In transportation, a release can occur anywhere along a route between the origin and destination. The unpredictability of the exact release location often requires the use of generalized approaches to limit the data needs and number of incident outcome cases. These generalized approaches may relate to one or more of the following:

- **Identification and selection of initiating events** – may utilize an aggregate incident rate or a limited breakdown, such as derailments and collisions, rather than a detailed breakout by failure mode.
- **Selection of incidents and incident outcomes** – particularly release sizes and rates, release orientation, material temperature and pressure at time of release. While a release in a facility is reasonably predictable in terms of the material conditions, these could change with the season changes.
- **Meteorological conditions for modeling** – wind roses and stability class distributions vary from location to location, as does the ambient temperature and humidity.
- **Ignition probabilities** – the number, type, and proximity of ignition sources vary along a route, and it may be very difficult to get route specific data.
- **Population distribution** –The population density around a traffic accident varies, for example, from large city to a rural area. In addition, traffic can build up behind an accident, resulting in a high number of victims surrounding the accident.

For fixed facilities, it is possible to eliminate or prevent risks but in transportation, risk reduction is the main aim. Most researchers estimated that 24- 47 % of hazardous material incidents are due to human error [74, 75]. The degree of variability and influence of human performance is often cited as being much greater for some modes of transportation than others especially for transportation compared to fixed sites. This is particularly true for road transportation where the route taken can vary from one trip to another.

### **2.5.3 Reason in Conducting TRA**

TRA is a powerful tool in HazMat transportation decision-making system. TRA is utilized in QRA and it provides a consistent and defendable decisions. It allows an effective evaluation of existing controls and procedures, but more important, its



capable to provide an insight on how to cost- effectively reduce the risk. It able to assist decision maker to choose a site for a facility or process relocation or expansion, by taking both fixed site and transportation risks into account. It is helpful in choosing alternative routes by providing information on the relative risks associated with each route therefore the appropriate mode of transportation or most effective container can be selected especially if additional protective measures are warranted.

In case if a transportation incident occurs, TRA could provide the emergency response plans. It can also help to understand the influence of material state on risks and make judgments about the tolerability of existing or increased movement levels.

## **2.6 Review of Previous Work on Transport Risk Analysis Models and Guidelines**

In the past two decades, attention has been focused on risk analysis of HazMat within transportation networks, and the techniques of QRA initially developed for fixed plants have been extended to TRA. Review of transportation risk analysis methodologies and consequences calculations for HazMats transportation, are mainly from major TRA guidelines and risk assessment handbooks such as CCPS Guidelines of Chemical Process Quantitative Risk Analysis, (2000), Netherlands Organization for Applied Scientific Research (TNO) (yellow book), TNO (purple book), CCPS Guidelines of Chemical Risk Transportation Risk Analysis, (1995), CCPS, Guidelines of Characteristics of Vapor Cloud Explosions (1994), CCPS, Vapor Cloud Dispersions (1987), Rhye [25] and BUWAL methodology recently developed by Swiss Federal Institute of Technology [11, 21, 22, 25, 26, 32, 76 -78].

### **2.6.1 Swiss Methodology (BUWAL) for Assessing the Risk of Hazardous Materials Transportation by Road**

In 1992 the Swiss Federal Office for Environmental Protection, Forestry and landscape (BUWAL) has issued a “Handbook III to the Regulations Concerning Incidents, - Guiding principles for Traffic ways” as below:



#### 2.6.1.1 *Subdivision of the Road Tracks into Road Segments*

As in the CCPS and Rhyne [21, 25] methodology the route is segmented to consider the variation of the characteristics along the route. The length of a segment is determined in such a way, that the architectural and technical configuration, the environment, the traffic and safety measures should be homogenous within the selected segment. Each length of a segment should not be less than a kilometer.

#### 2.6.1.2 *Data information*

**Population density** - The population density is to be indicated for the close-and-far-range along the road, and should mention the number of inhabitants per square kilometer (Inh. /km<sup>2</sup>). If there is no data available, than the population density could possibly be estimated as follows:

- Urban population density :> 5000 Inh. /km<sup>2</sup>
- Small-town population density: 2000 to 5000 Inh. /km<sup>2</sup>
- Village population density: 100 to 2000 Inh. /km<sup>2</sup>
- Slight or no settlement: < 100 Inh. /km<sup>2</sup>

**Traffic Rise** - The traffic volume is defined, as the average Daily traffic per 24 hours (ADT-24). The heavy Traffic Share (HTS) corresponding to this ADT-24 must be indicated.

**Average Daily Traffic per 24 Hour** - This is defined as the yearly total of vehicles at a certain road cross section divided through 365. This can be determined for certain through-roads from the published statistics of the Swiss traffic counting, which takes place every five years. Since such counts records catch hold of the ADT-24 data. A conversion is necessary. If records concerning the average (hourly) traffic of motor vehicles at day ( $N_d$ ) and night ( $N_n$ ) are available from the cantonal noise-pollution registers, then the ADT-24 data can be determined from such records.

**Traffic Composition**-In order to assess the composition of the Swiss traffic, one has to indicate the Share of Dangerous goods Traffic based on the Heavy traffic (SDH) and the ratio of the different SDR-classes corresponding to the dangerous goods traffic (RSC).



***Share of Dangerous Goods based on the Heavy Traffic (SDH)***- According to the latest road traffic survey of the year 1984, the share of the dangerous goods traffic related to the total heavy traffic amounts to 8% (Swiss average). Depending on road segment and regional particularities this proportion can vary between 5% and 15%.

***Ratio of the different SDR-Classes based on the Dangerous Goods Traffic (RSC)***. For transit roads, it can be assume the following distribution, which is based on the Swiss average (Table 2-2):

Table 2-2: Ratio of the different SDR-classes to the dangerous goods traffic (RSC)

| <b><i>SDR-class</i></b> | 1     | 2    | 3    | 4    | 5    | 6    | 7 | 8    | 9 |
|-------------------------|-------|------|------|------|------|------|---|------|---|
| <b><i>RSC</i></b>       | 0.001 | 0.07 | 0.70 | 0.07 | 0.01 | 0.07 | - | 0.08 | - |

Depending on the regional aspects (presence of a harbor, stores, loading/unloading station, chemical plant, or processing plan) the RSC-share corresponding to a given road segment may be corrected on the basis of estimates.

***Accident statistics*** - The Accident Rate of the total traffic is to be considered (*ART*). This is to be calculated according to Swiss VSS-directive, (1990). When some accident statistics are not available, the accident rate corresponding to different road categories can be selected from the data listed in Table (2-3), showing the accident rates, and in brackets, the confidence limit. However, if statistics concerning Accident Rates for Heavy traffic (*ARH*) are available for the different road segments. The data must be used for the calculation. Where this data are not available, the accidents to the total traffic accidents (Swiss average) is approximately half as large as the share of the heavy traffic to the total traffic. In special cases, e.g., strong ramp, this value can be higher and an appropriate correction must be made.



Table 2-3: Accident rates for the total traffic (average values *AR-total*) is based on empirical data collected in Switzerland.

| Road Type                       | Accident Rates                                     |
|---------------------------------|--|
| Highways                        | $0.45 (\pm 0.20) \times 10^{-6}/\text{Vehicle.km}$ |
| Semi-Highways                   | $0.50 (\pm 0.10) \times 10^{-6}/\text{Vehicle.km}$ |
| Main roads (outside localities) | $1.20 (\pm 0.40) \times 10^{-6}/\text{Vehicle.km}$ |
| Main roads (inside localities)  | $2.10 (\pm 0.40) \times 10^{-6}/\text{Vehicle.km}$ |

### 2.6.1.3 *Estimation of the likelihood of an Incident with Severe Consequences to People or Environment*

The goal of this assessment is to compare which road segments that will have high probabilities of severe damage to people and environment for further investigation. The methodology followed by the Swiss Authorities is based on the most actual national and international knowledge and experience in this field.. The method allows to coarsely assessing, for each road segment, the probability of an incident causing severe damage to people, groundwater resources, and surface waters, on the basis of representative incident scenarios. Unfortunately, this method cannot cope equally well with all kind of situations, like for instance very long tunnels. The frequency (per km and year) of representative incident scenarios is determined for each road segment as in Eq. (2-2), [32]:

$$F_s = ADT \cdot 365 \cdot HTS \cdot AR \cdot SDH \cdot RSC \cdot RRP \cdot RRI \cdot RSS \quad (2-2)$$

where,

$ADT = ADT(24)$  (i.e., Average Daily Traffic) is to be converted on a year basis, i.e., average number of vehicles per year (vhc. /year); assuming that a year has 365 days,

$AR$  = Accident Rate (vhc. /km)<sup>-1</sup>,

$F_s$  = Frequency of a representative incident scenario with severe damages [(km.year)<sup>-1</sup>],

$HTS$  = Heavy Traffic Share based on average daily traffic (ADT-24), (dimensionless),

$RRI$  = Relevant Release Rate, and for burning and explosion, the Ignition rate (dimensionless),



RRP = Ratio of the Relevant Product of the SDR-class applicable to the representative incident scenario (dimensionless),

RSC = Ratio of the different SDR-Classes corresponding to the dangerous goods traffic (dimensionless),

RSS = Ratio of the representative incident scenarios leading to severe damages (dimensionless), and

SDH = Share of Dangerous goods traffic based on the heavy traffic.

#### 2.6.1.4 *Frequency of incident with severe damages*

**Severe Damages to the Population:** one has to consider the sum of the frequencies of the incident scenarios burning, explosion and release of toxic gases.

#### 2.6.1.5 *Ratio of the relevant Product of the SDR-class Applicable to the representative Incident Scenario (RRP).*

This RRP-value is expressed as the ratio of the relevant products of the particular SDR-class representative of a given incident scenario.

**Relevant Release Rate and Ignition Rate:** It is assumed, that all materials relevant for a representative incident scenario are transported more or less in similar quantities and containers, so that a uniform release rate, and in the case of burning and explosion, that ignition will follow. This value is valid both for open rail tracks, as well as for tunnels.

**Ratio of the Representative Incident Scenarios leading to Severe Damages:** The RSS-factor stands for the probability of severe damage under the condition, that a relevant release, and for burning and explosion, the ignition has already occurred.

#### 2.6.1.6 *Assumptions concerning the representative incident scenario for the "Population"*

In this methodology, the total number of people which will be exposed to the potentially HazMat vehicle is based on relevant correlation of RRI impact for release rate, for burning and explosion over RSS ratio of severe damages from BUWAL published data.

#### 2.6.1.7 *Comparison risk by two routes only at one time*



The methodology has also proposed a short cut approach, if maximum two alternates route want to be compared. The probable number of fatalities from a road tanker carrying a HazMat load along the entire route can be calculated as in Eq. (2-3):

$$\text{fatality probability} = SI_L \sum_i P_{ai} D_i \quad (2-3)$$

$$\text{where, } SI_L = \sum_j \pi r_j^2 P_{sj} \quad (2-4)$$

$SI_L$  = Severity Index for a specific load, L ( $\text{km}^2$ )

$P_{ai}$  = Probability of the tanker involved in an accident in section, i (dimensionless),

$D_i$  = Population density in section, i (Inh. / $\text{km}^2$ ),

$P_{sj}$  = Probability of scenario j's occurrence (dimensionless), and

$r_j$  = Effect radius of scenario, j (km).

For each accident there is a number of possible accident scenarios, which may be considered to be fatal to individuals present within radius  $r_j$ . The number of people N, present at the location of the accident, which may be affected depends on the density of the population  $D_i$  is represent by  $N = \pi r_j^2 D_i$ . For any type of load, the term  $\pi r_j^2 P_{sj}$  as in Eq. (2-4) is constant which is independent of the route. This term is also called the Severity Index, SI. Since, the probable number of fatalities from a tanker carrying load L along sub segment i, is equal to  $(SI)_L P_{ai} D_i$ , therefore the probability of someone being killed, due to the passage of the tanker for the entire length of the route, is the sum of the probabilities for all possible accident scenarios which is equal to  $SI_L \sum_i P_{ai} D_i$  as in Eq. (2-3).

For any given load the smaller the values of  $SI_L$  and  $P_{ai} D_i$  as in Eq. (2-4) the safer the transport operation. Therefore it is possible to compare the relative risk of two alternatives routes by comparing the term  $\sum_i P_{ai} D_i$ , i.e. , the population density,  $D_i$ , along the route times the probability,  $P_{ai}$ , of an accident. The weakness of this methodology is because the standard coefficient or data used in the Eq. (2-2) to Eq. (2-4) is not suitable to be used for other country, because the accident rates and statistics, traffic volume and other data might differ considerably. Moreover the Swiss methodology used gasoline as the standard substance in all type of fire incident cases,



LPG represents any explosion incident cases while chlorine and ammonia represent any toxic release cases in the RRI and RSS calculations as in Eq. (2-2).

## 2.6.2 Rhyne Methodology for Assessing the Risk of Hazardous Materials Transportation by Road

In Rhyne methodology two important parameters, frequency and consequence are included. Similar to CCPS, the risk,  $R_i$ , for accident scenario  $i$  is a function of the scenario frequency,  $F_i$ , and the scenario consequence [21, 25].

$$R_i = f(F_i, C_i) \quad (2-5)$$

However the two parameters, frequency and consequences in Rhyne [25] consisting different subcomponent aggregation for both of the parameters used in the CCPS [21, 22]. As usual, the procedure for a quantitative transportation risk analysis is to divide the transport route into segments (also called links) along which the important parameters can be reasonably approximated by a single average value. A detailed expression for risk in Rhyne [25] can then be further defined:

$$R_i = f(F_{1a} \cdot M_a \cdot P_{2ab} \cdot P_{3bc} \cdot P_{4ad} \cdot P_{5ae}, N_{ad} \cdot A_{abc} \cdot X_{ace}) \quad (2-6)$$

where,

$F_i = f(F_{1a} \cdot M_a \cdot P_{2ab} \cdot P_{3bc} \cdot P_{4ad} \cdot P_{5ae})$ , frequency subcomponent parameters;

$C_i = f(N_{ad} \cdot A_{abc} \cdot X_{ace})$ , consequences subcomponent parameters;

$F_{1a}$  = frequency of an accident per mile in transport link  $a$  based primarily on highway (or rail track) type and conditions, vehicle type, and traffic conditions;

$M_a$  = number of miles, or miles per year, in link  $a$ ;

$P_{2ab}$  = probability that the accident in link  $a$  results in accident forces of type  $b$  (e.g., mechanical or thermal forces);

$P_{3abc}$  = probability that release class  $c$  occurs, given that the accident force type  $b$  occurs in link  $a$ , which depends on the force magnitude and the container's capability to resist the force;

$P_{4ad}$  = probability that population distribution class  $d$  occurs in link  $a$ ;

$P_{5ae}$  = probability that meteorological condition  $e$  occurs in link  $a$ ;

$N_{ad}$  = number of persons in affected area  $d$  in link  $a$ ;

$A_{abc}$  = release amount for release class  $c$ , given that force type  $b$  occurs in link  $a$ ;



$X_{ace,}$  = fraction of persons in the affected area which experience the specified health effect from a unit release of the hazardous material for meteorological condition  $e$  for release class  $c$ .

The overall risk (fatality per year) is obtained by summation of all scenarios for each link or for the entire route:

$$R = \sum R_i \quad (2-7)$$

The frequency component of risk in Eq. (2-6) consist of three main subcomponents: Firstly the accident frequency ( $F_{ai}$ ), which regard to how often the accident is likely to occur along the length route ( $M$ ). Second, the conditional probability of the release of contents given that an accident has occurred. That means how did the accident occur ( $P_{2ab}$ ), whether it is due to over speed, failure of the tanker or collision to another vehicles. Apart of that, second subcomponent of frequency is also considered, the seriousness level of the accident probability, based on the magnitude of accident force impact occurs ( $P_{3abc}$ ), such as considered, whether the magnitude is sufficient to cause container failure and thirdly, there is the conditional probabilities that arise from the consequence component such as the meteorological conditions influence toward population distribution [25]. For instance how the influence of wind direction will determine to which population is exposed (during indoors and outdoor or during night time or daytime) ( $P_{4ad}$ ), to a downwind plume, if 16 directions (each directions is  $1/16 = 0.0625$ ) are used to plot the probability that the wind ( $P_{5ae}$ ), will come from a particular direction and at particular speed. However, in most cases, the data are not specific for the a particular situation therefore the risk analyst will compensate for lack of specific data by using data from a broad class of situations, for example, failure probability for radioactive material containers, a hole produced by accident forces [25]. The consequences component of risk can be considered to consist of three sub component. First is the amount of material released. It is about the quantity of material being released out of the tanker ( $A_{abc}$ ). Second the number of people exposed, which means how many people are likely to be affected by the amout of material released ( $N_{ad}$ ), and finally the health of the exposure, ( $X_{ace}$ ), which means what risk would the people face with the hazardous material exposure.



For risk route comparison, Eq. (2-6) and Eq. (2-7) are produce a quantitative value for absolute (or complete) risk. It is useful to compute relative risk for two or more options using only a few of the parameters from Eq. (2-6) as a surrogate for risk. This approach is used frequently to compare routing options. Previously, the basic approach used the accident rate per mile times the number of miles in a highway segment as a surrogate for the frequency portion of Eq. (2-6) and the number of people in a 0.5 to 1-mile-wide band along the highway segment as a surrogate for the consequence portion of Eq. (2-6) The product of the two terms is a relative risk indicator, and the route with the lowest indicator has the lowest computed relative risk. Expressing the relative risk indicator approach mathematically is helpful. For simplicity of presentation, the following assumptions will be used: only one release class ( $c = 1$ ), one population distribution along each link type ( $d = 1$ ), with single meteorological condition ( $e = 1$ ). Thus,  $P_4 = P_5 = 1$ . If comparison of the relative risk of options route,  $x$  and  $y$  is desired, then the question is whether  $R^x$  is less than, greater than, or equal to  $R^y$ . Using Eq. (2-6) the question can be reformulated by comparing risk between the route  $x$  and  $y$  as follows:

$$F_1^x \cdot M^x \cdot P_2^x \cdot P_3^x \cdot P_4^x \cdot P_5^x \cdot A^x \cdot X^x \cdot N^x \text{ and } F_1^y \cdot M^y \cdot P_2^y \cdot P_3^y \cdot P_4^y \cdot P_5^y \cdot A^y \cdot X^y \cdot N^y \quad (2-8)$$

Since  $P_4 = P_5 = 1$  for both routes  $x$  and  $y$ , Eq. (2-8) is simplified into  $F_1^x \cdot M^x \cdot P_2^x \cdot P_3^x \cdot A^x \cdot X^x \cdot N^x$  and  $F_1^y \cdot M^y \cdot P_2^y \cdot P_3^y \cdot A^y \cdot X^y \cdot N^y$ . If some terms are the same for both options, if it would be the case for many routing studies (e.g., if  $P_2^x = P_2^y, P_3^x = P_3^y, A^x = A^y$ , and  $X^x = X^y$ , then Eq. (2-9) is became more simplified to the following expression for routing purposes:

$$\text{Compare } F_1^x \cdot M^x \cdot N^x \text{ and } F_1^y \cdot M^y \cdot N^y \quad (2-9)$$

To use of Eq. (2-9) as a safest risk route indicator includes some important assumptions such as the same container were used on all potential routes; therefore all related of the container safety factors such as failure threshold and response time to the accident force types must be also same.

### 2.6.3 CCPS-TRA Methodology for assessing the risk of hazardous Materials Transportation by Road



Transportation risk analysis (TRA) methodologies have existed for about the same time period as chemical process quantitative risk analysis (CPQRA) methodologies, but yet they are far less widely used and understood. TRA shares many of its tools and techniques with CPQRA, but distribution activities are often housed in a separate part of an organization and may not be aware of all the internal resources available in risk analysis. There are three basic types of risk measures which are developed for a semiquantitative or quantitative analysis for both CPQRA and TRA:

- **risk indices**, which are single numbers or scores.
- **individual risk measures**, which consider the risk to a particular person or at a particular location.
- **societal risk measures**, which consider the overall risk associated with an activity to a particular population.

Individual risk measures the risk to a person along a transportation route, and can be calculated for the most exposed individual at a specific locations along a route, or for an individual average risk in a potentially affected area. Societal risk considers the summation of likelihood of severe events occurring. It can be much higher for transportation movements than is commonly found for fixed facility operations, because of the multiplicative effect of route length and number of trips. In other cases, transportation risks can be much lower than facility risks if the route is remote from population, such as for some marine movements and pipelines.

The overall expression for annual risk at any specific location (such as x), assuming a constant accident rate, is thus [21,22]:

$$IR_{x,y} = T \cdot A \cdot \sum_{i=1}^n R_i \cdot \sum_{j=1}^m L_{i,j} \cdot W_j \cdot \sum_{k=1}^{S_i} P_{i,j,k} \quad (2-10)$$

where,

$IR_{x,y}$  = the total individual risk of fatality at geographical location x,y (chance of fatality per year)

T = trips per year

A = accident rate per mile

$R_i$  = release probability for release size  $i$

$n$  = number of released size considered

$L_{i,j}$  = length of release location zone  $j$  for release size  $i$  (in miles)

$m$  = number of release location zones and wind directions affecting location x,y



- $W_j$  = probability that wind blows in direction of concern for release location zone  $j$   
 (does not vary by release size)  
 $P_{i,j,k}$  = probability of a fatality at location  $x,y$  given that incident outcome  $k$  occurs in  
 release location zone  $l$  with appropriate wind direction, given release size  $i$   
 $S_i$  = number of incident outcomes for release size  $i$   
 $i$  = release size counter  
 $k$  = incident outcome counter

If the accident rate varies or if there are non-accident-initiated events to be considered as well, Eq. (2-10) can be modified accordingly by adjusting parameter,  $A$  or adding another term for fixed sources of risk where there is no length of a release location zone to be considered. The main difference between calculating societal and individual risk is in determining the consequences associated with an incident outcome. Individual risk essentially determines whether or not a particular location is involved in an incident outcome case, while societal risk considers how many people are involved in an incident outcome case.

Given the length of most transportation routes, it is suggested that the route first subdivided into segments over which the population density can be assumed to be uniform. If the route is divided into segments, then the frequencies and consequences can be obtained for each incident outcome case in each segment. The frequency of incident outcome  $k$  for release size  $i$  on segment  $g$  is defined as [21, 22]:

$$F_{g,i,k} = T \cdot A \cdot R_i \cdot L_g \cdot P_{i,k} \quad (2-11)$$

where,

$F_{g,i,k}$  = frequency of incident outcome  $k$  for release size  $i$  on segment  $g$  (per year)

$T$  = trips per year

$A$  = accident rate per mile

$R_i$  = release probability for release size  $i$

$L_g$  = length of segment  $g$  in miles

$P_{i,k}$  = probability of incident outcome  $k$  for release size  $i$

$g$  = segment counter

$i$  = release size counter

$k$  = incident outcome counter

$$N_{g,i,k} = CA_{i,k} \cdot PD_g \cdot PF_{i,k} \quad (2-12)$$

where,



$N_{g,i,k}$  = number of fatalities for incident outcome  $k$  for release size  $i$  on segment  $g$

$CA_{i,k}$  = consequence area associated with incident outcome  $k$  for release size  $i$

$PD_g$  = population density for segment  $g$

$PF_{i,k}$  = probability of fatality for incident outcome  $k$  for release size  $i$

$g$  = segment counter

$i$  = release size counter

$k$  = incident outcome counter

This calculation is repeated for all incident outcome cases. The results are then combined to construct societal risk F-N curve as described in Eq. (2-8). Eq. (2-9) can also include an additional term for wind direction. This might simply be set equal to 0.5 or might be calculated based on wind rose data. It is recognized that the release may originate in one segment but cause consequences in the next. This is generally insignificant as its occurrence is counteracted by releases in the previous segment which can cause consequences in the present segment. The only place that the crossing of segment boundaries is a significant concern is when the hazard length is much greater than the segment length.

## **2.6.4 Previous Trend on Development of Transportation Risk Analysis Model**

As mentioned by Lees [64], the work of Westbrook [65] was the earliest study in HazMat transportation to estimate the risks of chlorine to the road and pipeline. Then, in 1988, Ormsby and Le [90] proposed the use of frequency-number (F-N) curves for transport specific type of chemicals such as chlorine, LPG and natural gas. However, till year of 1990, there is no comprehensive guideline and procedure has been developed to manage risk of HazMat during transportation. To reduce the risk impacts from hazardous materials transportation, Health and Safety Executive of United Kingdom, 1991 [8], had published a first comprehensive report in ‘Major hazard aspects of the transportation of dangerous substances’.

Since 1991, several studies have been reported in literature related to hazardous materials such as the database development, selection criteria for designation of hazardous materials highway routes, risk assessment of HAZMAT transportation, hazard areas and safe distance for transporting hazardous materials by truck, accident rate model for routing and methodology to determine safe routes for hazardous



materials transportation [29, 39-53, 55, 79, 80-85]. Abkowitz and Cheng [86] identified that statistical accident database is the most commonly used method for estimating risk. Their methodology presumes that sufficient historical data must exist to determine the frequency and the consequences of the release incidents and those past observations can adequately be used in future. Vilchez et al. [74] also reported the same conclusion as Abkowitz and Cheng [86] on the use of major accident transportation statistic data method after comparing statistically the historical accident cases from major online or hardcopy databases such as MHIDAS, MAHRB, FACTS, and IChemE major accident database [87].

From the database analysis results, Vilchez et al. [74] have used the causal factors from the transportation of hazardous materials accident for ranking of the incident outcome (BLEVE, fireball, flash fire, pool fire, toxic dispersion). Harwood et al. [88] presented data analysis from several databases which identify that traffic accidents as a major cause of severe hazmat incidents and attempted to estimate the probability of a release given by an accident. Glickman [89] provided accident rate in transporting hazardous materials. Erkut and Verter [83] proposed a framework for quantitative risk assessment in hazardous materials transport. According to them in the case of an accident, all residents in the population center will experience the same consequences. However, their model is only will perform well if the hazardous materials route passes by a small population areas.

Till to date, most of risk modeling analyses have revolved around one, partially or all of the following criteria suggested by Erkut and Verter [79] such as (i) shortest travel distance, (ii) minimum population exposure, (iii) minimum societal risk, (iv) minimum DOT risk, (v) minimum accident probability, (vi) minimum incident probability. According to them, the shortest travel distance might not always be a best choice for transporting hazardous materials. Minimum population exposure as in criterion (ii) seems to exclude incident probabilities and find the path that exposes the fewest number of people to the hazardous materials. While a criteria (iii) is the traditional definition of risk, which uses the following formula to find the risk: Societal risk = (length of the exposure area per miles) X (accident rate probability per mile) X (conditional release probability given an accident) X (population/worker



density in the neighborhood of the exposure area-persons per sq. mile) X (pi-impact radius in miles-sq). Thus, the societal risk is the expected number of people who receive the accident impact as an important factor for risk. For criteria (iv) the definition of risk is according to the U.S. Department of Transportation (1989). By using this definition, mathematically it will affect the societal risk calculation with two differences, such as excluding conditional release probabilities, and computes population who are impacted by using a rectangle instead of a circle. Finally, criterion (v) is to find the path that minimizes the accident probability, has ignoring all other information.

In QRA, Rowe [90] characterized the quantitative risk analysis methodologies for transportation in three ways: (i) how they combine the two parameters to arrive at risk; (ii) the level of detail; and (iii) the methods for obtaining data and modeling parameters. As described in CCPS and Rhyne [11, 19, 21, 22, 25], usually the framework for TRA includes the following steps: (i) TRA scope definition; (ii) shipment description; (iii) hazard or initiating event identification; (iv) likelihood estimation; (v) consequence estimation; (vi) risk estimation; and (vii) utilization of risk estimation. In principle, these steps have to be repeated every time that any of the parameters involved in the above calculations changes along the itinerary, so usually a great deal of computation time is required to achieve the TRA goal [90]. Researchers in this field have executed substantial efforts to explore the practical and reasonable methods to measure the risk associated with HazMat transportation. Ang [91] suggested a general framework for risk analysis in transportation that decomposed the problem into three separate stages: (i) determination of an undesirable event (an accident involving the release of a hazardous material). (ii) estimation of the level of potential exposure, given the nature of the event and (iii) assessment of the magnitude of consequences (fatalities, injuries and property damage) given the level of exposure. These three stages produce one or more probability distributions, with the last two producing conditional distributions.

In practice, the process is seldom carried all the way through [53]. Frequently, the conditional probability distributions are ignored and the product of the probability of a release accident, and the extreme consequence of the accident, are used to estimate the risk. The potentially impacted population often represents the extreme



consequences. Abkowitz and Cheng [92] attempted to measure the risk of hazardous material transportation by summing the cost of fatalities, major injuries, minor injuries, and damage to property. The risk was expressed as a risk profile, which is a probability distribution of incident likelihood and severity. Purdy [29] estimated the impact to humans from flammable substances and toxic gases. The entire population that may be affected by a HazMat incident was considered in their model, including motorists on a road where an incident occurs, travelers on trains, and people who live near the transportation route [29]. Erkut and Verter [83] proposed that an assessment of HazMat transportation is a two-stage process that involves: (i) representation of risk via a quantitative model; and (ii) estimation of the model parameters. A basic model for risk assessment was presented in their work.

Kara et al. [93] pointed out that what differentiates HazMat transport models from other transport models is the explicit modeling of transport risk which usually consists of one or both of the following two factors: incident (i.e., spill, fire) probability and population impacted. They focused on modeling the incident probability and modeling the population exposure to quantify the risk along the transportation route [93]. Vayiokas and Pitsiava-Latinopoulou [84] developed a methodology for the risk assessment during road transportation of HazMat. Two critical factors have been taken into consideration: the probability of an outcome during incident occurrence and the consequences of the outcome. Theoretical risk source release model, exposure model, and consequence model were set up for the ultimate risk estimates [84, 93]. Fabiano et al. [94] developed a site-oriented framework of general applicability at local level. The evaluation of frequency took into account on one side inherent factors (e.g., slope, characteristics of neighborhood, etc.) and on the other side, factors correlated to the traffic conditions (e.g., dangerous goods trucks, etc.). The simple theoretical models were given to express both the incident frequency and the fatality number.

Rhyne [25] expressed the overall risk as obtained by summing over all scenarios; the scenario frequency computation usually is divided into three components: the accident frequency; the conditional probability of a release, given an accident; and the conditional probability of various consequence terms. The accident frequency starts with a value for accidents per mile and usually ends with accidents per year or



accidents per some unit of material delivered so that all analyses can be put on a common basis. The conditional probability of release may be subdivided into several components in the predictive approach or simply evaluated at this top level in the historical approach. The consequence analysis usually introduces some conditional probabilities into the frequency term, such as the probability that a certain meteorological condition exists, given that the accident has occurred. The terms in the mathematical formulation may vary with the specific analysis. The usual procedure for a quantitative transportation risk analysis is to divide the transport route into segments (also called links) along which the important parameters can be reasonably approximated by a single average value.

Ang and Briscoe [91] suggested a general framework for risk analysis in transportation, drawing heavily on the experience in the nuclear power industry. One of the key ideas in this approach is to break the problem into three separate stages: (i) determining the probability of an undesirable event (e.g., an accident involving release of hazardous material); (ii) determining the level of potential population and properly exposure, given the nature of the event; and (iii) estimating the magnitude of the consequences (i.e., fatalities, injuries and property damage), given the level of exposure. Although most hazardous materials incidents involve property damage only, it is the small but finite probability of a major disaster with multiple fatalities that attracts most of the attention in a risk analysis.

Conceptually, at least, each stage of the process described above, produces one or more consequences. These three types of distributions can then be combined to produce a resulting distribution of potential consequences from a specified activity. In practice, however, the process is seldom carried all the way through. A frequent shortcut is to compute only the expected value of each of the distributions, producing an "expected loss" as the measure of risk. In other cases, the sole focus is on the second stage, and population exposure to an assumed "worst case" event is used as the measure of risk, without regard for the likelihood of such an event, or the probability of various outcomes at a given exposure.



One method of summarizing a risk analysis is by using risk profile. The risk profile gives the probability of consequences that will exceed a given level. It is a multiple-measure method because it may produce varying probabilities of different levels of consequences, rather than a single measure such as "expected fatalities. For example, one study focused on six major types of potential events: corrosive or toxic liquid release, flammable liquid release, liquefied gas release, toxic gas release, asphyxiate gas release, and condensed phase explosion. For each type of event, probabilities of exceeding 1, 10 and 100 fatalities were estimated, as a means of creating a series of points along a risk profile as proposed by Considine et al. [95].

The U.S. Department of Transportation (USDOT) established a set of guidelines to be used in assessing the risks of transporting hazardous materials over specified routes. These guidelines have been used in several studies involving a variety of materials and sites. For example, Hobeika et al. [110] applied them to the movement of spent nuclear fuel between two power stations in Virginia for analyzing and developing evacuation plans around nuclear power stations. Kessler [97] performed a similar analysis for a wider variety of hazardous materials moving through the Dallas-Fort Worth metropolitan area in Texas. The work done for high-level nuclear wastes (spent fuel assemblies from commercial reactors) provides an example of risk analysis which includes a substantial effort on assessing risks that are associated with normal operations, rather than focusing only on incident-related risk. Cashwell et al. [96] provided an extensive report on risk analysis for transporting nuclear wastes, based on use of models developed at Sandia National Laboratories. This modeling takes a routing selection as input, and then assesses the level of risk to both workers and the public from movements along the route.

Unlike fixed HazMat facilities in which HazMat types, sources, and accident location conditions are all known, HazMat transportation risk assessment is associated with a road network and contains an element of uncertainty with regards to the expected location and condition of the accident site. The common approach to transportation risk analysis is to divide the HazMat route into portions where different parameters



can assume the same value. The average length of each route portion should be set according to the scope of the analysis and to the extent of accuracy and reliability of the available data. The smaller the portion, the greater the accuracy will be. However, this enhanced accuracy will lead to larger computational efforts. A review of various research topics associated with the transportation route, procedure for assessing risks from road transport and rail transport and how to obtain the minimum risk route of HazMat can be found in the related literatures [29, 48, 79, 83, 98-108].

Erkut and Verter [83] and Leonelli et al. [98] proposed that a path between a given origin-destination pair can be represented by a set of road segments, where the road characteristics are uniform within each segment. The risk imposed on an individual due to a HazMat shipment can be estimated as the probability of an incident during transport multiplied by the probability of the individual experiencing the consequence as a result of the incident. At the same year, Spadoni et al. [99] also proposed that the risk resulting from the transport of HazMat has to be calculated considering all the incidents occurring at any point of the road network, namely a set of linear source risk. The technique they used to perform linear source risk calculations is to divide each route into arcs, each then being considered as a point risk source. Next, a reassembling methodology has to be applied to perform calculations of indicators of the area risk [79, 99]. Bubbico et al. [100] proposed methodology allows an easy and rapid selection of the safest route for transporting dangerous substances by road. Depending on the scope of the analysis, approximate as well as detailed approaches to TRA can be used. The former could be kept as simple as possible, to carry out the analysis and to immediately use its results for a basic evaluation of the risk level for transport activity under consideration. The latter could be kept as accurate as possible, enabling a specialist to properly assess the risk, to investigate the presence of highly hazardous spots and to suggest effective mitigation measures. Bubbico et al. [100, 101, 103, 104] also proposed a simplified approach to TRA. From this approach only limited number of incident scenarios and release consequences need to be estimated in this simplified approach. Therefore, in this manner, TRA could be performed very rapidly to obtain the relevant risk measures, which can be used for a preliminary assessment of the case. Saccomanno and Chan [48] examined three strategies for routing of hazardous material shipments. These were: (i) minimize risk exposure, (ii)



minimize accident likelihood and (iii) minimize operating costs. Abkowitz and Chan [108] evaluated the use of five criteria for routing analysis: (i) minimize shipping distance, (ii) minimize travel time, (iii) minimize release-causing accident likelihood, (iv) minimize population exposure, and (v) minimize the product of accident likelihood and population. The first two criteria minimize economic cost, and the latter three maximize safety. The researchers found that routes that minimize risk may be so circuitous that they can be economically unfeasible, or at least impractical. His recommendation was that a routing analysis considers combinations of factors and use different weighting factors to evaluate trade-offs [48, 108].

Many risk models in the hazardous materials transport have used the concept of a danger zone. The assumption is that residents and workers inside a circle centered at the incident site, with a given impact radius, will experience the same undesirable consequence, and residents/workers outside this circle will experience no undesirable consequence. Although most researchers agree on the need to include risks in route selection for hazardous materials transport; they do not agree on how transport risk should be modeled.

Other prominent models include: traditional risk, population exposure, incident probability, perceived risk, and conditional risk. Some analysts use population exposure. Others multiply population exposure by the amount of material being shipped. Still others try to estimate the expected fatalities, injuries, environmental impacts, and dollar damages. When these latter measures are used, accident probabilities must be multiplied by conditional probabilities that other events will occur in succession (e.g. a catastrophic release given that an accident has occurred). The conditional risk model can be viewed as a multiplicative multi-attribute model, where the first attribute is traditional risk and the second attribute is incident probability.

## **2.7 Application of Geographic Information System in TRA**

According to Chang [111] a Geographic Information System (GIS) is a computer system for capturing, storing, querying, analyzing, and displaying geospatial data. This application also called geographically referenced data, geospatial data are data that describe both the locations and the characteristics of spatial features such as roads, land parcels, and vegetation stands on the earth surface.



In recent years GIS has been used for crime analysis, emergency planning, land records, market analysis, and transportation application. As for HAZMAT team GIS will performs search for optimum routes and provides navigation guidance to emergency vehicles for quickly reaching disaster sites. Its real-time traffic detection component acquires and up-dates dynamic traffic information such as route condition and traffic delays in real-time using various types of sensors.

Effective use of the GIS technology depends upon detailed knowledge of how real-world spatial objects and entities are represented. GIS supports three separate data models vector data, raster data and triangulated irregular networks (TINs). Vector data are represented with points, lines, or polygons. They can all be characterized by a series of  $X$ ,  $Y$  coordinate pairs. The representation of spatial data in a continuous coordinate space permits the closest approximation of the original spatial feature and thereby improves the accuracy of analysis. Therefore, the relationships among spatial entities are stored explicitly or can be computed when needed [112]. Raster data can either be a picture file, such as a bitmap file, or it can be a gridded data file represented with grids, where each cell in the grid has a particular value. TINs are particularly useful for surface representation and three-dimensional mapping. The data usually is stored in a file format called coverage or shape file. Individual coverage or theme can be displayed or removed depending on the intended application. Each of coverage is linked to an attribute table so that information is available on the individual features, or records, of the theme. The capacity to retain the spatial integrity of georeferenced data distinguishes a GIS from other computerized data management systems [113].

GIS software has integrated the algorithms into an analysis environment utilising a common spatial data model. The first phase of GIS development is exemplified by the development of analysis tools such as SYMAP (System of Map Analysis Package) and Map Algebra (Map Analysis Package) in the late 1960s and early 1970s at Laboratory of computer graphics and spatial analysis at Harvard Graduate School of Design. These early GIS packages were written for specific applications and required the mainframe computing systems found usually in government or university settings. In the 1970s, private vendors began offering off-the-shelf GIS packages.



M&S computing (later Intergraph) and Environmental Systems Research Institute (ESRI) emerged as the leading vendors of GIS software. In 1981, ESRI released Arc/Info, a standard package which ran on mainframe computers. As computing power increased and hardware prices plummeted in the 1980s, GIS became a viable technology for state and municipal planning. In 1992, ESRI released ArcView, a desktop mapping system with a graphical user interface that marked a major improvement in usability over Arc/Info's command-line interface. The GIS technology has extended to the current integration of topological data structures, and Relational Database Management System RDBMS such as ESRI's ARC/INFO and Intergraph's Modular GIS Environment (MGE). Virtually all GIS and image analysis software packages are sold with specific programming languages. Changes in the industry are supporting the need for knowledge of Visual Basic, VB.Net or other computer language, as it is the front end programming language for many software versions.

## **2.8 The Application of GIS for HAZMAT Transportation**

In order to perform an accurate TRA, the knowledge of territorial information of comparable accuracy is of paramount importance. Data for local distribution of population, incident rates, and weather conditions are gathered. Lepofsky et al. [109] have first proposed to integrate GIS into TRA to manage those kinds of information. GIS is a combination of computer software, hardware, and data that can be manipulates and to be analyzed, and presents information that is tied to a spatial location. GIS contain both geometry data (coordinates and topological information) and attribute data, i.e., information describing the properties of geometrical spatial objects such as points, lines, and areas.

In the work of Lepofsky et al. [109], GIS was employed to develop transportation networks that incorporate both physical and operational characteristics, and overlay these networks on other spatially referenced data. Fedra [114] proposed to employ GIS in the spatial TRA. GIS capable to map risks clearly and a powerful tool for risk assessment [113]. The integration of GIS and simulation models, together with the necessary databases and expert systems, within a common and interactive graphical



user interface could make for more powerful, easy-to-use and easy-to-understand risk information systems.

GIS is capable to become a central tool and user interface, databases of hazardous installations and hazardous chemicals which are linked in a hypertext structure. GIS application is also included as the tool for spatial risk assessment based on externally generated risk contours and it assist to describe the accidental and continuous atmospheric releases or toxic dispersions and transportation risk analysis.

## **2.9 The Application of GIS for Air Dispersion Consequences**

Atmospheric dispersion modelling is the mathematical simulation of how air pollutants disperse in the ambient atmosphere. It is performed with computer programs that solve the mathematical equations and algorithms which simulate the pollutant dispersion such as chlorine, ammonia and etc. Currently, there are five types of air dispersion models, which are normally used in computer simulations for calculating the effects of toxic gas dispersions [115]:

- *Gaussian model*: The Gaussian model is perhaps the oldest and the most accepted computational approach to calculate the concentration of a pollutant at a certain point. The origin of the Gaussian model is found in work by Sutton [116], Pasquill [117, 118], and Gifford [119, 120]. Gaussian models are most often used for predicting the dispersion of continuous, buoyant air pollution plumes originating from ground-level or elevated sources. Gaussian models may also be used for predicting the dispersion of non-continuous air pollution plumes (called *puff models*). A Gaussian model also assumes that one of the seven stability categories, together with wind speed, can be used to represent any atmospheric condition when it comes to calculating dispersion. There are several versions of the Gaussian plume model. A classic equation is the Pasquill-Gifford model. Pasquill [121] suggested that to estimate dispersion one should measure the horizontal and vertical fluctuation of the wind. Pasquill categorized the atmospheric turbulence into six stability classes named A, B, C, D, E and F with class A being the most unstable or most turbulent class, and class F the most stable or least turbulent class.



- *Lagrangian model:* a Lagrangian dispersion model mathematically follows pollution plume parcels (also called particles) as the parcels move in the atmosphere and they model the motion of the parcels as a random walk process. Lagrangian modelling well described by number of studies by Eliassen [122], Hanna [123] and Robert *et al.*, [124]. Lagrangian modelling is often used to cover longer time periods, up to years [125].
- *Box model:* The simplest approach to estimating pollutant concentrations over a given domain is to implement a single box model. As the name implies, the principle is to identify an area of the ground, usually rectangular, as the lower face of a cuboid which extends upward into the atmosphere [126]. Box models which assume uniform mixing throughout the volume of a three dimensional box are useful for estimating concentrations, especially for first approximations [127]. Box model is well discusses by Derwent *et al.*, [128] and Middleton [129, 130].
- *Eulerian model:* Eulerian dispersions model is similar to a Lagrangian model in that it also tracks the movement of a large number of pollution plume parcels as they move from their initial location. The most important difference between the two models is that the Eulerian model uses a fixed three-dimensional Cartesian grid.
- *Dense gas model:* Dense gas models simulate the dispersion of dense gas plumes (i.e., pollution plumes that are heavier than air). The most commonly used dense gas models are the DEGADIS model [131] developed by Dr. Jerry Havens and Dr. Tom Spicer at the University of Arkansas under commission by the US Coast Guard and the US Environmental Protection Agency.

By integrating air dispersion modelling as above, under GIS environment, the output of the pollutant records can be obtained in the form of spatial records. In the toxic dispersion impact model, it relationship to geographical data should be self evident. Thus, for more complex models that go beyond the classical Gaussian plume models,



topographic data, surface roughness, and surface temperatures are important input parameters [132]. The prediction of the magnitude of impacts is often undertaken by the application of simulation models [133]. The obtained result will most often be a map of the value of a given environmental descriptor (e.g., concentration of an air pollutant) at any location within the study area. The extension of environmental impacts can therefore be estimated from the spatial distribution of environmental quality values predicted for each alternative. Many models have been coupled with GIS in the past decade to simulate various environmental processes as described by Longley et al. [134].

In transportation risk analysis, the use of dispersion models were suggested by Zhang, et al [135] to incorporate route selection for HazMat transportation to find minimal risk paths on a network, while the Gaussian plume model is employed to model the air pollution dispersion. However, the analysis does not consider other parameters, such as accident rate, road tanker trip, traffic volume, and the sequence of the accident event, since an accident is normally propagated more than one incident outcomes.

The information on surrounding locations in the model is treated by adopting raster GIS framework. The raster framework transforms a continuous space into a discrete one by modeling it as a tessellation of square grid cells called pixels. Raster is commonly used to approximate continuous surfaces in GIS. Raster GIS are organized to a few number of layers, one assigned to each characteristic of interest. The traditional raster GIS overlay techniques were used to predict the spatial consequences of potential releases of airborne HazMat in a network.

Verter and Kara [136] set up a model to assess the total transport risk as well as the equity of its spatial distribution. They employed GIS to manage territorial information during the risk analysis of transportation network. A GIS-based model that was suitable for representing the HazMat transportation was constructed for Quebec and Ontario areas. Bubbico et al. [101, 104] which pointed out that the TRA tool developed based on the GIS approach allows risk assessment for various



transportation modes and permits to rapidly investigate possible benefits resulting from changes of routes.

## **2.10 Transportation Accident Trends Based on Available Accident Database**

Accident prevention and mitigation of consequences is the focus of a number of industry programmes and regulatory initiatives. There are two basic types of information; first is a database consisting of standardized fields of data usually for a large number of incidents and second is a database for a more detailed report on an individual incident. Analysis of these accident history databases can provide a better insight into accident prevention needs. While the analysis and conclusions obtained from the accident database is often limited by the shortcomings of the databases themselves, the fact remains that accident history databases are very useful and can be a powerful tool in focusing risk reduction efforts. The conclusions can be used to systematically identify the greatest risks to allow prioritization of efforts to improve process safety.

There are a number of major accident databases such as the Major Hazard Incidents Data Service (MHIDAS) [59], the Explosion Incidents Data Service (EIDAS) [64] and the Environmental Incidents Data Service (EnvIDAS) of the Safety and Reliability Directorate (SRD) [59, 64]; the Failure and Accident Technical Information System (FACTS) of TNO [57]; the Major Accident Reporting System (MARS) of the Commission of the European Communities (CEC) [58]; and World Offshore Accident Database (WOAD) of Veritas Offshore Technology [62] and many others.

Cannon and Bendell have developed an account of data banks and databases given in Reliability Data Banks [73]. As mentioned by Lees [64], Fragola [42] has reviewed reliability databases from a historical aspect, suggested the possible improvements of reliability database development [62]. So far, there are two main types of databases known as the incident database and the reliability database. The incident database does not have the inventory of items at risk and concentrates on the attributes and



development of the incidents. The information available is often limited to whatever is recorded at that particular time.

The reliability database may record the incidents better, and it treats them primarily as events from which statistical value on reliability, availability and maintainability can be derived [9]. Written report supported by graphics and photos are often published by various agencies and provided on governmental websites. There are also higher institutions and corporate organizations that compile the transportation hazardous incidents and publish them in their websites.

Since about 1996, the US Environmental Protection Agency (under the Chemical Emergency Preparedness and Prevention) has investigated and reported on many high profiles US chemical plant and refinery hazardous incident. As the result of these investigations, classifications of incidents have been developed [63] to assist in future investigation. Although there are many accident databases such as MHIDAS, MARS, NSTB, IChemE accident database, Unep/Apell/disaster etc. Perhaps, FACTS online database was the best major hazard online database for analyzing of accidents in the transportation of hazardous material study due to several reasons such as the information contained in FACTS is generally more complete and according to study requirement, compare from other databases and it is well structured for analyzing trends and obtaining general statistics. The abstracts are very accessible, so that even the most complex accidents are easy to comprehend as shown in Table (2-4), for comparison of major hazard online database basis.

According to the previous case studies from MHIDAS (Major Hazard Incident Data Service) database, [74] majority of HAZMAT transportation accidents occurred in a highly populated area (66%) compared to low populated areas (12%) and rural areas (22%) [137]. This trend is similar to the percentage obtained by other authors (Cheng Beng et al. [102], Planas et al [138], and the percentage have increased during the last decades as reported by Godoy et al. [139]. In the tunnels, the accident may develop differently and their consequences are very different from open-air route accident.



Table 2- 4: shows selected list of major accident database

| Name of accident database                                 | Developer  | Contents/ Features / Source of information  | Applications  |
|---|--|---|---|
| Failure and Accident Technical Information System (FACTS) | TNO, Netherlands   | <ul style="list-style-type: none"> <li>i) Contains more than 23,000 accidents records.</li> <li>ii) Gathered the information about near-misses, minor accidents and major accidents associated with hazardous materials (with tutorial on how to use the database)</li> <li>iii) The accidents are coded in abstracts making the existing data suitable for risk analysis, risk management, damage prevention and statistics. The abstracts are very accessible, so that even the most complex accidents are easy to comprehend.</li> <li>iv) Features of the database are a schedule of accident attributes and values and a hierarchical keyword structure. Another structure is the cause classification in which the course of the accident is translated into a sequence of occurrences.</li> <li>v) The information is often obtained from professional sources, such as accident reports made by companies, government agencies or from publications in technical periodicals and other literature. (Have free sample for unlicensed users of about ~ 80 records)</li> </ul> | <ul style="list-style-type: none"> <li>(i) Analysis of the role of instrumentation in accidents;</li> <li>(ii) analysis of incorrect human response and (iii) compilation of a reference book to trace incident causes (the Cause Book), giving a survey of incident causes which can occur in a large number of systems and operations. (Can perform statistical analysis according to specific circumstances, for each specific event). Application not for:- Nuclear materials and military activity are excluded</li> </ul> |
| Major Hazard Incidents Data Service (MHIDAS)              | Safety and Reliability (SRD)/ AEA Technology, UK Health Safety Executive | <ul style="list-style-type: none"> <li>i) Database was established in 1985</li> <li>ii) Contains coded information on reports of some 11,000 major accidents which are in the public domain. The database is updated quarterly and is available to users via various media including compact disc and internet.</li> <li>iii) Contains incident from over 95 countries throughout the world, particularly USA, UK, Canada, France, Germany and India.</li> <li>iv) No tutorial, and user guide on how to use the database</li> <li>v) No free sample of MHIDAS accident database and not free access.</li> </ul>  | Provide comprehensive accident database, involving the transportation, storage and processing of hazardous materials, which considered had the potential to cause off-site impact. Incidents which incurred casualties, required evacuation of either on-site or off-site personnel or caused damage to property or the natural environment, together with incidents. Application not for:-Types of incidents, involving radioactive materials for example, are specifically excluded from the database                         |
| Major Accident Reporting System (MARS)                    | European Union's, Major Accident Hazard Bureau (MAHB), Ispra, Italy      | <ul style="list-style-type: none"> <li>i) It is a hybrid between a database and a report-based system. The data is structured it contains extensive text descriptions of the incidents. In accordance with the call of the "Seveso II Directive" for a more open access to information on major accident hazards</li> <li>ii) Currently about 450 cases available to the public.</li> </ul>   | The Major Accident Reporting System (MARS) was established to handle the information on 'major accidents submitted by Member States of the European Union to the European Commission in accordance with the provisions of the 'Seveso Directive'  |

**Notes:** other major accident database: - a) UNITED NATIONS ENVIRONMENT PROGRAMME Industry and Environment Center (UNEP IE) This site contains the chemical accident database, APELL, compiled from various government sources by UNEP. b) Department of Transportation (DOT) \_Hazardous Material Incident Reporting System (HMIRS) This reporting system includes all modes of transportation except pipelines. c) Center for Chemical Process Safety (CCPS), maintains a private database. Only members that contribute incidents to the database are allowed to view the data. d) IChemE accident database covers accident of all sizes. The database contains over 12,000 records.



## **2.11 Smart Advisory System in HazMat TRA**

Recently, there have been quite a number of research studies related to the safety aspects of hazardous materials transportation which have shown that the transport of hazardous materials to and from factories plays an important role in determining the overall risk to an area. However, most of these research studies, concentrate mainly on the following areas: alternative HAZMAT routes [6, 98, 99, 102, 103, 141], risk assessment methodologies [143-145], dispersion and probabilistic models [100-107, 142, 146-148], and studies on transport guidelines and criteria.

Thus, in this section, the existing literatures are reviewed to assess risks from transportation of hazardous material by utilising smart advisory system (decision support system). Since historical evidence has shown that incidents due to hazardous materials (HazMat) releases during transportation can lead to severe consequences, the public and some agencies such as the Department of Transportation (DOT) express concern with regard to hazard associated with HazMat transportation. Many hazards can be identified, controlled or eliminated through use of risk analysis. The assessment of the hazard related to transportation of dangerous goods is a reasonable basis for any policy of risk management and reduction.

Spadoni et al. [99] reported that most of the features of risk assessment in transport networks are complex and a long computing time is required, compared to fixed plant risk assessment. An accident might occur at any point along the way, so that the analyst has to simulate at a different traveling accident point by considering linear risk source equivalent to a great number of point risk sources. In summary, when the risk sources are moving: this means that most of the parameters involved such as meteorological conditions, wind direction, population density and etc, change along the itinerary. This problem create a great obstacle to the wider use of TRA, therefore the need to limit the calculation burden imposes the need for the use of simplify assumptions and a fast running computer facility [98, 99]. Bubbico et al. [98,141] have also addressed and highlighted similar points of consequences and its uncertainties due to the applications of TRA methodology to determine the hazard represented by transportation of hazardous material [141]. Transportation Risk Analysis (TRA) presents in computer-aided approach is a powerful tool in HazMat



transportation decision support system. It is helpful in choosing alternate route/s by providing information on risks associated with each route, and in selecting appropriate risk reduction alternatives by demonstrating the effectiveness of various alternatives.

Spadoni et al [27, 145] used a computer program to assess transportation of hazardous material based on numerical procedure which overcomes the difficulties outlined from manual scrutiny calculations to evaluate risk levels and to test the suitability of alternatives choices using valid acceptability criteria in quantifying risk arising from road transport of either flammable or toxic substances [8,99]. Bubbico et al [28, 141] proposed TrHazGis as an integrated computer aided program approach, based on GIS Arcview 3.1 Map Risk software to TRA. The proposed program TrHazGis successfully perform more accurate risk estimates, substantial reduce the time required to perform the analysis, a simplification of the data input step, and able to display the result on the area map [141].

Chee Beng G. et al. [102] developed a methodology for the risk analysis of road transportation of hazardous chemicals (LPG) in Singapore. In these studies, the researchers used PHAST (Process Hazard Analysis Software Tools) version 4.1 to evaluate the fatality zone for each of the identified hazards for the various zones of the route. The calculations for the likelihood of release, and estimating event of the event frequencies were done via manual calculations. A group of researchers at Lawrence Livermore National Laboratory (LLNL), California State University have developed software tools for estimating the risk associated with truck and rail transport of hazardous cargos [149]. The software has been developed in conjunction with commercially available. S.M. Godoy et al.[139] have developed a software name STRAPP (Stochastic Toxic Release Risk Assessment Package) for risk assessment and emergency planning (safe distance calculation). STRAPP used Monte Carlo modeling approach in order to improve the system capabilities, for risk calculation of particulate matter diffusion and hazardous gas diffusion of light, neutral and heavy gases. STRAPP used DEGADIS software to present the Gaussian modified diffusion dispersion model. Godoy et al. [139] did not considered fire and explosions model in their research work.



Abkowitz and Associates, Inc. [150] in association with Vanderbilt University developed multimodal of hazardous materials management transport risk tool. The software is an integrated system database, map analysis modules and management reporting by identifying high-risk operation, evaluating risk reduction alternatives and emergency planning.

Other popular software models are CASRAM, Chemical Accident Stochastic Risk Assessment Model (Argonne National Laboratories, 2005), FIREPLUME, to predict consequences of toxic chemicals released from a vehicle fire that burns the hazardous material cargo (Argonne National Laboratories, 2005), SPILL, to estimate transient (including two-phased) release from a pressurized vessel (Oakridge National Laboratories, 2005), HEGADAS, to estimate the consequences of steady state or transient release of dense vapor, and to help to predict near-field and far-field consequences (Oakridge National Laboratories, 2005). These models have been used by United States Department of Transportation for carrying out risk assessment studies (Argonne National Laboratories, 2005; Oakridge National Laboratories, 2005) [150, 151].

Arthur Little Inc. [64] has developed transportation Risk Screening Model (ADLTRS) as a tool for determining risk to people and environment posed via chemical transportation operations. The program offers Microsoft PC and DOS 3 and greater based tools to evaluate and categorize the risks associated with differences between chemicals, transportation modes and routes. It offers rankings that can be used for a large number of movements. Easy-to-use techniques consider the chemical, transport mode, container type, distance, route characteristics and annual volume. Final results are placed in risk categories to establish relative ranking. Technica, Inc., Software Products Division has developed (SAFETI) software, which is an integrated set of computer programs designed to automate the risk assessment of chemical and petrochemical facilities involving the manufacture, storage, and transport of toxic and flammable materials.

The consequences calculation of possible accidental releases and their impact based on event frequency to produce measures of risk such as Risk Contour Plots and FN



curves. SAFETI is basically composed by DOS3.3 and higher, Math Microprocessor [5, 6, 152]. Yuanhua et al. developed decision support system of quantitative risk assessment for transportation hazardous material used fuzzy logic programming, CANARY software for consequences modeling, and GIS [152, 153]. Leonelli et al developed TRAT2 [27] software for the evaluation of hazardous materials transportation risk. TRAT2 is basically composed by tree executable codes (written in C++ and FORTRAN languages) and Microsoft access database to which communicate through direct access libraries. Based on the above mentioned, most of the research studies have shown that the analyses of transportation risk are depending on the availability of data/databases, commercially available software, and expert knowledge.

Abkowitz et al. [154] carried out a study on the use of GIS in managing hazardous materials, and have found that GIS is ideally suited for minimum path identification and risk computations, because it allows the integration of the transportation system with the environment. Saccomano et al. [155] presented an interactive model for routing transportation of dangerous goods through an urban road network. The model computes minimum risk routes based on each segment origin and destination, where risk is estimated considering accident rates, spill probability, spill impact area and population exposed. Many techniques have been proposed for solving multi-objective vehicle routing and scheduling problems. There are 3 main categories:-

- *Scalar Method*- These methods use mathematical transformation, like weighted linear aggregation. They have some disadvantages, like the difficulty of eliciting the weights and the facts that they may not be able to find all the Pareto optimal solutions. However, these techniques are quite simple to implement and can be used with any of the single-objective heuristics described in literature.
- *Pareto Methods*- These methods apply the notion of pareto dominance to evaluate solutions or to compare solutions. This concept is frequently used within evolutionary algorithms, and is becoming more popular.



- *Non-scalar and non-pareto algorithms*-These methods, which often consider the different objectives separately

Table 2-5 shows the routing management for hazardous materials transportation. Most of the researchers use GIS as a tool to map the location with several attributes within the origin to destination of the shipment. In 1994 the Sandia National Laboratory produces a software name MOSA (multi-objective spatial Analysis) [157]. As refer to Pawnhar et al. [156], they have explained the application of MOSA and RISKCHEM to demonstrate the analysis and to evaluate the consequences of hazmat risk after accident. The researchers such as Spadoni et al. [27, 44, 159, 160], Bubbico et al. [28, 141,142] have developed new software in order to enhance the previous software weaknesses. The development of ARIPAR-GIS software in year of 1990 for risk assessment which has some limitation of application forces the researcher to enhance the software application by producing TRAT2 [158]. TRAT2 provide the user with greater application in global risk assessment for HazMat transportation. With collaboration with researchers from Pisa University the main result is a standardized approach should be developed for the release characterization and the consequence assessment in quantitative hazardous material transportation risk analysis, in order to obtain significant and consistent values of the different risk indexes to be really useful for risk comparison and decision-making. The limitations of ARIPAR-GIS software encouraged the development of OPTIPATH software [159-160]. OPTIPATH determine alternative paths, whose risk values are lower than those of the routes usually chosen by drivers on the basis of economical and practical considerations. The OPTIPATH procedure is a risk-based routing methodology, which performs the evaluation of these alternative paths. It determines the flow of each chemical on each arc so as to send all trucks from their origin to destination while minimizing the total cost of transport and honoring risk acceptability criteria. Acknowledges by Scenna et al. [161] the awareness of dispersion of hazmat also develop the STRRAP software and its capability has been improved year by year. This tool is based on a method which lets the handling of stochastic uncertainty of atmospheric parameters, critical when calculating risk, especially when hazardous gases or particulate matter diffusions occur as a result of an accidental release or emission. The development of new



software for routing management nowadays helps most logistics company in reducing cost.

The product from ESRI which is Arc Logistics allows users to specify a route renewal point at any number of user specified locations. Arc Logistics Route solver functionality includes an advanced routing and scheduling algorithm that has proven itself in deployments across numerous industries. The benefits of Arc Logistics Route extend beyond calculating routes and being able to accommodate "normal" situations. Logistics management is seldom routine, and the assurance of having a robust and tested solver functionality will save time and money and conserve resources when demands are high. The Arc Logistics Route solver functionality accommodates a wide range of routing and scheduling problems. Lue and Colorni [162], explained the capability of DSS as a support system for hazardous material transport can be divide into two which are i. public decision making and ii. vehicle guidance. The development of software for routing management and risk analysis in supporting GIS for hazmat transportation is very important to ensure the safe condition for all. The different of location, type of product and populations make the necessary of enhancement of software as a decision support system to work in more precise and effective.



Table 2-5: Software and their features involved in chemical transportation risk analysis and routing management.

| Name of the software | Name of the establishment        | Available since | Routing Management | Risk Prediction | GIS | Method |        |                           | Coding language     | Hardware requirement  | Website address/Reference   |
|----------------------|----------------------------------|-----------------|--------------------|-----------------|-----|--------|--------|---------------------------|---------------------|---|---|
|                      |                                  |                 |                    |                 |     | Scalar | Pareto | Non-scalar/<br>non pareto |                     |   |   |
| MOSA                 | Sandia National Lab.             | 1995            | Yes                | No              | Yes | Yes    | No     | No                        |                     |   | <a href="http://www.sandia.gov">http://www.sandia.gov</a>   |
| MOLP                 | Sandia National Lab              | 1994            | Yes                | No              | No  |        |        |                           | C++                 |   |   |
| MPATHav              | Sandia National Lab.             | 1995            | Yes                | No              | Yes | No     | Yes    | No                        | C++                 |   | <a href="http://www.iaea.org/inis/collection/NCLCollectionStore/_Public/27/041/27041399.pdf">http://www.iaea.org/inis/collection/NCLCollectionStore/_Public/27/041/27041399.pdf</a>                                     |
| RISKCHEM             | Argonne National Lab.            | 1996            | No                 | Yes             | No  | No     | No     | No                        |                     |   | <a href="http://www.anl.gov/techtransfer/Available_Technologies/Transportation/transportation_portfolios.html">http://www.anl.gov/techtransfer/Available_Technologies/Transportation/transportation_portfolios.html</a> |
| TRAGIS               | The Oak Ridge National Lab.      | 2000            | Yes                | No              | Yes | No     | Yes    | No                        |                     | Microsoft Windows 32-bit  | <a href="http://www.ornl.gov/~webworks/cpr/v823/rpt/106749.pdf">http://www.ornl.gov/~webworks/cpr/v823/rpt/106749.pdf</a>   |
| ArcGIS 8.1           | ESRI                             | 2002            | Yes                |                 | Yes | No     | Yes    | No                        |                     | Windows 98  | <a href="http://www.esri.com/library/whitepapers/pdfs/arcgis_8.1.pdf">http://www.esri.com/library/whitepapers/pdfs/arcgis_8.1.pdf</a>   |
| Arc Logistics        | ESRI                             | 2004            | Yes                | No              | Yes | No     | Yes    | No                        |                     | Windows 98, Windows ME, Windows NT 4.0 with service pack 3, Windows 2000, and Windows XP. | <a href="http://www.esri.com/library/whitepapers/pdfs/alr-complete-rs-solution.pdf">http://www.esri.com/library/whitepapers/pdfs/alr-complete-rs-solution.pdf</a>   |
| STRAPP               | Godoy, Csenna & Santa Cruz       | 2007            | No                 | Yes             | No  | No     | No     | No                        | FORTRAN 90, DEGADIS | Windows 2000 and Windows XP.  | <a href="http://www.sciencedirect.com/science/article/pii/S0951832006000822">http://www.sciencedirect.com/science/article/pii/S0951832006000822</a>   |
| DSS                  | Alessandro Lue & Alberto Colorni | 2008            | Yes                | No              | Yes | Yes    | No     | No                        |                     |   | <a href="http://www.esri.com/library/whitepapers/pdfs/arcgis_8.1.pdf">http://www.esri.com/library/whitepapers/pdfs/arcgis_8.1.pdf</a>   |
| TriHazGis            | Bubbico et al                    | 2000            | Yes                | Yes             | Yes |        |        |                           | C++/Arc view 3.1    | Microsoft Windows 32-bit  |   |
| ADLTRS               | Arthur Little Inc.               |                 | Yes                | Yes             | Yes |        |        |                           |                     |   |   |
| TRAT 2               | Spadoni et al.                   | 2007            | Yes                | Yes             | Yes |        |        |                           | C++/FORTRAN         |   | <a href="http://www.springerlink.com/content/g2w0351504026452/">http://www.springerlink.com/content/g2w0351504026452/</a>   |
| OPTIPATH             | Erkut et al.                     | 2008            | Yes                | No              | Yes |        |        |                           |                     |   |   |

Continued to the next page



|            |                |      |     |     |     |  |  |  |  |  |  |
|------------|----------------|------|-----|-----|-----|--|--|--|--|--|--|
| ARIPAR-GIS | Spadoni et al. | 1990 | Yes | Yes | Yes |  |  |  |  |  |  |
|------------|----------------|------|-----|-----|-----|--|--|--|--|--|--|



## **2.12 Discussions Analysis for Proposed A Smart Advisory System of Hazardous Materials Transportation Risk Analysis Based on Malaysia Scenario.**

A thorough analysis was made as discussed in previous section in Chapter 2 on the current worldwide development and practice of Smart Advisory System (SAS) for hazardous materials transportation risk analysis; therefore it can be adopted into Malaysia scenario. Since the development of SAS for Hazmat TRA is dependent on the type of TRA model which is being used, therefore a careful analysis must be undertaken on the existing TRA model before it can be applied and programmed in SAS. The TRA may need to be modified and upgraded before it can be applied into the SAS. The correct selection of TRA software is vital, since the result of risk analysis for safest route for a HazMat transportation from a road network can be generated. The correct and reliable TRA software is also vital since the risk points which are need to be analyzed along the route are enormous and furthermore each HazMat carries a different level of consequences. Due to the differences in consequences, different model consequences are utilized for accident scenario involving fire, explosion and toxic release. Scenario can become more complicated if the collision involving more than 2 trucks which are transporting different hazardous material. In section 2.9, it is stated that there are few available software which are used in TRA model, however there are some limitation in the TRA software, such as DEGADIS (Fortran 90) which is used in STRAPP can only recognize the safe distance calculation for truck tanker which carry toxic release dispersion impact with no ignition such as chlorine, therefore it is not suitable for the fire and explosion cases. Meanwhile due to its chemical characteristics, chlorine has a potential to create an incident similar to UVCE incident especially if the ignition source spark within the chlorine zone release area. Therefore in this research, the aim is to develop a suitable SAS which is capable to analyze the impact of HazMat transportation accident according to Malaysia scenario. The proposed TRA model which is programmed into SAS must approximate to the actual HazMat risk on the road. Consideration on few factors will be discussed further in subsection 2.10.1 and 2.10.2 according to objective in Chapter 1.



### **2.12.1 Analisis from the existing TRA model of hazardous materials**

In Malaysia unfortunately, there is no TRA guideline available for reference. Therefore, the existing TRA guidelines have been reviewed, analyzed and modified before they are utilized in Malaysia as a guideline for hazardous materials transportation.

In this study, several major TRA guidelines were reviewed such as Center for Chemical Process Safety (CCPS), Risk Assessment Subcommittee (RASC) [11, 20-22, 25, 32, 33], Health Safety and Executive United Kingdom (HSEUK) for the assessment of societal risk for the road transportation of hazardous chemicals [8], Swiss federal Office for Environmental Protection, Forestry and Landscape (BUWAL) [32, 73] and others published TRA researchers work such as Rhyne [25], Leonelli et al. [44, 98], Spadoni et al. [99] and Bubbico et al. [100, 101, 103, 104, 141].

In order to recognize a suitable TRA guideline, all mathematical models in TRA analysis as in CCPS of the AIChE [11, 19-22], BUWAL [73] and other guidelines [25, 167] were reviewed. The review was done for the assumptions, parameters and definitions which were utilized in those TRA models. Subsequently, the possibilities, data and parameters which were required for the proposed model were recognized. Every changes made onto the proposed model were ensured that they did not alter the original objective of the particular model that is going to be developed. After the thorough review of the previous guidelines and TRA studies, few factors were considered for development of Malaysia TRA model;

- CCPS [21, 22], Rhyne [25] and BUWAL [73] methodology has introduced its owned method in determining the frequency of incident scenario. In CCPS [21], the formula model of frequency of incident scenario included trips per year. Every trips delivery is counted to get the average probability of accident rate to occur. The road is segmented less than one mile for suburban and urban area and longer than one mile for rural area or no settlement to define better potential accident rate along the route taken. The type of accident occurs such as collision, obstruction, and truck speeding also is take into account to



analyze the impact to human and surrounding areas and to verify the result of hole sizes gained from the impact. The length and number of release location zone, probability of wind blows direction and probability of fatality at the affected zone track are also introduced as the longer the track the higher the rate of accident. Thus, data of accurate route length, wind direction are needed in order to avoid uncertainty.

- While BUWAL [73] is proposing alternative way in identifying the frequency of accident rate by introducing parameter likes yearly number of accident goods. This parameter is used to estimate the number of transporting dangerous goods by dividing the annually transported quantity of dangerous good by the average of the road tanker. Probability of damages is also suggested by assuming that all materials relevant for a representative incident scenario are transported more or less in similar quantities and containers, so that a uniform release and ignition rate are introduced in the case of burning and explosion. The rate of release and ignition values is determined from the collected information sources and Swiss data. The Accident Rate of the total traffic (*ART*) is calculated according to Swiss VSS-directive, (1990). The accident rates of Runway Road Corresponding categories (highways; semi-highways; around roads (outside Localities) and main roads (inside and Federal)) are selected from the data as listed in the table (2-3). However, logically every accident that occurs at any point does not have the same accident rate. Therefore, the accident rate for different highway; semi-highway and mains road must have different value no matter in any place whatsoever. Thus, the accident rate value from Swiss VSS-directive can not be used in determine the transportation risk analysis at Malaysia.
- Rhyne [25] methodology used probability as a weightage value to estimate such as population distribution, meteorological condition, that the accident may occur from value 0 until 1. The worse accident may have high value of probability. However, probability factors indicator are not easily quantified, such as the presence of schools, very high building offices and hospitals that are not easily evacuated, the presence of reservoir at accident residential area (explosion might be can caused flooding as secondary or tertiary impact).



- Meanwhile, the difference in the CCPS-TRA methodology compared with other methods, CCPS complete extensive use of parameters for example length of release some of of LPG from the starting point until to the location of the accident. This length of road is introduced in calculation to find the accurate the rate accident before the gas release, the longer the track the higher the rate of accident. Thus the length of the release location is needed to avoid uncertainty. Probability of a fatality accident at the accident location are accounted for in accordance with wind direction and release location of hazardous material. If wind direction heading to high population, so the fatalities may higher. Therefore, road transportation can be divided into two segments which is urban and suburban areas. Urban areas may has the higher population compared to suburban areas, so this situation may affect fatality at some location. Moreover in CCPS the consequences area is calculated based on established models for fire, explosion, toxic gases as in CPQRA [11]. This consequences calculation method is much more better compared to BUWAL and Rhyne methodology. For instance, in BUWAL methodology, gasoline is used as the reference substance in all type of fire incident cases, LPG represents any explosion incident cases while chlorine and ammonia represent any toxic release cases in the RRI and RSS calculations as in Eq. (2-2). Thus the above assumptions create more uncertainty in the risk result calculation. Meanwhile in Rhyne [25] methodology the severity of consequences accident is based on probability value (according to numerical evaluation of truck accident scenario frequencies from selected state route in United State of America)
- The accident rate for CCPS is counting per segmented of mile while BUWAL in a measurement of kilometer. It should be no problem with the unit conversion. But, mathematically 1 mile give 1.6 km which is ideally 1 km per segmented will result better risk assessment of multiple ring display in GIS programming.
- Since transportation accident is unpredictable therefore it can occur at any time, any location and without warning. This situation will made the



calculations of consequences from the accident can become more complex since some parameters such as atmospheric stability class distributions, the ambient temperature and humidity (which are dominant contributors in the TRA analysis), are changing along the route. For example, to estimate the probability that wind blows in the direction concerns during HazMat transportation as in Eq. (2-10), the meteorological conditions such as wind direction must be determined from 16 probability of wind directions based on their weight age ratio; N, NNE, NE, ENE, E, ESE, SE, SSE, S, SSW, SW, WSW, W, WNW, NW and NNW.

- The severity of injury or damage caused by the release of hazardous materials depends on the number and the nature of population distribution surrounding the area. In the TRA model the injury, fatality, or damaged caused by the release of chemicals are difficult to be estimated due to population distribution (density) constantly changes along the selected route. Therefore, the calculation to estimate the population density as in Eq. (2-11) and the probability of fatality as in Eq. (2-12), should be repeated at every point of the road segment.

Spadoni et al. [99] and Bubbico et al. [28, 101, 141, 142] had simplified the calculation in the developed guidelines of Center for Chemical Process Safety of American Institute of Chemical Engineers [19-22] and proposed the application of GIS technology, in order to overcome the variation of the population density changes along the road. However those methodologies have a constraint on their capability to extract data (available data) such as accident rate, traffic volume or knowledge of territorial information of the selected route transportation from relevant organization due to their limited computer hardware capability.

- In reality, the population and environment closer to the source of an event is expected to experience more severe consequences than those farther than it. As the distance from the event increases, the consequences of such an event decreases. Thus the assumption of uniform distribution across the impact area used as in Eq. (2-10) – Eq. (2-12) in CCPS [21, 22], as in Eq. (2-8) in Rhyne



[25], and as in Eq. (2-2) – Eq. (2-4) in Swiss risk methodology (BUWAL) [73] may not correctly represent actual condition and may lead to a misrepresentation of risk.

- Based on the assumptions in CCPS guidelines [11, 21, 22] as reported in section 2.6, the individual risk,  $IR_{x,y}$  (chances per year), is defined as the probability that an individual will die or injured by the consequences of the transportation hazard at a specific geographical location, within each portion of route can be expressed as in Eq. (2-10). Equation (2-10) permits the estimation of how individual risk changes with variable distance from the route. According to CCPS guidelines [11, 21, 22], the value of  $P_{i,j,k}$  will be equal to 0, if the hazard does not reach location  $x, y$ . Therefore the term of  $P_{i,j,k}$  will be equal to the likelihood of the incident outcome multiplied by the chance of fatality at a given exposure to the hazardous outcome. Since researchers such as Spadoni et al. [99] and Bubbico et al. [141, 142] and guideline of Center for Chemical Process Safety of American Institute of Chemical Engineers [19-22] define the individual risk as the risk to a person in the vicinity of a hazard and includes the nature of the injury to the individual, the likelihood of the injury occurring and the time period over which the injury might occur. However, the use of injuries as a basis for risk evaluation, are very limited to the data available on the level of injuries. Therefore, none of the TRA technique publication and software of risk analysis have introduced problems associated with the degree of injury in comparison to different types of injuries (such as thermal radiation effects vs. explosion effects vs. toxic effects).
- It is realised that when different probit equations are used to estimate diverse consequences (for example, first-degree burns, second-degree burns, or lethality) on a given population, different categories will overlapped. Thus, all those individuals suffering second-degree burns will appear to have also suffered first-degree burns, and all those individuals who die due to thermal radiation will also have suffered second-degree burns. As a result, the percentage of people that can be affected by the accident will become more than 100%. Therefore to avoid doublecounting, the overall damage



probabilities must be equal to 1.0. Based on software risk analysis results, none of risk analysis software have been reported considered on this matter in the calculation [66, 182]

- Severity resulted from a thermal radiation affects the survival ability of a victim. However, existing research were still contain many loopholes as few important factors are not considered such as age, total body burn surface area, type of fabric respond to a particular incident flux, antibiotics and etc. This explains why many death records showed up after few days after the actual event happened. The absence of this factor reduces the accuracy of a risk analysis during transportation.
- For the thermal effects calculation, some researchers such as Bull et al. [163-165] and Curreri et al. [166] have studied thermal radiation impact accident, and demonstrating the relationship between mortality and probits. So far the first application of probit analysis to human mortality was proposed by Bull [164]. Bull [164] works is very relevance to reality since he applied the analysis to burn injury mortality data. According to Bull [164], in the majority of cases, the exact diagnosis of burn depth injury was often very difficult, and subject to healing stages revision, presence of infection and likely to vary with the judgement of different clinicians. Therefore, Bull has reviewed his mortality analyses several times since 1949 and finally successfully published his 'burn injury probability' chart [165]. Bull 's chart showed strong relationship between percentages of the total body surface area (TBS) burned and age with mortality. For instance, an injurious dose death relationship with a marked age effect such as elderly patients suffers a higher mortality for a given severity of injury. However, all of Bull [163-165], findings were not applied in the TRA risk software analysis such as TriHazGis [141], TRAT2 [159], since most of the researchers such Bubbico et. al [141-142], Spadoni et. al [159] are more comfort to programmed the existing TRA by using CCPS [21] and Rhyne [25].
- The effect model assesses the consequence from hazardous incidents in CCPS [21]. The damage caused to the vulnerable receptor in terms of injury, fatality,



level of burns and structural damage are dependent on the intensity of the impact experienced by a person, structures and the exposure duration. However, the probit table in CCPS [11], is unable to predict probit value which has a conversion less than 1%, and the percentage result is not in decimal point at the range of 1% to 99%. Furthermore, there is difficult to introduce data from figures and tables into a computer code.

- Accident rates are the most important components of a truck (HAZMAT) tanker risk analysis. Generally, the rate is affected by numerous parameters such as road conditions, environmental, trucking operation, types of road (urban, sub urban, rural and remote routes area). However, most of the truck tanker risk analyses are normally based on accident rates characteristic of broad classes of route types for which useful data are available [11, 20-22, 25, 100, 101, 103, 104, 141]. Since the work of Radin[169] has been the foundation of the Malaysian road accident analysis, thus his work and MIROS will be considered as the basis for the study.
- TRA model required a lot of data access. However, the data access has become more complicated since it may involve multi- agency and some informations are difficult to be gathered since they are depending on the efficiency of that particular department or organization in collecting, extracting, recording and updating their data. Therefore an efficient and accessible method of data storage also important since it can facilitate TRA analysis.
- With the previous computer hardware, there is difficult to extract information, data or database in relation to TRA in order to obtain result for the risk analysis such as low speed or memory. However this problem has been overcome after the discovery of computer processor technology, such as i7 technology millennium, which evolved from i5, i3, Core 2 Duo and become more efficient to upload more data and capable to read various data format [141, 142]. Unfortunately the current development of TRA analysis software which has developed is not in parallel with the development of the computer hardware. This is due to some of the version of TRA software is not upgraded



to be capable of converting and using directly the data format from available databases such as geo-data.

- It is recognized that the TRA method which has been used in TRA software are still the same for instance, even though Health Safety Executive (HSE) of United Kingdom [24, 54] has produced many independent review guidelines to improved risk analysis for societal and individual in reference to the Control of Major Hazard Installations Regulations 1999 (COMAH), the improvement only noted on the approaches, assumptions, methods and models used by HSE. This is also observed for the UK Chemical Industries Association (CIA), IChemE, UK and the UK Petroleum Industries Association (UKPIA). Therefore an updated development and an efficient designed TRA software technology are required for implementations which comply with recent guidelines review. The impact of above matter will lead to the minimization of loophole in the chain of TRA methodology development and TRA software technology development at implementation level.
- Most of the softwares that have been used by enforcement and research agencies in Malaysia such as Riskplot, Phast, Safeti, ALOHA, FRED in detailed Environmental Impact Assessment (EIA) study which involved hazardous materials installation, mainly focus on a fixed facility cases or pipeline of LNG. Based on the discussion with Department of Environment (DOE) Malaysia and analysis of Detailed Environmental Impact Assessment (DEIA) reports which was sent to DOE for licenses approval, it is concluded that none of TRA analysis software which have been used since EIA regulation 1989 has been enforced under the Environmental Quality Act law 1974 in Malaysia [168].

### **2.12.2 Requirement to develop and design proposed SAS for hazardous materials transportation**

Based on the above reasons and previous discussion in Chapter 2, a review on available guidelines and modification of TRA model were undertaken to fulfill the criteria for cases of transportation accident scenario in Malaysia as follows:



- The GIS technology will be applied to TRA, which capable to analyze the size, composition, distribution and change in population along the route. Moreover, GIS is a powerful tool for displaying and analyzing data during the planning, scoping, and problem formulation phases, during the exposure assessment, and displaying and evaluating the results of the risk characterization in tables and maps
- To facilitate the data and database access for Hazmat analysis requirement, it is noted that some organization and department in Malaysia are practicing online data access for humidity, temperature, wind speed, accident rate and land use. For example MIROS, had recorded data of death from the accident and other related safety issues and on road traffic accidents and if the data are not available in the database, the data could be determined via MIROS published mathematical model [169-171] which is commonly used for estimating accident rate from a particular route. Data from CCPS and other resources can be utilized if it is not available in Malaysia, for example probability data for initiating event and data for incident outcome.
- The accident rate mathematical model [169-171] is more suitable in the TRA analysis calculation in Malaysia compared to other models such as in CCPS of AIChE [11, 21, 22], BUWAL [73] and or other data [25, 32,33]. This is by considering some data such as accident rate, traffic flow etc depending on geographical characteristics and scenario accident in Malaysia. Data from CCPS, BUWAL and some other data from several researchers are only suitable to the geographical condition of that particular country. The above factors are the reasons of why some TRA software such as TrHazGis [141], TRAT2 [27], and STRAPP [139] are not suitable for Malaysia usage. The result of TRA calculation is more accurate by using local data of the studied area. Therefore it will give an accurate picture of Malaysia accident scenario, its consequences and acceptable risk for any transportation of hazardous materials activities in Malaysia.
- TRA analysis is usually involving a very wide territorial geographical. As a result, the risk analysis will require abundant interstate data, e. g accident rate,



population distribution and others. In Malaysia, in order to facilitate the data extraction for all states has been made by developing a single agency to control and update all data for each state in Malaysia e.g. MIROS for traffic information, JPBD for land use information, Department of Statistic for population density and others similar purpose organizations.

- Eventhough majority of risk assessments which have been conducted were based on fatal effects, however there are uncertainties on the exact fatal dose of thermal radiation, blast effect, or a toxic chemical to the severity of injury. Where it is desired to estimate injuries as well as fatalities, the calculation of the effect will be discussed in detail in section 3.2

### **2.13 Summary**

Assessing the accident risk of a region implies the use of a complex methodology, requiring a lot of information such as population density, incident probability, hazards health and environment. Moreover, till to date, actual evidence from various major accident databases such as FACTS, MHIDAS and etc., have reported the impact from hazardous substances could result in death or injury to people, property damage or damage to the biophysical environment, through the effects of fire, explosion or toxicity. Special attention has to be paid to the potential risk that may arise from the transport of hazardous materials (HazMat) through large territorial areas, which, in some cases, are heavily populated. and difficult to predict where and when the accident will be occurred.

An increasing number of transportation accidents involving dangerous substances have occurred worldwide, giving place to major awareness in government, industry and community ways to improve safety management of hazardous materials transportation.

Amongst the three major TRA guidelines, the CCPS Model is the most simplified. This acquires a simpler estimation of the model. If compared to the Rhyne Model, there are more parameter involves and it seems to give more accuracy of the



estimation. Since the Rhyne Model is more complicated, it needs special attention for the parameter to be selected. For the BUWAL Model, the parameter includes the traffic composition and volume. But BUWAL Model is more empirical, since the traffic composition and population are referring the Swiss conditions.

Based on the literature, no work has been conducted on the designing and developing on a smart advisory system for hazardous material transportation risk analysis using quantitative approach according to Malaysia scenario. The only road transportation analysis works in Malaysia which are nearly related to this study, are a study to identify the root cause of road accident in Malaysia as reported by Radin [169-171]. In his study, Radin [171] analyze the contributing factors of road accident by considering accident rate, traffic flows and road geometry. In other work of Radin [169], a mathematical model using log linear model was developed to forecast the number of road crashes. However, Radin et. al studies [169-171] were not considered the impact of hazardous material release during transportation which caused fire and explosion, wind direction release zone area, type and quantity of hazardous material transport, trip, population and property and environment damage within 1 km radius from source of accident. Other factors will be discussed in detail in Chapter3. Since Malaysia did not have its own TRA model for hazardous material transportation, CCPS-TRA methodology is likely more suitable to be used instead of other methods because estimated the accident consequences impact area by using such as established mathematical model to calculate fire and explosion incident, rather than use fix figure of consequences impact,. this model is more accurate in parameter since, the TRA model considered direction of wind and considered a length of release location zone. However, not all CCPS-TRA parameters can be used, this model should be modified in order to be used and consider the weather in Malaysia, pressure, Malaysia Population data and daily traffic in the highway. The accident rate per mile must be collected depending on the roadway in Malaysia. Moreover in section 2.10, none of TRA analysis software had been developed locally and used since EIA regulation 1989 has been enforced under the Environmental Quality Act law 1974 in Malaysia [168]'

Even though, several workers have developed a method of SAS TRA software for hazardous material. In section 2.9 and 2.10, the existing design and developed TRA



software which is a refinement on this work. Note that the existing TRA model guideline is limited to the consequences behavior observed only for fatality (death) impacts, the survival ability of an injury victim are not considered such as age, total body burn surface area, type of fabric respond to a particular incident flux, antibiotics and etc. This explains why many death records showed up after few days after the actual event happened. The absence of this factor reduces the accuracy of a risk analysis software during hazardous material transportation. The literature does not contain any detailed study to show how the various level of injury impact of the TRA model is integrate in designing the TRA risk analysis software. Detailed about the limitations of the existing TRA model and requirements to develop and design proposed SAS for hazardous material transportation have been address in section 2.9 and 2.10.

In conclusion, the future study must consider all of the required possibilities as discussed in Chapter 2, when designed and developed an effective decision making tool of Smart Advisory System (SAS) for hazardous materials transportation. Therefore this thesis will provide the first detailed study of the smart advisory system for hazardous materials transportation risk analysis via quantitative approaches for Malaysia scenario. The existing TRA model will be analyzed to rectify and identify possible parameters for the modification of TRA model apply, to Malaysia scenario. Further, the proposed TRA model will also be integrated and compute with established consequences model and databases to develop a smart advisory system for transportation risk analysis. Since most of data involved such as geographical data, land use development, road networking, accident rate are different among countries, and also crucial in the TRA analysis impact, therefore GIS is customize in SAS. Once the SAS TRA software is developed, a predicted result may be obtained and curve may be plotted, and compared with the results from published data in the literature and chemical risk software.



## CHAPTER 3

### METHODOLOGY

This chapter describes the methodology used for development of smart advisory system for hazardous materials transportation in relation to risk associated with potential incidents. As explained in Chapter 2, this system should to be capable minimize several loopholes and weaknesses which are existed in the current TRA guidelines. Thus, before compute the TRA model in the system, the entire requirement to design and develop a proposed SAS for transportation of hazardous materials which to be adopted for Malaysia scenario, will be followed the suggestions criteria as discussed in section 2.10.2 and 2.11. Basically, this chapter will provide the first procedure to improve the accuracy of transportation risk analysis software in Malaysia to determine the minimum exposure routes and to obtain the safest route for the transportation of hazardous material. To achieve this purpose, three main stages which consist of different aspects of risk analysis process are involved. In the first stage, the existing guidelines of TRA such as in CCPS [22], BUWAL [32, 73] and by Rhyne et al. [25] were reviewed, analyzed and modified to fit into Malaysia transportation risk characteristic scenario. All parameters, assumptions and constraint involved in the previous TRA model calculation were studied to identify the strength and weaknesses of the models. In the second stage, the proposed TRA method will be integrated with the established consequences models and the available data related to transportation of accident such as accident rate, traffic volume and population density. For thermal effects calculation, the severity of the accident impact on an individual or the society and the probability of a person surviving from the fire and explosion from the transportation accident; the age of the person and the percentage of total body surface (TBS) area burned are considered. In the third stage, the proposed system will be integrated to GIS, to enhance the visualization of the impact incident and to



determine the routes between the Origin-Destination (OD) pairs. The schematic diagram for the development of smart advisory system for transportation Risk Analysis (HazMat) is demonstrated in the Figure 3. 1. Meanwhile Figure 3.2 shows the flowchart of proposed TRA methodology for Malaysia HazMat scenario.

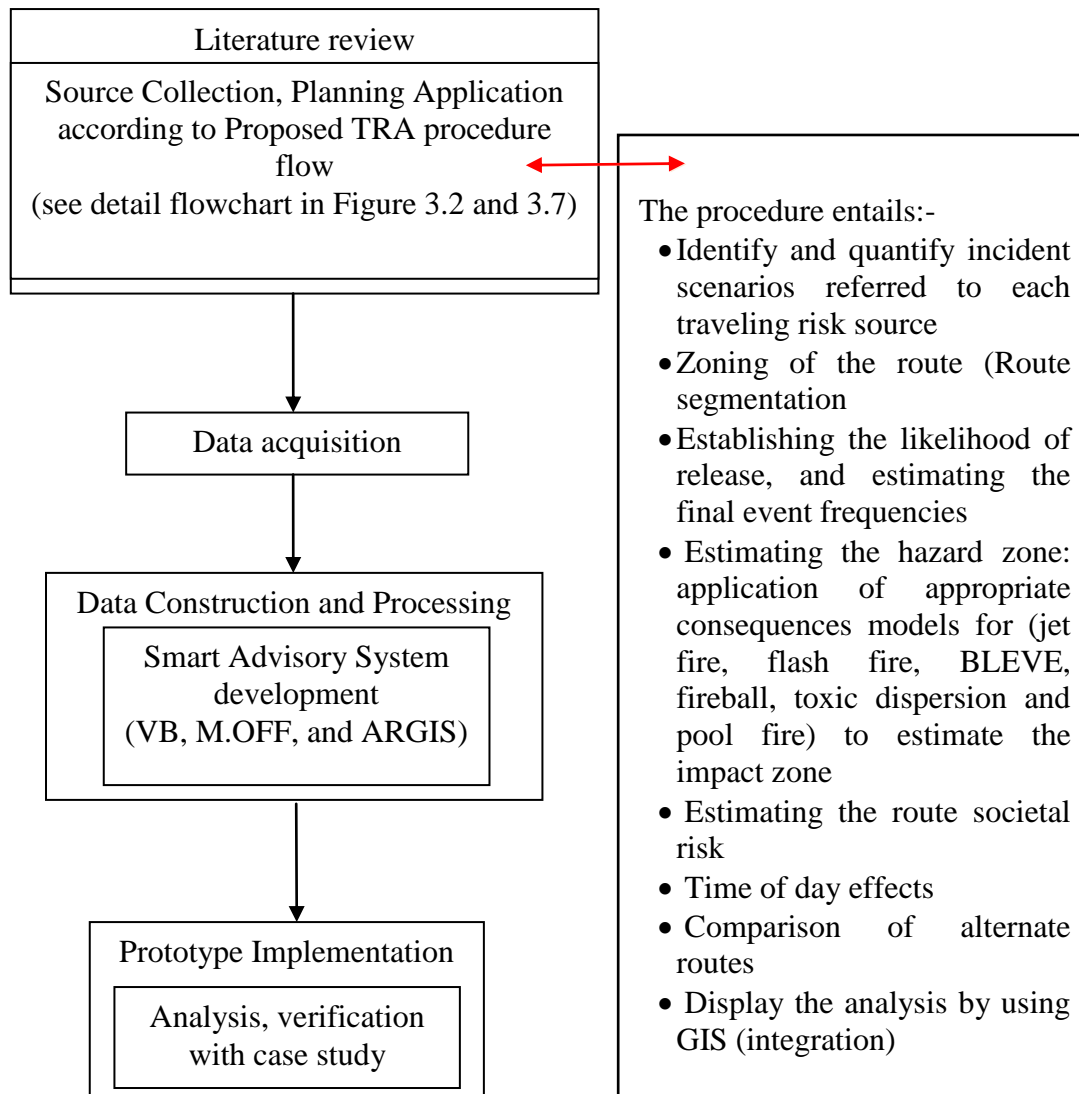


Figure 3.1 Flowchart shows the summary of the development of smart advisory system for transportation risk analysis (HazMat).



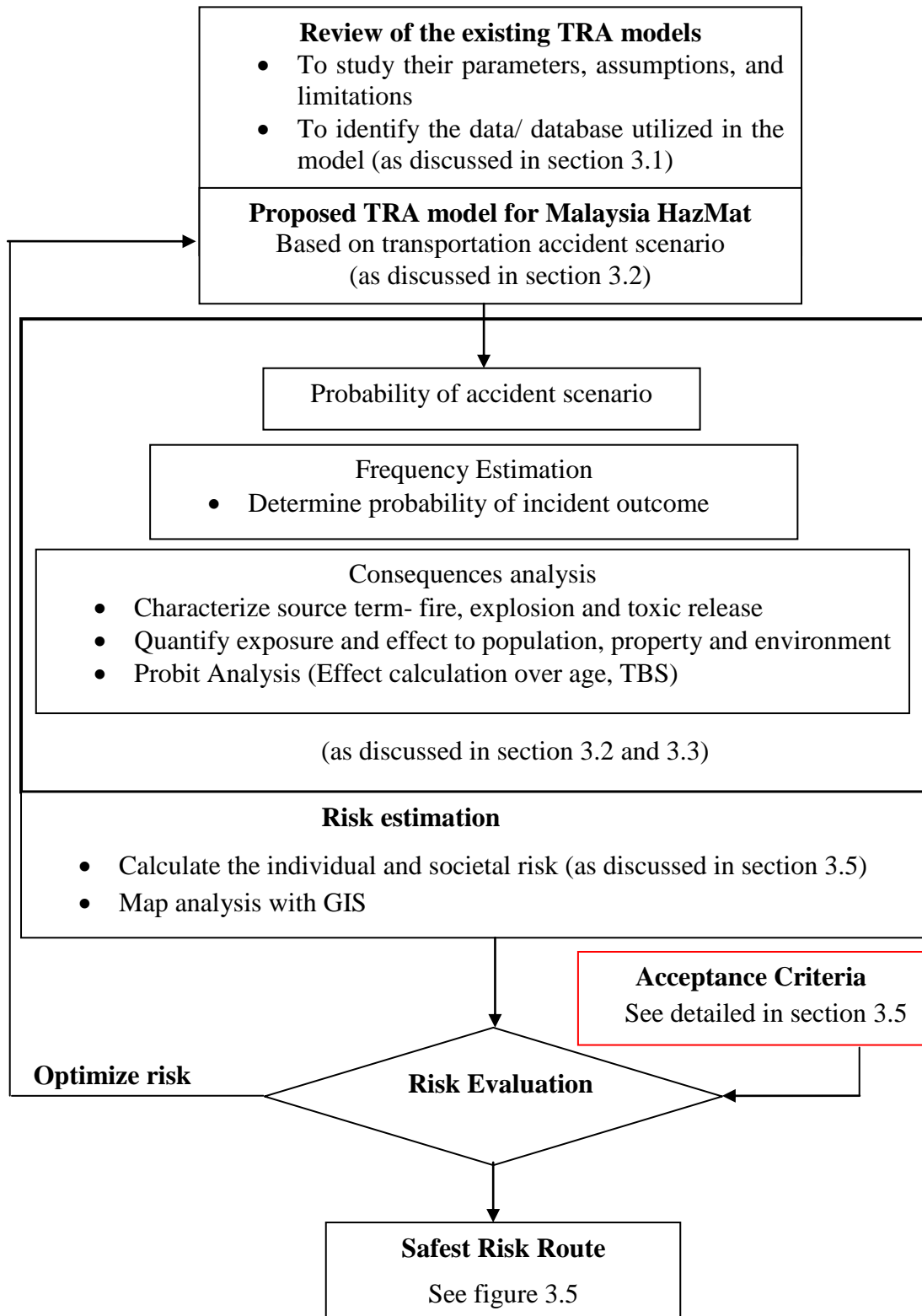


Figure 3.2 Overview flowchart of proposed TRA methodology for Malaysia HazMat scenario.



### **3.1 Review the existing TRA model of hazardous materials**

The detailed about this subject, have been discussed in section 2.10 and 2.11. As an overview, Rhyne methodology [25] is more accurate but the detailed information is not easily available, even in developed countries such as USA, Canada, and Europe. Whilst Buwal methodology [167] is more empirical, since all the calculated parameters in the model are based totally to Swiss condition. Compare to CCPS methodology, it only requires local information in order to obtained result as realistic as possible. Therefore, for Malaysia scenario, it is most suitable to use CCPS methodology because this model is more accurate in parameters such as direction of wind and consider a length of release location zone.

However slightly an additional modification should be introduce to suit Malaysia population data, weather condition, pressure, daily traffic in the highway and road trip for delivery. The accident rate per mile must be collected depending on the roadway in Malaysia. There will be much easier to collect the required data since only MIROS provided the service of freight wagon inventories for petroleum besides transporting other types of hazardous materials.

Since, this study considers improvement of several parameters in the risk model to enhance the quality of risk estimates and to better understand their focus and sensitivity of some assumptions. When parameters are limited so that a complete analysis of the entire models is not possible, statistical methodologies result will be used as suggested by Radin et. al [169].

### **3.2 Modification of TRA model for Malaysia**

As discussed in Chapter 2, any risk assessment dealing with multiple hazards, it is desired to estimate injuries as well as fatalities from each incidents in the risk calculation for example first and second degree burns, fragment injuries, and lung hemorrhage injuries due to thermal radiation intensity and explosion exposure. Thus, as in CPQRA guidelines, most of TRA risk analysis often estimate the risk of fatality by determine the appropriate levels of concern for overpressure, thermal radiation,



and toxicity hazards [11]. Therefore, these CCPS guidelines estimation [11, 21, 22] will open more space for inaccuracies in the TRA results evaluation. For example, most of the individual risk result in TRA considers the total individual risk of fatality by excluding the type injury, in assessing the level of risk from selected route of the transportation of hazardous materials. Moreover, according to CCPS model the numbers of death is depending on the fatality probability of an accident area multiplied with the population density.

The rational to include injury as in Eq. (3-3) in addition to fatality as used in CCPS have been discussed in detailed in section 2.10. In general, the severity of accident impacts towards human is not uniform, but the severity is varies depending on few factors such as the distance from source of accident, therefore a person closer to the accident event will receive the higher dose of death relationship, Other factors, which contribute to severity of injury such as physiological and pathological effect as reported by Bull [163-165] in detail, as discussed in section 2.10 which is also explain why few parameters are included in the Eq (3-1). Therefore by including those parameters in the Eq.(3-1), the result of transportation risk analysis will be more accurate. This opinion, is concluded based on the incidents which had happened in Bhopal, Seveso and other places which show that an increasing number of chronic disease after the accident. Moreover some incident, such as the effects of hot gases may have a significant contribution to an excess mortality especially in a confined situation such as inside the building.

The usage of fatality probability calculation in CCPS [11, 19-22], rather than the consequences model calculations as in Eq.(3-1) may yield a less accurate result for TRA analysis. For instances, if the level of exposures are assumed to yield probability of 0.3-0.4 fatalities (when the impact area have been protected by building structures or shelter, rapid escape, and clothing), the non-fatality results, is equal to the probability of 0.6-0.7 which mean that the incident area will be not affected by the accident. CCPS model does not give the probability of injury and unable to differentiate the different level of injury from the affected accident area, such as number of victim that will be affected by first or second degree burn, eardrum rupture and other impacts as shown in the Eq. (3-2) from the coordinate x,y against the



accident scenario. Besides that, the CCPS TRA model also cannot predict the projection number of road trip per year either increase or decrease over the years.

Accident rate is an important element in TRA analysis. However, the accuracy of TRA result is reduced, when the accident rate characteristics do not match with the geographical condition of the accident area during risk calculation. Therefore, Radin et. al [169] work is utilized as in Eq.(3.2). Detail about this subject will be discussed further in section 3.2.1.

In order to estimate the risk of injury and fatality, the Eq. (3-1) has been modified as follows:

$$IR_{x,y} = T \cdot T_{NYI} \cdot T_{TP\%} \left[ \frac{1}{T_{NYI} \cdot T_{TP\%}} \pm 1 \right] \cdot A_{MIROS} \cdot \sum_{i=1}^n R_i \cdot \sum_{j=1}^m L_{i,j} \cdot W_j \cdot \sum_{k=1}^{S_i} CorrectedP_{i,j,k} \cdot ratio(HD:MD:MiD:UE) \quad (3-1)$$

where,

$IR_{x,y}$  = the total individual risk of injury and fatality at specific geographical location x, y coordinate

T = number of trips per year

$T_{NYI}$  = number of year (after projected number of trip per year)

$T_{TP\%}$  = percentage of road trip projection (increase / decrease)

$A_{MIROS}$  = accident rate per kilometer according to Malaysian Institute of Road Safety Research

$R_i$  = release probability for ith release size

$L_{i,j}$  = length of release location zone j

$W_j$  = the probability that wind blows in the direction of concern

Corrected  $P_{i,j,k}$  = the probability of injury and fatality at coordinate x,y given that accident k occurs

m = number of release location zones and wind direction affecting coordinate x, y

n = number of release sizes considered

$S_i$  = number of incident outcomes for release size i



i = release size counter

j = release location zone counter

k = incident outcome counter

HD = Probability of the highest level of damage for Corrected  $P_{i,j,k}$  (fatality)

MD = Probability of major level of damage for Corrected  $P_{i,j,k}$  (injury or fatality)

MiD = Probability of minor level of damage for Corrected  $P_{i,j,k}$  (injury, such as first degree burn)

UED = Probability of no damage for Corrected  $P_{i,j,k}$  (no fatality and no injury)

By using Eq.(3-1), it is shown that the TRA analysis results is more accurate than CCPS, and the result is closer to the actual scenario consequences for transportation accident based on facts which were discussed before and in this section. Appropriate model is required in view of a rapid and continuous population growth leading to an increase in traffic and new development of industrial area with new findings in the chemical products. In the event of transportation accident, the information on the number of people affected is essential therefore an appropriate action or decision can be made especially during emergency cases such as the speed of hazard response team operation, the amount of medical supply and medical personnel involved.

A careful land use planning such as built- up of mixed development area or other related project must undergo EIA technical consensus from expertise, since they need to identify buffer or safe distance before any industry can be built within housing area.

### **3.2.1 Accident rates**

Accident rates are the most important components of a truck (HAZMAT) tanker risk analysis. Generally, the rate is affected by numerous parameters such as road conditions, environmental, trucking operation, types of road (urban, sub urban, rural and remote routes area). However, most of the truck tanker risk analyses are normally based on accident rates characteristic of broad classes of route types for which useful data are available. To calculate an accident rates in the modified TRA model as



demonstrated in Eq. (3-1), whereby several parameters are needed such as length of the road segment in kilometre, number of the registered vehicles and number of the truck accident.

The degree of accuracy in accident data relates directly to the size and quality of the database used to estimate rates. According to the literature review [25, 141, 142], most guidelines have utilised accident rates according to population density, type of road, road classes, and road area but the level tend to decrease as the conditions are made more restrictive. Therefore, to apply Eq.(3-3) in Malaysia, the accident data should be taken from Malaysian Institute of Road Safety Research (MIROS ), Jabatan Perancang Bandar dan Desa (JPBD) and others relevant data sources. For example, statistical data of the accident rates and road accident statistics are available from MIROS, Royal Police Malaysia, Highway Planning Unit (HPU) which provide the number of road deaths, number of road crashes, traffic volumes, for every 1 km of any motorway, express highway and major road in Malaysia.

Malaysia has experienced a remarkable period of economic expansion and growth in population, economy, industrialization and transportation. With the influence of rapid economic growth in Malaysia, the number of vehicles on the road, and highways are expected to increase. The total numbers of fatal road crashes were contributed by different type of modalities. In this study, road crashes are based MIROS formal data and Radin et al [171] statistics data whereby more than 58 % of fatal accident was constituted by motorcyclists, pedestrians constituted 12% of road fatalities, bicyclists constituted 5% of road fatalities, and truck crashes contributed 3-5% of road fatalities per year.

The mathematical models between Eq. (3-2) to Eq. (3-5) which were developed by Radin et al. [169] to forecast the number of road traffic deaths, number of road crashes and an accident rate, in Malaysia will be used in this study. The equations for predicting the number of road crashes and deaths for a given year are as follows:

Number of Road traffic deaths =

$$2289. e^{(0.0007 \text{ Vehicles } \times \text{ Population } \times \text{ Road})} . e^{0.2073 \text{ Data system}} \quad (3-2)$$



Number of Road crashes=

$$43478. e^{(0.00011 \text{ Vehicles} \times \text{Population} \times \text{Road})} . e^{0.2447 \text{ Data system}} \quad (3-3)$$

The above equations are included in Eq. (3-1). Data system factor in the above equations is equal to 1 for Peninsular Malaysia and 2 for East Malaysia. Estimated total number of vehicles in the year is expressed in millions. By applying Eq. (3-3), the total number of vehicles crashes in the year is obtained.

Both of the exponent model in Eq. (3-2) and Eq. (3-3) were established based on time series log-linear model, to explain the relationship between traffic deaths and traffic exposures, namely population, vehicles and road length. For reference, both of the models defined population as the estimated total number of people expressed in millions. Road means the estimated length total of roads expressed in thousands of kilometers.

Since the models established in 1994, Radin model is recognize as the best model which capable to accurately forecast the number of road traffic death and road crashes between year 1974 to 2000 [169] compared to the other popular models of traffic accident in Malaysia such as Rehan model and Aminuddin model [169].

Most probably, the assumptions parameter and criteria used in the Radin model was the most closest in explaining the actual traffic exposures in Malaysia. Amongst the assumptions which are considered in the Radin model were the number of vehicles per year, number of population per year, road length per year and standardization of accident data. Therefore the thesis used Radin et. al [169] model to incorporate in the Eq.(3-1), when some of the road accident statistic are not available in MIROS due to the rationale factors as below:-

- Malaysia is a developing country which is undergoing a dynamic growth in vehicle industry. This trend is approximating to developed country. In general, the growth for vehicle industry follows the ‘S’ curve which shows an exponential growth at the beginning and plateau when the each population



own about 2 vehicles per person. Based on this phenomena, we can predict that the improvement in the ‘S’ curve in 2020.

- It is known that the number of accident and death from an accident will increase with the increase in the number of population in a country. This is due to an increase in the number of traffic activities which directly increase the accident risk. Therefore the calculation of the number of population must be included in the model for road accident death.
- Exposure to accident also increases with the increase in the number of the road, road networking and road distance. These factors lead to an increase in the number of trips along the road especially with the increase in economic growth and commercialization activities in this country. Therefore the above factors must be taken in to consideration in the model calculation.
- Before 1981, only data on mortality, vehicle involved and route length throughout Peninsular Malaysia were reported. Only after 1981, all these information were integrated with Sabah and Sarawak datas. This explained why the statistic on the number of accident and death related accident suddenly showed a marked increment after 1980. Therefore, the effect of standardization in recording system must be considered in the calculation model.

However, the usage of Radin model has some limitation in the situation when the economic status is down whereby less people will buy vehicle. Therefore time series variable is more suitable for that condition [171].

For the state road portion, the average value of accident rate in year 2010 is  $5.3 \times 10^{-8}$ /km.yr.  $A_{miros}$  in Eq. (3-7) is also considered the relationships between accident, traffic flows and road geometry in the following mathematical expression as in Eq. (3-4) [169]:

$$Accident = 6.69 \exp^{0.3845Flow + 0.465LandUse - 0.4112LaneWidth + 0.5146Junction / kilometer}$$



(3-4)

Table (3-1) shows the structure and definition of independent variables for applying Eq. (3-4)

| Independent Variables | Description            | Level factors | Coding system  |
|-----------------------|------------------------|---------------|--|
| FL                    | Traffic Volume         | 2             | (1) Traffic Volume < 30,000<br>(2) Traffic Volume >30,000          |
| LW                    | Lane Width             | 2             | (1) Lane Width < 3.2 m<br>(2) Lane Width > 3.2 m                   |
| Jc                    | Nos. of Minor Junction | 2             | (1) Nos. Of minor junction < 15<br>(2) Nos. Of minor junction > 15 |
| LU                    | Adjacent Land Use      | 2             | (1) Kampong (rural/residential)<br>(2) Shop / commercial area      |

The structure of independent variables and their respective definitions are shown in Table (3-1). To find the accident rates, results from Eq. (3-4), will be used in the calculation as follows:

$$A_{miros} = \text{ratio of truck crashes} \left[ \frac{\text{Eq. (3-6)}}{\text{total number of vehicles}} \right] \left[ \frac{\text{length of (m) per year}}{1000(m)/(km)} \right] \quad (3-5)$$

Therefore by considering the traffic volume, number of junctions, lane width, and landuse, for the above model in this methodology enable to assess geometric factors contributing to accidents and select the safest route in their highway design.

### 3.2.2 Number of Road Tanker Trip

In Eq. (3-3), the number of road tanker trip is predicted based on the company product sales performance either increase or decrease over the years.



### 3.2.3 Probability Event from the Accident

According to CCPS [11, 19-22], Health Safety and Executive, United Kingdom [8-10, 24] and TNO guidelines [71, 76, 172] in order to estimate individual risk, various hypothetical events should be assessed. Each of these accident scenario events will have a predicted frequency of occurrence,  $f$  and a predicted number of persons harmed,  $N$ . The proposed TRA model will use the probability of the initiating event as described by Fisher et al. [174] as in appendix 3. Then from the initiating event, the incident will evolved to cause several potential accident scenarios outcomes, such as fireball, BLEVE or flash fire. The incident outcomes are depending on the sequence of the probability events. In Eq. (3-1), the length of release location zone  $j$ ,  $L_{i,j}$ , is estimated by using consequences model equation as in Eq. (A1- 1) to Eq. (A1-30) for explosion accident scenario, Eq. (A1- 31) to Eq. (A1-36) and Eq. (A1-81) to Eq. (A1-119) for fire accident scenario and Eq. (A1- 120) to Eq. (A1-165) for toxic release accident scenario. Meanwhile the value for release size probability,  $R_i$  is taken according to CCPS guidelines [21, 22]. Subsequently, to estimate the frequency of a potential accident scenario (in order to develop the propagation sequence of various scenarios) and to calculate the final frequency for each type of accident consequences, a selected Event Tree Analysis (ETA) is employed, as shown by Rhyne [25], CCPS [11] and Casal et al. [67]. Here the possible event tree of release magnitudes is based as follows:

- A rupture: release area equal to the area of a 4-inch diameter hole
- A puncture: release area equal to the area of a 1-inch diameter hole
- A leak: release area equal to the area of a 1/4 -inch diameter hole

### 3.2.4 Probability Damage Calculation

In reality, the population and environment closer to the source of an event is expected to experience more severe consequences than those farther than the event. Thus an assumption of a uniform distribution of consequences across the impact area may not be correctly representing the actual condition of risk. The proposed model is designed



to be capable to stratify the severity of injury and able to predict the number of fatalities and injuries associated with the event [11, 21, 22, 70, 76]. As shown in Eq. (3-1), the level of damage probability is categorized into four conditions which are fatality, major injury, minor injury and no damage.

In this study, the magnitude of the physical effects and the affected zone is estimated by using established consequences models such as in CCPS [11, 21,22], TNO [71, 76,172], Rhyne [25], Lees et al. [64], Casal [67] and Crowl and Louvar [153]. The damage is addressed by vulnerability models, using dose-response relations. The level of damage to human and property is dependent on the dose received and distance from the hazardous incident. Therefore, if the impact dose received by a person is low, it may not cause injury or death. The impact dose received is irreversibly proportionate to the distance, therefore as the distance increased; the dose received will be decreased. In the injury zone, a person situated at a various distance, will experience different level of injury such as minor or major injury.

### 3.2.5 Probit Analysis

In order to produce percentage of injury and fatality among humans in terms of the intensity of a hazardous event and duration of the exposure, probit based analysis are used to determine the fatality and injury levels to the exposed population.

The probit equation is as follows [70]:

$$Pr = k_1 + k_2 \ln D \quad (3 - 8)$$

Where, Pr is the probit and known as the probit value which is a measure of the percentage of the vulnerable resource which sustains injury or damage. The parameters,  $k_1$  and  $k_2$  are constants depending on the type of damage and derived from historical data published by Eisenberg et al. [173]. D is a function of the hazard dosage in terms of intensity and duration.

The probit value can then be converted into percentage. CCPS of AIChE [11], Crowl and Louvar [153], TNO Green Book [172], Finney [174] and Lees [64] have provided tables for converting probit value, P to percentage as in appendix 3.



The probit equations (Pr) as in Eq. (3-8) also can utilize to get the percentage of affected building and affected population (R, %) by using the probit table in appendix 3. The table also can be utilized for every probit equation. Unfortunately, the estimation of the number of people affected by an accident by using the conversion of probit variable to the percentage of people affected (as taken from tables and figures as in the appendix 3) has caused a significant problem. The problem encountered when the calculations are done using a computer program where an access to the numerical library is required and this can cause significant errors. Moreover, the probit value in the table [11, 64, 153, 172, 174] range between 2.67 to 8.09 which represent a percentage from 1% to 99% and 99.1% to 99.9%. Therefore the probit table is unable to predict probit value which has a conversion less than 1%, and the percentage result is not in decimal point at the range of 1% to 99%. Furthermore, there is difficult to introduce data from figures and tables into a computer code.

Even though Alonso et al. [175,176] has proposed analytical expressions to convert both probit variables to percentage and vice-versa by using R-Pr data from TNO (1989) and TNO (2005) as in Eq. (3-51), but the R values are only between ranges of 5% to 95%.

$$R = -3.25Pr^3 + 48.76Pr^2 - 206.60Pr + 270.35 \quad (3-9)$$

Therefore, the analytical expressions are used in this study to convert both probit variables to percentage of injured people and vice versa, as proposed by Vilchez et al. [137]. The Vilchez et al. [137] analytical equation is selected due to the excellent agreement between the values taken from the figures and tables proposed by Finney [174] which are commonly used to calculate the percentage of people injured in a given accident. Moreover these equations can predict the percentage of people affected with more than 1 decimal point value. The proposed equations [67, 137] also provide an easy way to convert values of the probit variable into percentage of people injured and vice versa.

The equation for the analytical expressions of probit value is shown in appendix 1, between Eq. (A1-43) to Eq. (A1-53). Application of the probit analysis for



consequences of fire, explosion and toxic exposure is presented using the following probit equation as in the Table (3-2). Table (3-2) lists a variety of probit equations for different types of exposures.

However, the probit equation as shown in the table (3-2) may not represent some type of injuries on human indoors such as death due to head impact, death due to whole body impact, impact of fragments and debris generated by the blast and building or structural collapse. Therefore, in considering the potential impacts on people and structures either direct and indirect effects from the blast, the probit equation in TNO [172] and several sources [67, 175, 176] can be used to predict the damage caused to these vulnerable receptor. Probit equations shown in the Table (3-3) and Table (3-4) are those applicable for different types of damage from explosions to building and on human outdoors.

Table (3-2) Probit Correlations for a variety of exposure (The causative variable is representative of the magnitude of the exposure.)

| Type of injury or damage              | Causative variable   | Probit parameters |       | Eq.    | References    |
|---------------------------------------|----------------------|-------------------|-------|--------|---------------|
|                                       |                      | $k_1$             | $k_2$ |        |               |
| Fire                                  |                      |                   |       |        |               |
| Burn deaths from flash fire           | $t_e I_e^{4/3}/10^4$ | -14.9             | 2.56  | (3-10) | [64, 173]     |
| Burn deaths from pool burning         | $t_I^{4/3}/10^4$     | -14.9             | 2.56  | (3-11) | [64, 173]     |
| First degree burn injury              | $t_I^{4/3}/10^4$     | -39.83            | 3.02  | (3-12) | [67, 173]     |
| Second degree burn injury             | $t_I^{4/3}/10^4$     | -43.14            | 3.02  | (3-13) | [67, 173]     |
| Lethality from thermal radiation      | $t_I^{4/3}/10^4$     | -36.38            | 2.56  | (3-14) | [67, 173]     |
| Protected (by clothing)               | $t_I^{4/3}/10^4$     | -37.23            | 2.56  | (3-15) | [67, 173]     |
| Explosion                             |                      |                   |       |        |               |
| Deaths from lung haemorrhage          | $p^o$                | -77.1             | 6.91  | (3-16) | [64, 173]     |
| Eardrum ruptures                      | $p^o$                | -15.6             | 1.93  | (3-17) | [64, 173]     |
| Deaths from impact                    | J                    | -46.1             | 4.82  | (3-18) | [64, 173]     |
| Injuries from impact                  | J                    | -39.1             | 4.45  | (3-19) | [64, 173]     |
| Injuries from flying fragments        | J                    | -27.1             | 4.26  | (3-20) | [64, 173]     |
| Structural damage                     | $p^o$                | -23.8             | 2.92  | (3-21) | [64, 173]     |
| Glass breakage                        | $p^o$                | -18.1             | 2.79  | (3-22) | [64, 173]     |
| Toxic release                         |                      |                   |       |        |               |
| Ammonia deaths <sup>a</sup>           | $\sum C^{2.0}T$      | -35.9             | 1.85  | (3-23) | [11, 20, 153] |
| Carbon monoxide deaths <sup>a</sup>   | $\sum C^{1.0}T$      | -37.98            | 3.7   | (3-24) | [11, 20, 153] |
| Chlorine deaths <sup>a</sup>          | $\sum C^{2.0}T$      | -8.29             | 0.92  | (3-25) | [11, 20, 153] |
| Ethylene oxide deaths <sup>a</sup>    | $\sum C^{1.0}T$      | -6.19             | 1.0   | (3-26) | [11, 20, 153] |
| Hydrogen chloride deaths <sup>a</sup> | $\sum C^{1.0}T$      | -16.85            | 2.0   | (3-27) | [153, 177]    |
| Nitrogen dioxide deaths <sup>a</sup>  | $\sum C^{2.0}T$      | -13.79            | 1.4   | (3-28) | [11, 20, 153] |
| Phosgene deaths <sup>a</sup>          | $\sum C^{1.0}T$      | -19.27            | 3.69  | (3-29) | [11, 20, 153] |
| Propylene oxide deaths <sup>a</sup>   | $\sum C^{2.0}T$      | -7.42             | 0.51  | (3-30) | [11, 20, 153] |
| Sulphur dioxide deaths <sup>a</sup>   | $\sum C^{1.0}T$      | -15.67            | 1.0   | (3-31) | [11, 20, 153] |



|  |                   |        |       |        |               |
|--|-------------------|--------|-------|--------|---------------|
| Toluene <sup>a</sup>                     | $\sum C^{2.5}T$   | -6.79  | 0.41  | (3-32) | [11, 20, 153] |
| Acrolein deaths <sup>a</sup>             | $\sum C^{1.0}T$   | -9.931 | 2.049 | (3-33) | [11, 20, 153] |
| Acrylonitrile deaths <sup>a</sup>        | $\sum C^{1.43}T$  | -29.42 | 3.008 | (3-34) | [20, 67]      |
| Benzene deaths <sup>a</sup>              | $\sum C^{2.0}T$   | -09.78 | 5.3   | (3-35) | [20, 67]      |
| Bromine <sup>a</sup>                     | $\sum C^{2.0}T$   | -9.04  | 0.92  | (3-36) | [20, 67]      |
| Carbon Tetrachloride deaths <sup>a</sup> | $\sum C^{2.5}T$   | -6.29  | 0.408 | (3-37) | [20, 67]      |
| Formaldehyde deaths <sup>a</sup>         | $\sum C^{2.0}T$   | -12.24 | 1.3   | (3-38) | [20, 67]      |
| Hydrogen Cyanide deaths <sup>a</sup>     | $\sum C^{1.43}T$  | -29.42 | 3.008 | (3-39) | [20, 67]      |
| Hydrogen Fluoride deaths <sup>a</sup>    | $\sum C^{1.0}T$   | -25.87 | 3.354 | (3-40) | [20, 67]      |
| Hydrogen Sulphide deaths <sup>a</sup>    | $\sum C^{1.43}T$  | -31.42 | 3.008 | (3-41) | [20, 67]      |
| Methyl Bromide deaths <sup>a</sup>       | $\sum C^{1.0}T$   | -56.81 | 5.27  | (3-42) | [20, 67]      |
| Methyl Isocyanide <sup>s</sup>           | $\sum C^{0.653}T$ | -5.642 | 1.637 | (3-43) | [20, 67]      |
| Acrolein death <sup>b</sup>              | $\sum C^{1.0}T$   | -9.93  | 2.05  | (3-44) | [20, 67]      |
| Ammonia <sup>b</sup>                     | $\sum C^{2.0}T$   | -9.82  | 0.71  | (3-45) | [20, 67]      |
| Carbon Tetrachloride                     | $\sum C^{0.5}T$   | 0.54   | 1.01  | (3-46) | [20, 67]      |
| Chlorine <sup>b</sup>                    | $\sum C^{2.75}T$  | -5.3   | 0.5   | (3-47) | [20, 67]      |
| Hydrogen Chloride <sup>b</sup>           | $\sum C^{1.0}T$   | -21.76 | 2.65  | (3-48) | [20, 67]      |
| Hydrogen Flouride <sup>b</sup>           | $\sum C^{1.0}T$   | -26.4  | 3.35  | (3-49) | [20, 67]      |
| Methyl Bromide <sup>b</sup>              | $\sum C^{1.0}T$   | -19.92 | 5.16  | (3-50) | [20, 67]      |
| Phosgene <sup>b</sup>                    | $\sum C^{1.0}T$   | -19.27 | 3.69  | (3-51) | [20, 67]      |

Note

s:

$t_e$  = effective time duration (s)

$I_e$  = effective radiation intensity (W/m<sup>2</sup>)

$t$  = time duration of pool burning (s)

$I$  = radiation intensity from pool burning (W/m<sup>2</sup>)

$p^o$  = peak overpressure (N/m<sup>2</sup>)

$J$  = impulse (N s/m<sup>2</sup>)

$C$  = concentration (ppm)

$T$  = time interval (min)

Table (3-3) probit equations for different degrees of damage to buildings and structures caused by explosions

| Type of damage  | Probit equations   | Eq.    | References     |
|---|--|--------|----------------|
| Minor damage (broken windows, displacement of doors and window frames, tile displacement, etc.) | $Y = 5 - 0.26 \ln \left[ \left( \frac{4600}{P_s} \right)^{3.9} + \left( \frac{110}{i} \right)^5 \right]$       | (3-52) | [64, 172, 178] |
| Major structural damage (cracks in wall, collapse of some walls)                                | $Y = 5 - 0.26 \ln \left[ \left( \frac{17500}{P_s} \right)^{8.4} + \left( \frac{290}{i} \right)^{9.3} \right]$  | (3-53) | [64, 172, 178] |
| Collapse (building partially or totally demolished)   | $Y = 5 - 0.22 \ln \left[ \left( \frac{40000}{P_s} \right)^{7.4} + \left( \frac{460}{i} \right)^{11.3} \right]$ | (3-54) | [64, 172, 178] |



Table (3-4) probit equations for different types of damage from explosions on human outdoors

| Type of damage                 | Probit equations  | Eq.    | References     |
|--------------------------------|---|--------|----------------|
| Eardrum rupture                | $Y = -12.6 + 1.524 \ln P_s$   | (3-55) | [64, 172]      |
| Death due to head impact       | $Y = 5 - 8.49 \ln \left( \frac{2430}{P_s} + \frac{4 \times 10^8}{P_s \times i} \right)$               | (3-56) | [64, 172, 178] |
| Death due to whole body impact | $Y = 5 - 2.44 \ln \left( \frac{7.38 \times 10^3}{P_s} + \frac{1.3 \times 10^9}{P_s \times i} \right)$ | (3-57) | [64, 177]      |
|                                | $Y = 5 - 4.82 \ln \frac{40267}{i}$  | (3-58) | [172, 177]     |
| Death due to lung haemorrhage  | $Y = 5 - 5.74 \ln \left( \frac{4.2 \times 10^5}{P_{ef}} + \frac{1694}{i} \right)$                     | (3-59) | [177]          |
|                                | $Y = 5 - 6.6 \ln \left( \frac{620550}{P_s} + \frac{2069}{i} \right)$                                  | (3-60) | [64]           |

It is realised that when different probit equations are used to estimate diverse consequences (for example, first-degree burns, second-degree burns, or lethality) on a given population, different categories will overlapped. Thus, all those individuals suffering second-degree burns will appear to have also suffered first-degree burns, and all those individuals who die due to thermal radiation will also have suffered second-degree burns. As a result, the percentage of people that can be affected by the accident will become more than 100%. Therefore to avoid doublecounting, the overall damage probabilities must be equal to 1.0. As mentioned earlier in this chapter, the existing model in the CCPS guidelines [11, 21, 22], Swiss methodology (BUWAL) guideline [73] and Rhyne et al. [25] unable to demonstrate the probability of injury and also cannot differentiate between the level of injury from the affected accident area, at the same given of x, y coordinate and accident scenario. For these reasons, the Eq. (3-2) has been modified to determine the probability of injury (by percentage) for different types of damage from explosions and thermal radiation on human outdoors.

#### 3.2.5.1 The damage to human from thermal radiation

In this section, steps to determine the damage from thermal radiation to human will be discussed in detailed. The proposed steps is developed to enable the estimation of the number of injuries as well as fatalities to the population affected from thermal radiation accident cases by taking into account the relationship between radiation intensity – time duration – distance variables as in the Eq. (3-3). To apply Eq. (3-3) for thermal radiation accident cases, the following steps must be carried out first in



order to obtained and to substituted the results of HD, MD, MiD, UED for CorrectedP<sub>ij,k</sub> into Eq. (3-3). The steps are as follows:

- Selected probit equations: in this case Eq. (3-12) – (3-15). Probit equations (P) are in general form shown by Eq. (3-8).

$$Pr = k_1 + k_2 \ln D = k_1 + k_2 \ln [f(I_e \cdot t_e)] \quad (3-61)$$

In the case of thermal radiation, D is the combination of effective radiation intensity,  $I_e$  (kW/m<sup>2</sup>) and effective time duration (s),  $t_e$ .

- Substitute the causative variable and probit parameters in Eq. (3-12) to Eq. (3-15) into Eq. (3-61), as follows:

$$Pr = -39.83 + 3.02 \ln [f(I_e \cdot t_e)] \quad \text{for first degree burn} \quad (3-62)$$

$$Pr = -43.14 + 3.02 \ln [f(I_e \cdot t_e)] \quad \text{for second degree burn} \quad (3-63)$$

$$Pr = -36.38 + 2.56 \ln [f(I_e \cdot t_e)] \quad \text{for lethality} \quad (3-64)$$

$$Pr = -37.23 + 2.56 \ln [f(I_e \cdot t_e)] \quad \text{for protected by clothing} \quad (3-65)$$

- The probit value in the Eq. (3-62) to Eq. (3-65), will be converted into percentage by using the analytical expressions of probit value as proposed by Vilchez et al. [137] as shown in appendix 1, between Eq. (A1-43) to Eq. (A1-53).
- To estimate the effects of thermal flux on individual burns and the severity of damage will depend on the intensity of the radiation (kW/m<sup>2</sup>) and the dose received and these must be recognized. Basically the impacts rapidly worsen as both radiation intensity and exposure duration increase. This will affect the injury levels and probability of fatality.
- Table (3-5) shows the approach to approximate the level of damage at different thermal flux [67, 179-181]. According to table (3-5), if the dose received by a person between 4.7 to 5.0 (kW/m<sup>2</sup>) and within the time duration of 20s to 30s, it can be assumed that the thermal flux can cause second degree burns. At continuous exposure with radiation intensity of 12.6 (kW/m<sup>2</sup>), 100% of population fatality can be predicted. Therefore a person who are exposed to radiation intensity of 2.1 (kW/m<sup>2</sup>), can be expected may suffer first degree burns. Based on the above assumptions, the impacts levels of thermal flux



damage is arranged from low to high impacts by using probit Eq. (3-62) to probit Eq.(3-65).

- Results from Eq. (3-62) - Eq. (3-65) must be corrected, since they are referring to different degrees for the same type of damage (thermal flux impact). Furthermore, different probit equations are used to estimate diverse consequences (for example, first-degree burns, second-degree burns, or lethality) on a given population which will cause overlapping of results for different categories damage. Thus, all those individuals suffering second-degree burns will appear to have first-degree burns and all those individuals who die due to thermal radiation also suffered from second-degree burns. As a results, the overall percentage of population injury and fatality from a single accident can become more than 100%. Therefore to avoid doublecounting, the overall percentage of damage must be equal to 100%.

Table (3-5) Approximate levels of damage for different radiation intensity

| Radiation Intensity<br>(kW/m <sup>2</sup> ) | Impact  |
|---|---|
| 1.4   | Harmless for individuals not wearing special protection   |
| 1.6   | Will cause no discomfort at long exposures  |
| 1.7   | Minimum required to feel pain   |
| 2.1   | Minimum required to feel pain after 1 min   |
| 4.0   | Enough to cause pain after an exposure of 20 s;<br>blistering of the skin is likely; 0% lethality |
| 4.7   | Causes pain in 15-20 s, 2nd degree burns after 30 s   |
| 7.0   | Maximum tolerable for firefighters who are totally<br>protected (classical protective clothing)   |
| 11.7  | Thin, partially insulated steel may lose its mechanical<br>integrity                              |
| 12.5  | Plastic insulation of electrical wires melts; melting of<br>plastic tubing; 100% lethality        |
| 15.0  | Critical radiation intensity* for wood (flame ignition  |



|      |  |
|------|--|
|      | without contact with the surface)  |
| 25.0 | Thin, insulated steel may lose its mechanical integrity                        |
| 35.0 | Critical radiation intensity for wood and textiles<br>(without flame ignition) |
|      | Threshold value for the ignition of buildings                                  |
| 37.5 | Damage to process equipment, collapse of structures                            |

---

- To correct the overall percentage of damage and to categorize the impacts levels of thermal flux damage from low to high impacts by using probit Eq. (3-62) to probit Eq. (3-65) as mentioned earlier, these steps are followed. By considering health effects related to radiation intensity doses, the distance between a person to the accident scenario plays a major factor. In which, a person who is closer to the source of an accident is likely to receive a greater dose and also likely to experience severe consequences than those further from it. Therefore the affected zone for first degree burn is expected to be larger than second degree burn and lethality. This conclusion is supported by San Juan Ixhuatepec, Mexico disaster in 1984 [57, 64] after a series of explosions occurred at a liquid petroleum gas (LPG) tank farm. The explosions demolished houses and propelled metal fragments over a distance ranging from a few meters up to 1.2 km, and also caused 500 to 600 people killed with 5,000 to 7,000 suffered severe injuries. The impact shows that most of the people affected by severe injuries is assumed to be further from the accident events up to 1.2 km and expected to receive low dose than those people who have died.
- In another case, Rashid et al. [182], estimated the impacts and effects from the LPG transportation accident and display the affected zones results via ArcGIS 9.3.1 version. For the case study evaluated, a 13,000kg (34.5 m<sup>3</sup>) LPG road tanker filled to 80% of its capacity is assumed to be involved in a series of events. By applying the probit equations for thermal radiation, the percentage of the population affected is predicted as in the table (3-6) below:



Table (3-6) shows the effects results of LPG transportation accident [182]

| Effect             | Area (range, m) | Percentage (affected) |
|--------------------|-----------------|-----------------------|
| First degree burn  | 0 – 700         | 99.24                 |
| Second degree burn | 0 – 450         | 18.87                 |
| Lethality          | 0 – 390         | 9.64                  |
| Protected          | 0 – 305         | 1.57                  |
| Total (%)          |                 | 129.32 > 100%         |

From Table (3-6), it is found that the different categories of effects showed overlap affected zone results. First degree burn shows the most affected impact area from the accident (0-700m).

- Since the affected zone of first degree burn is always higher due to low radiation intensity, probit Eq. (3-62) represent minor level of damage, known as  $Pr_{MiD}$ , followed by probit Eq. (3-63) which represent major level of damage and known as  $Pr_{MD}$ . Meanwhile, probit Eq. (3-64) represent highest level of damage to a person, known as  $Pr_{HD}$ , and probit Eq. (3-65) which represent lowest level of damage, recognized as,  $Pr_{LD}$ . The general results are obtained as:

$$Pr_{MiD} = -39.83 + 3.02 \ln[f(I_e \cdot t_e)], \text{ the probit value } Pr_{MiD} \text{ is convert into first degree burn percentage} = R_{MiD}\% \quad (3-66)$$

$$Pr_{MD} = -43.14 + 3.02 \ln[f(I_e \cdot t_e)], \text{ the probit value } Pr_{MD} \text{ is convert into second degree burn percentage} = R_{MD}\% \quad (3-67)$$

$$Pr_{HD} = -36.38 + 2.56 \ln[f(I_e \cdot t_e)], \text{ the probit value } Pr_{HD} \text{ is convert into lethality percentage} = R_{HD}\% \quad (3-68)$$

$$Pr_{LD} = -37.23 + 2.56 \ln[f(I_e \cdot t_e)], \text{ the probit value } Pr_{LD} \text{ is convert into protected by clothing percentage} = R_{LD}\% \quad (3-69)$$



- The above results must be corrected and re-arranged from the highest level of damage to the unaffected impacts. The HD = Probability of the highest level of damage for corrected  $P_{i,j,k}$  as in Eq. (3-3) is equal to the probit value conversion for the highest level of damage percentage,  $R_{HD}\%$  in Eq. (3-68).
- The MD=Probability of major level of damage for corrected  $P_{i,j,k}$  (injury or fatality) as in Eq.(3-3) which is equal to the probit value conversion for the actual effect of second degree burn percentage and also known as actual  $R_{MD}\%$ . The actual  $R_{MD}\%$  of second degree burn is obtained by subtracting the percentage result from Eq. (3-67) – Eq. (3-68) =  $Pr_{MD} - Pr_{HD}$ , as below:

$$Pr_{MD} - Pr_{HD} = \{-43.14 + 3.02 \ln [f(I_e, t_e)]\} - \{-36.38 + 2.56 \ln [f(I_e, t_e)]\} \quad (3-70)$$

Both probit values are converted into percentages without the need to simplify the Eq. (3-70) to get the actual percentage of second degree burn as in Eq. (3-71)

$$\text{Actual } R_{MD}\% = R_{HD}\% - R_{MD}\% \quad (3-71)$$

- The MiD=Probability of minor level of damage for corrected  $P_{i,j,k}$  (injury, such as first degree burn) as in Eq.(3-3) is equal to the probit value conversion for the actual effect of first degree burn percentage, known as actual  $R_{MiD}\%$ . The actual  $R_{MiD}\%$  of first degree burn is obtained by subtracting the percentage result from Eq. (3-66) over Eq. (3-67) and Eq. (3-68), as below:

$$\text{Actual } R_{MiD}\% = R_{MiD}\% - (R_{MD}\% + R_{HD}\%) \quad (3-72)$$

- The actual percentage for protected by clothing is obtained by subtracting the percentage result in Eq. (3-69) over Eq. (3-66), Eq. (3-67) and Eq. (3-68) as below:

$$Pr_{LD} - (Pr_{MiD} + Pr_{MD} + Pr_{HD}) \quad (3-73)$$



All probit values ( $Pr_{LD}$ ,  $Pr_{MiD}$ ,  $Pr_{MD}$  and  $Pr_{HD}$ ) must be converted into percentages before substituted into Eq. (3-73) to determine the actual percentage for protected by clothing as follows:

$$\text{The lowest level of damage, (actual } R_{LD}\%) - (R_{MiD}\% + R_{MD}\% + R_{HD}\%) \quad (3-74)$$

- The UED=Probability of no damage for Corrected $P_{i,j,k}$  (no fatality and no injury)  
as in Eq.(3-3) is obtained by subtracting the percentage result in Eq. (3-66), Eq. (3-67), Eq. (3-68) and Eq. (3-69) from 100% as below:

$$100\% - (Pr_{LD} + Pr_{MiD} + Pr_{MD} + Pr_{HD}) \quad (3-75)$$

All probit values,  $Pr_{LD}$ ,  $Pr_{MiD}$ ,  $Pr_{MD}$  and  $Pr_{HD}$  should first be converted into percentages before substituted into Eq. (3-75) to determine the actual number of people who are not affected in percentage as follows:

$$\text{The percentage, } R_{UED} = 100 - (R_{LD} + R_{MiD} + R_{MD} + R_{HD}) \quad (3-76)$$

The above methodology can also be applied to explosion accident cases.

### *3.2.5.2 The impact of thermal radiation to human from the influence of burn size distribution and ages.*

The use of probit analysis to determine of burn mortality was introduced in 1949 by Bull et al. [164]. This method is utilized to determine the severity of the accident impact on an individual by considering the age of the affected person and the percentage of total body surface (TBS) area burned in the second degree burn. The calculations are according to the steps as below:

- Result ( $R_{MD}\%$ ) from equation (3-67) should be used to determine the percentage of total body surface (%TBS) area burned in order to estimate the consequence of thermal flux on individual second degree burns. According to



Bull et al. [163-164] and Curreri et al. [166], the probability of surviving in thermal radiation impact is depends on the percentage of TBS and of the age of the person.

- Then, the probability of fatality were calculated by using binary logistic regression as below:

$$POD (Probability of Dying) = \frac{e^x}{1 + e^x} \quad (3-77)$$

$$\text{where, } X = B_0 + B_1 (age) + B_2 (\%TBS \text{ burn}) + B_3 (age)^2 \quad (3-78)$$

and the coefficients;  $B_0 = -5.22$ ;  $B_1 = -0.1041$ ;  $B_2 = 0.09843$  and  $B_3 = 0.002296$

An Eq. (3-77) and Eq. (3-78) are used to calculate the probability of a person surviving from second degree burn in the thermal radiation impact depending on the percentage of TBS and of the age of the person.

- From 1946 to 1971, there was correspondingly improved survival from large burns after introduction of a new treatment method of burn injury [183]. According to Bull et al. [163, 165], Curreri et al. [166] and Martin [184] whom confirmed that the 50% lethal area ( $LA_{50}$ ) is raised for all age groups. In the case of burns, a person who is affected 30% or more of the body surface area is expected to go into a state of shock and may die. Probit equations in Table (3-7) are used to calculate ( $LA_{50}$ ) according to age.

Table (3-7) Burn Mortality

| Age (years) | Probit equations        | $LA_{50}$ | 95% C. L. | Eq.    |
|-------------|-------------------------|-----------|-----------|--------|
| 0-14        | $Y = -1.4879 + 0.0670X$ | 62.5      | 55.4-69.5 | (3-79) |
| 15-44       | $Y = 1.9394 + 0.485X$   | 63.1      | 57.7-68.4 | (3-80) |
| 45-64       | $Y = 2.8918 + 0.0553X$  | 38.1      | 32.9-43.3 | (3-81) |
| >65         | $Y = 3.4398 + 0.0668X$  | 23.4      | 19.0-27.7 | (3-82) |



- The actual lethality percentage,  $R_{HD}\%$  will decreased, if medical treatment for second degree burn injury is capable to treat more than 30% of total body surface area burned by thermal radiation.

For the societal risk, the frequency of  $F_{g,i,k}$  of accident outcome, k for release size i on segment, g and the number of associated number of fatalities, therefore the  $N_{g,i,k}$  can be estimated as:

$$F_{g,i,k} = T \cdot A \cdot R_i \cdot L_g P_{i,k} \quad (3-83)$$

$$N_{g,i,k} = CA_{i,k} \cdot PD_g \cdot CorrectedPF_{i,k} \quad (3-84)$$

where,

$CA_{i,k}$  is the consequences area associated with incident outcome k,

$PD_g$  is the population density for g,

$PF_{i,k}$  is the probability for fatality and injury.

To obtain results for the entire route, the modified expressions of individual and societal risk is applied to every segment of the route by using Eq. (3-3), Eq. (3-83) and (3-84).

### 3.3 Consequence Analysis

Consequence analysis involves determining the effects of the events of interest in terms of their physical extent and their severity. The physical extent is determined by calculating the maximum distances from the source at which the people are affected. The severity of an event of interest is expressed as a level of harm (such as injury or fatality). The approaches taken by HSE [8-10], TNO [172], and CCPS [11, 20-22] to analyze consequence analysis are similar to that used by most risk analysts which comprised a number of sub-steps:

- Source term modelling (i.e., characterise the event in terms of the rate at which the dangerous substance is released such as the temperature, pressure, velocity and density of the substance);
- Dispersion modeling (i.e., calculate how the dangerous substance will move through the surroundings);



- Fire and explosion modeling (i.e., for releases of flammable substances which may be ignited); and,
- Effects modeling (i.e., determine the effect of the released will have on people or structures such as buildings).

For the source term modeling, the correct phase of the outflow is important because it affects the flow rate estimated for a given hole in a vessel, pipe, or other containment device. In the case of loss of confinement such as road tanker, the hazardous substance will be released into the open environment. The release rate depends on the thermodynamic state of the substance and the geometry of the hole. Outflow from vessels through small holes can in general be considered to be stationery, meaning that the outflow is controlled by the (constant) upstream pressure. If the upstream conditions are changing gradually with time, the flow may be considered quasi-stationery. In the case of total rupture of a vessel, the content is released in a very short time. These releases are regarded as instantaneous. All of the above situations are possible to be predicted by using several established consequences model in the CCPS [11, 77], TNO [76] and Lees [64].

However, the solution became more complex if the accident phenomena occur at pressured liquefied gases condition and the outflow from vessel very potential to exist in three phases; gas outflow, liquid outflow and two phases outflow. Therefore to distinguish the complex scenario and predicted the basic scenario cases, the TNO model [76] is the most suitable used as the estimation method for these types of the outflow in this thesis..

Apart from that, for explosion modeling, It has been common to classify a gas explosion from the environment where the explosion takes place: vapour cloud explosion (VCE), Boiling Liquid Expanding Vapour Explosion (BLEVE), and missiles. For VCE, varieties of prediction models have been developed to predict the blast effect at any given distance from an explosion source. However, these models have limited range of applications. The major explosion models can be classified into; numerical models, TNT equivalence model, TNO Multi-Energy model and Baker-Strehlow method. Most of the numerical methods use the Computational Fluid Dynamics (CFD) approach. CFD models are not easy to use and still require



significant computer power. This requirement increases the cost and time needed for the simulation of the explosion process. Since TNT, and TNO models are simplified models, both models are used in this study. The rationales to use the both models are based on several factors such as these models were developed based on experimental results. These models are also easy to use and have a wide range of application, therefore many investigations are reported using them in risk calculation to predict a blast effects from the explosion hazard. Moreover, in case of explosion models, it is not easy to develop a new method or to modify any one from the old models due to both models dependence on computational programming and series of very intensive experimental works. It is well to note that the blast effects from vapour cloud explosions from TNT models are determined not only by the amount of fuel burned but, more importantly, by the combustion mode of the cloud. For BLEVE scenario, point source model and solid plume model are used in this study to analyze static and dynamic conditions. The standard techniques as in point source model for evaluating the thermal radiation from BLEVE events assume that the radiant heat flux is constant over the duration of the BLEVE fireball. However the assumption from the point source model is not suitable to estimate dynamic condition and leads to overly conservative predictions of hazard zones for injuries (i.e., second-degree burns). Thus, solid plume techniques is more realistic assessment of hazard zones and rationale associated with burn injuries when detailed analysis need to be conducted, due to the time-dependent nature of thermal radiation generated by a BLEVE fireball.

When a flammable gas is released into the atmosphere, different kinds of fires may occur depending on the release mode and the degree of delayed ignition. Thus, it is convenient to divide gas fires into the following types; flash fire, jet fire, pool fire and fireball. The established mathematical models of fires allows prediction of size and shapes of flames and impact of the thermal radiation incident at a target. Since the CCPS [11] is the most comprehensive techniques for fire modelling then it is used in the study by incorporated the result to Eq. (2-12) and Eq. (3.1). The rationale to used the models are referred on strong considerations to suit in their level of complexity and the extent to which they attempt to account realistically for the physical and chemical processes when the combustion take place. Moreover the approach of models correlations based upon actual incidents and large scale field tests. Subsequently, the assessment of accidental release and dispersion of hazardous



chemicals have necessitated the development of a number of techniques and methodologies. A release of large toxic may give rise to the following effects on man: death; non-lethal injury; irritation. In order to estimate the effects of a toxic release it is necessary to know the relationship between the concentration-time profile and the degree of injury [64]. Meanwhile, there are hazardous gases such as hydrocarbons, chlorine and ammonia, and oxygen, are capable of resulting in a gas cloud which is heavier than air. The density difference may be expected to have an appreciable effect on the behaviour of the cloud. Hanna et al., [123] and Pasquill and Smith, [117,118,121] provide good descriptions of plume and puff discharges. The basis for the Pasquill-Gifford model is Gaussian dispersion in both the horizontal and vertical axes. The standard formula for dispersion during an elevated point source assuming no ground absorption or reaction to reduce the uncertainties. Detailed descriptions of consequences modelling and an example of process calculation analysis using the consequences models in sequence are presented in Appendix 4.

Each sub-step requires a detailed calculation. Therefore, with the availability of computer programming, these effects calculation models can be performed faster and more effective. For this reason, a software name as SACTRA is developed. The development of this software is discussed in detail in section 3.7. All related consequences model equations used in this study could be referred in the Appendix 1 and Appendix 2. The final sub-steps and effects modeling will require information as below:

- The toxicological effects that the dangerous substance has on people at a different concentrations; or,
- The effects of heat from fires; or,
- The effects of blast from explosions; or
- Other effects such as the impact by missiles generated from the explosions.

The outcome of a particular release is depending upon a large number of factors, including:

- The type and amount of dangerous substance involved;
- The conditions under which the substance is stored;
- The weather conditions at the time of the event;



- The size of the event (in terms of how quickly the material is released and the quantity released); and
- The nature of the surroundings (e.g. – whether the substance is spilt on to concrete or water).

An important factor in consequence analysis is to determine the level of harm which is called the ‘dangerous dose’. The dangerous dose is the cause of the following effects to an exposed population:

- Severe distress to almost everyone;
- A substantial proportion requires medical attention;
- Some people are seriously injured, requiring prolonged treatment; and
- Any highly susceptible people might be killed.

The main reason for using dangerous dose as a harm criterion instead of fatality are due to societal concern about risks of serious injury or other damage as well as death and also because there are technical difficulties in calculating the risks of death from a hazard to which individual members of a population may have widely varying vulnerabilities [64, 67]. This matter has been discussed in detail in section 2.10 and section 3.2.

### **3.4 Route Segmentation**

The characteristic of a particular route such as population density, weather condition, topography, accident frequency and etc, could vary from point to point. Therefore, to facilitate the analysis, the route is divided into different segments such as urban, rural or sub-urban. However, when one or more factors change, a new segment needs to be defined. A new segment is required whenever a small or moderate differences between route segments is giving significant effect on the final risk estimate [21, 22]. As the number of segment to be analyzed increases, the estimation of risk can become more accurate and better in reflecting the actual risks present along the given route. However, the number of incident outcome cases analysis also increases. Generally, the accident scenarios do not change along the route except for special locations such as rail yards and harbors. Meanwhile, the consequence modeling results remain the same unless there is a major changes in humidity, atmospheric temperature, terrain or



wind speed along the route. Therefore, if the meteorology and weather data remain the same, the main parameters that will influence the route segments are the population density and the accident/ release frequency. These include the differences in the magnitude of the consequence associated with a release in the middle of a large urban area versus a release in a sparsely populated rural area or a change in the road type.

In areas where the bandwidth is large enough to encompass several population densities, there are two options to get the magnitude of consequences. One option is to create a new average population density for the whole area and another alternative is to determine the relative likelihood of the different potential hazard distances. If most of the time the hazard is significantly less than the distance associated with the worst case, then it may only use the density associated with the nearer zone and apply it throughout the bandwidth.

In the example shown in Figure 3.3, variations in other parameters such as accident rates could cause the segments depicted to be further subdivided.

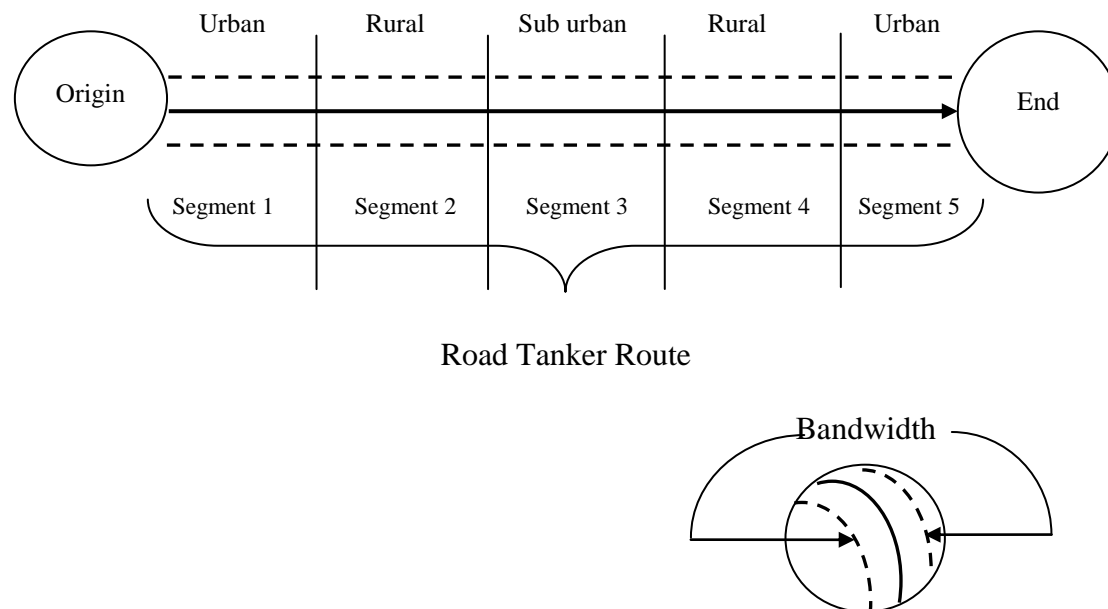


Figure 3.3 Route Segmentation.



### 3.5 Risk Estimation

In this section, the individual risk and societal risk are measured and explained in detail by using the proposed equations and parameters as demonstrated in section 3.2 and 3.3.

#### 3.5.1 Individual Risk

The individual risk at point  $Exp(x, y)$  is the sum of all risk sources from all links in the transportation route. The following steps should be employed to obtain the overall risk along a transportation route:

- Summing the risks created by all points on a link, and
- Summing the risks of all links in the route.

Figure 3.4, shows that as a vehicle transporting HazMat is passing through point  $Q(x, y)$  on link (l), a risk is posed on point  $Exp(x, y)$ . In order to calculate the annual individual risk (fatalities/year) at  $Exp(x, y)$ , the following input data are required:

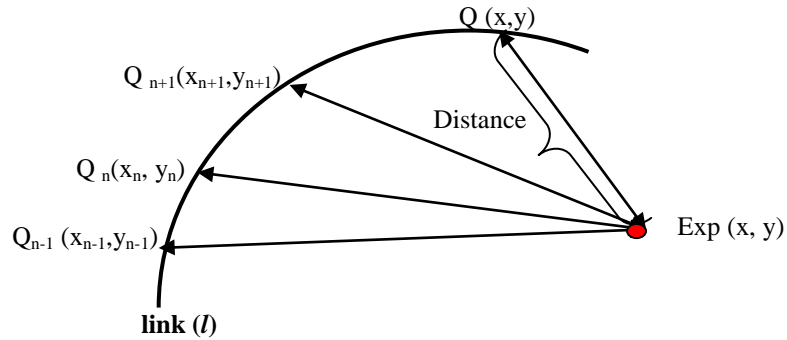


Figure 3.4 Diagram shows the relationships between link (l), point of release  $Q(x, y)$  and point of exposure  $Exp(x, y)$ .

- *Incident frequency.* It is a function of the following parameters: Lane width ( $x_1$ ), traffic volume ( $x_2$ ), adjacent of land use ( $x_3$ ), accident rate per kilometer ( $x_4$ ), meteorological condition ( $x_5$ ), surface condition ( $x_6$ ), truck trip ( $y_1$ ), container capacity ( $y_2$ ), container type ( $y_3$ ), type of truck ( $y_4$ ) and driver experience ( $y_5$ ). For a given transportation activity at a given route, all the parameters are constant, except the meteorological condition ( $x_5$ ), which is changing over the year. Therefore, the frequency at point  $Q(x, y)$  is a function of the meteorological condition or weather ( $x_5$ ) for a given transportation



activity.  $P_{\text{incident}}(\text{weather})$  denotes incident frequency. The number of weather conditions is denoted by  $N_{\text{weather}}$ , and the probability for each weather condition is  $P_{\text{weather}}$ . However, most of the parameters changed, if the same vehicle transporting HazMat is passing through various point of  $Q_{n-1}(x_{n-1}, y_{n-1})$ ,  $Q_n(x_n, y_n)$ ,  $Q_{n+1}(x_{n+1}, y_{n+1})$  on link (l).

- *Outcome probability.* If a release occurs following an incident, various outcomes caused by different magnitudes of release are possible. The probability of each outcome has been estimated using ETA as described in Appendix 3. The total number of outcomes is marked as  $N_o$ , and the probability for each outcome is marked as  $P_o$ .
- *Fatality.* The fatality or injury probability is a function of the consequence and of the exposure time (the exposure time is assumed constant for a given consequence scenario). The consequence can be the nature of the HazMat, type of release outcome, weather condition or wind direction. Therefore, for a given HazMat transportation, the fatality probability is a function of release outcome and the wind direction noted as  $F(\text{weather}, \text{accident rate}, r, w)$ . The number of wind directions is taken as  $N_w$ , and the probability of each wind direction is  $P_w$ .

The individual risk at point  $Exp(x, y)$  which is caused by the point risk source  $Q(x, y)$  is calculated by integrating the consequences associated with each wind direction over all wind directions, release outcomes, and weather conditions. This individual risk caused by a point risk source is known as a point individual risk (*PIR*):

$$PIR = \sum_l^{N_{\text{weather}}} \{P_{\text{weather}} \times P_{\text{incident}}(\text{weather}) \times \sum_l^{N_o=\max} \{P_o \times \sum_l^{N_w} [F(\text{weather}, o, w) \times P_w]\}\} \quad (3-85)$$

where,  $F(1.0) = (\text{ratio}(\text{HD}:\text{MD}:\text{MiD}:\text{UED})) = f_{\text{HD,MD,MiD,UED}}$ , therefore Eq. (3-85) can be applied as:



$$\sum_l^{N_w} F(weather, o, w) = \sum_l^{N_w} f_{HD,MD,MiD,UED} (weather, o, w) \quad (3-86)$$

And the total number of outcome release scenario can be calculated as:

$$(\sum_{j=1}^m L_{i,j} \cdot W_j \sum_{k=1}^{S_i} P_{i,j,k}) = (\sum_l^{N_o=max} P_0 \times \sum_l^{N_w} [F(weather, o, w) \times P_w]) \quad (3-87)$$

In Eq. (3-85), it is assumed that the vehicle is a stationary source at  $P(x, y)$ . However, whenever the vehicles are in motion, the effect of the velocity should be included into the model. A linear integration along the link, with respect to time ( $dt$ ), will include the component of travel time on the link risk value. The link individual risk ( $IR_l$ ) will then have the following form:

$$IR_l = \int_{origin, l=1}^{l=1, ends} PIR. dt \quad (3-88)$$

The sum of  $IR_l$  is along the entire transportation route will represent the total individual risk ( $IR$ ) posed on point  $Exp(x, y)$ . The total individual risk ( $IR$ ) then can be expressed as follows:

$$IR_{route} = \sum_{l=1}^{N_{link}} IR_l \quad (3-89)$$

Eq. (3-85) till Eq. (3-88), showed how the individual risk can be calculated to obtain the individual risk result along the link,  $l = 1$ . Whilst Eq. (3-89) is represent the number of links along the entire route. To simplify the TRA calculation results, the route is divided into segments in which the accident rate, population density, and other parameters contributing to the risk calculation are approximated adequately by a uniform distribution. Segment lengths are typically longer than the lethal distance arising from the worst scenario; therefore multiplying the route segment length by the accident rate will overestimate the risk frequency distribution. In this methodology, the risks from all scenarios occurring at a single point are computed and integrated along the link or route segment. Therefore, mathematically, the risk along a route segment or link is shown in Eq. (3-89), where the link starts at (*origin*,  $l=1$ ) and ends



at ( $l=1$ , ends). The effect area from a single lethality isopleths for a single scenario of all multiple locations along the route segment or link ( $l$ ) are illustrated in Figure 3.5. The effects area represent the outcome from concentrated flammable source, which can create an explosion and fire such as fireball, BLEVE, pool fire (in ring isopleths shape), and toxic material dispersion (in plume isopleths shape). From Figure 3.5 it was showed that the exposure point of x, y coordinate is originating from points P<sub>1</sub>, P<sub>2</sub>, and P<sub>3</sub>, but not in P<sub>4</sub>. All isopleths shape is identical for both fire explosion and toxic release accident scenario as shown in Figure. 3.5 and Figure 3.6.

To simplify the effects area calculation, this method will also use the assumption by Rhyne [25], which implies no azimuthally dependence of the isopleths calculation. According to Saccomanno and Shortreed [185], the accident frequency at point x, y can effect twice the lethality distance ( $d_1$ ) of the specific scenario release times the accident rate. This assumption is correct if the point is near to the route or link. However as value y approaches to  $d_1$ , the approximation decreases rapidly. Therefore, for a better approximation, the assumption proposed by Rhyne [25] is utilized which use the chord distance at x, y rather than twice the radius. The chord length at a distance y, from center of a circle radius r is:

$$\text{chord length} = 2\sqrt{r^2 - y^2} = 2r\sqrt{1 - f^2} \quad (3-90)$$

where  $y = f$  times  $r$  (radius),  $0 \leq f \leq 1$ . Parameter  $f$ , represent the changes probability of chemical release distance as value y approaches to  $d_1$ .

The chord length is combined with the accident rate to determine the frequency of release scenario,  $R_i$  from the transport container.



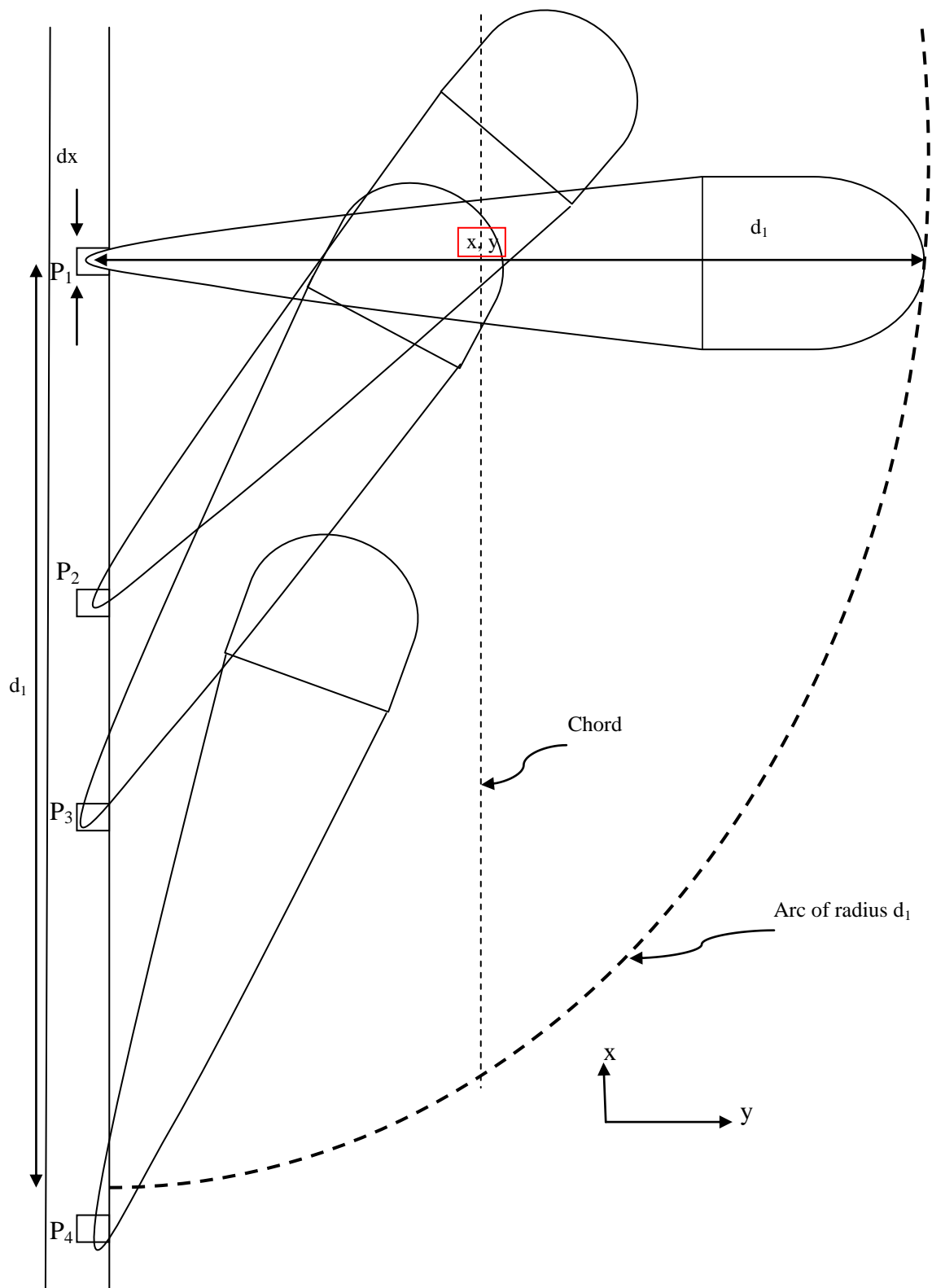


Figure 3.5 the individual risk for receptor at  $x, y$  coordinate of one scenario such as toxic release occurring at several locations



For the outcome of explosion and fire accident scenario such as fireball, BLEVE, and pool fire, the effect area for a single scenario at the point location 1 as shown in Fig. 3.6. The individual risk at  $x, y$  is same to  $x_1, y_1$  because the distance was same from point 1 to  $x, y, x_1, y_1$ . In this accident scenario, the outcome effects area is not influence by the wind direction.

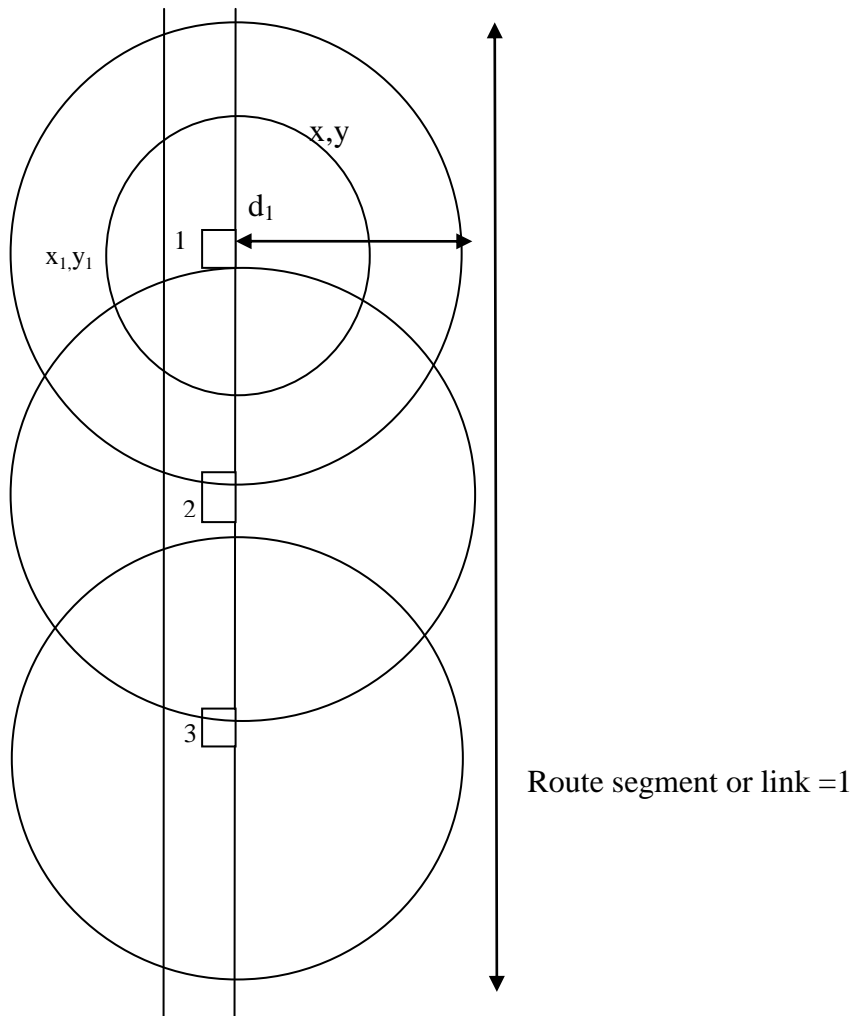


Figure 3.6 the individual risk for receptors at  $(x, y)$  and  $(x_1, y_1)$  coordinates of one scenario such as BLEVE occurring at several locations



### 3.5.2 Societal Risk Analysis

Societal risk is the risk to a population. It reflects the frequency of health effects (usually fatalities) in a specific population, as the result from exposure to a specific hazardous material. The societal risk is often expressed in terms of frequency distribution of multiple fatalities (f-N curve). The distribution of the population map for the transportation network is an essential input for societal risk calculation. The population map is composed of zones where people are assumed to be uniformly distributed. In this method, zones are defined based on shape, either rectangular or linear. Rectangular areas describe the off-route residential quarters, while linear zones represent the road network where motorists are present. Aggregation centers refer to particular areas where people are clustered, such as schools, hospitals, commercial centers, and other similar locations which are described as points or blocks. The total number of rectangle zones and the total number of linear zones in the network are marked as  $N_r$  and  $N_l$ , and the uniform population densities are denoted as  $\rho_r$  (persons/m<sup>2</sup>) and  $\rho_l$  (persons/m) respectively. The total number of aggregation centers is  $N_c$ , and the total number of persons in each center is  $P_c$ .

The number of fatalities in a linear zone is obtained by linear integration (first segment of Eq. (3-94) of the fatalities along the line or route, and it is a function of an outcome and a wind direction noted as  $F_l(wind, o, w)$ . In rectangular zones, the number of fatalities is obtained by integration (3-91) over the area of the rectangle noted as  $F_R(wind, o, w)$ . In an aggregation center, the number of fatalities is the fatality probability in the center multiplied by the number of people (third segment of Eq. (3-94) in the center noted as  $F_C(wind, o, w)$ . The number of fatalities over all zones, caused by a risk source  $Q(x, y)$ , under given release and given wind direction is calculated as follows:

$$N(\text{weather}, o, w) = \sum_{l=1}^{N_l} [\rho_l \times \int_L F_L(\text{weather}, o, w) dl] + \sum_{r=1}^{N_r} [\rho_r \times \int_A F_R(\text{weather}, o, w) dA] + \sum_{c=1}^{N_c} [P_c \times F_C(\text{weather}, o, w)] \quad (3-91)$$

By considering and applying an Eq. (3-3) for the injury impact from the outcome release to Eq. (3-91), along the line, rectangular area and aggregation centers, caused by a risk sources  $Q(x, y)$ , the new value of  $N(\text{weather}, o, w)$  is calculated as follows:



$$\begin{aligned}
N(\text{weather}, o, w) = & \sum_{l=1}^{N_l} [\rho_L \times (\int_L f_L^{HD}(\text{weather}, o, w) dl + \int_L f_L^{MD}(\text{weather}, o, w) dl + \\
& \int_L f_L^{MiD}(\text{weather}, o, w) dl + \int_L f_L^{UED}(\text{weather}, o, w) dl)] + \sum_{r=1}^{N_R} [\rho_R \times (\int_A f_R^{HD}(\text{weather}, o, w) \\
& dA + \int_A f_R^{MD}(\text{weather}, o, w) dA + \int_A f_R^{MiD}(\text{weather}, o, w) dA + \int_A f_R^{UED}(\text{weather}, o, w) \\
& dA)] + \sum_{c=1}^{N_C} [P_C \times (f_c^{HD}(\text{weather}, o, w) + f_c^{MD}(\text{weather}, o, w) + f_c^{MiD}(\text{weather}, o, w) + f_c^{UED} \\
& (\text{weather}, o, w))]
\end{aligned} \tag{3-92}$$

In this method,  $f$  is a probability of injury and fatality for four category of damages, whilst  $o$ , is a function of release outcome or  $S_i$  as in Eq. (3-3), which is influenced by parameters  $R_i$ ,  $L_{i,j}$ ,  $m$ , and  $n$  for the consequences area. The probability of having  $N$  fatalities under a given weather condition, release outcome, and wind direction is estimated by Eq. (3-93):

$$\begin{aligned}
F(N(\text{weather}, o, w)) = & T \cdot T_{NYI} \cdot T_{TP\%} \left[ \frac{1}{T_{NYI} \cdot T_{TP\%}} \pm 1 \right] \cdot A_{MIROS} \times P_{\text{incident}} \times P_{\text{weather}} \times P_{\text{outcome}} \\
& \times P_{\text{wind dir.}}
\end{aligned} \tag{3-93}$$

By considering all wind directions, it is possible to evaluate the probability of having  $N_n$  (or more) fatalities for a given weather condition and release outcome:

$$F(N_n(\text{weather}, o)) = \sum_l^{N_w} [P_{\text{weather}} \times \delta_n(\text{weather}, o, w)] \tag{3-94}$$

Where

$$\delta_n = \begin{cases} F(N(\text{weather}, o, w)), & N(\text{weather}, o, w) \geq N_n \\ 0, & N(\text{weather}, o, w) < N_n \end{cases}$$

In order to obtain the societal risk created by the motion of the vehicle over all the links or route segments on the consequences area is calculated as follows:

$$F(N_n) = \sum_{l=1}^{N_{\text{link}}} \sum_{o=k=1}^{N_{o=k}} \sum_{i=1}^{N_{\text{weather}}} \sum_{j=1}^{N_w} \int_L F(N_n(\text{weather}, o)) dt \tag{3-95}$$

Figure 3.7 shows how the societal risks are calculated for all routes to find the safest road network for transportation of hazardous materials.



### 3.5.3 Acceptability Risk

Outcome from risk assessment is usually compared to some criteria so that a decision can be made whether the risk is generally acceptable, tolerable or if it is unacceptable. Many countries throughout the world, including United Kingdom (UK), Netherlands, Hong Kong and Australia, have developed risk criteria or guidelines applicable to specific types of hazardous substance installation. In this study, the societal risk FN curves for various case studies are presented using U.K and Dutch governments societal risk guidelines. This is due to unavailability of societal risk guidelines developed by the Malaysian Government. For the assessment of the individual risk, the risk acceptability guidelines proposed by the Department of Environment (DOE) state that individual risks from an assessed facility should not exceed  $1 \times 10^{-6}$  fatalities per year for residential areas and  $1 \times 10^{-5}$  fatalities per year at neighbouring industrial sites are used for the acceptability risk result comparison to any hazardous materials activities and installation. Table (3.8) shows comparison of a few risk acceptability set by authorities in other countries.

Table (3-8) Acceptability Risk Criteria of Some Foreign Countries

| Country        | Broadly Acceptable<br>Region | Tolerable<br>Region  | Unacceptable<br>Region   |
|----------------|------------------------------|--|--|
| United Kingdom | $< 1 \times 10^{-6}$         | $> 1 \times 10^{-6}$ and $< 1 \times 10^{-5}$  | $> 1 \times 10^{-5}$ for public<br>$> 1 \times 10^{-3}$ for worker |
| Hong Kong      | -                            | -  | $> 1 \times 10^{-5}$ for public                                    |
| Netherlands    | $< 1 \times 10^{-6}$         | $> 1 \times 10^{-6}$ and $< 1 \times 10^{-5}$  | $> 1 \times 10^{-5}$ for public                                    |
| Singapore      | $< 1 \times 10^{-6}$         | $> 1 \times 10^{-6}$ - commercial<br>$> 5 \times 10^{-6}$ - industrial development<br>$5 \times 10^{-5}$ - plant site boundary | $> 5 \times 10^{-5}$ for public                                    |





114



### **3.6 Population Density**

Population density is an important parameter in the proposed TRA model. Therefore, the consideration the risk of injury or damage caused by the escape of hazardous materials to the surrounding population and area, or that might be caused by fire is crucial for risk analysis study. This is because the determination of the degree of injury and risk, which can be sustained, will depend on the extent of the presence and the nature of population distribution surrounding the area. Hence, an assessment of societal risk would require population data and information.

As the data relating to population at risk is important in risk assessment, head counts are paramount and are the leading protocol of work. The number of persons present is differentiated according to land use type and function (residential, commercial, industrial and recreational) as each varies in their nature of retaining people. As the occurrence of risk is full of uncertainty temporally, it implies a differential extent of exposure with regard to time (day or night) and location (indoors or outdoors).

#### **3.6.1 Population Data**

Population data is basically obtainable from population censuses. However, such data refers to macro situation in which the smallest administrative unit given in Malaysia Census is called 'mukim'. Hence it is little use for detailed population count and distribution analyses which is often needed for risk assessment. Nevertheless, they are invaluable source of information as initial and general population distribution and density in the area.

A more relevant source for detailed population analysis that relates to population census is population count at the smallest census unit (enumeration block). An enumeration block is a group of dwellings or households which are easily accessible without barrier such as crossing a major road, railway track, river, etc. Population data by enumeration block is obtainable on request from the Department of Statistics Malaysia, Department of Town and Country Planning Malaysia. Besides population



censuses, there are other secondary sources such as from published or unpublished data which are compiled in reports or files of various public or private authorities such as Local and Town Councils, municipalities, offices of housing developers, resort developers and Detailed Environmental Impact Assessment (DEIA) report.

#### *3.6.1.1 Population Data for Residential Area*

The determination of the number of people that might be affected within a calculated damage distance often refers to population data according to the type of residential area or buildings. The type of residential area or buildings requires determination of whether it is:

- Rural or remote or urban (density indication low for remote and high for urban)
- Sparse, linear or nucleated (indicative of distribution pattern)

In case of restricted nature or sensitive zone area, detailed population data is important. For determining rural population, besides field count, information on the number of households at village level could be obtained from the village heads committee. In Malaysia, the average number of persons per household was equal to 4.9~5.0 in the year 1991 and 4.6 in year 2000. However, it is recommended that the state average be utilized as the figure can vary from state to state according to the demographic feature of the respective state. In the case of large damage area; a more efficient method of data procurement would be via census with population breakdown according to enumeration blocks.

#### *3.6.1.2 Population Data for Commercial Area*

It is important to note on the onset of commercial activities that are present in the area. Generally, it is assumed that the daytime population size of the urban area or town of commercial areas is higher than the nighttime population. However, it is also important to note that townships in Malaysia often comprise shop houses, which signify higher night population as opposed to major central business districts that housed offices and shop lots which are normally devoid of population at night except for those that operate night shift.



#### *3.6.1.3 Population Data for Industrial Area*

Population of industrial area refers to those working in the surrounding industrial establishments. Population data for the industrial area is least complex as they can be obtained quite straightforwardly from the establishments.

#### *3.6.1.4 Population Data for Recreational Area*

Population of recreational area is refers to the type of recreational activities (in covered or open areas) and whether involve short stays such as in camping or with accommodation such as in resorts.

### **3.6.2 Population Present**

Although the present of the population is important to the calculation of both the individual and societal risk, but it is the time or when they are presence is more vital for risk calculation. It is known that the presence of population varies with time, as people travel out of their area to go to work, attend schools, window shopping or buying groceries and some are staying indoors. Therefore correct condition value has to be ascribed to calculating the time and the location of the population present.

#### *3.6.2.1 Day- time and Night- time population*

Daytime refers to the period from 7:00 hour to 19:00 hour GMT, whilst nighttime to the period 19:00 hour to 7:00 hour GMT. Some studies prefer 8.00 to 18.30 MET for day time and 18.30-8.00 MET for night time. Meanwhile, dividing the day and night hours to 12 hours apart each is based on the length of day and night around the equator which equal length of 12 hours each. As mentioned, population present varies with time; different values have to be used for the population during daytime and nighttime. In this method, residential area is defined as a land use in which the predominant use is housing (for habitant). These include single family housing, multiple family housing such as apartments, condominium, and townhomes. Zoning for residential use may permits some services or work opportunities or may totally exclude business and industry, which may either permit high density land uses or low density uses. The following rules are applied to determine the presence of population according to time:



- For residential areas the fraction of the population present during daytime ( $f_{\text{pop. night}}$ ) is set at 0.7 and the fraction present during nighttime ( $f_{\text{pop. night}}$ ) is 1.0 [76]. However it is recommended that a more refined basis for calculating the fraction of population present during daytime or nighttime for Malaysian cases. For instance the population present in the residential area during nighttime is approximately 100% at 1.00 a.m. Therefore GIS technology method such as IDW (Inverse distance weighted) is used to estimate presence of population may vary significantly for daytime and nighttime.
- The refinement refers to whether or not the residential area is rural or urban in nature as the occupational structure of the population in the two areas differ thus rendering a higher fraction for rural and a lower fraction for urban as more female go to work in the urban area. Even though in a low density area such differentiation may not be significant, in a high density area it can be considerable.
- In an urban area at least 3 out of 5 members are assumed to be away during the day either at work or attending school. Thus, the population present during daytime ( $f_{\text{pop. day}} = 0.4$ ) and the fraction present during nighttime or ( $f_{\text{pop. night}} = 1.0$ ). However, if the residential area is close to an industrial estate, it can be assumed that at least 0.05 household members are away from home working the night shift. In such case, the fraction of population present during nighttime is not 1.0 but 0.95. In rural area, the fraction of the population present during daytime and the fraction present during nighttime to 0.6 and 1.0 respectively.
- Another feature of residential area that has to be considered is the presence of either school or place of work or both.
- In commercial area, the calculation of population number, as stated earlier can be a loose estimation at best, especially in term of the transient population



such as commuters, shoppers etc. The fraction present during daytime is set at 1.0 and nighttime at 0.

- In industrial areas, the fraction of the population present during daytime is equal to 1.0. If some of the establishment carries out work in night shifts, the fraction of the population present during nighttime is the actual figure as determined by the field survey or a default value of 0.2 that is found to be characteristics of industrial area. If no work is done in night shifts, the fraction is equal to 0

#### *3.6.2.2 Indoor and Outdoor*

The location of the population either indoor or outdoor is matter in the calculation of societal risk. Populations at outdoors are exposed to higher risk than the population staying indoors. This is because it is normally assumed that indoors population would be partially protected by structures and clothing. Hence, different values are used for the fractions of the population dying indoors and outdoors whereby, fractions of the population present indoors is known as ( $f_{\text{pop. ind}}$ ) and outdoors as ( $f_{\text{pop. out}}$ ). Generally, more people are staying and working indoors than outdoors irrespective of time. Hence, the ( $f_{\text{pop. indoor}}$ ) is higher than the ( $f_{\text{pop. out}}$ ). Default parameter values used are 0.93 and 0.07 for day and 0.99 and 0.01 for nighttime for indoor and outdoor respectively.

### **3.6.3 Corrected Population Present**

The estimation of population present at the studied area is differentiated according to the type of land and its function. There are four types of land use which are known as residential, commercial, industrial and recreational. The institutions such as school, university and hostel are considered under residential land use. Firstly in order to establish the population data involved in the studied area, the total population of that particular area must be quantified. Secondly, the ratios between the different types of land use which is arranged from maximum to minimum ratio are adding up and the result is equal to 1.0. Thirdly, by following the above rules, the fraction of the population present during daytime and nighttime for each land is obtained.



In rural residential area, the fraction  $f_{\text{pop.day}} = 0.7$  during daytime, and 0.3 is away from home, at work or attending school and etc. In commercial area the fraction is 1.0 during daytime and this fraction value is also similar for industrial area and recreational area. The fraction value is equal to zero if the land use type was not existed at the studied area.

#### **3.6.4 Population Mapping**

The information regarding the population has to be mapped out before detailed distribution could be identified and determined. In this thesis, the population distribution is worked out into three phases: the spatial distribution, grid distribution and distribution by Risk Assessment Sector Diagram (RASD). Further discussion on this methodology, will be explained under the Geographic Information System (GIS) application.

### **3.7 Meteorology Condition**

The meteorological data records (Meteorological Department, Malaysia) available from the nearest meteorology station, which set the average weather conditions as follows: average temperature between 28 and 32°C in raining season and summer season with 70% humidity and a wind velocity of 3.3 to 5 m/s or 5.56 to 8.33 m/s. To get Malaysia meteorological condition included in transportation risk calculation, wind speed and stability should be obtained from local meteorological records whenever possible. Almost all meteorological data required can be found at Malaysian Meteorological Department (MMD) homepage as illustrated in Figure 3.8. Whenever these stability data are not available, Pasquill's simple table (Table 3-9) will permits atmospheric stability to be estimated from local sunlight and wind speed conditions. There are two type of weather combinations (stability and wind speed) which are used in many CPQRA guidelines such as D at 5 m/s (20 km/h) and F at 2 m/s (10 km/h). The first type is typically used for windy daytime situations and the latter for still nighttime conditions. Stability class D is more frequently used than class F because class D has produced satisfactory results and is easy to use [11, 21, 22].



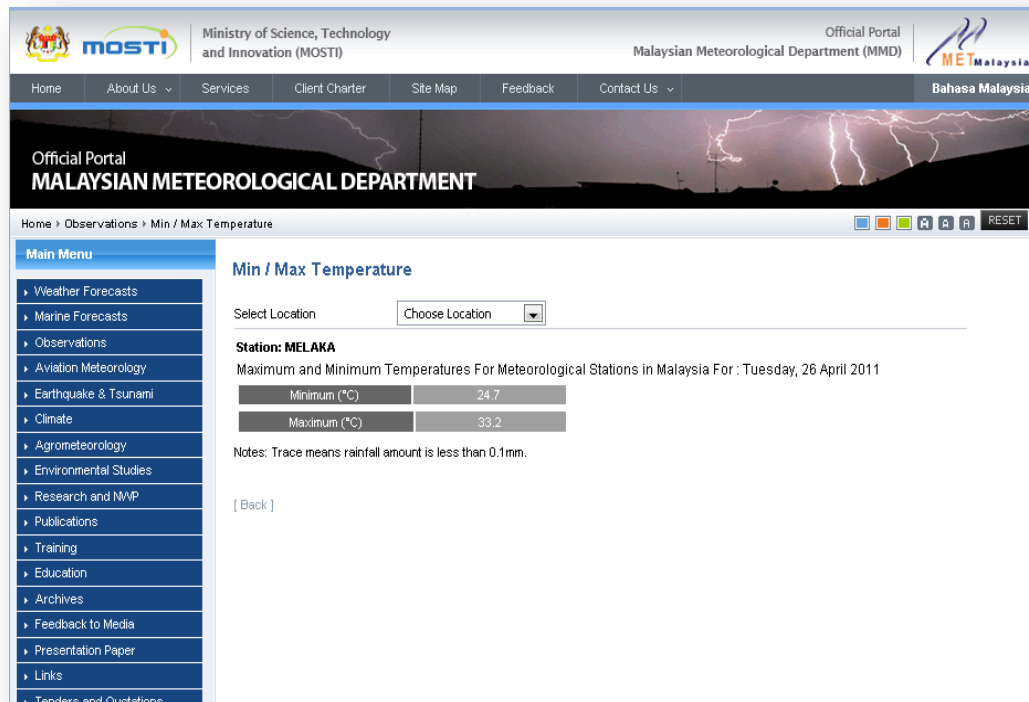


Figure 3.8 Malaysian Meteorological Department Homepage.

Table (3-9) Meteorological Conditions Defining the Pasquill- Gifford Stability Classes [20]

| Surface wind speed | Daytime insolation |          |        | Nighttime condition              |                       | Anytime |
|--------------------|--------------------|----------|--------|----------------------------------|-----------------------|---------|
|                    | Strong             | Moderate | Slight | Thin overcast or > 4/8 low cloud | > or = 3/8 cloudiness |         |
| < 2                | A                  | A-B      | B      | F                                | F                     | D       |
| 2-3                | A-B                | B        | C      | E                                | F                     | D       |
| 3-4                | B                  | B-C      | C      | D                                | E                     | D       |
| 4-6                | C                  | C-D      | D      | D                                | D                     | D       |
| > 6                | C                  | D        | D      | D                                | D                     | D       |

A = Extremely unstable condition  
 B = Moderately unstable condition  
 C = Slightly unstable condition

D = Neutral conditions  
 E = Slightly stable conditions  
 F = Moderately stable conditions



### **3.8 SMACTRA Description**

SMACTRA software is designed to be compatible with windows operating system (95, 98, XP, Microsoft Vista and Windows 7). The package is coded in VB language. The software is also designed to be able to work online by using php programming language to provide the accident impact analysis simulation results in the server. The package utilizes the latest ArcGIS version technique for geo-referencing and advance spatial analysis by performing the ArcGIS analytical model tool integrated with VB programming language under loose coupling technique.

SMACTRA consists of 7 main modules, namely: data, potential accident scenarios, event consequences, accident frequency analysis, event impact, risk estimation and risk evaluation. The data module handles general information related to the properties of the various chemicals, standard level of chemical risk exposure impacts and road characteristics. The potential accident scenario generation modules enables development of accident scenarios based on the properties of chemical involved, operating conditions and probability of the likelihood of road transportation accident and accident rates.

The event consequences analysis module is capable to forecast the nature and the severity of an accident. An accident frequency analysis module is a measure of the expected probability or frequency of occurrence of an event. This may be expressed as a frequency (e.g., events/year), a probability of occurrence at a particular time interval or conditional probability such as the probability of wind blows toward a populated area following the toxic gases release. The event impact module enables the estimation of the accident impact on human, environment and property. The risk estimation module combines the consequences and likelihood of incident outcomes from a selected incident to provide risk measurement. The risks for all selected incidents are individually estimated and summed to give an overall measure of risk. The risk evaluation module enables the results of a risk analysis to be used to make decisions either through a relative ranking of risk reduction strategies or through comparison of risk targets such as to find the safest route.



The functionality mapping and accident impact simulator (e. g . online BLEVE simulator) was developed to allow users to use SMACTRA as an effective graphical tool and capable to work online via PHP language programming. Users will be able to define accident cases by locating them on the maps and editing and then selecting them from the map. Therefore SMACTRA software makes it easy for process safety and risk assessment professionals to identify vulnerable locations as well as to integrate consequences results and develop the safest route.

The development of SMACTRA software can be divided into six distinct stages to enhance effective coordination of the various relevant activities:

- Planning the application;
- Designing the database;
- Building the graphical user interface (GUI);
- Writing the computer program;
- Integrate the ArcGIS Model Builder with SMACTRA application; and
- Testing and debugging the application (verification) through use of case studies.

### **3.8.1 Planning the Application**

At this stage, the objective is to identify various tasks that the application needs to perform. The second step is to identify how these tasks are logically related and to identify objects to which each task will be assigned. The third step is to classify the events required to trigger an object into executing its assigned tasks. Finally, a sketch of the graphical user interface is prepared. The application should have the capability to compute the hazards analysis from hazardous material transportation accidents. The application must be able to save the results in different formats and have the capability to generate graphs.

The next task was to identify information that is necessary for the execution of the program. The information was either user-provided information or internally generated information stored in a database in which the data can be retrieved. Analysis of this information assists in the selection of appropriate objects and controls therefore this information can be displayed on the GUIs and can accept input data from users.



The application was created by using some objects which were implemented through VB textboxes which allow data input by users and labels to provide identification of other objects in an interface. The VB has list boxes for displaying several options from which users can select the applicable options and command buttons that are used to initiate the event/s for each objects in the interface. Sketches of the GUIs for each procedure were made to show the expected structure of all the interfaces.

### **3.8.2 Designing Database**

In this study, many parameters are involved in the development and designing the software. Generally, the parameters are divided into several main components such as incident frequency, consequences model, risk estimation and evaluation, risk decision, and chemical products database. No database is required for risk estimation, evaluation and risk decision. But the database is essential to calculate the incident frequency and consequences model.

Since the hazardous transportation involved various types of chemical substances such as gasoline, liquefied petroleum gas, ammonia, liquefied natural gas, chlorine, therefore the material properties database is needed to show the physical and chemical properties characteristics of the chemical products. The physical and chemical properties data which has been used are based on the normal hazardous material transportation operation condition. However, the physical and chemical properties are dynamic according to meteorology condition such as humidity, atmospheric temperature and atmospheric pressure. To overcome this matter, several mathematical equations are used to calculate the result of physical and chemical properties such as density, volume, heat of combustion based on the meteorological changes. This is important to establish a precise result from the consequences model calculation. For example, to study the thermal radiation effect from a LPG tanker accident, the average value of the emissive power as the radiant heat emitted by the surface of the fireball has to be calculated. The calculation of emissive power is based on the theory of radiative fraction of the total heat of combustion as described by Robert and Hymes [20] in the Guidelines of CPQRA



[11, 19]. The heat of combustion ( $\Delta H_c^\circ$ )  $\text{kJkg}^{-1}$  is the energy which is released as heat when a compound undergoes complete combustion under a standard condition. The heat of combustion for fuels is expressed as the height heating value (HHV) and Low Heating Value (LHV). For emissive power calculation, the value of heat combustion is taken from LHV. The difference of the heating value depends on the chemical composition of the fuel. For instance, the value of the heat of combustion for propane by the road tanker transportation is in the range  $35000 \text{ kJkg}^{-1}$  to  $46500 \text{ kJkg}^{-1}$  depending on the country weather. Therefore the application uses Microsoft Access to store few common chemical substances in the database.

Information that is already recognised such as the physical and chemical properties of materials, special explosion properties, fire and toxic release are stored in the Microsoft Access and Microsoft Excel database and is automatically available to the application at run time making the retrieval and modification easier. For incident frequency, there are parameters such as accident rate, accident force types and force magnitudes, which are used in the calculation. The accident rate data is available from MIROS in which its application uses GIS databases to store the number of accident per vehicles and kilometre. Population density values relevant to each road were evaluated based on census, master plan project development report and published detailed EIA reports.

In SMACTRA, the data is store in GIS database or Microsoft Excel. However the phases of data acquisition and manipulation may be long, depending on the data format. For example different names or codes may be used in GIS database to identify the route segment, population density and land use activities. Figure 3.9 shows a flowchart of SMACTRA development.



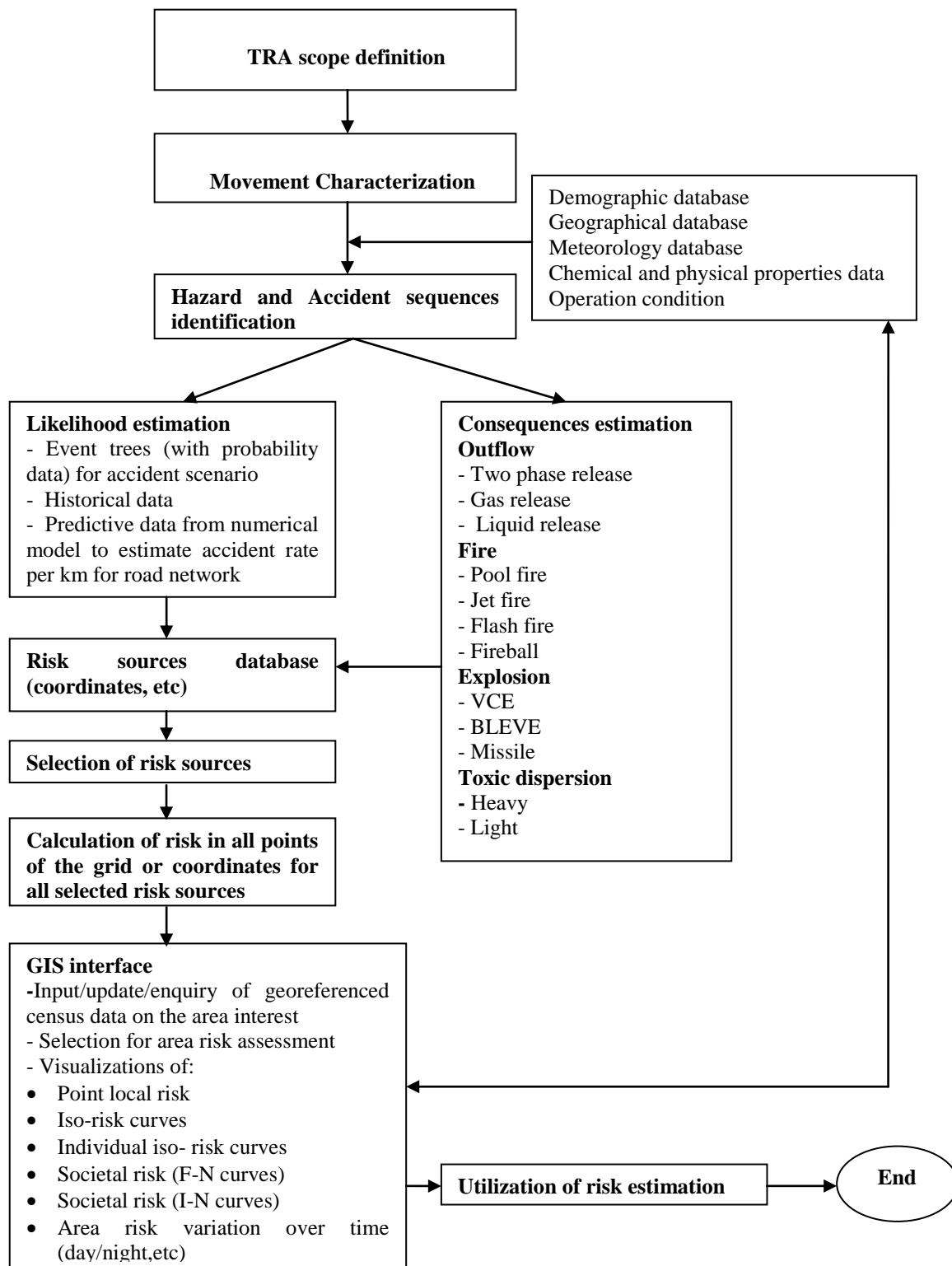


Figure 3.9 Flowchart of SMACTRA



### **3.8.3 Building the Graphical User Interface (GUI)**

A user interface is part of the program that is visible for human user. It can be as simple as a dos command line or as sophisticated as a virtual reality simulator. In the context of Visual Basic, the design of Graphical User Interfaces (GUIs) is based on object-oriented programming. It is displayed as one or more forms with attached tools such as text boxes, labels, buttons, picture boxes and etc. The tools are the objects and all the code which are associated with the object are written and attached to it therefore a form can be programmed. Each form has specific tasks defined by the functions of the objects placed on it. All the forms are logically connected. In all GUIs, information flows in the top to bottom and left to right fashion. VB is used to develop the application as front-end (GUI) and simulate the mathematical models for consequences modelling in the back-end (codes). The computation of the mathematical models for outflow, explosion, fire, toxic release, individual risk, societal risk are written in VB program, whilst the impact moving simulation are written in php online program by using JAVA script code. The main GUI component consists of project folder module, user create module, GUI control module and configuration setting module.

Error message is displayed by VB to assist the user while utilizing the system during programming. In this study, several interfaces were used for the different type of hazards calculations. To create an effective programme, a common code module can be added to a VB application. All programs written in this module and variables can be used by any GUI in the application.

### **3.8.4 General Interface**

The general interface is used to obtain selections for the user to evaluate the accident consequences. The general interface as shown in Figure 3.10 consists of eight menus; file, edit, view, scenarios, consequences models, risk assessment, database and help. These menus consist of submenus, which make “SMACTRA” user-friendly software. It also has a tool bar for fire, explosion, dispersion and etc. Figure 3.10 represents the main menu and available options of SMACTRA software. Further menus can be easily added in the future based on system requirements.



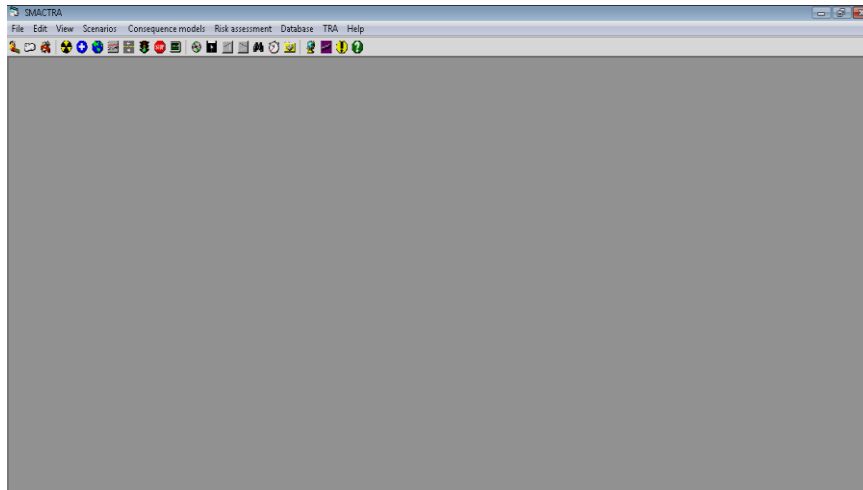


Figure 3.10: The main general interface.

### *File menu*

The file menu consists of several submenus shown as new, open, save, save as, print, and exit as shown in Figure 3.11. The submenus will appear by clicking on the main menus. For example, “Open” submenu will open the screen form as shown in Figure 3.12. “Save” submenu is used to save the current application under its original name while “Save as” submenu allows the user to save the current application under a new name without altering the original file. The “Print” submenu will print from either the current interface and its contents or a record from the output file. The “Exit” submenu will terminate the running application.

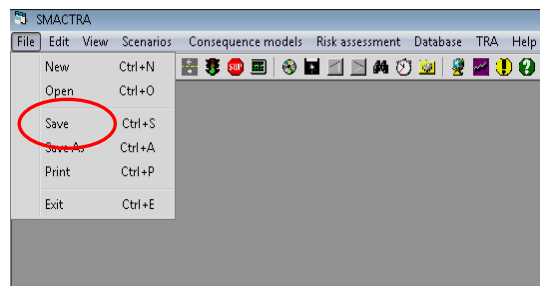


Figure 3.11: File submenus.



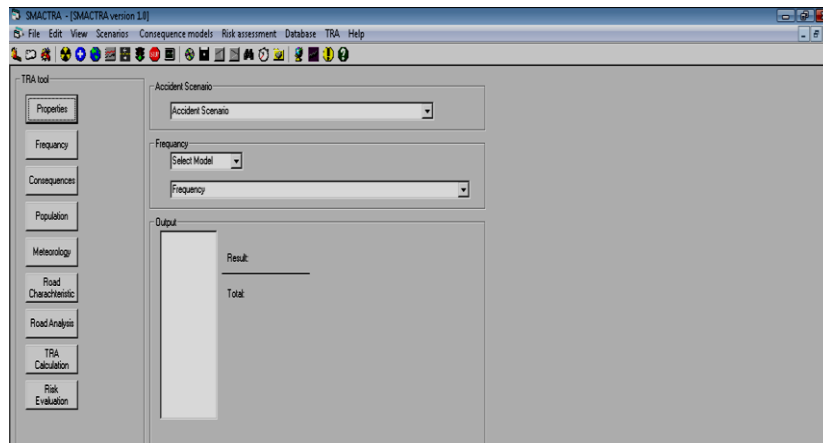


Figure 3.12: TRA interface form

### *Edit menu*

Edit menu consists of other submenus, such as cut, copy, paste, delete and select all. Fig 3.13 shows the submenus for the edit menu.

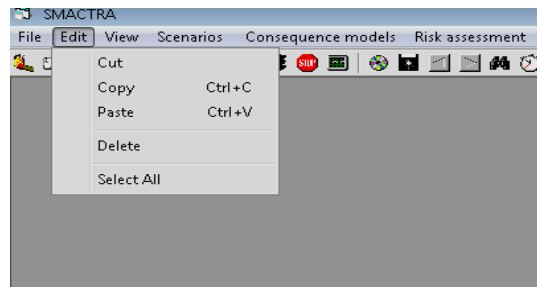


Figure 3.13 Edit submenus.

### *View menu*

Users can utilize the view submenus to select an image or images, to convert unit, calculator, toolbars, chemical and physical properties and impact. The impact describes the effect of transportation accident hazards to human and building structure. The image will display several types of chemical transportation hazards photos. Figure 3.14 illustrated the submenus for view menu

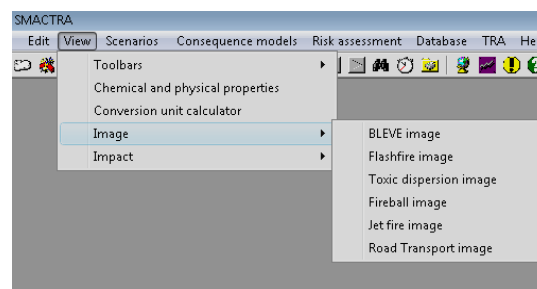


Figure 3.14: View submenus.



### Scenario menu

This application provides multiple options of accident scenario and its probability interest to start evaluation of the frequency of accident scenarios according to the model chosen. Figure 3.15, shows the scenario menus.

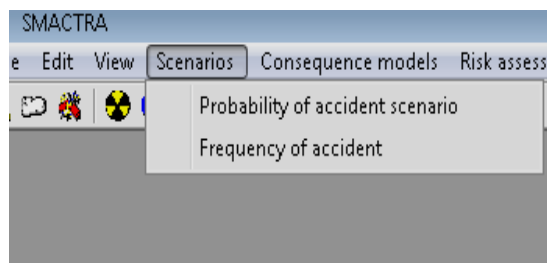


Figure 3.15: Scenario submenus.

### Consequence models menu

Consequence models menu consists of two main submenus which are consequences analysis models and vulnerability. The consequences analysis model is an important step in the risk management process. Therefore, after defined the accident scenario, source models are selected to describe how materials are discharged from the process. The source model describe the rate, total quantity (or total time of discharge) and the state of discharge either solid, liquid or vapor. For flammable releases, fire and explosion models will convert the source model information of the releases into energy hazard potentials such as thermal radiation and explosion overpressures. Figure 3.16 shows the example of consequences analysis model menu for heat radiation and combustion. From the submenus, user can define specific heat radiation model such as BLEVE (static case or dynamic case), fireball or pool fire. For pool fire, a user will have to options either pool fire analysis by using CCPS or Casal method [67].

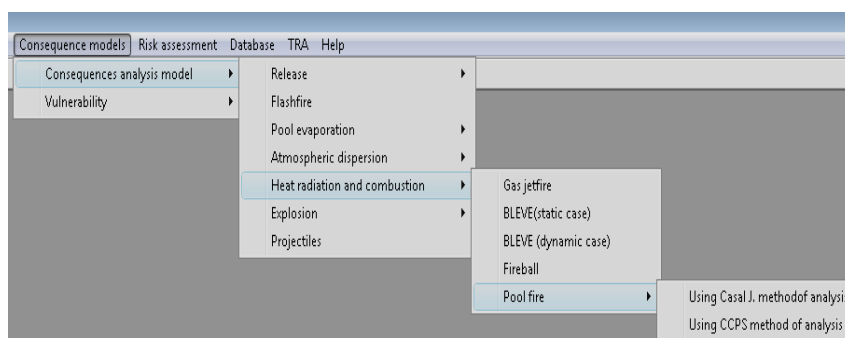


Figure 3.16 shows consequences analysis model menu.



The applications also provide vulnerability models which can predict the effect of an accident on human or property. Figure 3.17, shows the vulnerability submenus for toxic dispersion model which is subsequently will describe how the material is transported downwind and dispersed to different standard limits of concentration levels such as TLV, EPGL and IDLH.

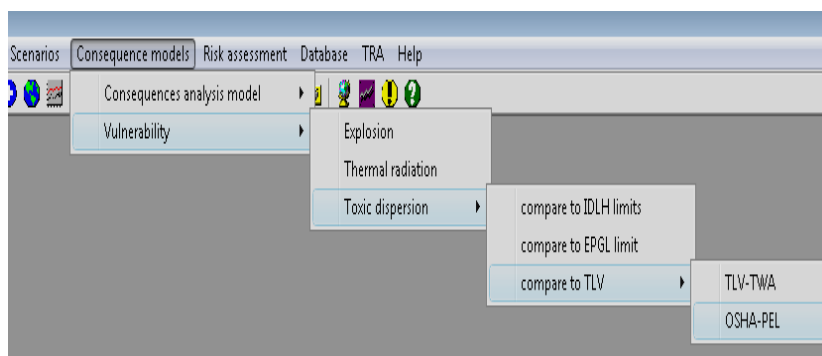


Figure 3.17 shows vulnerability main submenus.

#### *Risk assessment menu*

The final risk is determined by multiplying the consequences and the frequency of the accidents over time. The results of quantitative risk assessment are expressed as individual or societal risks. Figure 3.18 shows the risk assessment menu for the transportation risk analysis result.

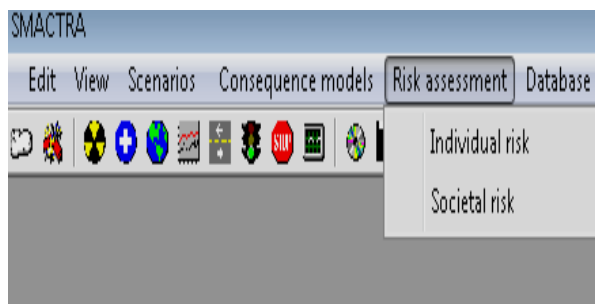


Figure 3.18 shows the risk assessment menu.

#### *Help menu*

This application is designed to provide a guide for the user while using the SMACTRA software. It also consists of other options to make the application more user-friendly such as; MSDS will help users to understand the characteristic of the transported materials. Users are highly encouraged to review SMACTRA's help to get more detail description of the models and their basis.



### 3.8.5 Incident Frequency Interface

The incident frequency interface has various profile selection for the accident scenarios. It provides the user many choices of accident scenarios, however only one accident scenario will be displayed at a time. Figure 3.19 shows an incident frequency interface which consist of 2 profiles selection box; accident scenario and frequency. For frequency profile selection box, a user has to choose the most suitable frequency model based on the characteristic of transported hazardous materials and the sequences of the incident. Event Tree Analysis (ETA) is advocated into the software programming to develop the propagation sequence of each scenario and to calculate the final probability for every type of consequences. The sequence of the incident events are based on three frequency models [22, 25, 67].

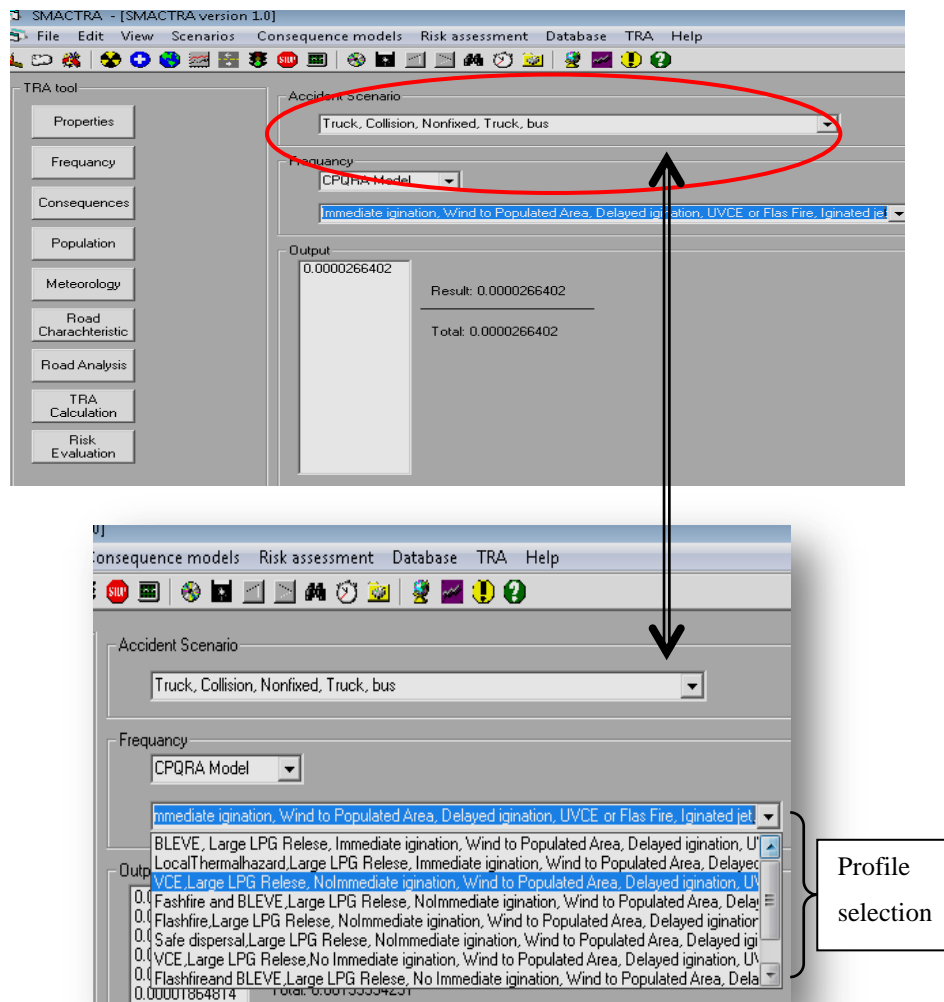


Figure 3.19 Accident scenario and frequency selection profile.



Users can calculate the total frequency for an accident scenario by pressing on the scroll down button on the keyboard until the total output value become constant. Figure 3.20 shows example of the frequency results.

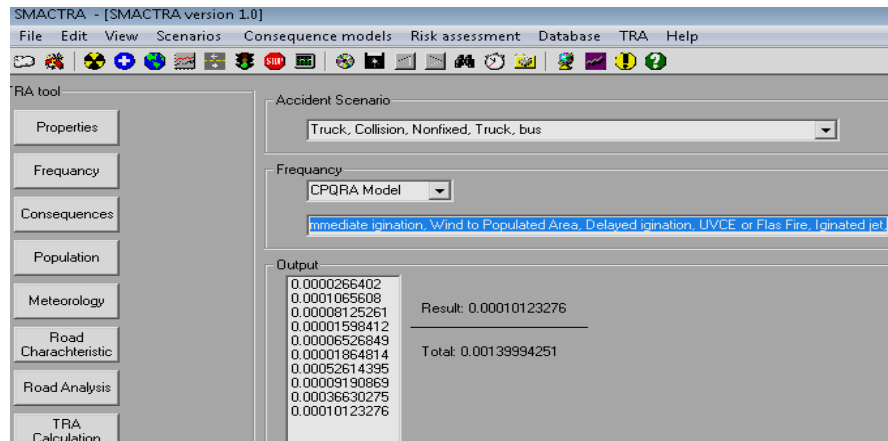


Figure 3.20 Final frequency output from the propagation sequence of the accident scenario.

### *Consequences scenario interface*

The consequences analysis interface is designed by using tabs control. It provides users many choices for selecting the type of hazards. Tab acts as an intermediate for other controls. Only one tab is active at a time, displaying the controls it contains to the user while hiding the other controls in the other tabs. Figure 3.21 shows consequences analysis interface which consist of four tabs; outflow, explosion, fire and toxic gas dispersion. The consequences analysis interface can be initiated by using the 'run' button or from the file menu.

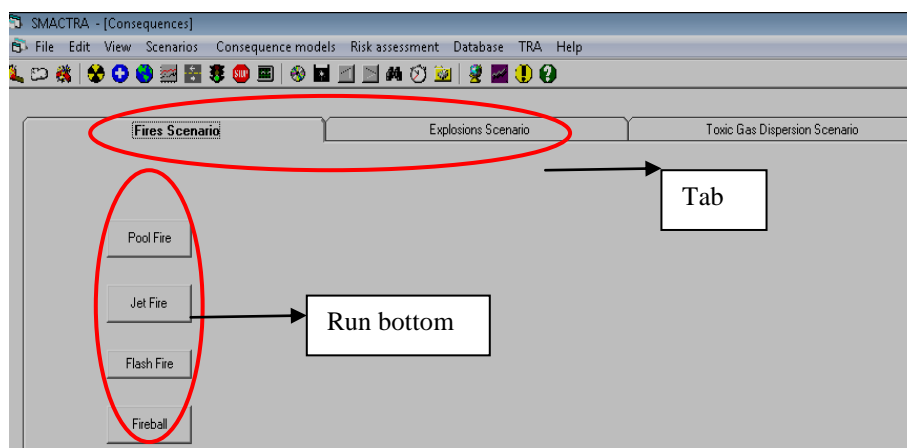


Figure 3.21 consequences analysis interface.



### 3.8.6 Fire Interface

Fire interface contains four buttons to estimate flash fire, jet fire, pool fire and fireball hazards. For example, if the user clicks on the pool fire button as in Figure 3.21, then the application will display the pool fire hazard form. Figure 3.22 shows the fire and pool fire forms. The pool fire form consists of many text boxes, inputs and outputs which allow the user to estimate the pool fire hazards.

#### Input Interface

This interface contains a list of various classifications and characteristics of material properties. The users can select their type of hazards and key in their inputs and properties to run the simulation process. The input values are typed in the textbox and the output will be displayed in the textbox (Figure 3.22) or list box (Figure 3.23).

The screenshot displays the SMACTRA - [Pool Fire] window. It features a menu bar (File, Edit, View, Scenarios, Consequence models, Risk assessment, Database, TRA, Help) and a toolbar. The main area is divided into several sections:

- Input Data:** Contains text boxes for Liquid leakage rate (0.1 m<sup>3</sup>/s), Heat of combustion of liquid (43700 kJ/kg), Heat of vaporization of liquid (300 kJ/kg), Boiling point of liquid (363 K), Ambient temperature (298 K), Liquid density (730 kg/m<sup>3</sup>), Constant heat capacity of liquid (2.5 kJ/kg.K), Dike diameter (25 m), Receptor distance from pool (50 m), Relative humidity (50 %), and Radiation efficiency for point source model (0.35 dimensionless).
- Point Sources Model:** Contains text boxes for Point source height (19.85869587197 m), Distance to receptor (77.58458482028 m), View factor (1.322023743473 dimensionless unit), Transmissivity (0.703710045794 dimensionless unit), and Thermal flux at receptor (6.118552163610 kW/m<sup>2</sup>).
- Result:** Displays calculated values for Vertical burning rate (1.19997837837 m/s), Mass burning rate (8.75984216216 kg/m<sup>2</sup>.s), Modified heat of vaporization (32.5737942524 kJ/kg), Diameter used in calculation (25 m), Area of pool (490.873852123 m), Flame H/D (1.58869566975 dimensionless unit), Maximum pool diameter (462.5 m), Flame height (39.7173917439 m), and Partial pressure of water vapor (1579.94709307 Pa).
- Solid Flame Model:** Contains text boxes for Source emissive power (25.97444820414 kW/m<sup>2</sup>), Distance flame axis to receptor (62.5 m), Flame radius (12.5 m), Flame H/D ratio (0.95151 dimensionless unit), Dimensionless distance from flame axis (0.732092976008 dimensionless unit), Transmissivity (0.732092976008 dimensionless unit), and Thermal flux at receptor (1.512648640563 kW/m<sup>2</sup>).

A callout box labeled "Text box" points to the "Flame H/D ratio" input field. At the bottom, there are buttons for "run", "CCPS analyst", "Casal analyst", and "Antoine eqns".

The screenshot displays the SMACTRA - [Physical and Chemical Database] window. It features a menu bar (File, Edit, View, Scenarios, Consequence models, Risk assessment, Database, TRA, Help) and a toolbar. The main area is titled "Constant Antoine Equation" and includes a "Select Chemical Substance" dropdown menu with "Propane" selected. Below this is a "Temperature" text box with the value "324". A "Calculated Result" section shows the "Saturation Vapor Pressure" as "17.48226152". A callout box labeled "Material properties" points to the "Select Chemical Substance" dropdown menu.

Figure 3.22 shows the pool fire forms.



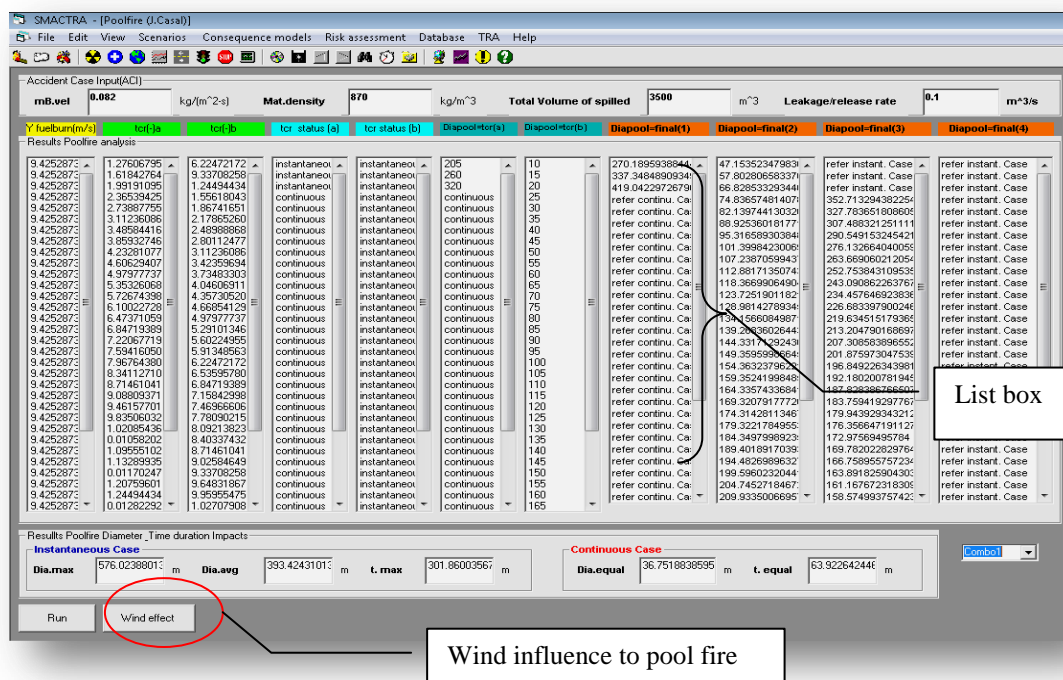


Figure 3.23 illustrates the calculation of pool fire hazard results via Casal method

### Output Interface

SMACTRA is designed to perform several calculation methods for different chemical hazards. The input factors are retrieved from the database and used for the analysis. The calculation results of pool fire hazard is presented in interfaces as demonstrated in Figure 3.20. The codes retrieve and process the information from the database and the result is displayed as GUI or text file which then can be printed or loaded in the Microsoft Excel or VB for plotting or GIS for mapping visualization.

By using SMACTRA, users can choose 2 types of analysis to calculate the hazard caused by pool fire by using either Casal (as in Figure 3.23) or CCPS method (as in Figure 3.24) [22, 67]. Figure 3.23 is also illustrates that the liquid spills can be defined into two categories known as instantaneous (as shown in blue font colour) or continuous spills (as shown in red font colour). SMACTRA has the capability to distinguish the spills categories by estimating a  $t_{cr}$  (i.e. critical time) over the duration and flow of the spill. Wind can have an influence on flame length however, recent study [67] found that the influence of wind on burning velocity,  $U_w$  is almost negligible at  $U_w < 2 \text{ m s}^{-1}$ . Wind can also tilt the flames and alter their bottom part (Figure 3-21), thus causing the flames to spill over the edge of the pool and elongating



the flame base. This can be highly significant if there is equipment nearby, as the level of thermal radiation will increased. The influence of wind to pool fire can be shown by clicking the wind effect button as illustrated in Figure 3.23. Figure 3.25 will be displayed when the wind effect button is on.

| dH <sup>a</sup> | y <sup>a</sup> max | mB        | Dia. max   | Dia. calc | Flame HD   | Pw         | Dist.receptor | Transmissivity | Es(t)      |
|-----------------|--------------------|-----------|------------|-----------|------------|------------|---------------|----------------|------------|
| 462.5           | 1.19997837         | 8.7598421 | 32.5737942 | 32.573794 | 1.46550588 | 1579.94709 | 85.95428362   | 0.69725150     | 8.38556689 |
| 462.5           | 1.19997837         | 8.7598421 | 32.5737942 | 32.573794 | 1.46550588 | 1643.14497 | 85.95428362   | 0.69479464     | 8.35572022 |
| 462.5           | 1.19997837         | 8.7598421 | 32.5737942 | 32.573794 | 1.46550588 | 1706.34286 | 85.95428362   | 0.69243868     | 8.32738708 |
| 462.5           | 1.19997837         | 8.7598421 | 32.5737942 | 32.573794 | 1.46550588 | 1769.54074 | 85.95428362   | 0.69017598     | 8.30017536 |
| 462.5           | 1.19997837         | 8.7598421 | 32.5737942 | 32.573794 | 1.46550588 | 1832.73862 | 85.95428362   | 0.68793869     | 8.27400294 |
| 462.5           | 1.19997837         | 8.7598421 | 32.5737942 | 32.573794 | 1.46550588 | 1895.93651 | 85.95428362   | 0.68569370     | 8.24879628 |
| 462.5           | 1.19997837         | 8.7598421 | 32.5737942 | 32.573794 | 1.46550588 | 1959.13439 | 85.95428362   | 0.68348253     | 8.22448927 |
| 462.5           | 1.19997837         | 8.7598421 | 32.5737942 | 32.573794 | 1.46550588 | 2022.33227 | 85.95428362   | 0.68131120     | 8.20102230 |
| 462.5           | 1.19997837         | 8.7598421 | 32.5737942 | 32.573794 | 1.46550588 | 2085.53016 | 85.95428362   | 0.68004524     | 8.17834141 |
| 462.5           | 1.19997837         | 8.7598421 | 32.5737942 | 32.573794 | 1.46550588 | 2148.72804 | 85.95428362   | 0.67822057     | 8.15639760 |
| 462.5           | 1.19997837         | 8.7598421 | 32.5737942 | 32.573794 | 1.46550588 | 2211.92593 | 85.95428362   | 0.67645348     | 8.13514529 |
| 462.5           | 1.19997837         | 8.7598421 | 32.5737942 | 32.573794 | 1.46550588 | 2275.12381 | 85.95428362   | 0.67474059     | 8.11454673 |
| 462.5           | 1.19997837         | 8.7598421 | 32.5737942 | 32.573794 | 1.46550588 | 2338.32169 | 85.95428362   | 0.67307879     | 8.09456166 |
| 462.5           | 1.19997837         | 8.7598421 | 32.5737942 | 32.573794 | 1.46550588 | 2401.51958 | 85.95428362   | 0.67146524     | 8.07515836 |
| 462.5           | 1.19997837         | 8.7598421 | 32.5737942 | 32.573794 | 1.46550588 | 2464.71746 | 85.95428362   | 0.66989733     | 8.05630096 |
| 462.5           | 1.19997837         | 8.7598421 | 32.5737942 | 32.573794 | 1.46550588 | 2527.91534 | 85.95428362   | 0.66837264     | 8.03796465 |
| 462.5           | 1.19997837         | 8.7598421 | 32.5737942 | 32.573794 | 1.46550588 | 2591.11323 | 85.95428362   | 0.66688694     | 8.02012143 |
| 462.5           | 1.19997837         | 8.7598421 | 32.5737942 | 32.573794 | 1.46550588 | 2654.31111 | 85.95428362   | 0.66544417     | 8.00274640 |
| 462.5           | 1.19997837         | 8.7598421 | 32.5737942 | 32.573794 | 1.46550588 | 2717.50900 | 85.95428362   | 0.66403642     | 7.98591696 |
| 462.5           | 1.19997837         | 8.7598421 | 32.5737942 | 32.573794 | 1.46550588 | 2780.70688 | 85.95428362   | 0.66266391     | 7.96931054 |
| 462.5           | 1.19997837         | 8.7598421 | 32.5737942 | 32.573794 | 1.46550588 | 2843.90476 | 85.95428362   | 0.66132459     | 7.95320844 |
| 462.5           | 1.19997837         | 8.7598421 | 32.5737942 | 32.573794 | 1.46550588 | 2907.10265 | 85.95428362   | 0.66001812     | 7.93749173 |
| 462.5           | 1.19997837         | 8.7598421 | 32.5737942 | 32.573794 | 1.46550588 | 2970.30053 | 85.95428362   | 0.65874185     | 7.92214311 |
| 462.5           | 1.19997837         | 8.7598421 | 32.5737942 | 32.573794 | 1.46550588 | 3033.49841 | 85.95428362   | 0.65749484     | 7.90714640 |
| 462.5           | 1.19997837         | 8.7598421 | 32.5737942 | 32.573794 | 1.46550588 | 3096.69630 | 85.95428362   | 0.65627584     | 7.89248643 |
| 462.5           | 1.19997837         | 8.7598421 | 32.5737942 | 32.573794 | 1.46550588 | 3159.89418 | 85.95428362   | 0.65508365     | 7.87814900 |
| 462.5           | 1.19997837         | 8.7598421 | 32.5737942 | 32.573794 | 1.46550588 | 3223.09206 | 85.95428362   | 0.65391718     | 7.86412078 |
| 462.5           | 1.19997837         | 8.7598421 | 32.5737942 | 32.573794 | 1.46550588 | 3286.28995 | 85.95428362   | 0.65277537     | 7.85038923 |

Figure 3.24 shows the pool fire hazard calculation following CCPS method.

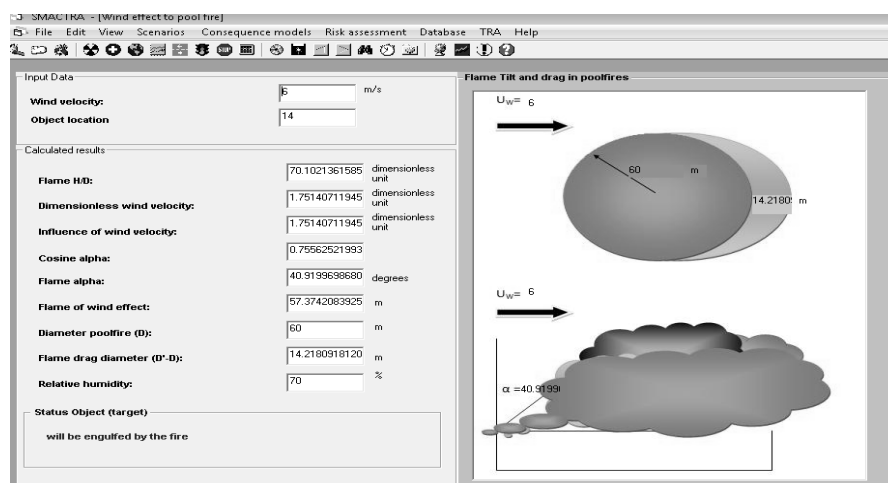


Figure 3.25 shows the wind influence to pool fire.

Jet or flare fires are characterized by highly turbulent diffusion flames. They exist from the accidental release of a fuel gas for example, through a broken pipe or a flange, from a relief valve or in process of emergency flaring. Accidental jet fires occurred in many parts of process plants or in transportation accidents and often impinge on the equipment. Therefore, large heat fluxes are produced from the high convective heat transfer caused by the combustion and the high flow velocities.



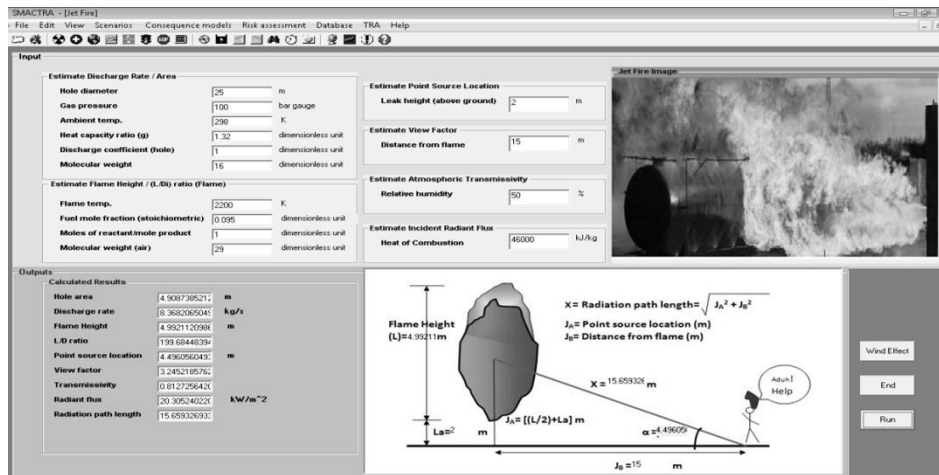


Figure 3.26 illustrates the calculation of jet fire hazard.

Wind can have a significant influence on the jet fire. The model proposed by Chamberlain [203, 204] describing the jet flames by the frustum of a cone (Figure 3.26) has been selected here.

### 3.8.7 Explosion Interface

The explosion interface is designed to calculate three types of hazards; Vapour Cloud Explosion (VCE), Boiling Expanding Vapour Explosion (BLEVE) and fragmentation. Each of these hazards has its own interface and each interface is capable of estimating different parameters. Figure 3.27 shows the parameters which can be calculated from the BLEVE hazard interface (i.e., the interface which appear in Figure 3.27 shows only the point source model to calculate the heat radiation from the BLEVE).

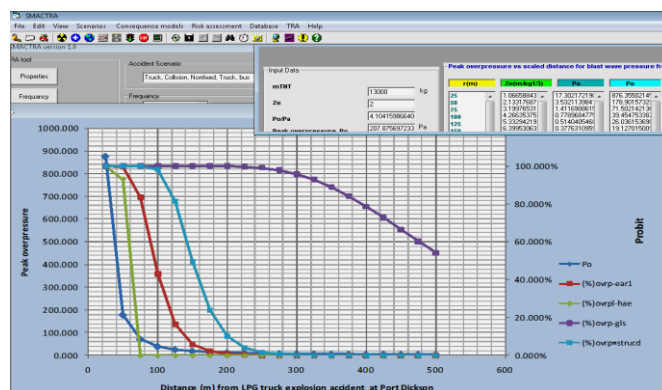


Figure 3.27 illustrates the calculation of BLEVE hazard with its graph analysis and output results for the incident scenario.



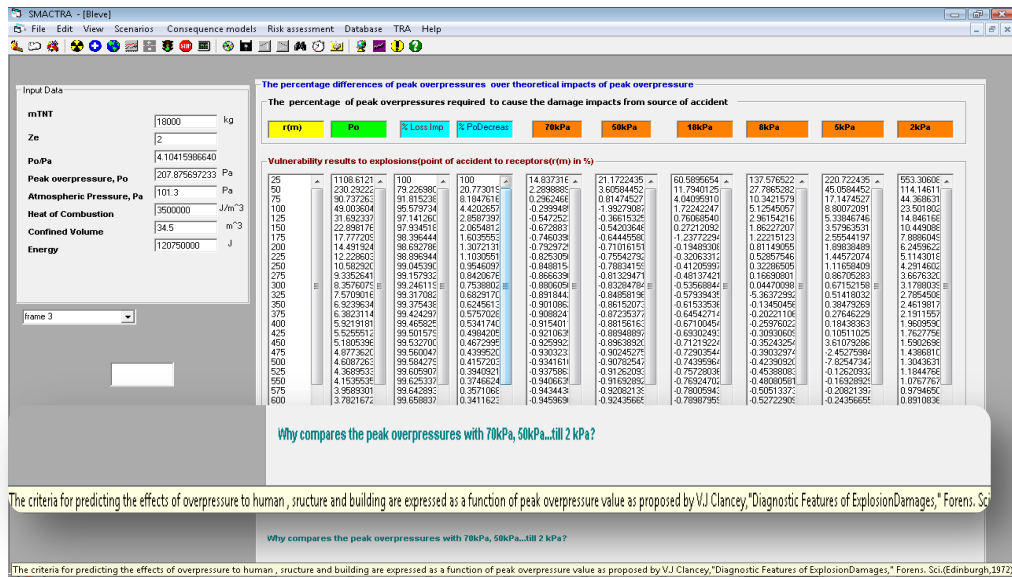


Figure 3.28 illustrates peak overpressure impact over the receptor distance to predict the effects of explosion to human, structure and building.

Figure 3.28 shows the relative percentage of peak overpressure impact over the receptor distance to predict the effects of explosion to human, structure and building in order to understand the vulnerability impact on the human and structure from various amount of (e.g. LPG) during HAZMAT accident.

SMACTRA can record the output result from BLEVE calculation. Any alteration to the input value for parameters such as mass of TNT (mTNT), scale distance (Ze), peak overpressure (Po), heat combustion ( $\Delta H_c^\circ$ ), confined volume and energy which can happen to the HAZMAT material can be analyzed by using comparison of graph effect calculation results as shown in Figure 3.29. For instance, based on Figure 3.29, as the input parameter mTNT increased from 3000 to 13000 or 20000 or 37000 kg of LPG, the damage zone on the human and building structure will also increased. This comparison can also be shown for only 4 data input. However VB can be programmed to analyze and compare more data input in a graphic form in a single interface. Figure 3.29 shows comparison analysis of the explosion effects calculation for road tanker carrying varies capacity of hazardous material over distance impact on human, structure and building



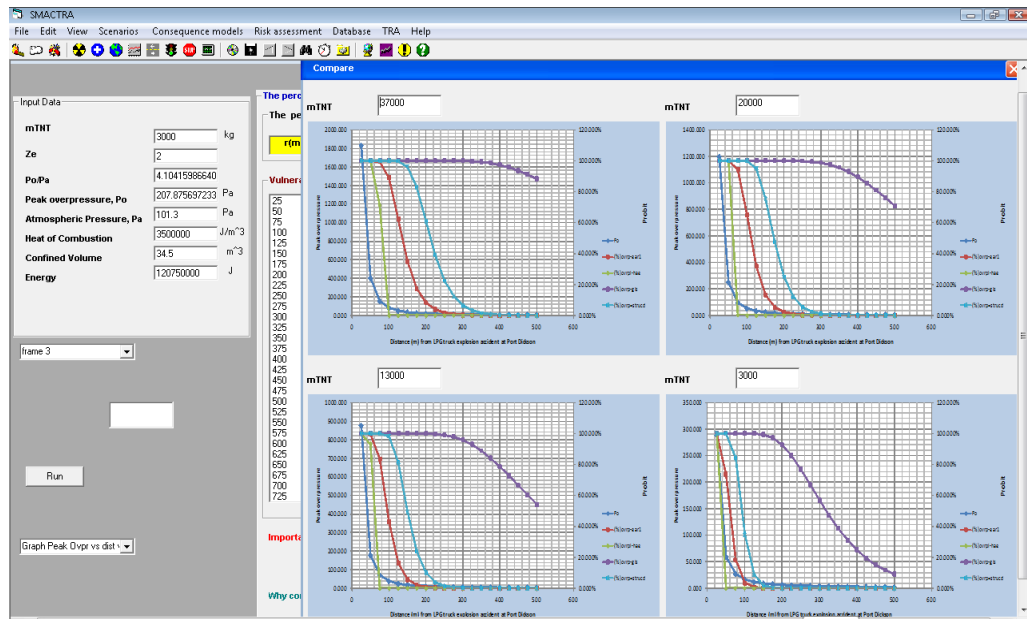


Figure 3.29 shows comparison analysis of the explosion effects calculation of road tanker carrying varies capacity of hazardous material over distance impact on human, structure and building.

SMACTRA can also perform fireball calculation by using various fireball models as shown in Figure 3.30. This figure also demonstrates the results of impact thermal radiation from fireball accident scenario towards receptor by calculating the amount of thermal radiation dose (DSE) in distance, time to feel pain ( $t_p$ ), vertical and horizontal thermal intensity. Graph analysis from the calculation result can be plotted from list of graphs analysis as chosen by the user.

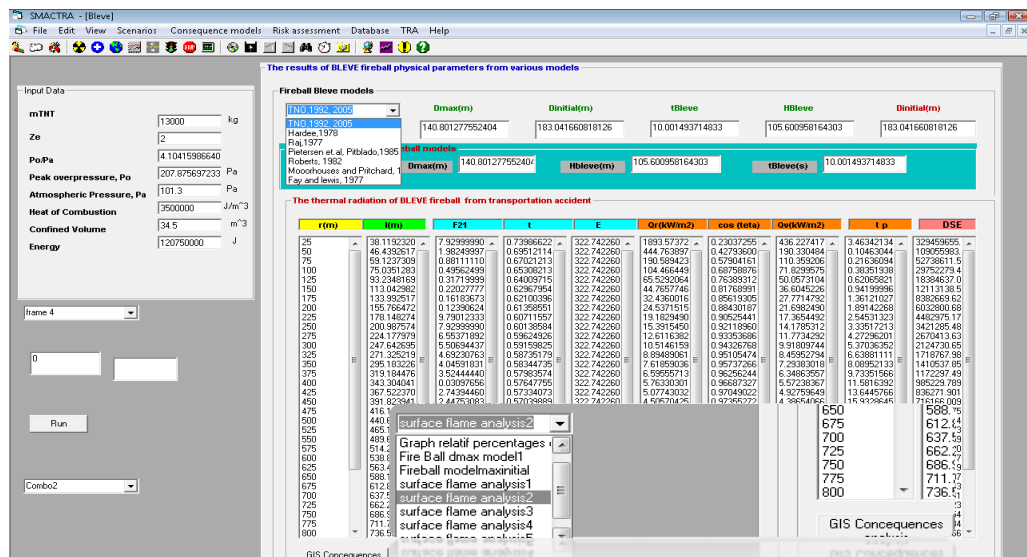


Figure 3.30 shows the BLEVE fireball and its vulnerability interface.



### 3.8.8 Toxic Release Interface

Toxic release interface is designed to estimate the effect of toxic material dispersion. The estimations are carried out for different atmospheric stabilities (stability A, B, C, D, E, and F). Figure 3.31 illustrates the toxic release interface. Input data and analytical results are shown in the text boxes. Toxic release zone from a tanker accident can be analyzed and shown on graph. For example, the graph below shows the toxic release zone in a plume shape graph.

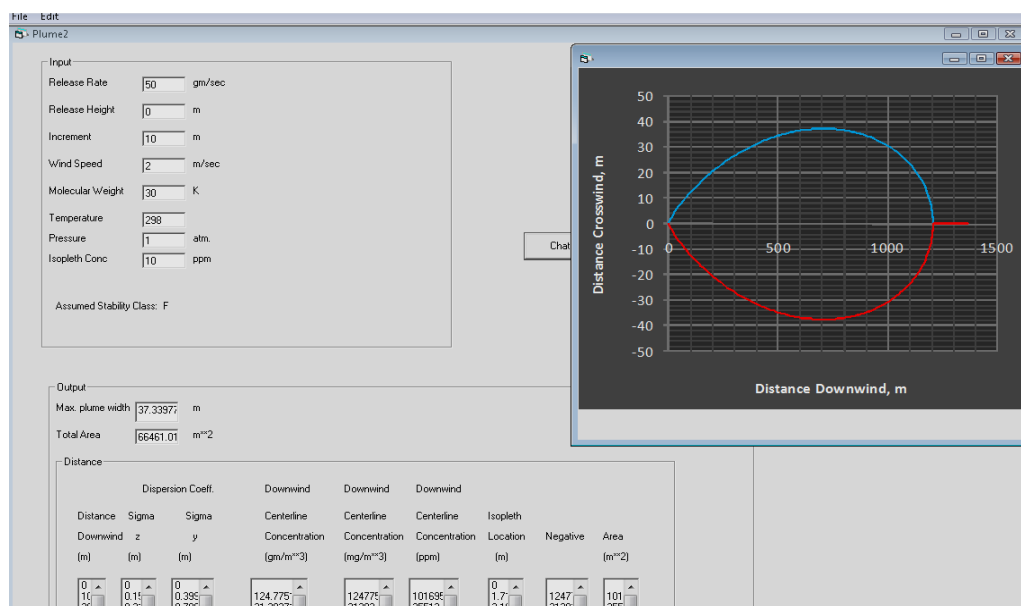


Figure 3.31 illustrates the toxic release interface.

### 3.8.9 Risk Impact Interface

Figure 3.32 shows the risk impact result from road tanker explosion. Within the interface, severity from fireball explosion is demonstrated based on duration and position of receptor from the source of accident. For example, the figure below shows that if the road tanker accident involved 13,000 kg of LPG, the maximum diameter for fireball duration can reach up to 10.01 s. By using SACTRA analysis, the severity of impact towards receptor according to  $t_{bleve}$  changes and the distance of the receptor from the source of an accident can be shown by colour risk indicator. Any receptor which received the highest risk impact, red colour will be shown as the risk output. For example, a receptor at a distance of 100m is expected to receive a very high risk impact at duration of 0.9s during the fireball accident event. Even though the risk colour impact showed a change between 0-10.01s but the effect of



impact on the receptor within 10.01s duration is perceived as the worst case scenario, which is red colour. However if the receptor is at 100m and appeared at the even after 9.01s during the fireball accident, the risk impact result will show that the receptor only suffer low risk impact. This is because during explosion a fireball growth phase is observed when the time,  $t_{bleve}$  reached, 9.01s the fireball is already located at 105m height from the ground level with the distance from the flame surface and the target,  $l_m$  is at 75.04m as calculated in Figure 3.30.

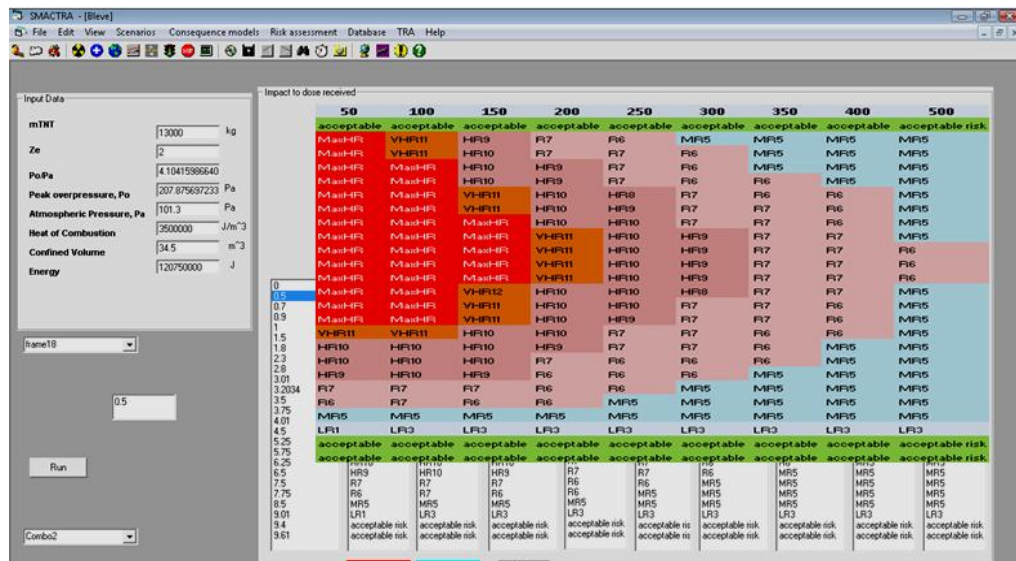


Figure 3.32 illustrates the risk impact interface.

### 3.8.10 Transportation Risk Analysis Simulation (TRIS) in SMACTRA

Simulation for transportation risk analysis as shown in Figure 3.33 till Figure 3.35 is for BLEVE fireball calculation case. By utilising this simulator, the risk impact from fireball road tanker accident bleve can be studied for a larger area since the map for the studied area requires the google online map. As an example, input simulator will ask the user to enter the information for the road tanker route (direction origin to destination) then the simulator will focus on the particular area on the map which needs to be analyzed. By using this simulator, the entire route involved during transportation with the route distance will be shown in detail. The route used by the simulated tanker will be shown in blue colour. The advantage of using this simulator, it creates a more interesting and interactive informative image for example all the building and surrounding environment will be shown as 2D or 3D image based on the map version.



### Control Simulation Driving Simulator

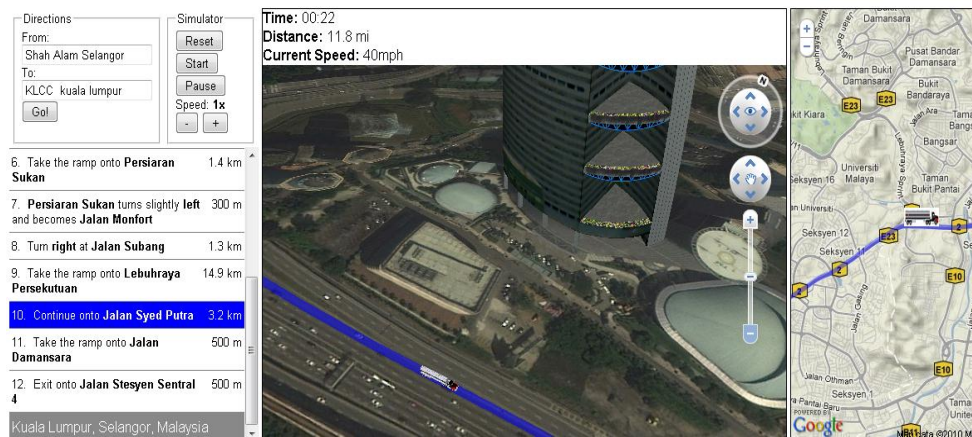


Figure 3.33 shows the online driving simulator.

The affected zone which involved the destruction of either buildings or infrastructures can be illustrated by the map as shown in Figure 3.34 and Figure 3.35.

### BLEVE Thermal Flux - Driving Simulator

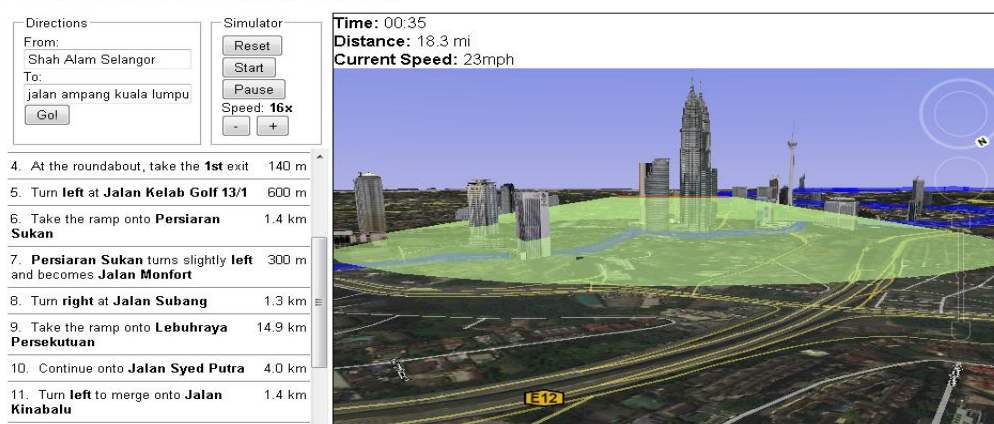


Figure 3.34 shows the BLEVE fireball impact using online simulation.

### BLEVE Thermal Flux - Driving Simulator



Figure 3.35 shows the BLEVE fireball impact at panoramic view.



### 3.8.11 SMACTRA Contour Panel for GIS Presentation

The contour display panel in SMACTRA will provide with geographic based analysis results. For example, in Figure 3.36 after the calculation of fireball consequences in VB, the result can be plotted in GIS interface by pressing on the GIS button which is available in SMACTRA. In GIS interface the consequences result can be plotted based on the X, Y coordinate input. With this method, a user can predict the affected zone with its content (houses, industrial zone, road etc) within the fireball diameter. All information are integrated in GIS by creating a map that shows location of the object (the house) and the range of land use in a specified colour coding. Unlike the common GIS system where the software has to manipulate every separate layer manually, SMACTRA can perform this task automatically. The SMACTRA software will create the base map (from the combination of map layers) which is also known as the background map and later will project into ArcGIS map via map projection method to present the coordinate.

In order to create and use the base map in SMACTRA consequences risk analysis, a user has to undergo a map projection method called georeferencing. Amongst the advantages of using the GIS application in SMACTRA is its capability to overlays the results of the models automatically on the base map at the right place and on the right scale. Line thickness, filling patterns and colors are set automatically and they can be modified afterwards whenever necessary.

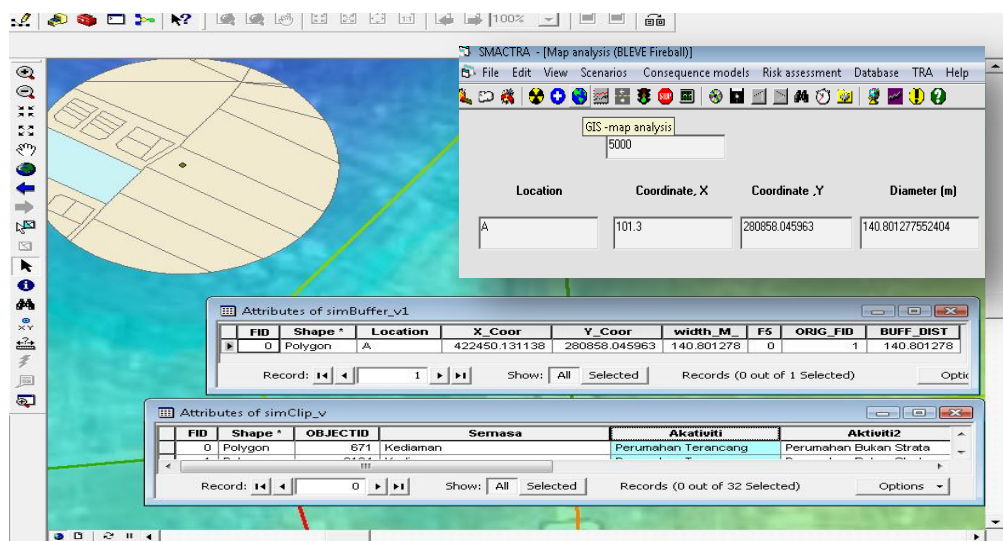


Figure 3.36 shows GIS map analysis using SMACTRA.



### **3.9 Writing the Computer Programme**

The SMACTRA program is written in the standard Microsoft Visual Basic 6.0 and distributed in an object format with the source code. After creating the interface for the SMACTRA application, a code is written to define the applications behaviour. VB makes code writing easier with features that can automatically fill in statements, properties and arguments. The computation of the mathematical models for the chemical hazards will be simulated using VB program (code).

For instance, once the user loads the pool fire hazard analysis form (Figure 3.19), a connection between the hazard analysis form and the database will be established. The product names will be listed into the product name combo list. The next calculation procedures for whole operations will depend on the selected product name (from product name: propane).

SMACTRA programme has several subroutines, which allow the users to simulate the scenarios. For example to estimate the impact of VCE to humans, the Run Click event performs two operations; first to retrieve the data from the database and second to run the mathematical models by using the input values. Finally it will display the outputs in the lists or text boxes. The graphs analyses for accident scenario output can be plotted by clicking on the chart button after calculate the input data. The Save Click event performs three operations; first, open the save dialog, second, set the filter of the save dialog to document or text, and third, create the output file.

### **3.10 Development of GIS**

GIS allows hazards of chemical materials and view all of the necessary deployment data in place. Data can be added, subtracted or modified with the computer mouse operations and the alternative plans can be created, analysed and modelled by using GIS. Although computerized mapping systems have been around for many years, recent improvements have made GIS software available on the desktop and on laptops. GIS software can now be used by non specialists to improve planning, analysis and response. These tools offer managers the ability to eliminate much of the guesswork that has been the norm in tasks such as sitting stations or deploying apparatus.



### 3.10.1 Integrating SMACTRA Application with GIS

The integration of the Visual Basic and ArcGIS 9.3.1 is required to integrate the map that is created in ArcGIS. The work flow diagram was shown in Figure 3.37

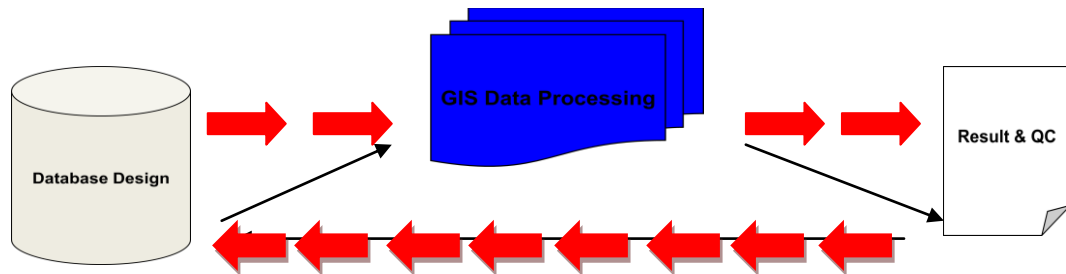


Figure 3.37 Work Flow of GIS Integration.

GIS can handle two types of data, vector and raster data. Vector data are defined as a pair of coordinate and present very accurate coordinate geometric information with small data storage requirement. Raster data are defined as a grid of cells and each cell represents a finite portion of geographic features. In GIS data processing as shown in Figure 3.35, the analyst will select the specific document or maps that need to be digitized (either scan map or Google map in jpeg\_file). Digitized is the transformation of raw information from analog format such as paper map to digital map, so that it can be stored and displayed in computer. To perform onscreen digitizing based on scanned topographic map, there are major tasks to be performed prior to the digitizing process as shown in Tables 3.38 and 3.39. These tasks are listed hereunder:

#### 3.10.1.1 Database Design

- *Data preparation and control point selection*

The analyst will select the specific document or maps that need to be digitized. The map should be inspected in term of scale, graphic, representation and implanted error. Control points are a set of point on the ground in which their





### Database Design

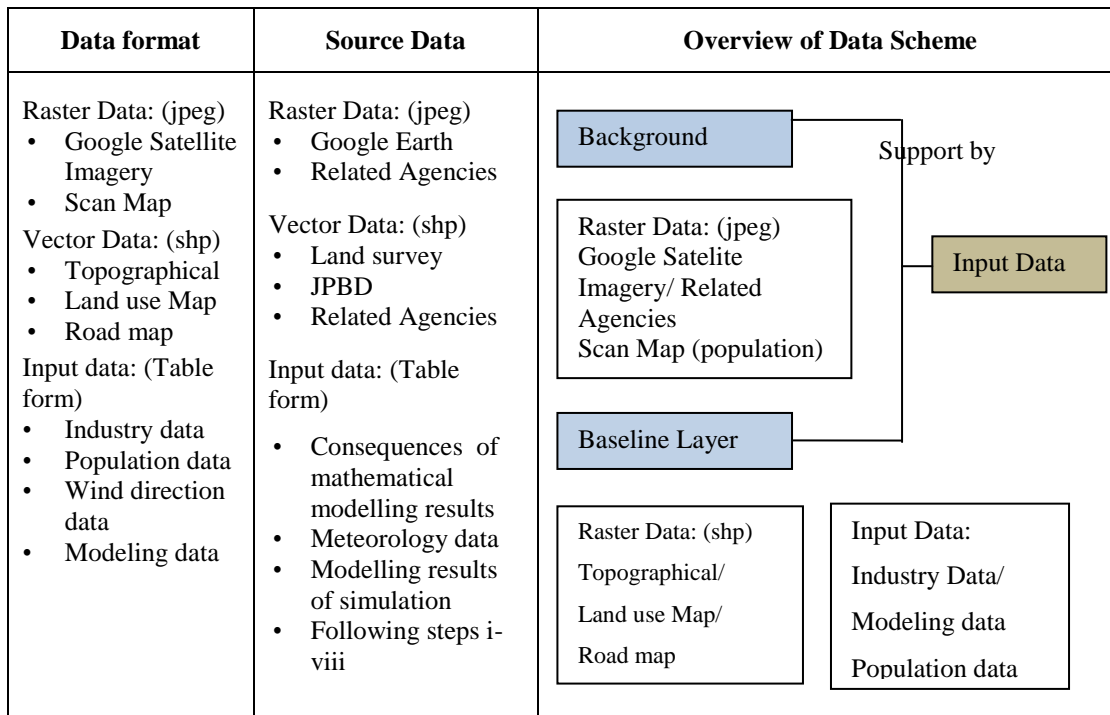


Figure 3.38 database design VB to Arc GIS.



### GIS Data Processing



### Result and Quality Control

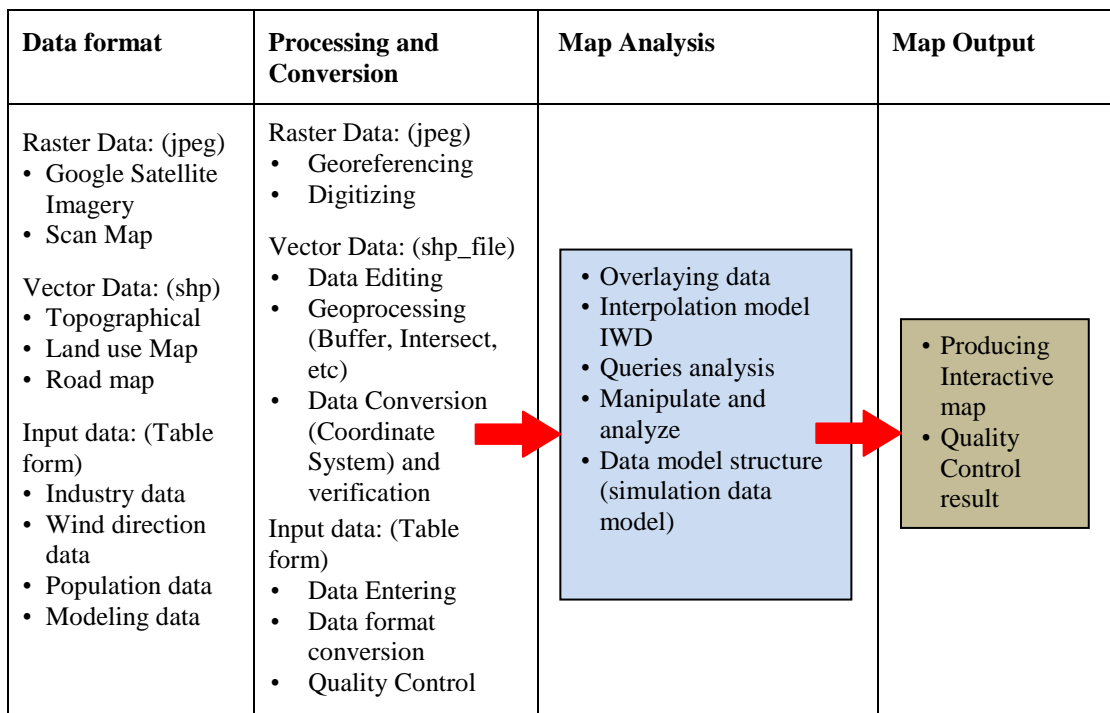


Figure 3.39 GIS Data Processing VB to ArcGIS Model builder tool.



horizontal and vertical location is known. The point is obtained from a known location with a coordinate or projection system. This study has used N. Sembilan map which was obtained from JPBD, DOE and related agencies with available data of the road, river, building, industries and topographical map.

- *Consequences from mathematical modeling road tanker accident results*  
The accident consequences results from VB will be integrated to ArcGIS model builder tool via loose coupling method. This method will be discussed in section 3.9.2.

#### **3.10.1.2 Data Processing**

- *Image registration and rectification*  
The raw data is processed by registering and rectifying them through powerful computer. It is performed using geo-referencing tool in ArcMAP to prepare the base map to initiate screen digitizing.
- *Database management and layer designation*  
The analyst will review the rectified image and identify the potential feature for digitizing such as contour, road, building, rivers, district area and etc. Then the database management and layer designation based on the analysis of the images are developed. Database management and layer designation task is conducted by using ArcCATALOG environment.
- *Digitizing and data editing*  
After the layer designation and database management have been conducted, the rectified image is digitized either by using ArcCATALOG or ArcMap environment. The objective of digitizing is to transform of information from analog format such as paper map to digital map. Features, events, and activities with a spatial component are modeled as points, lines, polygon, nets or links to form the geographical relational database. Lines are used to represent road, river, rail and something like a network. Polygons are used to model features of an area such as location, shape, dimension and building.



- *Attribute data editing*

Editing of attribute data is done by using ArcCATALOG which also capable to add new feature class to the data. This is important to extract out the information and do the analysis. This data is recorded in a table form and known as attribute data.

- *Map analysis and output*

Lastly, the analyst can do the analysis such as proximity analysis, buffer zone, and simulation, intersects and merges. Subsequently an interactive map is created based on the developer creativity.

### **3.10.2 Integrate VB Output to ArcGIS Model Builder**

Geographic information systems are the powerful computer-based tools to capture, store, manage, retrieve, query, analyze and present spatial data. GIS ability as spatial data processing and analyses tools can be used to manage a wide range of information. GIS also facilitates the integration of disparate data sets, creates new data sets, develops and analyze spatially explicit variables. In this study, all equations and parameters in the proposed TRA model such as consequences models, effect models, and risk calculations are programmed in VB 6. Loose coupling approach will be used to integrate the consequences and effect results calculations from VB6 to GIS. Loose coupling is an approach to interconnecting the components in a system so that those components, also called elements, depend on each other to the least extent practicable. The goal of a loose coupling is to reduce the risk that a change made within one element will create unanticipated changes within other elements. Furthermore by using loose coupling, all the consequences and effects from fire, explosion and toxic release incidents could be visualized and the entire surrounding environment such as schools, commercial area, residential area and industrial area can be identified. In order to do loose coupling, ArcObjects programming language files in ArcGIS 9.3.1 are shared between GIS and the Model. The optimization equation generated by VB platform would be used as an input. Then the input which is connected to Model builder tool is used to integrate the mathematical models written in VB6 programming language to GIS base map. Model builder is used to automate GIS processes by linking data input from VB6 result calculations, ArcGIS tools/functions and data



output. Basically, Model builder is part of the ArcGIS geoprocessing framework. The main advantage of using the model builder for GIS work is that the processes can be automated the GIS process can be saved and re-run at any time. This is good especially when an adjustment to the process or analysis is required. Rather than repeating the entire analysis, this can be simplified by changing the related parameter and rerun the model to produce new results. There are several steps to be carried out in order to link the data input (VB6) to GIS as follows:

- A model is built by using ArcToolbox window of ArcMap 9.4 and is named as Hazardous Buffer.
- Then model properties submenu is selected from the model builder menu to set a more specific info and name for the developing model such as in Figure 3. 40. After naming the developing model as “Hazard Region” and label it as “Hazard Region Analysis”, a description of event will be set and the user will know the expected consequences if the model is run as written in the Figure 3.40.

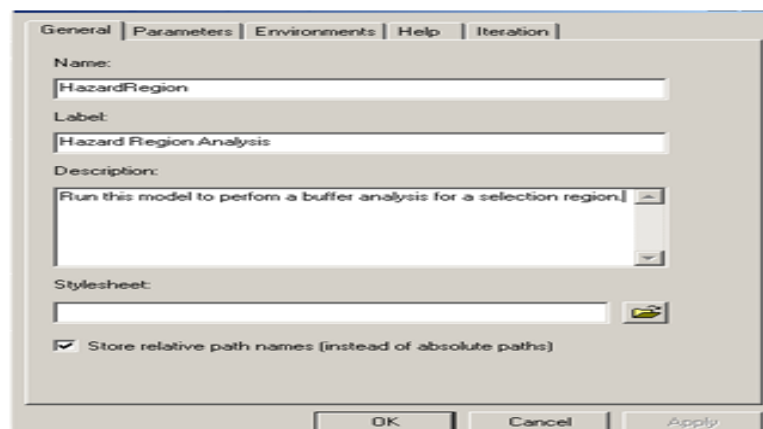


Figure 3.40 shows Model builder ArcGis submenu properties.

- In order to store the GIS data and locate the output from the model, the location of the hazard region model directory must be set under environment tab as in Figure 3.41, this directory set-up is to instruct the ArcGIS system to create the output from the model and to execute the model analysis. Therefore setting up the environment is a prerequisite before performing geo-processing tasks.



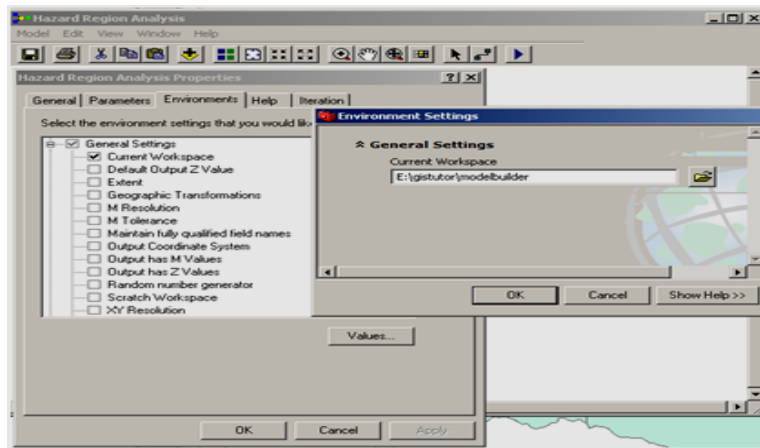


Figure 3.41 shows Hazard region analysis environment settings

- The analysis tool is added to automate the GIS process after the model directory is set-up. Basically, the model will have 2 data inputs: impacts boundary polygons from accident consequences and hazard point locations (road tanker coordinate x, y). Figure 3.42 shows the 2 input layers.

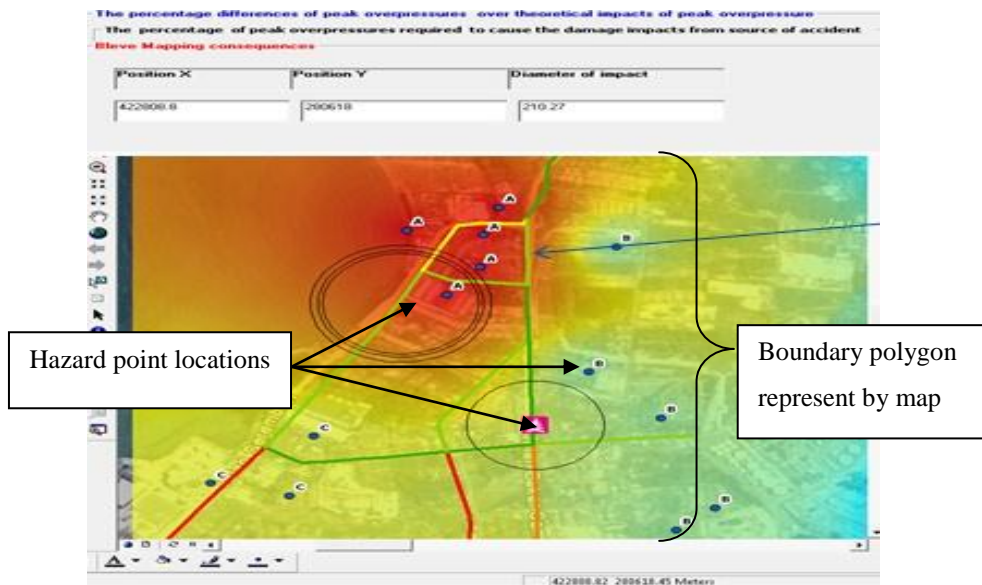


Figure 3.42 shows the boundary polygon and hazard point location.

- Then 4 ArcToolbox functions is utilized under the model builder tool such as spatial join, select, buffer and intersect which are link together in the model to allow flexibility for the model analysis. All the related input parameters will be filled-up under input parameters form. This will allow changing of the buffer radius distance in the ArcMap result after a new accident consequences input (in VB 6) is calculated therefore the output result can be filled in the



GIS model builder input parameter. Figure 3.43 shows the input setting parameter from VB calculation integrated into GIS model builder.

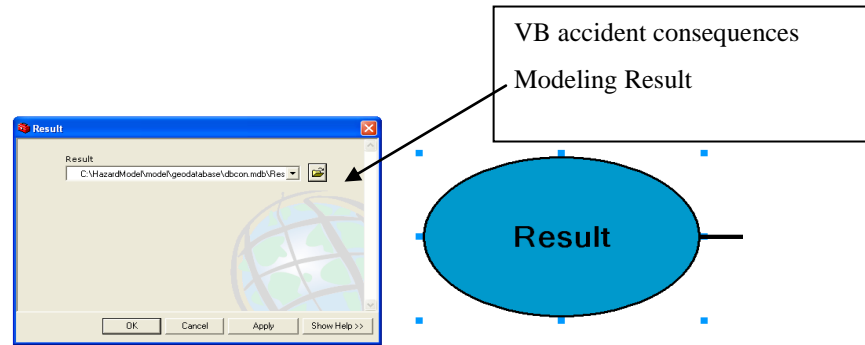


Figure 3.43 shows the input setting parameter from VB calculation integrated into GIS model builder.

- Hazards Spatial is included in the model to link and create variables from the parameters and join the boundary polygons and hazard point location input. This will give the attributes of the boundary polygons to all hazards point coordinate x, y within their boundaries. Hazard spatial joint tool is set under joint one to many, for the output class features joint operation. Therefore each boundary may have many hazards points. Figure 3.44 shows the selected coordinate x, y in VB which represent the accident point data on GIS.

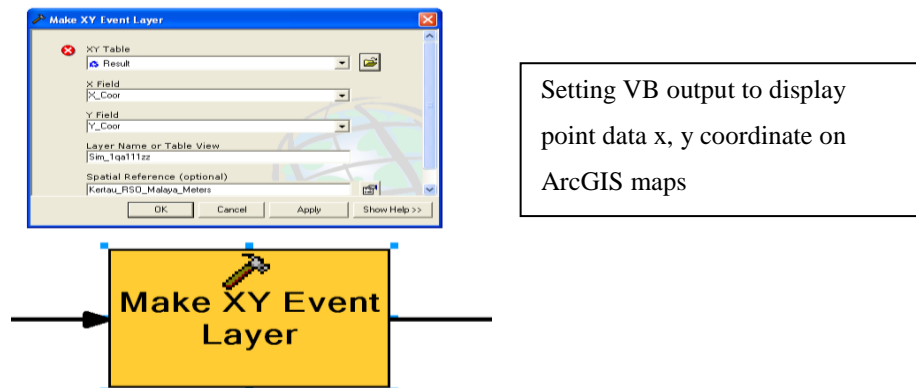


Figure 3.44 shows the selected coordinate x, y in VB which represent the accident point data on GIS.

- The selected coordinate x, y in VB is converted to GIS point data location at shape file point data as shown in Figure 3.45. The buffer radius from the tanker accident is generated from the selected coordinate x, y and stored in shape file point data as shown in Figure 3.46.



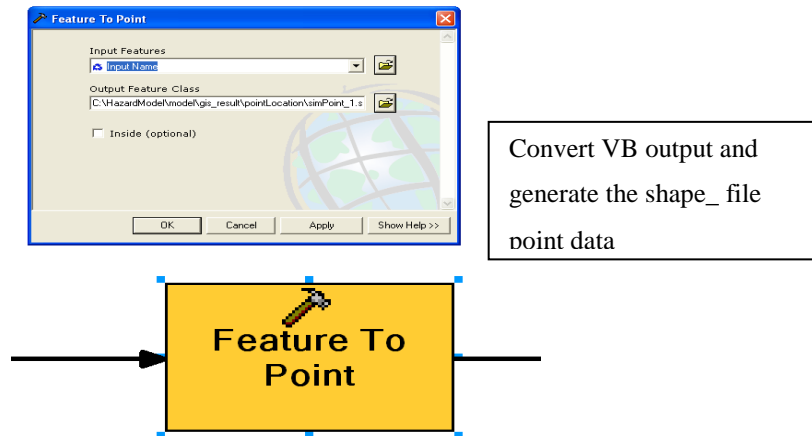


Figure 3.45 shows the selected coordinate x, y in VB is converted to GIS point data location at shape file

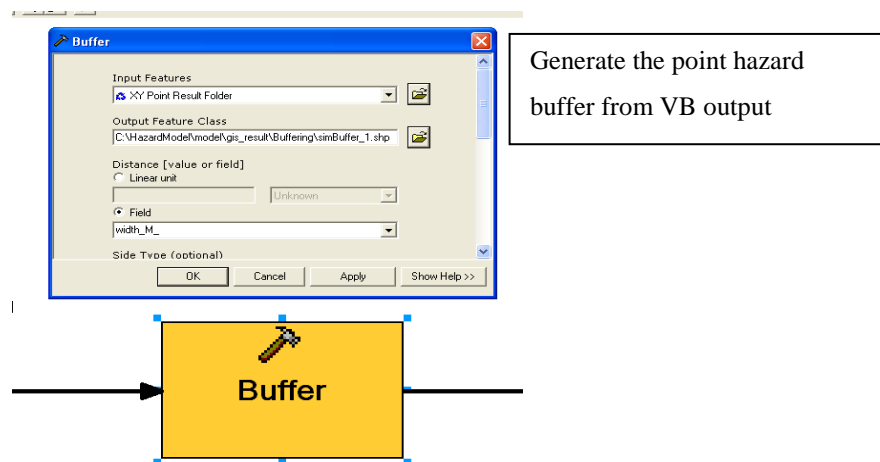


Figure 3.46 shows the buffer radius from the tanker accident will generated on GIS map via the input coordinate x, y in VB.

- If the boundary polygons and hazards point inputs in the model has no color to it and all elements are in white, this mean that the model is not ready to run. To run the model, the location of the data in the ArcGIS must be set. After setting the element files location, the model elements will have color to it and ready to be run. The blue round elements represent the inputs model, yellow rectangular elements are for tools and green round elements are for derived data for the output of the model.
- All of the selected coordinates for tanker accident consequences locations will have a buffer tool at the end of the model as the last output (hazards selectsection.shp).



- All output layers are intermediate and temporarily created while the model runs and deleted once the final output is obtained.
- All data which are gathered from the accident will be clipped to show the info involved such type of land-use or activities affected within the buffer, meanwhile index risk will show the severity of the impact accident within the boundary map as in Figure 3.47.

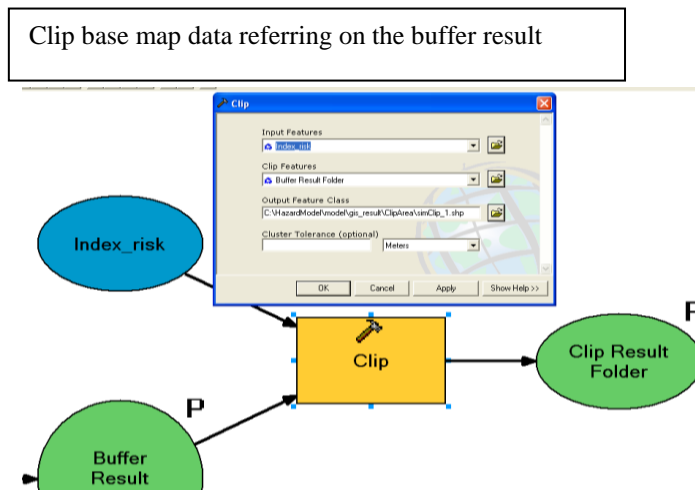


Figure 3.47 shows the Clip gathered the risk input data and buffer result.

- The model builder window is closed when the proposed analysis model created has completed.
- The model process flow as shown in Figure 3.48 represents the integration of VB output to ArcGis Model builder.



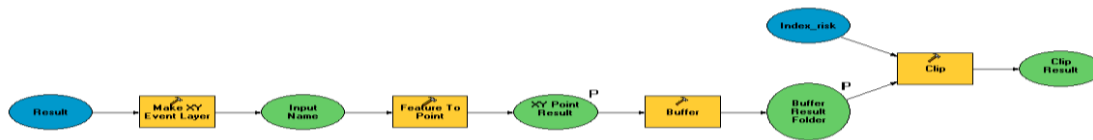


Figure 3.48 shows the process flow to integrate the VB output to ArcGis.

The above process flow summarized the stages for data model design. The blue circle represents the result for the process in the model by using VB output calculation. The result will become the input data to plot the buffer or affected zone area from the transportation accident that had occurred at a particular route. Clip GIS layer is used to demonstrate the risk for the coordinate area involved. Risk index is the risk calculation for the transportation activity along the selected route based on number of houses, industrial areas or commercial areas and also the population distribution (calculated based on IDW method) during day and night time.

### 3.11 Map Projection with Georeferencing

In GIS technology, geographic information can be divided into two classes: location and spatial data which also has known as vector and raster data. Vector data will record the location of a given object (point, line, or polygon) and attribute while raster data will describe the characteristics of an object or image. In this study, the information on the surrounding areas in the model is treated by adopting raster GIS framework. The raster framework transforms a continuous space into a discrete image by modelling it to tessellation of square grid cells called pixels. Tessellation refers to a finite number of objects/cells that cover a surface as discrete partitions. Raster is commonly used to approximate continuous surfaces in GIS. Raster GIS are organized in layers, each layer is assigned to a characteristic of interest. Raster data stored as raster datasets in matrix of square cells. ArcMap 9.3.1 Update version was used to model the HazMat release incident and the impact of the release of this toxic, hazardous chemical in the area surrounding. Layers including land use information (such as recreational area, industrial area, institutional area, development area, tourist area, settlement area, forest, airport and agricultural area), population density and roads are included in the map.



Satellite images from Google earth as in Figure 3.49, which are linked to a database are used to view actual map of accident location occur as in Figure 3.50 (for example at Port Dickson). Since data from different sources need to be combined and then used in an ArcGIS 9.3.1 update application, it is essential to have a common georeferencing system.

Georeferencing tasks are used since it capable to produce a new map by overlaying two or more different datasets together with the same coordinate of geographic locations. Georeferencing is a crucial task to make satellite image useful for GIS mapping application. To georeference an image, four major steps are involved, first to establish control points (at least 4 points) as in Figure 3.51, secondly to enter input of known geographic coordinates to the established control points, then to choose the coordinate system and other projection parameters and finally to minimize residuals.

Residuals are the difference between the actual coordinates of the control points (used by Google Earth) and the coordinates are predicted by the geographic model which is created in the GIS (known as WGS 1984 Mercator coordinate system) as in Figure 3.52. Figure 3.53 and Figure 3.54 illustrates the sequences or steps to integrate the transportation risk analysis accident input data with GIS application to produce an interactive map analysis. The Georeference process create and store control information that relates raster cells or vector and ArcGIS elements to a coordinate system and map projection. One of the easiest ways to establish georeference is to place control points on the input object using a reference object as in Figure 3.51 that already has georeference control.

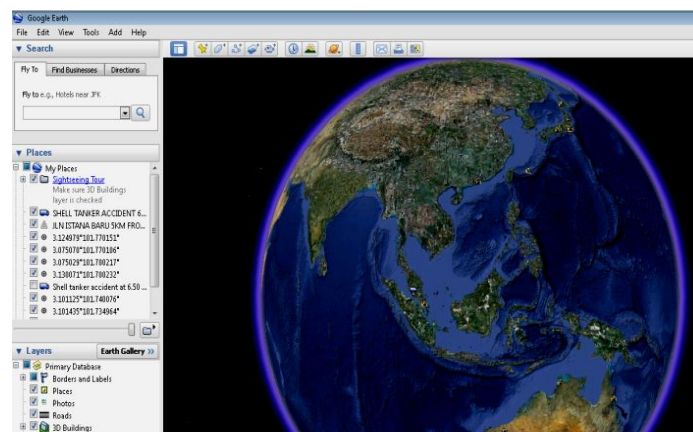


Figure 3.49 Google satellite image.



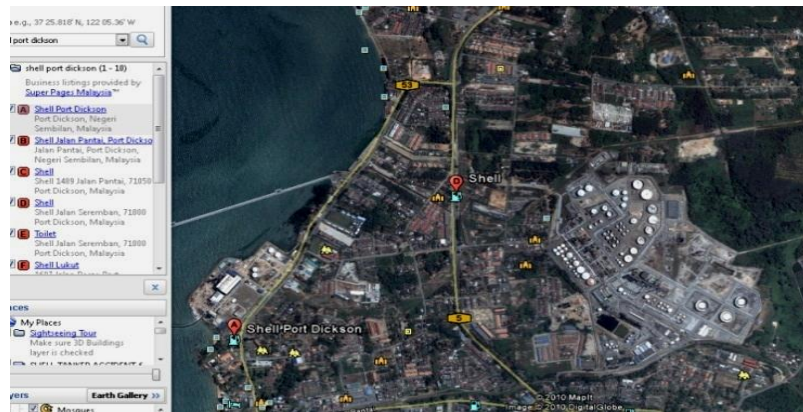


Figure 3.50 Search location of accident occurs (at Middle West Coast Refinery in Port Dickson) and zooms out the image.

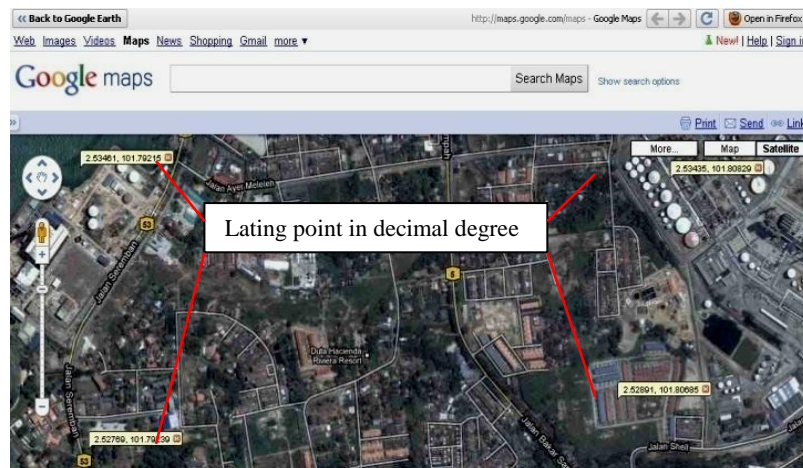


Figure 3.51 Add the lating of the position coordinate in decimal degree unit (at least 4 points).

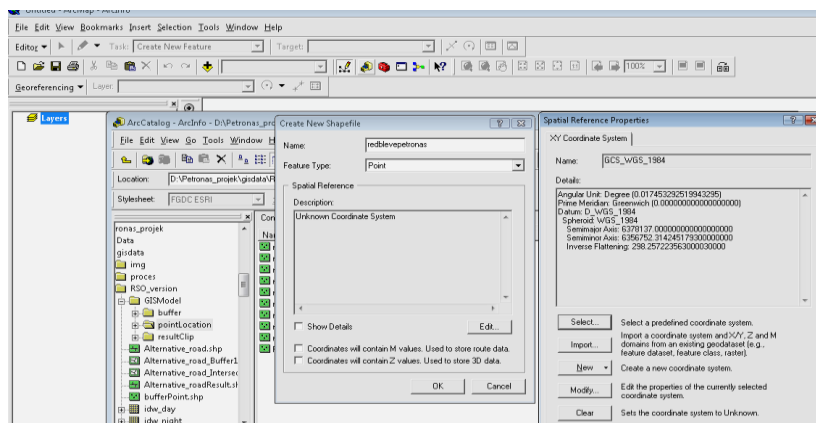


Figure 3.52 Projection Map from Different Spatial Reference World Geographic Coordinate System



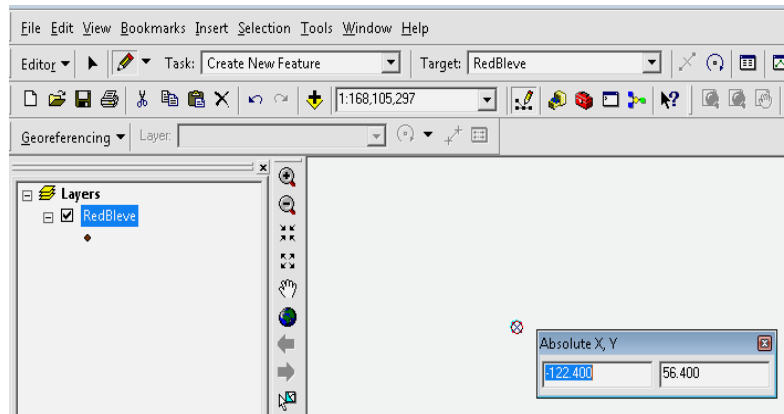


Figure 3.53 Adding Control from Reference Object.

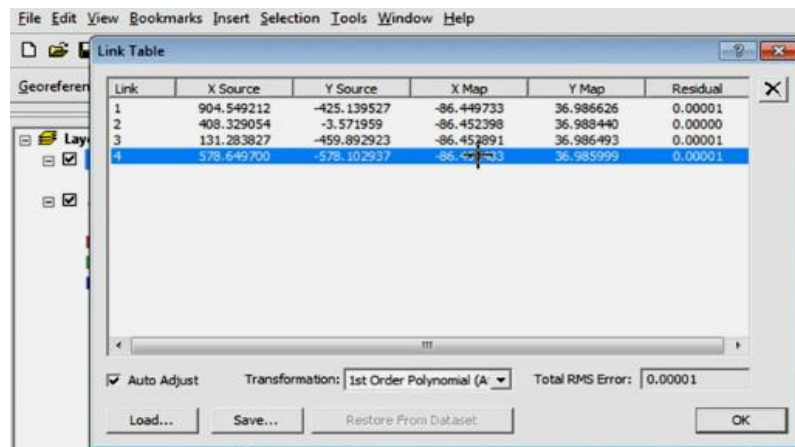


Figure 3.54 checked the coordinate residual (e.g 0.00001) subjected to georeferencing analysis.

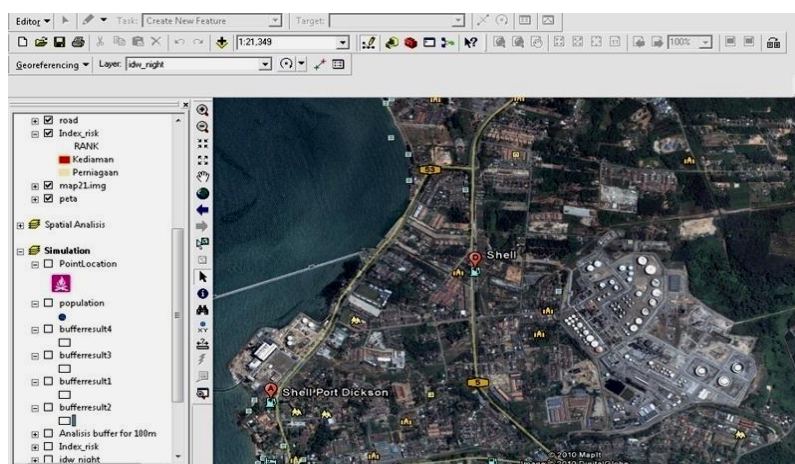


Figure 3.55 Result after Map projection and Georeferencing analysis processes (Image as background layer)



In this study, ArcGIS is used to project the GIS data from one map projection to another. Map projection involves taking spatial data defined on the curved surface of the earth prior to transforming it to the flat surface of a map and mathematical algorithm is used for this transformation. Figure 3.51 to Figure 3.55 illustrate some graphical user interface (GUI) involved during long georeferencing and map projection analysis. Figure 3.55 shows the result after minimization of the residuals coordinate system for map projection (as in Figure 3.54).

To perform a map analysis, various types of input data such as population distribution data, meteorology data and modeling data are used. An ArcGIS usually provides spatial analysis tools to calculate and carry out geoprocessing activities as data interpolation. Spatial interpolation is the process which uses points with known values to estimate values for unknown points. In this study, the technique of spatial data interpolation analysis is utilized to find the impact of BLEVE of hazmat of road transportation accident to population and surrounding environment via number of routes. In this research, interpolation method called Inverse Data Weighting (IDW) is used. Figure 3.56 illustrates how the inputs data points in ArcGIS RSO coordinates (Malaysian preferred coordinate instead of Kertau, and Cassini) are weighted during interpolation

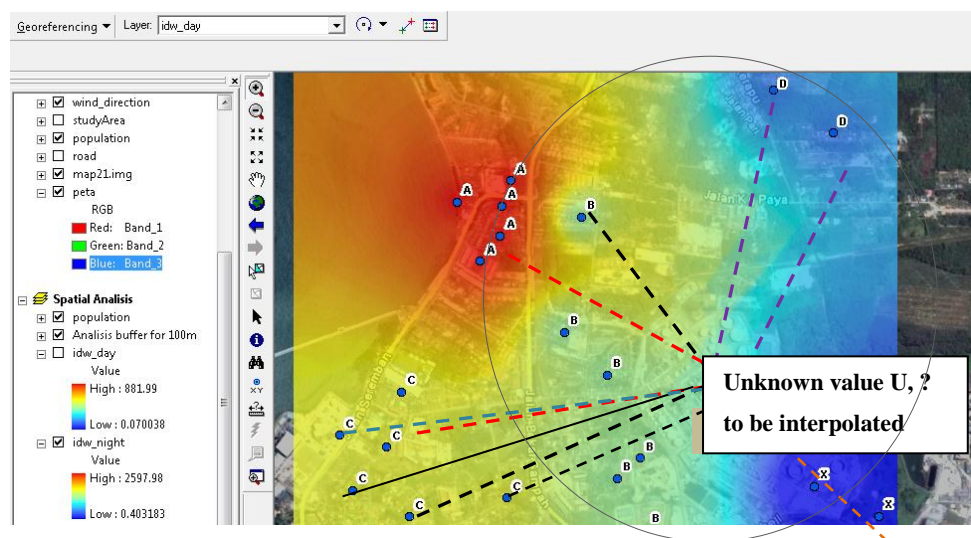


Figure 3.56 illustrate Inverse Distance Weighted (IDW) interpolation based on weighted sample point distance (left) from population density point over route.



In the IDW interpolation method, the sample points are weighted during interpolation such that the influence of one relative point (known as point A, point B, point C and point X) to another decline with distance from the unknown point (point U) can be estimated. Weighting is selected to sample points by using the weighting coefficient that controls how the weighting influence will drop off as the distance from new point increases. Within the interpolation area for unknown point U, it is noticed that the risk effect for the affected population is demonstrated by differentiating in color. Red color represent for high risk drop down to blue color for the low risk.

### **3.12 SMACTRA Validation and Verification**

Developers of computer codes, analysts who use the codes and decision makers who rely on the results of the analyses share the same concern on the accuracy of modeling and simulation assessment methods. Verification and validation of computational simulations are the primary methods to build confidence and quantify the results. Briefly, verification is the assessment of the accuracy of the solution to a computational model. Validation is the assessment of the accuracy of a computational simulation by comparison with experimental data. The Validation process confirms that the right system is being built (i.e., that the system requirements are unambiguous, correct, complete, consistent, operationally and technically feasible, and verifiable). The Verification process ensures that the design solution has met the systems requirement and that the system is ready for use in the operational environment for which it is intended.

### **3.13 Summary**

This chapter has been dedicated to describe the basic modeling technique and overall methodology. The basic idea of the proposed modified TRA methodology for Malaysia is to capture the matching data/databases available with TRA techniques and to set up an applicable framework to assess transportation risk step by step. Mathematical models and risk analysis techniques like ETA are employed for each risk component assessment. Numerical models are presented to measure individual risk and societal risk caused by HazMat transportation. The overall procedure to



develop and design a smart advisory system for hazardous materials transportation for Malaysia scenario could be simplified as follows:

*Identifying the hazards.* In order to identify and quantify incident scenarios referred to each traveling risk source and to predict the consequence of each incident scenario, the following parameters are required:

- The transportation conditions for each substance, i. e., the temperature and pressure values at which the substance is stored in the transportation vehicle container.
- The probability of the size of the equivalent holes, which have been chosen, to describe all possible releases from each vehicle typology. For each vehicle typology and for each rupture size including its physical aspects, outcome, a release rate, or a release quantity either instantaneous or continuous release, have to be evaluated.
- The final outcomes to which each hole size of each vehicle typology can lead such as toxic cloud, explosive or a pool flame, jet-fire and so on.
- The probability of having the final outcome once a release has occurred, i.e., the product of the probability of the release being of a specific equivalence size, once the release has occurred, and the probability of having final outcome, once the release of this specific equivalence hole has occurred.

*Zoning of the route* (Route segmentation): making a detailed analysis of the proposed route to segment it into zones of different topography, population density, (very much depending on the homogenous surrounding of the route), meteorological conditions, accident frequencies, etc.

All the parameters influencing the effects evaluation can vary from zone to zone of the impact area, especially when considering very large areas. The distribution of the population on the impact area is an essential input for calculating societal risk. A population map is composed of zones, where people may be considered uniformly distributed, and of aggregation centre, where people are clustered. The total numbers of these zones and centre and their population density need to be determined.



*Gathering accident data and movement data for the hazardous materials concerned:* establishing the likelihood of release, and estimating the final event frequencies using the modification event tree analysis and yield probabilities according to statistical analysis from major accident hazard databases available ( in case of transportation accident)

*Estimating hazard zones:* application of appropriate consequences models for jet fire, flash fire, BLEVE, fireball, toxic dispersion and pool fire to estimate the impact zone of human fatality and injury and damage of the structures and buildings for each of the identified hazards for the various zones of the route, and hence to evaluate the overall impacts for each of the zones of the route.

*Estimating the route societal risk:* estimates the risk to a group of people located in the effect zone of an accident, the result is normally represented by the Frequency – Number (F-N) curve.

*Time of day effects:* description for the variation of population between night, when most people are at home and day when most people are at work and more people are likely to be outside

*Comparison of alternate routes:* level of risk routes will be compared with risk acceptability criteria.

*Display the analysis by using GIS (integration):* GIS software such as Arc View 9.3.1, ArcGiS Engine and network analyst extension of the GIS software Arc View, are used to store roadway data and other socio-economic data for the county, identifying sensitive locations as well as to integrate them and develop the safest route.



## CHAPTER 4

### RESULT AND DISCUSSION

This chapter evaluates and discusses on the development and performance of Smart Advisory System for Chemical Transportation Risk Analysis (SMACTRA) software. This software uses mathematical models to evaluate explosion, fire, toxic release and risk estimation results for individual and society which have been successfully programmed and implemented in an interactive Visual Basic (VB) environment. It is also integrated with GIS visual mapping analysis and online spatial Map API for transportation risk analysis simulation. Since the SMACTRA software combines an interactive VB, GIS and Map API online, it is a very user friendly, able to assist and train users especially those who are non-experts in computer programming to evaluate hazards from chemical substances transportation. Therefore, the possibility of doing mistakes in the risk calculation is greatly reduced. For an expert, the software provides the risk information analysis of the hazardous material transportation in holistic approach. Furthermore, the software has the capability to identify vulnerable locations as well as to integrate risk consequences results and therefore the safest route can be selected.

#### **4.1 Software Validation**

Simulation techniques are used to prove the software's viability and can be used to compare 'real world' results to those simulated by the model. Validity of SMACTRA software to assess either the static or moving risk sources for the transportation of hazardous material has been confirmed. The SMACTRA calculation results have been tested by using an established data and compared with the results from published literature and chemical risk management software to check its validity of equations used and programmed. The results obtained by SMACTRA are found to be consistent and without significant deviation as in other trials. Thus, this newly developed



SMACTRA tool is compatible computational software for the consequence modeling of transportation of hazardous material. Figure 4.1 shows the software validation.

### **Verification the SMACTRA results**

To prove the software's viability as a reliable program and comparison of the calculation results are as below:

- Case studies and accident scenarios (as discussed in section 4.1 and 4.2)
- Risk assessment software (Effect 8.01, Canary)
- Other related and published data



### **Consequences Analysis**

Vapor cloud explosion impact (as discussed in section 4.3)

- Analyze road tanker accident hazard during transportation 13,000 kg of LPG or 34.5m<sup>3</sup> (commercial size)
- Analyze road tanker accident hazard at various capacities – 1000, 2000, 3000, 5000, 7000, 85000, 32000 kg of LPG
- Compare the SMACTRA results with Baker Strehlow Tang method, TNO Multi Energy method calculation results.

Pool fire impact (as discussed in section 4.3)

- Analyze road tanker accident containing 13,000 kg of LPG at constant leakage rate 0.0707m<sup>3</sup>/s or 43.5 kg/s and variable leakage rate using SMACTRA software and compare it with another published software analysis results
- Study the burning rate and spill time duration effect to pool fire diameter size during instantaneous and continuous spillage.
- Study thermal intensity, view factor, transmissivity, and thermal radiation dose effect over the receptor distance from accident source.

BLEVE fireball (as discussed in section 4.3)

- Analyze road tanker accident hazard at various LPG capacities (4000kg and 13,000kg) and compare the results with Effect 8.01.
- Comparison between fireball diameters with duration as calculated by SMACTRA and EFFECT 8.01 software. Also experimental and calculated their relationship as function of mass fuel.
- Study the time for the receptor to feel pain as a function of BLEVE fireball thermal radiation.
- Study the effect of fireball height, fireball diameter and emissive power as a function of BLEVE fireball duration time to receptor

Toxic gas release (as discussed in section 4.3)

- Analyze the consequences by using SMACTRA map API online for various capacities of ammonia release from tanker.

Continued to next page



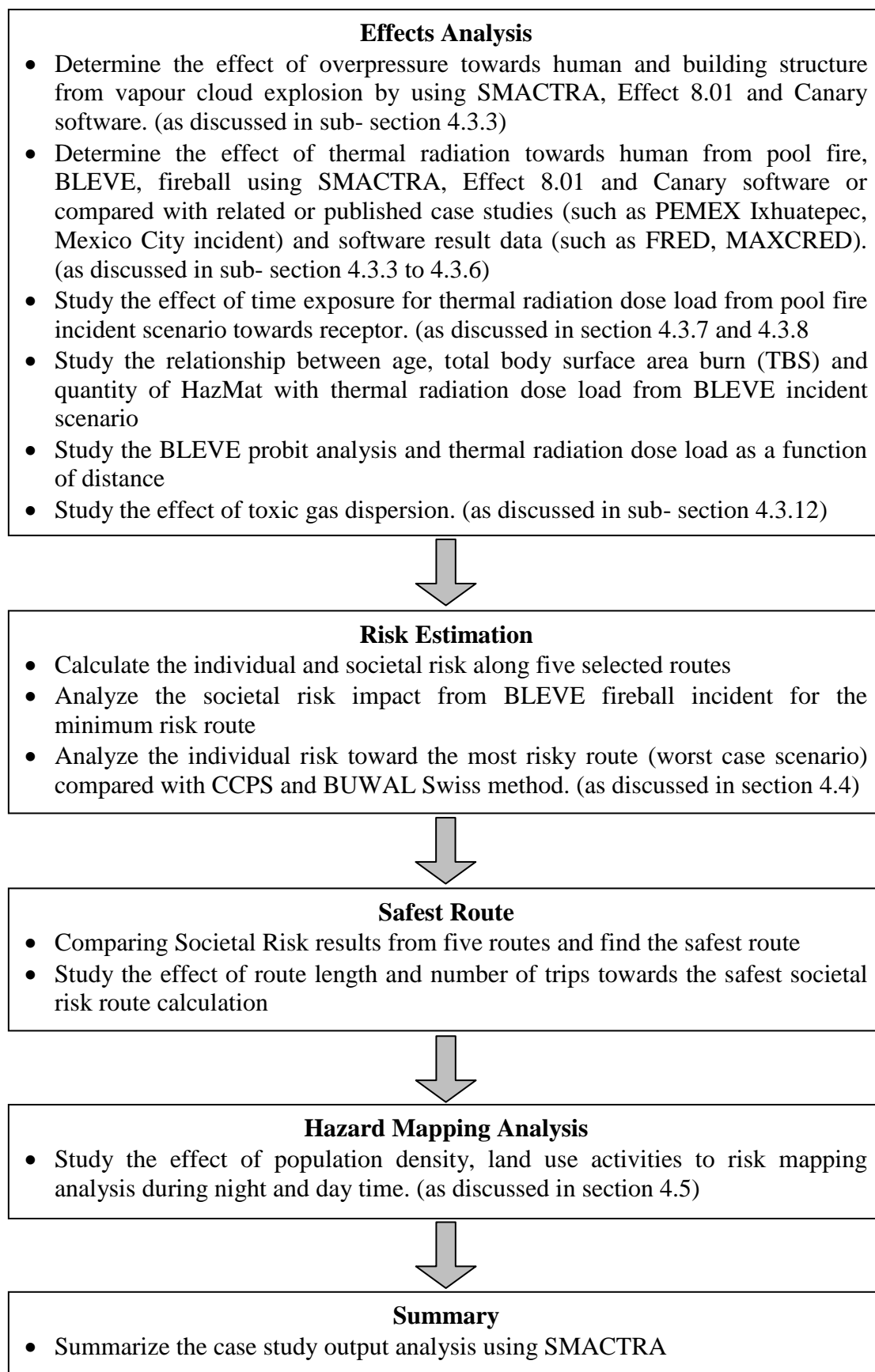


Figure 4.1 Software Validation



#### 4.1.1 Case Studies

It is known that the use of SMACTRA to predict the potential consequences from chemical hazards necessitates the review for several accident scenarios or case studies. Therefore, several case studies have been reviewed by other authors and those softwares results were compared with SMACTRA. Case study 1 was analysed by using SMACTRA and compared with case study 2, 3, 4 and 5. The descriptions for these studies are as follows:

*Case study 1: Environmental Impact Assessment of LPG transportation via road network for MCWR Port Dickson*

In this study, risk analysis was implemented to estimate and evaluate the risk impact from an accident involving LPG trucks. In order to estimate the risk related to LPG truck accident, the actual accident scenario was used. To make this case study relevant, the selection of accident scenario was based on the actual events that had occurred in Malaysia based on the information gathered from the database in National Institute of Safety and Health (NIOSH) and Malaysian Institute of Road Accident and Safety (MIROS) Bangi, Malaysia. Based on the review of NIOSH report, a specific accident scenario can be created according to the truck condition, time and features of the accident scene. During the accident, a truck with the composition 30,950 litre (tank volume 11995mm X 2480mm X 3500mm), carries Liquefied Petroleum Gas (LPG). There are few factors were considered during risk calculation such as Malaysia climate which is hot and wet with its temperature ranging from 28-32°C and humidity level about 70%. LPG comprises of two major components, propane and butane. In this case the percentage ratio of butane to propane is 70:30.

The truck accident scene was analyzed for five routes which involves a daily movement of 34.5 m<sup>3</sup> of LPG through approximately 15 to 20 km length route from Middle West Coast Refining (MWCR) Company in Port Dickson to Petrol and Gas service station in Port Dickson. The MWCR processed crude oil 55,000 barrels per stream day (BPSD) and produced the following products or domestic consumption for LPG, naphtha, mogas, kerosene, diesel and Low Sulphur Waxy Residue (LSWR). MCWR was built in 1963 on 101hectar area and located about 2km from Port Dickson. There is several residential housing close to the refinery with some of them



fringing the refinery fencing. Port Dickson is accessible via North South Highway and the coastal road along the west coast of Peninsular Malaysia. Access to MCWR site from the north which is from Seremban is possible via Port Dickson by using alternative roads without having to pass through the town. Access from the south is along Jalan Pantai but since this is a popular tourist destination, it experiences a substantial increase in vehicles especially during weekends and public holidays. Traffic volume counts are conducted regularly by the Highway Planning Unit of the Ministry of Works [169]. In 1996 vehicles flow rates for segments of the Seremban – Port Dickson bypass varies from 810 to 1314; whilst for the Port Dickson –Lubok Cina bypass, the figure is 1337. It is estimated that Seremban –Port Dickson highway will reach over its capacity in the future based on traffic growth projections.

Export of MCWR products by road currently generates approximately 400 lorry trips per day but with the commissioning of the multi product pipeline, the number of road trips is expected to be reduced to 219 per day. From 1998 to the year 2000, road trips are projected to increase by 6% per year. With the completion of the new highway linking Kuala Lumpur International Airport at Sepang (KLIA) to Port Dickson, it is expected that the road trips may increase to 8-10 % per year. At present, the loading activities are mainly during daytime, between 0800 and 1630 hours but this expected will be extend to longer hours in the future.

#### *Case Study 2: Effect version 8.01*

Effect version 8.01 software [188,189] is developed by TNO (Netherlands Organization for Applied Scientific Research) and is used to calculate the effect and consequences of accidental releases for Dutch government. All the consequences mathematical models used in the software are originated from the Yellow Book and Green Book, which provide solid scientific information and are recognized internationally as reference works for consequence analysis. The software is renewed and improved based on the developments in the safety knowledge and comments from the user.

#### *Case Study 3: Quest CANARY*

Quest CANARY software [190] package is developed by Quest Consultancy Incorporated, New York United States of America and is used to perform the



consequence modelling. CANARY includes application-specific models for vapour dispersion, fire radiation and vapour cloud explosions. CANARY able defines the hazard endpoints (e.g. gas concentration, radiant flux, and overpressure) that determine the extent of toxic or flammable gases. It also produces many forms of Risk Assessment and analysis and it uses a simple semi-quantitative method of Risk Assessment called Risk ranking up through a fully-Quantitative Risk Analysis—Quantitative risk analysis (QRA) for loads and radiation from several types of fires, or overpressure resulting from an explosion. This technique involves identification of hazardous events that could occur at a facility and estimate the possible consequences and probability of occurrence of each event.

#### *Case Study 4: Mexico City Ixhuatepec*

PEMEX LPG Terminal at San Juan Ixhuatepec, Mexico City where a disaster had occurred in 1984 which caused 650 fatalities and 6400 injuries. The incident occurred when a 200mm pipe between a storage cylinder and a sphere ruptured, releasing LPG. The release continued for 5 to 10 minutes resulting in a large gas cloud which ignited and caused an explosion and many ground fires. These ground fires led to a series of Boiling Liquid Expanding Vapor Explosions (BLEVEs) in the LPG terminal. The main cause for the escalation of the incident was the ineffective gas detection system and lack of emergency isolation. The accident also showed that BLEVEs were the important source of hazard.

#### *Case Studies: Others*

The results from published data such as from Lees compilation of case incident [64], related articles, journals [153, 191-193] and published results from risk software such as MAXCRED, FRED [194-202] are compared during the SACTRA validation results.

## **4.2 Accident Scenario (Sequence of Event)**

In the case of the loss of containment of a hazardous material, the possible damages can be due to its toxicity and/or its flammability. The evolution of an accident depends on a number of parameters such as the physical properties of the substance, its physical conditions during transport (pressure, temperature, degree of filling),



location and size of the release hole which will determine whether the spill is liquid, vapor or two-phase. The amount of material released is a function of:

- The total amount of transported material. Its depends on the size of the tank, and on the filling degree;
- The size of the release area (either leak from the relief valve, a pinhole, a larger fracture in the vessel wall, etc.);
- The release duration (whether it is continuous or instantaneous).

In case of immediate ignition, the flammable material will form a jet fire and its consequences are limited to a relatively small area near the release site. Even in this case, serious consequences may result, either because of the presence of many people nearby or from its secondary effects (domino effect), such as the heating effect on the tank itself or the impingement of the flame on other objects (collapsible structures, other vessels containing hazardous materials, buildings, cars, buses and so on). Factors affecting the generation of liquid pool from the liquid spill are the presence of immediate ignition, non-flammable material or the external (ambient) conditions. A vapor cloud will be produced either directly from the tanker or from pool evaporation. The whole sequence of events is represented in Figure 4.2.

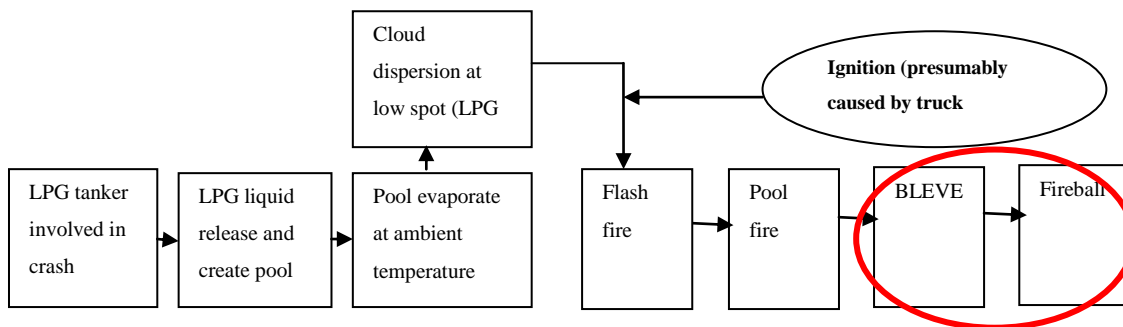


Figure 4.2 show the sequence of events based on LPG road tanker accident case study at Port Dickson

### *Population density*

Population density data are obtained from The Department of Statistics Malaysia records which is referred to the most recent census, 2010 and from Environmental Impact Assessment (EIA) report of MCWR [ 203]. Based on the data, the population density for region (called mukim in Malaysia) Port Dickson is 3.19756 people per



hectare. Mukim port Dickson is controlled by Port Dickson District Office and for District of Port Dickson; the population density is 1.6079 people per hectare. The population distribution is divided into 2 sets of population distribution: (i) day time population, and (ii) night time population. Table 4.1 shows the detail information of population distribution by point location.

Table 4.1 population distribution

| Point location | Day time population | Night time population |
|----------------|---------------------|-----------------------|
| A              | 517                 | 2598                  |
| B              | 280                 | 1400                  |
| C              | 882                 | 1743                  |
| D              | 408                 | 707                   |

Note: daytime refers to the period from 0700 hour to 1900 hour GMT, whilst nighttime to the period 1900 hour to 0700hour GMT.

In this case study, the information in Table 4.1 was mapped out before detailed distribution was identified and determined. The population distribution in Table 4.1 then was worked out into spatial distribution by risk assessment sector diagram (RASD) [70].

#### *Meteorology condition*

The meteorological data records (Meteorology Department, Malaysia) are available from the nearby Malacca meteorology station which allowed the setting of average weather conditions as follows: average temperature of 28 and 32°C in winter and in summer, respectively, with a humidity of 70% and a prevailing wind velocity of 3.3 to 5 m/s during hot season. The Pasquill atmospheric stability class was assumed as D (i.e. neutral) through the year.

#### *Release scenarios*

Two release scenarios were assumed: a spill from a hole 25 mm in diameter in the tank, lasting for 10-15 min and catastrophic rupture of the tank, with discharges of the entire content from > 250 mm hole in about 30 s. In both cases the possible consequences from the release include jet fire, pool fire, flash fire, UVCE and BLEVE fireball. The explosion of the tank, due to thermal decomposition of LPG,



may also occur in the event of a pool fire under the tank. The result will only show the explosion event for the catastrophic scenario.

### 4.3 Output from the Case Studies

#### 4.3.1 Results of the Vapor Cloud Explosion Consequences of LPG Transportation Accident (at the container capacity 34.5m<sup>3</sup>)

One of the main effects of an explosion is the development of a rapidly moving shock or pressure wave. This wave generates overpressures which can be divided into two categories; building damage and human damage. Blast wave damage is a common complication of overpressure and it is also known as a function for the rate of pressure rise and wave duration. Impulse is also used as a measure for blast damage. The principal parameters of the blast wave from Vapour Cloud Explosion (VCE) are the peak overpressure,  $p_0$ , the impulse of the positive phase duration,  $i_p$  and the duration of the positive phase,  $t_d$ . VCE is common consequences in transportation accident which can occur either in confined or unconfined area. Explosions effect modeling is generally based on TNT equivalence and TNO. The TNT model is easy to use for a known energy of a combustible fuel with an equivalent mass of TNT. The approach is based on the assumption that an exploding fuel mass behaves similar to exploding TNT with an equivalent energy basis [153]. TNT is the easier model and it is based on the assumption of equivalence between the flammable material and TNT, factored by an explosion yield term [16, 153]. The procedure of TNT calculation model is shown in Appendix 1 [27-33, 35]. The TNT equivalence predicts peak overpressure with distance. Crowl and Louvar [153], provides an equation for the scaled overpressure over scaled distance. It is noted that the pressure depends strongly on the distance between the place of the explosion and the structure. Therefore similar explosive charge may cause different overpressures depending on the location of the explosive charge. Pressure also depends on the location of the explosive charge above the ground. Table 4.2 shows the peak overpressure results at different distances for material release as predicted by SACTRA and Figure 4.2 shows the comparison of the overpressure at a given scenario predicted as a function of distance for the three methods (SACTRA –TNT- equivalency; Multi Energy method: blast strength; TNO



Multi Energy method using blast wave chart; Baker Strehlow-Tang method (at various radius from an explosion such as 25m till 500m) around LPG tank.

Table 4.2 Peak overpressure vs. scaled distance for blast wave pressure from an explosion using SMACTRA

| <b>r(m)</b> | <b>Ze(m/kg<sup>1/3</sup>)</b> | <b>P<sup>s</sup>(kPa)</b> | <b>P<sup>o</sup>(kPa)</b> | <b>r(m)</b> | <b>Ze(m/kg<sup>1/3</sup>)</b> | <b>P<sup>s</sup>(kPa)</b> | <b>P<sup>o</sup>(kPa)</b> |
|-------------|-------------------------------|---------------------------|---------------------------|-------------|-------------------------------|---------------------------|---------------------------|
| <b>25</b>   | 1.07                          | 17.30                     | 876.35                    | <b>525</b>  | 22.40                         | 0.08                      | 3.89                      |
| <b>50</b>   | 2.13                          | 3.53                      | 178.90                    | <b>550</b>  | 23.47                         | 0.07                      | 3.69                      |
| <b>75</b>   | 3.20                          | 1.41                      | 71.50                     | <b>575</b>  | 24.53                         | 0.07                      | 3.53                      |
| <b>100</b>  | 4.26                          | 0.78                      | 39.46                     | <b>600</b>  | 25.60                         | 0.07                      | 3.37                      |
| <b>125</b>  | 5.33                          | 0.51                      | 26.04                     | <b>625</b>  | 26.67                         | 0.06                      | 3.23                      |
| <b>150</b>  | 6.40                          | 0.38                      | 19.13                     | <b>650</b>  | 27.73                         | 0.06                      | 3.10                      |
| <b>175</b>  | 7.46                          | 0.29                      | 15.05                     | <b>675</b>  | 28.80                         | 0.06                      | 2.98                      |
| <b>200</b>  | 8.53                          | 0.25                      | 12.39                     | <b>700</b>  | 29.87                         | 0.06                      | 2.87                      |
| <b>225</b>  | 9.60                          | 0.21                      | 10.54                     | <b>725</b>  | 30.93                         | 0.06                      | 2.76                      |
| <b>250</b>  | 10.67                         | 0.18                      | 9.18                      | <b>750</b>  | 31.99                         | 0.05                      | 2.67                      |
| <b>275</b>  | 11.73                         | 0.16                      | 8.14                      | <b>775</b>  | 33.06                         | 0.05                      | 2.58                      |
| <b>300</b>  | 12.80                         | 0.14                      | 7.32                      | <b>800</b>  | 34.13                         | 0.05                      | 2.50                      |
| <b>325</b>  | 13.87                         | 0.13                      | 6.65                      | <b>825</b>  | 35.20                         | 0.05                      | 2.42                      |
| <b>350</b>  | 14.93                         | 0.12                      | 6.10                      | <b>850</b>  | 36.26                         | 0.05                      | 2.35                      |
| <b>375</b>  | 15.99                         | 0.11                      | 5.63                      | <b>875</b>  | 37.33                         | 0.05                      | 2.28                      |
| <b>400</b>  | 17.07                         | 0.10                      | 5.24                      | <b>900</b>  | 38.40                         | 0.04                      | 2.21                      |
| <b>425</b>  | 18.13                         | 0.09                      | 4.89                      | <b>925</b>  | 39.46                         | 0.04                      | 2.15                      |
| <b>450</b>  | 19.20                         | 0.09                      | 4.59                      | <b>950</b>  | 40.53                         | 0.04                      | 2.09                      |
| <b>475</b>  | 20.27                         | 0.09                      | 4.33                      | <b>975</b>  | 41.60                         | 0.04                      | 2.04                      |
| <b>500</b>  | 21.33                         | 0.08                      | 4.10                      | <b>1000</b> | 42.66                         | 0.04                      | 1.99                      |



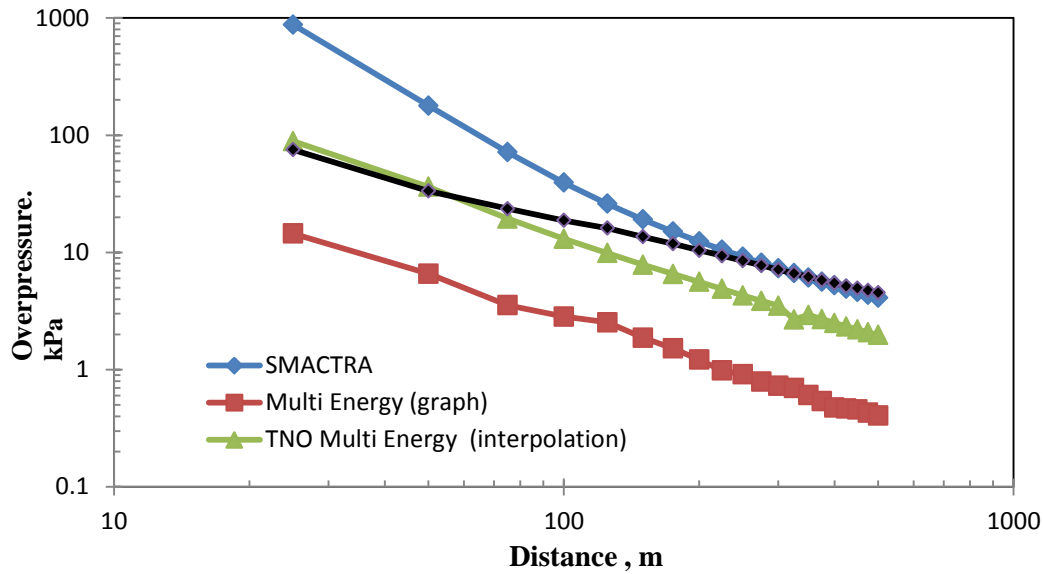


Figure 4.3 Comparison of the overpressure at a given scenario predicted as a function of distance for the three methods (SMACTRA –TNT- equivalency ( $\eta=10\%$  at 13000 kg propane); Multi Energy method: blast strength= 7 (interpolation from scaled overpressure); TNO Multi Energy method using blast wave chart; Baker Strehlow-Tang method:  $M_f= 0.662$  flame speed in Mach number).

From Table 4.2, it is shown that the receptors located at the distance 25 m from the source of accident will received the maximum impact value at 876.36 kPa. The peak overpressure value is drastically dropped to 178.90 kPa at the distance of 50 m. For the distance between 75m to 200m, this value dropped slowly. From 375m and above the peak overpressure value dropped to very minimum changes and subsequently showing constant impact value over distances.

Theoretically, the TNT-equivalency method assumes that the blast propagates in an ideal environment such as horizontal surface and excluding the presence of any obstacles. The multi-energy and the B-S-T method take into account the presence of congested zones to the generation of the blast. In the case of the SMACTRA –TNT equivalency method, it is necessary to select the explosion yield value and its result will change depending on the selected value. The value for explosion yield of an explosion event may range from 1% to 10%, but the most frequently used value is between  $\eta= 0.03$  to 0.05. For the multi-energy method, the initial blast strength must be chosen according to the degree of congestion in the area or areas covered by the



flammable cloud. According to Baker-Strehlow-Tang (BST) method, the Mach number of the flame speed and a function of the congestion must be specified. This specific correlation was established from the experimental data by Baker et al. [204]. He stated that the combined effect of fuel reactivity, obstacle density and confinement was associated with flame speed. Therefore, with this method the strength of the blast wave is proportionate to the maximum flame speed achieved within the cloud. Based on Figure 4.2, it is shown that at the short distance between 20 to 70m, the multi-energy method and BST predicts the maximum peak overpressures will be below than 89.08 kPa. SACTRA predicts that peak overpressure will drastically drop from 876 kPa at distance 25m to 178 kPa at distance 50m from an accident event. However SACTRA and Baker Strehlow Tang overpressure value shows a relatively similar value of peak overpressure at the distance between 200 m to 500 m with the overpressures range between 2 and 11 kPa.

The comparison results also shows the same conclusion as published by Lobato et al., [205] who applied the TNT-equivalency, the multi-energy and the BST methods for the explosion of a small cloud ( $264 \text{ m}^3$ ) which contain a mixture of hydrogen and air containing 1.08 kg of hydrogen, in a low congestion environment. According to their hypothesis if an explosion yield value was 10% for the TNT method (a conservative value); a blast strength of 10 instead of 7 due to the hydrogen explosion features for the multi-energy method; for the BST method, the flame expansion was assumed to be 2D and the obstacle density lower than 10%, so  $M_f = 0.662$ . They concluded that the TNT model predicts higher overpressures, while the multi-energy and the BST methods predict similar values but the overpressure values which were obtained were not significant for a very short distance (less than 70 m). Therefore the results of peak overpressure as predicted by BST and SACTRA are comparable for the VCE consequences of 13,000 kg of LPG at a distance between 175 m to 500 m as shown in Figure 4.2. However this is only applicable for the LPG capacity of 13000 kg which is equivalent to the commercial size of LPG road tanker with its confined volume  $34.5 \text{ m}^3$ . Similar comparison can also be made for other yield values, initial blast strength and flame speed. If those values are carefully selected, all three models will predict similar distances to the mid range overpressures. However, the model predictions may deviate substantially at higher and lower overpressures. Table 4.4 shows the results from the three models.



Table 4.3 Peak overpressure vs. scaled distance for blast wave pressure from an explosion (SMACTRA over other two models Baker Strehlow Tang and TNO Multi Energy Model at 13,000 kg of LPG.

| <b>r(m)</b> | <b>SMACTRA</b> | <b>Multi Energy</b> | <b>TNO<br/>Multi Energy</b> | <b>Baker Strehlow</b> |
|-------------|----------------|---------------------|-----------------------------|-----------------------|
| <b>25</b>   | 876.35         | 14.49               | 89.08                       | 75.21                 |
| <b>50</b>   | 178.30         | 6.59                | 36.31                       | 33.47                 |
| <b>75</b>   | 71.50          | 3.55                | 19.39                       | 23.61                 |
| <b>100</b>  | 39.46          | 2.84                | 13.05                       | 18.76                 |
| <b>125</b>  | 26.04          | 2.53                | 9.88                        | 16.11                 |
| <b>150</b>  | 19.13          | 1.87                | 7.85                        | 13.63                 |
| <b>175</b>  | 15.05          | 1.52                | 6.54                        | 11.86                 |
| <b>200</b>  | 12.39          | 1.22                | 5.62                        | 10.43                 |
| <b>225</b>  | 10.54          | 0.98                | 4.89                        | 9.36                  |
| <b>250</b>  | 9.18           | 0.91                | 4.29                        | 8.49                  |
| <b>275</b>  | 8.14           | 0.79                | 3.87                        | 7.76                  |
| <b>300</b>  | 7.32           | 0.73                | 3.51                        | 7.13                  |
| <b>325</b>  | 6.65           | 0.70                | 2.68                        | 6.62                  |
| <b>350</b>  | 6.10           | 0.61                | 2.92                        | 6.19                  |
| <b>375</b>  | 5.35           | 0.54                | 2.70                        | 5.81                  |
| <b>400</b>  | 5.24           | 0.48                | 2.50                        | 5.47                  |
| <b>425</b>  | 4.89           | 0.47                | 2.33                        | 5.16                  |
| <b>450</b>  | 4.59           | 0.46                | 2.20                        | 4.95                  |
| <b>475</b>  | 4.33           | 0.43                | 2.08                        | 4.75                  |
| <b>500</b>  | 4.10           | 0.41                | 1.97                        | 4.54                  |



#### **4.3.2 Results of the Vapour Cloud Explosion from LPG Transportation Accident at various truck capacities.**

Based on the previous works on transportation risk assessment, almost all works were conducted for fixed (constant) truck capacity. Hence it is crucial to evaluate the accuracy of the SACTRA software compared to the other models. Therefore in this chapter, the study decided to look into the impact of vapor cloud explosion for SACTRA peak overpressure result. In order to do that the truck capacities of LPG must be varied. Therefore in this study, LPG trucks with the capacity of 1000, 2000, 3000, 5000, 7000, 8500 and 32000 kg were chosen. Figure 4.3 till to 4.10 show the comparison of peak overpressure results at a given scenario predicted as a function of distance for the three methods (SACTRA –TNT- equivalency ( $\eta=10\%$ ); Multi Energy method: blast strength= 7 (interpolation from scaled overpressure); TNO Multi Energy method using blast wave chart; Baker Strehlow Tang method:  $M_f = 0.662$  flame speed in Mach number). The flame speed at 0.662 was used in the calculation, because the vapor cloud was enclosed beneath the storage tank and the flame can only expand in two directions.

In this study similar results were observed for SACTRA and multi energy model (for the VCE consequences) at the distance of 20 m to 500 m with 1000 kg of LPG as shown in Figure 4.3. The analysis showed that the SACTRA model predicts higher overpressures while TNO multi energy and Baker Strehlow Tang models predicted maximum peak overpressure that are less than 34.5 kPa when the distance is greater than 45 m. Predicted distances for the overpressures between 20.7 kPa to 6.9 kPa were quite similar for SACTRA and Baker Strehlow Tang. At the lowest overpressure at 1.0 kPa, the distance predicted by the TNO and Baker Strehlow Tang models were nearly 44.9%-51.6% and 3.2%- 21.2% greater, especially at the distance of 120 m to 200 m as shown in Figure 4.4.



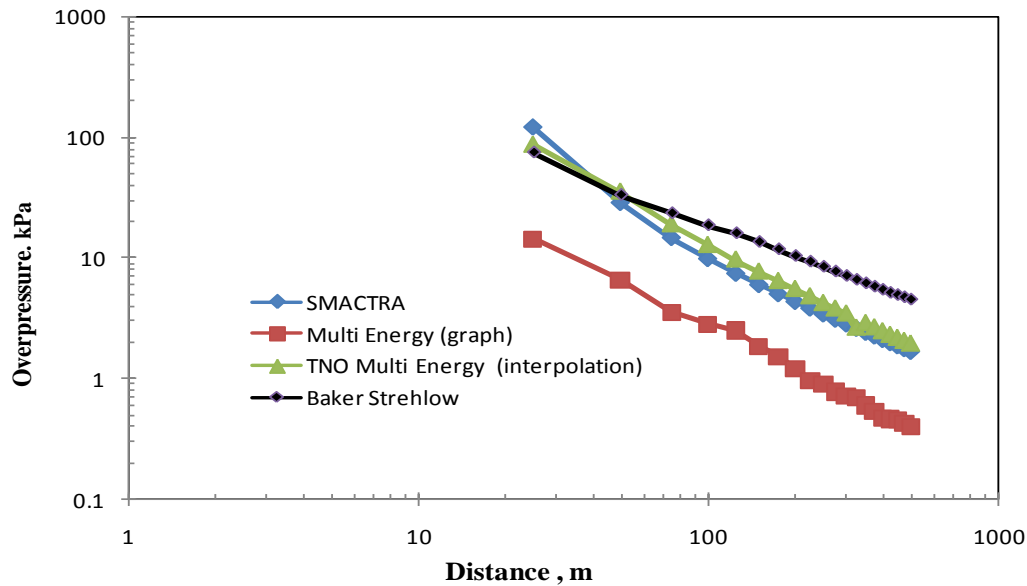


Figure 4.4 Comparison of the overpressure in a given scenario predicted as a function of distance for the three methods (SMACTRA –TNT- equivalency ( $\eta=10\%$  at 1000kg propane); Multi Energy method: blast strength= 7 (interpolation from scaled overpressure); TNO Multi Energy method using blast wave chart; Baker Strehlow-Tang method:  $M_f= 0.662$  flame speed in Mach number)

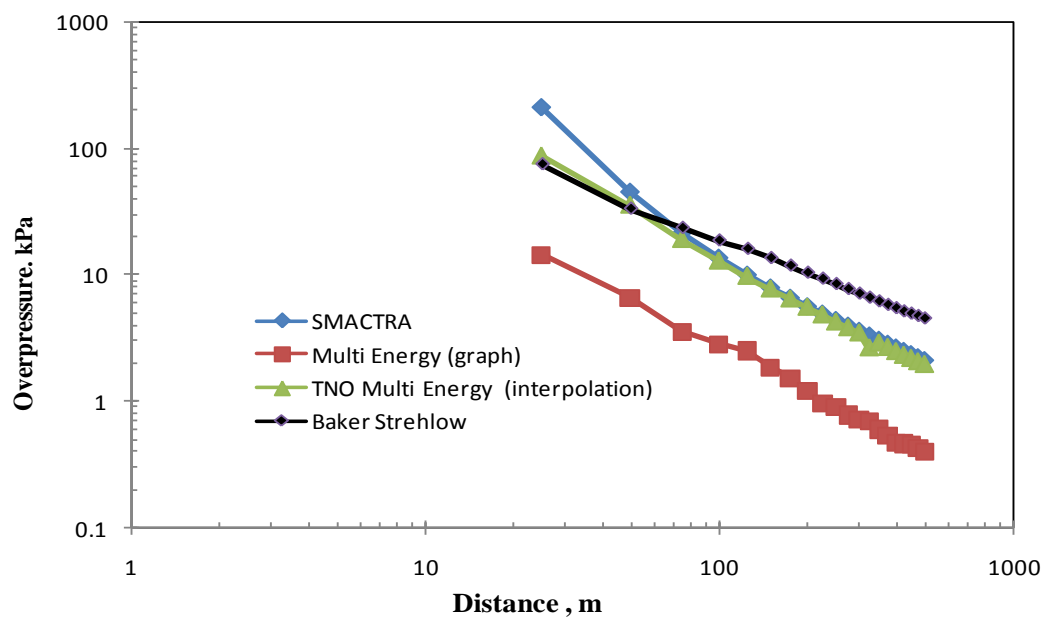


Figure 4.5 Comparison of the overpressure at a given scenario predicted as a function of distance for the three methods (SMACTRA –TNT- equivalency ( $\eta=10\%$  at 2000kg propane); Multi Energy method: blast strength= 7 (interpolation from scaled overpressure); TNO Multi Energy method using blast wave chart; Baker Strehlow-Tang method:  $M_f= 0.662$  flame speed in Mach number)



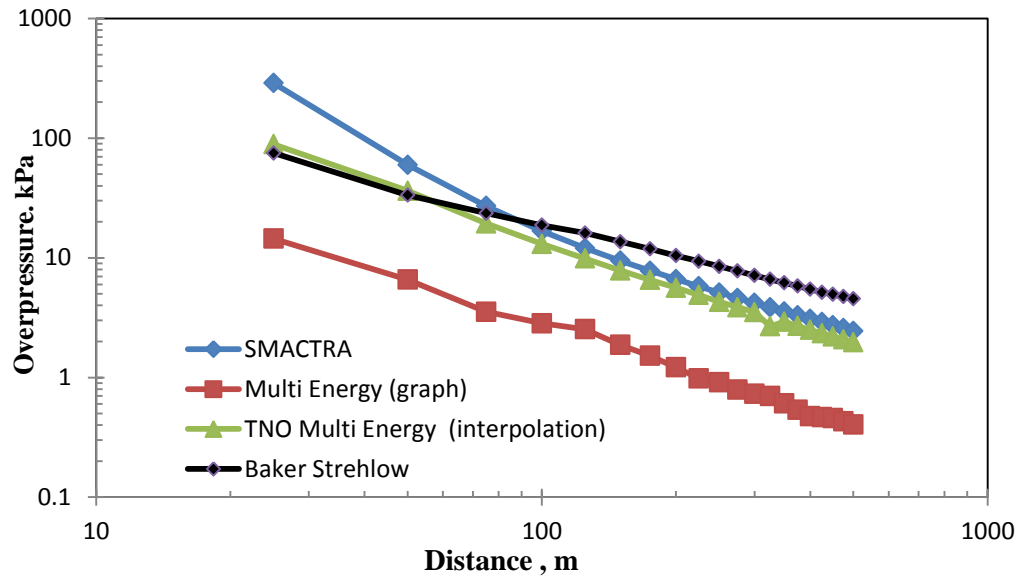


Figure 4.6 Comparison of the overpressure at a given scenario predicted as a function of distance for the three methods (SMACTRA –TNT- equivalency ( $\eta=10\%$  at 3000kg propane); Multi Energy method: blast strength= 7 (interpolation from scaled overpressure); TNO Multi Energy method using blast wave chart; Baker Strehlow-Tang method:  $M_f= 0.662$  flame speed in Mach number)

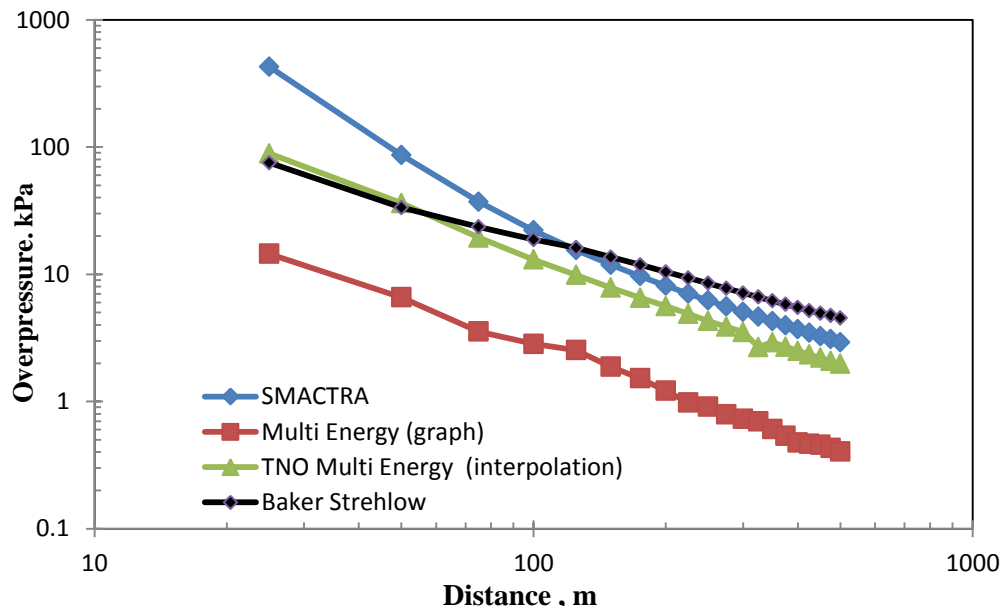


Figure 4.7 Comparison of the overpressure at a given scenario predicted as a function of distance for the three methods (SMACTRA –TNT- equivalency ( $\eta=10\%$  at 5000kg propane); Multi Energy method: blast strength= 7 (interpolation from scaled overpressure); TNO Multi Energy method using blast wave chart; Baker Strehlow-Tang method:  $M_f= 0.662$  flame speed in Mach number)



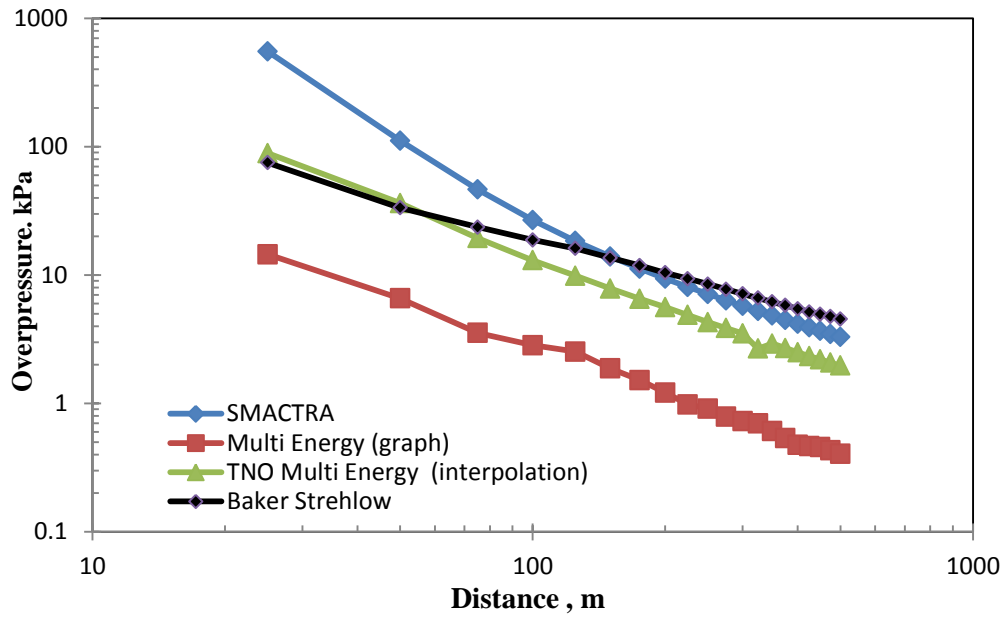


Figure 4.8 Comparison of the overpressure at a given scenario predicted as a function of distance for the three methods (SMACTRA –TNT- equivalency ( $\eta=10\%$  at 7000kg propane); Multi Energy method: blast strength= 7 (interpolation from scaled overpressure); TNO Multi Energy method using blast wave chart; Baker Strehlow-Tang method:  $M_f= 0.662$  flame speed in Mach number)

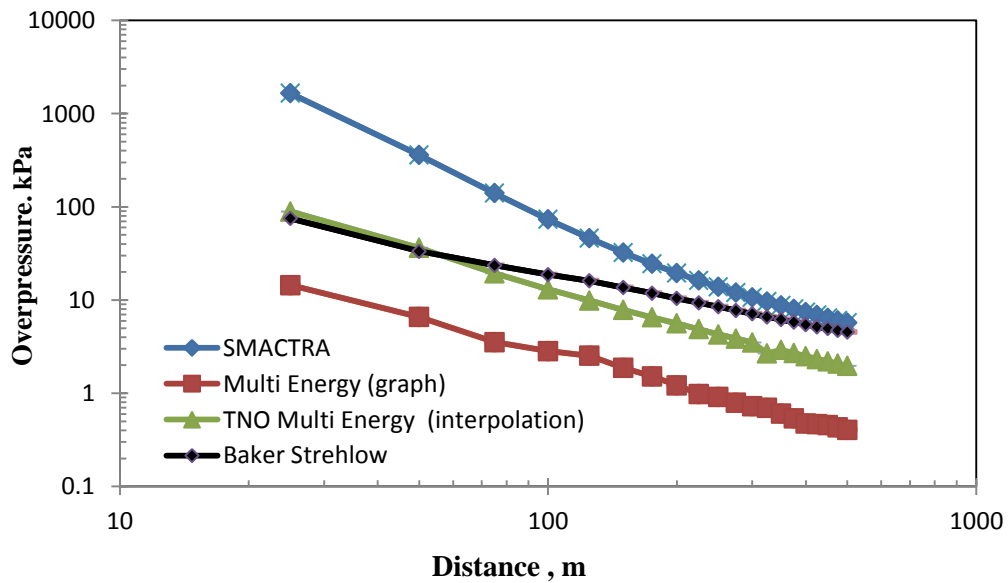


Figure 4.9 Comparison of the overpressure at a given scenario predicted as a function of distance for the three methods (SMACTRA –TNT- equivalency ( $\eta=10\%$  at 32000kg propane); Multi Energy method: blast strength= 7 (interpolation from scaled overpressure); TNO Multi Energy method using blast wave chart; Baker Strehlow-Tang method:  $M_f= 0.662$  flame speed in Mach number)



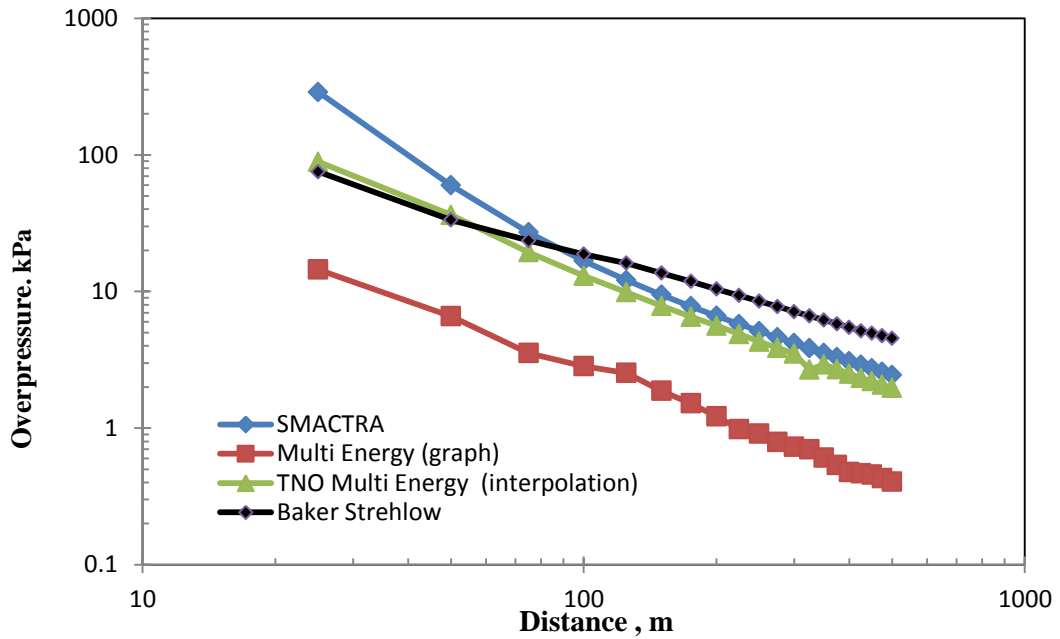


Figure 4.10 Comparison of the overpressure at a given scenario predicted as a function of distance for the three methods (SMACTRA –TNT- equivalency ( $\eta_t=10\%$  at 8500 kg propane); Multi Energy method: blast strength= 7 (interpolation from scaled overpressure); TNO Multi Energy method using blast wave chart; Baker Strehlow-Tang method:  $M_f=0.662$  flame speed in Mach number)

Based on the observation in Figure 4.4 and Figure 4.5, it is observed that the peak overpressure generated by SMACTRA software has a close approximated value to TNO Multi Energy VCE model, which is best at 2000 kg of LPG tanker capacity. However when the LPG capacity range is between 3000 to 8500 kg (Figure 4.6 till Figure 4.8, and Figure 4.10) the peak overpressure of SMACTRA result approaching to Baker Strehlow Tang model with the closest capacity at 8500 kg. With the value between 8500 to 32000 kg of LPG the approximation for peak overpressure value is decreasing and deviate further after 32000 kg of LPG from TNO Multi Energy and Baker Strehlow- Tang models (as shown in Figure 4.9). Therefore it can be concluded that SMACTRA software is applicable for commercial use in transportation risk analysis. Table 4.5 summarizes the comparison between the peak overpressure of SMACTRA result region and the two models.



Table 4.4 Summary of the comparison between the peak overpressure result region for SMACTRA and the two models (TNO Multi Energy and Baker Strehlow Tang).

| Result<br>P <sup>o</sup> (kPa) | Range<br>Radius (m) | Quantity<br>(kg) | Approximation to Model             |
|--------------------------------|---------------------|------------------|------------------------------------|
| 1.98-9.00                      | 125 – 500           | 1000             | SMACTRA $\leq$ TNO Multi Energy    |
| 1.90-10.05                     | 125 – 500           | 2000             | SMACTRA $\simeq$ TNO Multi Energy  |
| 2.08-12.08                     | 175 – 475           | 3000             | SMACTRA $\geq$ TNO Multi Energy    |
| 5.60- 16.0                     | 125 – 300           | 5000             | SMACTRA $\leq$ Baker Strehlow T.   |
| 5.00- 18.05                    | 125 – 375           | 7000             | SMACTRA $\simeq$ Baker Strehlow T. |
| 4.00 – 20.0                    | 125 – 500           | 8500             | SMACTRA $\simeq$ Baker Strehlow T. |
|                                | 500                 | > 32000          | SMACTRA deviate further            |

#### 4.3.3 Results of the Vapor Cloud Explosion Consequences of LPG Transportation Accident to Human and Structural Building Effects of Exposure to Overpressure

The magnitude of damage from an accident depends on various parameters such as the mass or energy involved in an accident, duration of accident which reflect the amount of energy released, type of hazardous material released and the degree of exposure. For example, the more the amount of toxic material and the longer the time of exposure the worst the effect can be expected.

The severity of damage from overpressure depends on the peak overpressure that reaches a given structure and the structure material. Similarly, the physiological effect of the overpressure depends on the peak overpressure that reaches human. Exposure to high overpressure levels may be fatal. For persons located outside the flammable cloud when it ignites it will expose them to a lower overpressure levels than persons who stay in the explosion cloud. Theoretically, if a person is far enough from the edge of the cloud, the overpressure is incapable to cause fatal injuries however in reality fatality can still occur due to injury from flying fragments or debris. In this study, the vapor cloud explosion overpressure analyzed by SMACTRA was also compared with CANARY software by Quest suite of models. Unlike potential fire hazards, persons who are exposed to overpressure have no time to react or to take shelter.



Health and Safety Executive, United Kingdom [8] has published probit relationship based on peak overpressure over fatality. Table 4.6 presents the probit results at range (0% to 100%) fatalities or for 1%, 50% and 99% fatalities. The graphical form of the overpressure probit result is presented in Figure 4.11 till 4.17. In this section, SMACTRA results is compared and validated with results from other published literatures and risk analysis softwares, such as EFFECT 8.01 and CANARY.

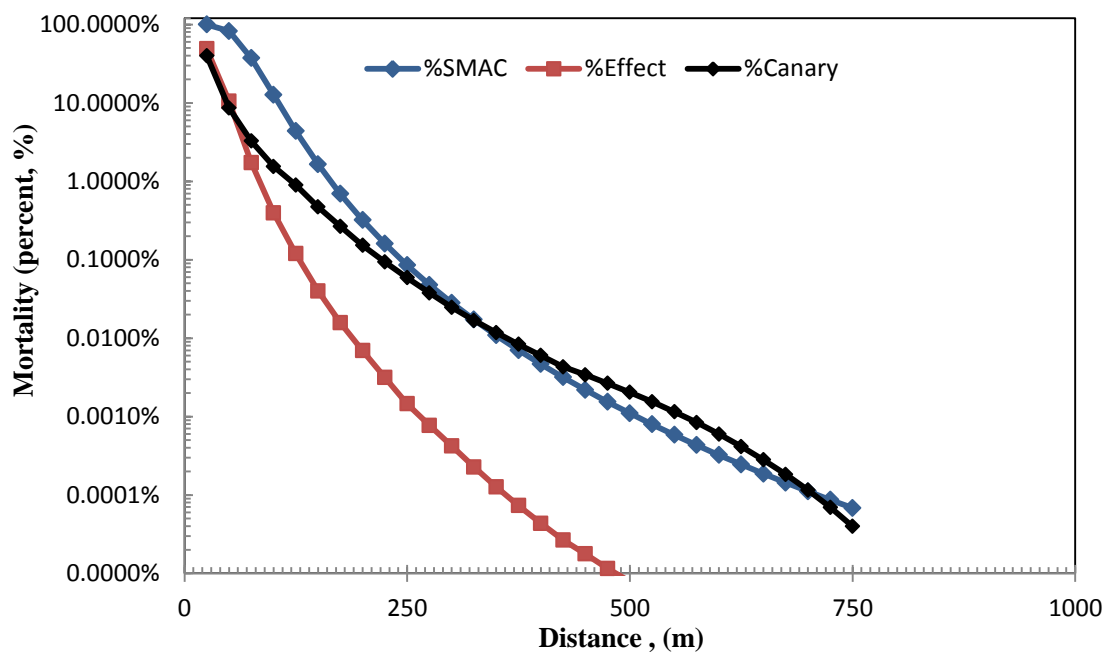


Figure 4.11 Comparison of the overpressure probit relation generated from an explosion of a road tanker containing 13000kg of LPG as a function of distance predicted by SMACTRA with others software.



Table 4.5 Comparison of mortality percentage (1%, 50% and 99%) to human from an explosion of a vessel containing various capacities of LPG as function of distance by using SACTRA and EFFECT Version 8.0 software

| Capacity<br>(kg) | Percentage | Distance (m) |             |         |
|------------------|------------|--------------|-------------|---------|
|                  |            | SACTRA       | Effect 8.01 | CANARY  |
| 13,000           | 99%        | 32           | 3(max. 57%) | 3 (94%) |
|                  | 50%        | 67           | 59          | 26.4    |
|                  | 1%         | 164          | 133.2       | 122.5   |
| 9119             | 99%        | 28           | 6(max. 57%) | 6(94%)  |
|                  | 50%        | 60           | 44.5        | 21      |
|                  | 1%         | 146          | 118         | 96.5    |
| 7000             | 99%        | 24           | (max. 57%)  |         |
|                  | 50%        | 54.7         | 31.5        | 19.2    |
|                  | 1%         | 134          | 108         | 88.4    |
| 5000             | 99%        | 20.3         | (max. 57%)  |         |
|                  | 50%        | 49           | 28.1        | 17.2    |
|                  | 1%         | 119.4        | 96.5        | 79      |
| 3000             | 99%        | 18.3         | (max. 57%)  |         |
|                  | 50%        | 41.3         | 23.6        | 14.5    |
|                  | 1%         | 100.5        | 81.5        | 66.7    |
| 2000             | 99%        | 16.5         |             |         |
|                  | 50%        | 36.1         | 34.1        | 12.7    |
|                  | 1%         | 88           | 85.2        | 58.2    |
| 1000             | 99%        | 13.2         | (max. 57%)  |         |
|                  | 50%        | 28.7         | 16.4        | 10.1    |
|                  | 1%         | 70           | 56.5        | 46.3    |

Note: the mortality results followed the explosion blast strength is equal to 7 (Effect 8.01)



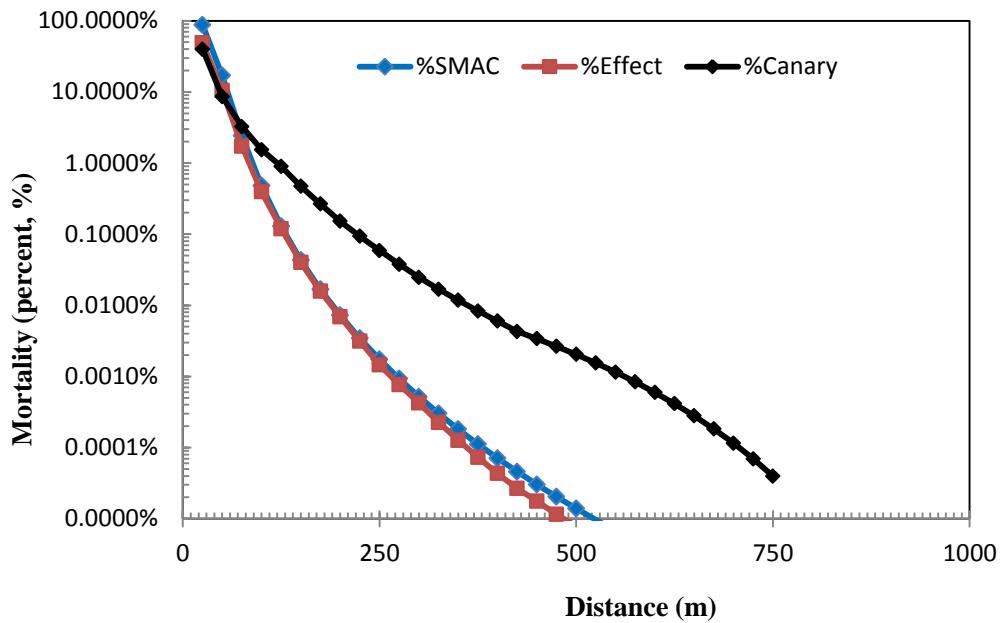


Figure 4.12 Comparison of the overpressure probit relation generated from an explosion of a road tanker containing 2000kg of LPG as a function of distance predicted by SMACTRA with others software.

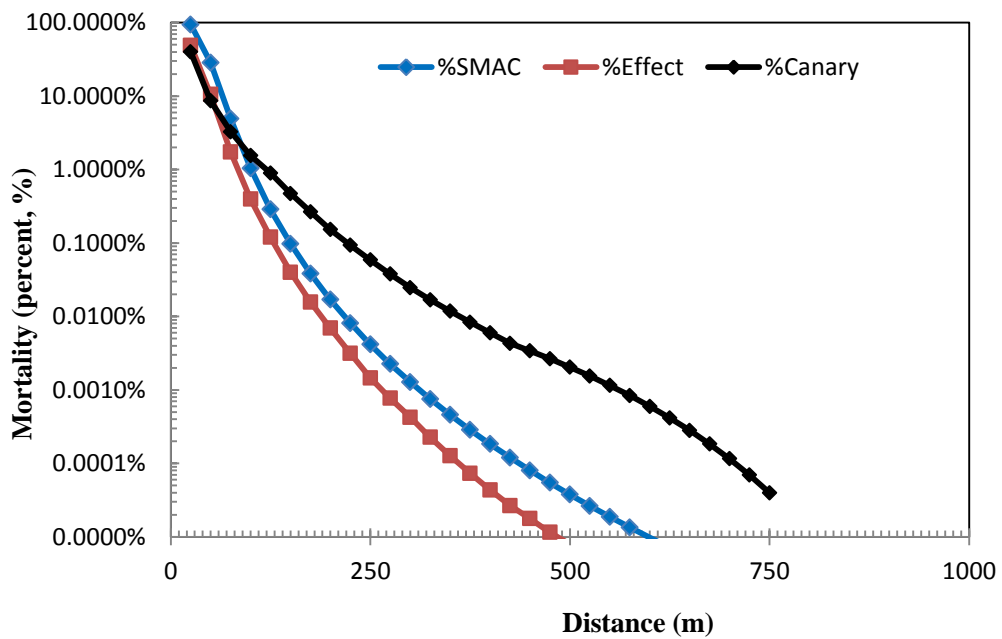


Figure 4.13 Comparison of the overpressure probit relation generated from an explosion of a road tanker containing 3000kg of LPG as a function of distance predicted by SMACTRA with others software.



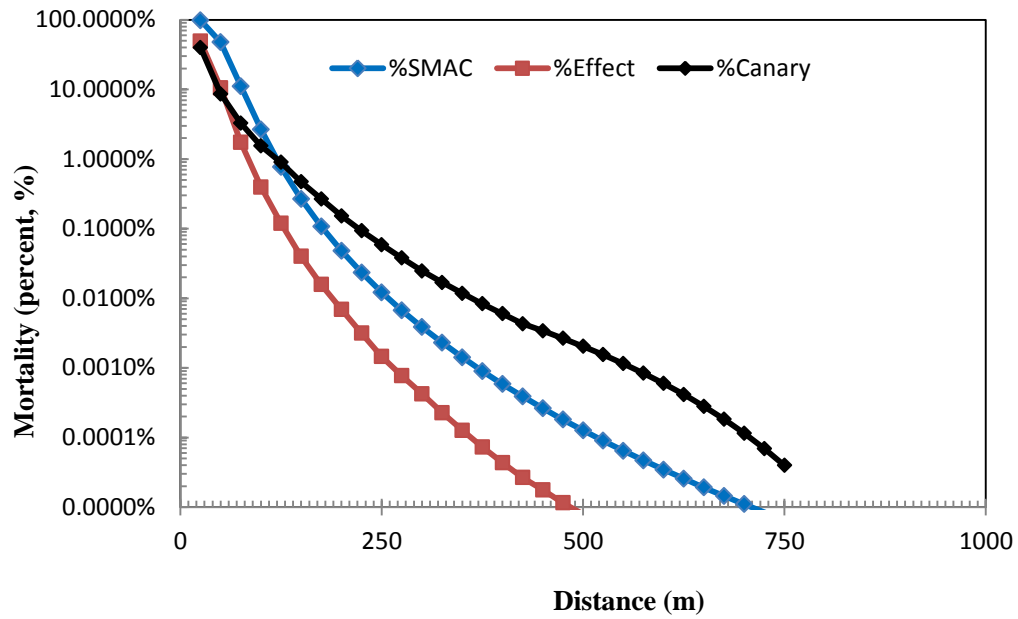


Figure 4.14 Comparison of the overpressure probit relation generated from an explosion of a road tanker containing 5000kg of LPG as a function of distance predicted by SMACTRA with others software

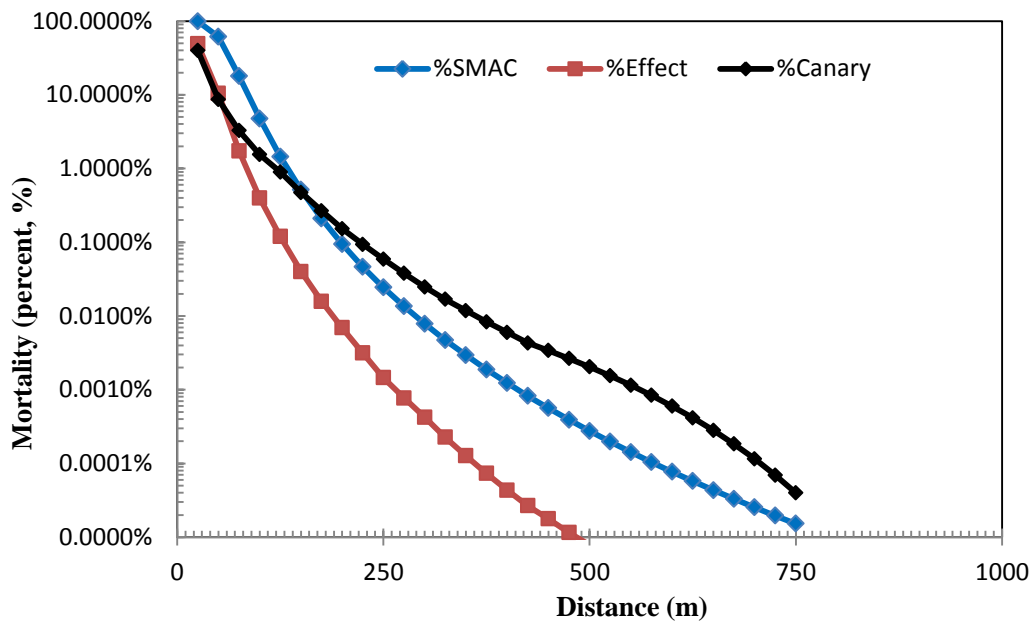


Figure 4.15 Comparison of the overpressure probit relation generated from an explosion of a road tanker containing 7000kg of LPG as a function of distance predicted by SMACTRA with others software



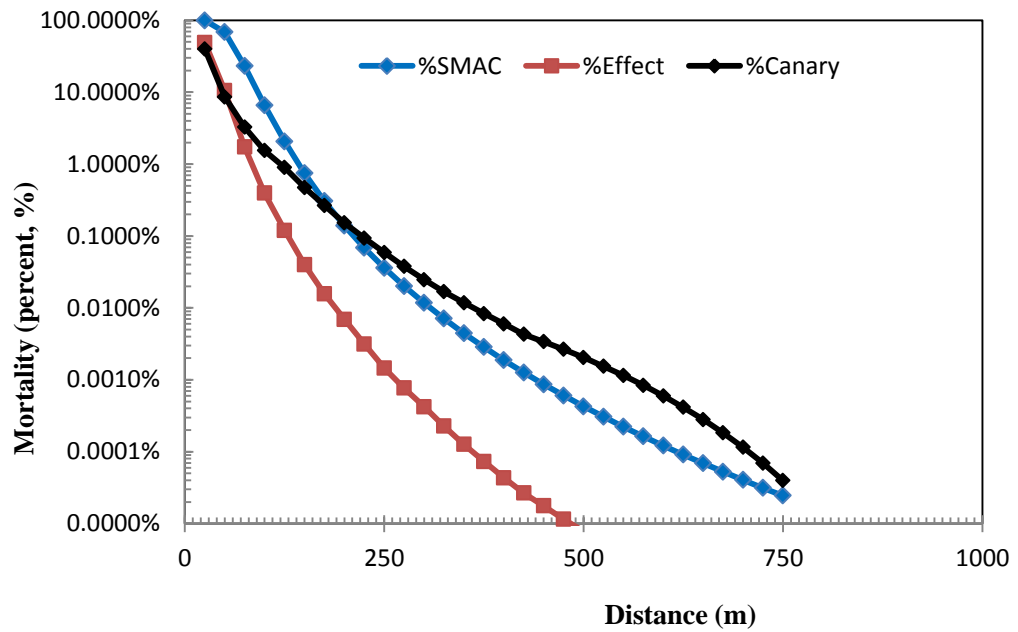


Figure 4.16 Comparison of the overpressure probit relation generated from an explosion of a road tanker containing 8500kg of LPG as a function of distance predicted by SMACTRA with others software

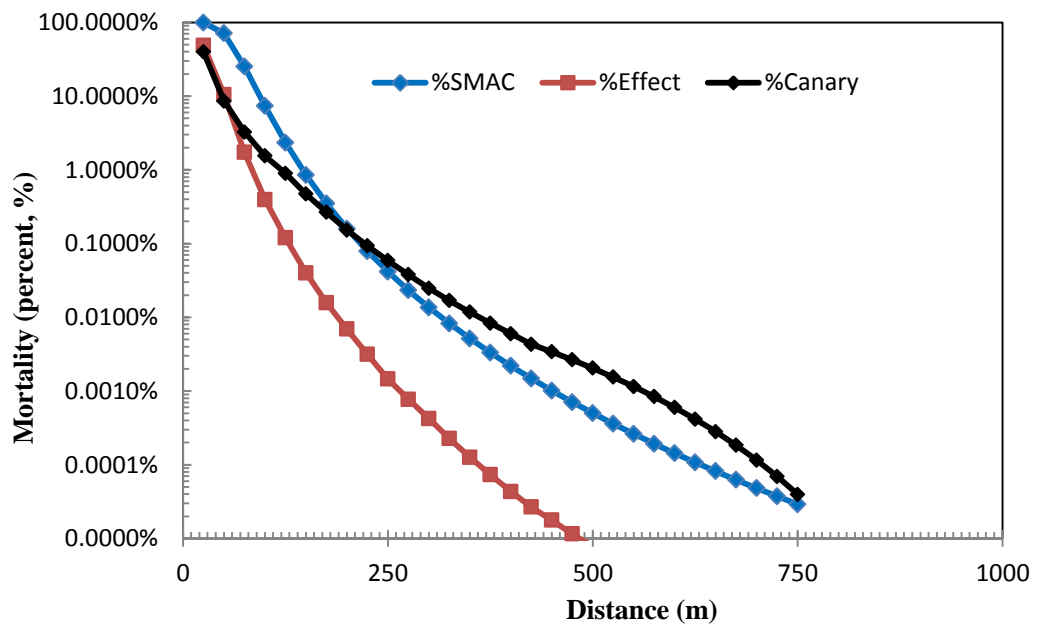


Figure 4.17 Comparison of the overpressure probit relation generated from an explosion of a road tanker containing 9119 kg of LPG as a function of distance predicted by SMACTRA with others software



In order to compare the results of the vapor cloud explosion consequences for LPG transportation accident over the physiological effects of overpressure exposure, LPG truck with capacities of 13000, 2000, 3000, 5000, 7000, 8500 and 9119 kg of LPG were selected. Figure 4.11 to 4.17 show the comparison results of the overpressure probit generated by road tanker explosion containing various quantity kg of LPG to the function of distance as predicted by SACTRA and others software. The analysis is important to determine the minimum safe operation distance between road tankers to human or building.

Table 4.6 and Figure 4.11 show the percentage of mortality from explosion from truck vessel containing 13,000 kg of LPG as predicted by SACTRA. The result is consistently approximated to EFFECT 8.01 software results for fatality which ranges between 3-100% for the distance ranges between 0 m to 75 m from the road tanker explosion containing 13,000 kg LPG. However it is shown that the mortality rate results for both SACTRA and EFFECT softwares deviate from each other as the distance increased and when the receptor point reaches more than 70 m. Probit results by SACTRA show 1% fatalities at a distance of 164m. Meanwhile mortality rate for EFFECT 8.01 and CANARY is 1% fatalities at the distance of 133.2 m and 123.5 m from the accident point. Both SACTRA and EFFECT 8.01 softwares calculated 50% fatalities between 59 to 67 m distance and 26.8m by CANARY software. With the distance greater than 185 m and on the curve for less 1% fatalities of the mortality rate, the result for both SACTRA and CANARY are consistently approximated to each other.

Meanwhile Figure 4.12 shows the graph curves for the mortality rate are approaching each other for the 3 softwares up to 2% fatalities. It is also shows that CANARY has calculated the explosive impact from 2000 kg of LPG road tanker explosion at a distance 110 m will cause 1% fatalities. In summary, the accident impact consequences results produced by SACTRA and EFFECT 8.01 approximated to each other at 3000 kg of LPG tanker. Figure 4.13 to 4.17 showing the comparison between the effects of overpressure probit generated by SACTRA, EFFECT 8.01 and CANARY for different LPG fuel capacity at 3000, 5000, 7000, 8500, and 9119 kg. Based on the mortality analysis from the accident impact of road tanker with



various capacities, it is demonstrated that the greater the amount of LPG content involved in the accident the larger the unsafe area for human. Based on the overpressures impact analysis it has been shown that the fatality percentage at 99%, 50% and 1% over distance increased exponentially with the increasing LPG capacity. For instance, for the 50% fatality curve from SACTRA it is recognised that unsafe distance for hazardous material transportation of LPG increased from 36.1 m at 2000 kg, 41.3 m at 3000 kg, 49 m at 5000 kg, 54.7 m at 7000 kg, 57 m at 8500 kg, 60 m at 9119 kg and 67 m 13,000 kg as shown in Table 4.6.

Comparison between SACTRA, EFFECT 8.01 and CANARY output analysis on the probabilities of accident impact to human physiology such as eardrum rupture, lung haemorrhage and to physical damage such as glass breakage and structural damage are shown in Table 4.7, 4.8 and 4.9. Table 4.7 shows the comparison between SACTRA, EFFECT 8.01 and CANARY probabilities impacts towards human and building generated from a vessel explosion containing 13000 kg of LPG. It is shown that the impact percentage of overpressure leading to glass breakage is highest for SACTRA and CANARY. From this table it is shown that the percentage of glass breakage from both models at the distance of 500 m is more than 50%. It is also shown that the predicted impact percentage towards human for eardrum rupture and lung haemorrhage is within 100 m and less than 25 m from the source of explosion. The above phenomenon is comparable with other studies [64, 67,179]. The percentage of glass breakage is still high even at the long distance due to its characteristics as the weakest part of the building and easily broken at a low pressures, 0.15-0.55 psi [64, 67, 179-181] compared to other components such as floors, walls, or column. It is reported from the literature [64, 67] that glass breakage may extend for miles from a large external explosion. Table 4.8 also shows the same characteristic of accident impact scenario as in Table 4.7 for a vessel explosion containing 2000 kg of LPG, but the unsafe zone is reduced. Even though fatal injury rate is demonstrated to be low by the 3 models as shown in Table 4.7- 4.10, the percentage is much greater in other reports [64, 67, 181, 206]. This is due to the high velocity glass fragments may become a major contributor to injuries in such incident. According to evidence based emergency medicine [206], it is reported that the flying projectiles can produce blunt trauma, depending of the size of the projectiles and the speed at which they travel.



According to SMACTRA it is estimated that the person who is standing at the distance of 500 m from explosion has the potential of having secondary blast injury from flying glasses at the percentage of 2.14% (4.09 kPa).

Secondary blast injury is the most common cause of death in blast victim. The flying glass causes 50% of secondary blast injury to human at a distance 250m for the capacity of 13,000 kg of LPG. This finding is consistent with the VCE case in Flixborough and Ixhuatepec, Mexico City [64], which showing that more than 40% of people injury is caused by secondary glass breakage effect. It is reported in the literatures [64, 181, 206, 207] that the penetrating injuries occur most often in the exposed areas, such as the head, neck, and extremities. Thoracic and intraabdominal injuries may occur when the fragments penetrate [64, 181, 206, 207]. It is estimated that up to 10% of blast survivors will have ocular injuries which can cause blindness and ruptured globes. The percentage of building structure damage is estimated to be 50% at 150 m distance by using SMACTRA and at 98 m with CANARY. The percentage of eardrum rupture is 50% for population at distance up to 90 m by using SMACTRA and 40 m by using CANARY for 13,000 kg of LPG explosion. Meanwhile none will get lung haemorrhage based on SMACTRA analysis at 55 m or more and at 25 m using CANARY. This result is consistent with explosion effect as proposed by Clancey and Glasstone [179-181] which shows that ear is the most easily damaged from primary blast injury.

According to Wightman et al. [208], most likely mechanism of primary blast injury is due to the irreversible effect related to the differences in tissue tensile strength and speed of the blast wave through the different tissues. Stress that exceeds tissue tensile strength probably predominates when blast surface loading exceeds velocities of 80-90 m/sec [208]. At the pressure of about 35 kPa (5 psi), human eardrum may rupture. With an overpressure of 100 kPa (14 psi), almost all eardrums will be ruptured. Meanwhile lungs are particularly susceptible to damage due to the extensive air/lung tissue interfaces. Blast lung is a direct consequence of the supersonic pressure wave generated by a high explosive [64, 67, 179-181]. It is the most common fatal injury caused by the primary blast among the survivors of the explosion. Eventhough, lung injuries may not be apparent immediately or externally, but the effect may lead to



death if not diagnosed and treated promptly [209, 210]. An overpressure of about 40 psi will cause lung injuries.

Table 4.9 comparing the result between SMACTRA and CANARY of 13,000 kg of LPG and EFFECT 8.01 at 2000 kg of LPG. Based on Table 4.7, Table 4.8 and Table 4.9 it is shown that the difference between the software results is in the range of 20%, up to 500 m distance is more than 80% fitted with the results with both CANARY and EFFECT 8.01 software. Table 4.9 will further re-emphasize on the result conclusion.



Table 4.6 Comparison of probabilities impacts to human and structural building generated from an explosion of a vessel containing 13000kg of LPG as function of distance by using SMACTRA and CANARY software

| SMACTRA |        |              |              |             |                | CANARY |              |              |             |                |
|---------|--------|--------------|--------------|-------------|----------------|--------|--------------|--------------|-------------|----------------|
| $r(m)$  | $P^o$  | (%)ovrp-ear1 | (%)ovrpl-hae | (%)ovrp-gls | (%)ovrp-strucd | $P^o$  | (%)ovrp-ear1 | (%)ovrpl-hae | (%)ovrp-gls | (%)ovrp-strucd |
| 25      | 876.36 | 100.00%      | 100.00%      | 100.00%     | 100.00%        | 75.21  | 85.77%       | 0.00%        | 100.00%     | 99.99%         |
| 50      | 178.90 | 99.70%       | 92.97%       | 100.00%     | 100.00%        | 33.47  | 31.11%       | 0.00%        | 100.00%     | 94.75%         |
| 75      | 71.50  | 83.46%       | 0.00%        | 100.00%     | 99.99%         | 23.61  | 12.17%       | 0.00%        | 100.00%     | 72.65%         |
| 100     | 39.46  | 43.06%       | 0.00%        | 100.00%     | 98.22%         | 18.76  | 5.37%        | 0.00%        | 99.99%      | 47.26%         |
| 125     | 26.04  | 16.42%       | 0.00%        | 100.00%     | 81.28%         | 16.11  | 2.85%        | 0.00%        | 99.99%      | 30.40%         |
| 150     | 19.13  | 5.79%        | 0.00%        | 99.99%      | 49.52%         | 13.71  | 1.34%        | 0.00%        | 99.98%      | 16.63%         |
| 175     | 15.05  | 2.09%        | 0.00%        | 99.99%      | 23.79%         | 11.90  | 0.64%        | 0.00%        | 99.90%      | 8.09%          |
| 200     | 12.39  | 0.80%        | 0.00%        | 99.93%      | 10.03%         | 10.43  | 0.31%        | 0.00%        | 99.67%      | 3.74%          |
| 225     | 10.54  | 0.32%        | 0.00%        | 99.70%      | 3.99%          | 9.36   | 0.16%        | 0.00%        | 99.21%      | 1.80%          |
| 250     | 9.18   | 0.14%        | 0.00%        | 99.08%      | 1.56%          | 8.51   | 0.09%        | 0.00%        | 98.41%      | 0.87%          |
| 275     | 8.14   | 0.06%        | 0.00%        | 97.84%      | 0.61%          | 7.76   | 0.05%        | 0.00%        | 97.05%      | 0.41%          |
| 300     | 7.32   | 0.03%        | 0.00%        | 95.77%      | 0.24%          | 7.13   | 0.03%        | 0.00%        | 95.07%      | 0.19%          |
| 325     | 6.65   | 0.02%        | 0.00%        | 92.76%      | 0.10%          | 6.62   | 0.02%        | 0.00%        | 92.59%      | 0.09%          |
| 350     | 6.10   | 0.01%        | 0.00%        | 88.80%      | 0.04%          | 6.20   | 0.01%        | 0.00%        | 89.63%      | 0.05%          |
| 375     | 5.63   | 0.00%        | 0.00%        | 84.02%      | 0.02%          | 5.83   | 0.01%        | 0.00%        | 86.21%      | 0.03%          |
| 400     | 5.24   | 0.00%        | 0.00%        | 78.57%      | 0.01%          | 5.50   | 0.00%        | 0.00%        | 82.36%      | 0.01%          |
| 425     | 4.89   | 0.00%        | 0.00%        | 72.66%      | 0.00%          | 5.25   | 0.00%        | 0.00%        | 78.72%      | 0.01%          |
| 450     | 4.59   | 0.00%        | 0.00%        | 66.51%      | 0.00%          | 5.01   | 0.00%        | 0.00%        | 74.88%      | 0.00%          |
| 475     | 4.33   | 0.00%        | 0.00%        | 60.31%      | 0.00%          | 4.78   | 0.00%        | 0.00%        | 70.50%      | 0.00%          |
| 500     | 4.10   | 0.00%        | 0.00%        | 54.22%      | 0.00%          | 4.55   | 0.00%        | 0.00%        | 65.56%      | 0.00%          |



Table 4.7 Comparison of probabilities impacts to human and structural building generated from an explosion of a vessel containing 2000 kg of LPG as function of distance by using SMACTRA and EFFECT Version 8.0 software

| SMACTRA |        |              |              |             |                | Effect Version 8.0 (TNO) |              |              |             |                |
|---------|--------|--------------|--------------|-------------|----------------|--------------------------|--------------|--------------|-------------|----------------|
| $r(m)$  | $P^o$  | (%)ovrp-ear1 | (%)ovrpl-hae | (%)ovrp-gls | (%)ovrp-strucd | $P^o$                    | (%)ovrp-ear1 | (%)ovrpl-hae | (%)ovrp-gls | (%)ovrp-strucd |
| 25      | 210.50 | 99.89%       | 99.53%       | 100.00%     | 100.00%        | 89.08                    | 91.88%       | 0.04%        | 100.00%     | 100.00%        |
| 50      | 45.32  | 53.69%       | 0.00%        | 100.00%     | 99.39%         | 36.31                    | 36.87%       | 0.00%        | 100.00%     | 96.85%         |
| 75      | 21.46  | 8.84%        | 0.00%        | 100.00%     | 62.68%         | 19.39                    | 6.11%        | 0.00%        | 100.00%     | 51.13%         |
| 100     | 13.70  | 1.33%        | 0.00%        | 99.97%      | 16.17%         | 13.05                    | 1.05%        | 0.00%        | 99.96%      | 12.97%         |
| 125     | 10.05  | 0.25%        | 0.00%        | 99.55%      | 2.94%          | 9.88                     | 0.22%        | 0.00%        | 99.48%      | 2.62%          |
| 150     | 7.97   | 0.06%        | 0.00%        | 97.52%      | 0.51%          | 7.85                     | 0.05%        | 0.00%        | 97.26%      | 0.45%          |
| 175     | 6.62   | 0.02%        | 0.00%        | 92.56%      | 0.09%          | 6.54                     | 0.01%        | 0.00%        | 92.09%      | 0.08%          |
| 200     | 5.67   | 0.00%        | 0.00%        | 84.42%      | 0.02%          | 5.62                     | 0.00%        | 0.00%        | 83.83%      | 0.02%          |
| 225     | 4.96   | 0.00%        | 0.00%        | 73.95%      | 0.00%          | 4.89                     | 0.00%        | 0.00%        | 72.52%      | 0.00%          |
| 250     | 4.42   | 0.00%        | 0.00%        | 62.47%      | 0.00%          | 4.29                     | 0.00%        | 0.00%        | 59.28%      | 0.00%          |
| 275     | 3.98   | 0.00%        | 0.00%        | 51.17%      | 0.00%          | 3.87                     | 0.00%        | 0.00%        | 47.79%      | 0.00%          |
| 300     | 3.63   | 0.00%        | 0.00%        | 40.88%      | 0.00%          | 3.51                     | 0.00%        | 0.00%        | 37.40%      | 0.00%          |
| 325     | 3.33   | 0.00%        | 0.00%        | 32.01%      | 0.00%          | 2.68                     | 0.00%        | 0.00%        | 27.75%      | 0.00%          |
| 350     | 3.08   | 0.00%        | 0.00%        | 24.67%      | 0.00%          | 2.92                     | 0.00%        | 0.00%        | 20.18%      | 0.00%          |
| 375     | 2.87   | 0.00%        | 0.00%        | 18.78%      | 0.00%          | 2.70                     | 0.00%        | 0.00%        | 14.45%      | 0.00%          |
| 400     | 2.68   | 0.00%        | 0.00%        | 14.16%      | 0.00%          | 2.50                     | 0.00%        | 0.00%        | 10.19%      | 0.00%          |
| 425     | 2.52   | 0.00%        | 0.00%        | 10.59%      | 0.00%          | 2.33                     | 0.00%        | 0.00%        | 7.16%       | 0.00%          |
| 450     | 2.38   | 0.00%        | 0.00%        | 7.88%       | 0.00%          | 2.20                     | 0.00%        | 0.00%        | 5.23%       | 0.00%          |
| 475     | 2.25   | 0.00%        | 0.00%        | 5.84%       | 0.00%          | 2.08                     | 0.00%        | 0.00%        | 3.70%       | 0.00%          |
| 500     | 2.13   | 0.00%        | 0.00%        | 4.32%       | 0.00%          | 1.97                     | 0.00%        | 0.00%        | 2.68%       | 0.00%          |



Table 4.8 Comparison between SACTRA result probabilities impacts to human and structural building generated from an explosion of a vessel containing 2000 and 13000kg of LPG as function of distance over CANARY and EFFECT Version 8.0 software (within 20% difference from SACTRA region value)

| CANARY (at 13000 kg of LPG) |              |             |             |                | EFFECT Version 8.0 (TNO) (at 2000kg of LPG) |             |             |                |
|-----------------------------|--------------|-------------|-------------|----------------|---|-------------|-------------|----------------|
| <i>r(m)</i>                 | (%)ovrp-ear1 | (%)ovrp-hae | (%)ovrp-gls | (%)ovrp=strucd | (%)ovrp-ear1                                | (%)ovrp-hae | (%)ovrp-gls | (%)ovrp=strucd |
| 25                          | in region    | 75%         | in region   | in region      | in region                                   | 74%         | in region   | in region      |
| 50                          | 44%          | 68%         | in region   | in region      | in region                                   | in region   | in region   | in region      |
| 75                          | 46%          | in region   | in region   | 2%             | in region                                   | in region   | in region   | in region      |
| 100                         | 13%          | in region   | in region   | 26%            | in region                                   | in region   | in region   | in region      |
| 125                         | in region    | in region   | in region   | 26%            | in region                                   | in region   | in region   | in region      |
| 150                         | in region    | in region   | in region   | 8%             | in region                                   | in region   | in region   | in region      |
| 175                         | in region    | in region   | in region   | in region      | in region                                   | in region   | in region   | in region      |
| 200                         | in region    | in region   | in region   | in region      | in region                                   | in region   | in region   | in region      |
| 225                         | in region    | in region   | in region   | in region      | in region                                   | in region   | in region   | in region      |
| 250                         | in region    | in region   | in region   | in region      | in region                                   | in region   | in region   | in region      |
| 275                         | in region    | in region   | in region   | in region      | in region                                   | in region   | in region   | in region      |
| 300                         | in region    | in region   | in region   | in region      | in region                                   | in region   | in region   | in region      |
| 325                         | in region    | in region   | in region   | in region      | in region                                   | in region   | in region   | in region      |
| 350                         | in region    | in region   | in region   | in region      | in region                                   | in region   | in region   | in region      |
| 375                         | in region    | in region   | in region   | in region      | in region                                   | in region   | in region   | in region      |
| 400                         | in region    | in region   | in region   | in region      | in region                                   | in region   | in region   | in region      |
| 425                         | in region    | in region   | in region   | in region      | in region                                   | in region   | in region   | in region      |
| 450                         | in region    | in region   | in region   | in region      | in region                                   | in region   | in region   | in region      |
| 475                         | in region    | in region   | in region   | in region      | in region                                   | in region   | in region   | in region      |
| 500                         | in region    | in region   | in region   | in region      | in region                                   | in region   | in region   | in region      |

Note: "in region" = the differences value is within or below than 20% from SACTRA result.



Table 4.9 Comparison between predicted peak side on overpressure versus distance curves for vessel containing 13000 kg of LPG using three models SMACTRA, CANARY and EFFECT Version 8.0 software

| Peak Overpressure |                           |                           |                                | Percentage of result difference |                          |                          |
|-------------------|---------------------------|---------------------------|--------------------------------|---------------------------------|--------------------------|--------------------------|
|                   |                           |                           |                                | $ (a-b)/a  \times 100\%$        | $ (a-c)/a  \times 100\%$ | $ (b-c)/b  \times 100\%$ |
| r(m)              | SMACTRA(kPa) <sup>a</sup> | CANARY (kPa) <sup>b</sup> | EFFECT 8.01 (kPa) <sup>c</sup> | (%)SMACTRA / CANARY             | (%)SMACTRA/EFFECT        | (%) CANARY/EFFECT        |
| 25                | 876.36                    | 75.21                     | 98.47                          | 91%                             | 89%                      | 24%                      |
| 50                | 178.90                    | 33.47                     | 47.51                          | 81%                             | 73%                      | 30%                      |
| 75                | 71.50                     | 23.61                     | 24.90                          | 67%                             | 65%                      | 5%                       |
| 100               | 39.46                     | 18.76                     | 16.30                          | 52%                             | 59%                      | 13%                      |
| 125               | 26.04                     | 16.11                     | 12.12                          | 38%                             | 53%                      | 25%                      |
| 150               | 19.13                     | 13.71                     | 9.68                           | 28%                             | 49%                      | 29%                      |
| 175               | 15.05                     | 11.90                     | 7.97                           | 21%                             | 47%                      | 33%                      |
| 200               | 12.39                     | 10.43                     | 6.83                           | 16%                             | 45%                      | 35%                      |
| 225               | 10.54                     | 9.36                      | 5.91                           | 11%                             | 44%                      | 37%                      |
| 250               | 9.18                      | 8.51                      | 5.27                           | 7%                              | 43%                      | 38%                      |
| 275               | 8.14                      | 7.76                      | 4.67                           | 5%                              | 43%                      | 40%                      |
| 300               | 7.32                      | 7.13                      | 4.20                           | 3%                              | 43%                      | 41%                      |
| 325               | 6.65                      | 6.62                      | 3.86                           | 0%                              | 42%                      | 42%                      |
| 350               | 6.10                      | 6.20                      | 3.56                           | 2%                              | 42%                      | 43%                      |
| 375               | 5.63                      | 5.83                      | 3.29                           | 3%                              | 42%                      | 44%                      |
| 400               | 5.24                      | 5.50                      | 3.04                           | 5%                              | 42%                      | 45%                      |
| 425               | 4.89                      | 5.25                      | 2.83                           | 7%                              | 42%                      | 46%                      |
| 450               | 4.59                      | 5.01                      | 2.64                           | 8%                              | 42%                      | 47%                      |
| 475               | 4.33                      | 4.78                      | 2.49                           | 9%                              | 43%                      | 48%                      |



500

4.10

4.55

2.34

10%

43%

48%



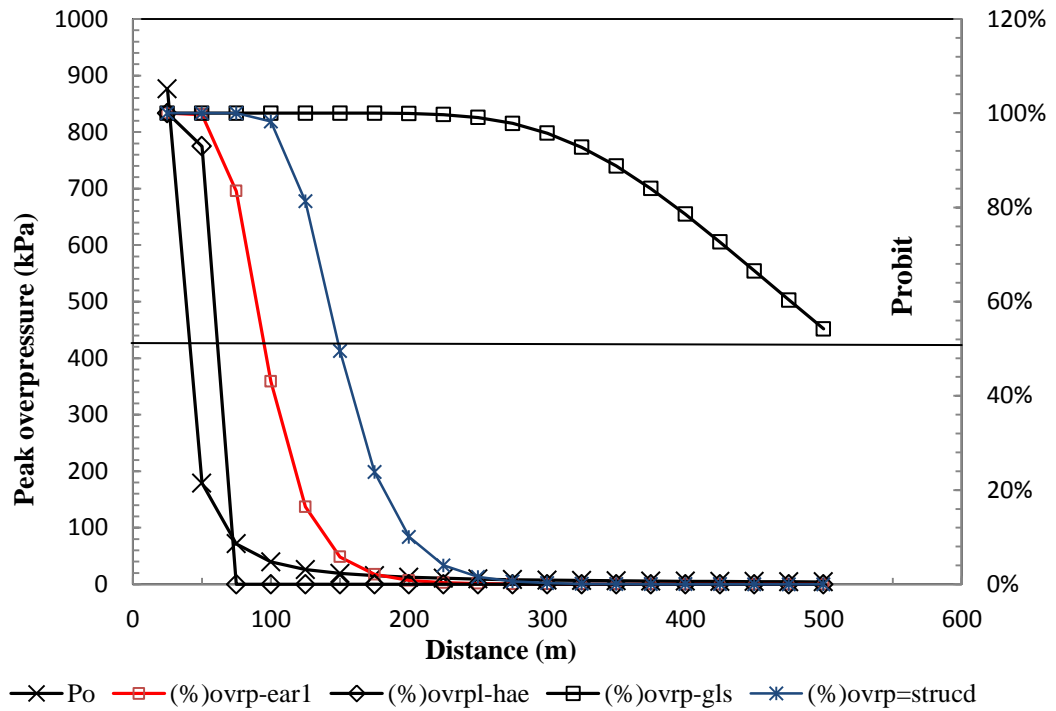


Figure 4.18 Consequences of an explosion from a road tanker containing 13000 kg of LPG as a function of distance predicted by SMACTRA software

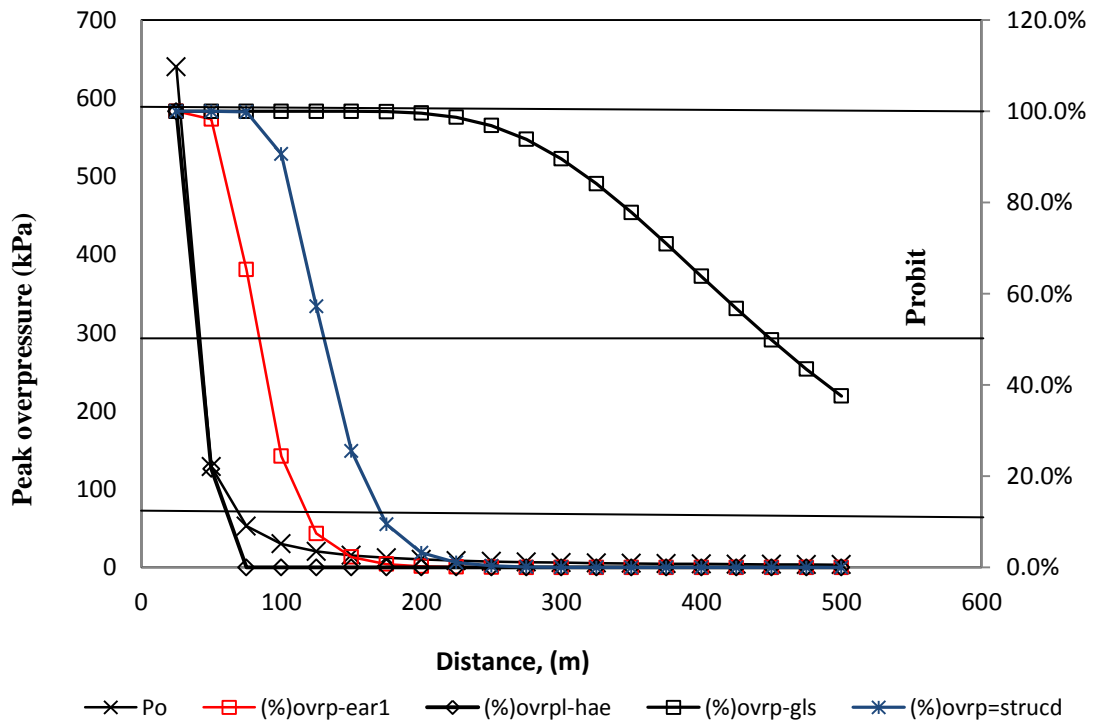


Figure 4.19 Consequences of an explosion from a road tanker containing 9119 kg of LPG as a function of distance predicted by SMACTRA software



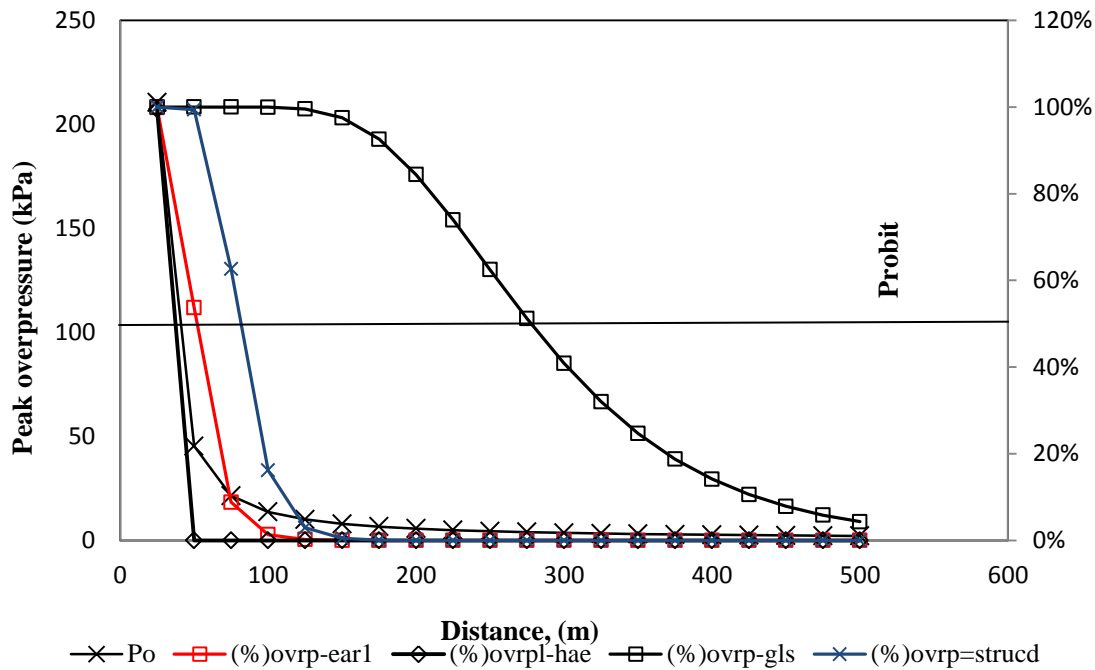


Figure 4.20 Consequences of an explosion from a road tanker containing 2000 kg of LPG as a function of distance predicted by SACTRA software.

Table 4.10 shows the comparison of overpressure percentages between SACTRA/CANARY, SACTRA/EFFECT and EFFECT/CANARY. The result for mortality percentages between SACTRA/CANARY shows a huge difference at 91% for the distance of 25m. However this percentage drops drastically to 52% for the distance of 100m. At the distance 170 to 500m the mortality percentage difference is below 0% at 325m and 11% at 175m. The combination of SACTRA/ CANARY at 13,000kg of LPG explosion impact shows a closer approximation compared to other combination (SACTRA/EFFECT and EFFECT/ CANARY) with the percentage difference of 40% at the distance between 200 to 500 m.

Figure 4.18 to 4.20, showing the graph analysis for consequences from a road tankers explosion containing 2000, 9119 and 13,000 kg of LPG against distance by using SACTRA. From the graph, the impact of the accident is clearly observed in Table 4.6 and 4.9, therefore it can be concluded that people who are staying within a radius of 62 m to 95 m from the incident are highly potential to have 50% chance of lung haemorrhage at 120 kPa and eardrum rupture at 42 kPa (13,000 kg of LPG). Meanwhile, most of the building is 50% damaged within the radius of 100 m to 200 m for all tanker capacities. More than 50 % of the glass breakage is estimated at the



distance 460 to 500 m. For the 2000 kg LPG, 50% of the glass damaged can be observed at 300 m distance. Based on the analysis on the impact of road tanker various capacities it can be concluded that the greater the amount of LPG content involved in the accident the larger the unsafe zone for human living and 500 m is considered the best distance of buffer zone for any transportation hazardous materials activities.

#### **4.3.4 Comparison results of the vapour cloud explosion consequences using SMAXTRA with published case studies and software risk analysis results.**

Comparison between vapour cloud explosion consequences results predicted by SMAXTRA with other established risk application softwares such as Effect 8.01 and Canary is discussed in section 4.2 and 4.3. Based on this comparison, it is concluded that SMAXTRA results are comparable with the two softwares. However, those results analysis only done for accident cases involving tanker carrying different LPG capacities as demonstrated in case study 1. Therefore in this section, additional analysis is made on different type of hazardous material such as butadiene and propane by using SMAXTRA and the outcomes are compared with published case studies and software risk analysis results as shown in Table 4.11. This section will also discuss on the effect calculation towards receptor and the results are also compared with other published result of impact explosion towards human and building structure as shown in Table 4.12 to 4.14. The overpressure, impulse and shock wave duration have been estimated by SMAXTRA software against distance are compared with other results from previous softwares and reported data from various accidents scenarios is shown in Table 4.10. According to the results in Table 4.11, for an explosion took place in a tank which contains 9,119 kg propane, the peak overpressure duration from SMAXTRA is at 6.54 kPa whereas the results from FRED software is 7 at kPa. The overpressure impulse for an explosion involving 100,000 kg butadiene is at 0.4 kPa/s by using SMAXTRA software, whereas the result from CANARY and MAXCRED software is at 0.223 kPa/s and at 0.6 kPa/s, which is closer than FRED result which is at 3.5 kPa/s. Meanwhile the result for LPG is comparable to other published results such as FRED and EFFECT. The explosion incident at PEMEX in Ixhuatpec at Mexico City is summarized in Table 4.11.



**Table 4.10** Comparison of peak overpressure from an explosion of propane, LPG, and butadiene with previous software and published data

| Variables  | Peak overpressure      |                      |       |           |        |                 |                               |                             |                       |
|--|------------------------|----------------------|-------|-----------|--------|-----------------|-------------------------------|-----------------------------|-----------------------|
|  | From previous software |                      |       |           |        |                 | From previous accidents       |                             | From current software |
|  | MAXCRED,<br>1997       | FRED, 2004           |       | BIS, 2003 | CANARY | EFFECT, 2009    | Analysis of Mexico City, 1984 |                             | SMACTRA               |
|  |                        | TNO                  | TNT   |           |        |                 | TNO                           | Baker <i>et. al.</i> , 1983 |                       |
| Chemical: <b>Propane</b><br>Quantity stored ( <i>kg</i> ): 9119<br>Volume of flammable gas/air cloud ( <i>m</i> <sup>3</sup> ): 119,719<br>Receptor distance ( <i>m</i> ): 293<br>Peak Overpressure: ( <i>kPa</i> )<br>Overpressure impulse: ( <i>kPa/s</i> )<br>Shock wave duration: ( <i>sec</i> )   | -                      | 13.5                 | 7.00  | 3.50      | 7.3    | 19              | -                             | -                           | 6.54                  |
|  | -                      | -                    | 0.01  | -         | -      | -               | -                             | -                           | -                     |
|  | -                      | -                    | 0.06  | -         | -      | -               | -                             | -                           | -                     |
| Chemical: <b>LPG</b><br>Quantity stored ( <i>kg</i> ):<br>Volume of flammable gas/air cloud ( <i>m</i> <sup>3</sup> ): 1200<br>Receptor distance ( <i>m</i> ): 50<br>Peak Overpressure: ( <i>kPa</i> )<br>Shock wave duration: ( <i>sec</i> )  | -                      | -                    | -     |           | 33.464 | 26.80           | 20.00                         | 29.00                       | 28.66                 |
| Chemical: <b>LPG</b><br>Quantity stored ( <i>kg</i> ): 250,000<br>Receptor distance ( <i>m</i> ): 300<br>Peak Overpressure: ( <i>kPa</i> )<br>Overpressure impulse: ( <i>kPa/s</i> )<br>Shock wave duration: ( <i>sec</i> )  | -                      | -                    | 35.60 |           | 4.55   | (10.13 - 25.33) | -                             | -                           | 47.06                 |
|  | -                      | -                    | -     |           | 1.2    | 0.87            | -                             | -                           | 3.9                   |
| Chemical: <b>Butadiene</b><br>Quantity stored ( <i>kg</i> ): 100,000<br>Storage pressure(atm): 3.5<br>Storage temperature: -25°C<br>Type of cylinder: pressurized cylinder<br>Volume of flammable gas/air cloud ( <i>m</i> <sup>3</sup> ):810,000<br>Receptor distance ( <i>m</i> ): 500<br>Peak Overpressure: ( <i>kPa</i> )<br>Overpressure impulse: ( <i>kPa/s</i> )<br>Shock wave duration: ( <i>sec</i> ) | 21.05                  | -                    | -     | -         | 8.71   | 4.08            | -                             | -                           | 5.62                  |
|  | 0.693                  | 6.90 (efficiency=1%) | 3.50  | -         | 0.223  | -               | -                             | -                           | 0.40                  |
|  | 41.09                  | -                    | -     | -         | -      | -               | -                             | -                           | -                     |



Table 4.11: Comparison the probabilities of fatalities from lung haemorrhage for a given overpressure.

| Probability of fatality | Peak overpressure ( <i>kPa</i> ) |                |         |
|-------------------------|----------------------------------|----------------|---------|
|                         | Eisenberg et al. [173]           | HSE [192]      | SMACTRA |
| 1%                      | 99.97                            | -              | 104.96  |
| 10%                     | 120.66                           | -              | 120.17  |
| 50%                     | 141.34                           | (137.9-172.4)  | 147.05  |
| 90%                     | 175.82                           | -              | 177.07  |
| 99%                     | 199.95                           | ( 206.8-241.3) | 205.08  |

Table 4.12: Comparison the probabilities of glass breakage for a given overpressure.

| Probability of glass breakage | Peak overpressure ( <i>kPa</i> ) |                      |                |            |           |              |         |
|-------------------------------|----------------------------------|----------------------|----------------|------------|-----------|--------------|---------|
|                               | Eisenberg, et. al., [173]        | Crowl & Louvar [153] | G. Wells [201] | FRED [195] | ATF [191] | HSE [192]    | SMACTRA |
| 1%                            | 1.70                             | -                    | -              | -          | -         | -            | 1.72    |
| 10%                           | -                                | 2.07                 | -              | -          | 2.07      | -            | 2.49    |
| 50%                           | -                                | -                    | (1.4-3)        | 2.00       | -         | (0.552-1.3)  | 3.95    |
| 90%                           | 6.20                             | -                    | (3-6)          | -          | -         | (4.62-11.03) | 6.25    |

Table 4.13: Comparison of the probabilities for construction damage at a given overpressure.

| Probability of construction damage | Peak overpressure ( <i>kPa</i> ) |                |            |               |         |
|------------------------------------|----------------------------------|----------------|------------|---------------|---------|
|                                    | Clancey [179]                    | G. Wells [201] | FRED [195] | HSE [192]     | SMACTRA |
| 10%                                | -                                | -              | -          | -             | 12.37   |
| 50%                                | 17.20                            | 35.00          | -          | (27.58-48.26) | 18.78   |
| 99%                                | 68.90                            | (80-260)       | 137.89     | -             | 52.16   |

Table 4.12 shows the comparison of physiological effect towards human and property from an explosion between SMACTRA software with results predicted by Eisenberg et al. [173] and FRED software [195]. As shown in Figure 4.18 and 4.20, the risk of lung haemorrhage are 10% and 99% for an overpressure of 120.17 kPa at a distance 52.8 m and 205.08 kPa at a distance 41.9 m as predicted by SMACTRA. This result is comparable with other researchers and published software results as shown in Table 4.12 [173].



Table 4.13 and 4.14 shows that, almost all probability results for glass breakage at low overpressure from other researchers and safety institutions are consistent with SACTRA probability result [8, 9, 10, 153, 173, 179, 191,192, 195, 201]. Table 4.13 shows the probability results predicted by SACTRA for glass breakage are 1% and 99% at very low and very high overpressure which are almost similar to Eisenberg [173], whereby results of 10%, and 50%, are comparable with Crowl and Louvar [153] and Wells [201] results. Comparison of the probabilities for construction damage at a given overpressure is shown in Table 4.14 and the results are comparable to the results published by Clancey [179].

#### **4.3.5 Results of the radiant heat from pool and torch fires of LPG transportation accident (at the container capacity 34.5m<sup>3</sup>)**

Pool fires are one of the most common occurrences in the process industries. This incident is normally occurring due to accidental releases of flammable material from storage or in transport situation. However, it is observed that for every release cases which are discussed in this study, the vapor cloud hazard zone is larger and more hazardous than the pool fire therefore the pool/flash fires rarely give an adverse affect the public.

Basically, pool fires occurring in industrial accidents are characterized by turbulent diffusion flames on a horizontal pool of fuel that is vaporized. The spillage liquid receives heat from the flames by convection and radiation and may lose or gain heat by conduction towards/from the solid or liquid substrate under the liquid layer. Once the fire reaches its steady state, there is a feedback mechanism that controls the feeding of fuel vapor to the flames. The amount of heat transferred between the fuel and the underlying interface will depend on the fuel and the substrate conditions. To analyze pool fire characteristic, a series of simplified relations key parameters are measured such as pool fire diameter and area, flame, length, angle of the flame drag and sag, radiation release, convective heat flux and hazard to human and structural building from heat radiation. These analyses were obtained by simulating several mathematical models as listed in Appendix 1.



For any LPG truck tanker collision release, there is a possibility of either torch fire, flash fire or pool fire may occur. As shown in Table 4.15 and 4.16, the pool fire size depends on the duration and the flow rate of the spill. Table 4.15 illustrated the effect of burning rate to pool fire as predicted by SMACTRA. From Table 4.15 it is observed that, the effect of burning rate results is consistent with Blinov and Khudiakov [211] conclusion on pool fire diameter characteristics, where the highest burning rates corresponded to the smaller pool diameters.

Table 4.14: Effect of burning rate of pool fire to pool fire diameter using SMACTRA

| Mass burning rate<br>$M_b, \text{kg/m}^2\text{-s}$ | Burning rate<br>$y_b, \text{m/s}$ | Diameter (pool fire)<br>m | time<br>s |
|--|-----------------------------------|---------------------------|-----------|
| 0.089  | $1.55 \times 10^{-4}$             | 28.68                     | 45.91     |
| 0.085  | $1.48 \times 10^{-4}$             | 29.35                     | 47.34     |
| 0.081  | $1.41 \times 10^{-4}$             | 30.06                     | 48.89     |
| 0.077  | $1.34 \times 10^{-4}$             | 30.83                     | 50.56     |
| 0.073  | $1.27 \times 10^{-4}$             | 31.67                     | 52.39     |
| 0.069  | $1.20 \times 10^{-4}$             | 32.57                     | 54.40     |
| 0.065  | $1.13 \times 10^{-4}$             | 33.56                     | 56.61     |

In SMACTRA, the liquid spill is divided into two categories, recognized as instantaneous spills and continuous spills. If the LPG spill is instantaneous, the pool fire will grow until it meets a physical barrier. However in the case of a continuous spill, the pool fire will grow until it finds a physical barrier or until the vaporization velocity or whenever it's burning rate is equal to spill rate. Therefore to differentiate between instantaneous and continuous spills, several researchers proposed a criterion [67, 213, 214]. SMACTRA differentiate the liquid spill based on criterion as proposed by K. Mudan et al. [212]. According to this criterion when critical time,  $t_{cr} < 2 \times 10^{-3}$ , spill is considered instantaneous and when  $t_{cr} > 2 \times 10^{-3}$  the spill is continuous. . Table 4.15 shows the results effect of time spillage to pool fire size diameter using SMACTRA. Table 4.16 shows the effect of time spillage to pool fire diameter at constant burning rate using SMACTRA.



Table 4.15: Effect of time spillage to pool fire diameter at constant burning rate using  
SMACTRA

| Mass burning<br>rate<br>$M_b$ , kg/m <sup>2</sup> -s | Duration of Spill<br>s | Critical time<br>s    | Diameter (pool fire)   |                     |
|--|------------------------|-----------------------|------------------------|---------------------|
|  |                        |                       | $m_a$                  | $m_b$               |
| $9.43 \times 10^{-5}$                                | 205                    | $1.28 \times 10^{-3}$ | $2.70 \times 10^2$     | refer instant. Case |
| $9.43 \times 10^{-5}$                                | 260                    | $1.62 \times 10^{-3}$ | $3.37 \times 10^2$     | refer instant. Case |
| $9.43 \times 10^{-5}$                                | 320                    | $1.99 \times 10^{-3}$ | $4.19 \times 10^2$     | refer instant. Case |
| $9.43 \times 10^{-5}$                                | 380                    | $2.37 \times 10^{-3}$ | refer continuous. Case | $3.53 \times 10^2$  |
| $9.43 \times 10^{-5}$                                | 440                    | $2.74 \times 10^{-3}$ | refer continuous. Case | $3.28 \times 10^2$  |
| $9.43 \times 10^{-5}$                                | 500                    | $3.11 \times 10^{-3}$ | refer continuous. Case | $3.08 \times 10^2$  |
| $9.43 \times 10^{-5}$                                | 560                    | $3.49 \times 10^{-3}$ | refer continuous. Case | $2.91 \times 10^2$  |
| $9.43 \times 10^{-5}$                                | 620                    | $3.86 \times 10^{-3}$ | refer continuous. Case | $2.76 \times 10^2$  |
| $9.43 \times 10^{-5}$                                | 680                    | $4.23 \times 10^{-3}$ | refer continuous. Case | $2.64 \times 10^2$  |
| $9.43 \times 10^{-5}$                                | 740                    | $4.61 \times 10^{-3}$ | refer continuous. Case | $2.53 \times 10^2$  |
| $9.43 \times 10^{-5}$                                | 800                    | $4.98 \times 10^{-3}$ | refer continuous. Case | $2.43 \times 10^2$  |
| $9.43 \times 10^{-5}$                                | 860                    | $5.35 \times 10^{-3}$ | refer continuous. Case | $2.35 \times 10^2$  |
| $9.43 \times 10^{-5}$                                | 920                    | $5.73 \times 10^{-3}$ | refer continuous. Case | $2.27 \times 10^2$  |
| $9.43 \times 10^{-5}$                                | 980                    | $6.10 \times 10^{-3}$ | refer continuous. Case | $2.20 \times 10^2$  |
| $9.43 \times 10^{-5}$                                | 1040                   | $6.47 \times 10^{-3}$ | refer continuous. Case | $2.13 \times 10^2$  |
| $9.43 \times 10^{-5}$                                | 1100                   | $6.85 \times 10^{-3}$ | refer continuous. Case | $2.07 \times 10^2$  |
| $9.43 \times 10^{-5}$                                | 1160                   | $7.22 \times 10^{-3}$ | refer continuous. Case | $2.02 \times 10^2$  |
| $9.43 \times 10^{-5}$                                | 1220                   | $7.59 \times 10^{-3}$ | refer continuous. Case | $1.97 \times 10^2$  |
| $9.43 \times 10^{-5}$                                | 1280                   | $7.97 \times 10^{-3}$ | refer continuous. Case | $1.92 \times 10^2$  |
| $9.43 \times 10^{-5}$                                | 1340                   | $8.34 \times 10^{-3}$ | refer continuous. Case | $1.88 \times 10^2$  |
| $9.43 \times 10^{-5}$                                | 1400                   | $8.71 \times 10^{-3}$ | refer continuous. Case | $1.84 \times 10^2$  |
| $9.43 \times 10^{-5}$                                | 1460                   | $9.09 \times 10^{-3}$ | refer continuous. Case | $1.80 \times 10^2$  |
| $9.43 \times 10^{-5}$                                | 1520                   | $9.46 \times 10^{-3}$ | refer continuous. Case | $1.76 \times 10^2$  |
| $9.43 \times 10^{-5}$                                | 1580                   | $9.84 \times 10^{-3}$ | refer continuous. Case | $1.73 \times 10^2$  |
| $9.43 \times 10^{-5}$                                | 1640                   | $1.02 \times 10^{-3}$ | refer continuous. Case | $1.70 \times 10^2$  |
| $9.43 \times 10^{-5}$                                | 1700                   | $1.06 \times 10^{-3}$ | refer continuous. Case | $1.67 \times 10^2$  |
| $9.43 \times 10^{-5}$                                | 1760                   | $1.10 \times 10^{-3}$ | refer continuous. Case | $1.64 \times 10^2$  |

The results in Table 4.16 show that, when the duration of spill is at 380 s and above, the spill is considered as continuous cases. The pool diameter will decrease while the pool size becomes smaller. Blinov and Khudiakov [211, 215] studied the behaviour of pool fires with different type of fuels and pool diameter and concluded that all fuels showed the same pool fire characteristic. Therefore it is expected that, the pool fire scenario will show similar result conclusion as shown in Table 4.15 and Table 4.16 if different type of fuel is analyzed by using SACTRA.



As illustrated in Table 4.17 and Table 4.18, the radiant heat from pool fire can cause secondary fires of other combustible materials, structural damage and injuries to exposed persons. The secondary fires can occur as the radiant heat from pool fire engulfed the tanker and heated the LPG inside the tank leading to the release of partial depressurized liquid as gas at atmosphere temperature. If the gas releases continue for a period of time, there is high possibility of an explosion to occur. Majority of explosion cases explosion such as BLEVE, fireball and VCE will leave a serious impact since the thermal radiation dose received by the receptor is high and the affected area is large.

Table 4.17 is related to the case study accident analysis for a road tanker containing 13,000 kg of LPG as predicted by SMAXTRA software for release of 40.65 kg/s LPG. By applying an input of release rate (40.65 kg/s) to assess pool fire by using SMAXTRA software, it estimates the flame length is equal to 40.72 m, the pool fire diameter is equal to 20 m, the area of the circular shaped pool is 314 m<sup>2</sup> and the tilt from vertical (43.86 deg.). The output results from SMAXTRA (as shown in table 4.16) have been compared with FRED software and the results are summarized in Table 4.18.

From Table 4.18, it can be concluded that the pool fire burns with cylindrical shaped, the flame height is usually twice the pool fire diameter (as shown in Table 4.17, when the diameter of pool fire is 20 m, the flame length is 40.72 m). The same findings have been reported by Khan and Abbasi [216] and Andreassen et al. [217].



Table 4.16: SACTRA input and output parameters for Pool fire hazard (34.5m<sup>3</sup> LPG).

|   | Value                 | Unit                                   |
|---|-----------------------|--|
| <b><i>Input parameters</i></b>                      |                       |  |
| Material name: Gasoline (petrol)                    |                       |  |
| Material release rate (=0.0707m <sup>3</sup> /s)    | 40.65                 | kg/s                                   |
| Heat of Combustion                                  | 46,400                | kJ/kg                                  |
| Heat of vaporization                                | 425.31                | kJ/kg                                  |
| Mass of material released (10-20%) before explosion | 1,300-2,600           | Kg                                     |
| Boiling point of liquid                             | 272.5                 | K                                      |
| Ambient temperature                                 | 298                   | K                                      |
| Liquid density                                      | 570                   | Kg/m <sup>3</sup>                      |
| Constant heat capacity                              | 1.528                 | kJ/kg.K                                |
| Receptor distance from pool (at 25m)                |                       |  |
| Relative humidity                                   | 70%                   |  |
| Radiation fraction                                  | 0.325                 | -                                      |
| Exposure time (sec)                                 | 4.5                   | sec                                    |
| Distance from pool fire                             | Open range            | M                                      |
| Modified heat vaporization                          | 386.35                | kJ/kg                                  |
| Vertical burning rate                               | 1.53x10 <sup>-4</sup> | m/s                                    |
| Mass burning rate                                   | 8.77x10 <sup>-2</sup> | kg/m <sup>2</sup> .s                   |
| Diameter of pool                                    | 20.00                 | m                                      |
| Area of pool  | 314.16                | m <sup>2</sup>                         |
| Flame H/D   | 1.70                  |  |
| Flame height  | 34.04                 | m                                      |
| Partial pressure of water vapour                    | 2211.93               | Pa                                     |
| <b><i>Output parameters</i></b>                     |                       |  |
| a) Point source model                               |                       |  |
|   | 17.02                 | m                                      |
| Point source height                                 | 3.44x10 <sup>-5</sup> |  |
| View factor   | 0.71                  | kW/m <sup>2</sup>                      |
| Transmissivity                                      | 10.18                 | (kW/m <sup>2</sup> ) <sup>4/3</sup> .s |
| Thermal radiation at receptor                       |                       |  |
| Thermal dose at receptor                            |                       |  |
| b) Solid plume radiation model                      |                       |  |
|   | 30.89                 | kW/m <sup>2</sup>                      |
| Source emissive power                               | 10                    | m                                      |
| Flame radius  | 3.40                  | m                                      |
| Flame H/R ratio                                     | 0.126                 |  |
| View factor   | 0.756                 | kW/m <sup>2</sup>                      |
| Transmissivity                                      | 9.62                  | (kW/m <sup>2</sup> ) <sup>4/3</sup> .s |
| Thermal radiation to receptor                       |                       |  |
| Thermal dose at receptor                            |                       |  |



Table 4.17: Comparison of the pool fire output results between SMACTRA and FRED software.

| Pool fire parameters                                | Results     |         |
|---|-------------|---------|
|   | FRED (2004) | SMACTRA |
| Fluid: LPG commercial (30:70 propane: butane % mol) |             |         |
| Pool fire Diameter (m)                              | 20.00       | 20.00   |
| Flame length (m)                                    | 31.73       | 40.72   |
| Flame clear length (m)                              | -           | 12.24   |
| Area of pool fire ( $m^2$ )                         | -           | 314.16  |
| Flame angle from vertical (Deg.)                    | 45.21       | 43.86   |
| Surface emissive power ( $kW/m^2$ )                 | 36.24       | 30.89   |
| Thermal radiation at 25 m                           | 8.5         | 9.62    |

#### 4.3.6 The effect from the radiant heat pool fire of LPG transportation accident (at the container capacity $34.5m^3$ ) to receptor.

To study the above effect, few parameters such as view factor, transmissivity, thermal flux and distance from receptor to pool fire are looked into detail. Based on the predicted result by SMACTRA (as shown in the Figure 4.21) whenever the distance from receptor to pool fire increased, thermal radiation flux reduced significantly. However the fire geometry is noted to be reduced and slightly constant. In this case, the atmospheric transmissivity is accounts as the absorption of the thermal radiation by the atmosphere, essentially by carbon dioxide and water vapour. From that factor, it is observed, the radiation is attenuated significantly, especially when reaches the target surface.

Meanwhile, view factor is a parameter which appears in practically in all thermal radiation calculation. By definition, view factor is the ratio between the amount of thermal radiation emitted by a flame and the amount of thermal radiation received by an object not in contact with the flame. Apart from that, this ratio is also dependent on the shape and size of the fire, the distance between the flame and the receiving element and the relative position of the flame and target surfaces. Therefore, whenever the size of the fire reduced, thermal flux is also reduced significantly.



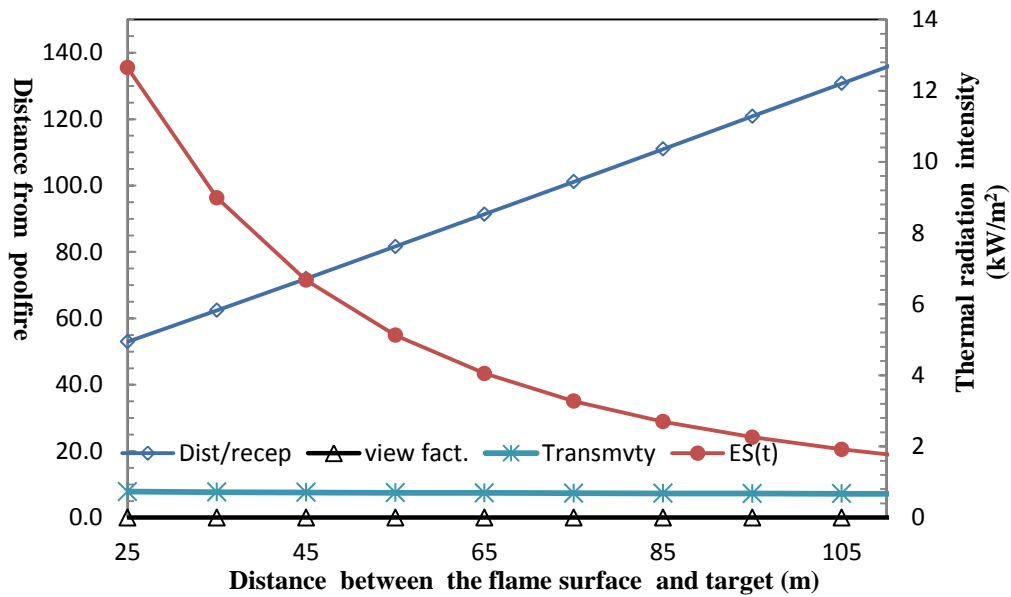


Figure 4.21 Thermal radiation intensity, view factor and transmissivity as a function of distance generated from consequences of pool fire from a road tanker containing 13,000 kg of LPG at leakage rate  $0.0707\text{m}^3/\text{s}$  or  $43.5\text{ kg/s}$  (predicted by SMACTRA software)

Graph in Figure 4.22 showing the analysis of leakage rate versus thermal dose. In the first condition known as  $Es(t)_2$ , leakage rate was constant at  $0.0707\text{m}^3/\text{s}$ . This has lead to a constant pool diameter and pool area. However, the distance of the receptor is getting further away from fire source. These also contribute to the reduction of transmissivity and view factor. With regard to view factor, when the fuel volume reduced, the fire size became smaller. However, for the second condition known  $Es(t)_3$ , the distance between fire source and receptor was nearer. As the leak rate increased, the area also became larger and getting nearer to receptor. It was shown, as in Figure 4.22, that thermal radiation intensity for second condition  $Es(t)_3$  is higher than the first condition,  $Es(t)_2$ . Therefore, based on SMACTRA predicted result as in Figure 4.23, the second condition will be getting more thermal radiation dose load in  $(\text{kW}/\text{m}^2)^{4/3}\text{-s}$ , when the leak rate is increased and the receptor distance is getting nearer to the fire source.



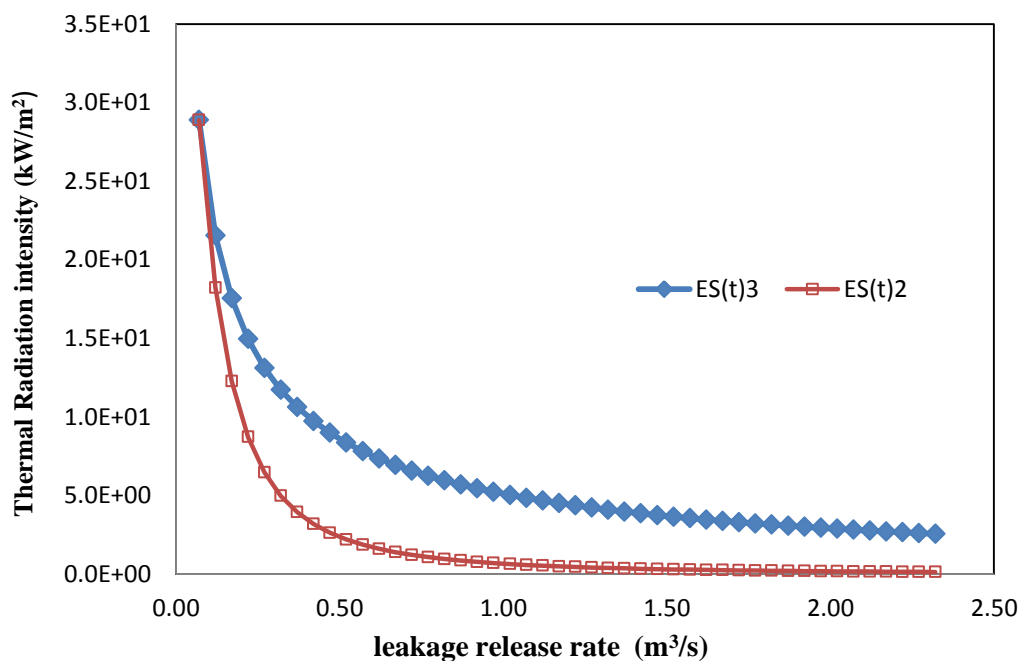


Figure 4.22 Thermal radiation intensity as a function of leakage rate release generated from consequences of pool fire from a road tanker containing 13000 kg of LPG (predicted by SMACTRA software)

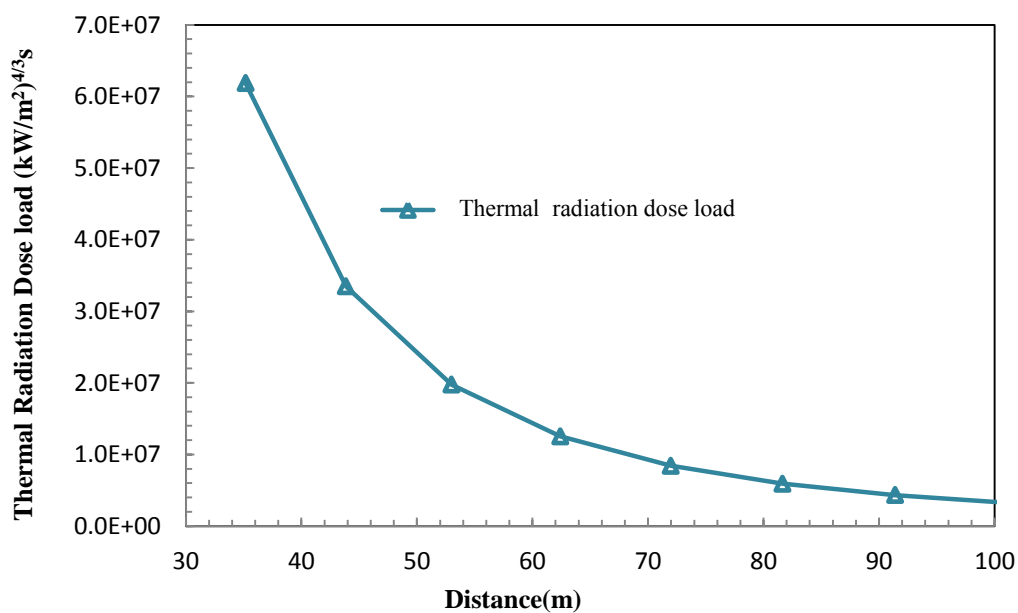


Figure 4.23 Thermal radiation dose loads as a function of distance generated from consequences of pool fire from a road tanker containing 13,000 kg of LPG at leakage rate 0.0707m³/s or 43.5 kg/s (predicted by SMACTRA software)



#### **4.3.7 The pool fire time exposure effect on thermal radiation dose load for LPG tanker incident (in capacity of 34.5m<sup>3</sup>) to Receptor**

Figure 4.24 to 4.30, demonstrate the probit function for pool fire thermal radiation at various exposure time 43.5s, 60s, 90s, 180s, 900s, and 1200s by using SACTRA. In the analysis, the association between duration of exposure and thermal radiation dose which is received by a human being is observed. According to accident and emergency medicine [163-166, 219] the impact of thermal radiation can be either 1<sup>st</sup> degree or 2<sup>nd</sup> degree burn and even mortality Based on the analysis, when the amount of dose thermal radiation received by an individual is increased, the percentage impact also increased as shown in Figure 4.24 till 4.29. It is also shown that the 1<sup>st</sup> and 2<sup>nd</sup> degree burn and lethality percentage are accelerated when the distance between the receiver and the source of explosion decreased.

Figure 4.28 and 4.29 show that at exposure time 900s (15 minute) and 1200s, approximately 100% of people around the accident zone (within 500m) will experience first degree burn. This is further confirmed by comparing the probabilities impact curves of thermal radiation as shown in Figure 4.24 to 4.29, the longer the time of exposure to thermal burns the more the thermal dose will be absorbed by the victim. The extent of burn damage depends on surface temperature and contact duration [218, 219]. Eventhough 1<sup>st</sup> degree burns are not life threatening, but it can cause a significant amount of pain for the victim. It is also observed that the dose thermal radiation curve  $(\text{kW/m}^2)^{4/3} \cdot \text{s}$  shifted from the range of  $1.0 \times 10^6$ -  $1.5 \times 10^6$   $(\text{kW/m}^2)^{4/3} \cdot \text{s}$  to  $1.7 \times 10^6$   $(\text{kW/m}^2)^{4/3} \cdot \text{s}$ . The above results are important to analyze the level of effectiveness for different agency/ies involved in emergency response from major accident hazard. Graph analysis in Figure 4.30 shows prediction by using SACTRA and the result is compatible to other literatures as reported by Mudan [212]. According to Mudan the time elapsed before one can feel pain is a function of the heat flux. From Figure 4.30 it is estimated that at  $5 \text{ kW/m}^2$  which is the time before one can feel pain is approximately 13s and by using SACTRA for poolfire leakage is at 43.5 kg/s or 0.0707 m<sup>3</sup>/s, this result is comparable to Eisenberg et al. [173].



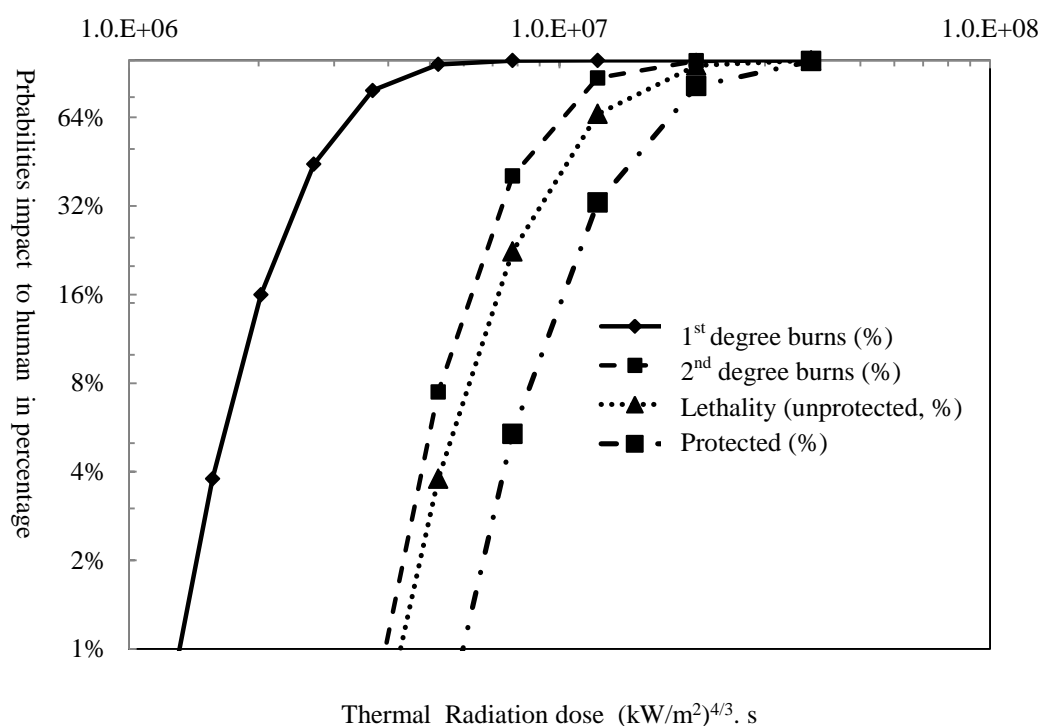


Figure 4.24 Probit functions for pool fire thermal radiation (at exposure time 43.5 sec. and  $\text{Dose}_{\text{human}} (\text{kW/m}^2)^{4/3} \cdot \text{s}$  (predicted by SACTRA software).

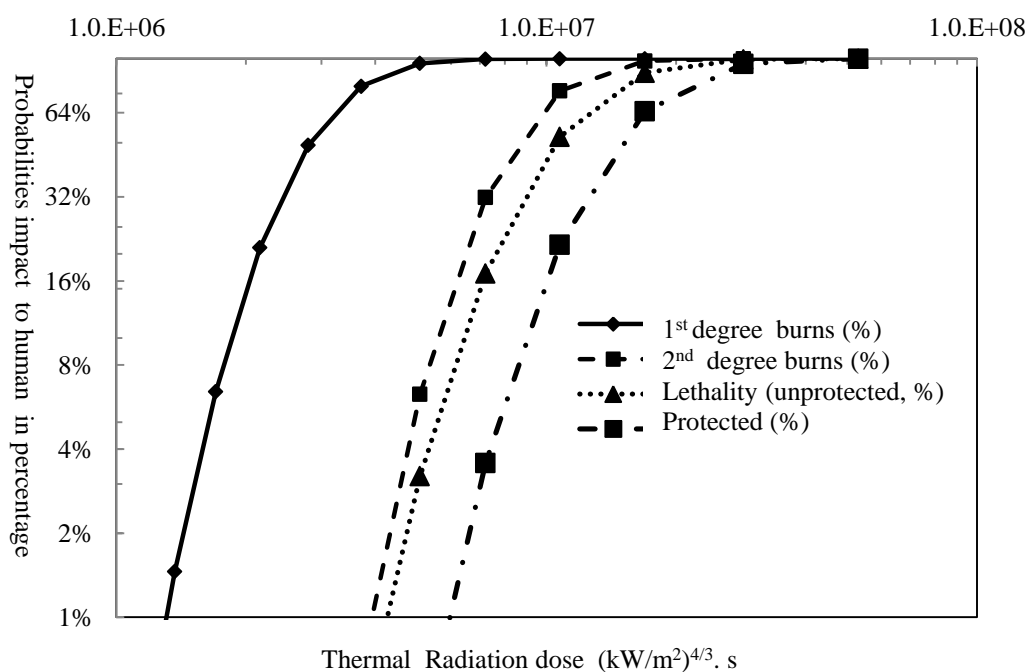


Figure 4.25 Probit functions for pool fire thermal radiation (at exposure time 60 sec. and  $\text{Dose}_{\text{human}} (\text{kW/m}^2)^{4/3} \cdot \text{s}$  (predicted by SACTRA software).



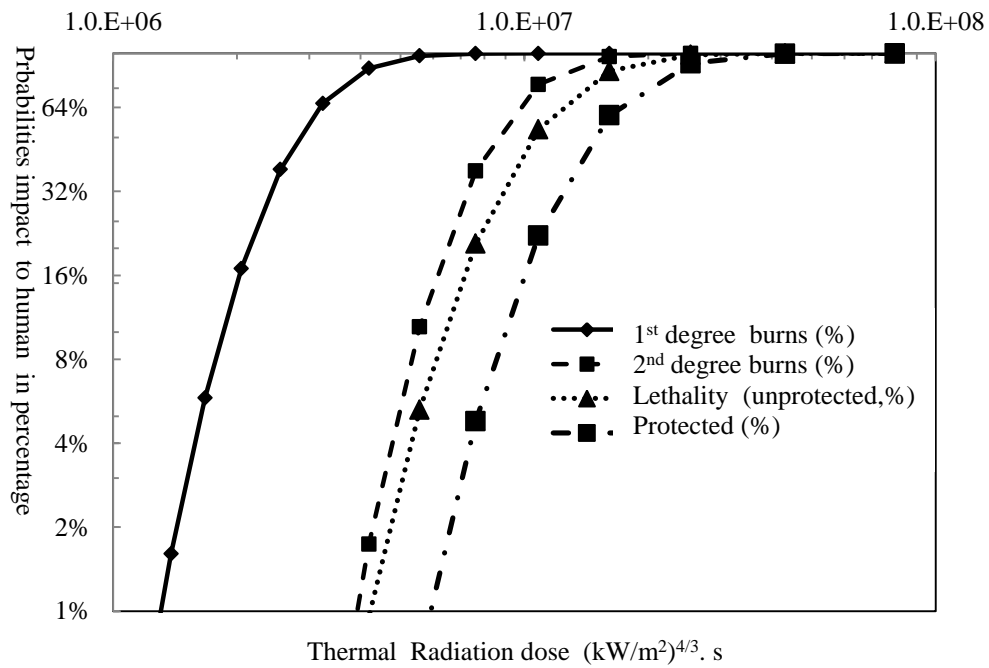


Figure 4.26 Probit functions for pool fire thermal radiation (at exposure time 90 sec.. and Dose<sub>human</sub> (kW/m²)<sup>4/3</sup>.s (predicted by SACTRA software).

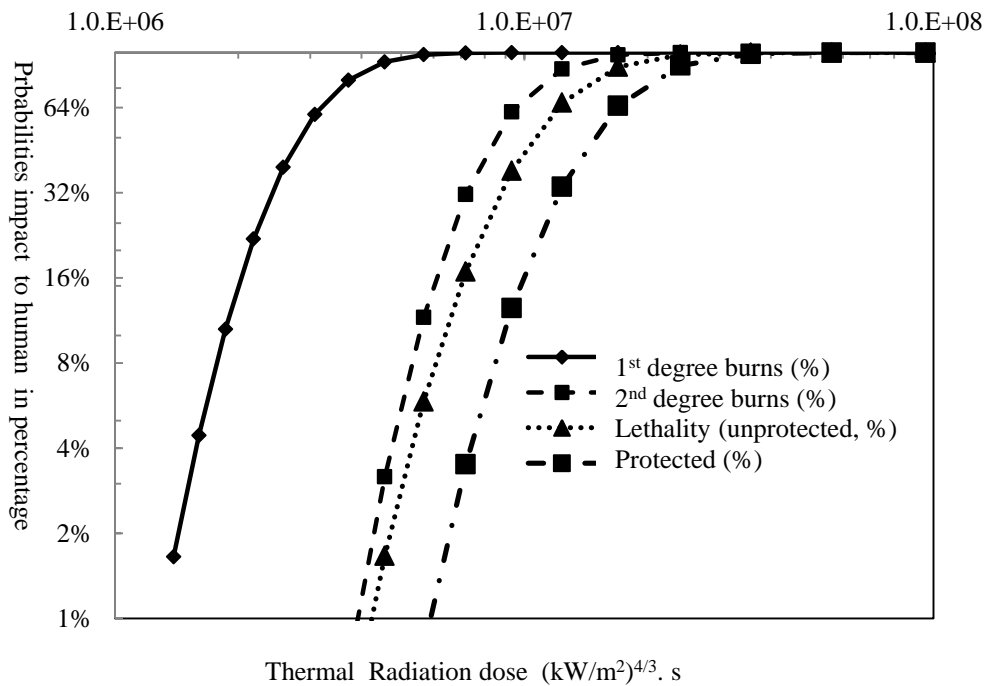


Figure 4.27 Probit functions for pool fire thermal radiation (at exposure time 180 sec.. and Dose<sub>human</sub> (kW/m²)<sup>4/3</sup>.s (predicted by SACTRA software).



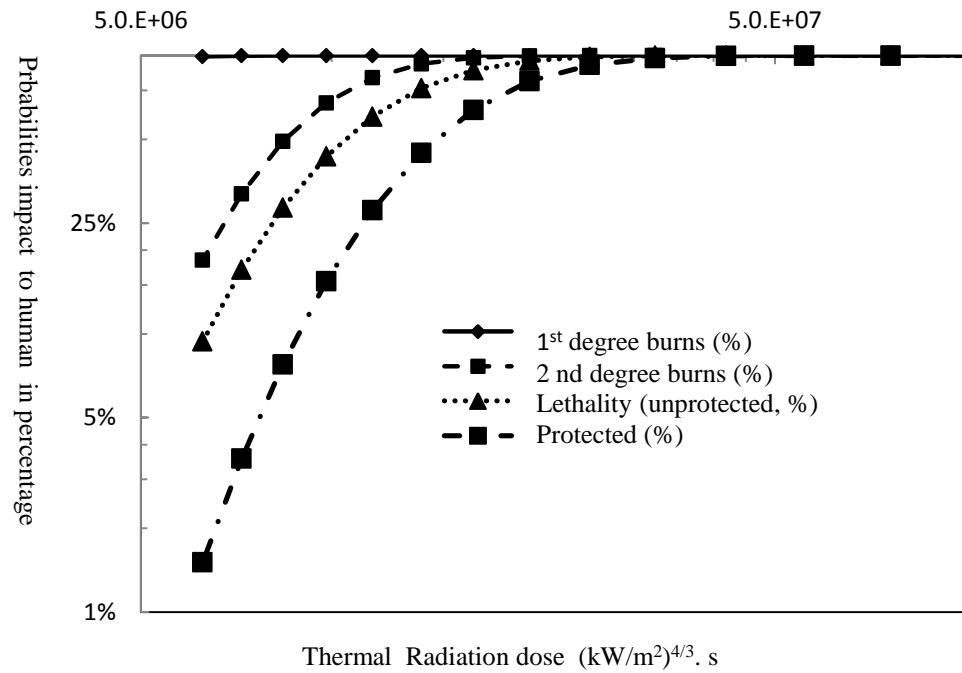


Figure 4.28 Probit functions for pool fire thermal radiation (at exposure time 900 sec. and  $\text{Dose}_{\text{human}} (\text{kW/m}^2)^{4/3} \text{s}$  (predicted by SACTRA software).

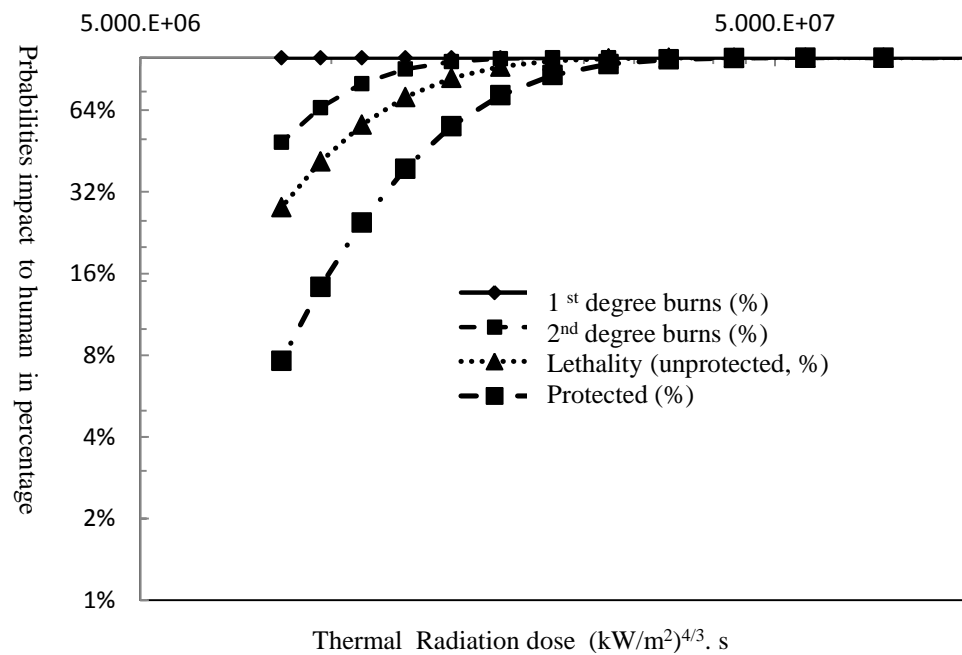


Figure 4.29 Probit functions for pool fire thermal radiation (at exposure time 1200 sec. and  $\text{Dose}_{\text{human}} (\text{kW/m}^2)^{4/3} \text{s}$  (predicted by SACTRA software).



In summary, the larger the exposure to dose thermal radiation to the human being, the higher the percentage of serious injury which may also lead to cost implication such as the treatment cost and insurance for compensation. Therefore the level of Key Performance Index (KPI) emergency response to accident between 900s and 15 to 20 minute should be re-evaluate due to, at the the particular time, individual or many people life may be jeopardice or possibility of acute, chronic or irreversible injury is high. Moreover, according to accident and emergency (A & E) medical research, the external heat can transfer from skin to internal organ including vascular system. Therefore, if a person stays for a long duration at a high thermal radiation area, this will cause an increase in core body temperature leading to severe dehydration and its complication [183].

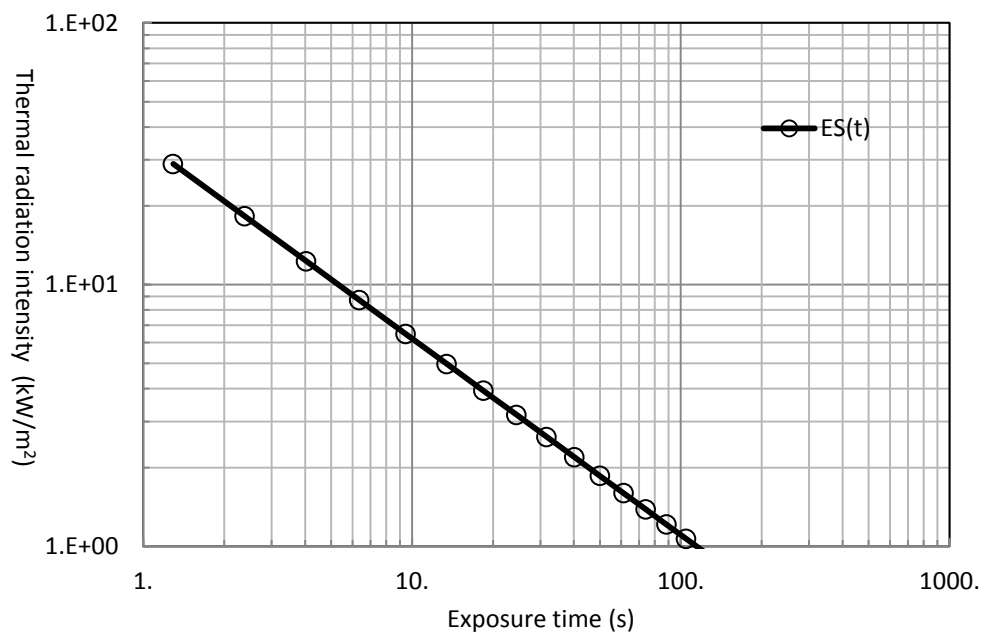


Figure 4.30 Time before one feels pain as a function of thermal radiation at 43.5kg/s or 0.0707m<sup>3</sup>/s caused from pool fire (predicted by SMACTRA software).

#### 4.3.8 Results of the BLEVE fireball consequences of LPG transportation accident

A Boiling Liquid Expanding Vapour Explosion (BLEVE) is the explosive release of expanding vapour and boiling liquid when a container holding a pressure-liquefied gas fails catastrophically. Catastrophic failure happens when a tank is ruptured and



releases its contents nearly instantaneously [221-223]. According to Lees [64], the cause and effects of a BLEVE depends on whether the liquid in the vessel is flammable or not. The initial explosion generates a blast wave and missiles. The flammable material causes a fire, which either transfer heat or form a vapor cloud and subsequently gives rise to a second explosion. A BLEVE can occur, due to sudden failure of containment allowing superheated liquid to flash and usually involves overheating of the container by fire. The combination of sudden expansion of compressed vapor in a large quantity will rapidly produce a large ball of liquid droplets and vapor. The formation of a road tanker BLEVE usually initiated by the external flame impinging on the shell of a vessel which is often above liquid level. Sudden rupture of tanker shell can happen if a tanker is exposed to fire for 30 minutes due to loss of tensile strength of the container and the fall of shell bursting pressure. The major risk of BLEVE is the radiation of heat from the fireball. The radiation of heat from the fireballs is characterized based on the size and dynamics of fireball. The standard techniques for evaluating the thermal radiation from BLEVE events assume that the radiant heat flux is constant over the duration of the BLEVE fireball. However, this assumption leads to overlyconservative predictions of hazard zones for injuries (i.e., second-degree burns).The SMACTRA software is designed by using Martinsen and Marx method [224] and method of TNO [76] to estimate the fireball height, to estimate the diameter and duration of fireball which account for the time-dependent nature of thermal radiation generated by aBLEVE fireball, and leading to a more realistic assessment of hazard zones associated with burn injuries.

There are several fireball formulas which have been considered in SMACTRA calculations. Further comparisons of the models correlations given by Bagster and Pitblado [225] showed that the TNO-model showed the best overall curve fit of the results. Comparison between seven different empirical models and software are shown in Figure 4.31 and 4.32. As predicted by SMACTRA, the fireball increases in diameter whenever the mass increases. The values predicted by SMACTRA as shown in Figure 4.31 and 4.32 are almost equal to the experimental works by Hardee et al. [226], Robert et al. [227] and EFFECT 8.01[188].



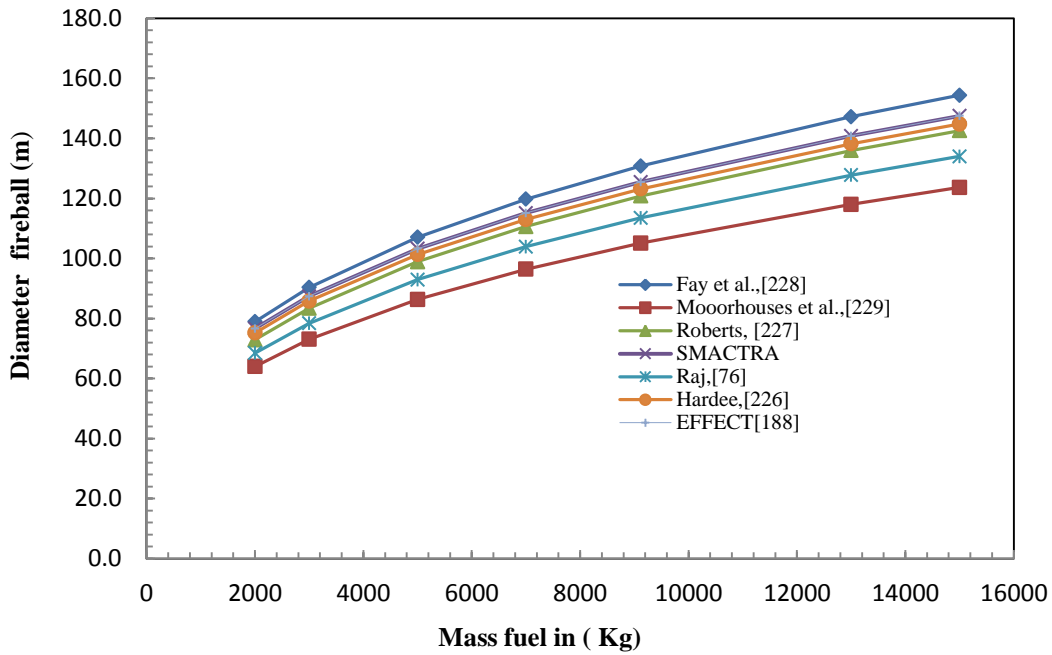


Figure 4.31 Comparison of Fireball diameters between SMACTRA over EFFECT 8.01 software and experimental and calculated relationship as function of mass fuel.

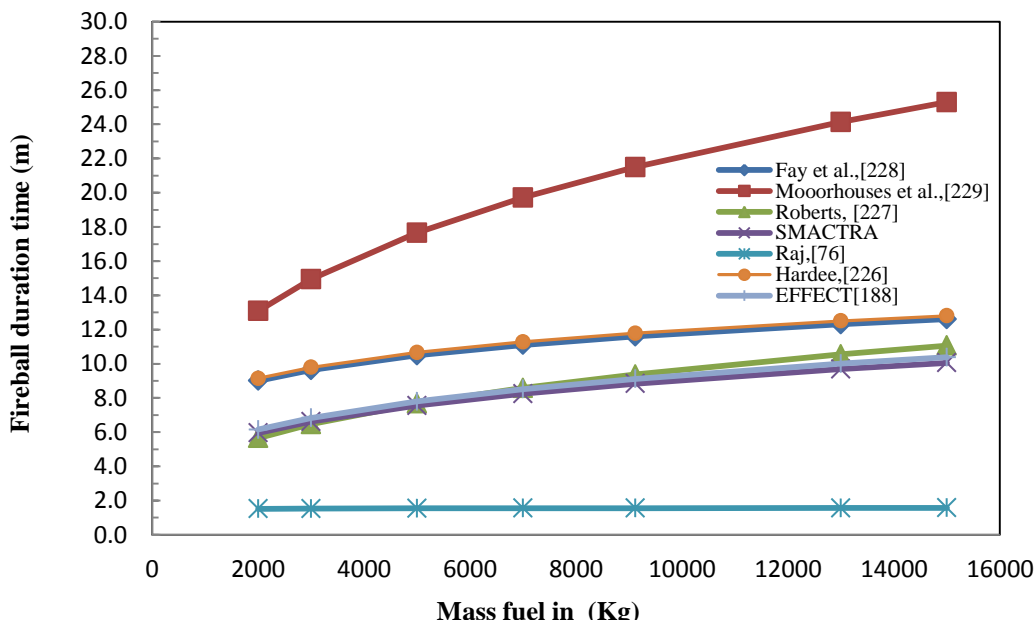


Figure 4.32 Comparison of Fireball duration time(s) between SMACTRA over EFFECT 8.01 software and experimental and calculated relationship as function of mass fuel.

Figure 4.33 and 4.34 are showing the time elapsed before one can feel pain as a function of the heat flux. From the Figure 4.33 it is estimated that at  $5\text{ kW/m}^2$ , the time



before one feels pain is approximately 11s. The time before one feels pain results for BLEVE is shorter than the pool fire case. From Figure 4.34, it is observed that the thermal radiation load is higher than the pool fire case which is ranges between  $1.0 \times 10^5 \text{ kW/m}^2$  to  $1.0 \times 10^6 \text{ kW/m}^2$ . The area zone for second degree burn and lethality curves is higher than the pool fire for the same capacity of LPG.

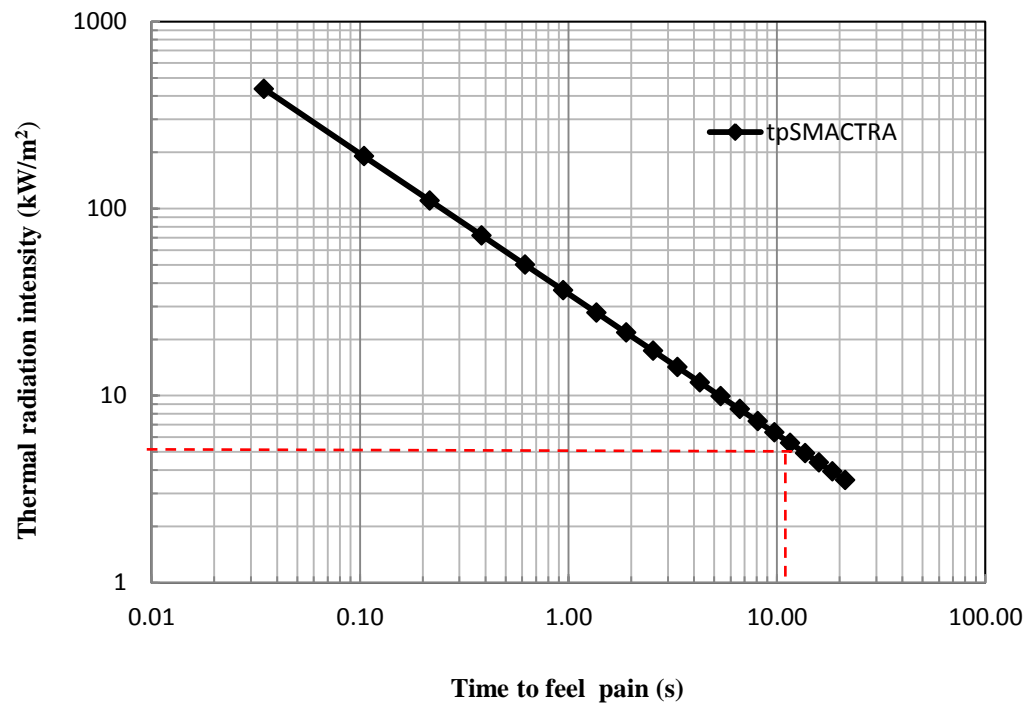


Figure 4.33 Time before one feels pain as a function of BLEVE fireball thermal radiation at truck tanker containing 13,000 kg (predicted by SMACTRA software)



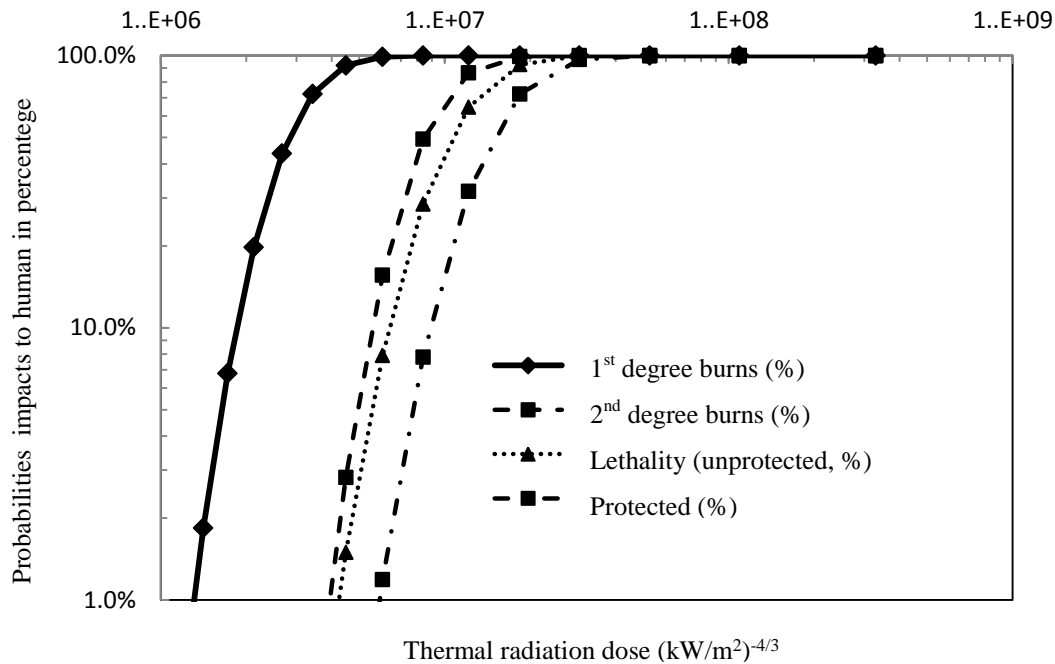


Figure 4.34 Probit functions for BLEVE fireball thermal radiation (at exposure time 9.61sec. and  $Dose_{human} (kW/m^2)^{4/3}$ s at truck containing 13,000 kg of LPG (predicted by SMACTRA software).

#### 4.3.9 The BLEVE time exposure effect over age and thermal radiation dose load for LPG tanker incident (in capacity of 34.5m<sup>3</sup>) to receptor

Figure 4.35 to 4.47 show the effect of duration of exposure towards probabilities impact percentage of thermal radiation to human. The analysis also include the discussion on the effect of total burn surface area (TBS) and age factor with fatality.

The medical treatment and management for burns injury are the most commonly observed aspect in research works such as by Bull et al.[163-165, 183], Curreri et al. [166] and others [220,230-233]. So far, none of the available risk analysis software can be utilised to predict and evaluate the fatality injury before the accident happens. Eventhough few risk analysis softwares such as SAFETI, EFFECT(TNO), CANARY, Risk plot, Riskcurves, ALOHA are capable to predict the effect of human mortality from thermal radiation, but these softwares did not include few factors such as age, TBS and medical related factors such as cost of treatment, insurance and the socio economic impact to the country. This confession is proved by TNO (which developed software EFFECT 8.01 and Risk curves) through email reply as shown in appendix 5.



In this section, few observations have been made on the effect of BLEVE towards age, TBS and LPG capacity by using SMACTRA software as follows:

- Analysis on the effect of age (69, 55, 45, 35, 15) towards 2<sup>nd</sup> degree burn injury at a constant TBS, 30% when a tanker is carrying 13,000 kg of LPG as shown in Figure 4.35 to 4.39.
- Analysis on the effect of age (69, 45, 15) towards 2<sup>nd</sup> degree burn injury at a constant TBS, 50% when the tanker is carrying 13,000 kg of LPG as shown in Figure 4.40 to 4.42.
- Analysis on the effect of age (69, 45, 15) towards 2<sup>nd</sup> degree burn injury at a constant TBS level, 10% when the tanker is carrying 13,000kg of LPG as shown in Figure 4.43 till 4.45.
- To study on the survival potential from 2<sup>nd</sup> degree burn injury at a different TBS level 10%, 30% and 50% (based on the comparison from the analysis as demonstrated in Figure 4.35 to 4.45 for age 15, 45 and 69).
- Analysis on the effect of age (80, 15) as shown in Figure 4.46 to 4.47, towards 2<sup>nd</sup> degree burn injury at a constant TBS, 10% when the tanker is carrying 4,000 kg of LPG.
- Analysis on the effect of age (80, 15) as shown in Figure 4.44 to 4.45, towards 2<sup>nd</sup> degree burn injury at a constant TBS, 10% when the tanker is carrying 13,000 kg of LPG.

The aim of the above analysis is to study on the survival potential for difference age groups; young, intermediate and old age. Therefore the age group range is selected according to Bull et al. [163-165, 183] and Curreri et al. [166]. The analysis will explain the effect of TBS when the level is higher or lower than the general standard 30% as proposed by Bull [163-165, 183] (this is the upper limit of survival potential for patient sustain 2<sup>nd</sup> degree burn based on the current advanced in medical treatment). The analysis is also to see the impact of LPG capacity towards survival potential.

Based on the graph analysis in Figure 4.35 to 4.47, as the thermal radiation dose curve shifted to the right on axis X, this mean the receptor will be exposed to a higher



radiation dose and possibly situated nearer to the source of accident. Meanwhile, as the probabilities of accident impact to human increased, the percentage value will be shifted upward on axis y. In general, receptor with 1<sup>st</sup> degree burn injury is shown in the left most curve (b1) which receive a low thermal radiation dose. The next curve is for receptor with 2<sup>nd</sup> degree burn injury and the last curve is for the protected receptor for example those in the building.

In the graphs, it is shown that two types of 2<sup>nd</sup> degree burn injury curve are overlapping to each other (red and black curves). The 2<sup>nd</sup> degree burn injury curve with black curve line is observed to end at the probability impact value 10%, 30% and 50%. The last point of this curve is noted to overlap on the TBS indicator dotted line which represent the percentage of total body surface area, which means the receptor may die if present above the dotted line. The blue curve represents the unprotected receptor which is located very close to the source of accident, therefore having a slim survival chance.

Figure 4.35 shows that the older age group receptor who sustain 2<sup>nd</sup> degree burn (69 years old) with TBS 30%, the survival potential from BLEVE accident scenario is lesser compared to the younger age groups for example 55, 45, 35, 15 years old as shown in Figure 4.36 to Figure 4.39. This is proven by the analysis in Figure 4.39, for younger age group such as 15 years old the blue curve is moving away from the red curve which mean better chance of survival. Meanwhile, for age 55 (as in Figure 3.36) and 45 (Figure 3.37), the blue and red curve nearly overlap to each other which mean the survival potential is 50:50. Younger patients with 2<sup>nd</sup> degree burn at TBS 50% have a higher survival percentage compared to older patient such as 69 years old, as shown in Figure 4.42 and Figure 4.35. Figure 4.35 to 4.39 analyzed the effect of age (69, 55, 45, 35, 15 years old) towards 2<sup>nd</sup> degree burn injury at a constant TBS, 30% and it can be concluded that younger age victims with 2<sup>nd</sup> degree of burn injury have high survival potential from 13,000 kg of LPG truck tanker explosion.



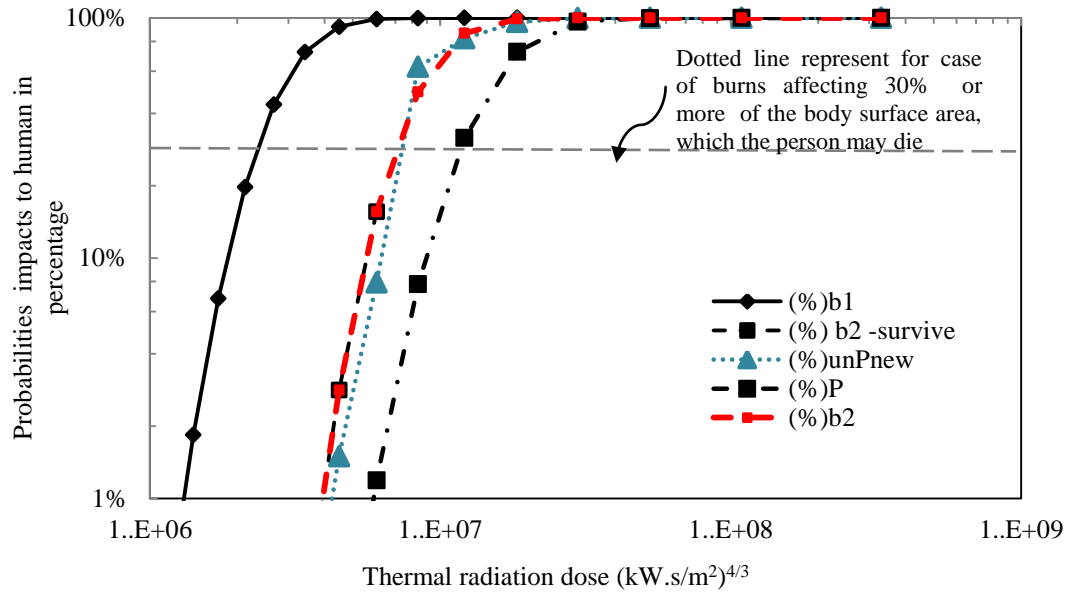


Figure 4.35 Probability of surviving from 2<sup>nd</sup> degree burn at the age of 69 for BLEVE fireball thermal radiation (at exposure time 10.01sec. and thermal dose load to human =  $\text{Dose}_{\text{human}} (\text{kW}/\text{m}^2)^{4/3} \text{s}$  at truck containing 13,000 kg of LPG (predicted by SMACTRA software): b1=1<sup>st</sup> degree burn; b2 = 2<sup>nd</sup> degree burn survived; unP<sup>new</sup> = lethality after revised (unprotected); P= protected.

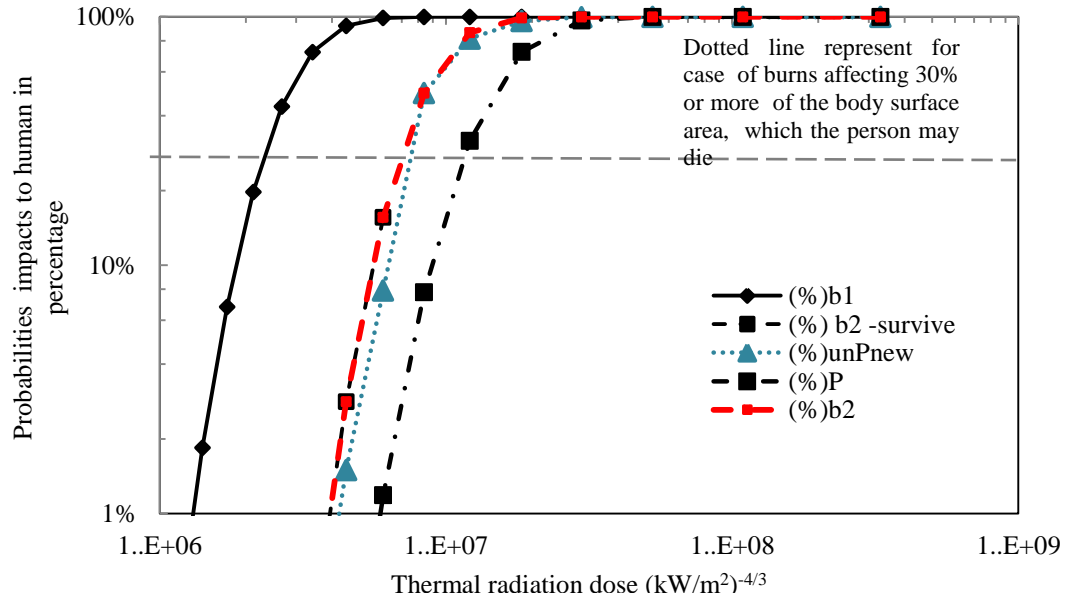


Figure 4.36 Probability of surviving from 2<sup>nd</sup> degree burn at the age of 55 for BLEVE fireball thermal radiation (at exposure time 10.01sec. and  $\text{Dose}_{\text{human}} (\text{kW}/\text{m}^2)^{4/3} \text{s}$  at truck containing 13,000 kg of LPG (predicted by SMACTRA software): b1=1<sup>st</sup> degree burn; b2=2<sup>nd</sup> degree burn survived; unP<sup>new</sup> = lethality after revised (unprotected); P= protected.



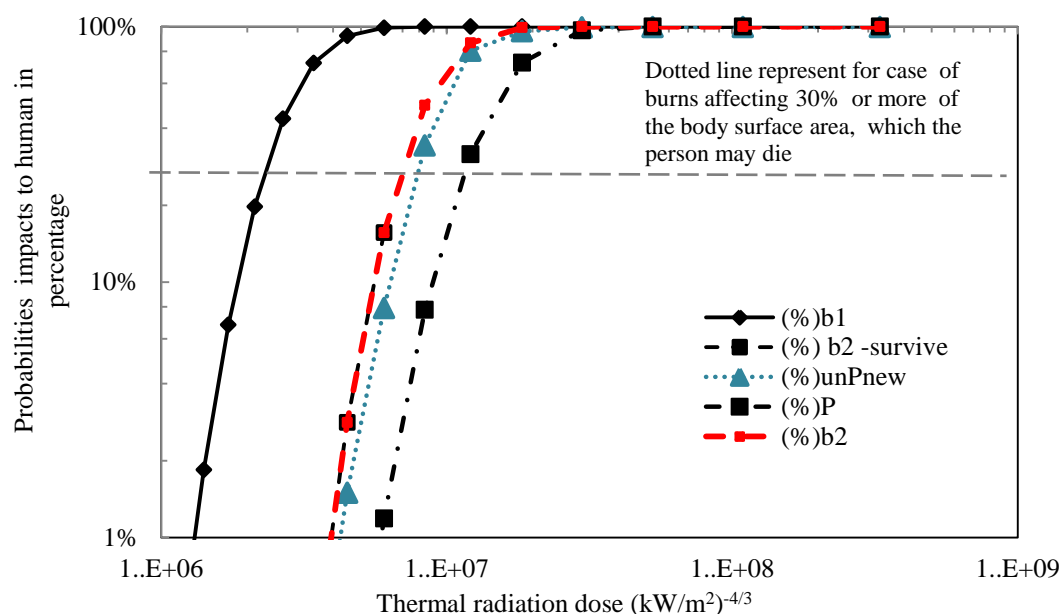


Figure 4.37 Probability of surviving from 2<sup>nd</sup> degree burn at the age of 45 for BLEVE fireball thermal radiation (at exposure time 10.01sec. and Dose<sub>human</sub> (kW/m<sup>2</sup>)<sup>4/3</sup>s at truck containing 13,000 kg of LPG (predicted by SMACTRA software): b1=1<sup>st</sup> degree burn; b2=2<sup>nd</sup> degree burn survived; unP<sup>new</sup> = lethality after revised (unprotected); P= protected.

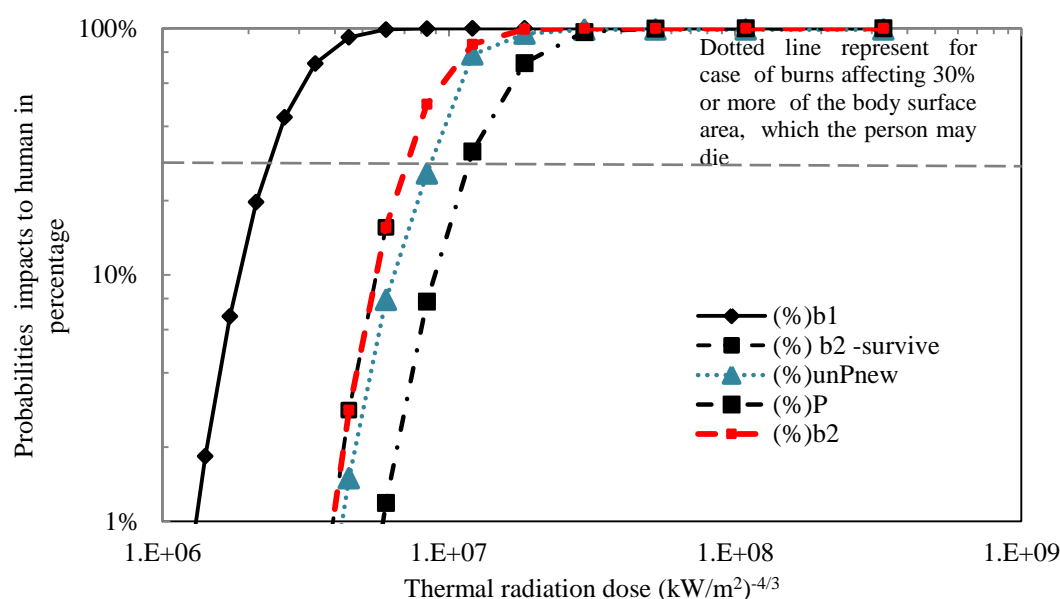


Figure 4.38 Probability of surviving from 2<sup>nd</sup> degree burn at the age of 35 for BLEVE fireball thermal radiation (at exposure time 10.01sec. and Dose<sub>human</sub> (kW/m<sup>2</sup>)<sup>4/3</sup>s at truck containing 13,000 kg of LPG (predicted by SMACTRA software): b1=1<sup>st</sup> degree burn; b2=2<sup>nd</sup> degree burn survived; unP<sup>new</sup> = lethality after revised (unprotected); P= protected.



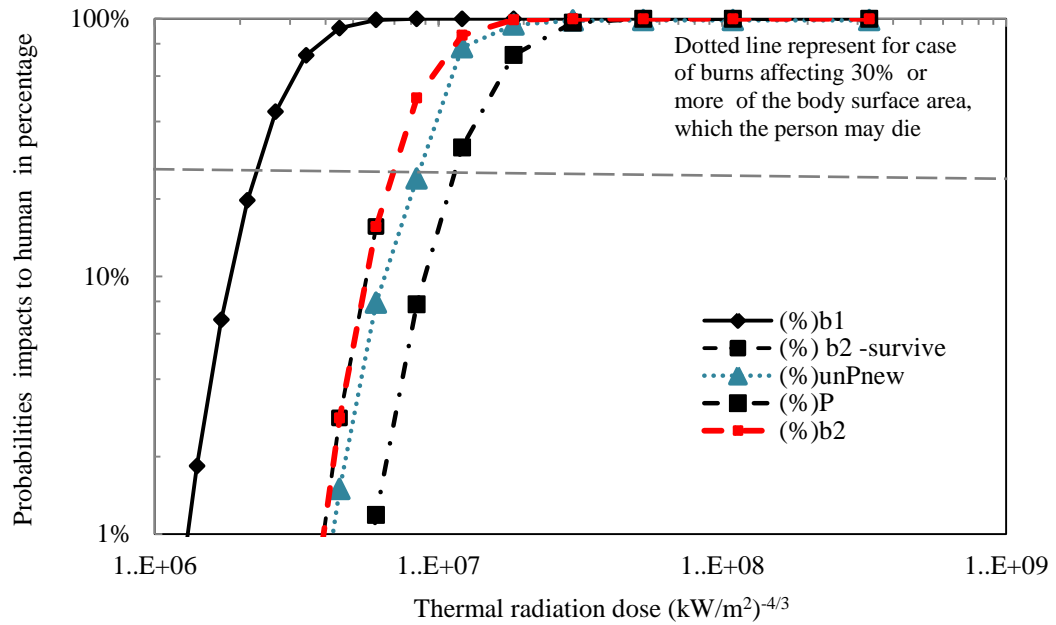


Figure 4.39 Probability of surviving from 2<sup>nd</sup> degree burn at the age of 15 for BLEVE fireball thermal radiation (at exposure time 10.01sec. and Dose<sub>human</sub> (kW/m<sup>2</sup>)<sup>4/3</sup>s at truck containing 13,000 kg of LPG (predicted by SACTRA software): b1=1<sup>st</sup> degree burn; b2=2<sup>nd</sup> degree burn survived; unP<sup>new</sup> = lethality after revised (unprotected); P= protected.

Figure 4.40 to 4.42 analyzed the effect of age (69, 55, 45, 35, 15 years old) towards 2<sup>nd</sup> degree burn injury when the percentage of TBS is increased to 50% while when the percentage of TBS is reduced to 10%, the analysis is shown in Figure 4.42 to 4.44. As shown in Figure 4.40, 4.41, and 4.42, when the % of TBS is increased to 50%, more life are salvaged which is probably due to the advancement in medical treatment for burn patient. This finding will become more obvious if the comparison of results for the age of 69 is made as in Figure 4.35 and 4.42. However, if the treatment ability is inadequate or poor, SACTRA predicted the survival percentage for 2<sup>nd</sup> degree burn injury will be reduced and the fatality percentage will be increased. Based on the SACTRA result analysis as shown in figure 4.35 to 4.39 and 4.46, young age group victims have a higher survival potential most likely due to their body capability to fight bacteria infections toward burn injury is better than those age 60 and above [184]. This result is consistent with most of the literatures in burn emergency medicine research [163-166, 183, 230-234].



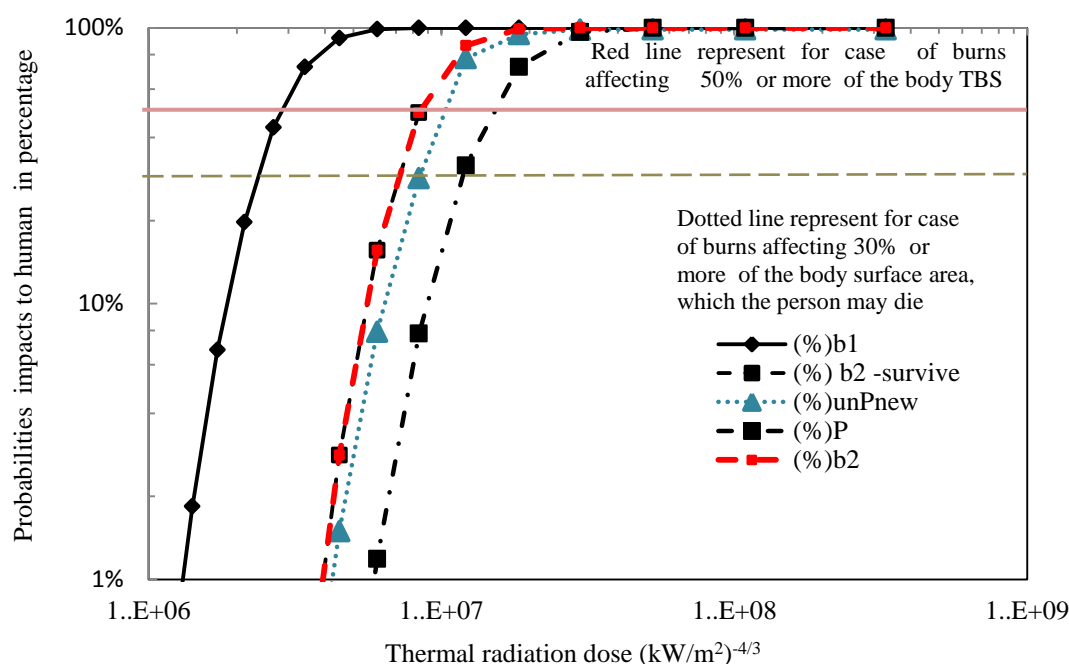


Figure 4.40 Probability of surviving from 2<sup>nd</sup> degree burn at the age of 14 for BLEVE fireball thermal radiation (at exposure time 10.01sec., 50% total burn surface area (TBS) and Dose<sub>human</sub> (kW/m<sup>2</sup>)<sup>4/3</sup> s ) for a truck containing 13,000 kg of LPG (predicted by SMACTRA software).

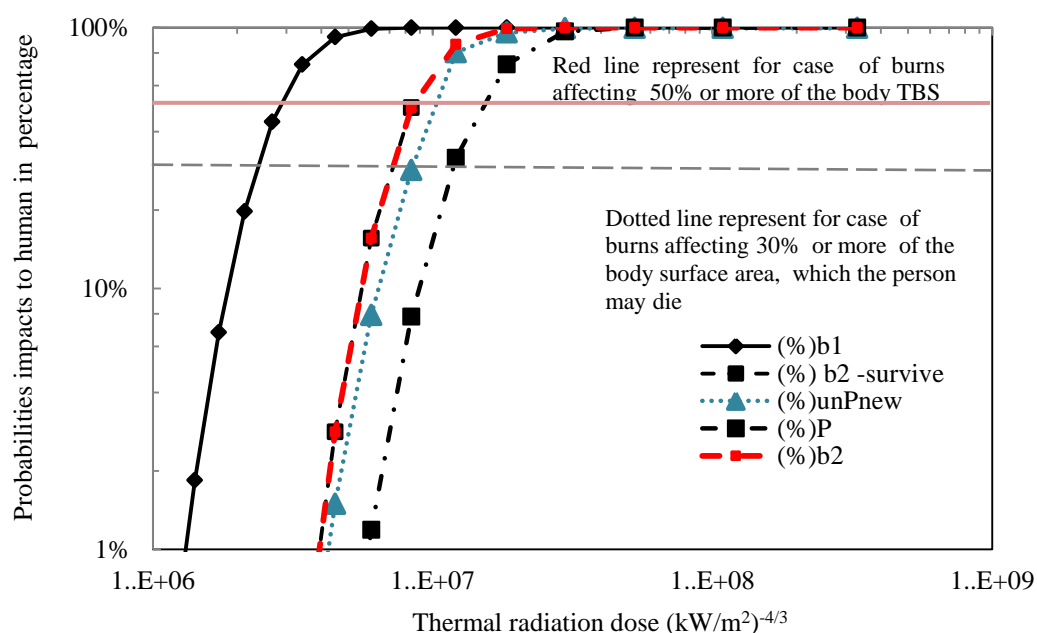


Figure 4.41 Probability of surviving from 2<sup>nd</sup> degree burn at the age of 45 for BLEVE fireball thermal radiation (at exposure time 10.01sec., 50% total burn surface area (TBS) and Dose<sub>human</sub> (kW/m<sup>2</sup>)<sup>4/3</sup> s at truck containing 13,000 kg of LPG (predicted by SMACTRA software).



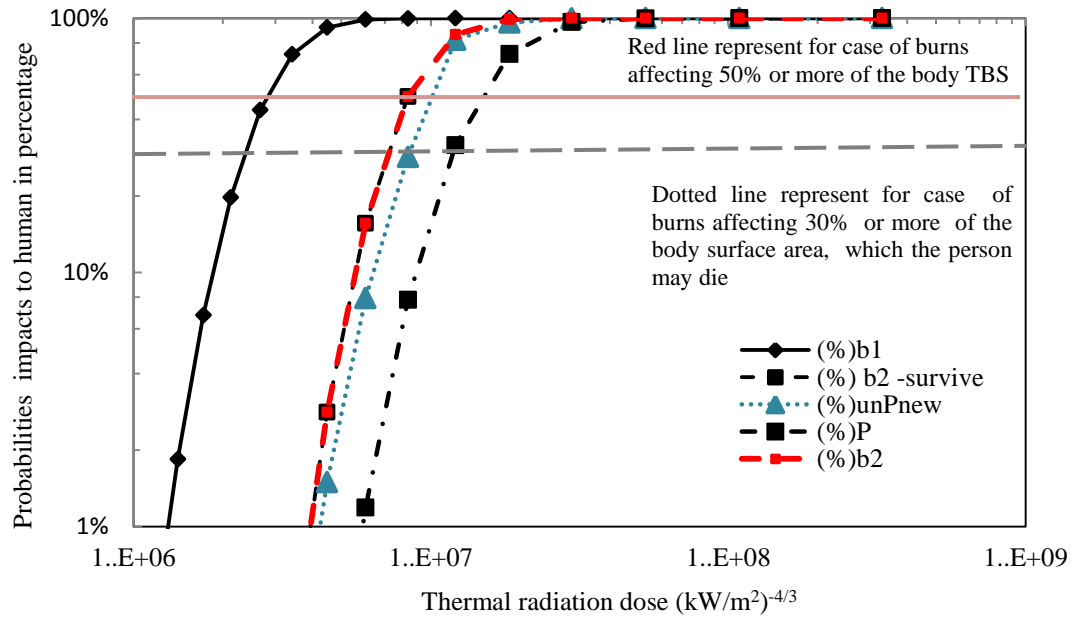


Figure 4.42 Probability of surviving from 2<sup>nd</sup> degree burn at the age of 69 for BLEVE fireball thermal radiation (at exposure time 10.01sec., 50% total burn surface area (TBS) and  $\text{Dose}_{\text{human}} (\text{kW}/\text{m}^2)^{4/3} \text{s}$  at truck containing 13,000 kg of LPG (predicted by SACTRA software).

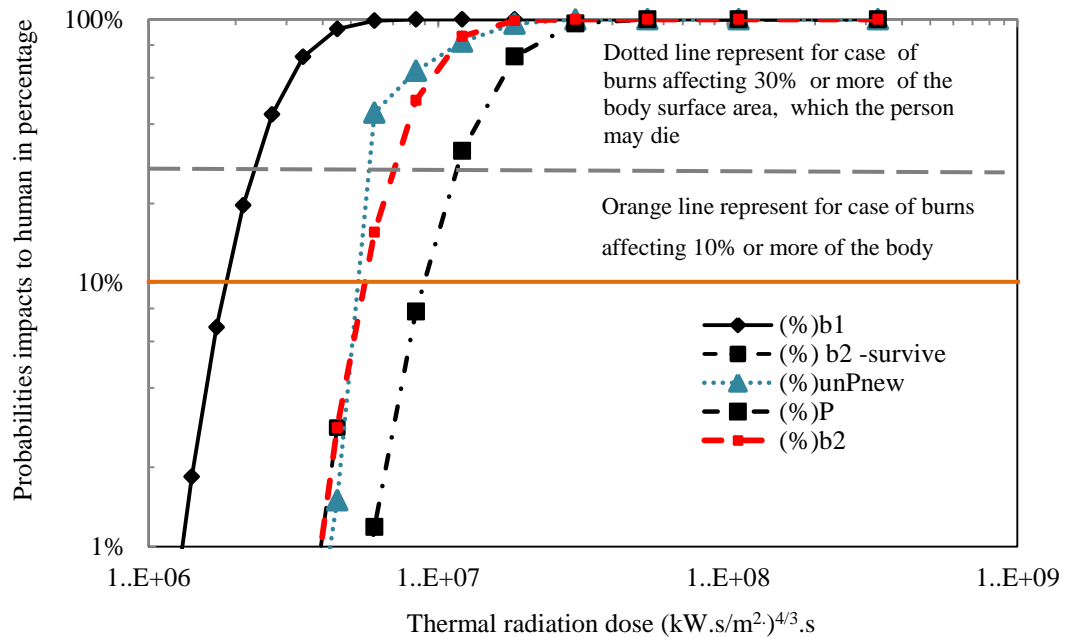


Figure 4.43 Probability of surviving from 2<sup>nd</sup> degree burn at the age of 69 for BLEVE fireball thermal radiation (at exposure time 10.01sec., 10% total burn surface area (TBS) and  $\text{Dose}_{\text{human}} (\text{kW}/\text{m}^2)^{4/3} \text{s}$  at truck containing 13,000 kg of LPG (predicted by SACTRA software).



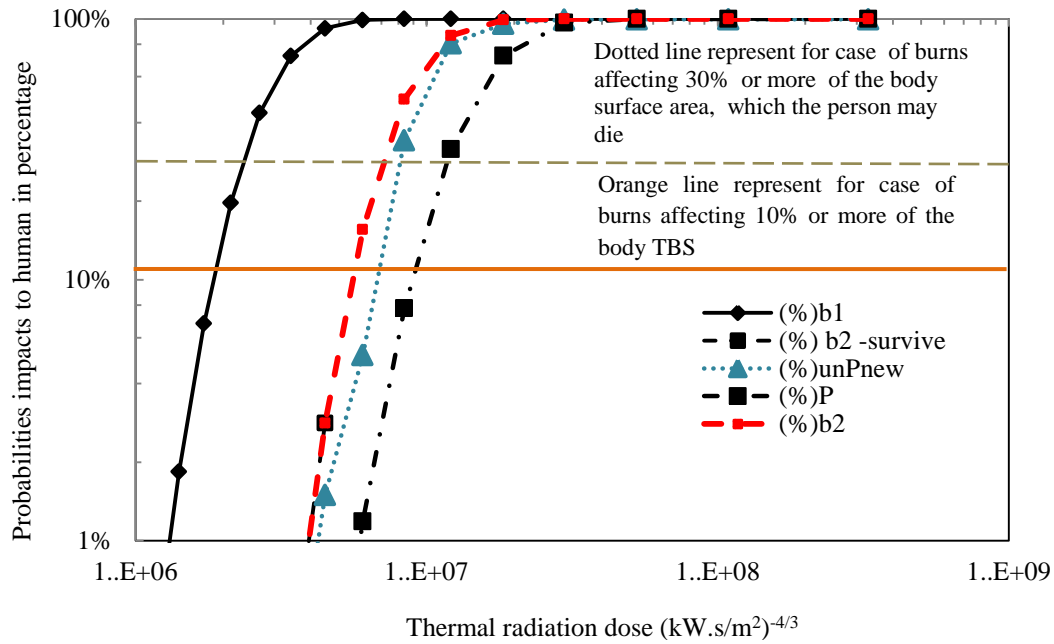


Figure 4.44 Probability of surviving from 2<sup>nd</sup> degree burn at the age of 45 for BLEVE fireball thermal radiation (at exposure time 10.01sec., 10% total burn surface area (TBS) and Dose<sub>human</sub> (kW/m<sup>2</sup>)<sup>4/3</sup>s) for a truck containing 13,000 kg of LPG (predicted by SACTRA software).

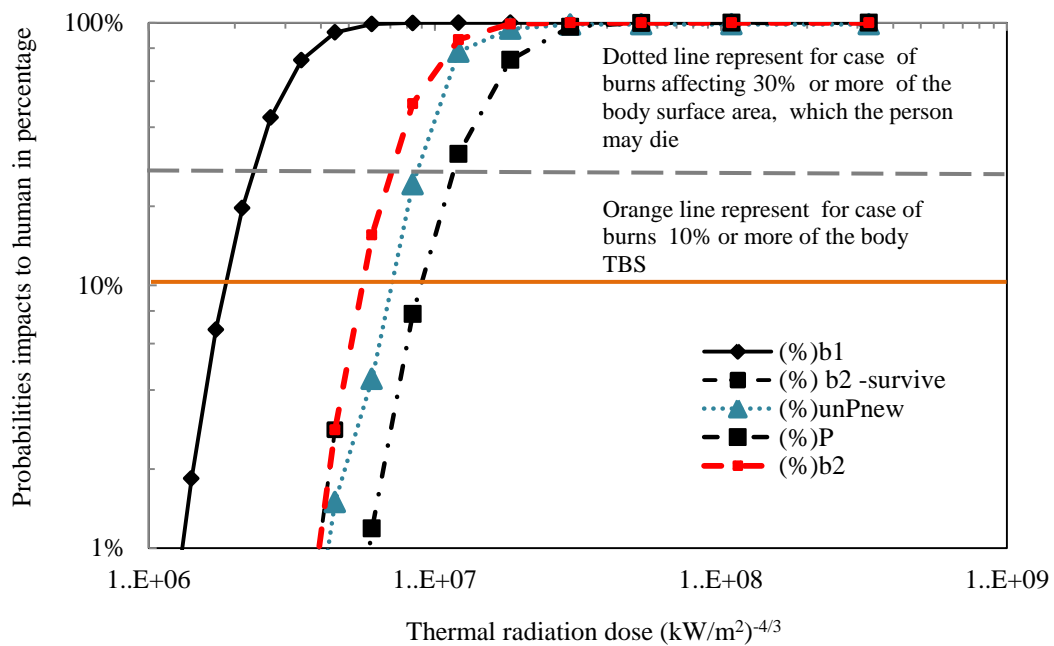


Figure 4.45 Probability of surviving from 2<sup>nd</sup> degree burn at the age of 14 for BLEVE fireball thermal radiation (at exposure time 10.01sec., 10% total burn surface area (TBS) and Dose<sub>human</sub> (kW/m<sup>2</sup>)<sup>4/3</sup>s) for a truck containing 13,000 kg of LPG (predicted by SACTRA software).



Figure 4.45 shows that if % TBS body area at or less than 10% and young age of victims, the percentage of survival potential is greater. It is also shown that the new lethality curve does not cross of curve for 2<sup>nd</sup> degree burn. If the lethality curve crosses the curve for 2<sup>nd</sup> degree burn, the lethality percentage will increase while 2<sup>nd</sup> degree burn survival potential will reduce.

Subsequently the analysis is made on the effect of truck tankers explosion towards victims if the LPG quantity is reduced to 4,000 kg from 13,000 kg at the same duration of 10.01s. As shown in Figure 4.46 and and in Figure 4.47, when the quantity of transported hazardous material is low, the severity of 2<sup>nd</sup> degree of burn injury is also low and the survival potential for victim age 80 tahun is higher. This result analysis is consistent with inherent safety analysis by Khan [216], Lees [64], Kletz [235] who concluded that as the hazardous material quantity is minimized, the hazard becomes lesser.

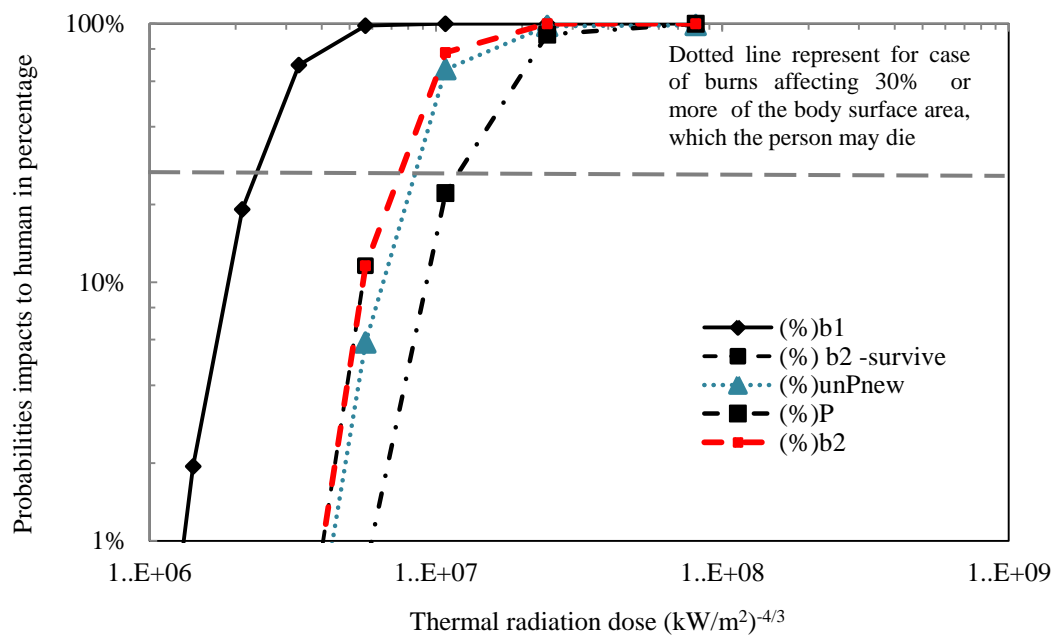


Figure 4.46 Probability of surviving from 2<sup>nd</sup> degree burn at the age of 14 for BLEVE fireball thermal radiation (at exposure time 10.01sec., 30% total burn surface area (TBS) and Dose<sub>human</sub> (kW/m<sup>2</sup>)<sup>4/3</sup>s) for a truck containing 4,000 kg of LPG (predicted by SMACTRA software).



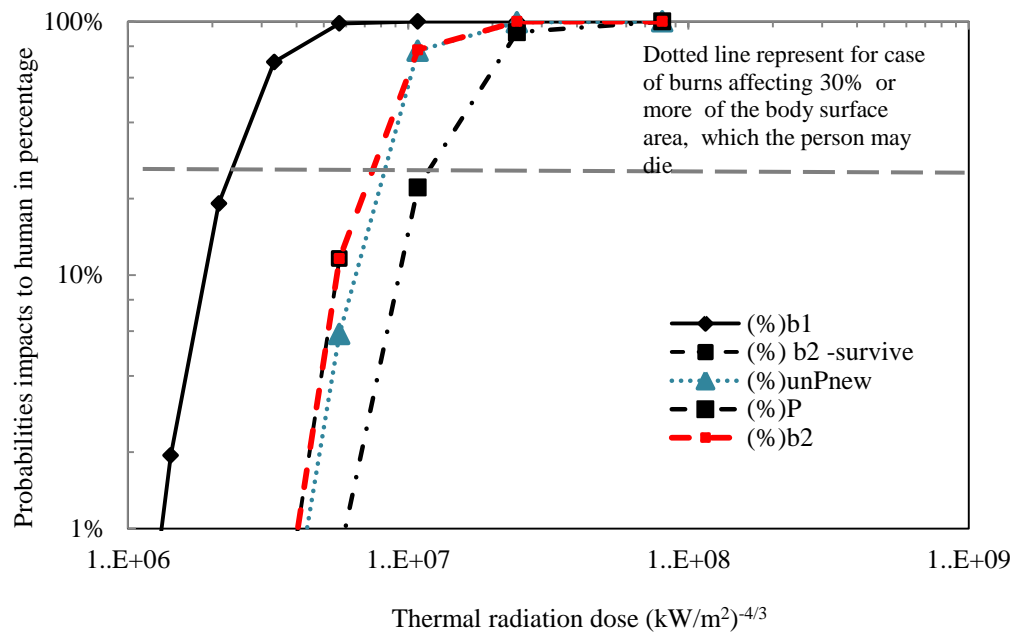


Figure 4.47 Probability of surviving from 2<sup>nd</sup> degree burn at the age of 80 for BLEVE fireball thermal radiation (at exposure time 10.01sec., 10% total burn surface area (TBS) and Dose<sub>human</sub> (kW/m<sup>2</sup>)<sup>4/3</sup>s) for a truck containing 4,000 kg of LPG (predicted by SMACTRA software).

In conclusion, for all developed and developing countries such as United States America, United Kingdom and other european country including Malaysia, many medical research are conducted to optimized patient health level through various treatment modalities such as antibiotic. This may not be applicable to underdeveloped countries in which the government budget is mainly for other things such as food and education. Therefore there is the possibility of delay in treatment, poor healing due to undertreatment from in adequate facilities and medication. Therefore socio economic factor of particular country or countries is a major contributor towards a better outcome for the burn injury victim. In general, with the development of SMACTRA burn analysis it is hoping that it can become a tool to save life and minimized the effect from explosion of hazardous volatile substances.



#### 4.3.10 The BLEVE probit analysis and thermal radiation dose load as a function of distance for LPG tanker incident (in capacity of 34.5m<sup>3</sup>) to receptor

This study is to analyze the effect of distance over the thermal radiation dose impact to human. Figure 4.48 till 4.53 showing the comparison between the effects of BLEVE fireball thermal radiation probit generated by SACTRA, at different LPG fuel quantity and capacity which are 3000 kg, 9119 kg and 13,000 kg.

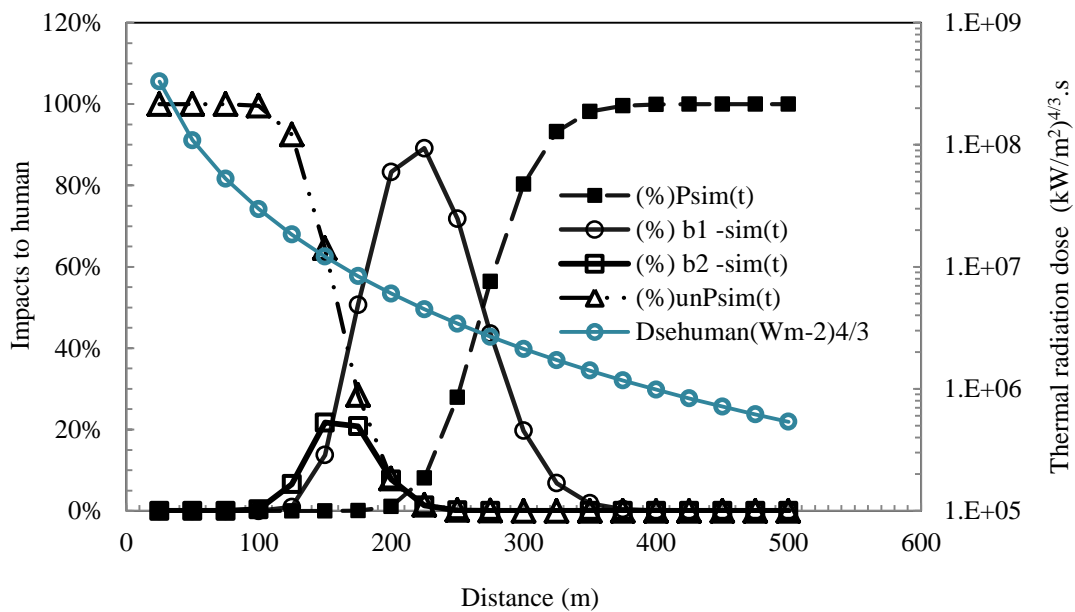


Figure 4.48 Consequences of BLEVE fireball thermal radiation as a function of the dose received by a person in  $Dose_{human} (kW/m^2)^{4/3} s$ , exposure distance (m) and probit functions at truck containing 13,000 kg of LPG (predicted by SACTRA software): b1=1<sup>st</sup> degree burn; b2=2<sup>nd</sup> degree burn; unP = lethality (unprotected); P= protected.



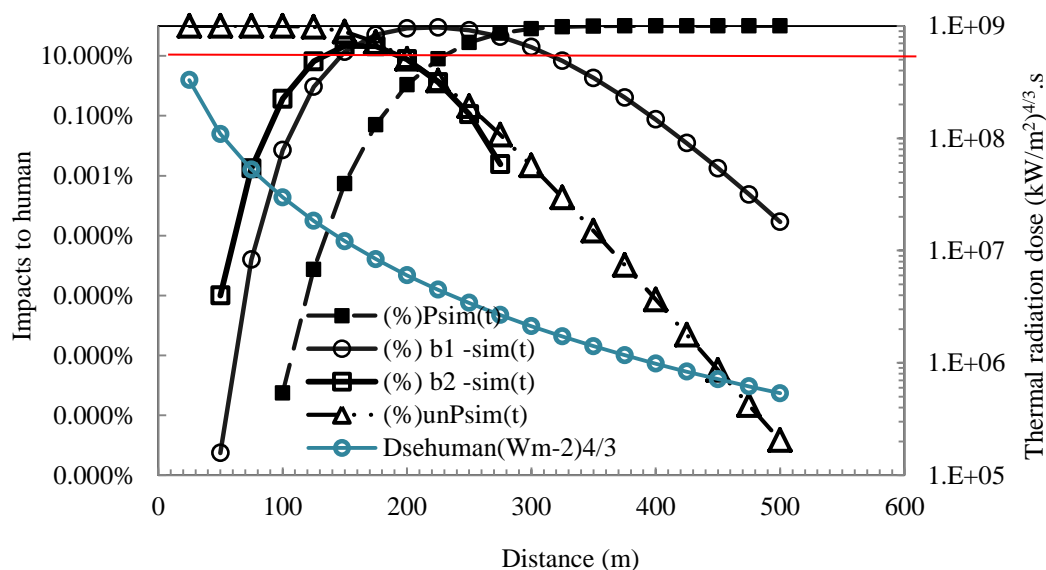


Figure 4.49 Consequences of BLEVE fireball thermal radiation as a function of the dose received by a person in  $Dose_{\text{human}} (\text{kW/m}^2)^{4/3} \cdot \text{s}$ , exposure distance (m) and probit functions (10% below) at truck containing 13,000 kg of LPG (predicted by SMACTRA software): b1=1<sup>st</sup> degree burn; b2=2<sup>nd</sup> degree burn; unP = lethality (unprotected); P= protected

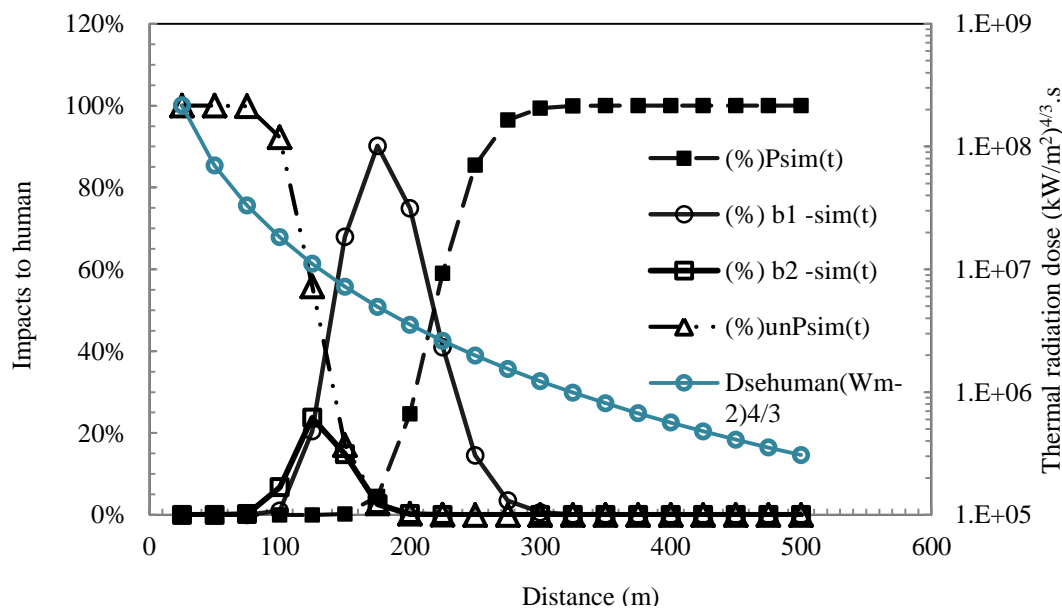


Figure 4.50 Consequences of BLEVE fireball thermal radiation as a function of the dose received by a person in  $Dose_{\text{human}} (\text{kW/m}^2)^{4/3} \cdot \text{s}$ , exposure distance (m) and probit functions at truck containing 9119kg of LPG (predicted by SMACTRA software): b1=1<sup>st</sup> degree burn; b2=2<sup>nd</sup> degree burn; unP = lethality (unprotected); P= protected



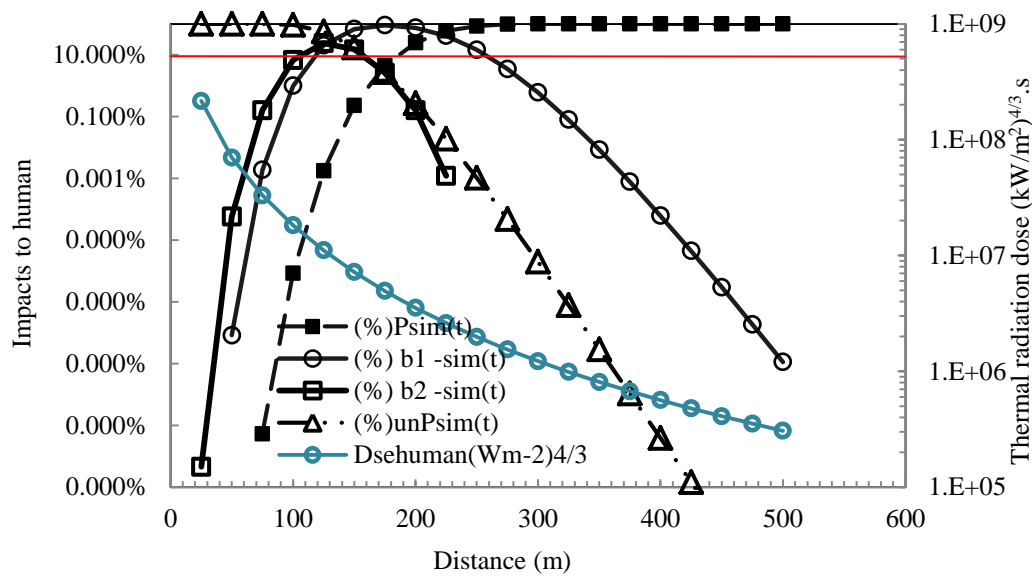


Figure 4.51 Consequences of BLEVE fireball thermal radiation as a function of the dose received by a person in  $\text{Dose}_{\text{human}} (\text{kW}/\text{m}^2)^{4/3} \text{s}$ , exposure distance (m) and probit functions (10% below) at truck containing 9119 kg of LPG (predicted by SACTRA software): b1=1<sup>st</sup> degree burn; b2=2<sup>nd</sup> degree burn; unP = lethality (unprotected); P= protected.

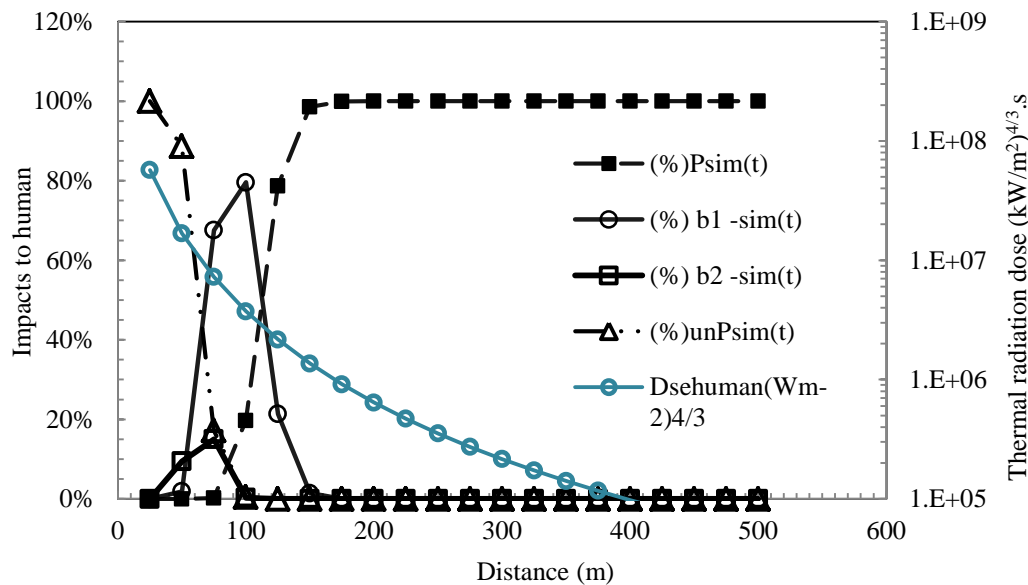


Figure 4.52 Consequences of BLEVE fireball thermal radiation as a function of the dose received by a person in  $\text{Dose}_{\text{human}} (\text{kW}/\text{m}^2)^{4/3} \text{s}$ , exposure distance (m) and probit functions at truck containing 3000 kg of LPG (predicted by SACTRA software): b1=1<sup>st</sup> degree burn; b2=2<sup>nd</sup> degree burn; unP = lethality (unprotected); P= protected.



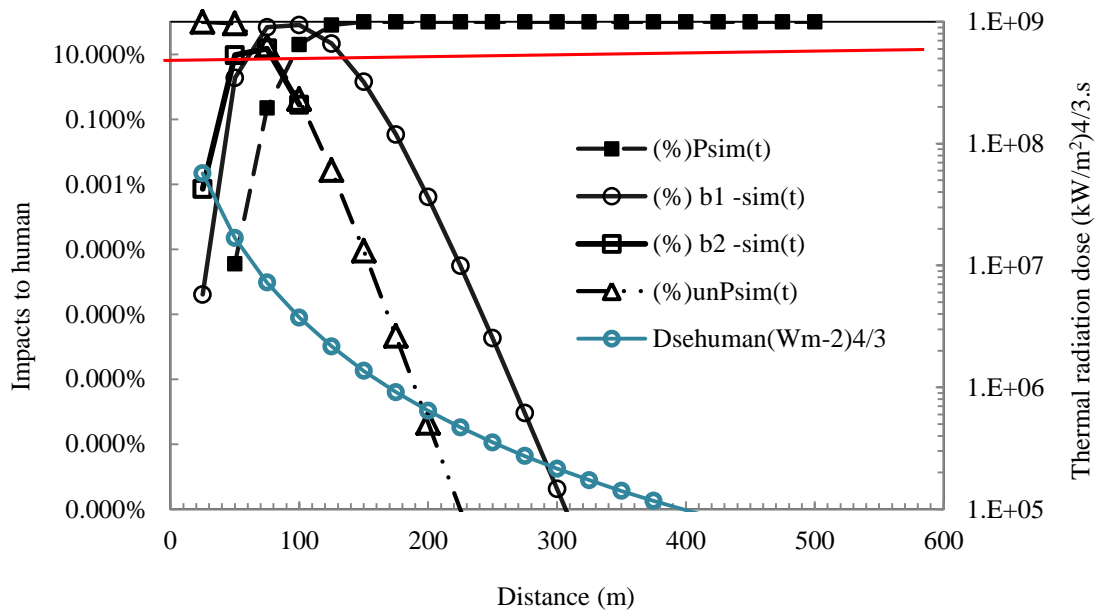


Figure 4.53 Consequences of BLEVE fireball thermal radiation as a function of the dose received by a person in  $\text{Dose}_{\text{human}} (\text{kW}/\text{m}^2)^{4/3} \text{s}$ , exposure distance (m) and probit functions (10% below) at truck containing 3000 kg of LPG (predicted by SMACTRA software): b1=1<sup>st</sup> degree burn; b2=2<sup>nd</sup> degree burn; unP = lethality (unprotected); P= protect

Based on the mortality analysis on the impact of road tanker at various capacities, the greater the amount of LPG content involved in the accident, the larger the unsafe area for human living. BLEVE thermal radiation impact analysis with the lethality percentage curve 100% at a distance 100 m and below is shown in Figure 4.48. However, the percentage reduced exponentially with the increasing distance. At 210 m radius, SMACTRA predicted less than 1% mortality. Although the percentage of death from thermal radiation impact is low at 210 m, the percentage for first degree injury case is almost 100%. It is also predicted from SMACTRA analysis that an individual may experience second degree injury between 100 m to 210 m. The distance between 350 to 500 m is considered to be the safe zone from accident impact. At 10% mortality and below, all probabilities results are declining, while protected curves shows the probability is 100% safe. When the transportation tanker carrying capacity decreased, all curves in Figure 4.48 to 4.53 are shifted to the left direction; this shows that whenever the capacity reduced, the unsafe zone radius would be minimized.



#### 4.3.11 The Effect of fireball height, fireball diameter and emissive power as a function of BLEVE fireball formation time for the LPG tanker incident (in capacity of 34.5m<sup>3</sup>) to receptor

This study will analyze the effect of fireball formation time over the fireball height, diameter and emissive power. Figure 4.54 till Figure 4.56 showing the comparison between emissive power, fireball height and fireball diameter as a function of time, for BLEVE (1195 mm X 2480 mm X 3500 mm) truck tanker generated by SMACTRA, at different LPG fuel quantity and capacity which are 3000, 9119, and 13,000 kg.

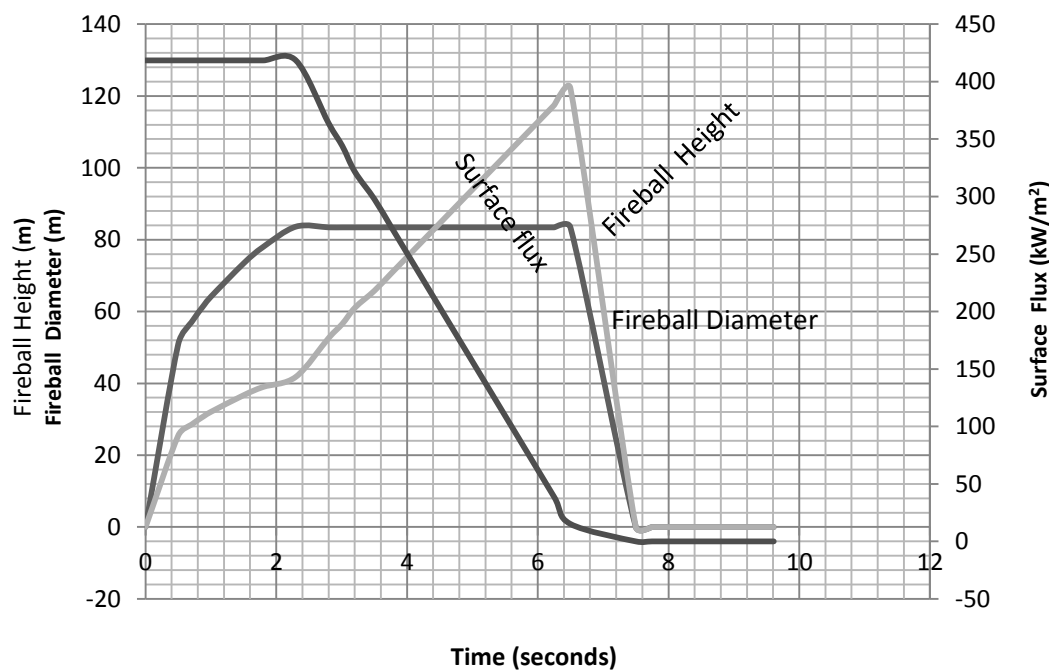


Figure 4.54: Emissive power, fireball height and fireball diameter as a function of time, for BLEVE of 3,000kg of LPG (1195 mm X 2480 mm X 3500mm) truck tanker.



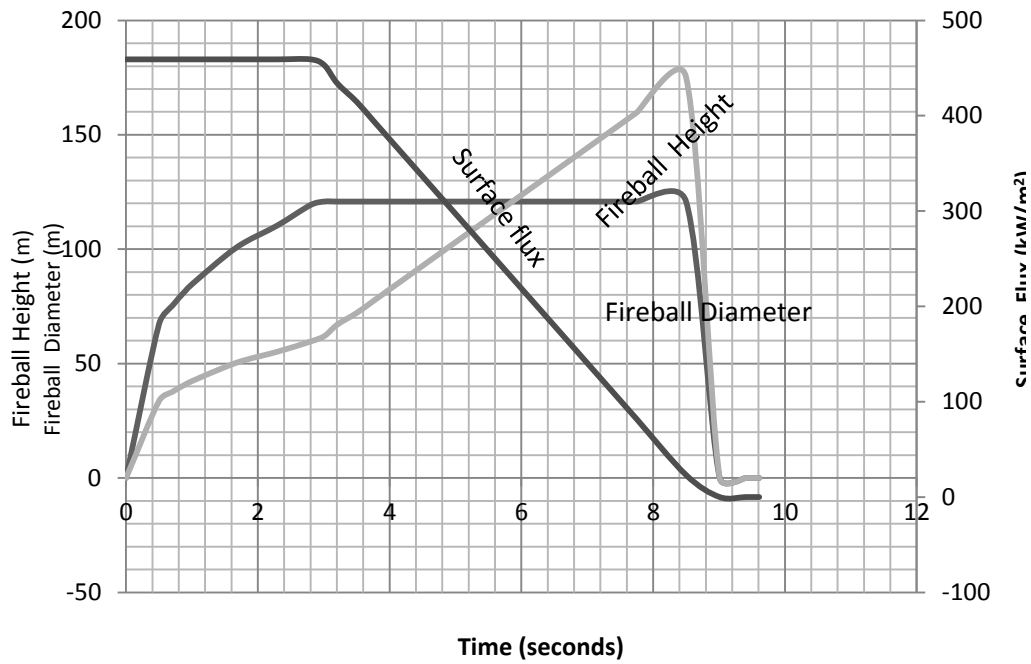


Figure 4.55: Emissive Power, fireball height and fireball diameter as a function of time, for BLEVE of 9119kg of LPG (1195 mm X 2480 mm X 3500 mm) truck tanker.

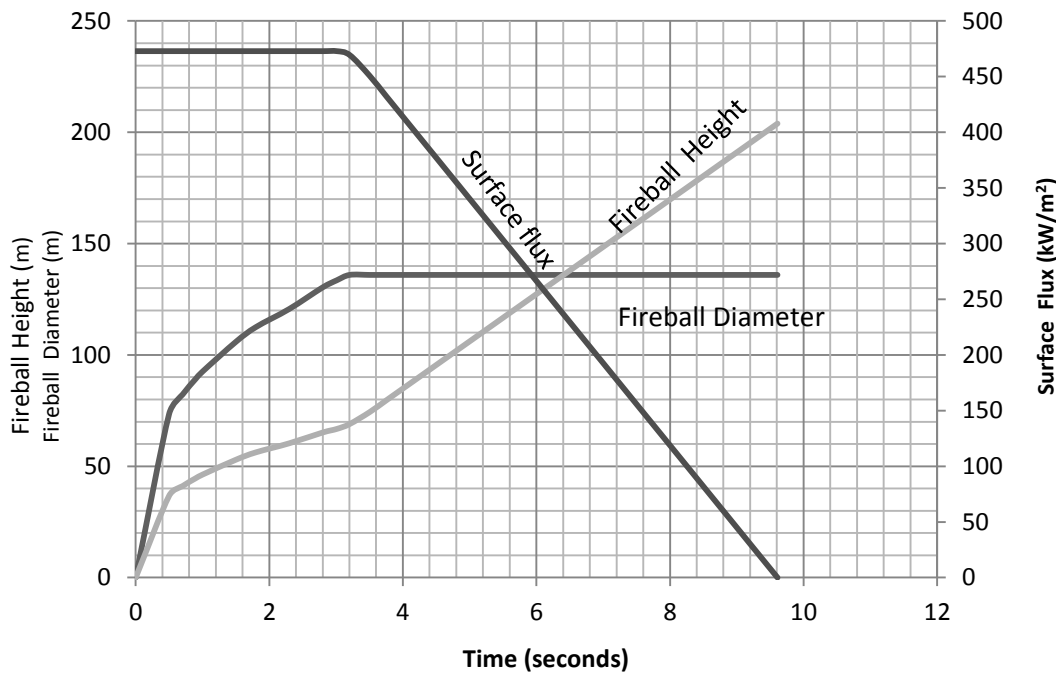


Figure 4.56: Emissive Power, fireball height and fireball diameter as a function of time, for BLEVE of 13,000kg of LPG (1195 mm X 2480 mm X 3500 mm) truck tanker.



The results of the atmospheric transmissivity ( $t$ ) between the fireball and the target are estimated by using the equations as described in the references [64, 67, 200, 35-52]. As shown in Figure 4.54 to Figure 4.56, during the early part of a fireball's formation, the dynamic model treats the fireball as a sphere that increases in diameter with time with the remaining tangent to grade as it grows. At the end of the growth phase, the fireball will reach its maximum diameter and begins to rise into the air.

The fireball is assumed to achieve its maximum diameter at the end of the first third of its formation duration. This is also the time at which lift-off is assumed to occur (i.e.  $t = t_d/3$ ) These assumptions are based on: experimental data from Hasegawa and Sato [236] and Maillette and Birk [222, 223], which indicate that peak radiation output occurs at the end of the first third of the fireball's duration; the work of Roberts [227], who noted that peak radiation output occurs when the fireball has grown to its maximum diameter; and experimental data from Hasegawa et al. [236] and Hardee et al. [226], which show the fireball begins to rise into the air once it reaches its maximum diameter. Thus, the center of the fireball moves upward at a constant rate from its pre-lift off position (one maximum radius above grade) to three times that elevation in the last two-thirds of the fireball's existence.

Based on SACTRA analysis results as shown in Figure 4.54 to 4.56, it is observed that when the LPG transportation capacity is increased, the fireball height, fireball diameter and surface flux is increased significantly. The persons who are exposed to excessive radiation heat from the fire may receive a fatal burn injury. Combustible structures might be ignited if exposed to radiant heat flux of  $31.5 \text{ kW/m}^2$  or more [32, 64, 67, 79-181]. Therefore for the worst case scenario of 13,000 kg of LPG, fatality is expected for all persons who are within  $31.5 \text{ kW/m}^2$  isopleths or greater with duration less than 9.2s.

#### **4.3.12 The effect of toxic gas dispersion as the result of propane and ammonia release from transportation accident by using SACTRA Map API online.**

This section will discuss on the dispersion of cloud of toxic gases into the atmosphere. The discussion will emphasize more on the consequences of toxic gas dispersion as the result of propane and ammonia release from transportation accident. The dispersion



models is classified according to the release sources for hazardous material either instantaneous or continuous. For instantaneous sources, the affected zone usually displayed as a circle shape which indicate that the released hazardous materials from truck accident will only burn for a short duration between 15 to 30s [64] before detonation of tanker occur. Meanwhile for continuous source, usually the released hazardous material is displayed as a plume shape. Usually the liquid material which is released from the tanker to atmosphere will be depressurized as gas. The gas which is released usually travel farther from the accident source known as downwind distance. Downwind distance is very much dependent on the influence of few parameters such as wind direction, wind velocity, atmospheric stability, material release rate and density towards air, humidity and meteorological condition. Figure 4.57 shows the accident location when a road tanker transporting hazardous material via Jalan Ampang after supplying the material at Petronas gas station and Hulu Kelang industrial area.

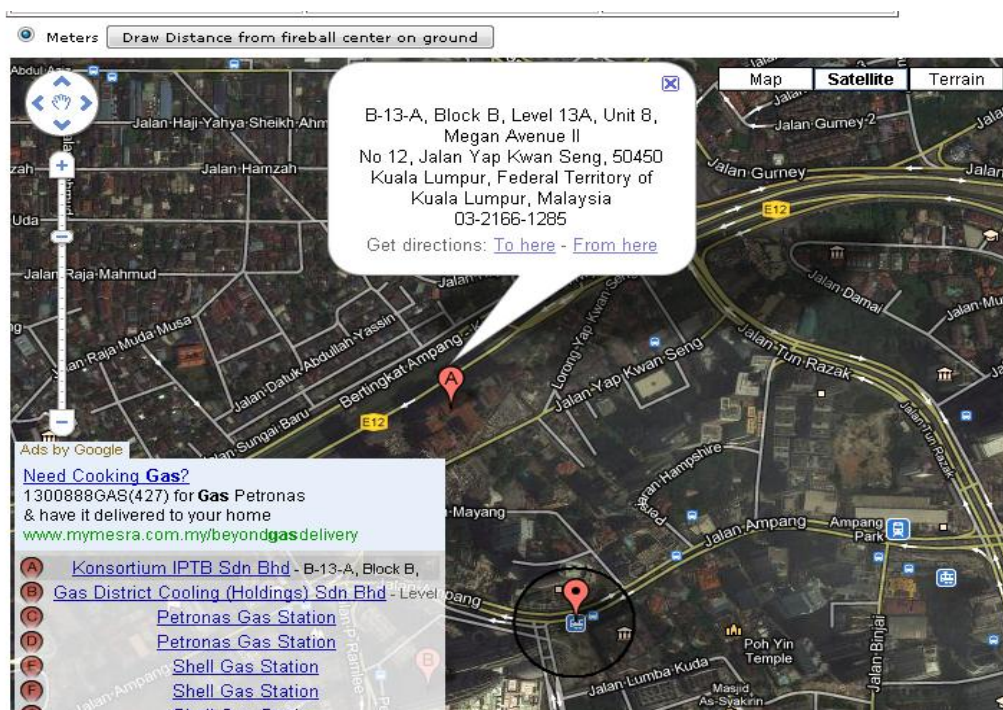


Figure 4.57 shows the accident location at Jalan Ampang involving a road tanker carrying hazardous materials



#### BLEVE Thermal Flux - Driving Simulator

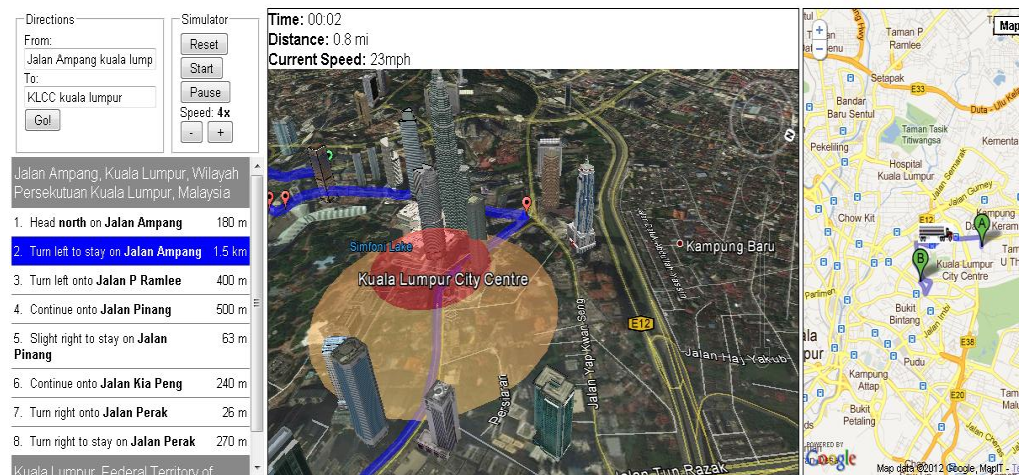


Figure 4.58 represents buffer zone from the impact of truck tanker explosion

Figure 4.57 represents buffer zone from the impact of truck tanker explosion in an accident while carrying propane by using SMACTRA map online driving simulator.

In order to recognize the severity of the condition experience by human and structure within the affected buffer zone, different buffer zone colour coding will be shown on the online map as shown in Figure 4.57 dan Figure 4.58. Figure 4.57 shows that for the case of propane fireball, receptor located within red buffer zone is expected to receive a lethal thermal radiation dose load at  $10 \text{ kW/m}^2$  at diameter 296 m. Meanwhile for a receptor located at diameter (418m - 296m) and (650m - 418m), the person will experience 1<sup>st</sup> and 2<sup>nd</sup> degree burn and pain.

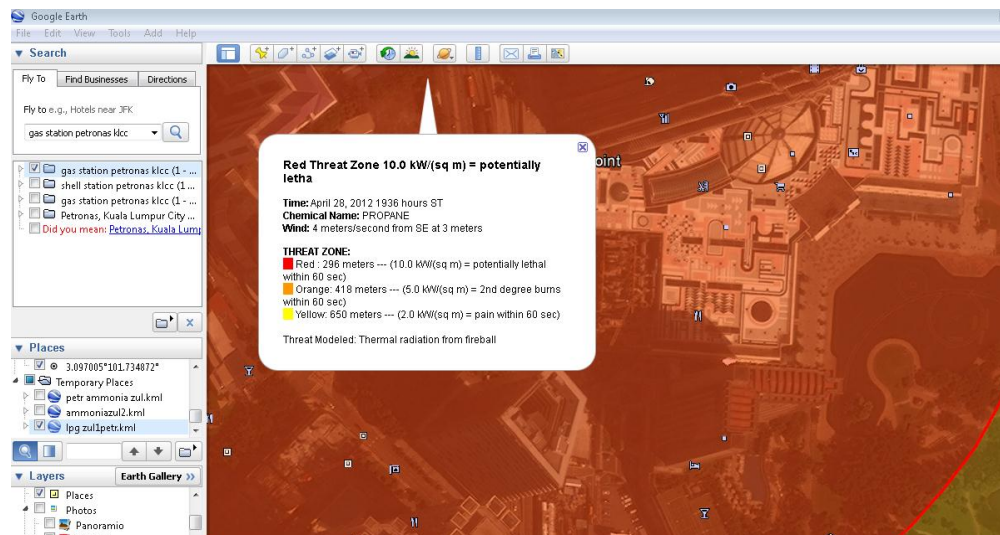


Figure 4.59 shows thermal radiation dose load from fireball impact.



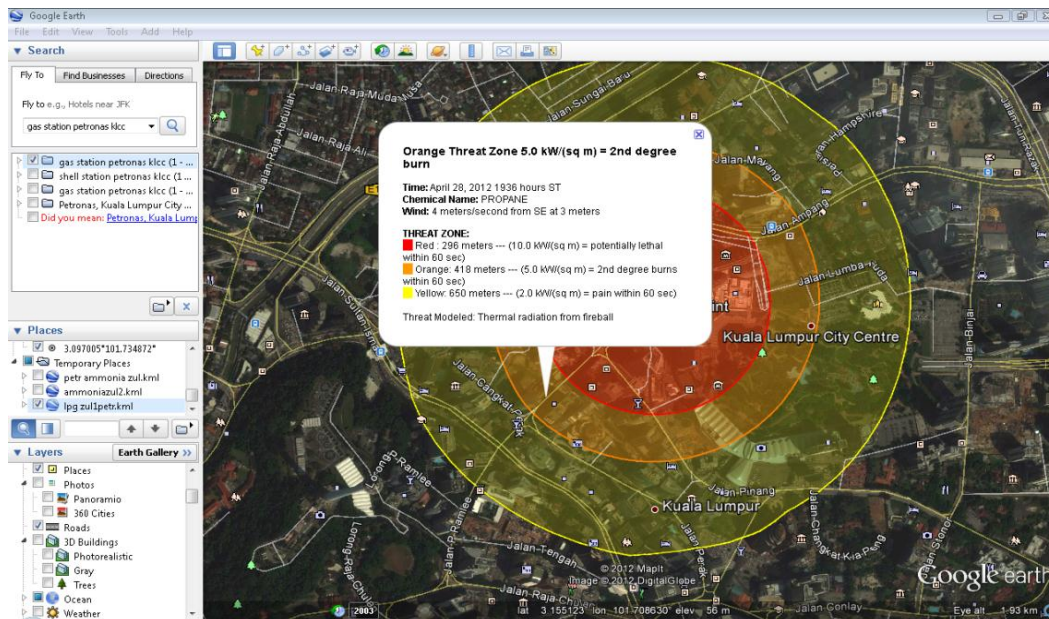


Figure 4.60 demonstrates an instantaneous case from ammonia gas release

Figure 4.59 and Figure 4.60 show the outcomes from an accident of truck tanker carrying liquid ammonia. Figure 4.59 demonstrates an instantaneous case from ammonia gas release just prior to tanker explosion. Human presence within the radius 352 m to 289 m from the explosion will experience a serious injury, with its highest peak of overpressure approximately at 3.5 psi and majority of the building within the red zone will have the worst destruction.

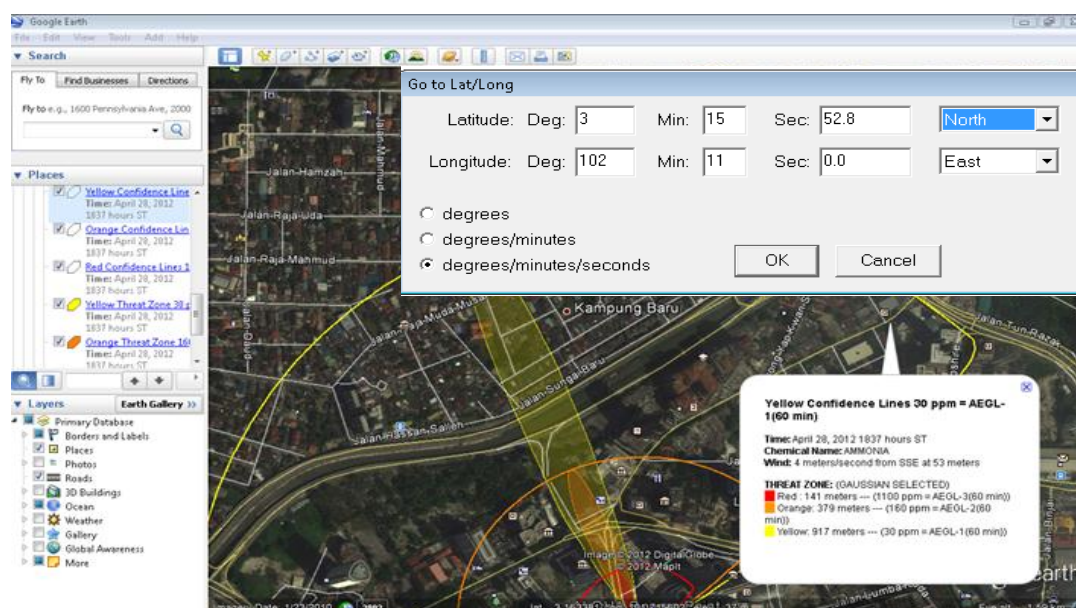


Figure 4.61 shows continuous case from ammonia gas release



For the second case, the location of longitude and latitude is similar to Figure 4.59. Figure 4.60 shows ammonia dispersion from truck tanker explosion, with wind direction to South East (SE), at 4 m/s. In this case, ammonia release did not explode but the gas disperses till 650 m from point of truck tanker accident. The effect of ammonia gas very much depending on its concentration level which reach a receptor. This phenomenon happens when ammonia is stored in a liquid form under refrigerated or pressurized condition is released and forms an aerosol or droplets along with ammonia vapor. Generally, ammonia gas has a density of  $0.778 \text{ kg/m}^3$  which is lower than air. However due to its aerosol formation, the effective density of ammonia gas becomes higher than air. Hence the dispersion of ammonia is treated as dispersion of heavy gas. The toxic exposure limits, which is defined as the toxic concentrations which lead to harmful effects to people who are exposed to ammonia.

In this figure, if the receptor is at 917 m from the plume isopleth source, a person has a possibility to experience either faint or no irritation after exposed to ammonia 30 ppm for 10 minute. However, according to Acute Exposure Guidelines Levels (AEGl) for selected airborne chemicals by National Research Council of United States (NRCU), it is expected that the toxic effect will not become more severe with the duration of exposure because adaptation will occur after prolonged exposure. To validate the result for plume isopleth of SMACTRA Map API online, result from ammonia explosion case in Houston, Texas in May 1976 [60] is used as a comparison. During the accident, the trailer was carrying 7,509 kg (19 tons) of ammonia, during spring season with temperature 26 degree celcius, humidity 79%, and wind velocity was 5.8 mph. Figure 4.60 shows the outcome map API online at Petronas Twin Tower, Jln Pinang, Kuala Lumpur.



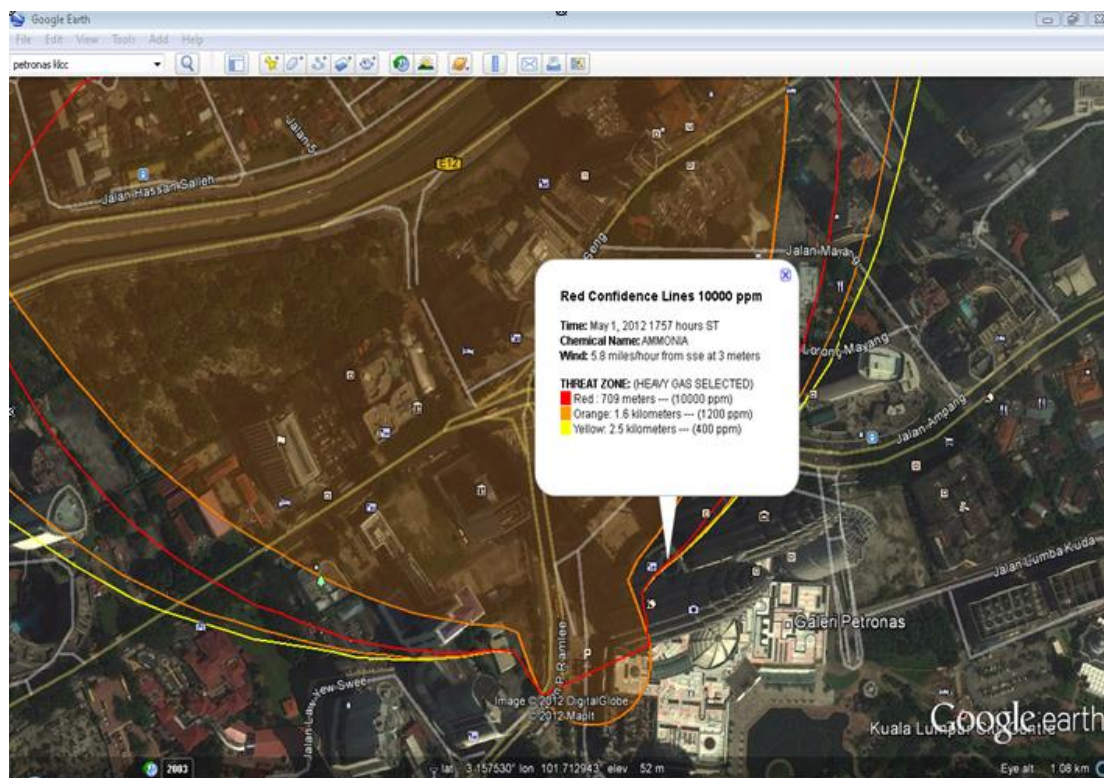


Figure 4.62 shows the outcome map API online at Petronas Twin Tower, Jln Pinang, Kuala Lumpur

Based on National Transportation safety Board of Houston in United States, ammonia toxic release accident at concentration 10,000 ppm ammonia cloud stretched up to 650 meters long and 350 meters wide, and at 1200 ppm ammonia concentration the cloud dispersed up to 1,200 meters long. By using the SMACTRA map online it shows that at concentration 10,000 ppm of ammonia is dispersed up to 709 meters, this value is comparable to the NTSB incident report [60] for houston texas ammonia incident in 1976. The detail outcome of analysis is shown in Table 4.19



Table 4.18: SMACTRA input and output parameters for ammonia gas release.

---

**Input:**

Location: PETRONAS Twin Tower, Malaysia.

Chemical Name: Ammonia.

Molecular Weight: 17.03 g/mol

AEGL-1(60 min): 30 ppm AEGL-2(60 min): 160 ppm AEGL-3(60 min): 1100 ppm

IDLH: 300 ppm LEL: 160000 ppm UEL: 250000 ppm

Ambient Boiling Point: -33.5° C

Vapor Pressure at Ambient Temperature: greater than 1 atm

Wind: 5.8 miles/hour from SSE at 3 meters

Air Temperature: 26° C

Stability Class: E

Relative Humidity: 79%

Leak from hole in horizontal cylindrical tank

Flammable chemical escaping from tank (not burning)

Tank Diameter: 2.48 meters

Tank Length: 11.99 meters

Tank Volume: 57.9 cubic meters

Tank contains liquid

Internal Temperature: 26° C

Chemical Mass in Tank: 19.1 tons

Tank is 49% full

Circular Opening Diameter: 0.25 meters

Opening is 0.12 meters from tank bottom

Release Duration: 1 minute

Max Average Sustained Release Rate: 287 kilograms/sec  
(averaged over a minute or more)

Total Amount Released: 17,212 kilograms

Note: The chemical escaped as a mixture of gas and aerosol (two phase flow).

**Outcomes**

Model Run: Heavy Gas

Red : 709 meters --- (10000 ppm)

Orange: 1.6 kilometers --- (1200 ppm)

Yellow: 2.5 kilometers --- (400 ppm)

---

#### **4.4 Risk Analysis for Hazardous Materials Transportation**

As mentioned earlier, the main objective of this study is to develop SMACTRA which capable to perform risk analysis for hazardous materials transportation. The expected results able to classify road by risk ranking, able to analyze and simulate the day and



night risk impact from data interpolation and spatial analysis. In this section, the discussion is limited to the BLEVE and fireball impact.

#### **4.4.1 Results of the road tanker accident analysis carrying 13,000kg of LPG (at the container capacity 34.5m<sup>3</sup>)**

The trend of the curves for road transportation (either via motorway, express highway or main road), depend on the relative probability for the final accident events and on the consequence analysis due to the high average value of the accident rate. The total risk with time is shown in Figure 4.62 which represents the overall individual risk at a particular time and distance. The area under the individual risk curves in Figure 4.62 represents total risk for 1<sup>st</sup> and 2<sup>nd</sup> degree burn, lethality risk and probability risk towards an individual who is protected by clothing and building. Figure 4.62 shows the total risk curves for road transport (route 1) with an individual risk value of  $2.49 \times 10^{-4}$  km/year at 3.2s, which is higher than individual risk at 0.9s, 1.0s, 1.8s, 2.8s, 3.01s, 3.5s and 9.61s. The individual risk value increases from time 0.9s to 3.1s and slowly decreased from time 3.5s to 9.61s. This value is constant from > 0 m up to 200 m distance from the source of accident. The individual risk starts to reduce from  $1.25 \times 10^{-4}$  km/year at 200m distance and drastically reduces to a negligible value at 400 m to 500 m with the individual risk value of  $3.51 \times 10^{-16}$  km/year. At 300 m the value is safe for human, building and property with the individual risk value of  $4.19 \times 10^{-7}$  km/year. This value is less than the tolerated value as stated in Malaysia guidelines for individual risk value which is at  $1.0 \times 10^{-6}$  km/year fatalities per year. Therefore at distances greater than 300 m, the risk value at  $4.17 \times 10^{-7}$  km/year injuries and fatalities indicates public acceptance of the existing risk. Based on these results, it can be concluded that the individual thermal radiation risk value is maximum at 3.2s and the “safe” zone starts at 290 m from the point of release.

To select the minimum risk for these five routes additional analysis is required to calculate societal risk. Societal risk results must be measured since most of transportation explosion incident usually give impact towards a group of people at that particular area. Therefore an input such as individual risk results as shown in Figure 4.62 is still insufficient. Usually input from individual risk results will be utilized to identify the worst acceptable risk by an individual at a particular time and



location from the source of accident. Further analysis is required to estimate safe buffer zone before any hazardous activity can be allowed for example to justify the safest route for the transportation of explosive material, radioactive or toxic. In this study, individual risk input is needed to calculate societal risk therefore safest route for HAZMAT transportation can be obtained. Kletz theory [235] such as 'worst case scenario' is used to simulate the condition and worst consequences which might occur from a disaster before any decision for the HAZMAT transportation safest route can be made and utilized. In this case study, the societal risk calculation for the worst case scenario was at 3.2s will be used as the reference in this analysis. The duration 3.2s is acceptable since 9.61s for a fireball incident is too short for an individual to escape to a safe place escape and therefore may suffer serious injury from the explosion incident.

From Figure 4.63 it is obvious that the F–N curve obtained for total impact from a BLEVE fireball is higher than those of individual BLEVE fireball impacts (for 1<sup>st</sup> degree burn, 2<sup>nd</sup> degree burn, lethality and protected). This results outcome is comparable with the outcomes results by other researchers such as Casal J. [67]. In Figure 4.63, the total societal risk result  $8.74 \times 10^{-4}$  /year is higher than the total individual risk results  $2.49 \times 10^{-4}$  /year as in Figure 4.62 at 3.2s. Therefore, it is expected all protected societal risk drastically increased and became unsaved from the accident impact between the duration of 0.1s to 3.2s. This phenomenon may be due to the maximum radiant heat emitted from the surface of the fireball between 0s and 3.2s as proposed by Martinsen and Marx [224]. According to a model proposed by Martinsen and Marx [224], Casal J. [67], fireball height, diameter and emissive power change as a function of time. The fireball reaches its maximum diameter during the first third of the fireball formation duration. At this point, the fireball tends to rise into the air and the diameter remains constant until the fireball dissipates. According to U.K. standards (Health and Safety Commission, 1991), the individual risk for road transport modalities run almost entirely in the ALARP zone, being higher than  $10^{-4}$  fatality/year with the number of fatalities and injuries increase to 1000 individuals. The road transport falls into the so called unacceptability zone ( $10^{-3}$ – $10^{-4}$  fatality/year) which is only applies to ALARP zones. The societal risk level appears globally higher than the individual one. The curves for road transport, which is the most hazardous



transport modality, fall within the UK limits for ALARP zone (Health and Safety Commission, 1991) (dotted lines). However, assuming the limits proposed by Dutch regulations (Dutch National Environmental Policy Plan, 1989) (dashed lines), it is observed that almost all curves exceed in their final part (i.e. in the high mortality zone) the intolerable zone limit.

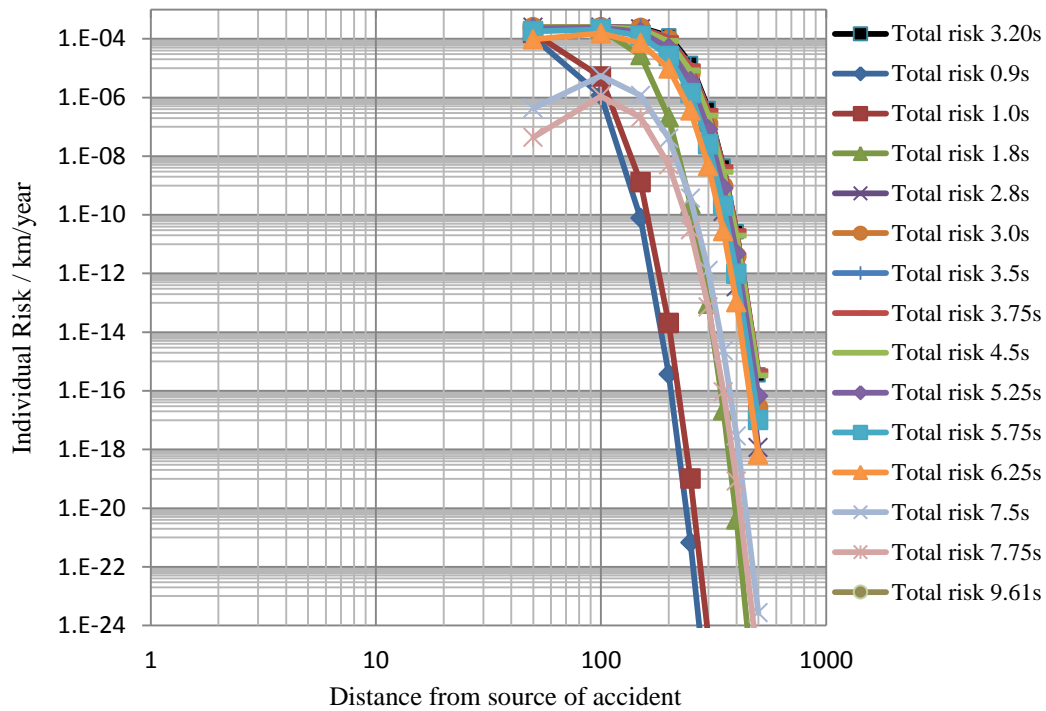


Figure 4.63 Individual risk vs. the distance from the route 1 for the LPG transport case varies with time.

This analysis provides an input for the decision-making process. The risks along each route can be compared and a decision on which route to be use is based solely on the fatality risk, environmental impacts and delivery time. If none of the results is tolerable, mitigation or a more rigorous analysis can be considered. Societal risks are used to define the routes. As shown in Figure 4.64, the fatality percentage is greatest for route 4. The lowest risk is route 2. Initially the societal risk is about the same for routes 1, 2, and 3; however the risks slowly become less than those for routes1 and 3. The maximum number of fatalities is limited to roughly 1000. Thus, if the goal is to reduce consequences, route 2 is the best choice. MCWR [203] will consider the potential benefits of an itinerary that does not cross towns or highly populated areas.



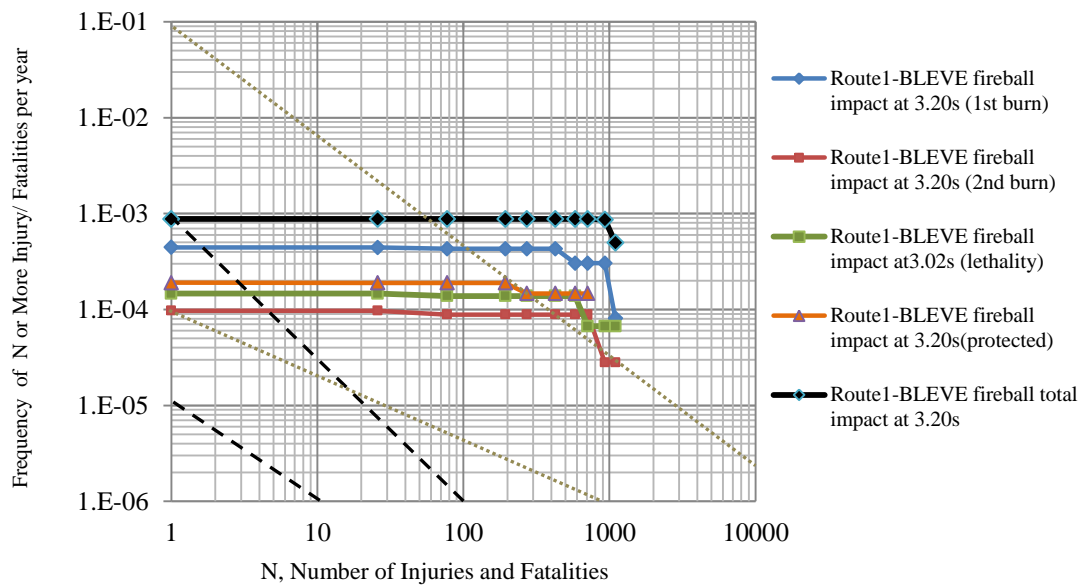


Figure 4.64 Societal risk for the LPG transport case at route 1; dashed lines: limits of the Dutch ALARP zone; dotted lines: limits of the U.K. ALARP zone.

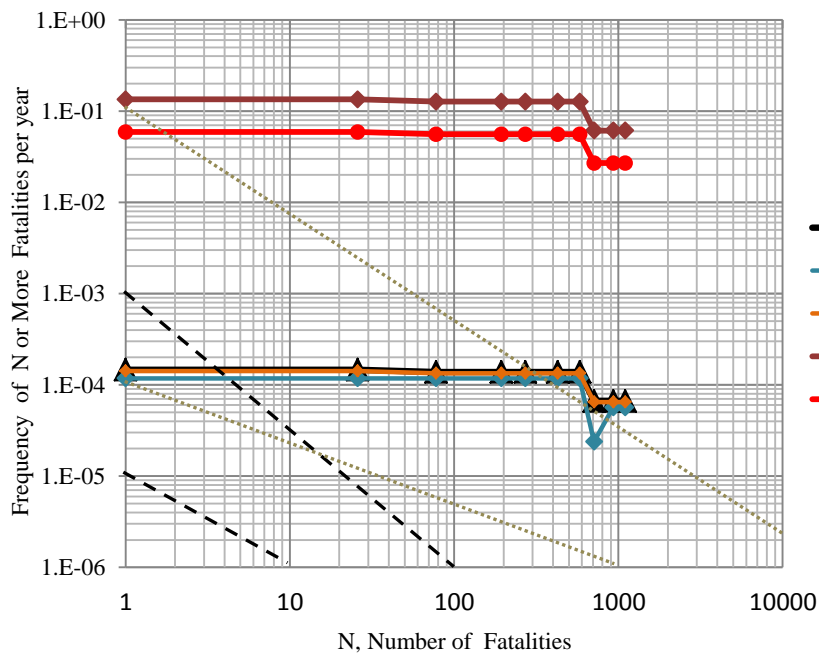


Figure 4.65 F-N curves for LPG tank truck via five routes as comparison

#### 4.4.2 Comparing results of societal risk route from LPG transportation accident (at the container capacity $34.5\text{m}^3$ )

In this section, the societal risk impact from LPG transportation accident by using different routes is shown in Figure 4.65 till Figure 4.68.



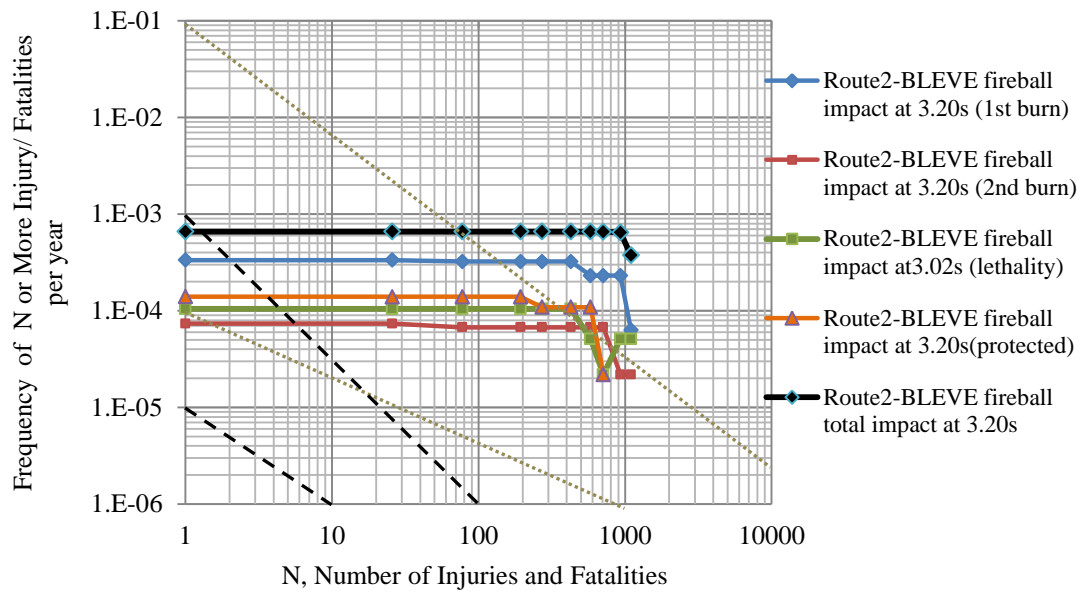


Figure 4.66 Societal risk for the LPG transport case at route 2; dashed lines: limits of the Dutch ALARP zone; dotted lines: limits of the U.K. ALARP zone.

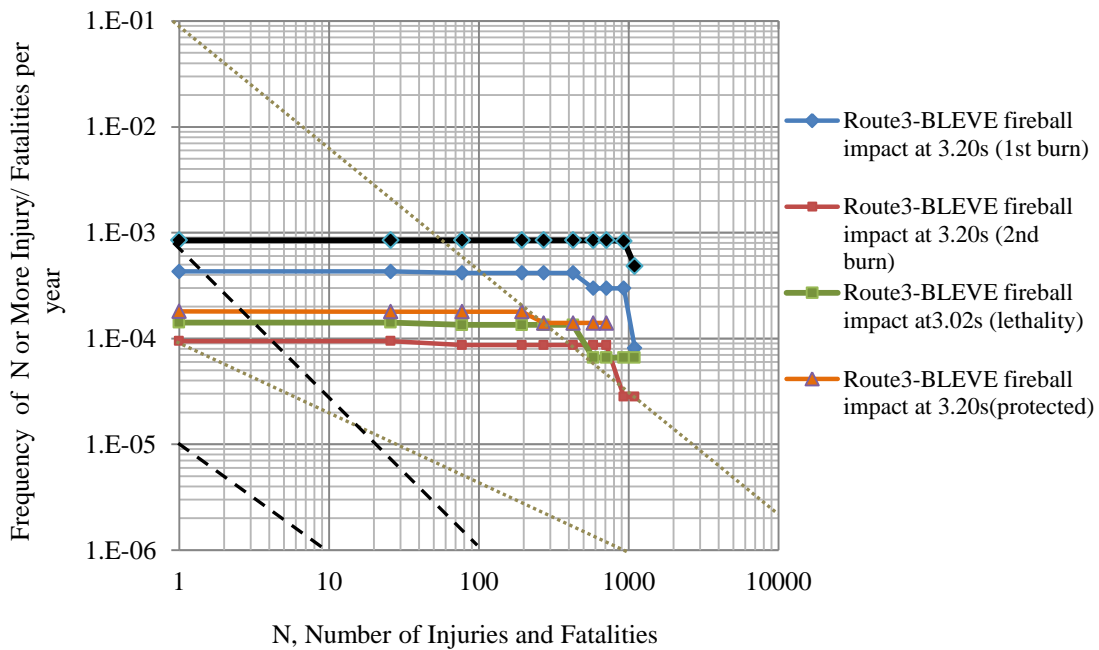


Figure 4.67 Societal risk for the LPG transport case at route 3; dashed lines: limits of the Dutch ALARP zone; dotted lines: limits of the U.K. ALARP zone.



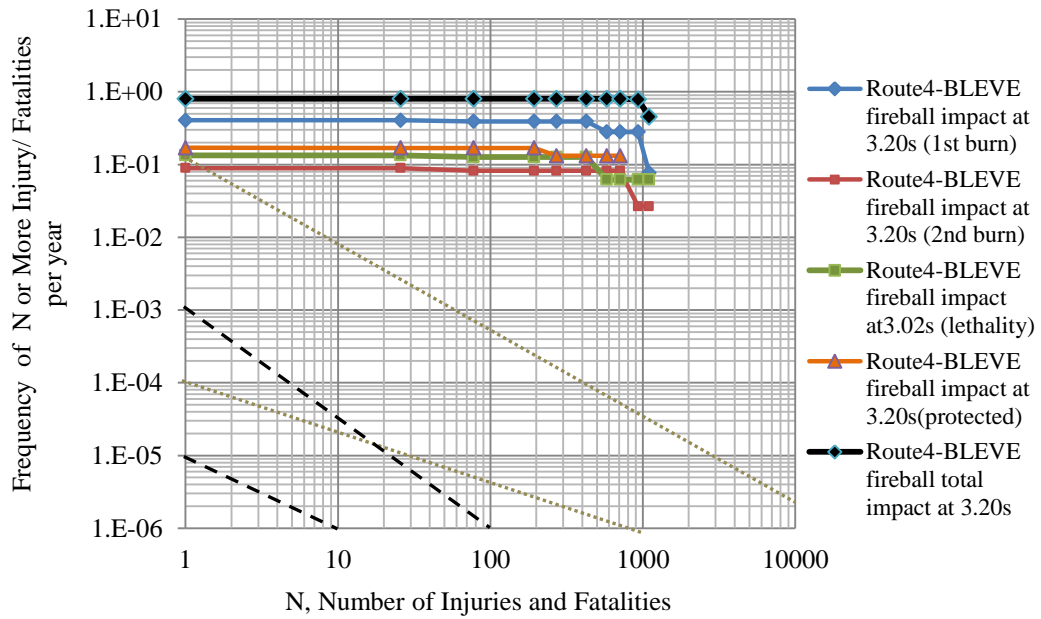


Figure 4.68 Societal risk for the LPG transport case at route 4; dashed lines: limits of the Dutch ALARP zone; dotted lines: limits of the U.K. ALARP zone.

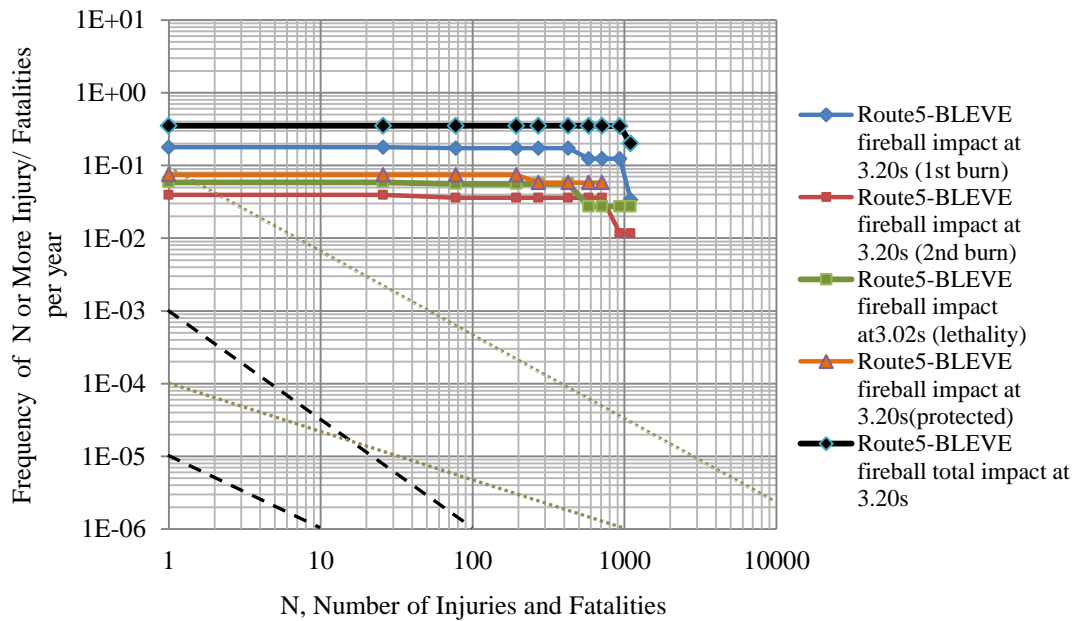


Figure 4.69 Societal risk for the LPG transport case at route 5; dashed lines: limits of the Dutch ALARP zone; dotted lines: limits of the U.K. ALARP zone.

From figure 4.65 till 4.68, SMACTRA predicted that all impacts of BLEVE, such as first degree, second degree and lethality for route 4 and 5 are located at an intolerable



region. This graph analysis results is shown in Table 4.16. From the table it is observed that the societal risk for route 4 and 5 are greater than  $1 \times 10^{-5}$  fatalities/injury per year (according to Malaysian standard). In conclusion route 2 is the safest route and the other routes are considered not saved for the transportation of 13,000 kg of LPG.

Table 4.19: Comparison results of five routes societal risk from BLEVE impact using SACTRA.

| <i>Fluid: Malaysia LPG commercial (30:70 propane: butane % mol)</i> |         |                        |                        |                       |                       |                       |
|---|---------|------------------------|------------------------|-----------------------|-----------------------|-----------------------|
| N, Number of fatalities   |         | Results                |                        |                       |                       |                       |
|   |         | 1 <sup>st</sup> degree | 2 <sup>nd</sup> degree | lethality             | protected             | total                 |
| Route 1   | 1       | $4.43 \times 10^{-4}$  | $9.76 \times 10^{-5}$  | $1.46 \times 10^{-4}$ | $1.86 \times 10^{-4}$ | $8.74 \times 10^{-4}$ |
|   | 25.85   | $4.43 \times 10^{-4}$  | $9.76 \times 10^{-5}$  | $1.46 \times 10^{-4}$ | $1.85 \times 10^{-4}$ | $8.74 \times 10^{-4}$ |
|   | 77.55   | $4.30 \times 10^{-4}$  | $8.94 \times 10^{-5}$  | $1.39 \times 10^{-4}$ | $1.85 \times 10^{-4}$ | $8.74 \times 10^{-4}$ |
|   | 193.87  | $4.30 \times 10^{-4}$  | $8.94 \times 10^{-5}$  | $1.39 \times 10^{-4}$ | $1.85 \times 10^{-4}$ | $8.74 \times 10^{-4}$ |
|   | 271.42  | $4.30 \times 10^{-4}$  | $8.94 \times 10^{-5}$  | $1.39 \times 10^{-4}$ | $1.45 \times 10^{-4}$ | $8.74 \times 10^{-4}$ |
|   | 426.52  | $4.30 \times 10^{-4}$  | $8.94 \times 10^{-5}$  | $1.39 \times 10^{-4}$ | $1.45 \times 10^{-4}$ | $8.74 \times 10^{-4}$ |
|   | 581.62  | $3.07 \times 10^{-4}$  | $8.94 \times 10^{-5}$  | $6.79 \times 10^{-5}$ | $1.45 \times 10^{-4}$ | $8.74 \times 10^{-4}$ |
|   | 710.87  | $3.07 \times 10^{-4}$  | $8.94 \times 10^{-5}$  | $6.79 \times 10^{-5}$ | $1.45 \times 10^{-4}$ | $8.73 \times 10^{-4}$ |
|   | 930.60  | $3.07 \times 10^{-4}$  | $2.90 \times 10^{-5}$  | $6.79 \times 10^{-5}$ | 0.00                  | $8.59 \times 10^{-4}$ |
|   | 1098.62 | $8.39 \times 10^{-5}$  | $2.90 \times 10^{-5}$  | $6.79 \times 10^{-5}$ | 0.00                  | $4.97 \times 10^{-4}$ |
| Route 2   | 1       | $3.35 \times 10^{-4}$  | $7.37 \times 10^{-5}$  | $1.05 \times 10^{-4}$ | $1.40 \times 10^{-4}$ | $6.60 \times 10^{-4}$ |
|   | 25.85   | $3.35 \times 10^{-4}$  | $7.37 \times 10^{-5}$  | $1.05 \times 10^{-4}$ | $1.40 \times 10^{-4}$ | $6.59 \times 10^{-4}$ |
|   | 77.55   | $3.24 \times 10^{-4}$  | $6.75 \times 10^{-5}$  | $1.05 \times 10^{-4}$ | $1.40 \times 10^{-4}$ | $6.59 \times 10^{-4}$ |
|   | 193.87  | $3.24 \times 10^{-4}$  | $6.75 \times 10^{-5}$  | $1.05 \times 10^{-4}$ | $1.40 \times 10^{-4}$ | $6.59 \times 10^{-4}$ |
|   | 271.42  | $3.24 \times 10^{-4}$  | $6.75 \times 10^{-5}$  | $1.05 \times 10^{-4}$ | $1.09 \times 10^{-4}$ | $6.59 \times 10^{-4}$ |
|   | 426.52  | $3.24 \times 10^{-4}$  | $6.75 \times 10^{-5}$  | $1.05 \times 10^{-4}$ | $1.09 \times 10^{-4}$ | $6.59 \times 10^{-4}$ |
|   | 581.62  | $2.32 \times 10^{-4}$  | $6.75 \times 10^{-5}$  | $5.12 \times 10^{-5}$ | $1.09 \times 10^{-4}$ | $6.59 \times 10^{-4}$ |
|   | 710.87  | $2.32 \times 10^{-4}$  | $6.75 \times 10^{-5}$  | $2.19 \times 10^{-5}$ | $2.19 \times 10^{-5}$ | $6.59 \times 10^{-4}$ |
|   | 930.60  | $2.32 \times 10^{-4}$  | $2.19 \times 10^{-5}$  | $5.12 \times 10^{-5}$ | 0.00                  | $6.49 \times 10^{-4}$ |
|   | 1098.62 | $6.33 \times 10^{-5}$  | $2.19 \times 10^{-5}$  | $5.12 \times 10^{-5}$ | 0.00                  | $3.75 \times 10^{-4}$ |
| Route 3   | 1       | $4.30 \times 10^{-4}$  | $9.47 \times 10^{-5}$  | $1.42 \times 10^{-4}$ | $1.81 \times 10^{-4}$ | $8.47 \times 10^{-4}$ |
|   | 25.85   | $4.30 \times 10^{-4}$  | $9.47 \times 10^{-5}$  | $1.42 \times 10^{-4}$ | $1.80 \times 10^{-4}$ | $8.47 \times 10^{-4}$ |
|   | 77.55   | $4.17 \times 10^{-4}$  | $8.67 \times 10^{-5}$  | $1.34 \times 10^{-4}$ | $1.80 \times 10^{-4}$ | $8.47 \times 10^{-4}$ |
|   | 193.87  | $4.17 \times 10^{-4}$  | $8.67 \times 10^{-5}$  | $1.34 \times 10^{-4}$ | $1.80 \times 10^{-4}$ | $8.47 \times 10^{-4}$ |
|   | 271.42  | $4.17 \times 10^{-4}$  | $8.67 \times 10^{-5}$  | $1.34 \times 10^{-4}$ | $1.40 \times 10^{-4}$ | $8.47 \times 10^{-4}$ |
|   | 426.52  | $4.17 \times 10^{-4}$  | $8.67 \times 10^{-5}$  | $1.34 \times 10^{-4}$ | $1.40 \times 10^{-4}$ | $8.47 \times 10^{-4}$ |
|   | 581.62  | $2.98 \times 10^{-4}$  | $8.67 \times 10^{-5}$  | $6.59 \times 10^{-5}$ | $1.40 \times 10^{-4}$ | $8.47 \times 10^{-4}$ |



---

|         |                       |                       |                       |                       |                       |
|---------|-----------------------|-----------------------|-----------------------|-----------------------|-----------------------|
| 710.87  | $2.98 \times 10^{-4}$ | $8.67 \times 10^{-5}$ | $6.58 \times 10^{-5}$ | $1.40 \times 10^{-4}$ | $8.47 \times 10^{-4}$ |
| 930.60  | $2.98 \times 10^{-4}$ | $2.81 \times 10^{-5}$ | $6.58 \times 10^{-5}$ | 0.00                  | $8.34 \times 10^{-4}$ |
| 1098.62 | $8.13 \times 10^{-5}$ | $2.81 \times 10^{-5}$ | $6.58 \times 10^{-5}$ | 0.00                  | $4.82 \times 10^{-4}$ |
| 1       | $4.06 \times 10^{-1}$ | $8.94 \times 10^{-2}$ | $1.34 \times 10^{-1}$ | $1.70 \times 10^{-1}$ | $8.00 \times 10^{-1}$ |
| 25.85   | $4.06 \times 10^{-1}$ | $8.94 \times 10^{-2}$ | $1.34 \times 10^{-1}$ | $1.70 \times 10^{-1}$ | $8.00 \times 10^{-1}$ |
| 77.55   | $3.93 \times 10^{-1}$ | $8.19 \times 10^{-2}$ | $1.27 \times 10^{-1}$ | $1.70 \times 10^{-1}$ | $8.00 \times 10^{-1}$ |
| 193.87  | $3.93 \times 10^{-1}$ | $8.19 \times 10^{-2}$ | $1.27 \times 10^{-1}$ | $1.70 \times 10^{-1}$ | $8.00 \times 10^{-1}$ |
| 271.42  | $3.93 \times 10^{-1}$ | $8.19 \times 10^{-2}$ | $1.27 \times 10^{-1}$ | $1.32 \times 10^{-1}$ | $8.00 \times 10^{-1}$ |
| 426.52  | $3.93 \times 10^{-1}$ | $8.19 \times 10^{-2}$ | $1.27 \times 10^{-1}$ | $1.32 \times 10^{-1}$ | $8.00 \times 10^{-1}$ |
| 581.62  | $2.81 \times 10^{-1}$ | $8.19 \times 10^{-2}$ | $6.22 \times 10^{-2}$ | $1.32 \times 10^{-1}$ | $8.00 \times 10^{-1}$ |
| 710.87  | $2.81 \times 10^{-1}$ | $8.19 \times 10^{-2}$ | $6.22 \times 10^{-2}$ | $1.32 \times 10^{-1}$ | $7.99 \times 10^{-1}$ |
| 930.60  | $2.81 \times 10^{-1}$ | $2.66 \times 10^{-2}$ | $6.22 \times 10^{-2}$ | 0.00                  | $7.87 \times 10^{-1}$ |
| 1098.62 | $7.68 \times 10^{-2}$ | $2.66 \times 10^{-2}$ | $6.22 \times 10^{-2}$ | 0.00                  | $4.55 \times 10^{-1}$ |
| 1       | $1.78 \times 10^{-1}$ | $3.93 \times 10^{-2}$ | $5.88 \times 10^{-2}$ | $7.49 \times 10^{-2}$ | $3.52 \times 10^{-1}$ |
| 25.85   | $1.78 \times 10^{-1}$ | $3.93 \times 10^{-2}$ | $5.88 \times 10^{-2}$ | $7.45 \times 10^{-2}$ | $3.52 \times 10^{-1}$ |
| 77.55   | $1.73 \times 10^{-1}$ | $3.59 \times 10^{-2}$ | $5.58 \times 10^{-2}$ | $7.45 \times 10^{-2}$ | $3.52 \times 10^{-1}$ |
| 193.87  | $1.73 \times 10^{-1}$ | $3.59 \times 10^{-2}$ | $5.58 \times 10^{-2}$ | $7.45 \times 10^{-2}$ | $3.52 \times 10^{-1}$ |
| 271.42  | $1.73 \times 10^{-1}$ | $3.59 \times 10^{-2}$ | $5.58 \times 10^{-2}$ | $5.81 \times 10^{-2}$ | $3.52 \times 10^{-1}$ |
| 426.52  | $1.73 \times 10^{-1}$ | $3.59 \times 10^{-2}$ | $5.58 \times 10^{-2}$ | $5.81 \times 10^{-2}$ | $3.52 \times 10^{-1}$ |
| 581.62  | $1.24 \times 10^{-1}$ | $3.59 \times 10^{-2}$ | $2.73 \times 10^{-2}$ | $5.81 \times 10^{-2}$ | $3.52 \times 10^{-1}$ |
| 710.87  | $1.24 \times 10^{-1}$ | $3.59 \times 10^{-2}$ | $2.73 \times 10^{-2}$ | $5.81 \times 10^{-2}$ | $3.51 \times 10^{-1}$ |
| 930.60  | $1.24 \times 10^{-1}$ | $1.17 \times 10^{-2}$ | $2.73 \times 10^{-2}$ | 0.00                  | $3.46 \times 10^{-1}$ |
| 1098.62 | $3.38 \times 10^{-2}$ | $1.17 \times 10^{-2}$ | $2.73 \times 10^{-2}$ | 0.00                  | $2.00 \times 10^{-1}$ |

---

#### 4.4.3 Analyze the effect of route length over societal risk from LPG accident (at the container capacity $34.5\text{m}^3$ ) by using SACTRA

The aim of this study is to analyze the effect of route length over societal risk from LPG accident. As concluded above, route 2 is the safest route, therefore this route can be used as a reference for the societal risk analysis effect at different length route. Based on the result of this analysis, the safety along route 2 can be monitor for HAZMAT transportation. Figure 4.69 till 4.74 showing the comparison between the effects of societal risk route at different route length as generated by SACTRA, for 13,000 kg LPG.



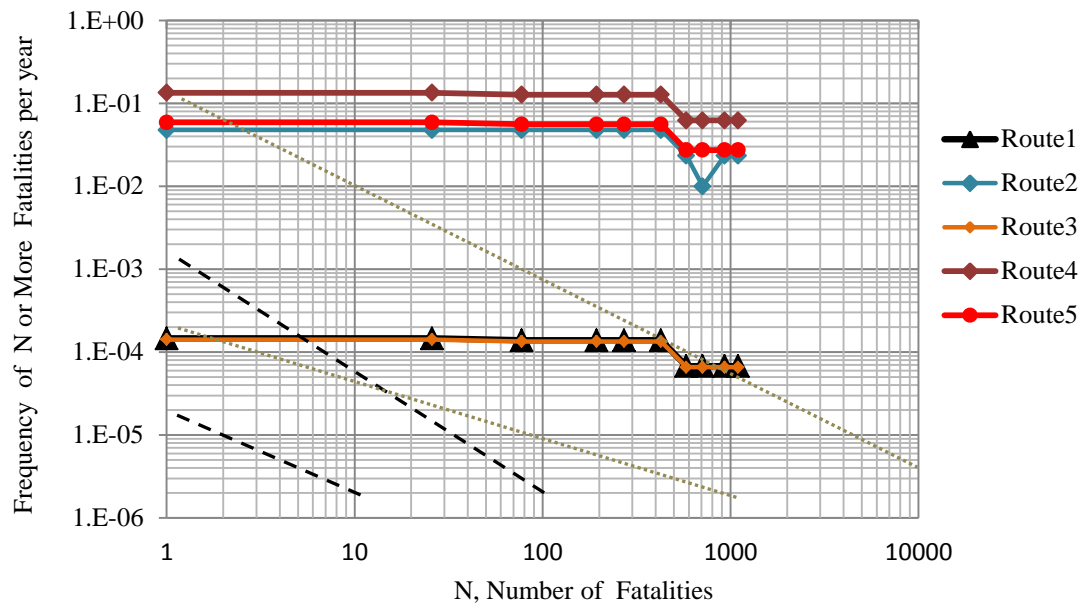


Figure 4.70 F-N curves for LPG tank truck via five routes as comparison on route 2 at length 34 km

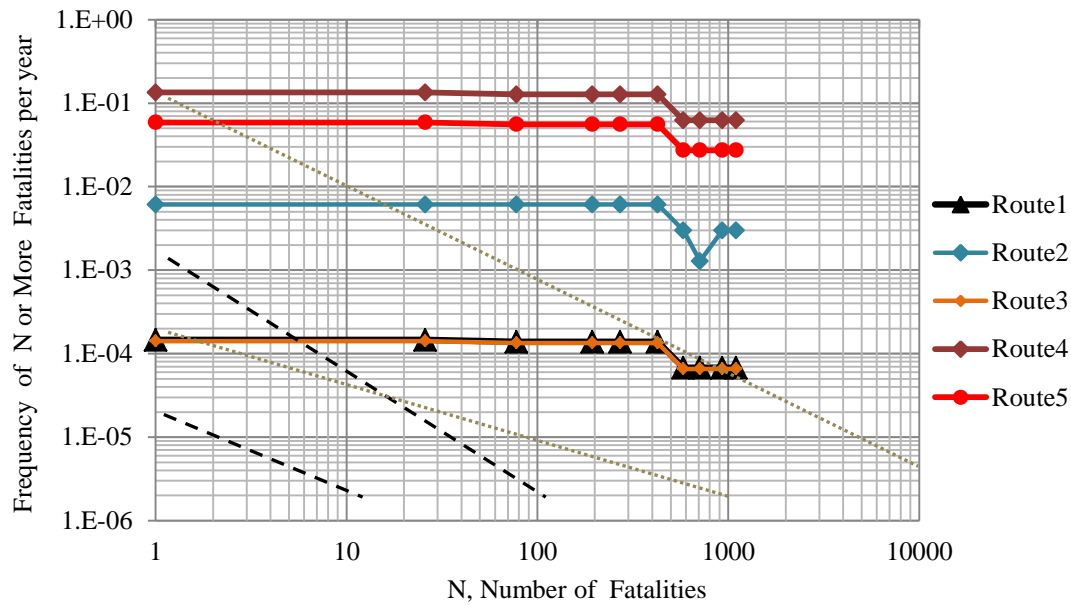


Figure 4.71 F-N curves for LPG tank truck via five routes as comparison with route 2 at length 20 km



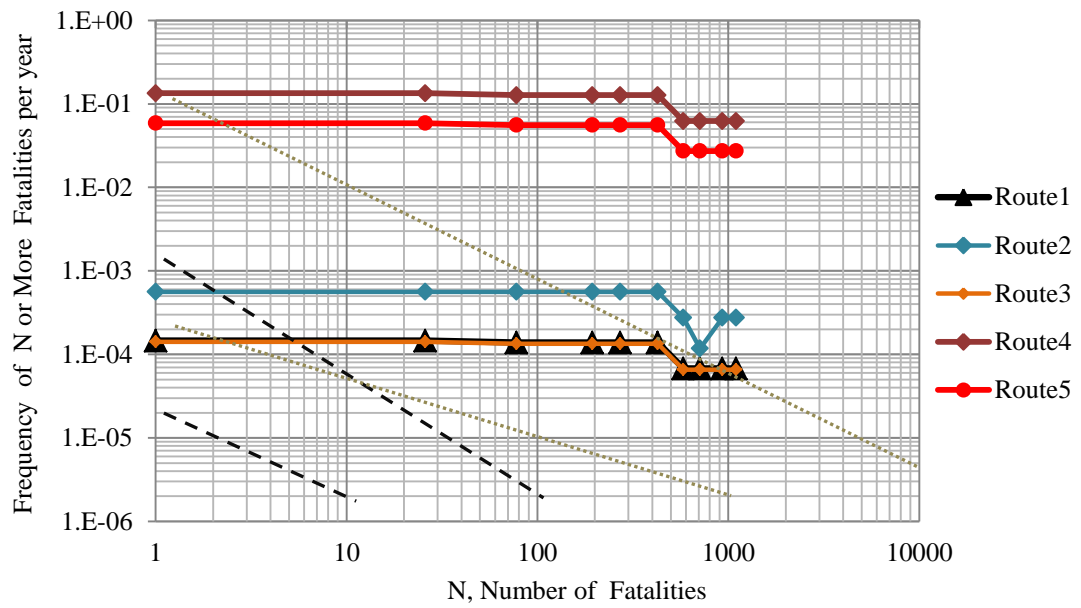


Figure 4.72 F-N curves for LPG tank truck via five routes as comparison on route 2 at length 14 km

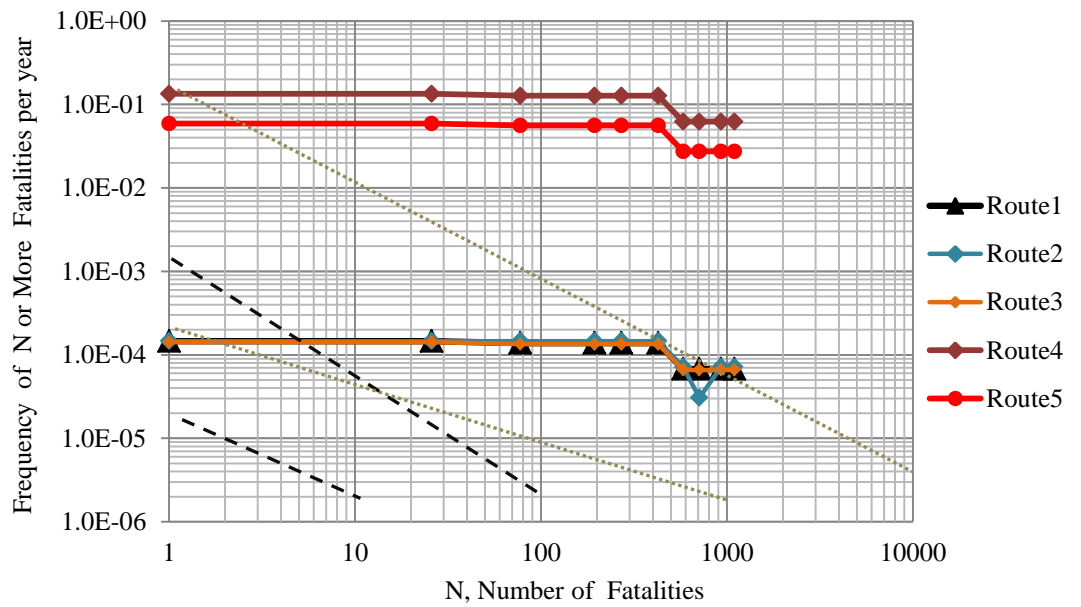


Figure 4.73 F-N curves for LPG tank truck via five routes as comparison on route 2 at length 10.458 km



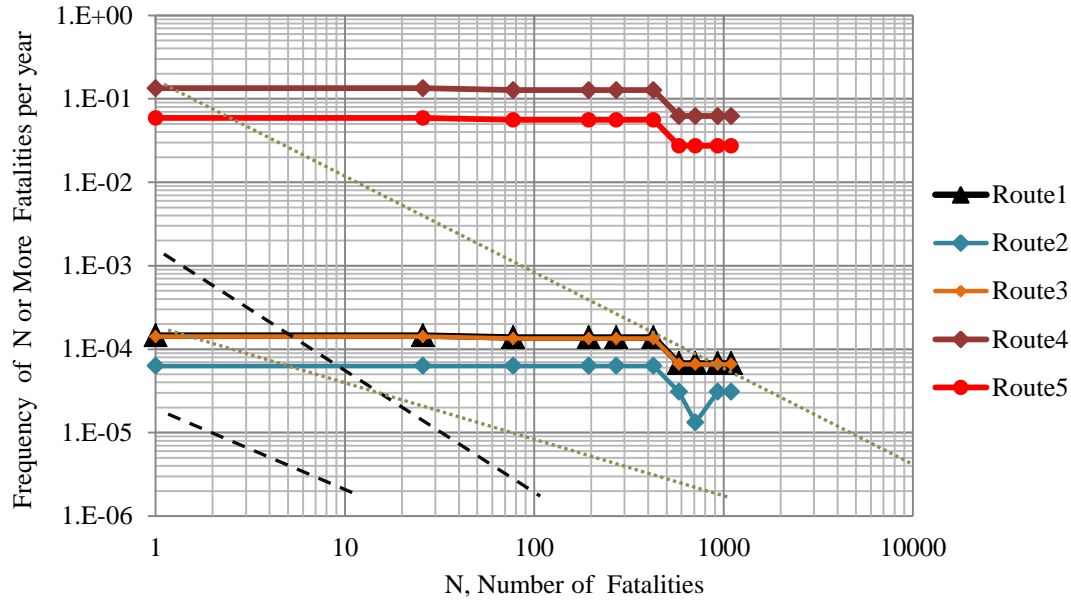


Figure 4.74 F-N curves for LPG tank truck via five routes as comparison on route 2 at length 4.458 km

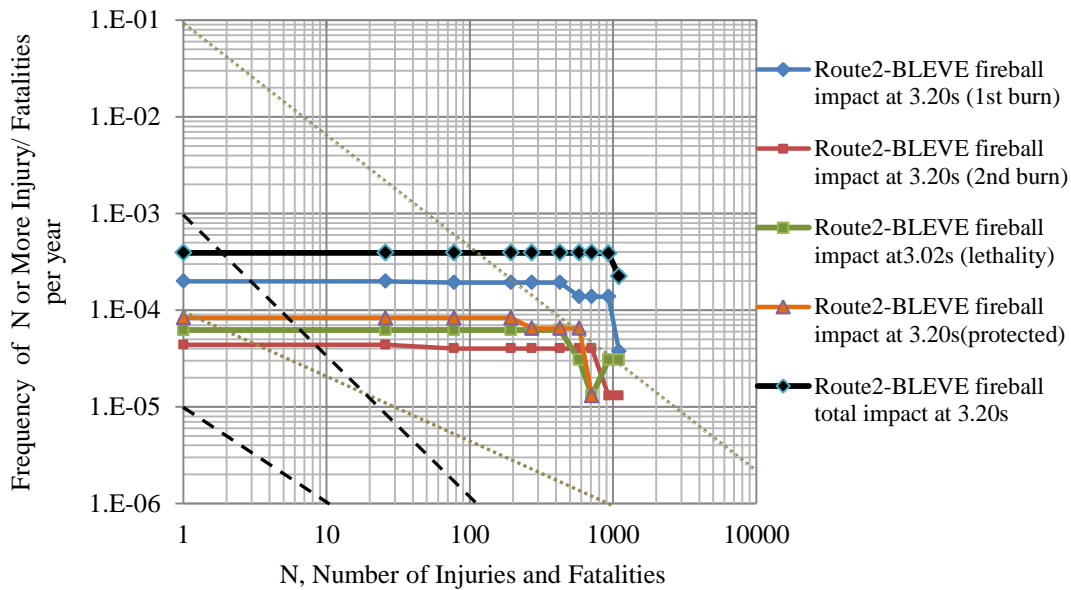


Figure 4.75 Societal risk for the LPG transport case at route 2, 4.458 km; dashed lines: limits of the Dutch ALARP zone; dotted lines: limits of the U.K. ALARP zone.

For the first scenario, SMACTRA predicted that the societal risk for route 2 is comparable to route 5 as the length for route 2 of LPG transportation increases from 10.46km to 34 km, with 400 trips per day. The length of route 5 is 4.024 km.



Therefore, when the length for route 2 increases, it is observed that the risk is also increased and at the journey of 34 km the risk level of route 2 is equivalent to risk level of route 4.

For second scenario, if route 2 length is reduced to 14 km, SMACTRA analysis predicted that about 50% reduction of risk level for route 2, from intolerable region to tolerable region. In UK legislation, Health and Safety Executive at work, 1974 guidelines [64], tolerable is also known as “As low As Reasonably Practicable (ALARP)”. It is define as the possible cost involved such as infinite time, effort and money to reduce the risk and would be grossly disproportionate to the benefit. Therefore, in order to reduce the risk factor for route 2, other than to reduced its length, but also other factors such as training to the drivers, production of the safe cryogenic tanker container and etc. For the third scenario, with the same journey surrounding, the length is reduced and approximated to route 5, which is 4.458 km. As a result, it is observed from Figure 4.73, that the risk is reduced further lower than the previous road tanker journey, which is 10 km for route 2. This value is totally lower than route 1 and 3 at 10.458 km as in Figure 4.72. Further analysis shown that when the length of a route 2 is reduce, the BLEVE impact to human is also reduce. Based on Figure 4.74, it is predicted that all probabilities impact of burn injury to human are shifted to a low tolerable region compared to societal risk analysis as in Figure 4.65.

In summary, route length should not become the sole risk indicator either high or low, since risk assessments involved many unforeseen or other factor which is can be unpredictable throughout the journey. . According to population distribution, taking into account outdoor and indoor population ratio, the surrounding environment between assigned localities generally does not change much for road trip in rural area, but it is vice versa with higher risk for transportation via urban zone population Therefore results obtained from Figure 4.69 to Figure 4.74 shows that when the surrounding environment along route 2 is constant, whenever the length route change, the societal risk also will change.



#### 4.4.4 The trips effect over the societal risk for five routes of LPG tanker incident (in capacity of $34.5\text{m}^3$ ) to receptor

The purpose of the analysis is to see the societal risk impact from five routes, when the number of transportation is increased or decreased than normal operation of MCWR.

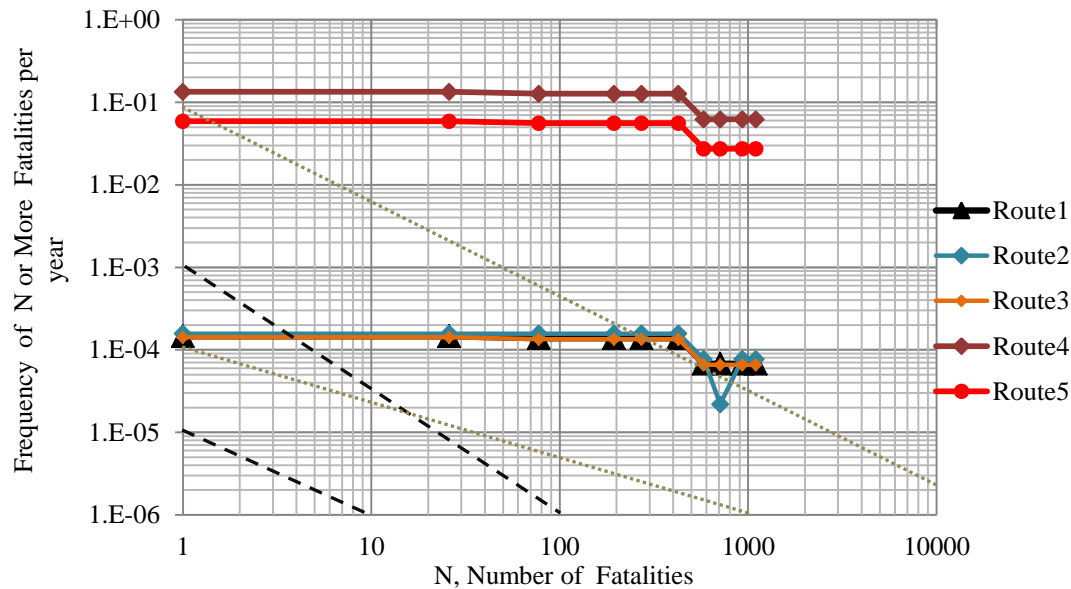


Figure 4.76 F-N curves for LPG tank truck via five routes as comparison on route 2 at 600 trips per day

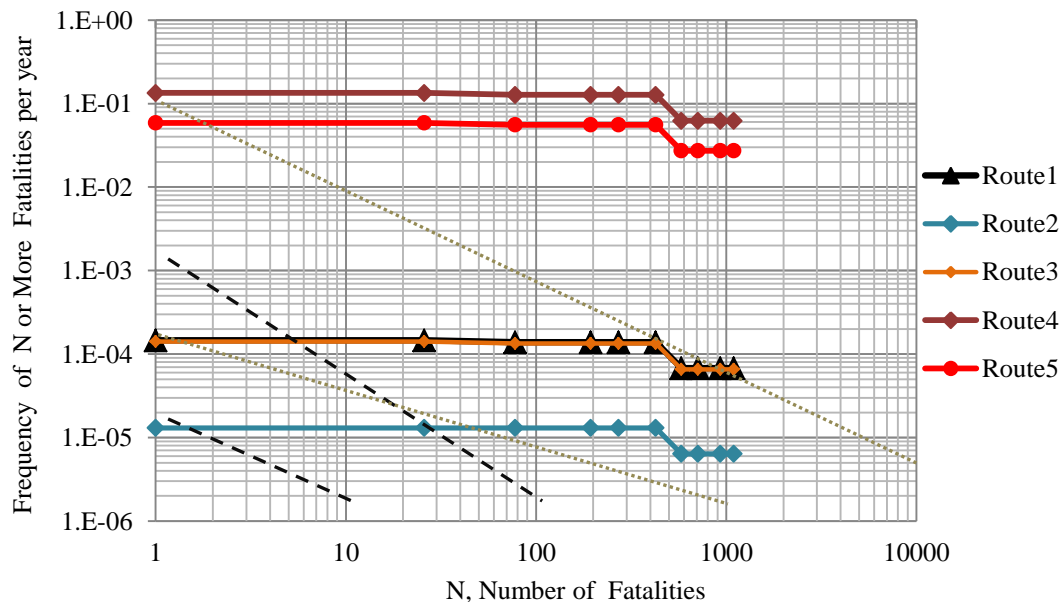


Figure 4.77 F-N curves for LPG tank truck via five routes as comparison on route 2 at 50 trips per day.



From figure 4.75, the number of trips for transportation of 13,000 of LPG tanker is increased from 400 to 600 trips. Whenever the transportation trip increased, the individual risk is also increased, and this is due to an increment in time contact per year. Route 2 in Figure 4.75, showing the societal risk curves is moving upward. Route 4 and 5 are observed situated at intolerable region with the value of  $1.0 \times 10^{-1}$  fatalities per year. Meanwhile the other three routes (1 to 3) are shifted greater than  $1 \times 10^{-4}$  fatalities per year which is still within UK tolerable region. As the trip is reduced to 50 trips, societal risk also reduced from the most risky to a tolerable risk. Whilst for several routes, the societal risk result is predicted changed from tolerable risk to acceptable risk, when the fatalities is below than 30 people. This result can be observed for route 2, as shown in Figure 4.76.

#### 4.4.5 Comparison the individual risk and societal risk results between SMACTRA, BUWAL and CCPS

In this section, the individual and societal risk results as predicted by SMACTRA are compared with the results produced by BUWAL [73] and CCPS [21, 22] method. Figure 4.77 till Figure 4.79 shows the comparison for individual risk result between SMACTRA/ BUWAL/ CCPS (AIChE). Meanwhile Figure 4.80 shows the comparison for societal risk results of SMACTRA/ BUWAL/ CCPS (AIChE).

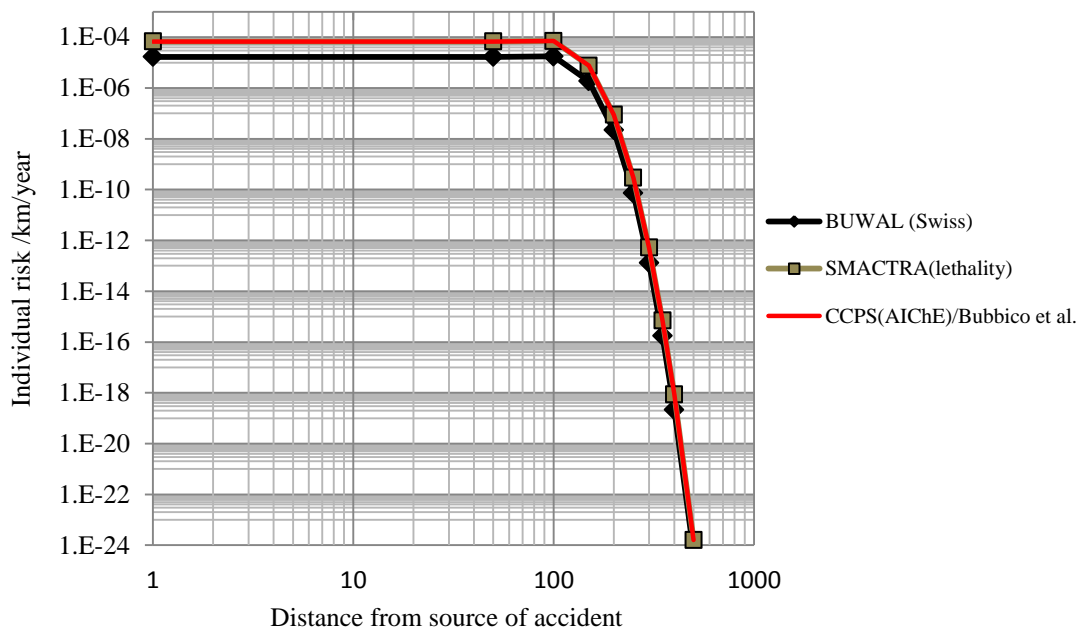


Figure 4.78 comparison the total individual risk results SMACTRA/ BUWAL/ CCPS (AIChE).



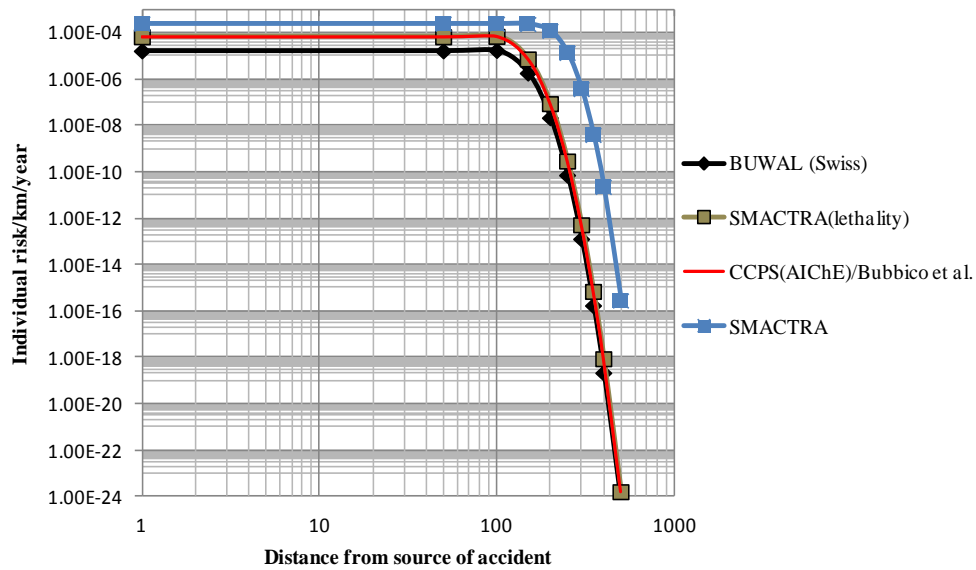


Figure 4.79 comparison the total individual risk results SMACTRA/ BUWAL/ CCPS (AIChE).

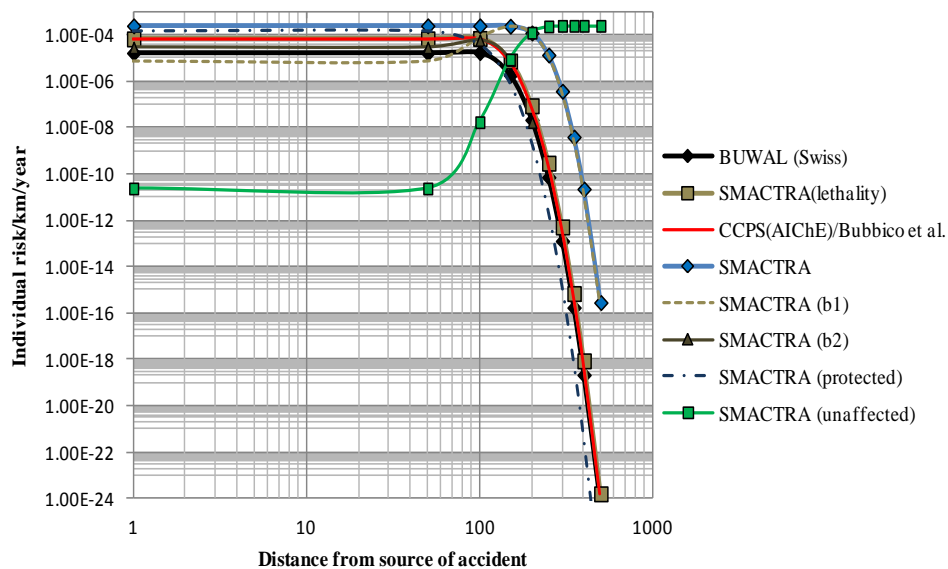


Figure 4.80 comparison the individual risk results SMACTRA/ BUWAL/ CCPS (AIChE).

Figure 4.78 shows that total individual risk results by SMACTRA (lethality) and CCPS (AIChE)- Bubbico et al. [101, 103,104] are overlapping to each other. However, the total individual risk result by BUWAL method is noted to be lower than SMACTRA (lethality) and CCPS. Meanwhile in figure 4.79 it is shown that total individual risk result SMACTRA is higher compared to total risk results by SMACTRA (lethality), BUWAL and CCPS method. As mentioned earlier, risk



impact from an accident is varies depend on distance from the accident source which is contradict to CCPS [21]. In reality, the population and environment closer to the source of an event is expected to experience more severe consequences than those farther than it. As the distance from the event increases, the consequences of such an event decreases. Thus the assumption of uniform distribution across the impact area used as in Eq.(2-10) – (2-12) in CCPS [21,22], as in Eq. (2-8) in Rhyne [25], and as in Eq. (2-2) – (2-4) in Swiss risk methodology (BUWAL) [73] may not correctly represent actual condition and may lead to a misrepresentation of risk which take risk impact is similar. Regardless of the receptor location, (as long as it's within the affected buffer zone) the receptor is considered to have a similar individual risk. SACTRA will calculate the probability of injury, as shown in Figure 4.78 and Figure 4.79 meanwhile the probability of no-injury as shown by graph analysis in Figure 4.77. Result in Figure 4.77 and 4.79, shows that total risk individual for SACTRA (lethality) and CCPS (AICHe)- Bubbico et al. [101] is overlapping. By using SACTRA, the individual risk for 2<sup>nd</sup> degree and 1<sup>st</sup> degree burn injury is shown under SACTRA blue curve line. Figure 4.79 shows that the individual risk calculated by SACTRA (unaffected), without any injury and survive are very slim between 0 till 150m from source of accident. At the distance more than 250 m from an accident event, it is expected that most of the people are saved.

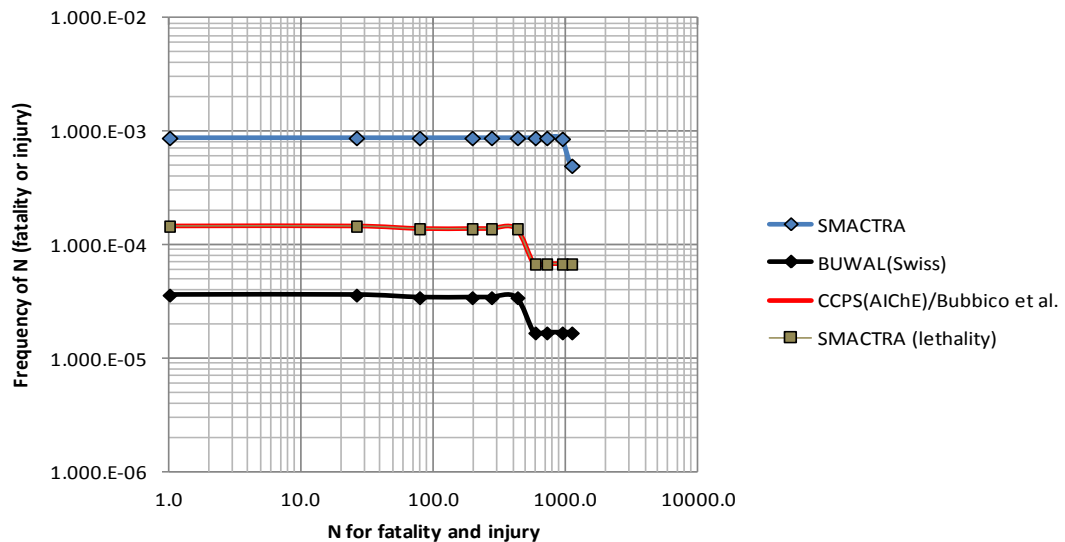


Figure 4.81 comparison the societal risk results SACTRA/ BUWAL/ CCPS (AICHe) for route 1 at 3.2s.



From Figure 4.80, the societal risk results for SACTRA are higher than BUWAL and CCPS. However results for SACTRA (lethality) and CCPS is observed to be overlapped.

#### **4.5 Hazard Mapping Analysis**

The use of information contained in the GIS application, coupled with those of the consequences transportation model calculation of SACTRA can be of great help in managing transportation risk analysis and emergencies. In fact, it is possible to view directly on the map the effect zones relevant to the various outcome cases possibly originated by an accident. Moreover, the impact areas shown on the map can take into account the severity of the accidental scenario (medium or catastrophic release) and local meteorological conditions at that moment, including wind direction. Since the trucks move along the road an accident could occur anywhere along this corridor, therefore there is an infinite series of possible sources of hazards. From Chapter 3 method, presents the routing hazard zone as a series of a circle around the series point of release from the source. People exposed closer to the road are exposed to more possible hazard sources than who are nearly 500 m from the road width. Previously this series of circle round presentation, referred to as a vulnerability zone, is misleading since everyone within the circle would be exposed to the same impact of the accident. Therefore with the proposed method in Chapter 3, and at least it will reduce the unnecessary gap of the impact results to human injury or at least this methodology can distinguish accident effect according to age and level of total body burn surface area.

Hazard zones can easily be displayed graphically on local maps that show vulnerable populations such as nearby houses, schools, nursing homes, businesses centers, parks and recreational areas. A more realistic illustration of the potential hazard zones as a series of accident events along the road is given by the following Figures 4.81 to Figure 4.85. The buffer zone in Figure 4.81 illustrates the hazard footprint that is expected after the rupture of a 13, 000 kg LPG tanker occurs. People who are exposed to explosion overpressures within the range of 0 to 75 m may die due to the high impact of overpressure (from 205.99 kPa to 876 kPa). More details about VCE, pool fire, BLEVE fireball hazards have been discussed in the previous section.





Figure 4.82 Vulnerable zone at the 300 m buffer from route 5 at 4.4024 km length (Grey color = residential zone, orange color= commercial zone, magenta = industrial zone).



Figure 4.83 Vulnerable zone at the 300 m buffer from route 4 at 9.16 km length (Grey color = residential zone, orange color= commercial zone, cyan color = industrial zone).





Figure 4.84 Vulnerable zone at the 300 m buffer from route 3 at 9.7 km length (Grey color = residential zone, orange color= commercial zone, dark blue color = industrial zone).



Figure 4.85 Vulnerable zone at the 300 m buffer from route 2 at 7.548 km length (Grey color = residential zone, orange color= commercial zone, green color = industrial zone).



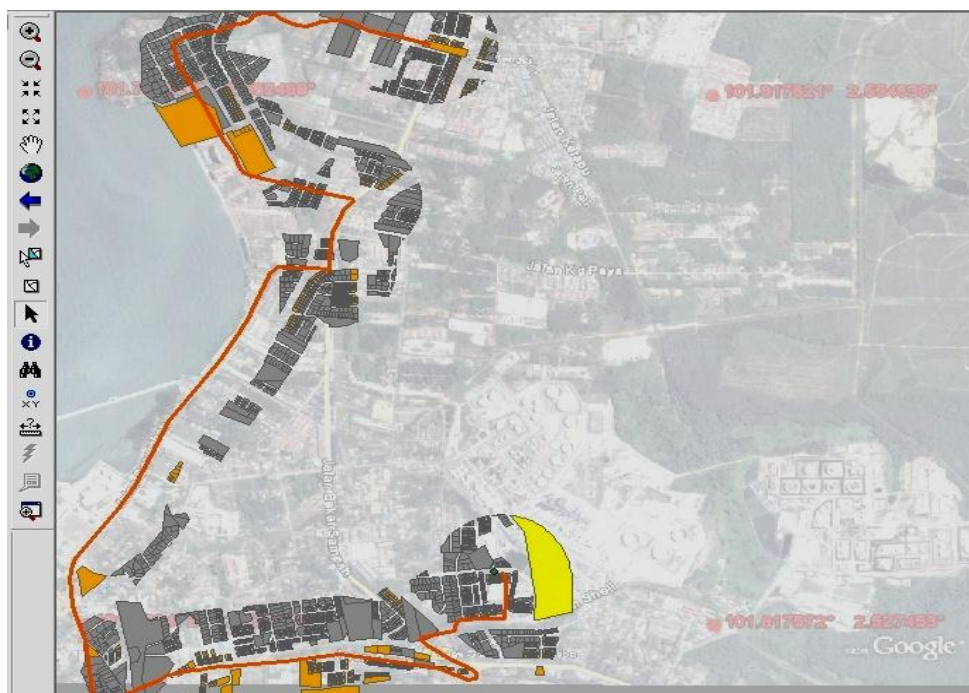


Figure 4.86 Vulnerable zone at the 300 m buffer from route 1 at 10 km length (Grey color = residential zone, orange color= commercial zone, yellow color = industrial zone).

Figure 4.81 show routes 5 is land use contributed with high residential zone area, followed by commercial and industrial area. Based on comparison to the land use area it is estimated that route 4 is the most occupied with the land use activities. The result is consistent with the results for population density distribution under the influence of wind as discussed in previous section. However, based on Figure 4.82 to Figure 4.85, the potential hazards from high to low based on area affected along the route is ranked, started with route 4 > route 3 > route 2 > route 1 > route 5 as in Table 4.21. Route 5 was concluded as the safest route since it has the smallest area. However, this conclusion is irrational since most of the time the HAZMAT truck will come across land use activities along 4.4024 km road. Table 4.22 shows that the potential hazards in  $\text{m}^2/\text{km}$  from high to low based on area affected per km the route is ranked, started with route 5 > route 4 > route 2 > route 1 > route 3. In this analysis, it is observed that the safety for HAZMAT transportation not only will depend on the route length but very much depend on the environment along the route.



Table 4.20 Comparison results of five routes based on area affected using SMACTRA and GIS Application.

| Route 5 (R1) | 100m | Area Affected (m <sup>2</sup> ) | 200m | Area Affected (m <sup>2</sup> ) | 300m | Area Affected (m <sup>2</sup> ) |
|--------------|------|---------------------------------|------|---------------------------------|------|---------------------------------|
| Residential  | 945  | 393543                          | 1605 | 740520                          | 2259 | 1064070                         |
| Commercial   | 173  | 62395                           | 365  | 109540                          | 464  | 134556                          |
| Industrial   | 0    | 0                               | 1    | 29209                           | 1    | 87536                           |
| TOTAL        |      | 455939                          |      | 879270                          | 2724 | 1286164                         |
| Route 4 (R2) | 100m |                                 | 200m |                                 | 300m |                                 |
| Residential  | 1053 | 378823                          | 1897 | 732619                          | 2773 | 1117960                         |
| Commercial   | 271  | 118629                          | 469  | 214764                          | 651  | 272565                          |
| Industrial   | 1    | 1816                            | 6    | 41449                           | 7    | 102742                          |
| TOTAL        |      | 499269                          |      | 988833                          | 3431 | 1493268                         |
| Route 3 (R3) | 100m |                                 | 200m |                                 | 300m |                                 |
| Residential  | 1072 | 442457                          | 1878 | 848451                          | 2742 | 1240130                         |
| Commercial   | 97   | 71255                           | 299  | 139984                          | 469  | 170764                          |
| Industrial   | 0    | 0                               | 1    | 30219                           | 1    | 90219                           |
| TOTAL        |      | 513712                          |      | 1018655                         | 3212 | 1501114                         |
| Route 2 (R4) | 100m |                                 | 200m |                                 | 300m |                                 |
| Residential  | 828  | 280524                          | 1627 | 578622                          | 2398 | 962776                          |
| Commercial   | 347  | 99672                           | 533  | 170492                          | 660  | 224550                          |
| Industrial   | 1    | 1816                            | 6    | 41601                           | 7    | 102443                          |
| TOTAL        |      | 382014                          |      | 790715                          | 3065 | 1289770                         |
| Route 1 (R5) | 100m |                                 | 200m |                                 | 300m |                                 |
| Residential  | 1386 | 598402                          | 2353 | 1096794                         | 3065 | 1440272                         |
| Commercial   | 242  | 115105                          | 406  | 202444                          | 602  | 254598                          |
| Industrial   | 0    | 0                               | 1    | 25882                           | 1    | 78490                           |
| TOTAL        |      | <u>713508</u>                   |      | <u>1325120</u>                  | 3668 | <u>1773362</u>                  |

Table 4.21 Comparison results of five routes based on area affected per km using SMACTRA and GIS Application

| Area affected (m <sup>2</sup> ) per km |        |        |        |        |        |
|--|--------|--------|--------|--------|--------|
| Route (R)                              | R1     | R2     | R3     | R4     | R5     |
|  | 155387 | 170875 | 153897 | 177336 | 292150 |



#### 4.5.1. The effect of population distribution to transportation risk hazards during day and night activities

This risk analysis is based on the population distribution using GIS application. From chapter 3, author has used Inverse Distance Weighted (IDW) interpolation technique based on weighted sample point distance from population density point over route. Interpolated IDW surface from elevation vector points (right). In the IDW interpolation method, the sample points are weighted during interpolation such that the influence of one point relative (known as point A, point B, point C and point X) to another declines with distance from the unknown point which can be created. Weighting is assigned to sample points through the use of a weighting coefficient that controls how the weighting influence will drop off as the distance from new point. The risk levels are rank by color. Red represented for highest risk route and dark blue for the lowest risk route. From Figure 4.86, it is predicted that most of residential area is considered as the most risky place to leave at night. Most probably, this is due to people culture, which was normally spent a lot of time at home, after struggling at the work place for the whole day. Therefore most of red color risk indicator is always come from residential area. Meanwhile, Figure 4.87 showing risk level distribution during day time, and it is noted that most of industrial and commercial area is predicted have more people, due to human activities in schools, offices, manufacturing factories, construction and project sites, and others.

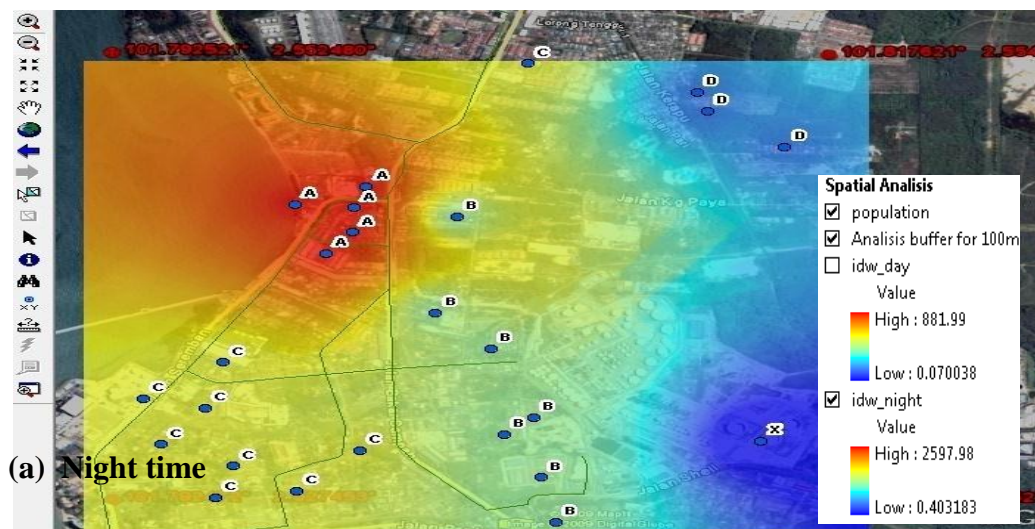


Figure 4.87 show the transportation risk hazards based on population density point at night.



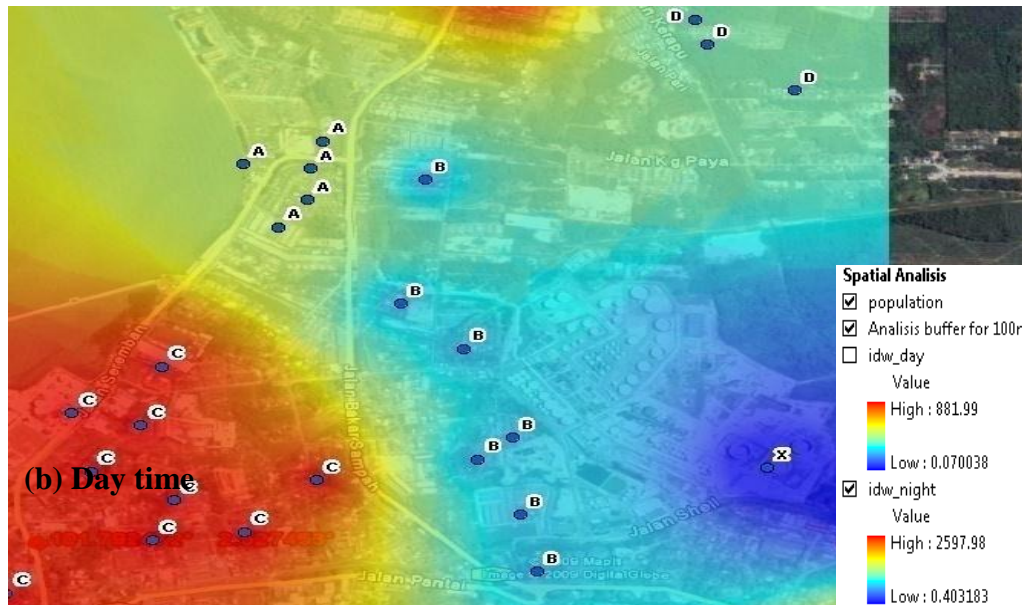


Figure 4.88 show the transportation risk hazards based on population density point at day time .

#### 4.5.2 The effect of LPG capacity during transportation accident using GIS application

In this section, effect of LPG tanker capacity will be study towards buffer hazard mapping using GIS application. Figure 4.89 shows buffer hazard from truck tanker fireball explosions when carrying 13,000 kg of LPG at coordinate,  $x$  (latitude: 422450.13 meters) and coordinate,  $y$  (longitude: 280858.05 meters). For 13,000 kg of LPG tanker explosion, may cause the buffer impact distance within 140.08 m diameter. If the quantity of transported LPG is added to become 50,000 kg, the impact diameter will also increase to 218.14 m as in Figure 4.90. By using GIS application, type of landuse activities, landuse area and other detail profile related to buffer hazard can be analyzed as shown in Table 4.23. In this analysis, the affected number of landuse activity is counted depending to the buffer size. Therefore, as the diameter for hazard area is increased, the affected number of landuse activities will be also increased. However, the effect of LPG tanker explosion towards the number of landuse activity is less obvious compare to the effect may be occur from explosion of nuclear accident source or earthquake point source.



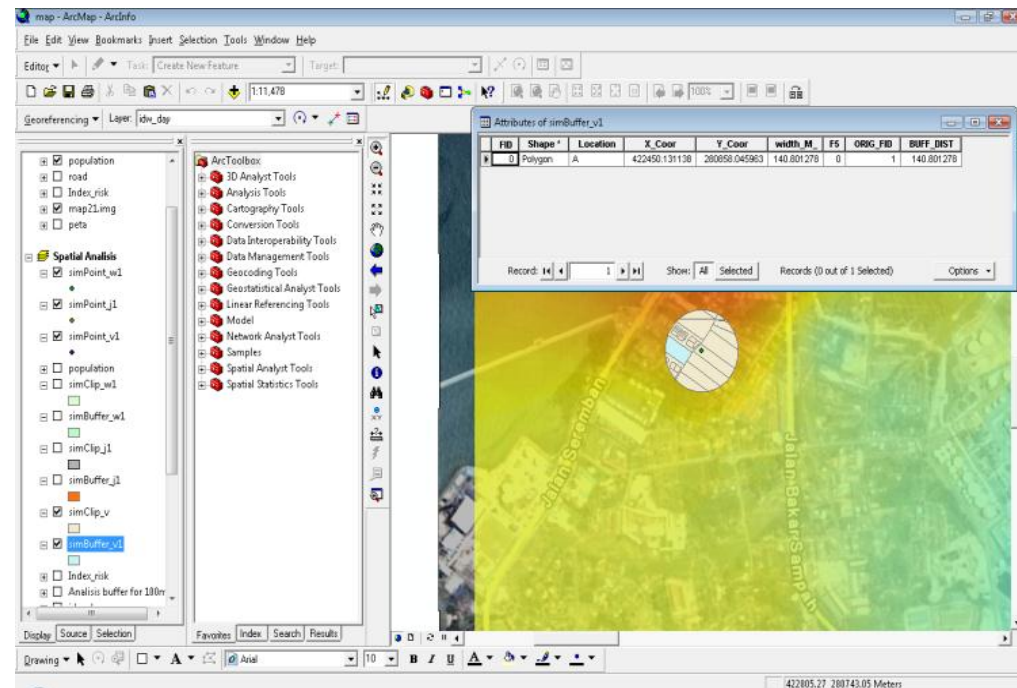


Figure 4.89 shows the buffer hazard impact from 13,000 kg of LPG tanker explosion.

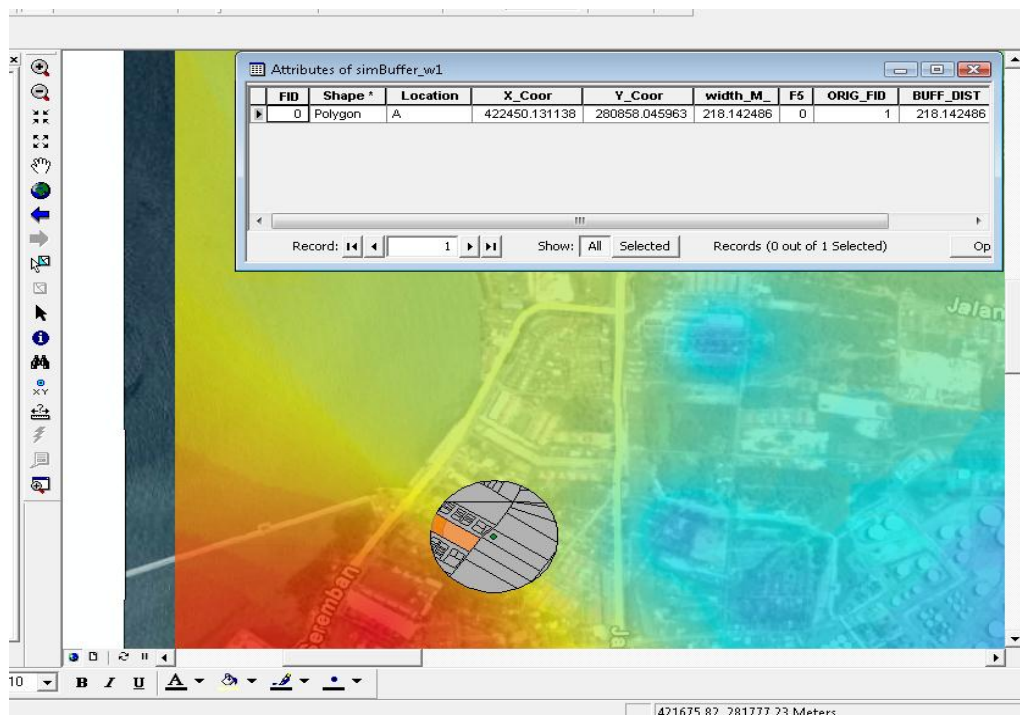


Figure 4.90 shows the buffer hazard impact from 50,000 kg of LPG tanker explosion.



Table 4.22 showing the characteristics of land use activities within the hazard point buffer for 13,000 kg of LPG tanker.

| SEMASA                       | AKTIVITI              | AKTIVITI2              | KOD_GTANAH | KELUASAN_H | OID | SEMASA_1                     | CNT_SEMASA | RANK | SHAPE_LENG | SHAPE_AREA   |
|------------------------------|-----------------------|------------------------|------------|------------|-----|------------------------------|------------|------|------------|--------------|
| Kediaman                     | Perumahan Terancang   | Perumahan Bukan Strata | TRM102     | 0.3        | 5   | Kediaman                     | 26642      | 1    | 456.191538 | 2353.996398  |
| Perdagangan dan Perkhidmatan | Perdagangan Terancang | Runcit                 | TPD102     | 0.74       | 8   | Perdagangan dan Perkhidmatan | 2638       | 2    | 473.224659 | 7383.240334  |
| Perdagangan dan Perkhidmatan | Perdagangan Terancang | Runcit                 | TPD102     | 0.73       | 8   | Perdagangan dan Perkhidmatan | 2638       | 2    | 449.117845 | 7251.41409   |
| Kediaman                     | Perumahan Terancang   | Perumahan Bukan Strata | TRM102     | 0.73       | 5   | Kediaman                     | 26642      | 1    | 453.149862 | 7304.87898   |
| Kediaman                     | Perumahan Terancang   | Perumahan Bukan Strata | TRM102     | 0.79       | 5   | Kediaman                     | 26642      | 1    | 465.56454  | 7862.760521  |
| Kediaman                     | Perumahan Terancang   | Perumahan Bukan Strata | TRM102     | 0.78       | 5   | Kediaman                     | 26642      | 1    | 464.783814 | 7802.549673  |
| Kediaman                     | Perumahan Terancang   | Perumahan Bukan Strata | TRM102     | 0.21       | 5   | Kediaman                     | 26642      | 1    | 212.935516 | 2071.243149  |
| Kediaman                     | Perumahan Terancang   | Perumahan Bukan Strata | TRM102     | 0.61       | 5   | Kediaman                     | 26642      | 1    | 454.886862 | 6059.99363   |
| Kediaman                     | Perumahan Terancang   | Perumahan Strata       | TRM101     | 0.42       | 5   | Kediaman                     | 26642      | 1    | 545.496882 | 4225.22285   |
| Kediaman                     | Perumahan Terancang   | Perumahan Bukan Strata | TRM102     | 0.05       | 5   | Kediaman                     | 26642      | 1    | 95.917945  | 469.919673   |
| Kediaman                     | Perumahan Terancang   | Perumahan Bukan Strata | TRM102     | 0.06       | 5   | Kediaman                     | 26642      | 1    | 104.596734 | 638.477028   |
| Kediaman                     | Perumahan Terancang   | Perumahan Bukan Strata | TRM102     | 0.87       | 5   | Kediaman                     | 26642      | 1    | 535.555792 | 8670.168329  |
| Kediaman                     | Perumahan Terancang   | Perumahan Bukan Strata | TRM102     | 1.11       | 5   | Kediaman                     | 26642      | 1    | 485.233355 | 11072.704907 |
| Kediaman                     | Perumahan Terancang   | Perumahan Bukan Strata | TRM102     | 1.26       | 5   | Kediaman                     | 26642      | 1    | 523.23499  | 12514.409836 |
| Kediaman                     | Perumahan Terancang   | Perumahan Bukan Strata | TRM102     | 0.04       | 5   | Kediaman                     | 26642      | 1    | 84.99243   | 420.182039   |
| Kediaman                     | Perumahan Terancang   | Perumahan Bukan Strata | TRM102     | 0.03       | 5   | Kediaman                     | 26642      | 1    | 86.034275  | 316.389424   |

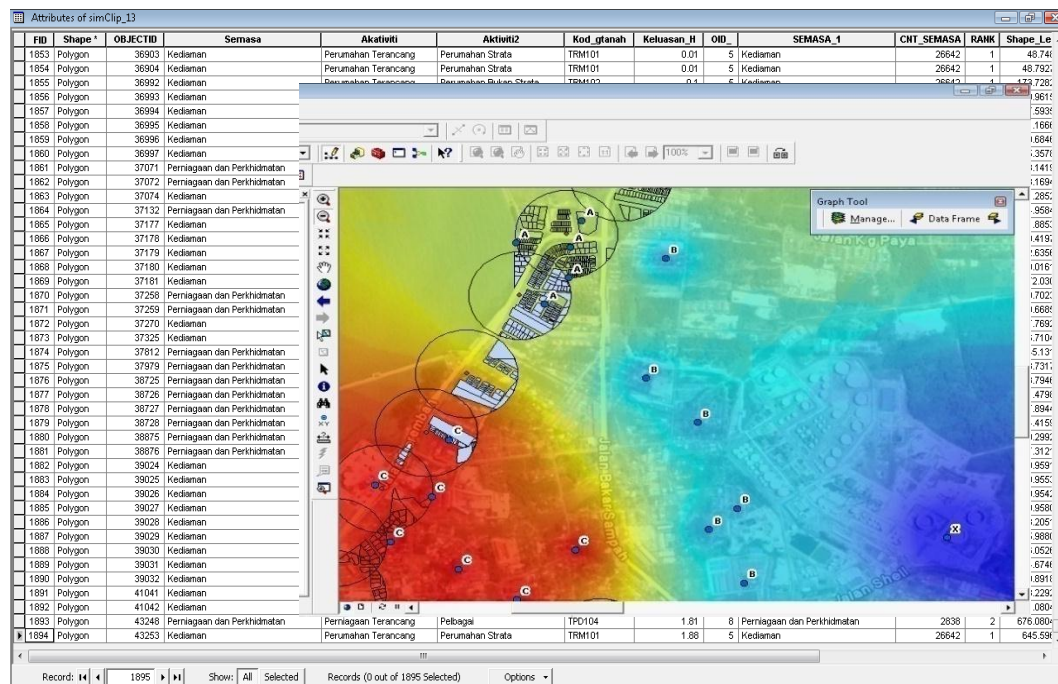


Figure 4.91 showing the detail characteristics of land use activities within the possible series sources of hazard point buffer along the transportation route.



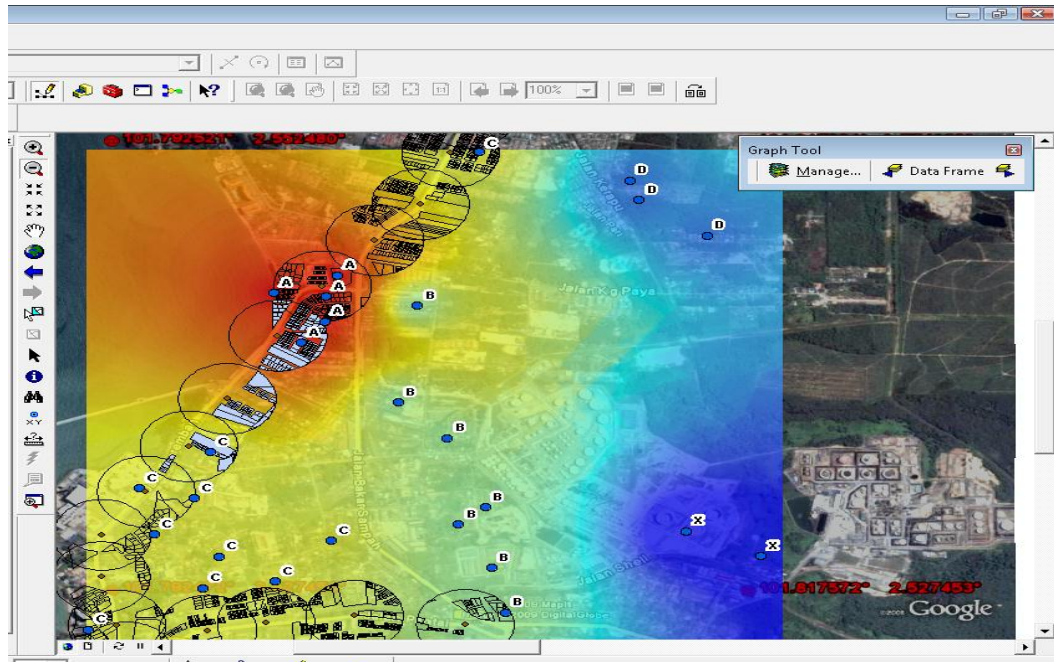


Figure 4.92 showing the detail characteristics of land use activities within the possible series sources of hazard point buffer along the transportation route.

In Figure 4.91 it is shown that the number of activities at landuse is 1895. The actual number probably more if recent data can be gathered. Detail of landuse activities within the possible series sources of hazard point buffer along the transportation route 2 as in Figure 4.92. The number of point buffer along the route is 16 as shown in Figure 4.93.

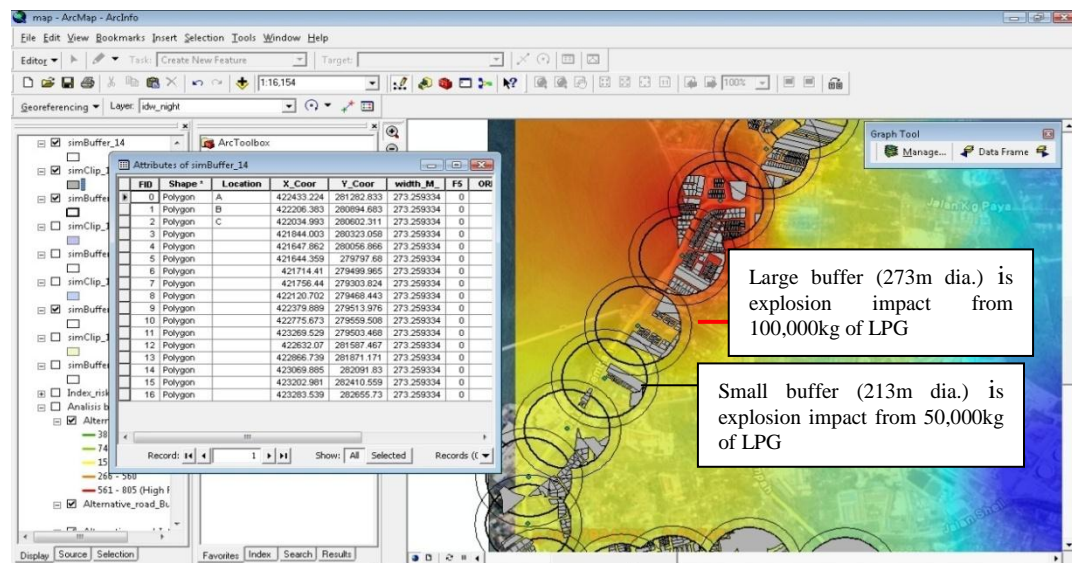


Figure 4.93 showing the detail characteristics of land use activities within the possible series sources of hazard point buffer (two rings) along the transportation route.



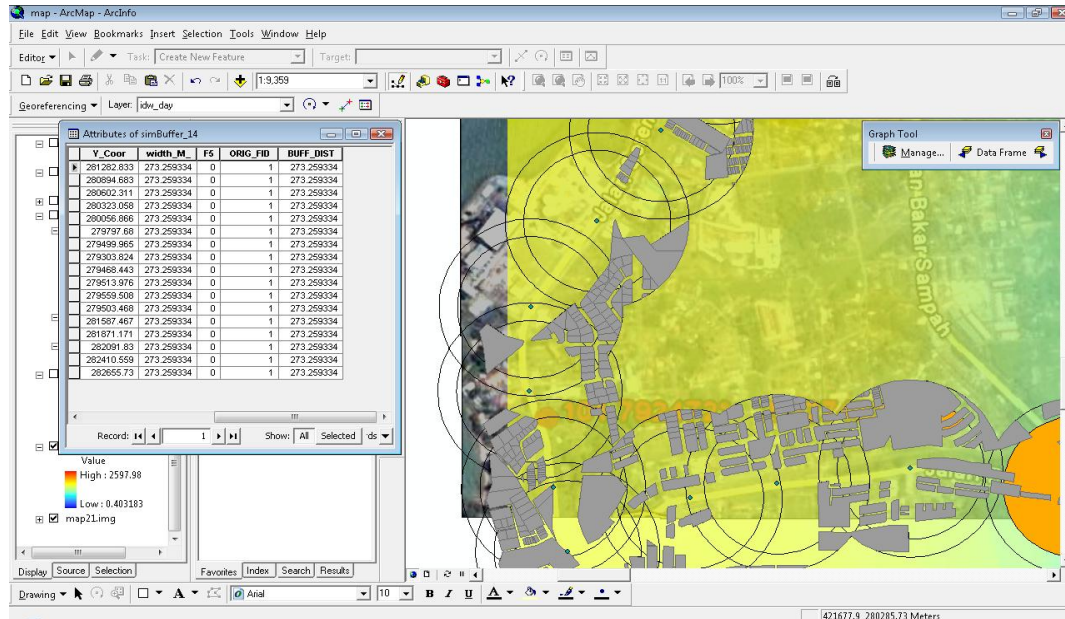


Figure 4.94 showing the effect of land use activities within the possible series sources of hazard point buffer along the transportation route at 100,000 kg of LPG.

Figure 4.94 shows an increasing point buffer diameter when LPG quantity increases.

## 4.6 Summary

This section summarizes, evaluates and discusses the performance results of SMACTRA software. SMACTRA software uses mathematical models to assist in evaluating consequences from an explosion, fire, toxic release and to provide risk estimation result for individual and society during HazMat transportation. The validation on the SMACTRA application is performed by comparing it's results with other risk softwares such as Effect 8.01, CANARY Quest, published results from several transportation accident case study such as PEMEX Mexico city, Houston Texas, published risk software results such as BIS, FRED, MAXCRED from journal, articles and books. It can be concluded that the results produced by SMACTRA software is comparable with the established risk analysis software in the market such as Effect 8.01 and CANARY.

Even though there is a large variation results (as discussed in section 4.3) for vapor cloud explosion case involving 13,000 kg of LPG tanker and noted that the peak overpressure value SMACTRA is much greater than Effect 8.01 and CANARY at 50 m from source accident, the scenario is observed to be more approximate. This is due



to at 50m usually the receptor has a fatality potential from severe internal organ concussion. At the distance more than 100 m, the value of peak over pressure (kPa) for both softwares is noted to be appropriate to quantity of transported LPG. The main advantage of SACTRA result it's provide a package software which capable to analyze both type of risk analysis such as static and moving risk sources in Malaysia. Other advantages of SACTRA are the application of TBS parameter, age factor, duration pain to identify the level of 2<sup>nd</sup> degree injury burn. This matter is approved by one of the TNO safety expert in his email to answer the researcher question during this study regarding the weakness in Effect 8.01, as shown in appendix 4. The impact analysis will consider the above parameters in order to estimate the level of 2<sup>nd</sup> degree burn injury towards receptor which is exposed to the fire and road tanker explosion. This will make the risk value results for any transportation accident to be more accurate and closely approximated to the actual scenario. For example, if age distribution and the receptor location along route five are known, therefore the survival probability for 2<sup>nd</sup> degree burn victim can be estimated, according to TBS percentage experience by the victim. As mentioned in this chapter, the larger the quantity, the more flammable and the more reactive the transported HazMat, the unsafe zone along its route will be increased and become more risky. The results are closer to the actual scenario compared to CCPS by assuming all victim 2<sup>nd</sup> degree burn are acceptably well, even though the victim suffer the effect of more than 30% TBS burn injury, however this is contradict with the statistic analysis for the burn injury survival at 30%TBS, which was proposed by burn injury analysis expertise such Bull et al. [163-165, 183], Curreri et al. [166] and Martin et al. [184]. They studies on the potential treatment for burn injury and antibiotic to cure patient with severe burn injury patient. Furthermore, SACTRA is capable to calculate the individual and societal results and the safest HazMat route. In general, the societal risk usually will consider fatality probability as produced by CCPS and BUWAL [21, 73]. However, total individual risk calculated by SACTRA has been shown to be higher compared to CCPS and BUWAL, since SACTRA will consider individual who might suffer injury when an accident occurs. The probability for an individual to be safe from an accident is also demonstrated in this analysis. SACTRA lethality results on individual risk are shown to be comparable with individual risk fatality by CCPS. Meanwhile BUWAL individual risk and societal risk always produce lower



results than SMACTRA and CCPS. This is contributed by coefficient or constant in BUWAL method which referred to the lower Swiss transportation traffic network and this is discussed in chapter 2. The usage of model builder ArcGIS in loose coupling technique with VB and ArcMap facilitate the calculation and therefore VB able to produce the outcome buffer hazards zone in ArcMap. SMACTRA also capable analysis of accident impact and plot the results on Map API online. The advantage of this map is that the point of accident can be moved to any location on it, therefore a new result will be displayed for the new potential damage of accident. SMACTRA also able to analyze risk and export the relevant data to GIS (Geographical Information Systems) for example ArcView ArcInfo, on line spatial Map API for transportation risk analysis simulation.



## CHAPTER 5

### CONCLUSION & FUTURE WORK

SMACTRA is a Smart Advisory System (SAS) which is designed and developed to perform risk analysis for road hazardous material transportation. Below are the conclusions which can be drawn from this study:

- Since the development of SAS for Hazmat TRA is dependent on the type of TRA model which is being used, therefore a thorough analysis must be undertaken on the existing TRA model before it can be applied and programmed in SAS. In this study, after reviewing various existing TRA models, a modified TRA model has been successfully developed. This modified TRA is integrated with the all possible requirement as discussed in Chapter 2 and 3 in this thesis, before a proposed SAS can be designed and developed for transportation of hazardous materials applicable for Malaysia scenario.
- In this modified TRA model, the individual and societal risk calculation for Malaysia accident data is established by using Eq. (3-2) to Eq. (3-5) (which were developed by Radin et al. [169]) as shown in Chapter 3 to forecast the number of Malaysia road traffic deaths. A detailed discussion on the rationality to use this model compared to the other popular model can be seen in section 3.2.1. Based on the discussion in section 3.2.1, the main reason for the use of Radin model [169] compared to other model is because the assumptions parameter and criteria used in Radin model is closest in explaining the actual traffic risk exposures in Malaysia.



- Some modifications for the road tanker trip parameters are discussed in Chapter 3, in which the frequency of trip is predicted based on the company product sales performance over the years. If the sales increase, the number of trips to sent the products will also increase. Therefore in this new model, the risk projection for the hazardous materials transportation for the next 2, 5 and 10 years can be analyzed. For example, to analyze the risk for LPG transportation between year 2013 to 2023 (10 years in the future), the statistical data for the LPG company sales performance from the previous years (1990 to 2010) must be reviewed (for example linear regression ( $Y$ : sales performance/ by year = ( $M$ :rate over year). ( $X$ : road tanker trips over the years ) + ( $C$ : constants)). Therefore the data can be utilized as a basis; to study the effects of trip toward the future trend of company transportation of hazardous materials risk analysis.
- Previously in order to analyze the impact from an accident, most TRA model such as CCPS, and Rhyne will only consider the number of death from the affected zone with the fatality probability between 0 till 1.0 and the standard transportation quantitative risk assessment focuses mainly on calculating the number of fatal victims as well as calculating the areas to be evacuated. The number of injured people is seldom evaluated, as this would involve significant additional effort. Therefore, in most cases little or no information on this is available. As discussed in chapter 3, the severity of injury for the victims is not uniform across the impact area. The severity of injury varies depending on several factors such as the distance of victims from the source of explosion; therefore a person closer to it will receive a higher chance of death or bad injury. Whilst other victim who are farther from the source of accident, the severity of injury will depend on few factors such as the percentage of body surface affected, the depth of burn and the age of the victim. Therefore, these factors which contribute to the variation in severity of injury are considered in the proposed TRA model.



- Different TRA model will have different approach and assumption and some of the reasons for these differences, are due to the variation in geographical factor, economic growth, infrastructure and road networking development and industrial growth of one country. In addition, risk calculation methods for road transport is more complex compared to stationary installations, therefore several differences exist between the basic principles in risk calculations for transport and for stationary installations. For instance, the frequency of catastrophic outcomes from road tanker transport is higher compared to stationary tanks. The impact of road tanker accident to the surrounding is not constant or unpredictable and varies depend on road tanker coordinate location on the geography. As discussed in Chapter 2, to develop an effective SAS for transportation of hazardous materials risk analysis, TRA model, consequences model and GIS are integrated into the system since various parameters such as meteorological condition, release scenario, and specific data such as accident rate and population distribution are need to be considered in the calculation. Therefore, to minimise error in the SAS TRA result calculation, all equations and parameters in the modified TRA model such as consequences models, effect models and risk calculations which are developed by using VB 6, have successfully integrated with ArcGIS9.3.1 geoprocessing data tool known as ArcGIS Model Builder. This integration technique is also known as loose coupling approach.
- The detail framework for developing and designing HazMat transportation risk analysis software is described in Chapter 3. The software is called Smart Advisory System for Chemical Transportation Risk Analysis (SMACTRA). The SMACTRA software is designed to be compatible with windows operating system (95, 98, XP, Microsoft Vista and Microsoft 2007). The software is also designed to be able to work online by using php programming language to produce accident impact analysis simulation results in the server.
- In order to validate results from SAS SMACTRA, by using combination of modified TRA model, consequences model and GIS; analysis of a simulated accident can be created such as when an accident involve LPG road tanker



with the capacity 13,000kg and 50,000kg. This is shown in Figure 4.89 and Figure 4.90, in which if the road tanker accident creates a BLEVE fireball explosion, it is calculated that the buffer radius for the hazard impact will increase from 140.08m diameter to 218.14 m diameter. This result proven that the modified TRA model and consequences model which are programmed with SAS TRA able to perform the risk calculation analysis in VB program and again has successfully display the result in ArcGIS as a hazard mapping results.

- To calculate transportation risk along the route, SACTRA is used to analyze the detail of land use activities at various hazard point buffer, as shown in Figure 4.92 till Figure 4.94. It is shown that, the results from the road tanker explosion cases will provide a detail condition regarding the population distribution from the affected zone and along the affected route. However, when some area in the hazard radius buffer are free from any landuse activities, or probably are not included and plotted in the map, this will make the population area affected within the total actual area for landuse activities for every radius buffer along route 2 (382014m<sup>2</sup>), as shown in Table 4.21 is smaller compared to the hazard radius of explosion cases created at 16 point buffer along route 2 (695345m<sup>2</sup>). In the calculation for societal risk along the route, this input is more accurate when fatality over consequences area affected is predicted based on the existence of population area affected not the hazard zone area.
- The validation of the SACTRA application is performed by comparing it's results with other risk softwares such as Effect 8.01, CANARY Quest, published results from several transportation accident case study such as PEMEX Mexico city, Houston Texas, published risk software results such as BIS, FRED, MAXCRED from journal, articles and books. It can be concluded that the results produced by SACTRA software is comparable with the established risk analysis software in the market such as Effect 8.01 and CANARY. Even though there is a large variation results (as discussed in section 4.3) for vapor cloud explosion case involving 13,000 kg of LPG tanker and noted that the peak overpressure value SACTRA is much greater than



Effect 8.01 and CANARY at 50 m from source accident, the scenario is observed to be more approximate. This is due to at 50m usually the receptor has a fatality potential from severe internal organ concussion. At the distance more than 100 m, the value of peak over pressure (kPa) for both softwares is noted to be appropriate to quantity of transported LPG.

- Meanwhile, for the case of ammonia toxic release, the same input and condition as Houston Texas incident are used in the calculation. By using the SMACTRA map online, it shows that at concentration 10,000 ppm of ammonia is dispersed up to 709 meters, this value is comparable to the NTSB incident report [60] for houston texas ammonia incident in 1976 690m. The detail outcome of analysis is shown in Table 4.19 as in Chapter 4.
- To validate the effect of thermal radiation on the pathological and physiological effect towards the survival of burn injury by using SMACTRA, Figure 4.35 shows that the older age group receptor who sustain 2<sup>nd</sup> degree burn (69 years old) with TBS 30%, the survival potential from BLEVE accident scenario is lesser compared to the younger age groups for example 55, 45, 35, 15 years old as shown in Figure 4.36 to Figure 4.39. This is proven by the analysis in Figure 4.39, for younger age group such as 15 years old the blue curve is moving away from the red curve which mean better chance of survival.
- Meanwhile, for age 55 (as in Figure 3.36) and 45 (Figure 3.37), the blue and red curve nearly overlap to each other which mean the survival potential is 50:50. Younger patients with 2<sup>nd</sup> degree burn at TBS 50% have a higher survival percentage compared to older patient such as 69 years old, as shown in Figure 4.42 and Figure 4.35. Figure 4.35 to 4.39 analyzed the effect of age (69, 55, 45, 35, 15 years old) towards 2<sup>nd</sup> degree burn injury at a constant TBS, 30% and it can be concluded that younger age victims with 2<sup>nd</sup> degree of burn injury have higher survival potential from 13,000 kg of LPG truck tanker explosion. As conclusions, the above results show that the older the victim, the lower the capability to recover from illness and the effect of TBS. The survival level for burn injury victim will be better if the efficacy of medical



treatment can be improved to treat burn injury patient who sustained TBS more than 30%.

- Since the new TRA model will include the injury effect such as thermal radiation effect, therefore the injury risk for 1st degree burn, second degree burn, lethality and burn wound can be calculated for societal risk and individual risk as shown in Figure 4.79 and Figure 4.80.
- Other main objective for this study is to design and develop a SAS TRA, which can become a useful risk assessment tool to identify the safest route for hazardous material transportation. In this study, the truck accident scene was analyzed along five routes which involves a daily movement of 34.5 m<sup>3</sup> of LPG through approximately 15 to 20 km length route from Middle West Coast Refining (MWCR) Company in Port Dickson to Petrol and Gas service station in Port Dickson as in the map of Figure 4.81 till to Figure 4.85. Based on the discussion in section 4.43, 4.4.4 and 4.5 (as in Table 4.21), the affected area does not depend on the length of the route. This is due to the division of the area which can be divided into three parts which are the residential, commercial and industrial zone. Thus, it does not mean that the longest route can affect larger area and vice versa. This explains why even though route 5 is the shortest in length but still is the second highest risk route; because along this route, there are a large residential area, a larger residential area means higher possibility for people involve in the accident consequences

In reference to the above conclusions, SMACTRA is a comprehensive quantitative tool for assessing process plant and HazMat transportation risk. It is capable to analyse complex consequences from accident scenarios based on local population and weather conditions and also capable to quantify the risks associated with the release of hazardous chemicals. The software also capable to analyze risk by calculating means of the most dominant contributor, construct all types of societal and individual risk curves, display risk contours, calculate transport risk per kilometer of route and export relevant data to GIS (Geographical Information Systems) like ArcView ArcInfo, on line spatial Map API for transportation risk analysis simulation.



The application is made user friendly by using software such as; MSDS for each material to help users understand and possess some knowledge about the materials, conversion units to convert units without using any external reference, internal help to guide users on how to use the software. Therefore SACTRA software is a useful tool and user friendly for environmental and safety professionals to identify hazards associated with accidental releases, fires, explosions and then describe the potential impacts of those risks.

The results, equations and programmes from the application is extensively validated with other commercial softwares such as EFFECT 8.01 (developed by TNO, 2008), BIS (developed by ThermDyne Technologies Ltd, 2003), CANARY (developed by QUEST 2009) and few other established data. The results for the SACTRA software is found to be consistent without any significant deviation from other trials. Thus, the developed smart TRA tool is good computational software for the consequence modeling of transportation of hazardous material. The SACTRA benefits to users:

- Provide accurate risk estimation with a substantial cut of time required to perform the analysis, simplify the data input step, possibility of displaying the results on the area map together with other information and useful in the case of an emergency (location of fire brigades stations, hospitals, etc.).
- Can be use for the future policy making processes and regulations related to transportation of hazardous material.
- Able to identify vulnerable locations as well as to integrate consequences results and develop the safest route with the minimum risk.
- Provide safety, health and environmental enforcer, environmental auditor CHRA assessor more information about HazMat transportation in a holistic approach.

Finally, this product is ideal for real-world applications, especially to assist in the decision making process for land-use planning to locate suitable hazardous installations, transportation of hazardous material and emergency response plan (ERP). It's also can be used as a teaching tool in process safety and environmental risk assessment studies.



### **Recommendation for Future Work**

Although this research has achieved its objective, it can be improved in order to extend the objective and include an analytical representation of waste management. For future research, this application still has to undergo a deem research to be more competent and consist more functions. The following recommendations are listed here:

- Extend the lethality probit analysis impact of human burn injury towards patient medical treatment and in antibiotic without limitation with age and total burn surface body area factors only. Perhaps other parameters which may contribute to the lethality probit analysis can be considered in the future. Even though it is reported in medical literature that patient with 30% TBS would survived, but there is recent medical treatment technology which capable to save people life which affected with more than 30% TBS of second degree burn injury.
- Extend the lethality probit analysis impact of human blast overpressure towards patient's treatment and not limited to prediction of getting lung haemorrhage, eardrum rupture and etc
- Integrate local government agency database to the similar type of software development. Therefore, the data can be easily updated and accessible by the hazardous material transportation and public transportation authority.
- Extend the transportation risk analysis to transportation hazardous material using aircraft, ship, train and pipelines.
- Develop online simulation methods to estimate appropriate composition region by using verified 3D-computational fluid dynamics (CFD) or any 3D tools in the market.
- Develop transportation risk analysis software for Emergency Response Plan using all related agency KPI (Key performance Index) benchmark with optimizes emergency response time.



## REFERENCES

- [1] RSPA, "The Role of Hazardous Material Placards in Transportation Safety and Security," Office of Hazardous Materials Safety and Volpe National Transportation Systems Center, Washington, D.C., January, 2003.
- [2] Transportation Research Board, "Special Report 283: Cooperative Research for Hazardous Materials Transportation: Defining the Need, Converging on Solutions," *Committee for a Study of the Feasibility of a Hazardous Materials Transportation Cooperative Research Program*, National Research Council, Washington, D.C., 2005.
- [3] Transportation Research Board Information Database, Office of Hazardous Materials Safety (OHMS), CFR 49.<http://www.myregs.com/dotrspa/2005>. 2009.
- [4] Office of Hazardous Material Safety (OHMS) (2005). Hazardous materials transportation guides. <http://ntl.bts.gov/DOCS/>
- [5] R. A. Zulkifli, H. E. Mohanad, Abdul Rashid Shariff, K.H. K.Hamid, H. Husin, "A Retrospective Study Of Smart Advisory System In The Transportation Of Hazardous Material (Hazmat)," *3th International Conferences on Chemical and Bioprocess Engineering in conjunction with 23nd Symposium of Malaysian Chemical Engineering (SOMChE)*, pp. 971-978, 2009.
- [6] R. A. Zulkifli, H. E. Mohanad, and Abdul Rashid Shariff, "A Significant Trend of Accident Scenario Consequences in the Transportation of Hazardous Materials (Hazmat): Analysis Study Based on the Available Accident Database," *TECHPOS*, Sunway, pp 1-23, 2009.
- [7] R. A. Zulkifli, H. E. Mohanad, Abdul Rashid Shariff, "Development and design of smart advisory system in the accident of transportation of hazardous material via quantitative risk approach," *12th conferences and exhibition for occupational safety and health, Sunway Pyramid convention center*, c: 1.7 A., pp 1-26, 2009
- [8] Health and Safety Executive Report, "ACDS Sub- Committee on the Major Hazard Aspects of the Transportation of Dangerous Substances," HSE Books, Sudbury, 1991.



- [9] Health and Safety Executive Report, "Advisory Committee on Major Hazards 'Second Report,'" HMSO publication, 1979.
- [10] Health and Safety Executive Report, Advisory Committee on Major Hazards 'Third Report, The Control of Major hazards', HMSO publication, 1984.
- [11] CCPS (Center for Chemical Process Safety), "Guidelines for Chemical Process Quantitative Risk Analysis," 2<sup>nd</sup> Edition. New York: American Institute of Chemical Engineers, 2000.
- [12] D. Egidi, D. Foraboschi, G. Spadoni, & A. Amendola, "The ARIPAR project: analysis of the major accident risks connected with industrial and transportation activities in the Ravenna area", *Reliability Engineering and System Safety*, 49, 75-79, 1995.
- [13] The Sun, "Traffic Cops Have Their Hands Full," [www.niosh.gov.my/Industrial accidents/library/index](http://www.niosh.gov.my/Industrial_accidents/library/index), 2003.
- [14] The Star, "PETRONAS to Find out Actual Cause of Blasts," [www.niosh.gov.my/Industrial accidents/library/index](http://www.niosh.gov.my/Industrial_accidents/library/index), 2006.
- [15] The Star, "Petroleum Laden Tanker Overturn Explodes," [www.niosh.gov.my/Industrial accidents/library/index](http://www.niosh.gov.my/Industrial_accidents/library/index), 1999.
- [16] The Star, "Potential Time Bombs on the Road," [www.niosh.gov.my/Industrial accidents/library/index](http://www.niosh.gov.my/Industrial_accidents/library/index), 2002.
- [17] Petronas Dagangan Berhad, <http://www.mymesra.com.my>, (access May 2008)
- [18] PETRONAS, "PETRONAS Adopts Aspen Tech's Solution for Fuels Marketing to Optimize Distribution of Fuels and Specialty Products," [http://www.aspentech.com/publication\\_files/pr9-15-03.htm](http://www.aspentech.com/publication_files/pr9-15-03.htm) (access January 2008)
- [19] CCPS (Center for Chemical Process Safety), "Guidelines for Developing Quantitative Safety Risk Criteria," 1<sup>st</sup> Edition. New York: American Institute of Chemical Engineers, 2009.
- [20] CCPS (Center for Chemical Process Safety), "Guidelines for Chemical Process Quantitative Risk Analysis," 1<sup>st</sup> Edition. New York: American Institute of Chemical Engineers, 1989.
- [21] CCPS (Center for Chemical Process Safety), "Guidelines for Chemical Transportation Risk Analysis," New York, American Institute of Chemical Engineers, 1995.



- [22] CCPS (Center for Chemical Process Safety), "Guidelines for Chemical Transportation Safety, Security and Risk Management," New York, American Institute of Chemical Engineers, 2009.
- [23] R. M. Bhanu Prakash and A. Bulgak, "A Simulation Study for Hazardous Material Transportation Risk Assessment," Master Thesis, 2000.
- [24] HSE (Health and Safety Executive), "The Safety Report Assessment Manual," 2007.
- [25] W. Rhyne, "Hazardous materials transportation risk analysis: Quantitative approaches for truck and train," New York, Van Nostrand Reinhold, 1994.
- [26] P. Carson and C. Mumford, "Transportation of chemicals," *Loss Prevention Bull.* vol. 170, pp. 11-17, 2003.
- [27] R. Lisi, M.F. Milazzo, G. Maschio, P. Leonelli, S. Bonvicini, G. Spadoni, "Risk analysis of the transportation of hazardous material: an application of theTRAT2 software to Messina," in *Loss Prevention and Safety Promotion in the Process Industries, 10<sup>th</sup> International Symposium, European Federation of Chemical Engineering*, Stockholm, Sweden, Elsevier Publications, 2001.
- [28] R. Bubbico, Cave, Guerieri, and B. Mazzarotta, "Best Routing Criteria for hazardous substances transportation," in *10th International Symposium: Loss Prevention and Safety Promotion in the Process Industries*, Stockholm, Sweden, EFCE and Elsevier Publications, pp.1029-1044, 19-21 June 2001.
- [29] G. Purdy, "Risk analysis of the transportation of dangerous goods by road and rail," in *J. Hazardous Material* , Vol. 33, pp. 229-259, 1993.
- [30] C R. Che Hassan, P. Balasubraniam, A.Z. Abdul Rahman, N. Z. Mahmood, F.C. Hung, N.M.Nik Sulaiman, "Inclusion of Human Errors Assessment in Failure Frequency Analysis- A Case Study for the Transportation of Ammonia by Rail in Malaysia," in *AIChE, Process Safety Progress*, Wiley Inter Sciences, vol. 28, No. 1, , pp 60-67, March 2009.
- [31] Department of Prime Minister of Malaysia, "Seventh Malaysia Plan 1996-2000," National Malaysian Printing Press, Kuala Lumpur , 1996.
- [32] M. N. Monier, A.V. Gheorghe, "Quantitative Risk Assessment of Hazardous Materials Transportation System. Rail, Road, Pipelines and Ship," in *Kluwer Academic Publications*, ISBN; 978-0-7923-3923-6, pp. 372, 1996.



- [33] A.V. Gheorghe, M. N. Monier, "Integrated Regional Risk Assessment: Continuous and Non- Point Source Emissions," Springer Kluwer Academic Publication, pp. 235, 1995.
- [34] Q. Yuanhua, "Decision Support System for Quantitative Risk Assessment for transportation hazardous material base on database," *PhD Thesis*, Texas A. and M., 2006.
- [35] Det Norske Veritas, "Risk Management for Dangerous Goods Transportation, DNV," Antwerp, 1995.
- [36] R.A. Zulkifli, A. B. Azil, A. J. Mohd, H. E. Mohanad, R. A. Norazah and S. M. Ayub, "Hazardous waste management: Current status and future strategies in Malaysia," in *International Journal of Environment and Waste Management (IJEWM)*, Indersciences, vol. 2, pp 139-158, 2010.
- [37] J. Arnaldos, J. Casal, H. Montiel, M. Sanchez-Carricondo, J.A. Vilchez, "Design of a computer tool for the evaluation of the consequences of accidental natural gas releases in distribution pipes," in *Journal of Loss prevention in the Process Industries*, vol. 11 pp135-148, 1998.
- [38] Petroleum (Safety Measures) Act 1984, Percetakan Nasional Malaysia Bhd., 2006.
- [39] Akgün, V., Parekh, A., Batta, R., Rump, C.M., "Routing of a hazmat truck in the presence of weather systems," in *Computers & Operations Research*, vol. 34 (5), pp. 1351–1373, 2007.
- [40] E. Erkut and A. Ingolfsson, "Catastrophe avoidance models for hazardous materials route planning," in *Transportation Science* 34 (2), 165–179, 2000.
- [41] Huang, B. and Cheu, R.L., "GIS and genetic algorithms for HAZMAT route planning with security considerations," in *International Journal of Geographical Information Science*, vol. 18 (8), pp. 769–787, 2004.
- [42] Fragola J.R, . R. J Borkowski, J.P.Drago, " The inplant reliability data system," Euredata vol. 4, 1983.
- [43] Erkut, E., Ingolfsson, A. (2005). Transport risk models for hazardous materials: Revisited. *Operations Research Letters* 33 (1), 81–89
- [44] Leonelli, P., Bonvicini, S., Spadoni, G., "Hazardous materials transportation: A risk-analysis- Based routing methodology," in *Journal of Hazardous Materials*, vol. 71, pp. 283–300, 2000.



- [45] K.G. Zografos, Vasilakis, G.M., I.M. Giannouli, "A methodological framework for developing a DSS for hazardous material emergency response operations," in *Journal of Hazardous Materials*, vol. 71, pp. 503–521, 2000.
- [46] B. Ashtakala and L.A. Eno, "Minimum risk route model for hazardous materials," in *Journal of Transportation Engineering – American Society of Civil Engineers (ASCE)*, vol. 122 (5), pp. 350–357, 1996.
- [47] E. Erkut, and T. Glickman, "Minimax population exposure in routing highway shipments of hazardous materials," in *Transportation Research Record*, vol. 1602, pp. 93–100, 1997.
- [48] F. Saccomanno, and Chan, A., "Economic evaluation of routing strategies for hazardous road shipments," in *Transportation Research Record*, vol. 1020, pp. 12–18, 1985.
- [49] M. Verma and V. Verter, "Rail transportation of hazardous materials: Population exposure to airborne toxins," in *Computers & Operations Research*, vol. 34 (5), pp. 1287–1303, 2007
- [50] T.S. Glickman, "Rerouting railroad shipments of hazardous materials to avoid populated areas," in *Accident Analysis and Prevention*, vol. 15 (5), pp. 329–335, 1983.
- [51] Iakovou, E., Douligieris, C., Li, H., Ip, C., Yudhbir, L., "A maritime global route planning model for hazardous materials transportation," in *Transportation Science*, vol. 33 (1), pp.34–48, 1999.
- [52] E. Weigkricht and Fedra, K., "Decision-support systems for dangerous goods transportation," in *INFOR*, vol. 33 (2), pp. 84–99, 1995.
- [53] G.F. List, Mirchandani, P.B., Turnquist, M.A., and Zografos, K.G., "Modeling and analysis for hazardous materials transportation-risk analysis, routing scheduling and facility location," in *Transportation Science*, vol. 25 (2), pp. 100–114, 1991.
- [54] Advisory Committee on Dangerous Substances, "Major hazard aspects of the transportation dangerous substances," London: Health and Safety Commission, 1991.
- [55] E. Erkut, S.A. Tjandra and V. Verter, "Chapter 9 Hazardous Materials Transportation," in *Handbooks in Operations Research and Management Science*, vol. 14, pp. 539-621, 2007



- [56] United Nations Environment Programme (UNEP), Division of Technology, Industry, and Economics Awareness and Preparedness for Emergencies at Local Level (APELL), [www.uneptie.org / pc/ apell / disasters /database/ disasters database. asp](http://www.uneptie.org/pc/apell/disasters/database/disasters_database.asp)
- [57] Failure and Accidents Technical information System (FACTS) online industrial accident database, TNO, Netherlands. <http://www.factconline.nl/>
- [58] Major Accident hazards Bureau, European Commission for the implementation of the Directive on the Major Accident Hazards of Certain Industrial Activities <http://mahbsrv.jrc.it/mars/Default>
- [59] Health and Safety Executive of United Kingdom (HSE) , Major Hazards of Incident Database (MHIDAS), <http://www.hse.gov.uk/infoserv/mhidas.htm>
- [60] National Safety and Transportation Board Database, [www. nstb. Gov / publication](http://www.nstb.gov/publication)
- [61] [http.www.nstb/hazmatdocs](http://www.nstb/hazmatdocs)
- [62] US Department of Transportation (US DOT) (2005). Incidents, deaths, and injuries by mode and incident year. [http://hazmat. dot.gov/pubs/ inc/data /tenyr.pdf](http://hazmat.dot.gov/pubs/inc/data/tenyr.pdf)
- [63] Office of Hazardous Materials Safety (OHMS) (2005c). Reported hazard doc [http.www.nstb/hazmatdocs](http://www.nstb/hazmatdocs) us materials incident. [http:// hazmat .dot.gov/spills](http://hazmat.dot.gov/spills)
- [64] Lees, F. P., “Loss Prevention in the Process Industries,” Butterworth Edited by Sam Mannan, 2005.
- [65] Westbrook G.W., “The bulk distribution of toxic substances:a safety assessment of the carriage of liquid chlorine,” in *Loss Prevention and Safety Promotion 1*, pp.197, 1974.
- [66] J. Marc Assael and Konstantinos E. K., “Fires, Explosions and Toxic Gas Dispersions: Effects Calculation and Risk Analysis,” CRC Press, Taylor and Francis Group Publishing, 2010.
- [67] J. Casal., “Evaluation of the Effects and Consequences of Major Accidents in Industrial Plants, Industrial Safety Series,” Elsevier, vol. 8, p. 363, 2008.
- [68] CCPS (Center for Chemical Process Safety, “Guidelines for Hazard Evaluation Procedures,” New York, American Institute of Chemical Engineers, 1992.



- [69] V.T. Covello and M.W. Merkhofer, "Risk Assessment Methods," Plenum Press, NY, 1993.
- [70] Department of Environment Ministry of Natural Resources and Environment, Malaysia, "Environmental Impact Assessment Guidelines for Risk Assessment," Putrajaya, 2004
- [71] Committee for the Prevention of Disasters, "Guidelines for Quantitative Risk Assessment (TNO Purple Book)," CPR 18E, The Hague, Holland, 1999
- [72] CCPS (Center for Chemical Process Safety), "Guidelines for Chemical Release Consequences Analysis. 1<sup>st</sup> Edition. New York: American Institute of Chemical Engineers, 1992.
- [73] Swiss Federal office for Environmental Protection, Forestry and Landscape (BUWAL), "Guiding Principles for Traffic Ways," in Handbook III, to the Regulations Concerning Incidents, 1992.
- [74] J. A. Vilchez, S Sevilla, H. Montiel and J. Casal, "Historical analysis of accidents in chemical plants and in the transportation of hazardous materials," *J Loss Prevention Process Ind.* vol. 8 no. 2 pp 87-96, 1995.
- [75] R. A. Zulkifli, H. E. Mohanad, K. H. Ku Hamid, A.R Shariff, A.B. Sheriff, "Development and design of smart advisory system in the accident of transportation of hazardous material via quantitative risk approach. A Review," in *Journal of Occupational Safety and Health*, vol.3, pp. 48- 67, 2009.
- [76] Committee for The Prevention of Disasters, Methods for the calculation of physical effects (TNO Yellow Book), CPR 18E, The Hague, 2005.
- [77] CCPS, (Center for Chemical Process Safety), "Characteristics of Vapor Cloud Explosions," American Institute of Chemical Engineers, 1994.
- [78] CCPS (Center for Chemical Process Safety), "Guidelines for, Vapor Cloud Dispersions," 1<sup>st</sup> Edition. New York: American Institute of Chemical Engineers, 1987.
- [79] E. Erkut and V. Verter, "Modeling of Transport Risk for Hazardous Materials," in *Operations Research*, Vol. 46 (5), 1998, pp. 625-641, 1998.
- [80] W. D. Rowe, "Risk assessment procedures for HazMat transportation," in *Transportation Research Board national cooperative highway research*



- program synthesis of highway practice report 103*. Washington, D.C.: Transportation Research Board, National Research Council, 1983.
- [81] J. B. Ang, "Development of a systems risk methodology for single and multimodal transportation systems," Final Report. Washington, DC: Office of University Research, US DOT NSTB, 1989.
  - [82] Abkowitz, M. P. and Cheng, P.D.M., "Developing a risk/cost framework for routing truck movements of hazardous materials, *Accident Analysis and Prevention*, vol. 20, no.1, pp. 39-51, 1998.
  - [83] E. Erkut, and V. Verter, V. "A framework for hazardous materials transport risk assessment," *Risk Analysis*, vol. 15, no.5, pp 589-601, 1995.
  - [84] N. Vayiokas, and M. Pitsiava-Latinopoulou, M. "Developing a framework for assessing risks involved in the transportation of dangerous goods," at *11th International Symposium: Loss Prevention and Safety Promotion in the Process Industries*, Praha, Czech Republic, pp. 4495-4503, 2004.
  - [85] B. Fabiano, F. Curro, Palazzi, E., and R. Pastorino, "A framework for risk assessment and decision-making strategies in dangerous good transportation," in *Journal of Hazardous Materials*, vol. 93, pp1-15, 2002.
  - [86] M. Abkowitz and P. Cheng, "Hazardous materials transportation risk estimation under condition of limited data availability", *Transportation Research Record*, vol. 1261, pp .35-39, 1989.
  - [87] Juan A. Vilchez, Sergi Sevilla, Helena Montiel and Joaquim Casal. 1995. Historical analysis of accidents in chemical plants and in the transportation of hazardous materials. *J Loss Prevention Process Ind*. Vol. 8 No. 2 pp 87-96
  - [88] D. W. Harwood, E. R. Russel and J. G. Viner, "Characteristics of accidents and incidents in highway transportation of hazardous materials", in *Transportation Research Records*, vol. 1245, pp. 23-33, 1990.
  - [89] T. S. Glickman, "An expeditious risk assessment of the highway transportation of flammable liquid in bulk," in *Transportation Research Records*, vol. 1193, pp. 22-28, 1991.
  - [90] Ormsby, R.W. and Le, N.B., "Societal risk curves for historical hazardous chemical transportation accident," in *Preventing Major Chemical and Related Process Accidents*, pp. 133, 1988.



- [91] J. B. Ang, "Development of a systems risk methodology for single and multimodal transportation systems," Final Report. Washington, DC: Office of University Research, US DOT NSTB, 1989.
- [92] M. Abkowitz, and P. D. M. Cheng, "Developing a risk/cost framework for routing truck movements of hazardous materials," *Accident Analysis and Prevention*, vol. 20 (1), pp. 39-51, 1998.
- [93] Kara, B., Erkut, E. and Verter, V. "Accurate calculation of hazardous materials transportation risks," *Operations Research Letters*, vol. 31, pp. 285-292, 2003.
- [94] Fabiano, B., Curro, F., Palazzi, E., and Pastorino, R. "A framework for risk assessment and decision-making strategies in dangerous good transportation," in *Journal of Hazardous Materials*, vol. 93, pp. 1-15, 2002.
- [95] M. Considine, "Risk Assessment of the Transportation of Hazardous Substances Through Road Tunnels," in *Recent Advances in Hazardous Materials Transportation Research: An International Exchange*, Washington, D.C., Transportation Research Board, pp. 178-185, 1986.
- [96] J. W. Cashwell, and K.S. Neuhauser, P.C. Reardon, and G. W. McNair, "Transportation Impacts of the Commercial Radioactive Waste Management Program," Report SANDS85-2715, Sandia National Laboratories, Albuquerque, N.M., 1986
- [97] D. Kessler, "Establishing Hazardous Materials Truck Routes for Shipments through the Dallas-Fort Worth Area," in *Recent Advances in Hazardous Materials Transportation Research: An International Exchange*, Washington, D.C., *Transportation Research Board*, pp. 79-87, 1986.
- [98] P. Leonelli, Bonvicini, S., and Spadoni, G., "New detailed numerical procedures for calculating risk measures in hazardous materials transportation," in *Journal of Loss Prevention in the Process Industries*, vol. 12, pp. 507-515, 1999.
- [99] Spadoni, G., Leonelli, P., Verlicchi, P., and Fiore, R. , "A numerical procedure for assessing risks from road transport of dangerous substances," in *Journal of Loss Prevention in Process Industry*, vol. 8, no. 4, pp. 245-252, 1995.
- [100] R. Bubbico, Cave, Guerieri, and Mazzarotta, "Best Routing Criteria for hazardous substances transportation," *10th International Symposium: Loss*



- Prevention and Safety Promotion in the Process Industries*, Stockholm, Sweden, EFCE and Elsevier Publications, pp1029-1044, 2001.
- [101] R. Bubbico, Cave, and Mazzarotta, "Risk analysis for road and rail transport of hazardous materials: a simplified approach", in *Journal of Loss Prevention in the Process Industries*, vol. 17, pp. 477-482, 2004.
  - [102] C. Beng Goh, Chi Bun Ching and Reginald Tan, "Risk analysis for the road transportation of hazardous chemicals in Singapore- a methodology," in *Journal of Loss Prevention in the Process Ind*, vol. 8, no. 1, pp.35-39, 1994.
  - [103] R. Bubbico, G. Dore and B. Mazzarotta, "Risk analysis study of road transport of ethylene oxide," in *Journal of Loss Prevention in the Process Industries*. vol. 11, pp. 49-54, 1998.
  - [104] R. Bubbico, C. Ferrari, and B. Mazzarotta, "Risk analysis of LPG transport of hazardous materials," in *Journal of Loss Prevention in the Process Industries*, vol. 13pp. 27-31, 2000.
  - [105] Fabiano, B., Curro, F., Palazzi, E., and Pastorino, R, "Risk assessment and decision making strategies in dangerous good transport. From Italian case-study to a general framework," in *10th International Symposium: Loss Prevention and Safety Promotion in the Process Industries*, Stockholm, Sweden, 19-21 June (2001), EFCE and Elsevier Publications, pp. 955-966, 2001.
  - [106] B. Ashtakala, Lucy A. Eno, "Minimum Risk Route Model for Hazardous materials," in *Journal of Transportation Engineering ASCE*, pp. 350, 1996.
  - [107] R. Bubbico, Maschio, Mazzarotta, Milazzo, Parisi, Risk management of road and rail transport of hazardous materials in Sicily," in *Journal of Loss Prevention in the Process Industries*, vol. 9, pp. 32-38, 2006.
  - [108] Abkowitz, M. and P. Chan, "Developing a Risk-Cost Framework for Routing Truck Movements of Hazardous Materials," *Accident Analysis Prevention*, vol. 20 (1), 39-51, 1998.
  - [109] Lepofsky, M., Abkowitz, M., and Cheng, P. "Transportation hazard analysis in integrated GIS environment," in *Journal of Transportation of Engineering-ASCE*, vol. 119(2), pp. 239-254, 1993.



- [110] G. Hobeika, Sigon Kim and Robert E. Beckwith, "A Decision Support System for Developing Evacuation Plans around Nuclear Power Stations", *Interfaces*, vol. 24, no. 5, pp. 22-35, 1994.
- [111] K.T. Chang, "Introduction to Geographic Information Systems," New York: Mc Graw Hill, 2008.
- [112] Liao, Hsiu-Hua, and Udoyara S. Tim, "Interactive Water Quality Modelling within A GIS Environment," in *Comput. Environ. and Urban Systems*. vol. 18, pp. 343-363, 1994.
- [113] J. Sauchyn, "GIS Modelling of Agricultural Soil Loss in a Plain Glacial Landscape," in *Quaternary International*. vol. 20, pp. 63-170, 1993.
- [114] K. Fedra, "Integrated risk assessment and management overview and state of the art," in *Journal of Hazardous Materials*, vol. 61, pp 5-22, 1998.
- [115] J. Colls, "Air Pollution," 2<sup>nd</sup> edition, Taylor & Francis, 2002.
- [116] Turner, Abkowitz D. B., "Workbook of atmospheric dispersion estimates," Office of Air Programs Pub. No. AP-26, Environmental Protection Agency, U.S.A, 1970.
- [117] F. Pasquill, "Some observed properties of medium-scale diffusion in atmosphere," in *Quart. J. R. Met. Soc*, vol. 88, pp. 70, 1962.
- [118] F. Pasquill, "Atmospheric Diffusion," 2<sup>nd</sup> edn. Ellis Horwood Ltd., Chichester, p. 228, 1974.
- [119] A. Gifford, "Relative atmospheric diffusion of smoke puffs," *J. Met.*, 14, 410, 1957.
- [120] A. Gifford, "Further data on relative atmospheric diffusion," in *J. Met.*, 14, pp. 475, 1957.
- [121] F. Pasquill, "The estimation of the dispersion of windborne material," in *Met. Mag.*, vol. 90, pp. 33, 1961.
- [122] A. Eliassen, "The study of long range transport of air pollutants: long range transport modelling," in *Atmos. Environ.*, vol. 12, pp. 479, 1978.
- [123] Hanna, S., "Lagrangian and Eulerian Time-Scale Relations in the Daytime Boundary Layer," in *Journal of Applied Meteorology*, vol. 20, no.3, pp. 242–249, 1981.
- [124] A. Robert, Tai Loy Yee, and Ritchie, H., "A Semi-Lagrangian and Semi-



- Implicit Numerical Integration Scheme for Multilevel Atmospheric Models. *Monthly Weather Review*”, vol. 113, no. 3, pp. 388–394 , 1985.
- [125] P. Builtjes, “Major Twentieth Century Milestones in Air Pollution Modelling and Its Application,” *Air Pollution Modelling and Its Application XIV*. Kluwer -Springer Publisher, 2004.
- [126] P. Cassini, “Road transportation of dangerous goods: quantitative risk assessment and route comparison,” in *J. Hazardous Materials*; vol. 61, pp. 133-138, 1998.
- [127] R. Bouble, Fox D., Turner B., “Fundamentals of Air Pollution,” in Academic Press. Elsevier, 1994.
- [128] G. Derwent, Middleton, R., Field A., Goldstone E., Lester, N. and Perry, R., “Analysis and interpretation of air quality data from an urban roadside location in Central London over the period from July 1991 to July 1992,” in *Atmospheric Environment* , vol. 29(8), pp. 923-946, 1995.
- [129] R.Middleton, (1995). “A new box model to forecast urban air quality: BOXURB,” in *Turbulence and Diffusion Note No 221*, 1995.
- [130] R. Middleton, “A New Box Model to Forecast Urban Air Quality: Boxurb. Environmental Monitoring and Assessment,” vol. 52, (1-2), pp. 315-335, 1998.
- [131] R. Beychok Milton, “Fundamentals of Stack Gas Dispersion,” 4<sup>th</sup> Edition, Irvine, California, USA, 2005.
- [132] K. Fedra, “GIS and Environmental Modelling,” in: M.F. Goodchild, B.O. Parks and L.T. Steyaert [eds.] *Environmental Modelling with GIS*, Oxford University Press, pp. 35-50, 1994.
- [133] K. Fedra, “Clean Air - Air Quality Modelling and Management. In: Mapping Awareness and GIS in Europe,” in Miles Arnold Publication, vol.7, no.6. pp. 24-27, 1993.
- [134] P.A. Longley, M. F. Goodchild, M. F., D. J. Maguire, and Rhind, D. W., “Geographic Information Systems and Science, John Wiley & Sons,” pp. 27–58, New York, 2001.
- [135] Zhang, J., Hodgson, J. and Erkut, E., “Using GIS to assess the risks of hazardous materials transportation in networks,” in *European Journal of Operational Research*, vol. 121, pp. 316-329, 2000.



- [136] Verter, V. and Kara, B. Y. , “ A GIS-based framework for hazardous materials transportation risk assessment, ” in *Risk Analysis*, vol. 21(6), pp1109-1120, 2001.
- [137] J. A. Vilchez, S. Sevilla, H. Montiel and J. Casal., “Analytical expressions for the calculation of damage percentage using the probit methodology,” in *J. Loss Prevention Process Ind.*, vol.14, pp. 193-197, 2001.
- [138] E. Planas Cuchi, Montiel H. and J. Casal, “A survey of the origin, type and consequences of fire accidents in process plants and in the transportation of hazardous materials,” in *Process Safe Environ Protect*; Issue 75, pp. 3-8, 1997.
- [139] S.M. Godoy, A.S. M. Santa Cruz, N.J. Scenna, “STRAPP system- A software for hazardous materials risk assessment and safe distances calculation,” *Reliability Engineering & System Safety*, vol.92, pp. 847-857, 2007.
- [140] Fischer L. E., “Shipping Container Response to Severe Highway and railway Accident Condition,” in NUREG/CR-4829, Lawrence Livermore National laboratory, 1987.
- [141] R. Bubbico, Sergio Di Cave, B. Mazzarotta, “Computer aided transportation risk assessment,” in *European Symposium on Computer Aided Process Engineering*, Vol. 8, pp 769-774, 2000.
- [142] R. Bubbico, Sergio Di Cave, B. Mazzarotta, “Risk analysis for road and rail transport of hazardous materials: a GIS approach,” in *Journal of Loss Prevention in the Process Industries*, issues 17, pp. 483-488, 2004.
- [143] J.P. Haile, “Quantified risk assessment in railway system design and operation,” in *Qual. Reliability Eng Inter*, vol. 11 pp 439–443, 1996.
- [144] E. Alp, “Risk based transportation planning practice: Overall methodology and a case example,” *INFOR* 33, pp. 4–19, 1995.
- [145] H.M. Tweeddale, “Maximizing the usefulness of risk assessment,” *Probabilistic Risk and Hazard Assessment* ISBN 9054103493, R.E. Melchers and M.G. Stewart, (Editors), Aa Balkema, USA pp. 1–11, 1993.
- [146] D.W. Pepper and J.A. Marino, “A set of integrated environmental transport and diffusion models for calculating hazardous releases,” in *Nucl. Tech.*, vol. 113, pp. 190–203, 1996.



- [147] P. Franchon, "Use of probabilistic models in risk assessments," in *INFOR* 33, 1996.
- [148] L. Helmersson, "Consequence Analysis of Different Accident Scenarios in Transport of Hazardous Materials by Road and Rail, Swedish Road and Transport Research Institute, p. 4, 1994.
- [149] [https://wwweng.llnl.gov/sys\\_dec/sys\\_dec\\_transportation.html](https://wwweng.llnl.gov/sys_dec/sys_dec_transportation.html)
- [150] Argonne National Laboratories, "Modeling Simulation and Visualization," Chicago, IL: University of Chicago, 2005, <http://www.dis.anl.gov/msv/enviro>
- [151] Oakridge National Laboratories, "Overview of HGSYSTEM," Oak Ridge, TN: HGSYSTEM, 2005, <http://www.hgsystem.com/summary.html>
- [152] J.R. Taylor, "Risk Analysis for process plant, pipelines and transport, Chapter 16," Computer Software for risk analysis, pp 401-409, 1994.
- [153] D. A. Crowl, and J.F. Louvar, "Chemical Process Safety, Fundamental with Applications," 2nd Edition, Prentice Hall Publication, 2002.
- [154] M. Abkowitz, P. D. Chen and M. Lepofsky, "Use of geographical information systems in managing hazardous materials shipment", in *Transportation Research Record*, vol. 1261, pp. 35-39, 1990.
- [155] F. F. Saccomano, Van Aerde M and Queen D., "Interactive selection of minimum risk routes for dangerous goods shipments", in *Transportation Research Records*, pp. 1148: 9-17, 1987.
- [156] S.T. Panwhar, R. Pitt and M.D. Anderson, "Development of A GIS- Based Hazardous Materials Transportation Management System: A demonstration Project," in *Transportation Research Board of the National Academics*, UTCA Final Report 99244, 50 p, 2000.
- [157] J. H. Ganter and J.D. Smith, "MPATHav: A Software Prototype for Multi Objective Routing in Transportation Risk Assessment," in Sandia National Laboratories, New Mexico, 1995.
- [158] M. Trepanier, M. H. Leroux and N. M. Warin, "Cross-Analysis of Hazmat Road Accident Using Multiple Databases," in *Accident Analysis and Prevention*, vol.41, Issues 6, pp1192-1198, 2009.
- [159] G. Spadoni and S. Bonvicini, "ARIPAR-GIS, TRAT, OPTIPATH, EHHRA-GIS: Features and Applications of some tools for assisting decision-makers in



- risk management,” in *Integrated Risk and Vulnerability Management Assisted by Decision Support Systems*, Springer Publication, vol.8, pp.349-360, 2005.
- [160] D. Egidi, F.P. Foraboschi, G. Spadoni and A. Amendola, “The ARIPAR Project: Analysis of the Major Accident Risks Connected with Industrial and Transportation Activities in the Ravenna Area,” in *Reliable Eng. Syst. Saf.* Vol. 49, pp. 75-89.
- [161] S. M. Godoy, A. S. M. Santa Cruz and N.J. Scenna, “A System for Risk Analysis Considering Atmospheric Parameters Uncertainty,” in *2<sup>nd</sup> Mercosur Congress on Chemical Engineering in conjunction with 4<sup>th</sup> Mercosur Congress on Process System Engineering*, Enpromer, Brasil, pp. 1-10, 2005
- [162] A. Lue and A. Colorni, “A Multicriteria Spatial Decision Support System for Hazardous Material Transport,” pp. 1-13, 2008.
- [163] J. P. Bull and A. J Fisher, “A Study of Mortality in a Burn Unit: A Revised Estimate,” in *Annals of Surgery*, pp. 269-274, March 1954.
- [164] J. P. Bull and J. R. Squire, “A Study of Mortality in a Burn Unit,” in *Annals of Surgery*, pp. 160, 1949.
- [165] J. P. Bull, “Revised Analysis of Mortality due to Burns,” in *The Lancet*, pp. 1133-1134, 1971.
- [166] P. William Curreri, A. Lutterman, W. Braun and G. Thomas Shires, “Burn Injury: Analysis of Survival and Hospitalization Time of 937 Patients,” in *Annals of Surgery*, pp. 472-477, 1980.
- [167] L. Nardini, L. Aparicio, A. Bandoni, S.M. Tonelli, “Regional risk associated with the transport of hazardous materials,” in *Latin American Applied Research*, vol. 33, pp. 213-218, 2003.
- [168] Environmental Quality Act, 1974, ILBS publishing, 2005
- [169] R. S. Radin Umar and H. Hamid, “Time Series Multivariate Traffic Accidents and Fatality Models in Malaysia,” in *REAAA Journal*, pp. 15-20, January 1998.
- [170] M. N. Mustaffa, “Overview of Current Road safety in Malaysia,” Highway Planning Unit, road Safety Section, Ministry of Works, Malaysia Reports, 2006.



- [171] R. S. Radin Umar, "Updates of Road Safety Status in Malaysia," in *IATSS Research*, vol. 29, pp. 78-80, 2005
- [172] Committee for The Prevention of Disasters, "Determination of the damage effects (TNO Green Book)," CPR 18E, The Hague, 2008. 1998.
- [173] N. A. Eisenberg, C. J. Lynch and R. J. Breding, "Vulnerability Model: A Simulation System for Assessing Damage Resulting from Marine Spills," in USCG, AD/A-015 245, NTIS Report n. CG-D-137-75, 1975.
- [174] D. J. Finney, "Probit Analysis," London, Cambridge University Press.
- [175] F.D. Alonso, E. G. Ferradas, T.J. Sanchez, A.M. Aznar, J.R. Gimeno and J.M. Alonso, "Consequence analysis to determine the damage to humans from vapour cloud explosions using characteristic curves," in *Journal of Hazardous Materials*, vol.150, pp.146-152, 2008.
- [176] F.D. Alonso, E. G. Ferradas, T.J. Sanchez, A.M. Aznar, J.R. Gimeno and M.D. Minarro, "Consequence analysis to determine the damage to buildings from vapour cloud explosions using characteristic curves," in *Journal of Hazardous Materials*, vol.159, pp.264-270, 2008.
- [177] R.W. Prugh, "Quantitative evaluation of fireball hazards," in *Process Safety Prog.*, vol.13, pp. 83-91, 1994.
- [178] W.E. Baker, P.A. Cox, P.S. Westine, "Explosion Hazards and Evaluation," in Elseviers scientific publishing company, 1983
- [179] V.J. Clancey, "Diagnostic features of explosion damage," Paper Presented at the *Sixth International Meeting of Forensic Sciences*, Edinburgh, 1972.
- [180] S. Glasstone and P.J. Dolan, "The Effects of Nuclear Weapons," in *Atom Energy Comm.*, Washington D.C., 1977.
- [181] S. Glasstone and P.J. Dolan, "The Effects of Nuclear Weapons," in 3<sup>rd</sup> Edition, Tonbridge Wells, Castle House Publications, 1980.
- [182] R. A. Zulkifli, H. E. Mohanad, A. Rashid Sharif, "Assessment on the consequences of Liquefied Petroleum Gas Release Accident in the Road Transportation," in *Journal of Applied Sciences*, vol. 10, issue 12, pp. 1157-1165, 2010.
- [183] J. P. Bull, D.M. Jackson, E. J.L. Lowburry, "The Recent Burn," in *The Lancet (Letter to Editor)*, vol. 10, pp. 161, 1954.



- [184] A. Martin, "Centennial Perspective on Burn Treatment," in *Journal of the American College of Surgeons*, vol.200, pp. 814, 2005.
- [185] F. Saccomanno, and J.H. Shortreed, "Societal individual risk for hazmat transportation," In *State and local Issues in Transportation of Hazardous Waste Materials: Towards a National Strategy*, ed., American Society of Civil Engineers, New York pp. 220-245, 2006, 1991.
- [186] G.A. Chamberlain, "Developments in design methods for predicting thermal radiation from flares," in *Chem. Engng Res.*, vol., 65, pp. 299, 1987.
- [187] G.A. Chamberlain. " An experimental study of large scale compartment fires," in *Hazards, XII*, pp. 155, 1994.
- [188] EFFECT, Version 8.01, "Model for computing the physical effects of the escape of hazard materials," (TNO, The Netherland), 2009.
- [189] EFFECT, Version 8.01 Manual, "Model for computing the physical effects of the escape of hazard materials," Department of Industrial and External Safety (TNO, The Netherland), 2009.
- [190] CANARY Quest Software, "Consequences Modelling software," Quest Consultancy Incorporated, New York United States of America, 2007
- [191] ATF, 2003. Alcohol, Tobacco and Fire: from technically speaking, Palmtop Emergency for Chemicals (PEAC) by John S. Nordin, [www.atf.teas.gov/pub/fire-explo\\_pub/i54001.htm](http://www.atf.teas.gov/pub/fire-explo_pub/i54001.htm).
- [192] HSE, "Development of method to assess the significance of domino effects from major hazard sites," Health and Safety Executive. Report 183, 1998.
- [193] I. Hymes, W. Boydell, and B. Prescott, "Thermal Radiation: Physiological and Pathological effects (Major hazards monograph)," Institute of Chemical Engineers (IChemE), Rugby, Warwickshire, U.K., 1996.
- [194] F. Khan and S. Abbasi, "MAXCRED-a new software package for rapid risk assessment in chemical process industries," in *Environmental Modelling and Software*, vol.14, pp. 11-25, 1998.
- [195] M.A. El Harbawi, " Design and Development of an Integrated Chemical Accident System for Monitoring Potential Risk of Hazard Installation," in *PhD Thesis*, Universiti Putra Malaysia, 2006.



- [196] F. Khan and S. Abbasi, "Risk Analysis of Chloralkali Industry Situated in a Populated Area Using the Software Package MAXCRED II chemical process industries," in *Process safety Progress*, vol.16, no. 3, pp. 172-184, 1997
- [197] I. Hymes, "The physiological and pathological effects of thermal radiation," SRD R 275, 1983.
- [198] M. Pieterse, "Analysis of the LPG Incident in San Juan Ixhuatepec, Mexico City, 19 November 1984," in *Rep. 85-0222. TNO, Apeldoorn, The Netherlands*, 1985.
- [199] B.J. Wiekema, "Vapour cloud explosions-An analysis based on accidents. II," in *Journal of Hazardous Materials*, vol.8, issue 4, pp. 313-329, 1984.
- [200] B.J. Wiekema, "Vapour cloud explosions-An analysis based on accidents. I," in *Journal of Hazardous Materials*, vol.8, issue 4, pp. 295-311, 1984.
- [201] G. Wells, "Major hazards and their management," Institution of Chemical Engineers, IChemE, UK, 1997.
- [202] G. Wells, "Hazard Identification and Risk Assessment," Institution of Chemical Engineers, IChemE, UK, 1996.
- [203] DNV, "Environmental Impact Assessment of Proposed LRCCU Project for Middle West Coast Refinery (MWCR)," for DOE Putrajaya: Malaysia 1996.
- [204] M.J. Tang, Q.A. Baker, "A new set of blast curves from vapour cloud explosion," in *Process Safety Progress*, vol. 18, no.3, pp. 235–240, 1999.
- [205] J. Lobato, P. Cañizares, M. Rodrigo, C. Saez and J. Linares, "A comparison of hydrogen cloud explosion models and the study of the vulnerability of the damage caused by an explosion of H<sub>2</sub>," in *Int. J. Hydrogen Energy*, vol. 31, pp. 1780–1790, 2006.
- [206] C. Stewart, A. Jagoda and J. M. Howell, "Blast Injuries: Preparing for the Inevitable," in *An Evidence Based of Emergency Medicine Practice*, vol. 8, no. 4, pp.1-28, 2006.
- [207] E. Hinman, "Blast safety of the Building Envelope," in *Whole Building Design Guide*, National Institute of Building Structures, 2012.
- [208] J.M. Wightman, Gladish SL, "Explosions and blast injuries," in *Ann Emerg Med (Review article)*, vol. 37, no.6, pp. 664-678, 2001.



- [209] J. Yelverton, "Blast biology. In: Cooper C, Dudley H, Gann D, eds.," *Scientific Foundations of Trauma*. 1st ed. Oxford, UK, Butterworth-Heinemann, pp. 189-199, 1997.
- [210] D. Leibovici, Gofrit ON, Stein M, et al., "Blast injuries: bus versus open-air bombings--a comparative study of injuries in survivors of open-air versus confined-space explosions," in *J Trauma (Retrospective review, 297 patients)*, vol.41, no.6, pp. 1030-1035, 1996.
- [211] V. Blinov and G. Khudiakov, "Certain laws governing diffusive burning of liquids," in *Academia Nauk, SSSR Doklady*, vol. 113, pp. 1049, 1957.
- [212] K. S. Mudan, "Thermal radiation hazards from hydrocarbon pool fire," in *Progress in Energy and Combustion Science*, vol. 10, pp. 59-80, 1984
- [213] K. S. Mudan, Croce, P. A., "Fire Hazard Calculations for Large Open Hydrocarbon Fires," in *The SFPE Handbook of Fire Protection Engineering*, NFPA-SFPE. Boston, 1988.
- [214] J. M. Chatris, Quintela, J., Folch, J., Planas, E., Amaldos, J., Casal, in *J. Comb. and Flame*, vol. 126, pp. 1373, 2001.
- [215] H. Hottel, "Certain laws governing diffusive burning of liquids," in *Fire Res. Abs. Revs*, vol. 1, pp. 41, 1958.
- [216] F. Khan and S. Abbasi, "Major Accidents in Process Industries and an Analysis of causes and Consequences," in *Journal of Loss Prevention in the Process Industries*, vol.12, pp. 361-378, 1999.
- [217] M. Andreassen, B. Bakken, U. Danielsen, H. Haanes, G. Solum, J. Stenssas, J., Thon, H., and Wighus, R., "Handbook for fire calculations and fire risk assessment in the process industry. Scandpower A/S. Sintef-Nbl, Lillestrom, 1992.
- [218] R.L. Sheridan, "Burns," *Critical Care Med.*, vol. 30, no. 11(Supplement), pp. 500-514, 2002.
- [219] B.R. Taira, Singer AJ, Thode HC, Lee C., " Burns in the Emergency Department: A National Perspective," in *J Emerg Med.*, vol. 39, no. 1, pp. 1-5, 2010.
- [220] R. Sheridan, "Outpatient burn care in the emergency department," in *Pediatr. Emerg Care.* , pp. 449, 2005.
- [221] A. Birk, "BLEVE Response and Prevention," *Technical Documentation*, 1995



- [222] A. Birk, and Cunningham M., "The Boiling Liquid Expanding Vapour Explosion," in *Journal of Loss Prevention in the Process Industries*, vol. 7, pp. 474-480, 1994.
- [223] A. Birk, A. and Cunningham M., "Liquid Temperature Stratification and its Effects on BLEVEs and their Hazards," in *Journal of hazardous Materials*, vol. 48, pp. 219-237, 1996.
- [224] W. Martinsen W. and J. D. Marx, "An Improved Model for the Prediction of Radiant Heat from Fireballs," in *International Conference and Workshop on Modelling Consequences of Accidental Releases of Hazardous Materials*, San Francisco, California, pp. 605-621, 1999.
- [225] D.G Bagster and R.M. Pittblado, "The Thermal Hazards in the Process Industries," in *Chemical Engineering Progress*, pp. 69-75, 1989.
- [226] H. Hardee, Lee, D. and Benedick W., "Thermal hazards from LNG fireballs," in *Combust. Sci. Technol.*, vol. 17, pp. 189, 1978.
- [227] A.E. Roberts, "Thermal Radiation Hazards from Release of LPG from Pressurized Storage," in *Fire Safety J.*, vol. 4, no., pp. 97-212, 1981.
- [228] Fay A. and Lewis H., "Unsteady Burning of Unconfined Fuel Vapour Clouds," in *Sixteenth Symp. on Combust.* (Pittsburgh Pa.: Combustion Inst.): pp.1397, 1977.
- [229] J. Moorhouse and Pritchard, "Scaling Criteria for pool fires derived from large fire experiments," in *I. Chem. E. Symposium Series*, no.71, pp. 165-179, 1982.
- [230] K. Vassilia, Eleni P, Dimitrios T., "Firework-related childhood injuries in Greece: a national problem," in *Burns*, vol. 30, pp. 151-153, 2004.
- [231] D. Jones D, Lee W, Rea S, et al., " Firework injuries presenting to a national burn's unit," in *Ir Med J.* , vol. 97(8), pp. 244-245, 2004.
- [232] Consumer Product Safety Commission, "Flammable Fabrics Act: Children's Sleepwear," Federal Registrar Online via GPO access: Federal Registrar; September, vol. 61(175), 1996.
- [233] R.J. Perry, Moore CA, Morgan BD, Plummer DL., "Determining the approximate area of a burn: an inconsistency investigated and re-evaluated," in *BMJ*, vol. 312(7042), pp. 1338, 1996.
- [234] Department of Commerce, "Chapter12: Biological Effect," National technical Information services, Springfield, Virginia 22161, pp. 541-628.



- [235] T. Kletz, "Process plants: a handbook for inherently safer design," Taylor & Francis Publisher, 1998.
- [236] K. Hasegawa and K. Sato, "Study on the Fireball Following Steam Explosion of *n*-Pentane," in *Proceedings of the Second International Symposium on Loss Prevention and Safety Promotion in the Process Industries*, Heidelberg, Germany, September, pp. 297-304, 1977.
- .



## List of Publications and Awards

### Journals

- 1) R. A. Zulkifli, H. E. Mohanad, Abdul Rashid Sharif, 'Assessment on the consequences of Liquefied Petroleum Gas Release Accident in the Road Transportation', *Journal of Applied Sciences*, 10(12): pp. 1157-1165, 2010 (Scopus and Thomson index).
- 2) R. A. Zulkifli, H. E. Mohanad, Abdul Rashid Shariff. 2009. Development and design of Smart Advisory System in the accident of transportation of hazardous material via quantitative risk approach. A Review', *Journal of Occupational Safety and Health*, 6(12): pp. 48-67
- 3) Mohanad El Harbawi, S. Mustapha, Z. Abdul Rashid, Thomas S. Y. Choong, S. Abdul Rashid and A.A.Sherif, "SCIA:GIS- Based Software for Assessing the Impacts from Chemical Industrial Accidents," ASCE Journal., *Pract. Periodical of Haz., Toxic, and Radioactive Waste Mgmt.* vol. 14, pp.104, 2010
- 4) R. A. Zulkifli, H. E. Mohanad, K. Hamid Sherif Abdul bari, "New technique for Risk Analysis of road transportation of hazardous chemicals in Malaysia,". IAENG, DOAJ : Journal in Lecture Notes in Engineering and Computer Science, Vol, 2191, Issues 1, pp. 1270-1275, (ISSN: 20780958, EISSN: 20780966) EBSCHO ,DOAJ, 2011.
- 5) R. A. Zulkifli, H. E. Mohanad, Sherif Abdul bari, Jamaluddin Osman, RE Intan Hamdan Ismail, "The Application of GIS and GPS on Emergency Response for hazardous materials Transportation Incident in Malaysia" in *Journal of Environment of Science and Technology* (review MISC-11\_20) Scopus index

### International papers

- 6) R. A. Zulkifli, H. E. Mohanad, Abdul Rashid Shariff, K.H. K.Hamid, H. Husin, "A Retrospective Study of Smart Advisory System in the Transportation Of Hazardous Material (Hazmat)," in 23rd Symposium of Malaysian Chemical Engineering (SomChE), Kota Kinabalu, Sabah, pp. 971-978, 2009.



- 7) R. A. Zulkifli, H. E. Mohanad, Abdul Rashid Shariff, "Assessment on the consequences of Liquefied Petroleum Gas Release Accident in the Road Transportation," in *International Conference on Process Engineering and Advanced Materials (ICPEAM 2010) in conjunction with 24th Symposium of Malaysian Chemical Engineering. A Conference of World Engineering, Science & Technology Congress (ESTCON)*, 15-17 June 2010.
- 8) R. A. Zulkifli, H. E. Mohanad, Abdul Rashid Shariff, "Development and design of smart advisory system in the accident of transportation of hazardous material via quantitative risk approach," in *12th conferences and exhibition for occupational safety and health (COSH)*, Sunway Pyramid Convention Center, C: 1.7A: pp. 1-26, 2009.
- 9) R. A. Zulkifli, H. E. Mohanad, and Abdul Rashid Sharif, "A Significant Trend of Accident Scenario Consequences in the Transportation of Hazardous Materials (Hazmat): Analysis Study Based on the Available Accident Database," in *TECHPOS Legend Hotel*, 14-15 December 2009.
- 10) R. A. Zulkifli, H. E. Mohanad, A. R. Shariff, K. H. K. Hamid and H. Husin, "A Study on the capabilities of Decision Support System (DSS) for transportation of Hazardous Material (Hazmat) in performing an effective Transportation Risk Analysis (TRA)," CHEMECA, Adelaide, Australia, 26-29 September 2010 pp. 3535-3544, ISBN 9780858259713. Informit: ENGINEERS AUSTRALIA.
- 11) R. A. Zulkifli, H. E. Mohanad, A. R. Shariff. SMACTRA-1 : As a Smart Advisory System for a Reliable Consequences Analysis, HAZARDS Asia Pacific 2011, conference, 27-29 September 2011, Intercontinental Hotel KL.
- 12) R. A. Zulkifli, H. E. Mohanad, A. R. Sharif, IEEE Symposium on Industrial Electronics and Applications, incorporating Colloquium on Humanities, Sciences and Engineering Research, Park Royal, Hotel Penang, 3-5 October 2010
- 13) R. A. Zulkifli, H. E. Mohanad, Sherif Abdul bari, Jamaluddin Osman, RE Intan Hamdan Ismail "Risk Analysis for the road transportation of hazardous chemicals in Malaysia via modified," IChemE, CHEMECA International Conferences, Sydney Hilton Hotel, New South Wales, Australia, ISBN:



- 9780858259676, Informit: ENGINEERS AUSTRALIA, 18-21 September 2011,
- 14) R. A. Zulkifli, H. E. Mohanad, Sherif Abdul Bari, "A New technique for Risk Analysis of road transportation of hazardous chemicals in Malaysia,". *IAENG, World Congress Engineering, ICSSE, Imperial College London, South Kensington United Kingdom*, 5-9, July, 2011
  - 15) R. A. Zulkifli, H. E. Mohanad, Sherif Abdul Bari, "Risk Analysis for the road transportation of hazardous chemicals in Malaysia. A Methodology," in *IEEE* normally indexed by Scopus, National Postgraduate Conference (NPC), UTP, 19-20 September 2011
  - 16) R. A. Zulkifli, H. E. Mohanad, Sherif Abdul Bari, Jamaluddin Osman, RE Intan Hamdan Ismail, "A Review: Enhancing The Emergency Response via GIS based routing analysis for hazardous Materials Transportation Incident," at ICCEIB- IChemE, SomChe conference at UMP, 28 November – 1 Disember, 2011, Pahang
  - 17) R. A. Zulkifli, H. E. Mohanad, Sherif Abdul Bari, A. B. Alias, Fadrimar Peling, "SMACTRA: A Smart Tool for Assessing Risk from hazardous material transportation," at Process System Engineering Asia Pacific (PSEASIA) conference at Best Western Hotel, Kuala Lumpur, June 2013.

#### Awards

- 18) **Gold Medal** at Innovation, Invention and Design Exhibition (IID) 2010 Annex, UITM, Product: R. A. Zulkifli, H. E. Mohanad, A. R. Sharif, Sherif A.A., Syafique H., K. H.K. Hamid, A Smart Advisory System for Hazardous Transportation Risk Analysis (TRA).
- 19) **Bronze Medal** at Malaysian Technology Expo (International Exhibition) 2011KLCC, Product: R. A. Zulkifli, H. E. Mohanad, A. R. Sharif, Sherif A.A., Syafique H., K. H.K. Hamid, A Smart Advisory System for Hazardous Transportation Risk Analysis (TRA).



Appendix 1: shows the consequences models use in the physical effect calculation

| Sequences of analysis  | Description of analysis   | Consequences model   | No.of equations   | Sources   |
|--|---|--|---|---|
| Explosions effect modelling is generally based on TNT equivalence and TNO models | TNT model is based on the assumption of equivalence between the flammable material and TNT, factored by an explosion yield term. The TNTequivalence predicts peak overpressure with distance  | TNT Equivalency calculation involved:-<br>$m_{TNT} = \frac{\eta m \Delta H_c}{E_{TNT}}, Z_e = \frac{r}{(m_{TNT})^{1/3}},$ TNT overpressure curve or by equation (1, 2)<br>TNO Multi Energy Explosion<br>$\bar{R} = \frac{R}{(E/P_0)^{1/3}}, P^o = \Delta \bar{P}_{sPa}$  | (1), (2)<br>(3), (4)  | [11, 20, 64, 67, 72,76, 153]<br>[11, 20, 64, 67, 72,76, 153]  |
| The radiation received by a target (for the duration of the BLEVE incident)      | The atmospheric transmissiity accounts of the thermal radiation by the atmosphere. The atmospheric transmissivity depends on distance between the flames and target, temperature and atmospheric humidity.<br><br>The BLEVE equations (5-17) is given by Pieteron and Huaerta (1985), Robert (1981) and TNO (1992) by considering the radiation received by a target for the duration of the BLEVE accident.<br><br>The radiation fraction, $F_{rad}$ was given by Roberts (1981), is equal to 0.25-0.4. As the effects of a BLEVE mainly relate to human injury, a geometric view factor for a sphere to the surface normal to the sphere (not the horizontal or vertical components) should be used (Pieteron and Huaerta, 1985). | BLEVE<br>$D_{max} = 6.48 M^{0.325}$ $t_{BLEVE} = 0.825 M^{0.26}$ $D_{initial} = 1.3 D_{max}$ $H_{BLEVE} = 0.75 D_{max}$<br>Point source model:<br>$Q_R = \tau E F_{21}$ $\tau = 1.53(P_w l)^{-0.06}, \text{ for } P_w l < 10^4 \text{ Nm}^{-1}$ $\tau = 2.02(P_w l)^{-0.09}, \text{ for } 10^4 \leq P_w l \leq 10^5 \text{ Nm}^{-1}$ $\tau = 2.85(P_w l)^{-0.12}, \text{ for } P_w l > 10^5 \text{ Nm}^{-1}$ where<br>$P_w = P_{wa} \frac{H_R}{100}$ $\ln P_w = 23.18986 - \frac{3816.42}{(T - 46.13)}$<br>The path length, distance from flame surface to target is:<br>$l = (H_{BLEVE}^2 + r^2)^{0.5} - (0.5 D_{max})$ Thermal radiation is usually calculated using surface emitted flux, $E$ :<br>$E = \frac{F_{rad} M \Delta H_c}{\pi (D_{max})^2 t_{BLEVE}}$ $F_{21} = \frac{D_{max}^2}{4r^2}$ $F_{rad} = 0.00325. P^{0.32}$ | (5)<br>(6)<br>(7)<br>(8)<br>(9)<br>(10)<br>(11)<br>(12)<br>(13)<br>(14)<br>(15)<br>(16)<br>(17)<br>(18) | [11, 20, 64, 67, 72,76, 153]<br>[11, 20, 64, 67, 72,76, 153]<br>[11, 20, 64, 67, 72,76, 153]<br>[11, 20, 64, 67, 72,76, 153]<br>[11, 20, 64, 67, 72]<br>[11, 20, 64, 67]<br>[11, 20, 64, 67]<br>[11, 20, 64, 67]<br>[11, 20, 64, 67]<br>[11, 20, 64, 67]<br>[11,67, 227]<br>[11, 227]<br>[11,67, 227]<br>[11, 67] |







| Sequences of analysis | Description of analysis   | Consequences model  | No.of equations  | Sources  |
|-----------------------|---|---|--|--|
|                       | <p>The protective effect of clothing. By considering the threshold value of the ignition of clothing (<math>t = 20s</math>) is approximately <math>35 \text{ kW.m}^{-2}</math>, The thermal radiation from BLEVE fireball by a point source target is known as <math>Q \text{ (kW/m}^{-2}\text{)}</math>.</p> <p>Personnel injuries resulting from exposure to a BLEVE fireball are dependent upon the thermal dose (<math>Q_{\text{dose}}</math>).</p> <p>Person feels pain when the skin reaches a temperature of <math>45^{\circ}\text{C}</math> at a depth of <math>0.1\text{mm}</math></p> <p>Analytical expressions for converting both probit variables to percentages affected people and percentages of affected people to probit variables [137].</p> | <p>Protected , <math>Y = -37.23 + 2.56 \ln(Q_{\text{dose}}^{4/3} t)</math></p> $Q_{\text{dose}}(x) = \int_0^{t_d} Q_{th}(x, t) dt$ <p><math>t_d = (35/Q)^{4/3}</math>, time elapsed before one feels pain in seconds</p> <p>From Gaussian distribution equations, <math>P = \frac{1}{\sqrt{2\pi}} \int_{-\infty}^{Y-5} \exp\left[-\frac{V^2}{2}\right] dV</math></p> $Y = a + b \ln V$ <p>From equations (43) and (44) expressed the expressions below[ ]:</p> $s = \frac{1}{1 + r Y - 5 }$ $m = (b_1 s + b_2 s^2 + b_3 s^3 + b_4 s^4 + b_5 s^5) \left[ \frac{1}{\sqrt{2\pi}} \exp\left[-\frac{(Y - 5)^2}{2}\right] \right]$ $u = \sqrt{\ln\left(\frac{1}{p^2}\right)}, u = \sqrt{\ln\left(\frac{1}{(1-p)^2}\right)}, w = u - \frac{c_0 + c_1 u + c_2 u^2}{1 + d_1 u + d_2 u^2 + d_3 u^3}$ <p>or</p> $P_r = \left[ 1 + \frac{Y - 5}{ Y - 5 } \operatorname{erf}\left[\frac{ Y - 5 }{\sqrt{2}}\right] \right]$ $\operatorname{erf}(x) \approx 1 - (a_1 \phi + a_2 \phi^2 + a_3 \phi^3) \exp(-X^2) + \varepsilon$ $\phi = \frac{1}{(1 + \alpha x)}, \text{ where } \alpha = 0.47047, a_1 = 0.34802, a_2 = -0.09587, a_3 = 0.74785 \text{ and } \varepsilon \leq 2.5 \times 10^{-5}$ | <p>(40)</p> <p>(41)</p> <p>(42)</p> <p>(43)</p> <p>(44)</p> <p>(45)</p> <p>(46)</p> <p>(47-49)</p> <p>(50)</p> <p>(51)</p> <p>(52)</p> <p>(53)</p> | <p>[67, 172]</p> <p>[67, 137]</p> <p>[67, 137]</p> <p>[67, 137]</p> <p>[67, 137]</p> <p>[67, 137]</p> <p>[67, 137]</p> <p>[11, 67, 153]</p> <p>[67, 137]</p> <p>[67, 137]</p> <p>[67, 137]</p> |



| Sequences of analysis  | Description of analysis  | Consequences model  | No.of equations | Sources      |
|--|--|---|-----------------|--------------|
| Vulnerability to explosions. The effects to human beings and structures. | The probit equation for eardrum rupture.   | $Y = -15.6 + 1.93 \ln P_o$  | (54)            | [67, 172]    |
|  |  | or  |                 |              |
|  |  | $Y = -12.6 + 1.524 \ln P_o$   | (55)            | [67, 172]    |
|  |  | $Y = -77.1 + 6.91 \ln P_o$  | (56)            | [67, 172]    |
|  |  | $Y = -18.1 + 2.79 \ln P_o$  | (57)            | [67, 172]    |
|  | The probit equation for lung haemorrhage   | $Y = -23.8 + 2.92 \ln P_o$  | (58)            | [67, 172]    |
|  | The probit equation for glass breakage.  |   |                 |              |
|  | The probit equation for large building and structures.   |   |                 |              |
|  | Fragments, missiles projectiles and debris. The distance reached by projectiles from cylindrical tanks is usually greater than that reached by fragments from spherical vessels.   | $r_d = 634 (m) 0.1667$<br>where :                                   | (59)            | [67, 172]    |
|  |  | $r_d$ is range (m) and m is weight of explosive material (kg)       |                 |              |
|  |  | $r_s = 120 m_{TNT}^{0.33}$  | (60)            | [11, 77, 78] |
|  |  | $H_p = 0.286 \ln [0.01m] e^{-0.01r}$<br>where:                      | (61)            | [11, 77, 78] |
|  |  | $r_s$ is the safety distance from missiles, (90 m minimum)          | (62)            | [11, 77, 78] |
|  |  | $H_p$ is the average fatality probability for humans                | (63)            | [11, 77, 78] |
|  |  | For tanks < 5m <sup>3</sup> in capacity: $I = 90. M^{0.33}$         |                 |              |
|  |  | For tanks > 5m <sup>3</sup> in capacity: $I = 465. M^{0.1}$         |                 |              |
|  | The prediction of the range of cylindrical tank projectiles (tube fragments).  | Find velocity of fragments (vessel rupture):                        |                 |              |
|  |  | $P_{scaled} = \frac{(P - P_o)V}{M_c a_o^2}$                         | (64)            | [11, 77, 78] |
|  |  | $a_o = \left( \frac{T \gamma R g}{M} \right)^{1/2}$                 | (65)            | [11, 77, 78] |
|  |  | $K = 1.306 \times (\text{Fragment Mass Fraction}) + 0.308446$       | (66)            | [11, 77, 78] |
|  |  | $\ln \left( \frac{v_i}{K a_o} \right) = a \cdot \ln P_{scaled} + b$ | (67)            | [11, 77, 78] |
|  |  | $V = \left( \frac{\pi}{4} \right) D^2 \cdot L$                      | (68)            | [11, 77, 78] |
|  | The prediction of initial fragment velocity for cylindrical vessels bursting. According to Baker et. al [178 ], requires knowledge of the internal pressure (P), internal volume (V <sub>o</sub> ), mass of container/ fragment (M <sub>c</sub> ), ratio of gas heat capacities (γ), and the absolute temperature of the gas at burst (T <sub>o</sub> ). |   |                 |              |
|  |  |   |                 |              |
|  |  |   |                 |              |
|  |  |   |                 |              |



| Sequences of analysis                            | Description of analysis  | Consequences model   | No.of equations | Sources      |
|--|--|--|-----------------|--------------|
| The effects of fragments to humans.              | Estimate the flying objects or fragment in air (distance).   | $P_o = \frac{PM}{R_g T}$ , to determine ambient air density                                  | (69)            | [11, 77, 78] |
|  |  | Calculate the surface area of the fragment,  | (70)            | [11, 77, 78] |
|  |  | $A_D = \frac{\pi D^2}{4}$  | (71)            | [11, 77, 78] |
|  |  | $U_{scaled} = \frac{P_o C_D A_D u^2}{M_f g}$   | (72)            | [11, 77, 78] |
|  | Determine fragments effects on humans. Two types of fragments are essentially considered: cutting and non-cutting fragments. Cutting fragments-e.g. glass fragments-penetrate the skin. Non-cutting fragments or debris, e.g. a brick-cause high compressive stresses in the body. | $R_{scaled} = \frac{P_o C_D A_D r}{M_f}$ , where, r is actual range                          | (73)            | [77, 78]     |
|  |  | $r_{max} = \frac{u^2}{g}$  | (74)            | [77, 78]     |
|  |  | The probability of fatality for mass fragment > 4.5 kg<br>$Y = -13.19 + 10.54 \ln v_i$       | (75)            | [77, 78]     |
|  |  | For mass fragments, 0.1 kg < m <sub>f</sub> < 4.5 kg<br>$Y = -17.56 + 5.30 \ln S$<br>where : |                 |              |
|  |  | $S = \frac{1}{2} m_f \cdot v_i^2$  | (76)            | [67, 77, 78] |
|  |  | For mass fragments, 0.001kg < m <sub>f</sub> < 0.1 kg<br>$Y = -29.15 + 2.10 \ln S$ , where : | (77)            | [67, 77, 78] |
| The vulnerability of thermal radiation (escape). | The dose received by an individual who escapes, for an open area.  | $S = m_f \cdot v_i^{5.115}$  | (78)            | [67, 77, 78] |
|  |  | or<br>$v_{50} = 1247 \cdot k^{2/3} \cdot m_f^{2/3} + 22.03$ , where :                        | (79)            | [67]         |
| Equation Jetfire                                 |  | $v_{50}$ = penetration velocity at which 50% of fragments penetrate the skin.                |                 |              |
|  | The wind can have a significant influence on the jet fire. The model proposed by Chamberlain [186, 187], relatively complex, describing the jet flames by the frustrum of a cone   | Dose = $I_o^{4/3} \cdot t_{eff} = I_o^{4/3} \cdot t_r + \int_{t_r}^t I(t)^{4/3} \cdot dt$    | (80)            | [67]         |
|  |  | $0.024 \left( \frac{g d_s}{u_j^2} \right)^{1/3} Y^{5/3} + 0.2 Y^{2/3} - c_c = 0$             | (81), (82)      | [67]         |
|  |  | $c_c = (2.85 / c_{st-mass})^{2/3}$   | (83)            | [67]         |
|  |  | $L_{b_0} = Y d_s$  | (84)            | [67]         |
|  | Measured flame length Under wind influence, $\theta_{jv}$ is the angle between the hole axis and the wind vector (o).  | $L_b = L_{b_0} (0.51 e^{-0.4 u_w} + 0.49) (1 - 6.07 \times 10^{-3} (\theta_{jv} - 90))$      | (85)            | [67]         |



| Sequences of analysis | Description of analysis   | Consequences model   | No.of equations   | Sources   |
|-----------------------|---|--|---|---|
|                       | <p>Lift off distance</p> <p><math>R_w</math> is the ratio of wind speed to jet velocity.</p> <p>Length of the flames (length of frustrum)</p> <p>If <math>R_w &lt; 0.05</math>, the tilt angle can be calculated using Eq. (92)</p> <p>and if <math>R_w &gt; 0.05</math>, using Eq. (93)</p> <p>where <math>Ri_{Lbo}</math> is the Richardson number based on <math>L_{bo}</math>, <math>\Omega</math> is the angle between the wind direction and the normal perpendicular to the pipe in the horizontal plane; <math>\theta_j</math> is the angle between the hole axis and the horizontal in the vertical plane. Finally, the width of frustrum (base and tip, respectively) can be calculated with Eq. (89)</p> <p><math>Ri_{ds}</math> is the Richardson number based on the source diameter and <math>C'</math> is a function of <math>R_w</math></p> | $s = L_b \frac{\sin \left( (0.185e^{(-20R_w)} + 0.015)\alpha \right)}{\sin \alpha}$ $R_w = u_w / u_j$ $s = 0.2L_b$ $A = \frac{\pi}{2} \left( \frac{W_1 + W_2}{2} \right)^2 + L\pi \left( \frac{W_1 + W_2}{2} \right)$ $\eta_{rad} = 0.21e^{-0.00323u_j} + 0.11$ $L = \sqrt{L_b^2 - s^2 \sin^2 \alpha} - s \cos \alpha$ $\alpha = (\theta_{jv} - 90)(1 - e^{-25.6R_w}) + 8000 \frac{R_w}{Ri_{Lbo}}$ $\alpha = (\theta_{jv} - 90)(1 - e^{-25.6R_w}) + \frac{(134 + 1726(R_w - 0.026)^{1/2})}{Ri_{Lbo}}$ $Ri_{Lbo} = L_{b0} \left( \frac{g}{d_s^2 u_j^2} \right)^{1/3}$ $\cos \theta_{jv} = \cos \Omega \cos \theta_j$ $W_1 = d_s (13.5e^{-6R_w} + 1.5) \left[ 1 - \left[ 1 - \left( \frac{\rho_{air}}{\rho_j} \right)^{1/2} \frac{1}{15} \right] e^{-70Ri_{ds}CR_w} \right]$ $W_2 = L_b (0.18e^{-1.5R_w} + 0.31)(1 - 0.47e^{-25R_w})$ $Ri_{ds} = d_s \left( \frac{g}{d_s^2 u_j^2} \right)^{1/3}$ $C = 1000e^{-100R_w} + 0.8$ | <p>(86)</p> <p>(87)</p> <p>(88)</p> <p>(89)</p> <p>(90)</p> <p>(91)</p> <p>(92)</p> <p>(93)</p> <p>(94)</p> <p>(95)</p> <p>(96)</p> <p>(97)</p> <p>(98)</p> <p>(99)</p> | <p>[67]</p> <p>[67]</p> <p>[67]</p> <p>[67]</p> <p>[67]</p> <p>[67]</p> <p>[67]</p> <p>[67]</p> <p>[67]</p> <p>[67]</p> <p>[67]</p> <p>[67]</p> <p>[67]</p> <p>[67]</p> |



| Sequences of analysis | Description of analysis   | Consequences model   | No.of equations   | Sources   |
|-----------------------|---|--|---|---|
| View factor analysis  | <p>The radiant intensity from the flame center is calculated by the spherically symmetric inverse.</p> <p>The thermal radiation field around a fire is based on the radiation originates from the hot products of combustion.</p> <p>Eq. (103) till Eq. (105), show how the contour integral approach has been used to determine the geometric view factors.</p> <p>The vertical view factor Fv and the horizontal view factor Fh are given by the following expressions as in Eq. (106) till</p> | $\dot{q}_r'' = \frac{\dot{Q}}{4\pi X^2}$ $\dot{Q} = \eta \dot{m} \Delta H_c$ $\dot{q}_r'' = E F_\tau$ $F_{dA_1 \cdot A_2} = \frac{1}{\pi} \iint_{A_2} \frac{\cos \beta_1 \cos \beta_2}{r^2} dA_2$ $F_{dA_1 \cdot A_2} = \frac{1}{2\pi} \oint \frac{(z_2 - z_1) dy_2 - (y_2 - y_1) dz_2}{r^2} + \frac{m}{2\pi} \oint \frac{(x_2 - x_1) dz_2 - (z_2 - z_1) dx_2}{r^2} + \frac{n}{2\pi} \oint \frac{(y_2 - y_1) dx_2 - (x_2 - x_1) dy_2}{r^2}$ $r = [(x_2 - x_1)^2 + (y_2 - y_1)^2 + (z_2 - z_1)^2]^{1/2}$ $\pi F_v = -\frac{a \cos \theta}{(b - a \sin \theta)} \tan^{-1} \left( \frac{b-1}{b+1} \right)^{1/2} + \frac{a \cos \theta}{(b - a \sin \theta)}$ $\times \frac{a^2 + (b+1)^2 - 2b(1 + a \sin \theta)}{[a^2 + (b+1)^2 - 2a(b+1) \sin \theta]^{1/2} [a^2 + (b-1)^2 - 2a(b-1) \sin \theta]^{1/2}}$ $\times \tan^{-1} \left\{ \left[ \frac{a^2 + (b+1)^2 - 2a(b+1) \sin \theta}{[a^2 + (b-1)^2 - 2a(b-1) \sin \theta]^{1/2}} \right]^{1/2} \left( \frac{b-1}{b+1} \right)^{1/2} \right\} + \frac{\cos \theta}{[1 + (b^2 - 1) \cos^2 \theta]^{1/2}} \times$ $\left\{ \tan^{-1} \left[ \frac{ab - (b^2 - 1) \sin \theta}{(b^2 - 1)^{1/2} (1 + (b^2 - 1) \cos^2 \theta)^{1/2}} \right] + \tan^{-1} \left[ \frac{(b^2 - 1) \sin \theta}{(b^2 - 1)^{1/2} (1 + (b^2 - 1) \cos^2 \theta)^{1/2}} \right] \right\}$ $\pi F_h = \tan^{-1} \left( \frac{b+1}{b-1} \right)^{1/2} + \frac{\sin \theta}{[1 + (b^2 - 1) \cos^2 \theta]^{1/2}} \left\{ \tan^{-1} \left[ \frac{ab - (b^2 - 1) \sin \theta}{(b^2 - 1)^{1/2} (1 + (b^2 - 1) \cos^2 \theta)^{1/2}} \right] + \tan^{-1} \left[ \frac{(b^2 - 1) \sin \theta}{(b^2 - 1)^{1/2} (1 + (b^2 - 1) \cos^2 \theta)^{1/2}} \right] \right\}$ $- \frac{[a^2 + (b+1)^2 - 2(b+1 + ab \sin \theta)]}{[a^2 + (b+1)^2 - 2a(b+1) \sin \theta]^{1/2} [a^2 + (b-1)^2 - 2a(b-1) \sin \theta]^{1/2}}$ $\times \tan^{-1} \left[ \left( \frac{b-1}{b+1} \right)^{1/2} \left\{ \frac{a^2 + (b+1)^2 - 2a(b+1) \sin \theta}{a^2 + (b-1)^2 - 2a(b-1) \sin \theta} \right\}^{1/2} \right]$ | <p>(100)</p> <p>(101)</p> <p>(102)</p> <p>(103)</p> <p>(104)</p> <p>(105)</p> <p>(106)</p> <p>(107)</p> | <p>[212, 213]</p> <p>[212, 213]</p> <p>[212, 213]</p> <p>[212, 213]</p> <p>[212, 213]</p> <p>[212, 213]</p> <p>[212, 213]</p> |



| Sequences of analysis | Description of analysis   | Consequences model   | No.of equations                        | Sources   |
|-----------------------|---|--|--|---|
|                       | <p>When the angle of tilt is zero, Eq. (106) and in Eq. (107), the view factors is reduce to the following Eq.(108) and Eq. (109).</p> <p>When the observer is in the crossind direction (i.e., perpendicular to the direction of tilt), the horizontal and the vertical view factors are given by Eq. (110) and Eq.(111)</p> | $\pi F_v = \frac{a}{b} \frac{a^2 + b^2 + 1}{[a^2 + (b+1)^2]^{1/2} [a^2 + (b-1)^2]^{1/2}} \tan^{-1} \left[ \left\{ \frac{a^2 + (b+1)^2}{a^2 + (b-1)^2} \right\}^{1/2} \left( \frac{b-1}{b+1} \right)^{1/2} \right] + \frac{1}{b} \tan^{-1} \frac{a}{(b^2-1)^{1/2}} - \frac{a}{b} \tan^{-1} \left( \frac{b-1}{b+1} \right)^{1/2}$ $\pi F_h = \tan^{-1} \left( \frac{b+1}{b-1} \right)^{1/2} - \frac{a^2 + b^2 - 1}{[a^2 + (b+1)^2]^{1/2} [a^2 + (b-1)^2]^{1/2}} \times \tan^{-1} \left\{ \left[ \frac{a^2 + (b+1)^2}{a^2 + (b-1)^2} \right]^{1/2} \left( \frac{b-1}{b+1} \right)^{1/2} \right\}$ $2\pi F_h = 2 \tan^{-1} \left( \frac{b-1}{b+1} \right)^{1/2} + \frac{(b^2-1)^{1/2} \sin \theta}{(b^2 - \sin^2 \theta)^{1/2}} \left\{ \tan^{-1} \left[ \frac{ab}{(b^2-1)^{1/2} + \sin \theta} \right] - \tan^{-1} \left[ \frac{ab}{(b^2-1)^{1/2} - \sin \theta} \right] - 2 \tan^{-1} \left[ \frac{\sin \theta}{(b^2 - \sin^2 \theta)^{1/2}} \right] \right\} - \frac{a^2 + b^2 - 1}{[(a^2 + b^2 + 1)^2 - 4(b^2 + a^2 \sin^2 \theta)^2]^{1/2}} \left\{ \tan^{-1} \left[ \frac{(a^2 + (b+1)^2) \left( \frac{b-1}{b+1} \right)^{1/2} - 2a \sin \theta}{(a^2 + b^2 + 1)^2 - 4(b^2 + a^2 \sin^2 \theta)^{1/2}} \right] + \tan^{-1} \left[ \frac{(a^2 + (b+1)^2) \left( \frac{b-1}{b+1} \right)^{1/2} + 2a \sin \theta}{(a^2 + b^2 + 1)^2 - 4(b^2 + a^2 \sin^2 \theta)^{1/2}} \right] \right\}$ | <p>(108)</p> <p>(109)</p> <p>(110)</p> | <p>[212, 213]</p> <p>[212, 213]</p> <p>[212, 213]</p> |



| Sequences of analysis | Description of analysis   | Consequences model  | No.of equations | Sources    |
|-----------------------|---|---|-----------------|------------|
|                       | In determining thermal radiation hazard zones, it is customary to use a view factor maximized as regards the orientation of the receiving element. The maximum view factor is the vectorial sum of the horizontal and vertical view factors | $2\pi F_v = -\frac{a^2 \sin \theta \cos \theta}{2(a^2 \sin^2 \theta + b^2)} \ln \left[ \frac{a^2 + b^2 - 1 - 2a \frac{(b^2 - 1)^{1/2}}{b} \sin \theta}{a^2 + b^2 - 1 + 2a \frac{(b^2 - 1)^{1/2}}{b} \sin \theta} \right]$ $+ \frac{\cos \theta}{(b^2 - \sin^2 \theta)^{1/2}}$ $\times \left[ \tan^{-1} \left\{ \frac{\frac{ab}{(b^2 - 1)^{1/2} + \sin \theta}}{(b^2 - \sin^2 \theta)^{1/2}} \right\} + \tan^{-1} \left\{ \frac{\frac{ab}{(b^2 - 1)^{1/2} - \sin \theta}}{(b^2 - \sin^2 \theta)^{1/2}} \right\} \right] - \frac{2ab \cos \theta}{(b^2 + a^2 \sin^2 \theta)}$ $\times \tan^{-1} \left( \frac{b-1}{b+1} \right)^{1/2} + \frac{ab \cos \theta}{(b^2 + a^2 \sin^2 \theta)} \frac{a^2 + b^2 + 1}{[(a^2 + b^2 + 1)^2 - 4(b^2 + a^2 \sin^2 \theta)]^{1/2}}$ $\times \left\{ \tan^{-1} \left[ \frac{(a^2 + (b+1)^2) \left( \frac{b-1}{b+1} \right)^{1/2} - 2a \sin \theta}{[(a^2 + b^2 + 1)^2 - 4(b^2 + a^2 \sin^2 \theta)]^{1/2}} \right] + \right.$ $\left. \tan^{-1} \left[ \frac{(a^2 + (b+1)^2) \left( \frac{b-1}{b+1} \right)^{1/2} + 2a \sin \theta}{[(a^2 + b^2 + 1)^2 - 4(b^2 + a^2 \sin^2 \theta)]^{1/2}} \right] \right\}$ $F_h = \left\{ \tan^{-1} \frac{1}{Q} - \frac{Q}{(P^2 + Q^2)^{1/2}} \times \tan^{-1} \frac{1}{(P^2 + Q^2)^{1/2}} \right\}$ $F_v = \frac{1}{\pi} \left\{ \frac{P}{(P^2 + Q^2)^{1/2}} \tan^{-1} \frac{1}{(P^2 + Q^2)^{1/2}} - \frac{1}{\pi} \right.$ $\left. + \frac{1}{(1 + Q^2)^{1/2}} \tan^{-1} \frac{P}{(1 + Q^2)^{1/2}} \right\}$ <p>Where; <math>P=2H/L</math> and <math>Q=2X/L</math></p> $F_h = \frac{1}{\pi} \left\{ \tan^{-1} \frac{1}{Q} + \frac{(P \cos \beta - Q)}{(P^2 + Q^2 - 2PQ \cos \beta)^{1/2}} \times \tan^{-1} \left[ \frac{1}{(P^2 + Q^2 - 2PQ \cos \beta)^{1/2}} \right] + \right.$ $\left. \frac{\cos \beta}{(1 + Q^2 \sin^2 \beta)^{1/2}} \times \left[ \tan^{-1} \left\{ \frac{P - Q \cos \beta}{(1 + Q^2 \sin^2 \beta)^{1/2}} \right\} + \tan^{-1} \left\{ \frac{Q \cos \beta}{(1 + Q^2 \sin^2 \beta)^{1/2}} \right\} \right] \right\}$ $F_v = F_v(H_1) - F_v(H_2)$ | (111)           | [212, 213] |
|                       |   |   | (112)           | [212, 213] |
|                       |   |   | (113)           | [212, 213] |
|                       |   |   | (114)           | [212, 213] |
|                       |   |   | (115)           | [212, 213] |
|                       |   |   | (116)           | [212, 213] |
|                       |   |   |                 | Continued  |



| Sequences of analysis         | Description of analysis   | Consequences model   | No.of equations | Sources    |
|-------------------------------|---|--|-----------------|------------|
| Air flow simulation           | The analysis is applicable to compute the thermal radiation in a crosswind direction    | $F_h = \frac{1}{2\pi} \left\{ \cos \theta \tan^{-1} \left( \frac{W}{X} \right) - \frac{X \cos \theta}{A} \left[ \tan^{-1} \left( \frac{L \sin \theta}{A} \right) + \tan^{-1} \left( \frac{W - L \sin \theta}{A} \right) \right] \right\}$  | [117]           | [212, 213] |
| Dynamic characteristic length |   | $F_v = \frac{1}{2\pi} \left\{ \frac{L \cos \theta}{A} \left[ \tan^{-1} \left( \frac{W - L \sin \theta}{A} \right) + \tan^{-1} \left( \frac{L \sin \theta}{A} \right) \right] + \frac{W \cos \theta}{B} \times \left[ \tan^{-1} \left( \frac{L - W \sin \theta}{B} \right) + \tan^{-1} \left( \frac{W \sin \theta}{B} \right) \right] \right\}$ | (118)           | [212, 213] |
|                               |   | Where; $A = [L^2 \cos^2 \theta + X^2]^{1/2}$ and $B = [W^2 \cos^2 \theta + X^2]^{1/2}$   | (119)           | [212, 213] |
| Particle transfer             |   | $\frac{\partial \bar{u}_i}{dx_i} = 0$  | (120)           | [11]       |
|                               |   | $\frac{\partial \bar{u}_i}{\partial t} + \frac{\partial \bar{u}_i \bar{u}_j}{dx_j} = - \frac{\partial \bar{p}}{\partial x_i} - \frac{\partial \tau_{ij}}{\partial x_j} + \frac{1}{Re} \frac{\partial^2 \bar{u}_i}{\partial x_j \partial x_j} + S_i$  | (121)           | [11]       |
|                               |   | $\tau_{ij} = -2v_{sgs} \overline{S_{ij}} + \frac{1}{3} \tau_{kk} \delta_{ij}$  | (122)           | [11]       |
| Emission Factor (EF)          | LES was used to simulate flow and turbulence distributions, assuming incompressibility. | $\frac{\partial \bar{c}}{\partial t} + \frac{\partial ((\bar{u}_i + \partial_{i,3} V_s) \bar{c})}{dx_i} = - \frac{v + v_{sgs}}{Sc} \frac{\partial^2 \bar{c}}{\partial x_i \partial x_j} + S_o$   | (123)           | [11]       |
|                               |   | $V_s = \frac{\rho_p d^2 g C_c}{18 \eta}$   | (124)           | [11]       |
|                               |   | $EF = 0.0069 \times NDV\% + 0.1250 \times DV\% + 0.0449$<br>Where NDV% and DV% represent the percentages of  | (125)           | [11]       |
|                               |   | NDV and DV respectivel   | (126)           | [11]       |
|                               |   |  |                 | Continued  |



| Sequences of analysis          | Description of analysis   | Consequences model  | No.of equations | Sources   |
|--------------------------------|---|---|-----------------|-----------|
| Plume Model                    | The model was used to simulate particle transfer for the finite particle inertia.   | $Ve = N\pi(Re)^2 v_e$   | (127)           | [11]      |
| Visible length                 |   | $F_e = gV_e \frac{T_e - T_a}{T_e + 273}$  | (128)           | [11]      |
| Buoyancy flux                  | The EF are calculated using experimental data. The EF defined as the mass of specific pollutants produced in a unit kilometer.                  | $R(x) = \beta z_p(x)$   | (129)           | [11]      |
| Radius of the plume            |   | $z_p(x) = \left(\frac{3}{2\beta^2}\right)^{1/3} \left(\frac{F_e}{\pi}\right)^{1/3} \frac{x^{2/3}}{u}$   | (130)           | [11]      |
| Centreline height of the Plume | The calculation of the plume rise and subsequent dispersion of the plume in the atmosphere.   | $D(x) = \frac{V_x}{V_c}$  | (131)           | [11]      |
| Dilution                       |   | $T(x) = T_a + \frac{T_e - T_a}{D(x)}$   | (132)           | [11]      |
| Ambient air condition          | It is assumed that the plumes from individual cells forming a bank of cooling towers interact with one another to form a single combined plume. | $w(x) = w_s(T_a) \frac{RH}{100} + \frac{r[w_s(T_e) - w_s(T_a)] \left(\frac{RH}{100}\right)}{D(x)}$  | (133)           | [11]      |
| Water Content                  |   | $w(x_c) = w_s(T(x_c))$  | (134)           | [11]      |
| Water vapour concentration     | The dilution of the water vapour plume after travelling the distance  | $T_{atmos}(z) = T_a - 0.0098z$  | (135)           | [11]      |
| Atmospheric temperature        |   | $\frac{\partial C}{\partial t} = D_x \frac{\partial^2 C}{\partial x^2} + D_y \frac{\partial^2 C}{\partial y^2} + D_z \frac{\partial^2 C}{\partial z^2} - \bar{u}_x \frac{\partial C}{\partial x} - \bar{u}_y \frac{\partial C}{\partial y} - \bar{u}_z \frac{\partial C}{\partial z}$ | (136)           | [11]      |
| Advection Dispersion Equation  |   | $\frac{\partial C}{\partial t} = D_x \frac{\partial^2 C}{\partial x^2} + D_z \frac{\partial^2 C}{\partial z^2} - \bar{u}_x \frac{\partial C}{\partial x}$   |                 | [11]      |
|                                |   |   |                 | Continued |



| Sequences of analysis               | Description of analysis  | Consequences model   | No.of equations | Sources |
|-------------------------------------|--|--|-----------------|---------|
| <u>Liquid Discharge</u>             |  | $\frac{P_2 - P_1}{\rho} + \frac{g}{g_c}(z_2 - z_1) + \frac{1}{2g_c}(v_2^2 - v_1^2) + \sum e_f + \frac{W_s}{m} = 0$   | (137)           | [11]    |
| Normal pressure of liquid discharge |  | $\dot{m} = AC_D \sqrt{2\rho g_c(P_1 - P_2)}$   | (138)           | [11]    |
|                                     |  | $C_D = \frac{1}{\sqrt{1 + \sum K_f}}$  | (139)           | [11]    |
|                                     |  | $t = \frac{1}{AC_D \sqrt{2g}} \int_{v_2}^{v_1} \frac{dV(h)}{\sqrt{h}}$   | (140)           | [11]    |
|                                     |  | $\dot{m} - \rho v A = \rho AC_D \sqrt{2 \left( \frac{g_c P_g}{\rho} + g h_L \right)}$  | (141)           | [11]    |
| <u>Gas Discharge</u>                |  | $\dot{m} = C_D A P_1 \sqrt{\frac{2g_c M}{R_g T_1} \frac{k}{k-1} \left[ \left( \frac{P_2}{P_1} \right)^{2/k} - \left( \frac{P_2}{P_1} \right)^{(k-1)/k} \right]}$ | (142)           | [11]    |
| Hole gas discharges                 | The pressure integral in the mechanical energy balance can be integrated directly to result in the equation. | $m_{choked} = C_D A P_1 \sqrt{\frac{k g_c M}{R_g T_1} \left( \frac{2}{k+1} \right)^{(k+1)/(k-1)}}$   | (143)           | [11]    |
|                                     | The equation assumes an ideal gas, no heat transfer and no external shaft work.                              | $\frac{P_{choked}}{P_1} \left( \frac{2}{k+1} \right)^{k/(k-1)}$  | (144)           | [11]    |

d



| Sequences of analysis   | Description of analysis  | Consequences model  | No.of equations | Sources   |
|---|--|---|-----------------|-----------|
| Two phase discharge   | Two-phase flow usually requires a larger relief area compared to all-vapour venting.   | $\dot{m} = A \sqrt{G_{SUB}^2 + \frac{G_{ERM}^2}{N}}$  | (145)           | [11]      |
| <u>External Fire to Vessel</u>  | NFPA58 basically covers LPG of molecular weight btwn 30 to 58.   | $G_{SUB} = C_D \sqrt{2\rho_f g_c (P - P^{sat})}$  | (146)           | [11]      |
| Heat flux prediction  |  | $G_{ERM} = \frac{h_{fg}}{v_{fg}} \sqrt{\frac{g_c}{TC_p}}$   | (147)           | [11]      |
|   |  | $Q_f = 34,500 F A^{0.82}$   | (148)           | [11]      |
| Puff model<br>*neutral case   | The Puff model describes near instantaneous releases of material. It depends on the total quantity of material released, the atmospheric conditions, the height of the release above ground and the distance from the release. | $\dot{m} = Q_f / h_{fg}$  | (149)           | [11]      |
| Recommended Equations for Pasquill-Gifford dispersion coefficient for plume dispersion as in Appendix 2 (Table 1) |  | $\langle C \rangle(x, y, z, t) = \frac{G^*}{(2\pi)^{3/2} \sigma_x \sigma_y \sigma_z} \exp \left[ -\frac{1}{2} \left( \frac{y}{\sigma_y} \right)^2 \right] x \left\{ \exp \left[ -\frac{1}{2} \left( \frac{z+H}{\sigma_z} \right)^2 \right] \right\}$  | (150)           | [11]      |
|   |  | $\exp \left[ -\frac{1}{2} \left( \frac{x-ut}{\sigma_x} \right)^2 \right]$   | (151)           | [11]      |
|   | If the coordinate system is fixed at the release point, use the factor.  | $y = \sigma_y \sqrt{2 \ln \left( \frac{\langle C \rangle(x, 0, 0, t)}{\langle C \rangle(x, y, 0, t)} \right)}$  | (152)           | [11]      |
|   | Isopleths  | $\langle C \rangle(x, y, z) = \frac{G}{2\pi\sigma_y\sigma_z u} \exp \left[ -\frac{1}{2} \left( \frac{y}{\sigma_y} \right)^2 \right] x \left\{ \exp \left[ -\frac{1}{2} \left( \frac{z-H}{\sigma_z} \right)^2 \right] + \exp \left[ -\frac{1}{2} \left( \frac{z+H}{\sigma_z} \right)^2 \right] \right\}$ | (153)           | [11]      |
| Plume model<br>*neutral case  | This model describes a continuous release material. It depends on the rate of release, the atmospheric conditions, the height of the release above ground and the distance from the release.                                   | $\sigma_z = \frac{H}{\sqrt{2}}$   | (154)           | [11]      |
| Recommended Equations for Pasquill-Gifford dispersion coefficient for puff dispersion as in Appendix 2 (Table 2)  |  | $\langle C \rangle_{max} = \frac{2G}{e\pi u H^2} \left( \frac{\sigma_z}{\sigma_y} \right)$  | (155)           | [11]      |
|   | Min ground level release   |   |                 |           |
|   | Max ground level release   |   |                 | Continued |



| Sequences of analysis  | Description of analysis                         | Consequences model                         | No.of equations | Sources |
|--|---|--|-----------------|---------|
| Pasquill-Gifford Gaussian Models<br>*neutral case  | This is the simplified of dispersion modelling. | $L^* = \left( \frac{Q_m}{u(C)^*} \right)$  | (156)           | [11]    |
| Table 3 in appendix 2 show the curve fit for downwind distance and isopleth area                   | Dimensionless downwind distance                 | $x^* = \frac{x}{L^*}$                      | (157)           | [11]    |
|  | Dimensionless area                              | $A^* = \frac{A}{(L^*)^2}$                  | (158)           | [11]    |
|  |   | $g_0 = \frac{g(\rho_0 - \rho_2)}{\rho_2}$  | (159)           | [11]    |
|  | Initial buoyancy                                | $D_c = \left( \frac{q_0}{u} \right)^{1/2}$ | (160)           | [11]    |
| *dense gas dispersion  |   | $D_i = (V_0)^{1/3}$                        | (161)           | [11]    |
| Table 4 and 5 in appendix 2 provides equations for the correlation of dense cloud plumes and puffs | Continuous releases                             | $\frac{g_0 q_0}{u^3 D_c} \geq 0.15$        | (162)           | [11]    |
|  | Instantaneous releases                          | $\frac{g_0 V_0}{u D_i} \geq 0.20$          | (163)           | [11]    |
|  | Dense cloud continuous releases                 |  |                 |         |
|  | Dense cloud instantaneous releases              |  |                 |         |



## Appendix 2

Table 1: Recommended Equations for Pasquill-Gifford Dispersion Coefficients for Plume Dispersion

| Pasquill-Gifford Stability Class | $\sigma_y(m)$               | $\sigma_{zy}(m)$            |
|----------------------------------|-----------------------------|-----------------------------|
| <b>Rural Conditions</b>          |                             |                             |
| A                                | $0.22x(1 + 0.0001x)^{-1/2}$ | $0.20x$                     |
| B                                | $0.16x(1 + 0.0001x)^{-1/2}$ | $0.12x$                     |
| C                                | $0.11x(1 + 0.0001x)^{-1/2}$ | $0.08x(1 + 0.0002x)^{-1/2}$ |
| D                                | $0.08x(1 + 0.0001x)^{-1/2}$ | $0.06x(1 + 0.0015x)^{-1/2}$ |
| E                                | $0.06x(1 + 0.0001x)^{-1/2}$ | $0.03x(1 + 0.0003x)^{-1}$   |
| F                                | $0.04x(1 + 0.0001x)^{-1/2}$ | $0.016x(1 + 0.0003x)^{-1}$  |
| <b>Urban Conditions</b>          |                             |                             |
| A-B                              | $0.32x(1 + 0.0004x)^{-1/2}$ | $0.24x(1 + 0.001x)^{+1/2}$  |
| C                                | $0.22x(1 + 0.0004x)^{-1/2}$ | $0.20x$                     |
| D                                | $0.16x(1 + 0.0004x)^{-1/2}$ | $0.14x(1 + 0.0003x)^{-1/2}$ |
| E-F                              | $0.11x(1 + 0.0004x)^{-1/2}$ | $0.08x(1 + 0.0015x)^{-1/2}$ |

Note: The distance downwind units x, is in meters

Table 2: Recommended Equations for Pasquill-Gifford Dispersion Coefficients for Puff Dispersion

| Pasquill- Gifford Stability Class | $\sigma_x$ or $\sigma_y$ | $\sigma_z$     |
|-----------------------------------|--------------------------|----------------|
| A                                 | $0.18x^{0.92}$           | $0.60x^{0.75}$ |
| B                                 | $0.14x^{0.92}$           | $0.53x^{0.73}$ |
| C                                 | $0.10x^{0.92}$           | $0.34x^{0.71}$ |
| D                                 | $0.06x^{0.92}$           | $0.15x^{0.70}$ |
| E                                 | $0.04x^{0.92}$           | $0.10x^{0.65}$ |
| F                                 | $0.02x^{0.89}$           | $0.05x^{0.61}$ |

Note: The distance downwind units x, is in meters



Table 3: Curve fit equations for downwind reach and isopleths area. These values are used in the equation form:

$$\ln y = c_0 + c_1 \ln(L^*) + c_2 [\ln(L^*)]^2 + c_3 [\ln(L^*)]^3$$

| y                         | Stability Class | C <sub>0</sub> | C <sub>1</sub> | C <sub>2</sub>           | C <sub>3</sub> |
|---------------------------|-----------------|----------------|----------------|--------------------------|----------------|
| $x^* = \frac{x}{L^*}$     | B               | 1.28868        | 0.037616       | -0.0170972               | 0.00367183     |
|                           | D               | 2.00661        | 0.016541       | 1.42451X10 <sup>-4</sup> | 0.0029         |
|                           | F               | 2.76837        | 0.0340247      | 0.0219798                | 0.00226116     |
| $A^* = \frac{A}{(L^*)^2}$ | B               | 1.35167        | 0.0288667      | -0.0287847               | 0.0056558      |
|                           | D               | 1.86243        | 0.0239251      | -0.00704844              | 0.00503442     |
|                           | F               | 2.75493        | 0.0185086      | 0.0326708                | 0.00392425     |

Table 4: Equations used to approximate the curves in the Britter-McQuaid correlations provided for plumes

| Concentration Ratio<br>C <sub>m</sub> /C <sub>0</sub> | Valid range for<br>$\alpha = \log_{10} \left( \frac{g_0^2 q_0}{u^5} \right)$ | Equation for<br>$\beta = \log_{10} \left( \frac{x}{(q_0/u)^{1/2}} \right)$ |
|---|--|--|
| 0.1   | $\alpha \leq -0.55$  | $\beta = 1.75$   |
| 0.1   | $-0.55 < \alpha \leq -0.14$  | $\beta = 0.24\alpha + 1.88$  |
| 0.1   | $-0.14 < \alpha \leq 1$  | $\beta = 0.50\alpha + 1.78$  |
| 0.05  | $\alpha \leq -0.68$  | $\beta = 1.92$   |
| 0.05  | $-0.68 < \alpha \leq -0.29$  | $\beta = 0.36\alpha + 2.16$  |
| 0.05  | $-0.29 < \alpha \leq -0.18$  | $\beta = 2.06$   |
| 0.05  | $-0.18 < \alpha \leq 1$  | $\beta = 0.56\alpha + 1.96$  |
| 0.02  | $\alpha \leq -0.69$  | $\beta = 2.08$   |
| 0.02  | $-0.69 < \alpha \leq -0.31$  | $\beta = 0.45\alpha + 2.39$  |
| 0.02  | $-0.31 < \alpha \leq -0.16$  | $\beta = 2.25$   |
| 0.02  | $-0.16 < \alpha \leq 1$  | $\beta = 0.54\alpha + 2.16$  |
| 0.01  | $\alpha \leq -0.70$  | $\beta = 2.25$   |
| 0.01  | $-0.70 < \alpha \leq -0.29$  | $\beta = 0.49\alpha + 2.59$  |
| 0.01  | $-0.29 < \alpha \leq -0.20$  | $\beta = 2.45$   |
| 0.01  | $-0.20 < \alpha \leq 1$  | $\beta = 0.52\alpha + 2.35$  |
| 0.005   | $\alpha \leq -0.67$  | $\beta = 2.40$   |
| 0.005   | $-0.67 < \alpha \leq -0.28$  | $\beta = 0.59\alpha + 2.80$  |
| 0.005   | $-0.28 < \alpha \leq -0.15$  | $\beta = 2.63$   |
| 0.005   | $-0.15 < \alpha \leq 1$  | $\beta = 0.49\alpha + 2.56$  |
| 0.002   | $\alpha \leq -0.69$  | $\beta = 2.60$   |
| 0.002   | $-0.69 < \alpha \leq -0.25$  | $\beta = 0.39\alpha + 2.87$  |
| 0.002   | $-0.25 < \alpha \leq -0.13$  | $\beta = 2.77$   |
| 0.002   | $-0.13 < \alpha \leq 1$  | $\beta = 0.50\alpha + 2.71$  |



Table 5: Equation used to approximate the curves in the Britter-McQuaid correlations provided for Puff

| Concentration Ratio<br>$C_m/C_o$ | Valid range for<br>$\alpha = \log_{10}\left(\frac{g_o^2 q_o}{u^5}\right)$ | Equation for<br>$\beta = \log_{10}\left(\frac{x}{(q_o/u)^{1/2}}\right)$ |
|----------------------------------|---|---|
| 0.1                              | $\alpha \leq -0.44$   | $\beta = 0.70$  |
| 0.1                              | $-0.44 < \alpha \leq 0.43$  | $\beta = 0.26\alpha + 0.81$   |
| 0.1                              | $-0.43 < \alpha \leq 1$   | $\beta = 0.93$  |
| 0.05                             | $\alpha \leq -0.56$   | $\beta = 0.85$  |
| 0.05                             | $-0.56 < \alpha \leq -0.31$   | $\beta = 0.26\alpha + 1.0$  |
| 0.05                             | $0.31 < \alpha \leq 1.0$  | $\beta = 0.12\alpha + 1.12$   |
| 0.02                             | $\alpha \leq -0.66$   | $\beta = 0.95$  |
| 0.02                             | $-0.66 < \alpha \leq -0.32$   | $\beta = 0.36\alpha + 1.19$   |
| 0.02                             | $-0.32 < \alpha \leq 1$   | $\beta = 0.26\alpha + 1.38$   |
| 0.01                             | $\alpha \leq -0.70$   | $\beta = 1.15$  |
| 0.01                             | $-0.71 < \alpha \leq -0.37$   | $\beta = 0.34\alpha + 1.39$   |
| 0.01                             | $-0.37 < \alpha \leq 1$   | $\beta = 0.38\alpha + 1.66$   |
| 0.005                            | $\alpha \leq -0.52$   | $\beta = 1.48$  |
| 0.005                            | $-0.52 < \alpha \leq -0.24$   | $\beta = 0.26\alpha + 1.62$   |
| 0.005                            | $-0.24 < \alpha \leq 1$   | $\beta = 0.30\alpha + 1.75$   |
| 0.002                            | $\alpha \leq -0.27$   | $\beta = 1.83$  |
| 0.002                            | $0.27 < \alpha \leq 1$  | $\beta = 0.32\alpha + 1.92$   |
| 0.001                            | $\alpha \leq -0.10$   | $\beta = 2.075$   |
| 0.001                            | $-0.10 < \alpha \leq 1$   | $\beta = -0.27\alpha + 2.05$  |

Table 6: Relationship between the probit variable and the percentage [137, 174].

| %  | 0    | 1    | 2    | 3    | 4    | 5    | 6    | 7    | 8    | 9    |
|----|------|------|------|------|------|------|------|------|------|------|
| 0  |      | 2.67 | 2.95 | 3.12 | 3.25 | 3.36 | 3.45 | 3.52 | 3.59 | 3.66 |
| 10 | 3.72 | 3.77 | 3.82 | 3.87 | 3.92 | 3.96 | 4.01 | 4.05 | 4.08 | 4.12 |
| 20 | 4.16 | 4.19 | 4.23 | 4.26 | 4.29 | 4.33 | 4.36 | 4.39 | 4.42 | 4.45 |
| 30 | 4.48 | 4.50 | 4.53 | 4.56 | 4.59 | 4.61 | 4.64 | 4.67 | 4.69 | 4.72 |
| 40 | 4.75 | 4.77 | 4.80 | 4.82 | 4.85 | 4.87 | 4.90 | 4.92 | 4.95 | 4.97 |
| 50 | 5.00 | 5.03 | 5.05 | 5.08 | 5.10 | 5.13 | 5.15 | 5.18 | 5.20 | 5.23 |
| 60 | 5.25 | 5.28 | 5.31 | 5.33 | 5.36 | 5.39 | 5.41 | 5.44 | 5.47 | 5.50 |
| 70 | 5.52 | 5.55 | 5.58 | 5.61 | 5.64 | 5.67 | 5.71 | 5.74 | 5.77 | 5.81 |
| 80 | 5.84 | 5.88 | 5.92 | 5.95 | 5.99 | 6.04 | 6.08 | 6.13 | 6.18 | 6.23 |
| 90 | 6.28 | 6.34 | 6.41 | 6.48 | 6.55 | 6.64 | 6.75 | 6.88 | 7.05 | 7.33 |
| -  | 0.0  | 0.1  | 0.2  | 0.3  | 0.4  | 0.5  | 0.6  | 0.7  | 0.8  | 0.9  |
| 99 | 7.33 | 7.37 | 7.41 | 7.46 | 7.51 | 7.58 | 7.65 | 7.75 | 7.88 | 8.09 |



Table 7: Relationship between percentage of body area burned, age and mortality by Bull et al.[163-165].

| %<br>area<br>burned | Age  |     |       |       |       |       |       |       |       |       |       |       |       |       |       |       |    |
|---------------------|------|-----|-------|-------|-------|-------|-------|-------|-------|-------|-------|-------|-------|-------|-------|-------|----|
|                     | year |     |       |       |       |       |       |       |       |       |       |       |       |       |       |       |    |
|                     | 0-4  | 5-9 | 10-14 | 15-19 | 20-24 | 25-29 | 30-34 | 35-39 | 40-44 | 45-49 | 50-54 | 55-59 | 60-64 | 65-69 | 70-74 | 75-79 | 80 |
| ≥93                 | 1    | 1   | 1     | 1     | 1     | 1     | 1     | 1     | 1     | 1     | 1     | 1     | 1     | 1     | 1     | 1     | 1  |
| 88-92               | .9   | .9  | .9    | .9    | 1     | 1     | 1     | 1     | 1     | 1     | 1     | 1     | 1     | 1     | 1     | 1     | 1  |
| 83-87               | .9   | .9  | .9    | .9    | .9    | .9    | 1     | 1     | 1     | 1     | 1     | 1     | 1     | 1     | 1     | 1     | 1  |
| 78-82               | .8   | .8  | .8    | .8    | .9    | .9    | .9    | .9    | 1     | 1     | 1     | 1     | 1     | 1     | 1     | 1     | 1  |
| 73-77               | .7   | .7  | .8    | .8    | .8    | .8    | .9    | .9    | .9    | 1     | 1     | 1     | 1     | 1     | 1     | 1     | 1  |
| 68-72               | .6   | .6  | .7    | .7    | .7    | .8    | .8    | .8    | .9    | .9    | .9    | 1     | 1     | 1     | 1     | 1     | 1  |
| 63-67               | .5   | .5  | .6    | .6    | .6    | .7    | .7    | .8    | .8    | .9    | .9    | .9    | 1     | 1     | 1     | 1     | 1  |
| 58-62               | .4   | .4  | .4    | .5    | .5    | .6    | .6    | .7    | .7    | .8    | .9    | .9    | 1     | 1     | 1     | 1     | 1  |
| 53-57               | .3   | .3  | .3    | .4    | .4    | .5    | .5    | .6    | .7    | .7    | .8    | .9    | .9    | 1     | 1     | 1     | 1  |
| 48-52               | .2   | .2  | .3    | .3    | .3    | .3    | .4    | .5    | .6    | .6    | .7    | .8    | .9    | 1     | 1     | 1     | 1  |
| 43-47               | .2   | .2  | .2    | .2    | .2    | .3    | .3    | .4    | .4    | .5    | .6    | .7    | .8    | 1     | 1     | 1     | 1  |
| 38-42               | .1   | .1  | .1    | .1    | .2    | .2    | .2    | .3    | .3    | .4    | .5    | .6    | .8    | .9    | 1     | 1     | 1  |
| 33-37               | .1   | .1  | .1    | .1    | .1    | .1    | .2    | .2    | .3    | .3    | .4    | .5    | .7    | .8    | .9    | 1     | 1  |
| 28-32               | 0    | 0   | 0     | 0     | .1    | .1    | .1    | .1    | .2    | .2    | .3    | .4    | .6    | .7    | .9    | 1     | 1  |
| 23-27               | 0    | 0   | 0     | 0     | 0     | 0     | .1    | .1    | .1    | .2    | .2    | .3    | .4    | .6    | .7    | .9    | 1  |
| 18-22               | 0    | 0   | 0     | 0     | 0     | 0     | 0     | .1    | .1    | .1    | .1    | .2    | .3    | .4    | .6    | .8    | .9 |
| 13-17               | 0    | 0   | 0     | 0     | 0     | 0     | 0     | 0     | 0     | .1    | .1    | .1    | .2    | .3    | .5    | .6    | .7 |
| 8-12                | 0    | 0   | 0     | 0     | 0     | 0     | 0     | 0     | 0     | 0     | .1    | .1    | .1    | .2    | .3    | .5    | .5 |
| 3-7                 | 0    | 0   | 0     | 0     | 0     | 0     | 0     | 0     | 0     | 0     | 0     | 0     | .1    | .1    | .2    | .3    | .4 |
| 0-2                 | 0    | 0   | 0     | 0     | 0     | 0     | 0     | 0     | 0     | 0     | 0     | 0     | 0     | .1    | .1    | .2    | .2 |



### Appendix 3

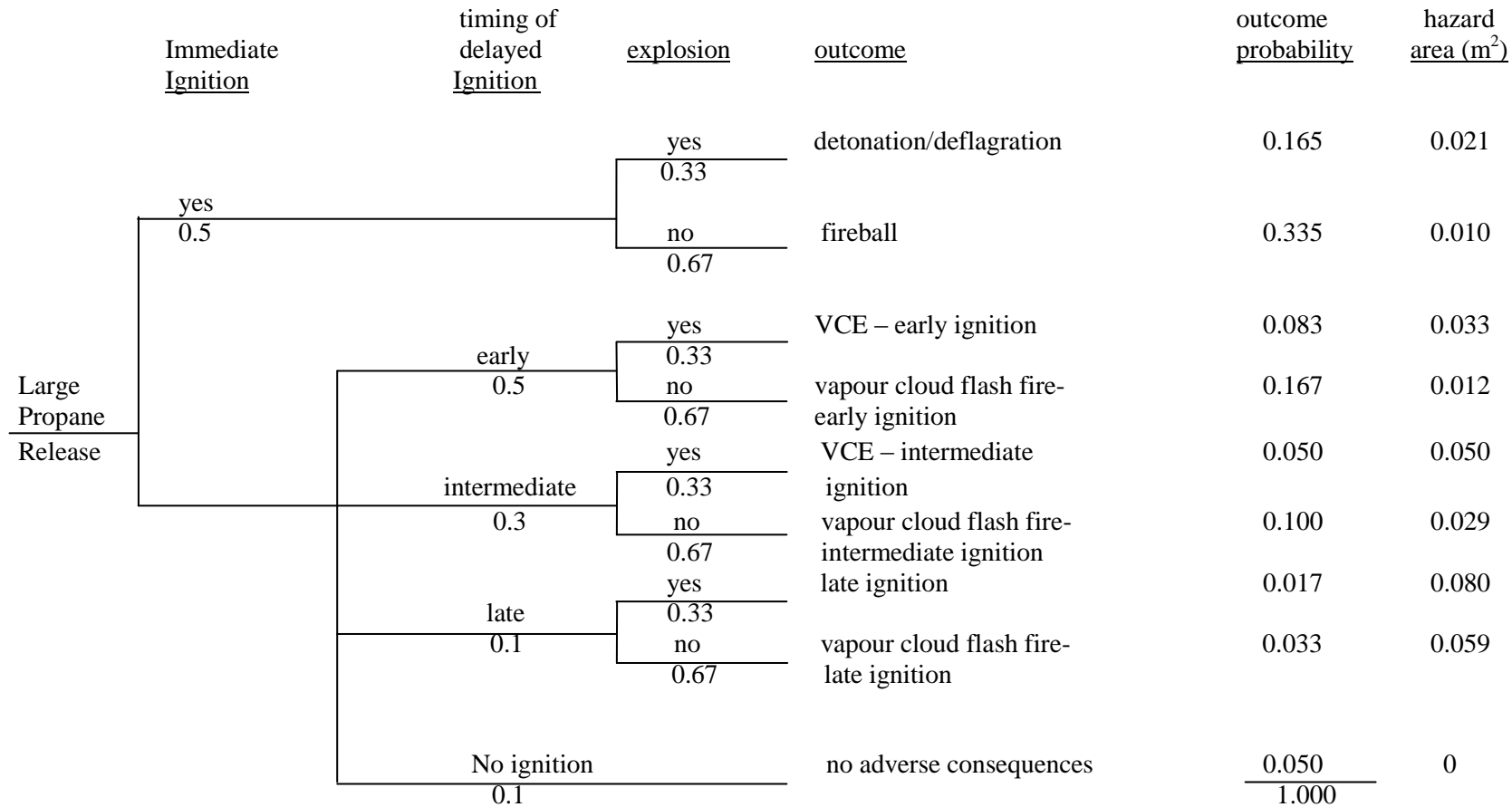


Figure 1 Event Tree for a Large Release from a Propane Tank Truck (by Rhyne) [25]..



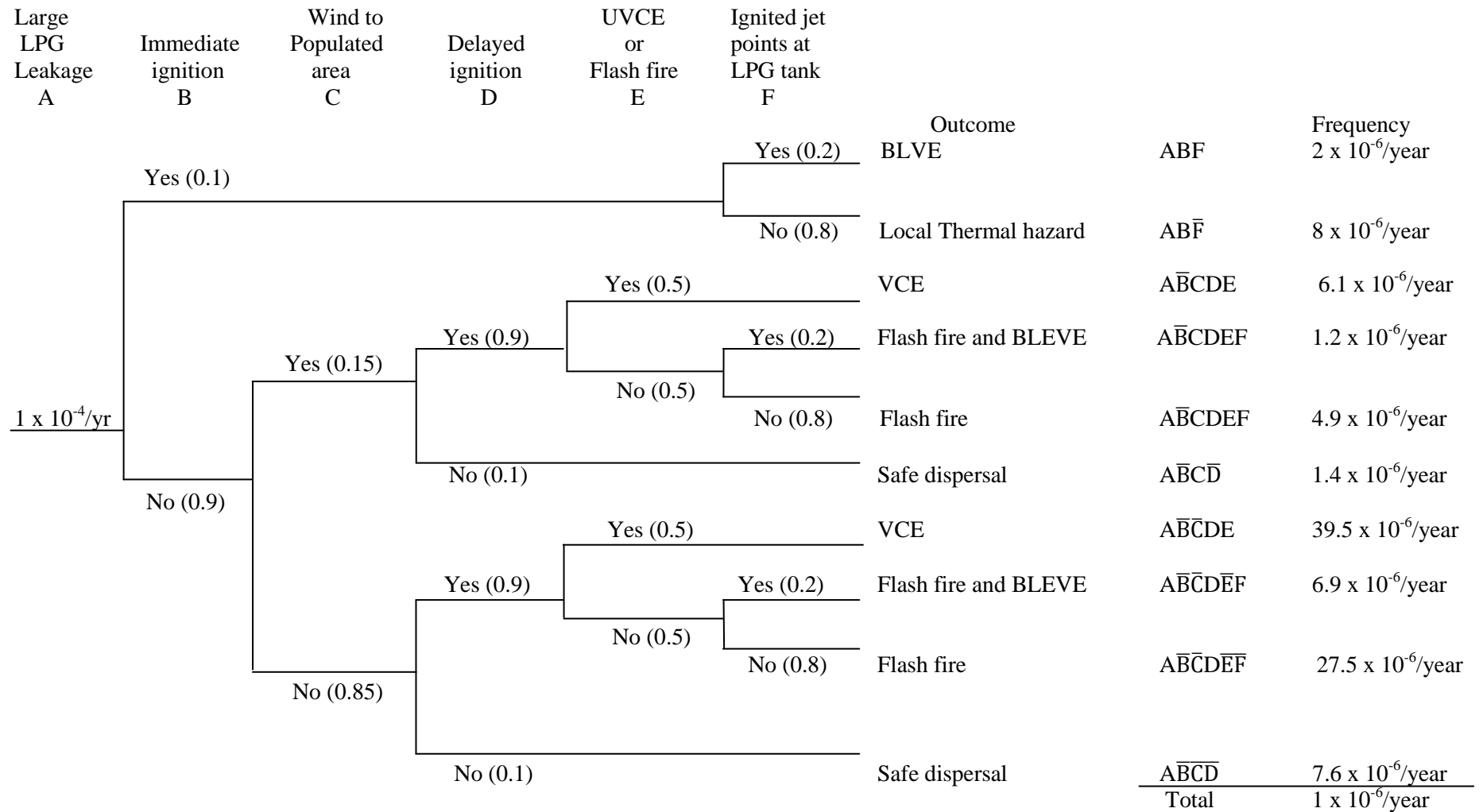


Figure 2 Event tree outcomes for LPG tanker accident (by CCPS) [11, 20-22] .



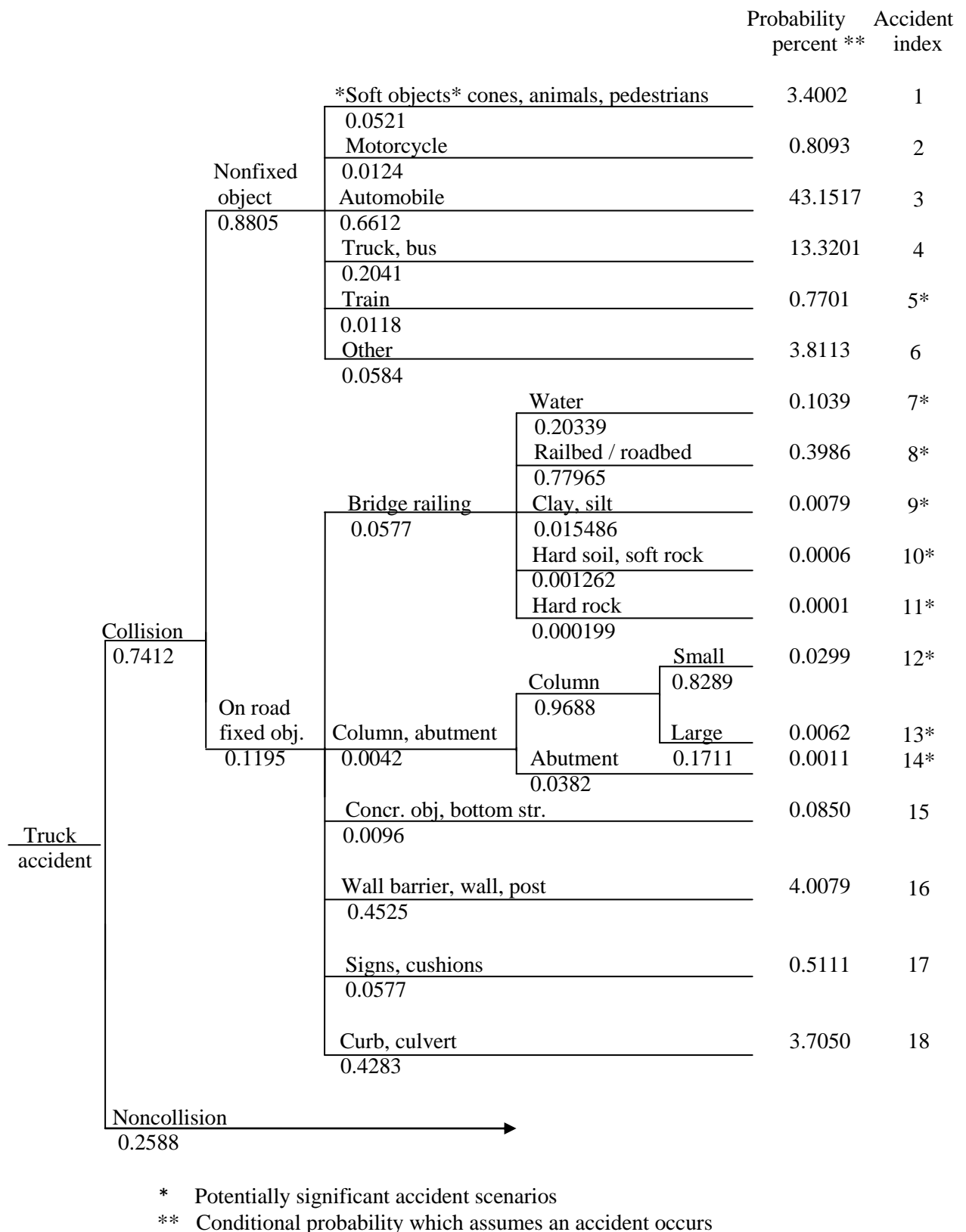
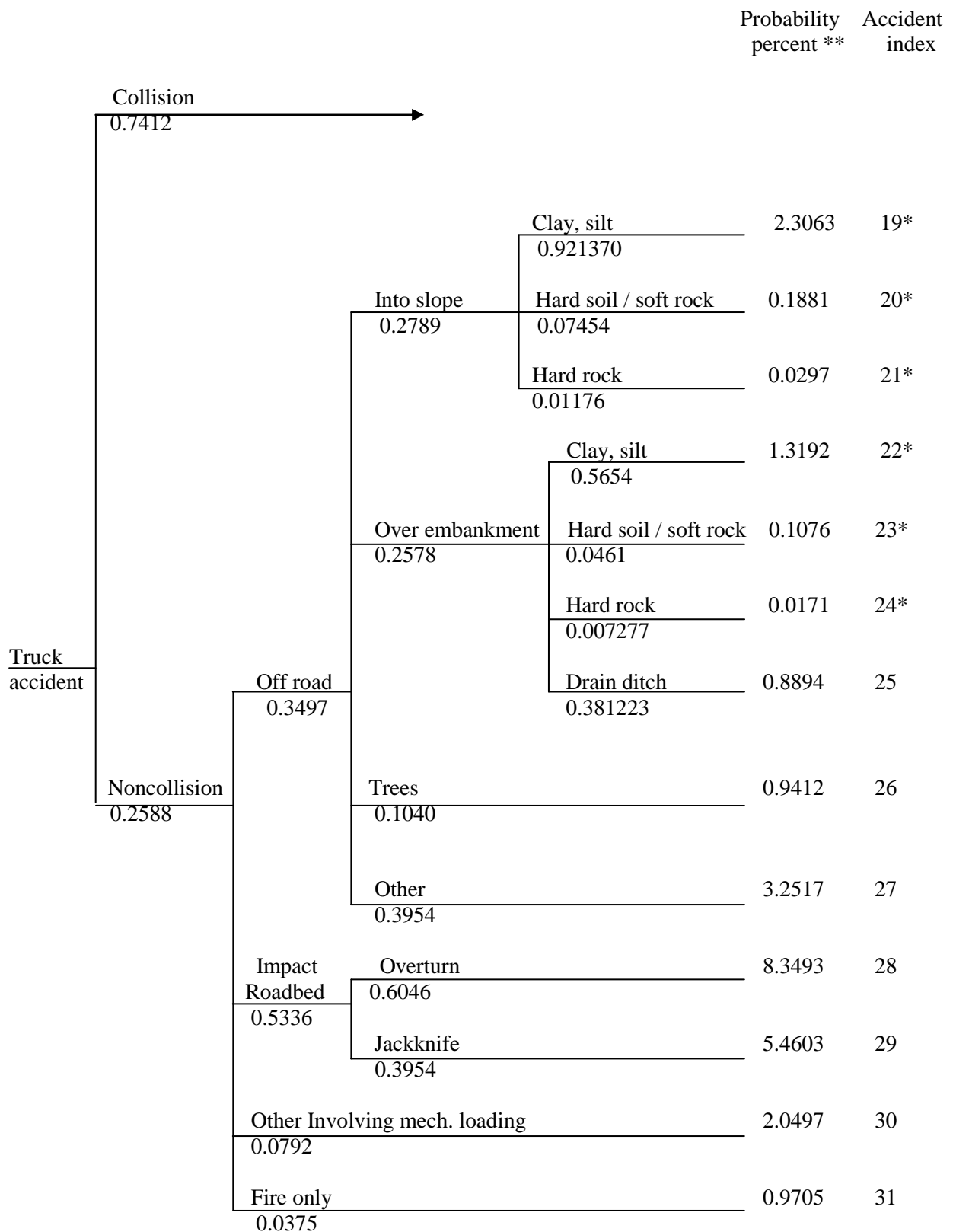


Figure 3 Truck accident scenarios and their percent probabilities.





\* Potentially significant accident scenarios

\*\* Conditional probability which assumes an accident occurs

Figure 4 (Continued)



## Appendix 4

### **Description on the consequences modeling process flow calculation for LPG transportation**

There are several factors need to be considered in order to calculate the risk of hazardous materials transportation during road tanker accident. Among the factors need to be considered is the frequency of accident whereby how often is the road tanker accident loaded with hazardous material can occur over a period of time. Other factors affected are consequences from the road tanker accident towards human and area vicinity.

The statistic information such as probability of accident from various causes (e.g. collision, overturn) collected for the road accident is based on the database information of major accident online likes Major Hazard Incident Data Service (MHIDAS), FACTS, United Nations Environment Programme (UNEP) and BUWAL transportation risk analysis guidelines. As further study, model equations which is introduced by CCPS by AIChE, and Green Book or Yellow Book Guidelines published by TNO will be used to predict the consequences of road tanker accident.

As in flowchart 1, it is showing the sequences of the rail tanker accident during transportation.

Level of road tanker catastrophic accident is depends on the type of product loading, the quantity and the condition of hazardous materials (HAZMAT) being stored during transportation. So, there are some parameters need to take into account in calculating the model of consequences such as heat capacity ratio of gas, ( $C_p/C_v$ ), hole size, ambient temperature and also the stored temperature in the tank, and its product molecular weight. The hole sizes analysis can be within 1.5'', 2'' – 6'' and 8'' – 12''. Normally, for road tanker case, they are using hole size of 8'' – 12'' and for tank truck case they are using 2'' – 6'' hole size. The hole sizes is varies from 5mm, 25mm, and 100mm in estimating the corresponding of gas release and it is noted that the hole size above 100mm will contribute to the catastrophic case.

For gas discharges through holes, Eq. (143) in Appendix 1 is integrated along an isentropic path to determine the mass discharge rate. This equation assumes an ideal



gas, no heat transfer and no external shaft work. However, majority of the gas releases from the road tanker occur from the hole size less than 25mm will initially be sonic or choked due to the pressure drop competition. The gas pressure release at upstream and downstream will decrease and until at one point, the velocity will reach its maximum level to flow on either side of the phase and this maximum velocity phenomenon is known as sonic or choked velocity. For instance, if the gas release at upstream, the maximum of mass flow will tend to flow at the upstream phase. Thus, Eq. (145) in Appendix 1 will be used in demonstrating the pressure ratio required to achieve choking condition. Whilst, the Eq.(144) in Appendix 1 will be used to calculate the consequence model of sonic gas discharge to the atmosphere.

For gases such as LPG is characterized as dense gas dispersion because the molecular weight of propane (content in LPG) is greater than the molecular of air at ambient surrounding. The released gas is then will move towards upwind and downwind direction according to wind velocity at that current time. Naturally, the gas disperses will directly down to the ground level. Thus, from this consequence, the downwind distance of the gas release travel can be calculated. There three options in calculating this model namely Raman box model [ 11 ], K -  $\epsilon$  theory model [ 11 ] and Britter and McQuaid model [ 11 ]. In this study, we are using Britter and McQuaid model [11] as in Eq. (161) till Eq. (164) in the Appendix 1, Table 4 and Table 5 in the Appendix 2, to approximate the curves in the model correlations for plumes and puffs condition. The rationale to used this model are because it is simple and easy model besides its ability in expecting precise and consistent prediction even though the gaseous release could be at rapid or continuous conditions.

Meanwhile, the rest models have their own weaknesses. For instance, Raman (1986) box model is not been chosen because any lack of data will tremendously affected the whole data. The parameters needed in running the calculation are thermodynamic process; gravity slumping and air entrainment which is difficult to obtained the exact results. While, for K -  $\epsilon$  theory model, it is only allow the prediction on flat terrain surface and no obstruction. Logically, our earth surface is filled with tress, building, vehicles and many more. Thus, this only complicates the problem of solving.

In calculating downwind distance using Britter and McQuaid Model [ 11 ], initial buoyancy ( $g_0$ ) of model Eq. (160) in Appendix 1, or generally known as at first velocity accelerate the gas cloud disperse to atmosphere is calculated. The gas



dispersion will then cover certain portion of circumstances and this is illustrated as source dimension by Gaussian et al.[ ] as in Eq. (151) till Eq. (156) in the Appendix 1 are used with both tables in Table 1 and Table 2 in Appendix 2, for type of continuous gas cloud release in determining the source dimension, for parameter,  $D_c$ . as in Eq. (161) in the Appendix 1. For further study, Eq.(163) in Appendix 1 will determine whether the value obtained from the previous equations is satisfactorily for dense densities of continuous gas cloud release at which it supposed to be more or greater than 0.15. If the value obtained satisfies the criterion, Table 4 as in Appendix 2, of Britter McQuaid model for dispersion of dense cloud plumes can be used in estimating the downwind distance. However if , the value obtained suitable in determining the downwind distance from puff cloud, Table 5 as in Appendix 2 equation can be refer in approximating the curve. While the gas disperses, any ignition to this flammable cloud gases, or satisfies zone within the range between the upper or the lower flammability limit before the cloud is diluted, a vapor cloud explosion.

There are four indications have been cited from AIChE of CCPS [11] of vapor cloud behavior in order for a vapor cloud explosion (VCE) to occur. The first indication is the release materials must be combustible. The second indication is the sufficient vapor cloud forming for it to ignite. The third indication for VCE to occur is the sufficient gas cloud within the flammable range. Lastly, the vapor flow undergoes the confinement place plus move in turbulence mixing. There are 3 methods in calculating the vapor cloud explosion (VCE), either by using TNT equivalent model, TNO multi-energy model or Modified Baker Model. Among of those methods, TNT equivalent model is practically been used because it is only requires an input parameters of mass of fuels and explosion efficiency. In additions, the ease of this model is also described by Baker et al (1983), Stull (1977) Decker (1974), and Lees (1986, 1996) and yet it is using widely in CPQRA[ ]. These parameters obtained also can be easily predicting the consequences of overpressure and impulse distance prior the vapor cloud explosion is known.

The input parameters needed in TNO multi-energy are type of confinement and relative blast strength. While, for Baker-Strethlow method requires chemical reactivity, geometry and obstacle densities. Both methods are difficult to determine vapor concentration profile due to the congested process area.



In determining VCE using TNT equivalent model, the mass and vapor gas cloud is estimated prior to calculate the TNT mass,  $m_{\text{TNT}}$  using as in Eq. (1) and Eq. (2). Then, the scaled distance,  $Z_e$  of Eq.(2) is used to estimate the explosion parameters such as scaled overpressure ( $p_s$ ), arrival time ( $t_a$ ), Impulse ( $I_p$ ) and duration ( $t_d$ ) during the road tanker accident. For further particular, the number of significant figures in CCPS [11] is used to obtain the correlation relationship between the explosion parameters and scaled distance,  $Z$ . Common structure of overpressure within 0 – 69 kPa have their own damages. For instance, 0.14 kPa of VCE consequence the rail tanker accident will contribute to annoying noise while the maximum overpressure will lead to catastrophic case by buildings destruction.

In determining overpressure using TNO multi-energy model, some standard procedure need to take into account and this is described in AIChE/CCPS [11]. The gas cloud result from gas release from hole size is examined by assuming no obstruction at affected circumstances and it is noted that the dense densities will directed to downhill..From the gas dispersion around the atmosphere, many potentials assumptions and possibilities need to figure out in predicting the strong blast within the source dimension areas. The potential strong blast could be at congested area likes chemical plant or refineries, multilevel car parking, and tunnels. Thus, by knowing the possible strong blast, energy absorb (E,J)at each source can be estimated by multiply the individual volume of mixture by  $3.5 \times 10^6 \text{ J/m}^3$ . Once the strong blast of potential source and energy combustion (E) is estimated, the Sachs scaled quantities of Eq. (3) in the Appendix 1, gives the blast side on overpressure,  $P_s$  as in Eq. (4) in the Appendix 1. Positive phase duration,  $t_d$ , the  $\Delta P_s$  and  $\bar{t}_d$  is read from the blast chart in CCPS [11].

While, for Baker-Strehlow Model the flame speed can be used to determine the interpolated pressure by referring Figure 1 impulse by referring Figure 2 as in Appendix 2. This model is the combination of TNO multi-energy Model in determining the energy term as the flame speed is reliant on chemical reactivity, obstruction and confinement. Particularly in this model, confinement is based on three symmetries namely as point-symmetry (3D), line-symmetry (2D) and plane-symmetry (1D). Point-symmetry is denoted as unconfined geometry and it is less pressure for free moving flame. Line-symmetry is illustrated as cylindrical flame between two plates for instance space beneath cars. Thus the moving flame effect is stronger than



point-symmetry. Last but not least, plane-symmetry is describing as planar flame in a tube for example tunnels. This flame moving will result on overpressure and impulse at catastrophic case.

Consequence of the road tanker accident also could result on pool fires wherein the beginning of the occurrence is due to thermal radiations from the flame source in the affected vicinity. The pool fires severity is dependent on the spill volume and fuel properties. Knowledge of the burning rate allows the heat output per unit area and the duration of the fire to be estimated (CCPS, 1992). The mass-burning rate is dependent on the diameter of the pool and the specific fuel type. For pool below 0.03 m in diameter, the flames are laminar, and the rate of burning decreases with increase in diameter. For large diameter ( $>1$  m) pools, the burning rate becomes independent of diameter; the flames are now fully turbulent (DOW, 1993). The mass burning rate for a particular fuel has been reported by following correlation, based on work of Babrauskas (1983), to relate the actual burning rate to the maximum burning rate for a fuel as in Eq.( 32) in Appendix 1. It can be seen that the burning rate asymptotes to a maximum mass burning rate at large diameters. This can be explained by assuming that vaporisation of fuel from the pool surface is due predominantly to radiation from the fire. As the flame grows it reaches a characteristic size at which it is said to have become optically thick and any further increase in size does not produce an increase in emitted radiation. Thus there is a diameter at which the radiative feedback to the pool surface reaches a maximum. The pool diameter at which this occurs varies with fuel type and thus  $k$  in Eq.(32) in the Appendix 1, values are also fuel dependent (Rew and Hulbert, 1996).

The pool surface area determines the shape of the radiation source, in case of pool fire. For circular pools the source can be considered cylindrical (TNO, 1992). In most cases, pool size is fixed by the size of release and by local physical barriers (e.g., dikes, sloped drainage areas). For a continuous leak, on an infinite flat plane, the maximum diameter is reached when the product of burning rate and surface area equal the leakage rate. Critical pools are normally assumed: where dikes lead to square or rectangular shapes, an equivalent diameter may be used (Andreassen, 1992).

For unconfined continuous releases, it can be assumed that the pool increases in diameter until the release rate is balanced by the burning rate (Rew and Hulbert, 1996) as in



Eq (33) and in Eq. (34) in Appendix 1. The Thomas (1963) correlation as in Eq.(35) in Appendix 1, is widely used for models which use a mean surface emissive power over the entire envelope. The correlation based on the dimensionless mass burning rate of the fire under quiescent conditions.

Heat transfer from fires incident includes both thermal radiation heat transfers from the flames to the surrounding objects as well as convection heat transfer. Convection heat transfer from the flames to engulfed objects is important particularly in calculating the response of boundaries to the fire (Kashef *et. al.*, 2002). Thermal radiation is considered one of the more dramatic hazards related to hydrocarbon pool fires. According to Mudan *et al.*, (1995), the quantification of the thermal properties of fires can be accurately obtained from basic principles that consider the mixing dynamics and the chemical processes of burning fuel with the oxygen in air. Estimating thermal radiation field surrounding a fire involves determining the burning rates, the physical dimensions and radiative properties of the fire and, the radiant intensity at a given location.

Basically, there are two models in calculating the fire radiation effects which are Solid Plume Radiation Model and Point Source Radiation Point Source Model is more simplicity compare to solid plume radiation.

In point source model, the surface emitted power is based on total combustion energy release and may ends to BLEVE consequence. Schulz-Forberg et al (1984) had discussed about the BLEVE consequence and this is supported by Baum (1984) in defining the missiles velocities from vessel bursting. Prior proceeding to BLEVE calculations, the incident radiant flux should be determined first. Radiant fraction from the energy release due to accident crushed can be referred in Mudan and Croce (1988) discoveries by divided the radiated power by flame of surface area. The radiant fraction propane (content in LPG) is 0.30. Then, Eq.(17) in Appendix 1 is used to estimate the point source where the road tanker accident occurred. Gas release from the point source will cause the thermal radiation absorbed throughout the atmosphere at the affected vicinity. Pietersen and Huerta (1985) have developed a correlation of Eq. (13), Eq. (14) and Eq. (11) in the Appendix 1 in determining the atmospheric transmissivity which recommend a correlation formula that accounted humidity. The path length, and distance from the flame surface to the target is calculated using



Eq.(15) as in Appendix 1. Finally, the thermal flux of Eq. (9) is calculated using surface emitted flux as in Eq. (16) prior the BLEVE catastrophic happened.

BLEVE is a sudden release of a large mass flow of pressurized superheated liquid to the atmosphere from the rupture pressure vessel. From CPQRAs said, “The beginning incident of the occurrence is the external flame or pool fire has impinging near the shell vessel above the liquid level, weakening the container and leading to a sudden bursting vessel”. The blast wave produced by the BLEVE is dependent on type of fluid release, rate of energy release, shape of vessel, type of rupture and the reflecting surfaces at the affected vicinity. The input data required in approximating the BLEVE severity is the amount of fuel carried during transportation, atmospheric humidity, material heat of combustion and the vapor pressure.

Eq. (5) till Eq. (8) are used to correlate the BLEVE diameter and the combustion duration.. These equations are used widely in estimating BLEVE consequence from the flammable materials. In addition, consequences from the blast wave of the BLEVE and VCE have leading to human injury in the vicinity and the geometric view factor of Eq.(17) as proposed by Pietersen and Huerta [ ] and the radiation fraction as given by Robert [ ] is equal to (0.25-0.4) are used to determine the oriented target of road tanker accident. Thus, the gas release from the estimated geometric view factor is then been used in determining the emissive radiative flux received by a black body receptor as in Eq. (9) in the Appendix 1. Solid Plume model presents the most recent analysis techniques for evaluating the blast (overpressure, impulse, etc.), time-dependent thermal radiation, and missile generation consequences of a BLEVE event. In this model, the thermal radiation generated from a BLEVE fireball is assumed as a spherical ball that rises into the air as the flammable material is burned. The time-dependent diameter and height of the fireball and the duration of the fireball are estimated using empirical relationships. The duration of combustion ( $t_d$ ) for the BLEVE fireball is estimated using (Martinsen and Marx 1999) model as in Eq. (19) in the Appendix 1, where  $t_d$  is in sec and  $M_{FB}$  is the mass of released flammable material in the fireball in kg. The fireball diameter is time-dependent. Based on experimental observations, the fireball tends to reach its maximum diameter during the first third of the fireball duration. At this point, the fireball tends to rise into the air and the diameter remains constant until the fireball dissipates. Martinsen and Marx



(1999) present an Eq.(20) in the Appendix 1, for estimating the fireball diameter during the growth phase.

At the end of the growth period, the fireball is assumed to achieve its maximum diameter ( $D_{\max}$ ) as given by the following equation (Roberts 1981-1982) as in Eq.(21), where  $D_{\max}$  is in m. The initial ground flash radius ( $R_{f_{\text{lash}}}$ ) associated with a BLEVE fireball is approximated using an Eq. (22). This radius represents the distance that may be engulfed in flames during the initial development of the BLEVE fireball. The height of the center of the fireball is also time-dependent. Based on experimental observations (Martinsen and Marx 1999) the center of the fireball rises at a constant rate from its lift-off position to three times the lift-off position during the last two-thirds of the fireball duration. This leads to the following equations for the height of the center of the fireball ( $H_{\text{FB}}$ ) as in Eq. (23) and Eq.(24) in the Appendix1.

The thermal radiation emitted from the surface of the fireball is also time-dependent. The fireball surface emitted flux is assumed to be constant during the growth period, and then is assumed to linearly decrease from its maximum value to zero during the last two-thirds of fireball duration. The maximum surface emitted thermal flux ( $E_{\max}$ ) during the growth phase is given by the following (Martinsen and Marx 1999) as in Eq.(25) in the Appendix 1, where  $E_{\max}$  is in  $\text{kW/m}^2$ . Fire research suggests that the maximum surface emitted flux  $E_{\max}$  will not exceed some upper limit ranging from 300 to 450  $\text{kW/m}^2$ . A value of 400  $\text{kW/m}^2$  is suggested as a limiting value (Martinsen and Marx 1999). Therefore, the lesser of the surface emitted flux given by Equation 16 or 400  $\text{kW/m}^2$  should be used. During the last two-thirds of the fireball duration, the surface emitted flux (ES) is given by Eq. (27) as in Appendix1. The thermal flux incident upon a target object is a function of the geometric view factor between the fireball and the target. For a target at ground level, the maximum geometric view factor (F) for a spherical emitter is given by Eq. (28) as in Appendix 1, where F is dimensionless and D,  $H_{\text{FB}}$ , and x are in m.

The atmospheric transmissivity (g) between the fireball and the target is estimated from Eq. (29), where g is dimensionless, R is the fractional relative humidity (e.g., for 70% relative humidity, R is 0.7), and  $P_v$  is the saturated vapor pressure of water at the ambient temperature in Pa.



In order to estimate the consequences of an accident on people and the damage caused by the accident, the best method is probit analysis. Usually, the method used is the probit analysis, which relates the probit (from “probability unit”) variable to the probability. The probit variable  $Y$ , is a measure of the percentage of a population submitted to effect with a given intensity ( $V$ ) which will undergo certain damage. This variable follows a normal distribution, with an average value of 5 and a normal deviation of 1.

Abramowitz and Stegun (1965) have given a rational approximation for digital computation as in Eq. (43) till Eq. (53). Most of the previous works about probit analysis have been given by Finney, (1971); Eisenberg *et. al.*, (1975); TNO, (1990); Weber, *et. al.*, (1990); Schubach, (1995); Casal, *et. al.*, (1999) and Vélchez, *et. al.*, (2001).

In short, this procedure should be carried out in approximating the thermal impact in order to predict the level of injury and number of fatality from a specified radius circumstances affected.



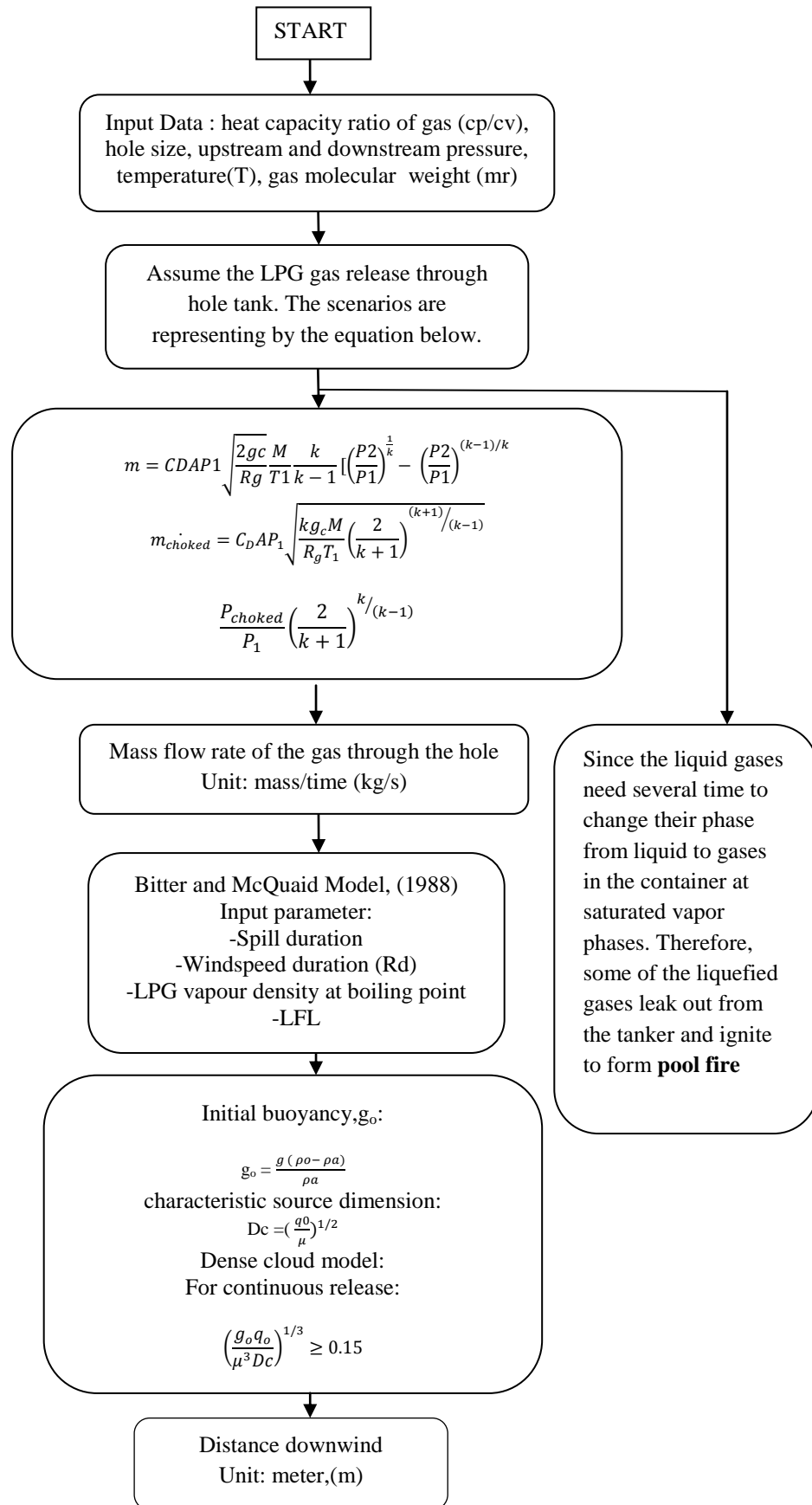
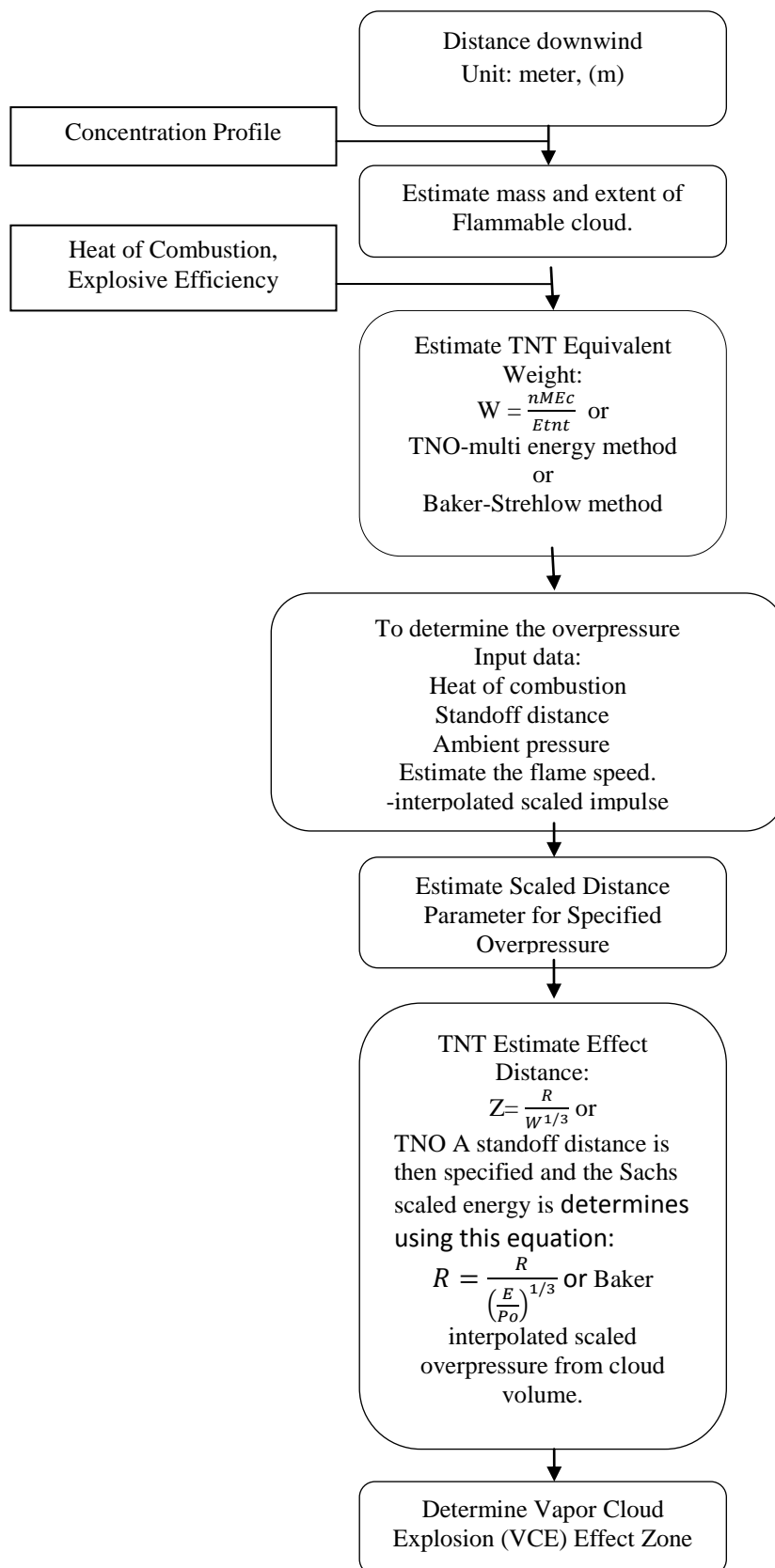
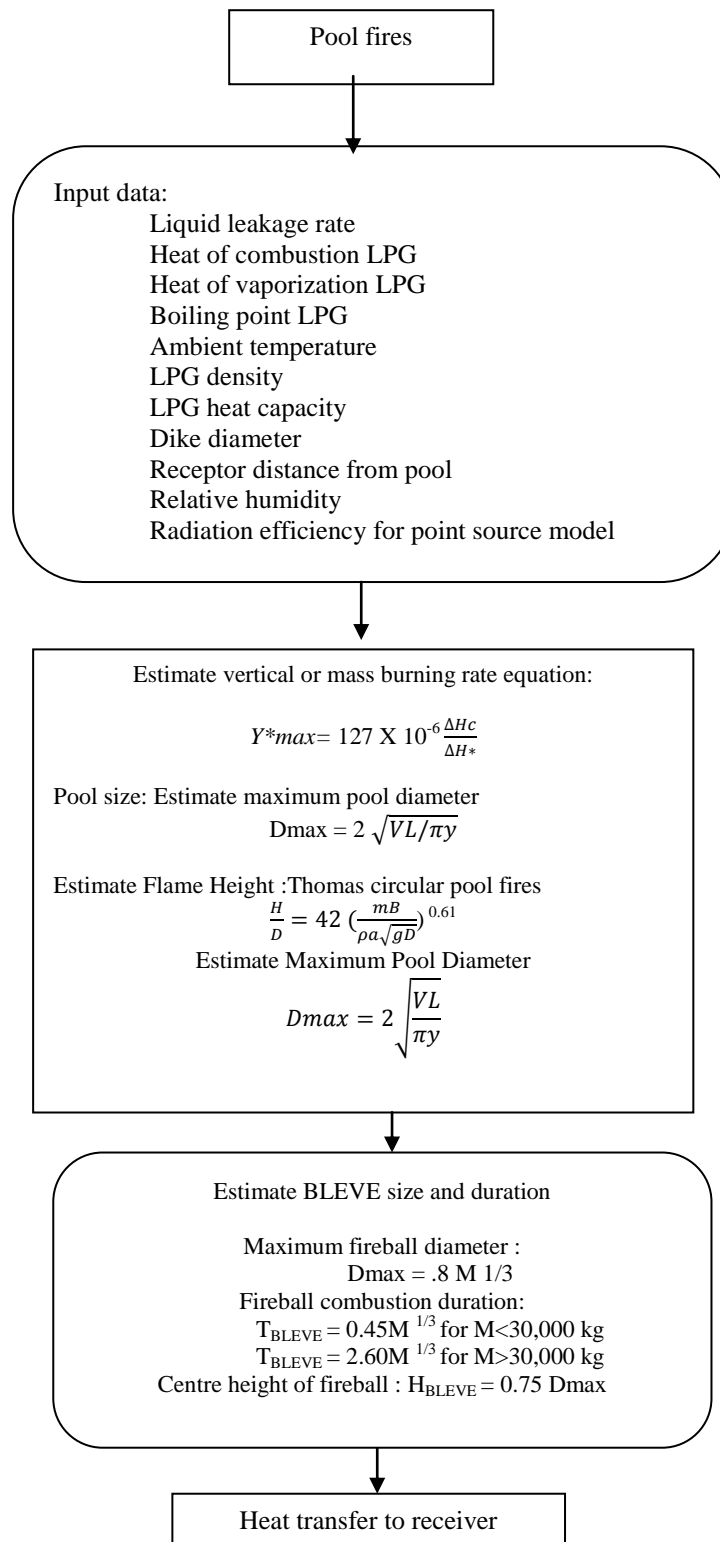


Figure 1 Flowchart of Tank truck accident Analysis carrying hazardous materials

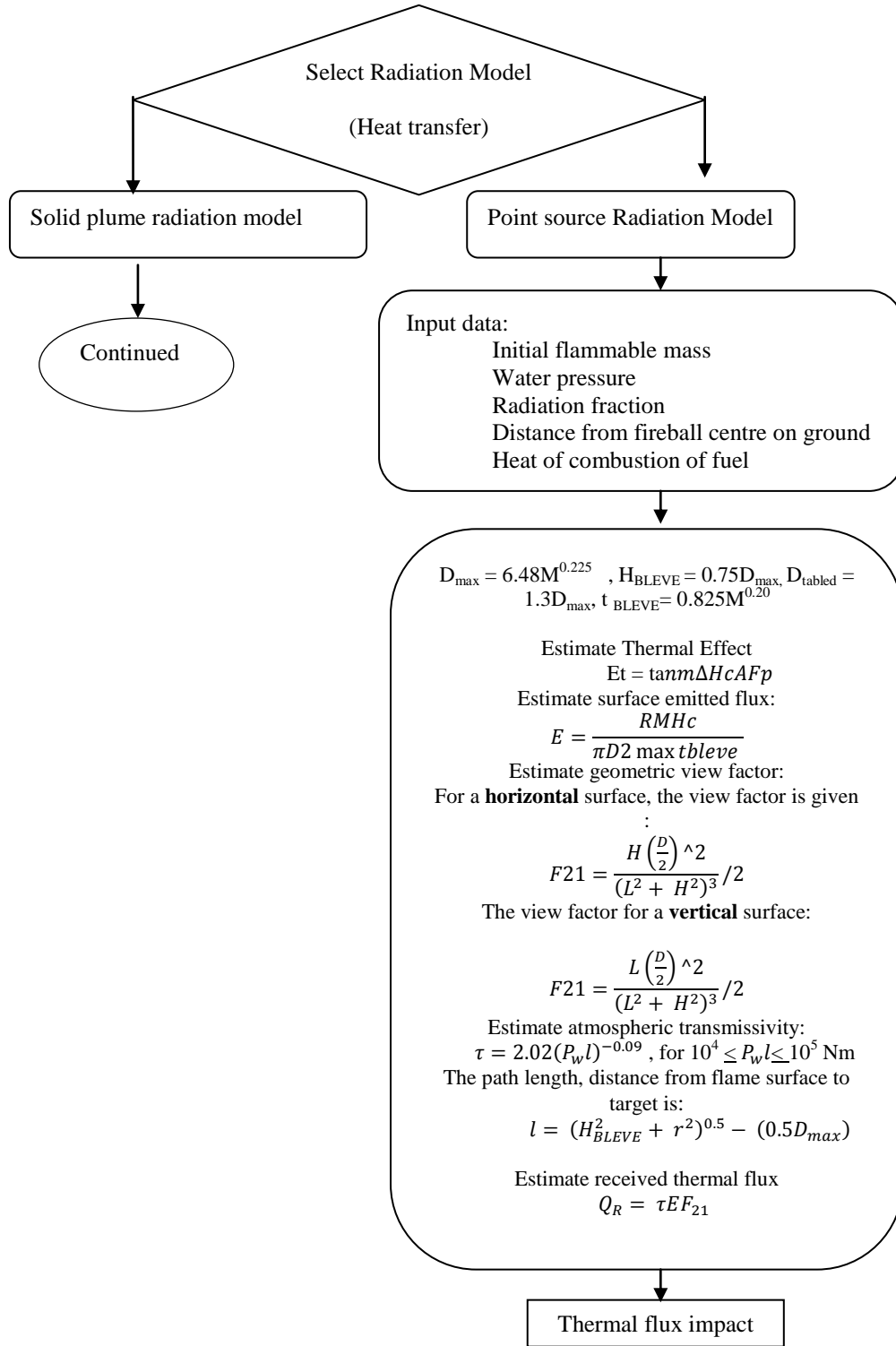




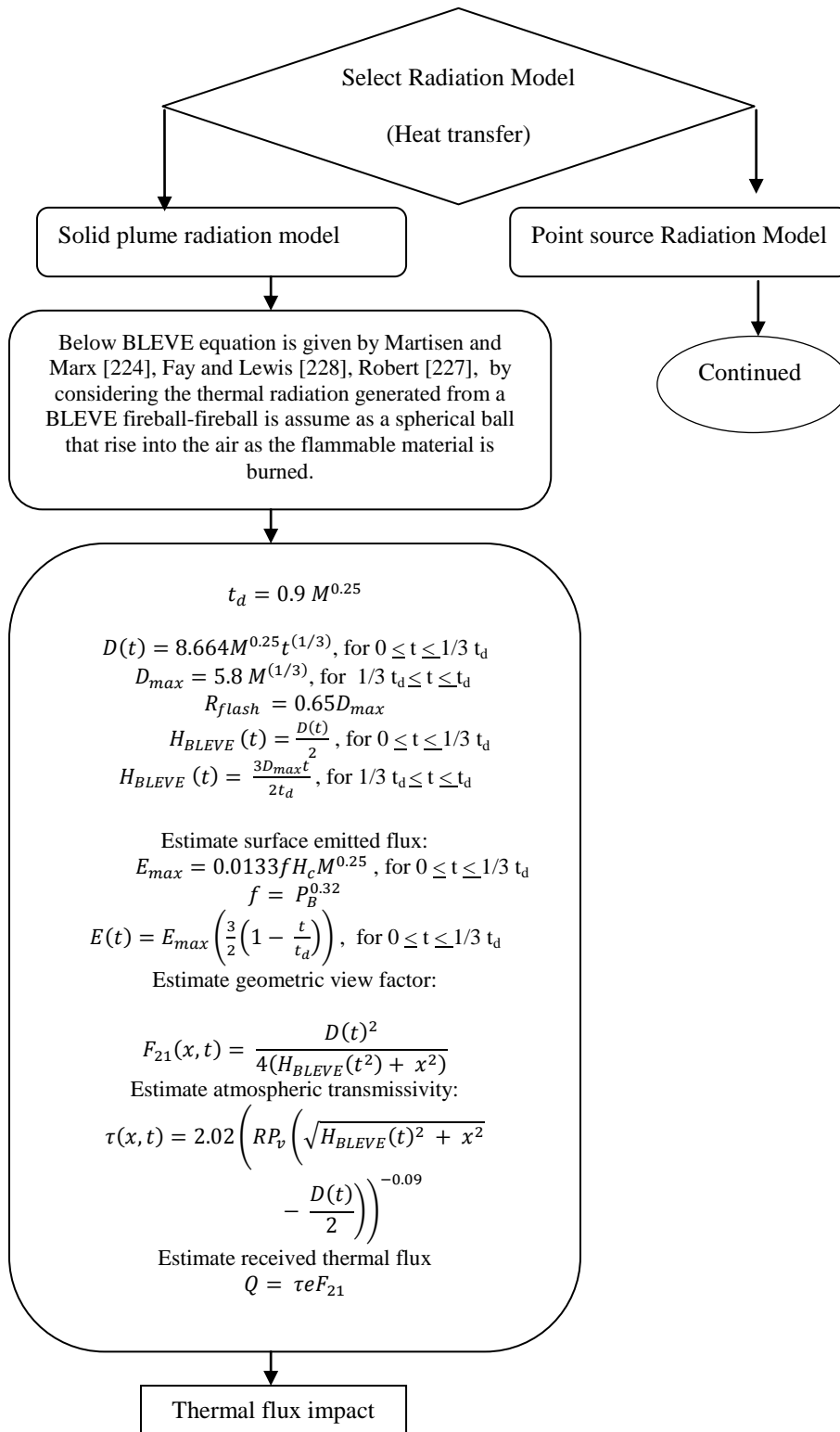




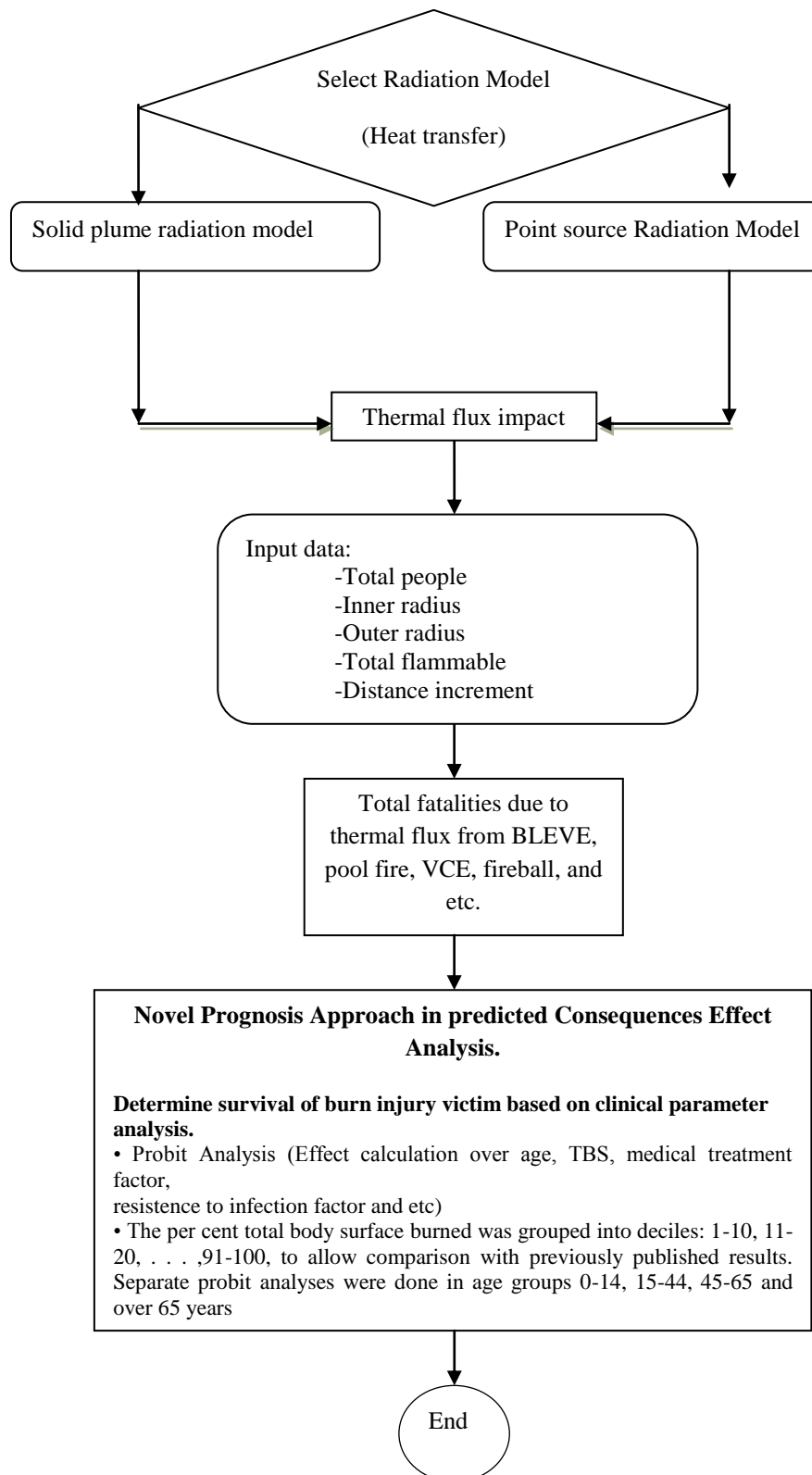














## Unconfined and Confined Vapour Cloud Explosions

An unconfined vapour cloud explosion (UVCE) is the result of a unique sequence of events UVCE can be both very spectacular and very dangerous. This is because the leak is into the open air, and with the right meteorological conditions, truly large clouds of combustible mixture can be produced before ignition occurs. Confined vapour explosions (VCEs) is defined as explosions within tanks, process equipment, pipes, in culverts, sewage systems, closed rooms and in underground installations. UVCE was used to describe explosions in open areas such as process plants. The main distinction between confined and unconfined explosions is confined explosions are those occur within some type of containment. Often the explosion is in a vessel or pipework, but explosions in buildings also come within this category [64].

Models of VCE have been discussed in many articles. The most common models are: TNT, TNO and TNO Multi-Energy models. The TNT equivalent model has been widely used to model the vapour cloud explosions. An early application was that of Brasie and Simpson (1968), who used it to study the damage from three accidental explosions. The TNT model was also used by Decker (1974), Stull (1977), Baker *et al.* (1983) and Lees (1996). The TNT model is well established for a high explosion and it is applied in flammable vapour clouds (CCPS, 1994). Crowl and Louvar (2002) used TNT method to estimate the damage for common structures and process equipment whereby this damage is a result of the explosion. The explosion involves peak overpressure and flammable material. Three models of explosion have been developed by TNO. The first of these is the shock wave model described in the TNO yellow book (TNO, 1992). The Netherlands Organization for Applied Scientific Research (known as TNO) published a book entitled *Methods for the Calculation of the physical Effects of the Escape of Dangerous Material*, which outlines models to be used for calculating the consequences of many types of hazardous release scenarios. This model is applicable to most flammable materials of medium reactivity. It allows the peak overpressure and the duration time of the explosion to be estimated. The second TNO model is the correlation model; this is described in the TNO yellow book (TNO, 1992). This model allows an estimate to be made of the radius of defined damage circles. It does not give explosion parameters such as peak



overpressure or duration time. The third TNO model is the Multi-Energy model described by van den Berg (1985) and updated model in 1996. This model allows the peak overpressure and duration of time to be estimated. The TNT equivalent model is easy to use. Neither it, nor the TNO model, is solidly based on theory, but they predict well the observed UVCE incidents. In the TNT approach an explosion yield must be selected. A weakness of the TNT model is the substantial physical difference between detonations and UVCE deflagrations. The TNO correlation model is based on actual UVCE incidents and employs one of two defined explosion yields, but it is limited to flammable materials of medium reactivity. The TNT model has the advantage of being easy to use. It considers the uncertainty of the calculations to determine the amounts of a flammable release, efficiency factors, and the impact of wind velocity on the vapour cloud (CCPS, 1994).

Baker-Strehlow Method was developed to provide estimation of blast pressure from vapour cloud explosions. The methodology consists of a number of steps, i.e. assessing flame speed, fuel reactivity, confinement, and etc. The blast pressure and impulse are then read from a series of graphs.

### **Boiling Liquid Expanding Vapour Explosion (BLEVE)**

A Boiling Liquid Expanding Vapour Explosion (BLEVE) is the explosive release of expanding vapour and boiling liquid when a container holding a pressure-liquefied gas fails catastrophically. Catastrophic failure means that the tank is fully opened to release its contents nearly instantaneously. In most cases, this means that the tank is flattened on the ground after the BLEVE (Birk and Cunningham, 1996). BLEVE occurs when there is a sudden loss of containment of a pressure vessel containing a superheated liquid or a liquefied gas. The primary cause is usually an external flame impinging on the shell of a vessel above the liquid level weakening the container and leading to sudden shell rupture. If the released liquid is flammable, a fireball may result. The resulting thermal radiation is intense and has the potential to cause severe health-damage even loss of life as well as other material damage.(Papazoglou and Aneziris, 1999).



In a BLEVE the hazardous loadings are liquefied gases such as LPG, ammonia, chlorine, and vinyl chloride. These materials are gases at atmospheric pressure and normal temperature but are liquefied by pressurization for storage and transportation. However, there are some hazardous liquid materials such as methanol, propanol, and acetone that are flammable and used as fuel and raw materials in chemical plants. These liquids also have a potential to cause catastrophic damage if an accident occurs. Birk and Cunningham (1996) described the mechanism of occurrence of BLEVE. Heating of a closed vessel in a fire leads to elevation of the temperature of the liquid to values exceeding the normal boiling temperature. The vapour pressure is increased to a value much greater than atmospheric pressure. Heating of the walls of dry tanks causes reduction in the tensile strength of the metal, leading to destruction of the tank. A rapid pressure decrease causes propagation into the liquid of a rarefaction wave, which is followed by a liquid boiling wave with the associated pressure elevation.

The steps below show the conditions that produced the BLEVE from the propane storage tank :

- After the propane begins leaking from the tank and flows along the ground surface.
- Soon after ignition of the leaking propane, a fire burns out of control in the vicinity of the tank.
- The fire heats the propane inside the tank, causing it to boil and vaporize.
- The pressure inside the tank increases as the temperature of the propane increases.
- When pressure inside the tank reaches about 250 *psi*, the relief valves open to vent the tank. The propane escaping from the relief valves ignites and burns.
- As boiling continues, the pressure inside the tank exceeds 250 *psi*, the temperature of the tank wall increases, and the strength of the steel used to construct the tank decreases.



- At some point, the weakened steel can no longer resist pressure-induced forces inside the tank so the wall of the tank ruptures, allowing propane to escape rapidly into the surrounding atmosphere.
- Immediately following rupture, the escaping propane ignites, resulting in an explosion that causes the tank wall to separate to numbers of pieces. Fire quickly consumes the remaining propane.
- Tank fragments are propelled at a high velocity in many different directions.

Lees [64] states that the cause and effects of a BLEVE depend on whether the liquid in the vessel is flammable or not. In all the cases the initial explosion may generate a blast wave and missiles. If the material is flammable, it may cause a fire, which radiates heat or may form a vapour cloud, which then gives rise to a second explosion. Lees [64] also indicated that the BLEVE can occur with both flammable and non-flammable materials, such as water. In all cases the initial explosion may generate a blast wave and missiles. The best-known type of BLEVE involves LPG. Once a fire impinges on the shell above the liquid level, the vessel usually fails within 10-20 *min*. Birk *et al.* (1993) and Birk and Cunningham (1996) conducted a series of medium scale tests using 320 and 400 litre automotive propane tank. The tests involved exposing instrumented test tanks filled with 80% liquid propane. The authors defined a BLEVE as the explosive release of boiling liquid and expanding vapour resulting from the catastrophic failure of a vessel holding a pressure liquefied gas. Three types of tank failure were categorized based on observing the event and outcome of tests. The authors suggest that the BLEVE event can be explained by using simple thermodynamics and stress analysis. The authors performed and described a tank deformation analysis, a BLEVE mechanism and the factors related to the consequences from a BLEVE hazards, including the suggestions for emergency response.

Lees (1996) has considered some features of BLEVEs from an empirical viewpoint, the time of BLEVE, the model of rupture, the blast effects, the fireball, the missiles and the



release of flammable fluids. Time of BLEVE defined as the time between the occurrence of the engulfing or torch fire and BLEVE. For storage vessels the time to BLEVE has been of the order of 5-30 min. Blything (1986) studied the horizontal cylindrical storage vessel holding butane, with actual capacity of 75 tonnes. The time of BLEVE is between 4 and 48 minutes. Time to BLEVE for tanks in transport accidents, particularly rail tank have also been mainly in the range 5-30 minutes (Lees, 1996).

The vessel can lead to rupture if it is exposed to overpressure, mechanical failure and fire engulfment (Birk, 1995). The overpressure can be calculated from any of these methods, TNT, TNO, Strehlow, and Congestion Assessment Methods. The mechanical failure of vessel occurs, which may be due to a metallurgical defect, corrosion or impact [64]. Failure due to fire engulfment is a typical scenario of a BLEVE.

The blast wave is the result of an explosion in air that is accompanied by a very rapid rise in pressure. Pressure effects are usually limited in magnitude and are thus of interest mainly for prediction of domino effects on adjacent vessels and equipment rather than to cause harm to neighbouring communities. The blast wave generated by a BLEVE event may cause building damage or personnel injury. Personnel may be injured as a result of direct or indirect effects of a BLEVE. Direct effects result from direct exposure to the blast wave generated from a BLEVE. For example, eardrum rupture and lung haemorrhage can occur from direct exposure to excessive overpressures. The missiles may occur in any incident involving high pressure gases or superheated liquids. These can travel to distances up to the order of kilometres. Missiles are considered physical hazards which will be discussed as below.

### **Physical Explosion**

Physical explosion occurs when two liquids at different temperatures are violently mixed or a finely divided hot solid material is rapidly mixed with a much cooler liquid. No chemical reactions are involved; instead, the explosion occurs when the cooler liquid is converted to vapour at such a rapid rate that localized high pressures are produced (Baker *et. al.*, 1983). The physical explosion usually results from the production of large volumes of gases by non-chemical means, or the sudden release of gases already existing. They can be as destructive and dangerous as an explosion resulting from chemical



reactions. The outcome of explosions depends on the nature of the explosion. If no ignition occurs and vessel rupture results due to overpressure, the explosion is considered to be a physical explosion and shock wave and projectiles are the consequences. When this occurs, there is maximum amount of energy found in the bursting vessel waiting to be released. Basically there are two kinds of projectiles from BLEVEs:

- Primary projectiles which are major pieces of the tank and
- Secondary projectiles which are generated by the acceleration of nearby objects (attached pipe, support legs, other attachments, adjacent structures or objects, etc.).

Objects or their fragments may be turned to missiles as a result of energy delivered to them by an explosion and can cause significant damage to the bodies they hit. Typically a BLEVE involving a ductile steel tank will result in only a few primary projectiles (typically less than five, as reported by Baum (1998) depending on the strength of the BLEVE and the design of the tank). The risk of the small projectiles is often low. However, if a large projectile impacts there is a good chance for a domino event to result. It would usually be assumed that being hit by a large projectile will result in death or severe damage to construction. A calculation for hazards posed by pieces of metal tank that are scattered when a tank ruptures are difficult to quantify and it can be made to estimate the amount of energy released when the rupture occurs. However, uncertainties concerning how much of this energy is transmitted to the metal tank pieces, size and weight of fragments, etc., are of such a magnitude that one can have little confidence in the prediction of hazards due to flying fragments or rocketing tubs. The direction is difficult to predict but there is some evidence that cylindrical vessels tend to be more likely to travel in the direction of their longitudinal axis. The risk of missile damage is often low because the probability of being hit is very low. However, if a large missile impacts there is a good chance for a domino event to result. It would usually be assumed that being hit by a large missile will result in death or severe damage to construction. There are basically many kinds of projectiles from BLEVEs:

- Primary projectiles from the casing,
- Projectiles from the vehicle.



- Projectiles ejected from the carter,
- Secondary projectiles set in motion by the blast.
- Falling masonry and glass, and
- Flying glass.

In many process plant installations, the system contains cylindrical vessels which contain high pressure, high temperature fluids. If a pressure vessel does rupture, missiles (i.e. fragments), shock wave and energy may be generated and equipment in the vicinity is put at risk. The energy release in a chemical explosion is considered first high explosive and then flammable gases and fluids. Explosion can also be caused by gas or liquid under high pressure. The physical energy may take such forms as pressure energy in gases, strain energy in metals or electrical energy. The important physical form is thermal energy (Less, 1996). Bjerketvedt *et al.* (1997) defined a shock wave as a fully developed compression gas wave of large amplitude, across which density, pressure, and particle velocity change drastically. A shock wave propagates at supersonic velocity relative to the gas immediately ahead of the shock. The propagate velocity of the shock wave depends on the pressure ration across the wave. Increasing pressure gives higher propagation velocity. Lees (1996) defined the shock wave as a very rapid rise in pressure, and the shape of this pressure profile near the centre of the explosion depends on the type of the explosion involved. The initial shape differs for explosions of high explosives, nuclear weapons and flammable vapour clouds. The initial pressure profile for nuclear explosion is probably the most readily defined. The pressure at the edge of the fireball is approximately twice compared to that at the centre. The most common models to calculate the shock waves are the TNO, TNT and Baker-Strehlow models.

## **Fire**

The major hazards which the chemical industry is concerned are fire, explosion and toxic release. Fire is most common but explosion is more significant in terms of its damage potential. Toxic release has perhaps the greatest potential to kill a large number of people. Fire is normally regarded as having a disaster potential less than explosion or toxic release. Fire, or combustion, is chemical reaction in which a substance combines with



oxygen and heat is released. Usually fire occurs when a source of heat comes in contact with a combustible material. There are three conditions essential for a fire: fuel, oxygen and heat. If one of the conditions is missing, fire does not occur and if one of them is removed, fire is extinguished (Less, 1996). Fuel can be in solid, liquid, or vapour form, but vapour and liquid fuels are generally easier to ignition. The combustion always occurs in the vapour phase; liquids are volatilised and solids are decomposed into vapour before combustion (Crowl and Louvar, 2002). Fire is normally the result of fuel and oxygen coming together in suitable properties and with a source of heat. The consumption of a material by fire is a chemical reaction in which the heated substance combining with oxygen.

Within the petrochemical industries, many flammable gases are stored as liquid under pressure. Flammable gases are usually very easily ignited if mixed with air. Flammable gases are often stored under pressure, in some cases as a liquid, whereby even a small leak of a liquefied flammable gas from relatively large quantities of gas, which is ready for combustion. The major distinction between fires and explosions is the energy release rate. Fires release energy slowly, whereas explosion release energy rapidly in the order of microseconds. Fires can also result from explosions, and explosions can result from fires (Crowl and Louvar, 2002). Fires can take several different forms, including flash fires, jet fires, pool fires, and fireball. A jet fire would appear as a long narrow flame produced. A pool fire would be produced if a material release from a storage tank into a bund ignited. A flash fire could occur if an escape of gas released a source of ignition and rapidly burnt back to the source of the release.

### *Flash Fires*

A flash fire is a non-explosive combustion of an unconfined vapour cloud resulting from a release of flammable fuel into the atmosphere, which, on mixing with air, ignites. On ignition, the fire propagates through the vapour cloud and burns as a flash fire. A flash fire occurs when a vapour cloud, formed from a leak, is ignited without creation of significant overpressure. Such flash fires are not uncommon in chemical process industries. If the ignition is prompted the cloud may be modest in size, but if the cloud



has time to spread over an appreciable part of the site and is then ignited, a major vapour cloud fire may result.

Generally the damage caused by flash fires is less widespread or spectacular than that caused by “Vapour Cloud Explosions” (VCEs), and in many cases it is not clear whether a flash fire develops into a VCE or not.

### *Jet Fire*

A jet fire occurs when flammable gas emitting from a pipe or equipment then ignited and burns on the orifice (Lees 1996). A jet fire may result from a high-pressure leakage of gas from process plants or storage tanks. Storage tanks or process vessels containing, for example LPG which is exposed to an enveloping fire, after a very short period of time vent their contents through a relief valve. If the released gas is ignited, a jet fire may occur (Andreassen, *et al.* 1992). Jet flames can occur in chemical process industries, either by design or by accident. They occur intentionally in burners and flares. Ejection of flammable fluid from a vessel, pipe or pipe flange can give rise to a jet flame if the material ignites.

### *Pool Fire*

Pool fires can occur when a significant quantity of liquid is released and immediately ignited. A pool fire may also occur on the surface of a flammable liquid spilled onto water. These can be confined or unconfined. Pool fires are a result of spillage or leakage from tanks, pipelines, or valves. A pressurised release of either vapour or two-phase mixture may result in a fire whereas the momentum from a liquid release is more likely to be destroyed, and the release will form a pool fire. A pool fire is a type of turbulent diffusion flame, which burns above a pool of vaporising fuel where the fuel vapour has negligible initial momentum. Many industrial fires involve hydrocarbon fuels. Depending on the release rate and ignition of these fuels, various types of gas or liquid pool fires may occur. Event trees, which provide guidance as to which type of fire will occur for a given set of ignition and release conditions, can be found in fire protection engineering handbooks. A confined pool fire is one in which there is a dike or other barrier that does



not allow the fuel to spread beyond a certain diameter, whereas an unconfined pool fire is a fire where there is no barrier to prevent the fuel from spreading. Pool fires may also be classified on the basis of the rate and duration of the spill of fuel that burns. An instantaneous pool fire is a fire in which the spill of fuel occurs in a very short period of time, while a continuous pool fire is a fire in which the spill of fuel occurs at a given rate for a relatively long period of time. There are many experimental works done related to pool fire in the last century. Most work of pool fire deals with circular pools. A particular type of circular pool fires is the storage tank fire (Lees, 1996). Much of the early work was done on relatively small diameter pool fire. Subsequent studies indicate that the effect of pool diameter is important and that it is preferable to carry out studies on large pool fires. This initial works appeared to focus and concentrate on determining the liquid burning rate of heat transfer to the liquid surface and of the fraction of heat radiated. Experimental studies on these aspects were conducted by by Blinov and Khudiakov (1957). This work covered a wide range of pool diameters.

### *Fireball*

Another significant fire hazard is that from fireballs. A fireball occurs when there is a release of some considerable violence and vigorous mixing and rapid ignition take place. The fire is burning with sufficient rapidity as to cause the burning mass to rise into the air as a cloud or ball. The sudden release of superheated flammable liquid from a storage tank or process vessel is the beginning of a complex event that often ends in the formation of a short-lived fireball. The event starts with a major failure of the container. Because the pressure in the container is greater than atmospheric pressure, much of the liquid is quickly expelled into the atmosphere. In response to this rapid drop in pressure, a portion of the liquid flashes to vapour nearly instantaneously. This vapour expands rapidly, shattering some of the remaining liquid into small drops, thereby creating a turbulent aerosol cloud consisting of vapour, liquid drops, and air (Martinsen and Marx, 1999). Ignition of this cloud creates a fireball that grows rapidly until it reaches its maximum size. The fireball becomes buoyant and lifts off the ground as the heat of the fire vaporizes the liquid drops and increases the temperature of the remaining mixture of vapour, air and reaction products. As it rises, the limited fuel supply is consumed and the fireball ceases to exist (Marx and Martinsen, 1999).



The fireball grows larger and moves upward continuously because of buoyancy. The duration of the fireball is small (<40 sec), but the radiation levels are intense e.g. the radiation at fireball surface can be up to  $200 \text{ kW/m}^2$ . Within the radius of the fireball there will be severe damage to process equipment and buildings. Beyond this, the danger is mainly for the people that may be affected by the radiation. Therefore, the fireball radius is defined as the domino effects radius (Petrolekasa and Andreoub, 1999).

### **Toxic Release**

The third of the major hazards is the release of toxic chemicals. The hazard presented by a toxic substance depends on the conditions of exposure and on the chemical itself. It ranges from a sudden brief exposure at high concentration to prolonged exposure at low concentrations over a working life (Lees, 1996). Toxicity is a general term used to indicate adverse effects produced by poisons. These adverse effects can range from slight symptoms like headaches or nausea, to severe symptoms like coma and convulsions or death.

The worst accident in the history of the process industries occurred on the third December 1984 at Bhopal, where water entered a storage tank of methyl isocyanate, causing overheating and release of methyl isocyanate vapour which spread over a shanty town close to the works and killed some 4000 people. There have been a number of major accidents involving chlorine. A list of major chlorine accidents world-wide has been provided by Lees (1996).



## Appendix 5

Delete

Reply

Forward

Spam

Print

Confirmation of your inquiry 1

772

39

37

1

+

Dear Ms. / Mr. zulkifli abdul rashid,  
We have received your email. It has been forwarded to the correct contact within TNO: Mr. / Ms. J.V.Q. (Victor) van Swinderen

You will receive a reaction as soon as possible.

If you have not received a response after five days, please contact the TNO Infodesk: [wegwijzer@tno.nl](mailto:wegwijzer@tno.nl)

Your question was:

I am interested with your product which provide a comprehensive risk assessment tool. As a person involve in EIA consultancy work the tool is essential this is especially in matters related to the impact of a particular activity toward population around it and environment. For the effect tool there is availability to measure thermal radiation from BLEVE. Does it able to distinguish between victim with second degree burn and first degree burn. It is well established in the medical world the survival level of burn activity will depend on total body burn surface area and age. Does the tool able to tell the severity level of the victim who had the impact according to age and total body surface area burn TBS and also the survival rate of the victim based on the depth of burn injury?

Yours sincerely,

Webmaster TNO  
Communication

P +31 (0)88 866 86 34  
F +31 (0)15 262 73 35  
E [webmaster@tno.nl](mailto:webmaster@tno.nl)

[Location](#)  
[Disclaimer](#)

TNO innovation for life

X (3023)

CONTACTS

SEARCH: tno

TNO

Delete

Reply

Forward

Spam

Print

TNO 2 Show Details

772

39

37

1

+

Dear Rashid,

Regarding:  
*I am interested with your product which provide a comprehensive risk assessment tool. As a person involve in EIA consultancy work the tool is essential this is especially in matters related to the impact of a particular activity toward population around it and environment. For the effect tool there is availability to measure thermal radiation from BLEVE. Does it able to distinguish between victim with second degree burn and first degree burn. It is well established in the medical world the survival level of burn activity will depend on total body burn surface area and age. Does the tool able to tell the severity level of the victim who had the impact according to age and total body surface area burn TBS and also the survival rate of the victim based on the depth of burn injury?*

Thank you for your interest in our software. The software will distinguish between 1<sup>st</sup>, 2<sup>nd</sup> and lethal burns. These relations derive from "The Green Book" which you can download here: [www.tno.nl/COLOUREDBOOKS](http://www.tno.nl/COLOUREDBOOKS). If you installed the EFFECTS software (as a demo), you can open the attached project file to see the results. In this case I set the observer distance to 50m and choose the "dynamic bleve" model. A second one is calculated with "protective clothing" set to ON. You can compare them by selecting both sessions.

We do not distinguish for specific age, amount of skin burnt and survival rate. Green Book, chapter 1 (Heat radiation); pages 11-36 gives background information.

Hope this helps.

Kind regards,

**Victor van Swinderen**  
TNO Urban Environment & Safety  
E-mail [victor.vanswinderen@tno.nl](mailto:victor.vanswinderen@tno.nl)